DEVELOPMENTS IN PRECAMBRIAN GEOLOGY 7
ADVISORY EDITOR B.F. WINDLEY

DEVELOPMENTS AND INTERACTIONS OF THE PRECAMBRIAN ATMOSPHERE, LITHOSPHERE AND BIOSPHERE

B. NAGY, R. WEBER, J.C. GUERRERO AND M. SCHIDLOWSKI
(EDITORS)

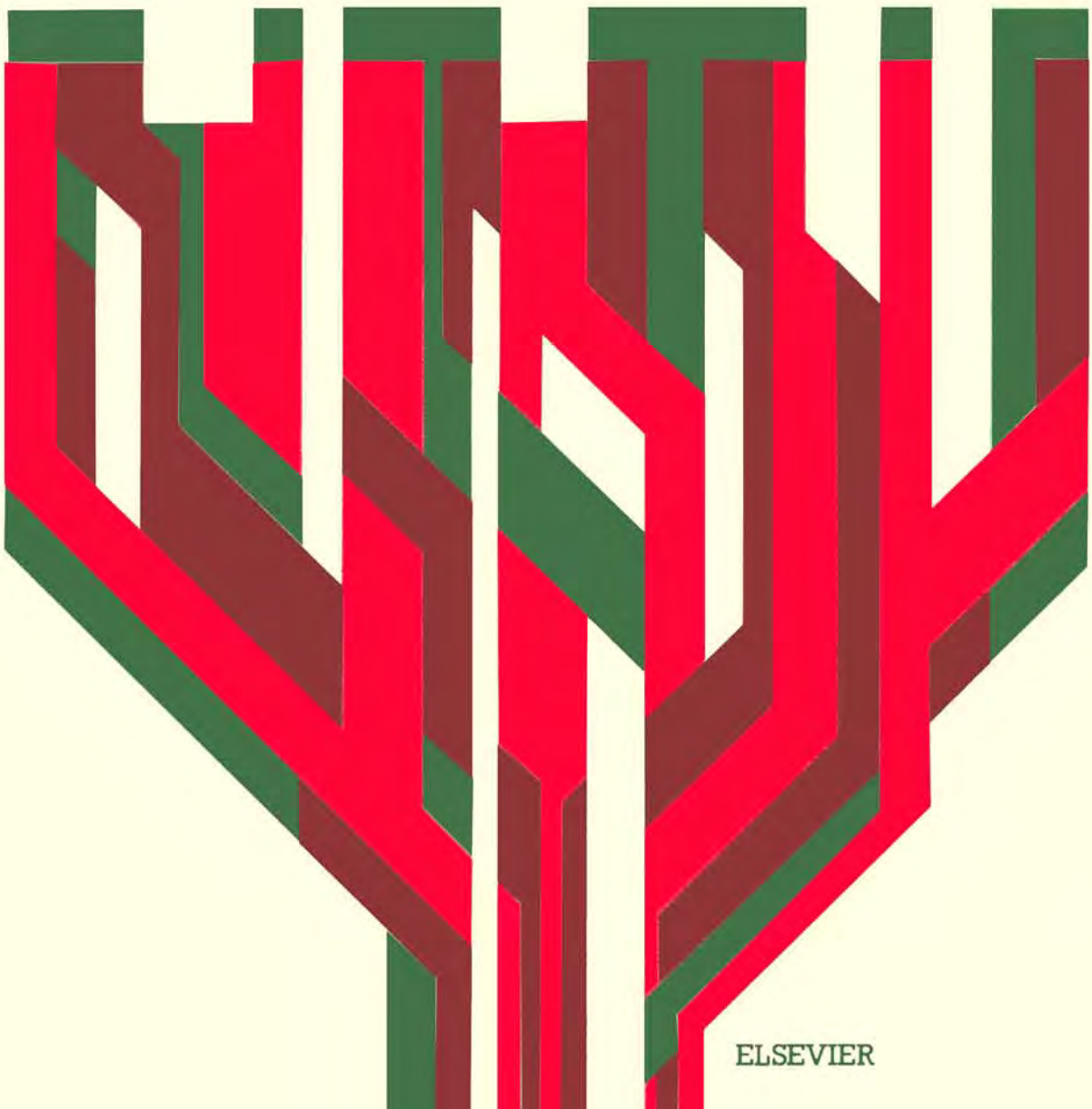

ELSEVIER

Developments in Precambrian Geology 7

DEVELOPMENTS AND INTERACTIONS OF THE PRECAMBRIAN ATMOSPHERE, LITHOSPHERE AND BIOSPHERE

DEVELOPMENTS IN PRECAMBRIAN GEOLOGY
Advisory Editor B.F. Windley

Further titles in this series

1. B.F. WINDLEY and S.M. NAQVI (Editors)
   Archaean Geochemistry
2. D.R. HUNTER (Editor)
   Precambrian of the Southern Hemisphere
3. K.C. CONDIE
   Archean Greenstone Belts
4. A. KRONER (Editor)
   Precambrian Plate Tectonics
5. Y.P. MEL'NIK
   Precambrian Banded Iron-formations. Physicochemical Conditions of Formation
6. A.F. TRENDALL and R.C. MORRIS (Editors)
   Iron-Formation: Facts and Problems

DEVELOPMENTS IN PRECAMBRIAN GEOLOGY 7

DEVELOPMENTS AND INTERACTIONS OF THE PRECAMBRIAN ATMOSPHERE, LITHOSPHERE AND BIOSPHERE

Compilation of papers based on the presentations of participants at, or contributed by authors unable to attend, the IGCP Projects 157 and 160 meeting at the Universidad Nacional Autonoma de Mexico in Mexico City, Mexico, January 11–14, 1982.

Edited by
B. NAGY
Department of Geosciences, University of Arizona, Tucson, Arizona, U.S.A.

R. WEBER AND J.C. GUERRERO
Institut di Geologia, Universidad Nacional Autónoma de México, México City, Mexico

and
M. SCHIDLOWSKI
Max-Planck-Institut für Chemie, Mainz, F.R. of Germany

reprinted from *Precambrian Geology,* vol. 20, nos. 2–4

IGCP Project Nos. 157 and 160

ELSEVIER, Amsterdam – Oxford – New York – Tokyo 1983

ELSEVIER SCIENCE PUBLISHERS B.V.
Molenwerf 1, 1014 AG Amsterdam
P.O. Box 211, Amsterdam, The Netherlands

Distributors for the United States and Canada:

ELSEVIER SCIENCE PUBLISHING INC.
52, Vanderbilt Avenue
New York, N.Y. 10017

Library of Congress Cataloging in Publication Data
Main entry under title:

Developments and interactions of the Precambrian atmosphere, lithosphere, and biosphere.

(Developments in Precambrian geology ; 7)
"Reprinted from Precambrian geology, vol. 20, nos. 2-4."
"IGCP Project nos. 157 and 160."
Bibliography: p.
1. Geology, Stratigraphic--Pre-Cambrian--Addresses, essays, lectures. I. Nagy, Bartholomew, 1927- II. Series.
QE653.D47 1983 551.7'1 83-16520
ISBN 0-444-42240-4

ISBN 0-444-42240-4 (Vol. 7)
ISBN 0-444-41719-2 (Series)

Printed in The Netherlands

CONTENTS

Foreword

This volume contains articles which resulted from the joint meeting of International Geological Correlation Program Projects 157 and 160, held in Mexico City. Pertinent details of the scope and organization of the meeting are described in the Prefaces.

For introduction, it seems appropriate to quote from the Presidential Address of Robert Etheridge, F.R.S. to the Geological Society of London. "Time and life are two subjects that at once arrest the attention of all earnest students. Our knowledge of the commencement of either is as indefinite now as in the days of the earliest investigators. With the succession of sedimentary rock masses in the outer framework of the globe we are perhaps partly familiar . . . yet yearly some new light is thrown upon the obscure history of the earliest rocks with which we believe ourselves acquainted". Some of the ideas presented in this are new, and are indeed novel. These should be challenged in print; this is how new scientific insight is acquired. Studies of the Precambrian, having sufficiently wide scope and great depth are still not common. This is a relatively new field of scientific endeavor. As in all young fields of inquiry, entrenched ideas occasionally hamper the evolution of heterodox concepts. This is noteworthy in context of Robert Etheridge's munificent Presidential Address, which was published in 1881 — one hundred and two years ago.

BARTHOLOMEW NAGY

This Page Intentionally Left Blank

Preface

This volume contains a set of papers resulting from the second joint meeting of Projects 157 and 160 of the International Geological Correlation Program held in January, 1982, in Mexico City, under the general title "Development and Interactions of the Precambrian Lithosphere, Biosphere and Atmosphere". In addition, the issue contains some articles by authors who had been invited, but, because of various circumstances were unable to attend the meeting.

In 1980, rather surprisingly, the participants of the first common workshop of IGCP Projects 157 and 160, held at Santa Barbara, California, invited the Geological Institute of the National University of Mexico (UNAM) to organize and host the second common meeting of these projects. Manfred Schidlowski and Erich Dimroth, the chairmen of these projects at the time of the Santa Barbara workshop, provided us with an excellent opportunity to bring together a large group of outstanding researchers, and to present to this audience the results of several research programs in Precambrian geology, paleontology and the origins of life, which are being carried on in Mexico.

About 40 specialists in astrophysics, microbiology, oceanography and a wide array of geological disciplines, particularly geochemistry, sedimentology and paleontology, from Brazil, Canada, China, Denmark, France, Germany, Great Britain, Mexico, the Soviet Union, the United States of America and Yugoslavia contributed many conventional and "unconventional" ideas to the wide field of Precambrian research. The central point of the discussions was the problem of oxygen partial pressures, especially in the early history of the Earth. A new orthodoxy seems to have emerged, i.e., that the early atmosphere was richer in oxidized species than previously suspected.

The meeting was organized with the financial support of the International Union of Geological Sciences and the International Geological Correlation Program (IUGS—IGCP), the National Council of Science and Technology (CONACyT) of Mexico, and the National Autonomous University of Mexico (UNAM). Many institutions gave additional support to the meeting through individual grants to the participants, and some individuals made considerable efforts to participate despite insufficient public funding. All these colleagues and institutions helped to make the meeting successful, and the organizers offer them their most sincere thanks.

The meeting took place in the auditorium of the Institute of Biomedical Research and the Seminar Unit "Ignacio Chávez", both of the UNAM. During the days in Mexico City, the Faculty of Engineering of the UNAM provided a bus for the transportation of the participants to the meeting places. We express our sincere gratitude to the academic and administrative authorities of these institutions for their invaluable help and constant attention to our, sometimes, very hasty requests.

Finally, we acknowledge the interest and efforts of Bartholomew Nagy to have the proceedings of the meeting incorporated into the scientific literature, which hopefully will continue to be stimulating for a long time.

REINHARD WEBER and JOSE C. GUERRERO
Instituto de Geologia,
Universidad Nacional Autónoma de México,
Ciudad Universitaria,
04510 MEXICO, D.F.

Preface

It is, indeed, gratifying for the organizers of the second common workshop of IGCP Projects 157 and 160 to see the proceedings of this meeting appear as a special issue of *Precambrian Research.* The workshop, entitled "Development and Interactions of Precambrian Lithosphere, Biosphere and Atmosphere", was held from 11—14 January 1982, in Mexico City, with local organization by Reinhard Weber and José Guerrero from the Institute of Geology, Universidad Nacional Autónoma de México (UNAM).

It goes without saying that the topic of the meeting reflects one of the foremost current frontiers in the earth sciences and one which has long represented a challenge not only to the geological community, but also to the biological and physical sciences. Therefore, it was timely that a multidisciplinary task force, of the type assembled in these two IGCP Projects, engaged in these problems whose relevance to a number of questions related to economic geology specifically calls for the involvement of "Third World" countries. Accordingly, it is hoped that this conference will, in the long run, also provide a stimulus for Mexican colleagues to intensify relevant programmes in this field.

Considering the intricacies of the Precambrian (and notably the Archaean) record and dealing, in part, with model-dependent assumptions, it was not surprising that a heterogeneous assembly did not achieve a universal consensus on all current issues. Such a consensus was neither expected nor aimed at. In fact, it was generally agreed among the organizers to deliberately structure the workshop so as to encourage creative conflict and to allow opportunities for the presentation of "unconventional" ideas. This policy was eventually implemented by Reinhard Weber who had assumed the heavy burden of organising the scientific programme of the conference. In this way, the stage was set for the refreshing controversies which considerably added to the conference and helped to clarify respective standpoints. By presenting personal challenges to one another, those engaged in lively discussions constantly needed to re-think their own positions. Not every standpoint defended during these controversies is likely to withstand critical scrutiny, but it is hoped that this publication of the proceedings will contain some ideas that stand the test of time.

I would like to express my sincere gratitude on behalf of our community to Reinhard Weber and José Guerrero for having responded so warmly to the call of the IGCP. Their technical organization of the workshop was excellent — from the provision of lavish open-air meals in the Botanical Garden, and the prevention of increased hotel tariffs, to coping with the logistics of an excursion some 1800 km from the site of the conference. It is, furthermore, a pleasure to acknowledge the generous support received from the University and from the Consejo Nacional de Ciencia y Tecnología (promoted by José Guerrero as Director of the Institute of Geology of UNAM). Together with

the modest IGCP budget, this support catered for the needs of those participants who had difficulty with their travel grants. Finally, special thanks are due to the members of the IGCP community, since it is primarily their unfailing commitment and enthusiasm that continues to keep our meetings at the forefront of current research.

MANFRED SCHIDLOWSKI
Chairman, IGCP Project 157,
Paleoatmosphere Research Group,
Max-Planck-Institut für Chemie (Otto-Hahn-Institut),
D-6500 Mainz,
WEST GERMANY.

OXYGEN AND OZONE IN THE EARLY EARTH'S ATMOSPHERE

V.M. CANUTO[1], J.S. LEVINE[2], T.R. AUGUSTSSON[2] and C.L. IMHOFF[3]

[1]*NASA, Goddard Institute for Space Studies, New York, NY 10025 (U.S.A.)*

[2]*NASA, Langley Research Center, Hampton, VA 23665 (U.S.A.)*

[3]*C.S.C., NASA, Goddard Space Flight Center, Greenbelt, MD 20771 (U.S.A.)*

ABSTRACT

Canuto, V.M., Levine, J.S., Augustsson, T.R. and Imhoff, C.L., 1983. Oxygen and ozone in the early Earth's atmosphere. Precambrian Res., 20: 109—120.

The precise amount of O_2 and O_3 in the Earth's prebiological paleoatmosphere has been a topic of considerable discussion in the past. Since the photolysis of H_2O and CO_2, the prebiological mechanisms to produce O_2, depends on the ultraviolet (UV) flux from the Sun, a reliable quantification of the problem requires detailed knowledge of such flux. Using the most recent astronomical observation of young stars from the International Ultraviolet Explorer, as well as a detailed photochemical model of the paleoatmosphere, we find that the amount of O_2 in the prebiological paleoatmosphere may have been as much as 10^6 times greater than previously estimated.

Some of the implications of this new value are discussed.

INTRODUCTION

Interaction among biologists, biochemists and geologists, as well as astronomers and atmospheric scientists, provides a unique opportunity to consider two fundamental questions about the prebiological paleoatmosphere: (1) what were the levels of atmospheric oxygen (O_2) and ozone (O_3) during the Earth's first billion years, and (2) what was the source of this early oxygen? The laboratory simulation experiments on chemical evolution discussed by the biochemists preclude the presence of free oxygen, while the geologists conclude that they could accept "some" oxygen. We believe that it is possible for the first time to quantify the levels of atmospheric oxygen during the Earth's first billion years. Recent astronomical measurements, coupled with recent developments in atmospheric reaction rates and in the photochemical modeling of the atmosphere, have provided powerful tools to consider the question of oxygen in the early atmosphere. The basic inputs in this study include:

(1) recent measurements of the ultraviolet (UV) radiation from young stars (representing the Sun over its first few million years) obtained with the International Ultraviolet Explorer (IUE);

(2) a detailed one-dimensional photochemical model of the paleoatmosphere consisting of 34 atmospheric gases and 102 chemical processes (25 photolysis reactions and 77 chemical reactions). The molecular absorption cross sections needed for the photolysis calculations and the reaction branching ratios and reaction rates needed for the chemical calculations are based on laboratory measurements.

THE AMOUNT OF CO_2

Standard stellar evolutionary models unequivocally predict that the Sun was dimmer in the past (Newman and Rood, 1977). In its early history, the Sun was composed almost entirely of hydrogen, which, over 4.5 Ga, has been partially converted into heavier elements. Since the luminosity of a star is a strong function of the mean molecular weight, μ, i.e.

$$L \sim \mu^8 \tag{1}$$

then

$$L(4.5 \text{ Ga-ago}) = 0.72\ L \text{ (today)} \tag{2}$$

where L is the solar luminosity. A decrease of 30% may seem a rather small change. However, when translated into a decrease in the effective temperature T of the Earth, the result is that

$$T(4.5 \text{ Ga-ago}) = 238°\text{K} \tag{3}$$

i.e., T was below the freezing point of seawater. Since the increase in the Sun's luminosity is a slow process, the prediction is that the Earth's effective temperature may have been below freezing for at least 2 Ga, contrary to the well established fact that stromatolites have been found which are 3.5 Ga-old, indicating the presence of liquid water (Sagan and Mullen, 1972; Sagan, 1977).

A widely accepted solution to the "Dim Sun Paradox" may be that the prebiological paleoatmosphere contained considerably more CO_2 than the present atmosphere (Owen et al., 1979). These authors have suggested that the early atmosphere may have contained as much as three orders of magnitude more CO_2 than the present atmosphere.

THE UV DATA

Since the Sun's total luminosity was lower in the past, it has sometimes been assumed that the UV flux was also correspondingly lower. This, however, does not appear to be the case. Recent UV data on young (T-Tauri) stars, obtained with IUE, have indicated that the formation of a stellar chromosphere is accompanied by large UV fluxes (Imhoff and Giampapa, 1980, 1981, 1982). Since young T-Tauri stars are believed to be a good representation of the initial stages of the early Sun, it is concluded from the IUE data that the young Sun was emitting much more UV radiation than it does today.

To quantify the statement, we present in Table I the ratio of stellar to solar UV fluxes intercepted at the distance of the Earth. As can be seen, the UV fluxes were 10^3—10^5 times larger than their present values. This datum is, however, not sufficient because the duration of such an enhanced flux also needs to be known. Therefore, in Table II we present the estimated UV fluxes as a function of stellar age, and see that at the main sequence entrance time, 5×10^7 y, the UV flux was still 100 times larger than today's value (Canuto et al., 1982).

TABLE I

Ratios of stellar to solar UV line fluxes intercepted at the distance of the Earth

λ(A)	Ident	T Tau	DR Tau	RW Aur	GW Ori	CoD-35°10525	RU Lup	S CrA
1240	NV	2.5(5)*		⩽4.0(3)	2.3(5)	6.1(4)	2.4(3)	
1304	OI, SI	1.3(5)		9.4(3)	9.9(4)	3.0(4)	6.5(3)	
1335	CII	7.8(4)		9.6(2)	4.3(4)	1.7(4)	1.9(4)	
1400	Si IV	2.2(5)	5.5(4)	1.2(4)	2.3(5)	2.0(4)	3.3(4)	2.4(4)
1550	CIV	1.4(5)	8.8(4)	3.2(3)	1.5(5)	2.9(4)	1.2(4)	8.1(3)
1640	He II	1.4(5)	5.9(4)	⩽1.5(3)	2.0(5)	2.6(4)	5.8(3)	⩽7.7(3)
1813	Si II.SI	2.9(4)	1.9(4)		1.1(4)	2.8(3)	5.1(3)	5.6(3)

*2.5(5) = 2.5 x 10^5.
The radii of the stars have been taken as (in solar radii): 6.8, 4.7, 3.1, 8.4, 3.4, 2.6, and 3.2, respectively.

TABLE II

Stellar UV flux as a function of age

Age (years)	UV enhancement
10^6	10^4
10^7	500
5 x 10^7	100
10^8	32
5 x 10^8	8
10^9	4
5 x 10^9	1

THE PHOTOCHEMICAL MODEL

Prior to the origin and evolution of photosynthetic activity, the formation of oxygen was initiated by the photolysis of water vapor (H_2O), accompanied by the exospheric escape of atomic hydrogen (H) and atmospheric reactions involving the hydroxyl radical (OH), and by the photolysis of carbon dioxide (CO_2)

($\lambda \leqslant 240$ nm) $H_2O + h\nu \rightarrow OH + H$ (4)

$OH + OH \rightarrow O + H_2O$ (5)

($\lambda \leqslant 230$ nm) $CO_2 + h\nu \rightarrow O + CO$ (6)

The atomic oxygen (O) formed in reactions 5 and 6 produces molecular oxygen (O_2) via reactions 7 and 8 (M represents any third body)

$O + O + M \rightarrow O_2 + M$ and (7)

$O + OH \rightarrow O_2 + H$ (8)

Atmospheric ozone (O_3) is produced via a reaction involving O_2 and O

$O + O_2 + M \rightarrow O_3 + M$ (9)

Atmospheric oxygen is destroyed via photolysis by solar ultraviolet radiation and by chemical reactions, e.g., with molecular hydrogen (H_2) resulting from volcanic activity. To calculate the vertical distributions of O, O_2, O_3, H_2O, H, OH, CO_2 and H_2, Levine et al. (1981, 1982) developed a detailed photochemical model of the paleoatmosphere. This model, which was originally developed to study the effect of anthropogenic perturbations on future levels of O_3, has been used to study the origin and evolution of O_3 for specified levels of paleoatmosphere O_2 ranging from 10^{-4} of the present atmospheric level (PAL) to the present atmospheric level (1 PAL) (Levine et al., 1981). The model was modified such that O_2, CO_2, and H_2, which were previously specified as input parameters, are now considered as chemically-active species whose vertical profiles are calculated using coupled species continuity/flux equations containing both chemical production and loss terms, and vertical eddy transport (Levine et al., 1982). The inclusion of O_2, CO_2, and H_2 as chemically-active species brings the total of species whose vertical profiles are solved simultaneously by coupled species—continuity/flux equations to 31. The other calculated species are: O_3, O, N_2O, N, NO, NO_2, NO_3, N_2O_5, HNO_2, HNO_3, H_2O, H, OH, HO_2, H_2O_2, CH_4, CO, CH_3OOH, CH_2O, CH_3, HCO, CH_3O_2, CH_3O, Cl, ClO, HCl, CH_3Cl, and $ClNO_3$. Very short-lived species assumed to be in instantaneous photochemical equilibrium include: $O(^1D)$, ClO_2, and Cl_2. The model now includes 25 photochemical processes listed in Table III, and 77 chemical reactions listed in Table IV. The U.S. Standard Atmosphere Mid-Latitude Spring/Fall temperature profile is specified in the troposphere. A primordial temperature profile that decreases linearly from the troposphere. A primordial temperature This profile is based on coupled photochemical/radiative equilibrium temperature calculations in the O_3-deficient paleoatmosphere (Levine and Boughner, 1979). Water soluble species, e.g., HNO_3, H_2O_2, CH_3OOH, HCl, ClO, and $ClNO_3$ are lost via rainout, with a rainout coefficient of 1.0×10^{-6} s^{-1}. The model extends from the surface up to 53.5 km with the tropopause at a height of 14.5 km. Photodissociation rates are diurnally averaged for a latitude of 30° and solar declination of 0°. The model includes the flux of radiation from the present Sun, which is between 110—735 nm (Ackermann, 1971).

TABLE III

Photodissociation reactions and diurnally-averaged rates at 53.5 km for a latitude of 30° (equinoctial conditions) (for present atmosphere)

Reaction no.	Reaction	Destruction (cm^{-3} s^{-1})
J1	$O_2 + h\nu \rightarrow O + O$	1.41×10^{6}
J2	$O_3 + h\nu \rightarrow O + O_2$	4.40×10^{6}
J3	$O_3 + h\nu \rightarrow O(^1D) + O_2$	7.07×10^{7}
J4	$H_2O + h\nu \rightarrow OH + H$	5.32×10^{2}
J5	$N_2O + h\nu \rightarrow O(^1D) + N_2$	1.29×10^{2}
J6	$HNO_3 + h\nu \rightarrow OH + NO_2$	2.63×10^{0}
J7	$NO_2 + h\nu \rightarrow O + NO$	1.33×10^{4}
J8	$H_2O_2 + h\nu \rightarrow OH + OH$	2.52×10^{2}
J9	$HNO_2 + h\nu \rightarrow OH + NO$	4.31×10^{1}
J10	$NO_3 + h\nu \rightarrow NO + O_2$	7.85×10^{-1}
J11	$NO_3 + h\nu \rightarrow NO_2 + O$	7.85×10^{0}
J12	$N_2O_5 + h\nu \rightarrow NO_2 + NO_3$	5.21×10^{-4}
J13	$HCl + h\nu \rightarrow H + Cl$	1.47×10^{0}
J14	$ClO_2 + h\nu \rightarrow ClO + O$	6.41×10^{-3}
J15	$ClO + h\nu \rightarrow Cl + O$	1.45×10^{2}
J16	$Cl_2 + h\nu \rightarrow Cl + Cl$	1.43×10^{-6}
J17	$ClNO_3 + h\nu \rightarrow ClO + NO_2$	4.77×10^{-4}
J18	$CCl_4 + h\nu \rightarrow 2Cl + products$	1.27×10^{-5}
J19	$CH_3Cl + h\nu \rightarrow CH_3 + Cl$	1.09×10^{-2}
J20	$CH_2O + h\nu \rightarrow H + HCO$	4.00×10^{1}
J21	$CH_2O + h\nu \rightarrow H_2 + CO$	4.15×10^{1}
J22	$CH_3CCl_3 + h\nu \rightarrow Cl + products$	1.20×10^{-5}
J23	$CH_3OOH + h\nu \rightarrow CH_3O + OH$	1.82×10^{0}
J24	$NO + h\nu \rightarrow N + O$	9.12×10^{1}
J25	$CO_2 + h\nu \rightarrow CO + O$	4.51×10^{-1}

As already noted, the complete photochemical model contains 34 species and 102 photochemical/chemical processes listed in Tables III and IV. This model has been adopted for photochemical studies of the prebiological paleoatmosphere by appropriate choices of the boundary conditions for various species. In these calculations, the prebiological paleoatmosphere consists of present-day levels of nitrogen (N_2) and water vapor (H_2O), and preindustrial levels (280 parts per million by volume — ppmv) of carbon dioxide (CO_2). The H_2O profile based on the U.S. Standard Atmosphere Mid-Latitude Spring/Fall is specified in the troposphere, and is calculated using a H_2O continuity/flux equation in the stratosphere. The surface flux of gases resulting from biological activity, e.g., CH_4, N_2O, and CH_3Cl, and those gases resulting from anthropogenic activity, e.g., NO_x (NO + NO_2), CCl_4, CH_3CCl_3 are set equal to zero in these calculations. The surface flux of CO assumed to result from volcanic activity is set equal to 3.2×10^{8} cm^{-2} s^{-1} (Walker, 1977). The surface flux of HCl assumed to result from sea salt spray and volcanic activity

TABLE IV

Chemical reactions

No.	Reaction	Rate constant (cm^3 s^{-1} or cm^6 s^{-1})
1	$O + O_2 + M \rightarrow O_3 + M$	$1.1 \times 10^{-34} \exp(510/T)$
2	$O + O_3 \rightarrow 2O_2$	$1.5 \times 10^{-11} \exp(-2218/T)$
3	$O(^1D) + O_2 \rightarrow O + O_2$	$3.2 \times 10^{-11} \exp(67/T)$
4	$O(^1D) + N_2 \rightarrow O + N_2$	$1.8 \times 10^{-11} \exp(107/T)$
5	$N_2O + O(^1D) \rightarrow 2NO$	6.6×10^{-11}
6	$N_2O + O(^1D) \rightarrow N_2 + O_2$	5.1×10^{-11}
7	$NO + O + M \rightarrow NO_2 + M$	$1.6 \times 10^{-32} \exp(584/T)$
8	$NO + O_3 \rightarrow NO_2 + O_2$	$2.3 \times 10^{-12} \exp(-1450/T)$
9	$NO_2 + O \rightarrow O_2 + NO$	9.3×10^{-12}
10	$NO_2 + O_3 \rightarrow NO_3 + O_2$	$1.2 \times 10^{-13} \exp(-2450/T)$
11	$NO + HO_2 \rightarrow NO_2 + OH$	$3.5 \times 10^{-12} \exp(250/T)$
12	$NO_2 + OH + M \rightarrow HNO_3 + M$	*See JPL Publication 81-3 (1981)
13	$HNO_3 + OH \rightarrow NO_3 + H_2O$	$1.5 \times 10^{-14} \exp(650/T)$
14	$H_2O + O(^1D) \rightarrow 2OH$	2.2×10^{-10}
15	$H + O_2 + M \rightarrow HO_2 + M$	$2.1 \times 10^{-32} \exp(290/T)$
16	$H + O_3 \rightarrow OH + O_2$	$1.4 \times 10^{-10} \exp(-470/T)$
17	$OH + O \rightarrow H + O_2$	$2.3 \times 10^{-11} \exp(110/T)$
18	$OH + O_3 \rightarrow HO_2 + O_2$	$1.6 \times 10^{-12} \exp(-940/T)$
19	$OH + OH \rightarrow H_2O + O$	$4.5 \times 10^{-12} \exp(-275/T)$
20	$HO_2 + O \rightarrow OH + O_2$	4.0×10^{-11}
21	$HO_2 + O_3 \rightarrow OH + 2O_2$	$1.1 \times 10^{-14} \exp(-580/T)$
22	$HO_2 + OH \rightarrow H_2O + O_2$	4×10^{-11}
23	$HO_2 + HO_2 \rightarrow H_2O_2 + O_2$	2.5×10^{-12}
24	$H_2O_2 + OH \rightarrow HO_2 + H_2O$	$2.7 \times 10^{-12} \exp(-145/T)$
25	$OH + NO + M \rightarrow HNO_2 + M$	See JPL Publication 81-3 (1981)
26	$NO + NO_3 \rightarrow 2NO_2$	2.0×10^{-11}
27	$O(^1D) + N_2 + M \rightarrow N_2O + M$	3.5×10^{-37}
28	$O(^1D) + H_2 \rightarrow OH + H$	9.9×10^{-11}
29	$O(^1D) + CH_4 \rightarrow OH + CH_3$	1.4×10^{-10}
30	$NO_2 + O + M \rightarrow NO_3 + M$	1.0×10^{-31}
31	$NO_2 + NO_3 \rightarrow N_2O_5$	$1.5 \times 10^{-13} \exp(861/T)$
32	$N_2O_5 \rightarrow NO_2 + NO_3$	$1.2 \times 10^{14} \exp(-10319/T)$
33	$N_2O_5 + H_2O \rightarrow 2HNO_3$	1.0×10^{-20}
34	$N_2O_5 + O \rightarrow 2NO_2 + O_2$	3.0×10^{-16}
35	$N + NO_2 \rightarrow N_2O + O$	$2.1 \times 10^{-11} \exp(-800/T)$
36	$N + O_2 \rightarrow NO + O$	$4.4 \times 10^{-12} \exp(-3220/T)$
37	$N + NO \rightarrow N_2 + O$	3.4×10^{-11}
38	$N + O_3 \rightarrow NO + O_2$	1.0×10^{-15}
39	$Cl + O_3 \rightarrow ClO + O_2$	$2.8 \times 10^{-11} \exp(-257/T)$
40	$ClO + O \rightarrow Cl + O_2$	$7.7 \times 10^{-11} \exp(-130/T)$
41	$ClO + NO \rightarrow Cl + NO_2$	$6.5 \times 10^{-12} \exp(280/T)$
42	$Cl + CH_4 \rightarrow HCl + CH_3$	$9.6 \times 10^{-12} \exp(-1350/T)$
43	$Cl + H_2 \rightarrow HCl + H$	$3.5 \times 10^{-11} \exp(-2290/T)$
44	$Cl + HO_2 \rightarrow HCl + O_2$	4.8×10^{-11}
45	$Cl + H_2O_2 \rightarrow HCl + HO_2$	$1.1 \times 10^{-12} \exp(-980/T)$
46	$Cl + HNO_3 \rightarrow HCl + NO_3$	$1.0 \times 10^{-11} \exp(-2170/T)$
47	$Cl + CH_2O \rightarrow HCl + HCO$	$9.2 \times 10^{-11} \exp(-68/T)$

TABLE IV (*continued*)

No.	Reaction	Rate constant ($cm^3\ s^{-1}$ or $cm^6\ s^{-1}$)
48	$HCl + OH \rightarrow Cl + H_2O$	$2.8 \times 10^{-12} \exp(-425/T)$
49	$HCl + O \rightarrow Cl + OH$	$1.1 \times 10^{-11} \exp(-3370/T)$
50	$Cl + O_2 + M \rightarrow ClO_2 + M$	See JPL Publication 81-3 (1981)
51	$ClO_2 + M \rightarrow Cl + O_2 + M$	$2.7 \times 10^{-9} \exp(-2650/T)$
52	$Cl + ClO_2 \rightarrow 2ClO$	8.0×10^{-12}
53	$Cl + ClO_2 \rightarrow Cl_2 + O_2$	1.4×10^{-10}
54	$OH + OH + M \rightarrow H_2O_2 + M$	See JPL Publication 81-3 (1981)
55	$H_2O_2 + O \rightarrow OH + HO_2$	$2.8 \times 10^{-12} \exp(-2125/T)$
56	$OH + CH_4 \rightarrow CH_3 + H_2O$	$2.4 \times 10^{-12} \exp(-1710/T)$
57	$ClO + NO_2 + M \rightarrow ClNO_3 + M$	See JPL Publication 81-3 (1981)
58	$O + ClNO_3 \rightarrow ClO + NO_3$	$3.0 \times 10^{-12} \exp(-808/T)$
59	$O(^1D) + HCl \rightarrow OH + Cl$	1.4×10^{-10}
60	$H_2 + OH \rightarrow H_2O + H$	$1.2 \times 10^{-11} \exp(-2200/T)$
61	$CH_3 + O_2 + M \rightarrow CH_3O_2 + M$	See JPL Publication 81-3 (1981)
62	$CH_3O_2 + HO_2 \rightarrow CH_3OOH + O_2$	$7.7 \times 10^{-14} \exp(1300/T)$
63	$CH_3O_2 + NO \rightarrow CH_3O + NO_2$	7.4×10^{-12}
64	$CH_3O + O_2 \rightarrow CH_2O + HO_2$	$9.2 \times 10^{-13} \exp(-2200/T)$
65	$CH_2O + OH \rightarrow HCO + H_2O$	1.0×10^{-11}
66	$CH_2O + O \rightarrow OH + HCO$	$3.0 \times 10^{-11} \exp(-1550/T)$
67	$HCO + O_2 \rightarrow CO + HO_2$	5.0×10^{-12}
68	$CO + OH \rightarrow H + CO_2$	See JPL Publication 81-3 (1981)
69	$CH_3Cl + OH \rightarrow Cl +$ products	$1.8 \times 10^{-12} \exp(-1112/T)$
70	$CH_3OOH + OH \rightarrow CH_3O_2 + H_2O$	$2.1 \times 10^{-12} \exp(-145/T)$
71	$OH + CH_3CCl_3 \rightarrow Cl +$ products	$5.4 \times 10^{-12} \exp(-1820/T)$
72	$O + O + M \rightarrow O_2 + M$	$2.8 \times 10^{-34} \exp(710/T)$
73	$H + H + M \rightarrow H_2 + M$	8.3×10^{-33}
74	$H_2 + O \rightarrow OH + H$	$3.0 \times 10^{-14} \exp(-4480/T)$
75	$H + HO_2 \rightarrow O_2 + H_2$	4.7×10^{-11} (x0.29)
76	$H + HO_2 \rightarrow H_2O + O$	4.7×10^{-11} (x0.02)
77	$H + HO_2 \rightarrow OH + OH$	4.7×10^{-11} (x0.69)

*Chemical Kinetic and Photochemical Data for Use In Stratospheric Modelling. JPL Publication 81-3, Jet Propulsion Laboratory, California Institute of Technology, Pasadena, California, Jan 15, 1981, 124 pp.

is set equal to 1×10^{10} cm^{-2} s^{-1} (Levine et al., 1981). Oxygen (O_2) is considered as a chemically-active species and has a specified zero flux lower boundary condition, while molecular hydrogen (H_2) has a prescribed surface mixing ratio of 17 ppmv, both identical to the boundary conditions of Kasting and Walker (1981). We have studied the sensitivity of prebiological O_2 and O_3 to the level of CO_2 by performing calculations for the preindustrial level of CO_2 (280 ppmv) and for 10—100 times this value, which is considerably below the paleoatmospheric level of CO_2 suggested by Owen et al. (1979). We have used five values for calculating the flux of solar UV radiation ($\lambda < 300$ nm), i.e., the present value (Ackermann, 1971), and multiples of 10, 30, 100 and 300 times the present value.

THE RESULTS

The calculated O_2 and O_3 profiles are presented in Figs. 1—4 for different UV fluxes and CO_2 levels. The case of 280 ppm of CO_2, corresponding to the preindustrial value, is included to highlight the difference brought about by a 10^2 increase of CO_2, i.e., a CO_2 level of 28000 ppm.

At ground level, the O_2 mixing ratio increases from 10^{-15} (Fig. 1) to 10^{-9} (Fig. 2) for a UV flux of 300 and a CO_2 enhancement of 100: the larger UV flux together with the enhancement of CO_2, produce an increase of six

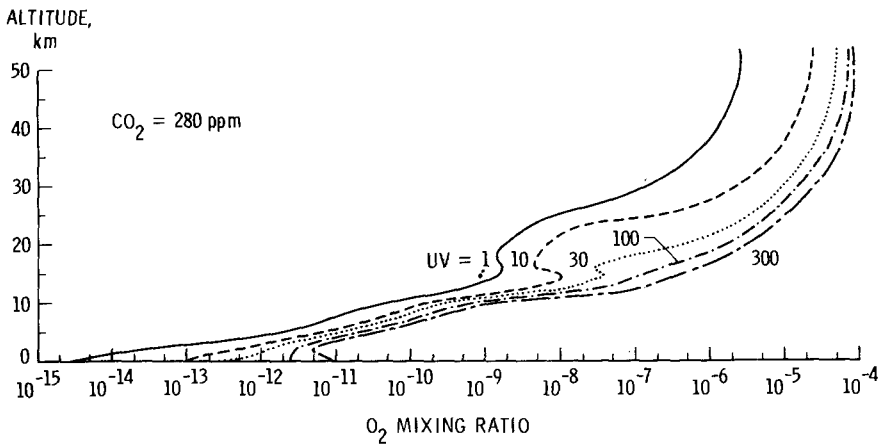

Fig. 1. Vertical distribution of O_2 in the prebiological paleoatmosphere for levels of solar UV from 1 to 300 times the present value for a CO_2 level of 280 ppmv.

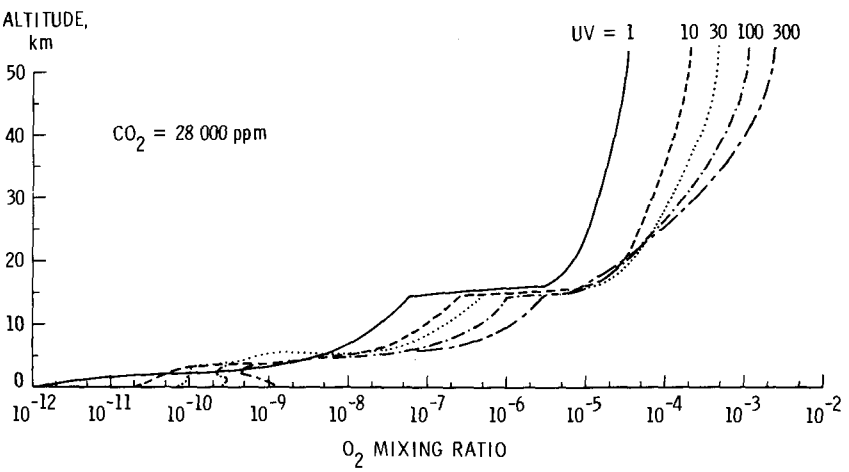

Fig. 2. Vertical distribution of O_2 in the prebiological paleoatmosphere for levels of solar UV from 1 to 300 times the present value for a CO_2 level of 28000 ppmv.

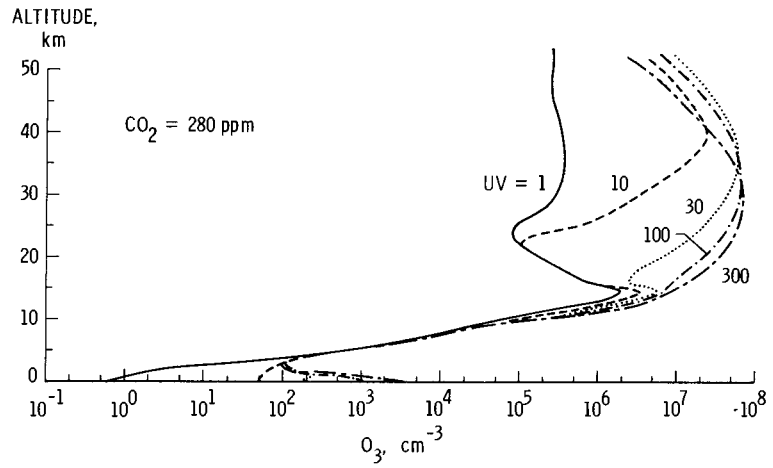

Fig. 3. Vertical distribution of O_3 in the prebiological paleoatmosphere for levels of solar UV from 1 to 300 times the present value for a CO_2 level of 280 ppmv.

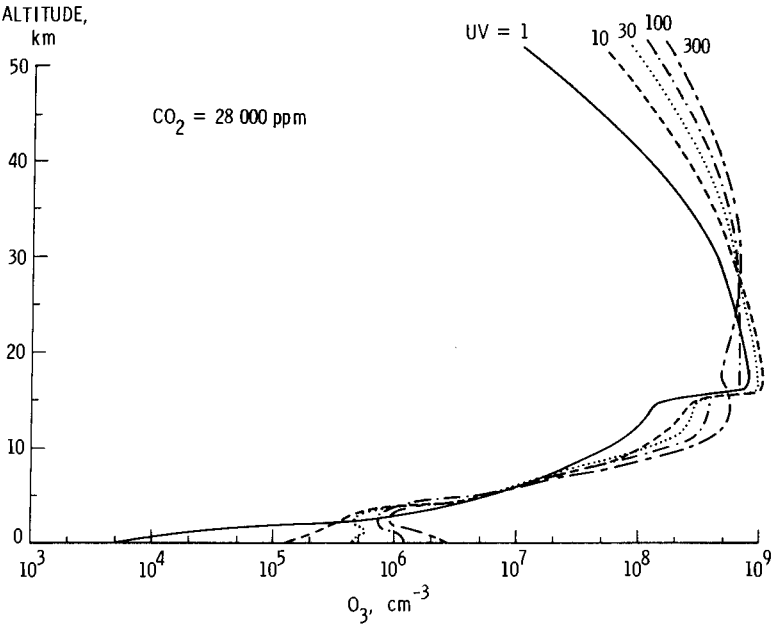

Fig. 4. Vertical distribution of O_3 in the prebiological paleoatmosphere for levels of solar UV from 1 to 300 times the present value for a CO_2 level of 28 000 ppmv.

orders of magnitude in the O_2 content at the Earth's surface. It is important to stress that this O_2 increase by a factor of 10^6 has been achieved without resorting to photosynthetic production of oxygen, i.e., a completely abiological production. Equally important are the O_3 profiles of Figs. 3 and 4, as

well as the values for the total O_3 column presented in Table V. In this table it is clearly seen that for a 300 UV flux and a CO_2 level 100 times the present value, the O_3 column density is

$$2.2 \cdot 10^{15} \text{ cm}^{-2} \tag{10}$$

TABLE V

Column density of ozone (O_3) in the prebiological paleoatmosphere for various combinations of atmospheric CO_2 and solar UV flux

Solar UV flux	CO_2 (ppmv)	O_3 column, cm^{-2}
1[a]	1[b]	1.72 (12)[c]
	10	2.49 (14)
	100	1.38 (15)
10	1	3.94 (13)
	10	5.36 (14)
	100	1.95 (15)
30	1	1.50 (14)
	10	7.81 (14)
	100	2.06 (15)
100	1	1.76 (14)
	10	8.15 (14)
	100	2.04 (15)
300	1	1.52 (14)
	10	9.41 (14)
	100	2.19 (15)

[a]Present value of solar ultraviolet flux (Ackermann, 1971). Other values represent multiples of present value.
[b]Preindustrial level of CO_2(ppmv). Other values represent multiples of this value.
[c]1.72 (12) is read as 1.72×10^{12}

to be contrasted with the value

$$1.7 \cdot 10^{12} \text{ cm}^{-2} \tag{11}$$

calculated for present level of UV flux and preindustrial CO_2. The gain is of a factor of 10^3, a considerable step toward, but short of the value

$$7 \cdot 10^{18} \text{ cm}^{-2} \tag{12}$$

frequently noted as the one needed for a biologically effective screening of UV radiation (Ratner and Walker, 1972).

Our calculated increase in ground level concentration of O_2 by six orders of magnitude places O_2 concentrations in the ppbv range. At this range, ground level concentrations of O_2 are comparable to ground level concentration values of NO_x, HNO_3, NH_3, H_2O_2, and HCO in the present atmosphere. Although these five gases are at ppbv levels, they are all of great environmental and photochemical significance in the present atmosphere.

CONCLUSIONS

The relevance and reliability of the results presented here depends to a large extent on the quality of the input data, which, as we have discussed, were recently obtained from the IUE observations of young T-Tauri stars.

We believe that the enhanced amount of O_2 that results from our analysis, while it may not hamper the chemical evolution process, is large enough to help explain the oxidation reduction state of ancient rocks. In fact, it is interesting to note that the higher value of O_2 reported here falls within the lower (10^{-13}) and upper (10^{-3}) O_2 values arrived at in order to explain the simultaneous existence of oxidized iron and reduced uranium in the oldest rocks (Kline and Bricker, 1977; Towe, 1978; Grandstaff, 1980).

ACKNOWLEDGEMENTS

V.M.C. and J.S.L. thank Dr. K.M. Towe for his helpful comments on earlier versions of this manuscript. C.L.I. thanks Dr. H.S. Giampapa for his assistance. J.S.L. and T.R.A. thank Dr. M. Natarajan for his assistance and comments on the photochemical calculations.

REFERENCES

Ackermann, M., 1971. Ultraviolet solar radiation related to mesospheric processes. In: G. Fiocco (Editor), Mesospheric Models and Related Experiments. Reidel, Dordrecht, Holland, pp. 149—159.

Canuto, V.M., Levine, J.S., Augustsson, T.R. and Imhoff, C.L., 1982. UV radiation from the young Sun and levels of O_2 and O_3 in the prebiological paleoatmosphere. Nature, 296: 816—820.

Grandstaff, D.E., 1980. Origin of uraniferous conglomerates at Elliot Lake, Canada and Witwatersrand, South Africa: implications for oxygen in the Precambrian atmosphere. Precambrian Res., 13: 1—26.

Imhoff, C.L. and Giampapa. M.S., 1980. The UV-spectrum of T-Tauri star RW Aurigae. Astrophys. J. (Letters), 239: L115—119.

Imhoff, C.L. and Giampapa, M.S., 1981. The UV variability of T-Tauri stars RW-Auriga in the universe at ultraviolet wavelengths. In: R.D.Chapman (Editor), The First Two Years of IUE. NASA Conf. Publ. No. 2171, pp. 185—189.

Imhoff, C.L. and Giampapa, M.S., 1982. Far UV and X-ray evidence concerning the chromospheres and coronae of T-Tauri stars. In: M.S. Giampapa (Editor), Proceedings at the Second Cambridge Workshop on Cool Stars, Stellar Systems and the Sun. Smithsonian Astrophys. Observ. Special Rep. No. 392, Vol. 2, pp. 175—180.

Kasting, J.F. and Walker, J.C.G., 1981. Limits on oxygen concentration in the prebiological atmosphere and the rate of abiotic fixation of nitrogen. J. Geophys. Res., 86: 1147—1158.

Kline, C. and Bricker, O.P., 1977. Some aspects of the sedimentary and diagenetic environment of Protorozoic banded iron formation. Econ. Geol., 72: 1457—1470.

Levine, J.S., Augustsson, T.R., Boughner, R.E., Natarajan, M. and Sacks, L.J., 1981. Comets and the Photochemistry of the Paleoatmosphere. In: C. Ponnamperuma (Editor), Comets and the Origin of Life. Reidel, Dordrecht, pp. 161—190.

Levine, J.S., Augustsson, T.R. and Natarajan, M., 1982. The prebiological paleoatmosphere: stability and composition. Origins Life, 12: 245—259.

Levine, J.S. and Boughner, R.E., 1979. The effects of paleoatmospheric ozone on surface temperature. Icarus, 39: 310—314.

Newman, M.J. and Rood, R.T., 1977. Implications of solar evolution for the Earth's early atmosphere. Science, 198: 1035—1037.
Owen, T., Cess, R.D. and Ramanathan, V., 1979. Enhanced CO_2 greenhouse to compensate for reduced solar luminosity on early Earth. Nature, 277: 640—642.
Ratner, M.I. and Walker, J.C.G., 1972. Atmospheric ozone and the history of life. J. Atmos. Sci., 29: 803—808.
Sagan, C. and Mullen, G., 1972. Earth and Mars: evolution of atmospheres and surface temperatures. Science, 177: 52—56.
Sagan, C., 1977. Reducing greenhouses and the temperature history of Earth and Mars. Nature, 269: 224—226.
Towe, K.M., 1978. Early Precambrian oxygen: a case against photosynthesis. Nature, 274: 657—661.
Walker, J.C.G., 1977. Evolution of the Atmosphere. Macmillan, New York, 318 pp.

PHOTOCHEMISTRY OF METHANE IN THE EARTH'S EARLY ATMOSPHERE

J.F. KASTING*
National Center for Atmospheric Research, P.O. Box 3000, Boulder, CA 80307 (U.S.A.)

K.J. ZAHNLE

Department of Astronomy and Department of Atmospheric and Oceanic Science, The University of Michigan, Ann Arbor, MI 48109 (U.S.A.)

J.C.G. WALKER

Space Physics Research Laboratory and Department of Atmospheric and Oceanic Science, The University of Michigan, Ann Arbor, MI 48109 (U.S.A.)

ABSTRACT

Kasting, J.F., Zahnle, K.J. and Walker, J.C.G., 1983. Photochemistry of methane in the Earth's early atmosphere. Precambrian Res., 20: 121—148.

A detailed model is presented of methane photochemistry in the primitive terrestrial atmosphere along with speculation about its interpretation. Steady-state CH_4 mixing ratios of 10^{-6}—10^{-4} could have been maintained by a methane source of about 10^{11} cm^{-2} s^{-1}, which is comparable to the modern biogenic methane production rate. In the absence of a source, methane would have disappeared in $< 10^4$ years, being either oxidized, or polymerized into more complex hydrocarbons. The source strength needed to maintain a steady CH_4 mixing ratio and the degree to which methane could have polymerized to form higher hydrocarbons depend upon the amount of CO_2 present in the early atmosphere. The dependence on H_2 is much weaker. Infrared absorption by methane, and especially by other hydrocarbon species, may have supplemented the greenhouse warming due to carbon dioxide. A radiative model is needed to establish this effect quantitatively. The destruction of the methane greenhouse early in the Proterozoic may have triggered the Huronian glaciation.

These calculations also suggest that atmospheres rich in both CO_2 and CH_4 may be photochemically unstable with respect to conversion to CO.

INTRODUCTION

Theoretical calculations by several investigators have led to plausible models for the composition of the Earth's primitive atmosphere (Walker, 1977; Yung and McElroy, 1979; Kasting et al., 1979; Kasting and Walker, 1981; Pinto

*Now at NASA-Ames Research Center, Moffett Field, CA 94035, U.S.A.

et al., 1980). The model atmospheres considered in these studies consist primarily of N_2, CO_2 and H_2O, along with smaller concentrations of H_2 and CO, and only trace amounts of O_2. This type of weakly reducing early atmosphere is consistent with both the geological record and with the present understanding of volcanic emissions and the escape of hydrogen to space.

The factors controlling climate on the early Earth are less well understood. Models of stellar evolution predict that the ancient Sun was considerably less luminous than it is today (Newman and Rood, 1977). Since the Earth does not appear to have been extensively glaciated during the first half of its history (Frakes, 1979), several authors have suggested that the atmospheric greenhouse effect must have been substantially larger in the remote past. Sagan and Mullen (1972) originally proposed ammonia as the key primordial greenhouse constituent. However, calculations by Kuhn and Atreya (1979) and Kasting (1982) indicate that ammonia is photochemically unstable with respect to conversion to N_2 and is, therefore, unlikely to have played a major role in warming the Earth's surface.

Carbon dioxide is a more promising candidate. Owen et al. (1979) have shown that CO_2 concentrations of 100—1000 PAL (present atmospheric level) could have provided the required warming. Walker et al. (1981) have proposed a mechanism by which enhanced CO_2 levels could have been maintained in the distant past. The rate of loss of CO_2 through silicate weathering depends upon rainfall and is, therefore, likely to be a strong function of surface temperature. At global surface temperatures lower than today's, the CO_2 loss rate should decrease and more CO_2 should accumulate in the atmosphere. The Earth's climate may be effectively buffered by this mechanism, so that even relatively large decreases in solar luminosity may result in only small decreases in average surface temperature.

We suggest here, that the early greenhouse effect may have been further augmented by the presence of atmospheric methane. Donner and Ramanathan (1980) have shown that the 1.4 ppm (parts per million) of methane in today's atmosphere contribute about 1.4 K to the present globally-averaged surface temperature. The absorption due to the 7.4 μ band of methane increases linearly with CH_4 concentration up to a mixing ratio of about 0.7 ppm, then more slowly above this level as the center of the band becomes saturated. Thus, methane could have made a modest contribution towards heating the early atmosphere if its mixing ratio was $>\sim 10^{-6}$. Perhaps more significantly, methane may also have polymerized in response to solar ultraviolet radiation, creating higher hydrocarbon compounds which should also have been absorbed in the infrared. If several of these compounds were each able to provide a small amount of heating, the combined effect could have been of major climatic significance. With this in mind, we have investigated the photochemical behavior of methane in the early atmosphere to determine how much CH_4 might have been present and what types of higher hydrocarbons could have been formed.

THE MODEL

The one-dimensional photochemical model used in this study is similar to that described by Kasting (1982), except that the focus is on hydrocarbon photochemistry rather than the photochemistry of ammonia. Diffusion equations were solved simultaneously for 22 different species: O_3, O, H_2O, OH, HO_2, H_2O_2, H, O_2, H_2, CO_2, CO, HCO, H_2CO, CH_4, C_2H_6, C_3H_8, C_4H_{10}, C_2H_2, C_2H_4, CH_3, $^3CH_2$ and C_2H_5. Another 12 species, including $O(^1D)$, $^1CH_2$, excited C_2H_2 (C_2H_2*), C_2H, C_2H_3, C_3H_6, C_4H_8, C_3H_7, C_4H_9, CH_3CHO, C_2H_5CHO and C_3H_7CHO, were assumed to be in photochemical equilibrium. The equations were integrated in time-dependent fashion until a steady-state solution was approached, which typically required 10—100 years of model time. More time was required for certain 'high CO' cases, as will be discussed later.

The altitude grid used in the model extends from 0 to 80 km in 1 km increments. The assumed boundary conditions for most species were zero flux at the ground and at 80 km. At the top the upward fluxes of CO_2 and O_2 required to compensate for photodissociation were balanced by downward fluxes of CO and O. Constant ground-level mixing ratios were assumed for H_2O, H_2, CO_2 and CH_4. The tropospheric H_2O mixing ratio was fixed at values ranging from 1.5×10^{-2} at the ground to 3.8×10^{-6} at 10 km. Assumptions concerning temperature and eddy diffusion profiles, lightning production of O_2, and rainout of H_2O_2 and H_2CO were the same as in Kasting and Walker (1981).

Photolysis rates were calculated for a solar zenith angle of 57.3° and then multiplied by 0.5 to approximate a diurnal average. Rayleigh scattering was treated using the method of Yung (1976). The importance of Rayleigh scattering in the context of primitive terrestrial atmospheres has been described by Kasting (1982). Its primary effect is to reduce solar ultraviolet fluxes in the lower troposphere which, for this model, means that H_2O photolysis is slowed relative to photolysis of well-mixed species such as CO_2.

The reaction scheme describing hydrocarbon formation is based on sequences proposed by Lasaga et al. (1971), Strobel (1973), Yung and Pinto (1978), Yung and Strobel (1980) and Allen et al. (1980). Reactions (R) and rate constants are listed in Table I.

In the anaerobic atmosphere, the oxidizing radicals O and OH are produced throughout the atmosphere by photolysis at $\lambda \lesssim 2050$ Å of CO_2 and H_2O:

$CO_2 + h\nu \rightarrow CO + O$ (R29); $H_2O + h\nu \rightarrow H + OH$ (R25).

These radicals initiate methane photochemistry in the lower atmosphere via

$CH_4 + OH \rightarrow CH_3 + H_2O$ (R47) and $CH_4 + O \rightarrow CH_3 + OH$ (R48).

The resultant methyl radicals may react with atomic hydrogen to reform methane

$CH_3 + H + M \rightarrow CH_4 + M$ (R50),

or they can react with another OH or O radical to produce formaldehyde

$CH_3 + OH \rightarrow H_2CO + H_2$ (R51); $CH_3 + O \rightarrow H_2CO + H$ (R52).

TABLE I

Reactions and rate constants

Reaction	Rate constant ($cm^3\ s^{-1}$)	Reference
(1) $H_2O + O(^1D) \rightarrow OH + OH$	2.3×10^{-10}	JPL, 1979
(2) $H_2 + O(^1D) \rightarrow OH + H$	9.9×10^{-11}	JPL, 1979
(3) $H_2 + O \rightarrow OH + H$	$3.0 \times 10^{-14}\ T \exp(-4480/T)$	Hampson and Garvin, 1977
(4) $H_2 + OH \rightarrow H_2O + H$	$1.2 \times 10^{-11} \exp(-2200/T)$	JPL, 1979
(5) $H + O_3 \rightarrow OH + O_2$	$1.4 \times 10^{-10} \exp(-470/T)$	JPL, 1979
(6) $H + O_2 + M \rightarrow HO_2 + M$	$5.5 \times 10^{-32} (300/T)^{1.4}$ [M]	JPL, 1979
(7) $H + HO_2 \rightarrow H_2 + O_2$	4.7×10^{-11} ($\times 0.29$)	Hack et al., 1978, 1979
(8) $H + HO_2 \rightarrow H_2O + O$	4.7×10^{-11} ($\times 0.02$)	Hack et al., 1978, 1979
(9) $H + HO_2 \rightarrow OH + OH$	4.7×10^{-11} ($\times 0.69$)	Hack et al., 1978, 1979
(10) $OH + O \rightarrow H + O_2$	4.0×10^{-11}	JPL, 1979
(11) $OH + HO_2 \rightarrow H_2O + O_2$	4.0×10^{-11}	JPL, 1979
(12) $OH + O_3 \rightarrow HO_2 + O_2$	$1.6 \times 10^{-12} \exp(-940/T)$	JPL, 1979
(13) $HO_2 + O \rightarrow OH + O_2$	3.5×10^{-11}	JPL, 1979
(14) $HO_2 + O_3 \rightarrow OH + 2O_2$	$1.1 \times 10^{-14} \exp(-580/T)$	JPL, 1979
(15) $HO_2 + HO_2 \rightarrow H_2O_2 + O_2$	2.5×10^{-12}	JPL, 1979
(16) $H_2O_2 + OH \rightarrow HO_2 + H_2O$	$1.0 \times 10^{-11} \exp(-750/T)$	JPL, 1979
(17) $O + O + M \rightarrow O_2 + M$	$2.76 \times 10^{-34} \exp(710/T)$ [M]	Campbell and Thrush, 1967
(18) $O + O_2 + M \rightarrow O_3 + M$	$6.2 \times 10^{-34} (300/T)^{2.1}$ [M]	JPL, 1979
(19) $O + O_3 \rightarrow 2O_2$	$1.5 \times 10^{-11} \exp(-2218/T)$	JPL, 1979
(20) $OH + OH \rightarrow H_2O + O$	$1.0 \times 10^{-11} \exp(-500/T)$	Hampson and Garvin, 1977
(21) $O(^1D) + N_2 \rightarrow O + N_2$	$2.0 \times 10^{-11} \exp(-107/T)$	JPL, 1979
(22) $O(^1D) + O_2 \rightarrow O + O_2$	$2.9 \times 10^{-11} \exp(-67/T)$	JPL, 1979
(23) $O_2 + h\nu \rightarrow O_2 + O(^1D)$	J_{O_2}	Kasting et al., 1979
(24) $\rightarrow O + O$		
(25) $H_2O + h\nu \rightarrow H + OH$	J_{H_2O}	Kasting et al., 1979
(26) $O_3 + h\nu \rightarrow O_2 + O(^1D)$	J_{O_3}	Kasting et al., 1979
(27) $\rightarrow O_2 + O$		
(28) $H_2O_2 + h\nu \rightarrow OH + OH$	$J_{H_2O_2}$	Kasting et al., 1979
(29) $CO_2 + h\nu \rightarrow CO + O$	J_{CO_2}	Kasting et al., 1979
(30) $CO + OH \rightarrow CO_2 + H$	$6.0 \times 10^{-13} [0.25 + A[M]] / [1 + A[M]]$ [a]	Hampson and Garvin, 1977
(31) $CO + O + M \rightarrow CO_2 + M$	$6.5 \times 10^{-33} \exp(-2180/T)$ [M]	Hampson and Garvin, 1977
(32) $H + CO + M \rightarrow HCO + M$	$2.0 \times 10^{-33} \exp(-850/T)$ [M]	Baulch et al., 1976
(33) $H + HCO \rightarrow H_2 + CO$	1.2×10^{-10}	Hochanadel et al., 1980
(34) $HCO + HCO \rightarrow H_2CO + CO$	2.3×10^{-11}	Hochanadel et al., 1980
(35) $OH + HCO \rightarrow H_2O + CO$	5.0×10^{-11}	Baulch et al., 1976
(36) $O + HCO \rightarrow H + CO_2$	1.0×10^{-10}	Hampson and Garvin, 1977
(37) $O + HCO \rightarrow OH + CO$	1.0×10^{-10}	Hampson and Garvin, 1977
(38) $H_2CO + h\nu \rightarrow H_2 + CO$	J_{H_2CO}	Calvert et al., 1972
(39) $\rightarrow HCO + H$		
(40) $HCO + h\nu \rightarrow H + CO$	$1.0 \times 10^{-2}\ s^{-1}$	Pinto et al., 1981
(41) $H_2CO + H \rightarrow H_2 + HCO$	$2.8 \times 10^{-11} \exp(-1540/T)$	JPL, 1979

Table I (*continued*)

Reaction	Rate constant ($cm^3 s^{-1}$)	Reference
(42) $CO_2 + h\nu \rightarrow CO + O(^1D)$	J_{CO_2}	Kasting et al., 1979
(43) $H + H + M \rightarrow H_2 + M$	$2.6 \times 10^{-33} \exp(375/T)$ [M]	Liu and Donahue, 1974
(44) $HCO + O_2 \rightarrow HO_2 + CO$	4.0×10^{-12}	Reilly et al., 1978
(45) $H_2CO + OH \rightarrow H_2O + HCO$	$1.7 \times 10^{-11} \exp(-100/T)$	JPL, 1979
(46) $H + OH + M \rightarrow H_2O + M$	$6.1 \times 10^{-26}/T^2$ [M]	Hampson and Garvin, 1977
(47) $CH_4 + OH \rightarrow CH_3 + H_2O$	$2.4 \times 10^{-12} \exp(-1710/T)$	JPL, 1979
(48) $CH_4 + O \rightarrow CH_3 + OH$	$2.3 \times 10^{-11} \exp(-2620/T)$	Hampson and Garvin, 1977[m]
(49) $CH_4 + O(^1D) + CH_3 + OH$	1.3×10^{-10}	JPL, 1979
(50) $CH_3 + H + M \rightarrow CH_4 + M$	$3.3 \times 10^{-10}/[1 + 1/(2 \times 10^{-19}$ [M])]	Cheng and Yeh, 1977
(51) $CH_3 + OH \rightarrow H_2CO + H_2$	1.0×10^{-10}	Estimated[b]
(52) $CH_3 + O \rightarrow H_2CO + H$	1.0×10^{-10}	Hampson and Garvin, 1977
(53) $CH_3 + CH_3 + M \rightarrow C_2H_6 + M$	Min [5.5×10^{-11}; $1.7 \times 10^{-17} T^{-2.3}$ [M]]	Van den Bergh, 1976; Troe, 1977
(54) $C_2H_6 + OH \rightarrow C_2H_5 + H_2O$	$1.86 \times 10^{-11} \exp(-1230/T)$	Hampson and Garvin, 1977
(55) $C_2H_6 + O \rightarrow C_2H_5 + OH$	$4.1 \times 10^{-11} \exp(-3200/T)$	Hampson and Garvin, 1977
(56) $C_2H_6 + O(^1D) \rightarrow C_2H_5 + OH$	1.3×10^{-10}	Estimated[c]
(57) $C_2H_5 + H \rightarrow CH_3 + CH_3$	Min [$1.8 \times 10^{-10} \exp(-435/T)$; $1.0 \times 10^{-20} T^{-3.3}$ [M]]	Teng and Jones, 1972
(58) $C_2H_5 + OH \rightarrow CH_3CHO + H_2$	1.0×10^{-10}	Estimated[b]
(59) $C_2H_5 + O \rightarrow CH_3CHO + H$	1.0×10^{-10}	Estimated[b]
(60) $C_2H_5 + CH_3 + M \rightarrow C_3H_8 + M$	(=R53)	Benson, 1964
(61) $C_2H_5 + C_2H_5 + M \rightarrow C_4H_{10} + M$	(=R53)	Benson, 1964
(62) $CH_3CHO + h\nu \rightarrow CH_3 + HCO$	$4.2 \times 10^{-5} s^{-1}$	Demerjian et al., 1974
(63) $C_3H_8 + OH \rightarrow C_3H_7 + H_2O$	$1.8 \times 10^{-11} \exp(-900/T)$	Estimated[d]
(64) $C_3H_8 + O \rightarrow C_3H_7 + OH$	$1.6 \times 10^{-11} \exp(-2900/T) + 2.2 \times 10^{-11} \exp(-2250/T)$	Hampson and Garvin, 1977
(65) $C_3H_8 + O(^1D) \rightarrow C_3H_7 + OH$	1.3×10^{-10}	Estimated[c]
(66) $C_3H_7 + H \rightarrow CH_3 + C_2H_5$	(=R57)	Estimated
(67) $C_3H_7 + OH \rightarrow C_2H_5CHO + H_2$	1.0×10^{-10}	Estimated[b]
(68) $C_3H_7 + O \rightarrow C_2H_5CHO + H$	1.0×10^{-10}	Estimated[b]
(69) $C_3H_7 + CH_3 + M \rightarrow C_4H_{10} + M$	(=R53)	Benson, 1964
(70) $C_2H_5CHO + h\nu \rightarrow C_2H_5 + HCO$	$4.2 \times 10^{-5} s^{-1}$	Estimated[e]
(71) $C_4H_{10} + OH \rightarrow C_4H_9 + H_2O$	$1.76 \times 10^{-11} \exp(-560/T)$	Hampson and Garvin, 1977
(72) $C_4H_{10} + O \rightarrow C_4H_9 + OH$	$1.6 \times 10^{-11} \exp(-2900/T) + 4.4 \times 10^{-11} \exp(-2250/T)$	Hampson and Garvin, 1977
(73) $C_4H_{10} + O(^1D) \rightarrow C_4H_9 + OH$	1.3×10^{-10}	Estimated[c]
(74) $C_4H_9 + H \rightarrow C_2H_5 + C_2H_5$	(=0.5 × R57)	Estimated
(75) $C_4H_9 + H \rightarrow C_3H_7 + CH_3$	(=0.5 × R57)	Estimated
(76) $C_4H_9 + OH \rightarrow C_3H_7CHO + H_2$	1.0×10^{-10}	Estimated[b]

Table I (*continued*)

Reaction	Rate constant ($cm^3\ s^{-1}$)	Reference
(77) $C_4H_9 + O \rightarrow C_3H_7CHO + H$	1.0×10^{-10}	Estimated[b]
(78) $C_3H_7CHO + h\nu \rightarrow C_3H_7 + HCO$	$4.2 \times 10^{-5}\ s^{-1}$	Estimated[e]
(79) $CH_4 + h\nu \rightarrow {}^1CH_2 + H_2$	J_{CH_4}	Mount et al., 1977
(80) $C_2H_6 + h\nu \rightarrow C_2H_2 + 2H_2$	$J_{C_2H_6}$	Mount and Moos, 1978 Strobel, 1973
(81) $\rightarrow C_2H_4 + 2H$		
(82) $\rightarrow CH_4 + {}^1CH_2$		
(83) $C_3H_8 + h\nu \rightarrow C_3H_6 + H_2$	$J_{C_3H_8}$ ($\times 0.4$)[f]	Okabe and McNesby, 1962
(84) $\rightarrow C_2H_4 + CH_4$	($\times 0.3$)	Calvert and Pitts, 1966
(85) $\rightarrow CH_3 + C_2H_5$	($\times 0.3$)	
(86) $C_4H_{10} + h\nu \rightarrow C_4H_8 + H_2$	$J_{C_4H_{10}}$ ($\times 0.3$)[f]	Okabe and Becker, 1963
(87) $\rightarrow 2C_2H_4 + H_2$	($\times 0.16$)	Calvert and Pitts, 1966
(88) $\rightarrow C_3H_6 + CH_3 + H$	($\times 0.07$)	
(89) $\rightarrow C_2H_6 + C_2H_2 + H_2$	($\times 0.10$)	
(90) $\rightarrow CH_3 + C_3H_7$	($\times 0.25$)	
(91) $\rightarrow 2C_2H_5$	($\times 0.12$)	
(92) $C_2H_4 + h\nu \rightarrow C_2H_2 + H_2$	$J_{C_2H_4}$	Zelikoff and Watanabe, 1953
(93) $\rightarrow C_2H_2 + 2H$		Strobel, 1973
(94) $C_3H_6 + h\nu \rightarrow C_2H_2 + CH_3 + H$	($=J_{C_2H_4}$)	Estimated
(95) $C_4H_8 + h\nu \rightarrow C_2H_2 + C_2H_5 + H$	($=J_{C_2H_4}$)	Estimated
(96) $C_2H_2 + h\nu \rightarrow C_2H_2^*$	$J_{C_2H_2}$	Nakayama and Watanabe, 1964
(97) $C_2H_2^* \rightarrow C_2H_2 + h\nu$	$3.0 \times 10^5\ s^{-1}$	Becker et al., 1971; Stief et al., 1965
(98) $C_2H_2^* \rightarrow C_2H + H$	$1.0 \times 10^5\ s^{-1}$	Takita et al., 1968, 1969; Strobel, 1973
(99) $C_2H_2^* + N_2 \rightarrow C_2H_2 + N_2$	4.0×10^{-11}	Estimated[g]
(100) $C_2H_2^* + O_2 \rightarrow 2HCO$	1.0×10^{-10}	Estimated[h]
(101) ${}^1CH_2 + H_2 \rightarrow CH_3 + H$	7.0×10^{-12}	Braun et al., 1970
(102) ${}^1CH_2 + CH_4 \rightarrow CH_3 + CH_3$	1.9×10^{-12}	Braun et al., 1970
(103) ${}^1CH_2 + O_2 \rightarrow H_2CO + O$	3.0×10^{-11}	Laufer and Bass, 1974
(104) ${}^1CH_2 + N_2 \rightarrow {}^3CH_2 + N_2$	5.0×10^{-13}	Bell, 1971
(105) ${}^3CH_2 + H_2 \rightarrow CH_3 + H$	5.0×10^{-14}	Braun et al., 1970
(106) ${}^3CH_2 + CH_4 \rightarrow CH_3 + CH_3$	5.0×10^{-14}	Braun et al., 1970
(107) ${}^3CH_2 + O_2 \rightarrow H_2CO + O$	1.5×10^{-12}	Laufer and Bass, 1974
(108) ${}^3CH_2 + {}^3CH_2 \rightarrow C_2H_2 + 2H$	5.3×10^{-11}	Russell and Rowland, 1979
(109) ${}^3CH_2 + CH_3 \rightarrow C_2H_4 + H$	5.0×10^{-11}	Pilling and Robertson, 1975
(110) ${}^3CH_2 + C_2H_2 \xrightarrow{M} C_3H_4$	7.5×10^{-12}	Laufer and Bass, 1974
(111) $C_2H_2 + OH \rightarrow CO + CH_3$	$2.0 \times 10^{-12}\ \exp(-250/T)$	Hampson and Garvin, 1977

Table I (*continued*)

Reaction	Rate constant ($cm^3 s^{-1}$)	Reference
(112) $C_2H_2 + H + M \rightarrow C_2H_3 + M$	Min [$9.2 \times 10^{-12} \exp(-1205/T)$; $10^{-30} \exp(-770/T)$ [M]]	Payne and Stief, 1976
(113) $C_2H_3 + H \rightarrow C_2H_2 + H_2$	7.0×10^{-12}	Benson and Haugen, 1967
(114) $C_2H_3 + H_2 \rightarrow C_2H_4 + H$	$3.0 \times 10^{-13} \exp(-5570/T)$	Yung and Strobel, 1980
(115) $C_2H_3 + CH_4 \rightarrow C_2H_4 + CH_3$	$3.0 \times 10^{-13} \exp(-5370/T)$	Estimated[i]
(116) $C_2H_3 + C_2H_6 \rightarrow C_2H_4 + C_2H_5$	$3.0 \times 10^{-13} \exp(-5170/T)$	Estimated[i]
(117) $C_2H_4 + OH \rightarrow H_2CO + CH_3$	$2.2 \times 10^{-12} \exp(385/T)$	Hampson and Garvin, 1977
(118) $C_2H_4 + O \rightarrow HCO + CH_3$	$5.5 \times 10^{-12} \exp(-565/T)$	Hampson and Garvin, 1977
(119) $C_2H_4 + H + M \rightarrow C_2H_5 + M$	Min [$3.7 \times 10^{-11} \exp(-1040/T)$; 3.0×10^{-30} [M]]	Lee et al., 1978
(120) $C_3H_6 + OH \rightarrow CH_3CHO + CH_3$	$4.1 \times 10^{-12} \exp(540/T)$	Hampson and Garvin, 1977
(121) $C_3H_6 + O \rightarrow 2CH_3 + CO$	$4.1 \times 10^{-12} \exp(-38/T)$	Hampson and Garvin, 1977[h]
(122) $C_3H_6 + H + M \rightarrow C_3H_7 + M$	(=R119)	Estimated
(123) $C_4H_8 + OH \rightarrow C_2H_5CHO + CH_3$	(=R120)	Estimated
(124) $C_4H_8 + O \rightarrow CH_3 + C_2H_5 + CO$	(=R121)	Estimated
(125) $C_4H_8 + H + M \rightarrow C_4H_9 + M$	(=R119)	Estimated
(126) $C_2H + O_2 \rightarrow CO + HCO$	1.0×10^{-10}	Estimated[h]
(127) $C_2H + H_2 \rightarrow C_2H_2 + H$	$3.0 \times 10^{-11} \exp(-1600/T)$	Estimated[j]
(128) $C_2H + CH_4 \rightarrow C_2H_2 + CH_3$	$3.0 \times 10^{-11} \exp(-1400/T)$	Estimated[j]
(129) $C_2H + C_2H_6 \rightarrow C_2H_2 + C_2H_5$	$3.0 \times 10^{-11} \exp(-1200/T)$	Estimated[j]
(130) $C_2H + H + M \rightarrow C_2H_2 + M$	(=R50)	Estimated
(131) $C_2H + C_2H_2 \rightarrow C_4H_2 + H$	3.1×10^{-11}	Laufer and Bass, 1979
(132) $C_3H_4 \rightarrow$ dust	1.0×10^{-10}	Assumed[k]
(133) $C_4H_2 \rightarrow$ dust	1.0×10^{-10}	Assumed[k]
(134) $CH_3 + h\nu \rightarrow {}^3CH_2 + H$	5.0×10^{-5}	Estimated[l]

[a] $A = 1.82 \times 10^{-20}$.
[b] Assumed equal to R52.
[c] Assumed equal to R49.
[d] By comparison with R54 and R71.
[e] Assumed equal to R62.
[f] Branching ratios assumed to be wavelength independent.
[g] Assumed equal to half the rate measured by Becker et al. (1971) for quenching by H_2.
[h] Products uncertain.
[i] By comparison with R114, with correction for the expected difference in activation energies.
[j] Estimated by Allen et al. (1980) based on results of Laufer and Bass (1979).
[k] See text.
[l] By comparison with rate estimated by Allen et al. (1980) for Titan.
[m] Barassin and Combourie (1974) give $5.8 \times 10^{-11} \exp(-4450/T)$.

A third possibility is recombination with another methyl radical to form ethane

$CH_3 + CH_3 + M \rightarrow C_2H_6 + M$ (R53).

Reaction R53 occurs at the high-pressure limiting rate all the way up to 80 km, so ethane can be formed efficiently throughout the model atmosphere.

Ethane, once formed, can undergo a sequence of reactions which are analogous to those of methane (R54—R61), the only essential difference being that the reaction of H with an ethyl radical

$C_2H_5 + H \rightarrow CH_3 + CH_3$ (57)

produces two methyls rather than reforming ethane. The recombination of ethyl radicals can then lead to the formation of propane and butane

$C_2H_5 + CH_3 + M \rightarrow C_3H_8 + M$ (R60); $C_2H_5 + C_2H_5 + M \rightarrow C_4H_{10} + M$ (R61).

According to Benson (1964) these reactions occur at essentially the same rate as the recombination of two methyl radicals (R53). The entire sequence of higher alkanes can, presumably, be generated in this fashion, so our exclusion of species heavier than butane might be expected to cause trouble in some circumstances. The effects of cutting off the alkane sequence at $n = 4$ will be discussed in a later section. The polymerization process can also be reversed by the reaction of H with alkyl radicals, producing two smaller alkyls, as is the case for ethane.

The higher alkanes may be oxidized to form higher aldehydes in much the same way that methane is oxidized to formaldehyde. Since the C—O bonds formed in this process cannot be broken again within the atmosphere, each aldehyde molecule formed corresponds to a net loss of one methane molecule. The loss of methane via such oxidation processes must be balanced by a ground-level source of methane in order to maintain a constant CH_4 mixing ratio in the atmosphere.

At altitudes above about 40 km methane may also be destroyed by direct photolysis

$CH_4 + h\nu \rightarrow {}^1CH_2 + H_2$ (R79).

Since the photolysis of methane (and the higher alkanes) requires wavelengths shorter than 1600 Å, this process is responsible for only a small fraction of total methane destruction. The by-products of methane photolysis may react to form unsaturated hydrocarbons such as acetylene and ethylene via

${}^3CH_2 + {}^3CH_2 \rightarrow C_2H_2 + 2H$ (R108); ${}^3CH_2 + CH_3 \rightarrow C_2H_4 + H$ (R109).

Acetylene, in particular, is potentially important because it can catalytically destroy atomic hydrogen by

$C_2H_2 + H + M \rightarrow C_2H_3 + M$ (R112); $C_2H_3 + H \rightarrow C_2H_2 + H_2$ (R113).

In these models, however, the catalytic cycle involving CO is much more important

$CO + H + M \rightarrow HCO + M$ (R32); $HCO + H \rightarrow CO + H_2$ (R33).

Acetylene can also react with different radical species to produce polyunsaturated hydrocarbon compounds. We have identified two such pathways in the model

${}^3CH_2 + C_2H_2 + M \rightarrow C_3H_4 + M$ (R110) and $C_2H + C_2H_2 \rightarrow C_4H_2 + H$ (R131).

Reaction R110 forms methylacetylene and allene in roughly a 1:2 ratio (Laufer and Bass, 1974) and is the largest source of polyunsaturated compounds in our model. Reaction 131 yields butadiene, which has been suggested as a precursor to the formation of Danielson dust on Titan (Allen et al., 1980). In this model we assume, somewhat arbitrarily, that both C_3H_4 and C_4H_2 are eventually removed from the atmosphere by conversion to some solid polymer. This assumption yields an estimate for the maximum possible loss of methane that can result from these two processes.

RESULTS

One of the difficulties in conducting a study of this kind is that the atmospheric mixing ratios of hydrogen and carbon dioxide are not known. Indeed, both H_2 and CO_2 levels are likely to have varied during ~2 Ga prior to the development of an oxygenic atmosphere. Reasonable values for the H_2 mixing ratio range from 10^{-5} to 10^{-3} (Kasting and Walker, 1981), while the CO_2 mixing ratio was probably between one and several hundred PAL (Owen et al., 1979; Walker et al., 1981). The calculations described here assume a range of possible mixing ratios for each of these gases.

As an initial experiment, the ground-level H_2 and CO_2 mixing ratios were fixed at 10^{-4} and 4.17×10^{-4}, respectively. (This is the equivalent of 1 PAL of CO_2 since the total atmospheric pressure is only 0.8 bars.) Calculations were performed for CH_4 mixing ratios ranging from 10^{-6} to 5×10^{-4}. Plotted in Fig. 1 are the calculated atmospheric residence time for methane and the ground-level methane source required to maintain the atmosphere in steady

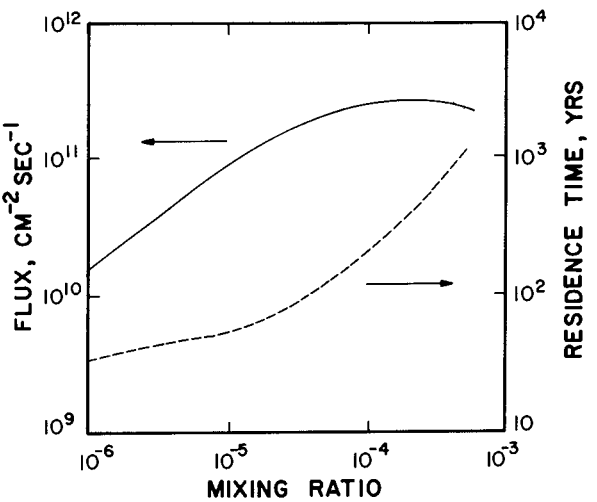

Fig. 1. Methane flux (solid curve) and atmospheric residence time (dashed curve) as a function of ground-level CH_4 mixing ratio. The assumed H_2 and CO_2 mixing ratios are 10^{-4} and 1 PAL, respectively.

state. Figure 1 illustrates several important points. First, the CH_4 residence times range from a few tens to a few thousands of years. Similar values were encountered over the entire range of different background atmospheres examined. Since a few thousand years is insignificant on a geological time scale, it is clear that only steady-state scenarios with a constant source for methane are of interest here. Second, the methane source required to maintain a CH_4 mixing ratio of several ppm is in the order of 10^{11} CH_4 molecules cm^{-2} s^{-1}. This figure is roughly equivalent to estimates for the present-day source of atmospheric methane (Koyama, 1963; Baker-Blocker et al., 1977; Ehhalt and Schmidt, 1978; Kasting and Donahue, 1980). We shall argue later that a source of this magnitude could have existed throughout much of the Archean. A third point — one that is considerably less certain — is the suggestion that the required methane flux reaches a maximum as the methane mixing ratio is increased above $\sim 3 \times 10^{-4}$, actually beginning to decrease for higher mixing ratios. The explanation is that interconversions among the hydrocarbon species are consuming a larger percentage of the oxidizing radicals. This phenomenon might disappear, however, in a model which included alkanes higher than $n = 4$.

Figure 2 shows altitude profiles of CO and the dominant hydrocarbon species for a methane mixing ratio $f(CH_4) = 10^{-5}$. The higher alkanes are all poorly represented, while C_2H_2 and C_2H_4 are confined almost exclusively to the upper atmosphere. A few features concerning the overall structure of the atmosphere deserve comment. First, the lower atmosphere is more highly reduced than the upper atmosphere. Second, the main photolysis paths begin with the dissociation of H_2O below 20 km, and of CO_2 above 10 km. Third, CO is much less abundant in the troposphere than in the stratosphere. Tropospherically produced OH (R25) is the main sink of this gas, via

$CO + OH \rightarrow CO_2 + H$ (R30).

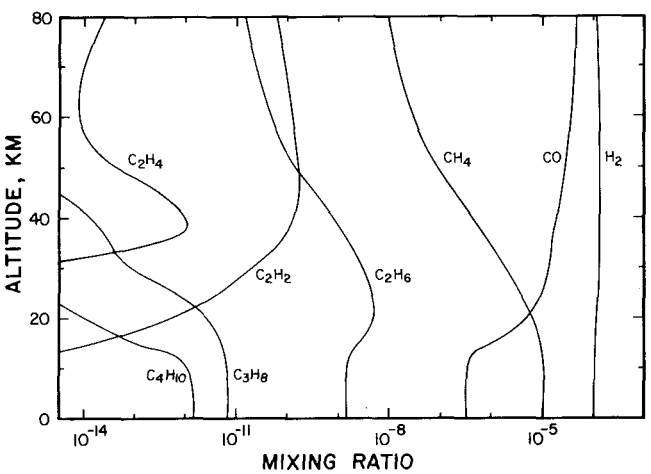

Fig. 2. Mixing ratio profiles of major reduced species at $f(CH_4) = 10^{-5}$, $f(H_2) = 10^{-4}$, and $f(CO_2) = 1$ PAL.

Figure 3 shows alkane mixing ratios for $f(CH_4) = 10^{-4}$. The alkanes have all become quite prominent and acetylene has begun to appear in the troposphere. The CO mixing ratio has also increased substantially in the troposphere, as the increasingly reduced conditions have greatly lowered the O and OH densities. Increasing CO acts to decrease H, by means of the catalytic cycle R32—R33, and thus, tends to increase the efficiency of alkane polymerization. The prediction that the tropospheric C_4H_{10} density exceeds that of C_3H_8 is an artifact of our truncated alkane sequence. In the lowest 20 km of the atmosphere shown in Fig. 3 the densities of the alkyl radicals tend to increase with increasing molecular weight. This would result, in a more complete model, in the formation of significant amounts of still higher alkanes. Our results are, therefore, not very meaningful for CH_4 mixing ratios above 10^{-4}.

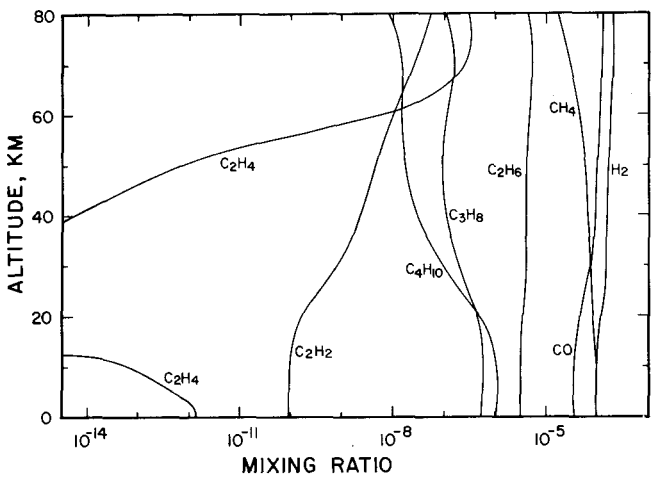

Fig. 3. The same as Fig. 2, except $f(CH_4) = 10^{-4}$.

The effects on the CO and C_2H_6 mixing ratios of varying methane mixing ratio at 1 PAL CO_2 and $f(H_2) = 10^{-4}$ are summarized in Fig. 4. All mixing ratios here refer to ground-level.

The trend towards alkane polymerization at high methane levels is accompanied by increased production of polyunsaturated hydrocarbons. Figure 5 shows column-integrated production rates for C_3H_4 and C_4H_2 as a function of methane mixing ratio. The rate of polymerization via these two channels becomes substantial at CH_4 mixing ratios near 10^{-4}, although it never exceeds a few percent of the methane oxidation rate (Fig. 1). We have not attempted to determine the subsequent fate of C_3H_4 and C_4H_2 in this model. It is conceivable, however, that they may have led to the formation of stratospheric dust in much the same fashion as has been suggested to occur in the atmosphere of Titan (Allen et al., 1980).

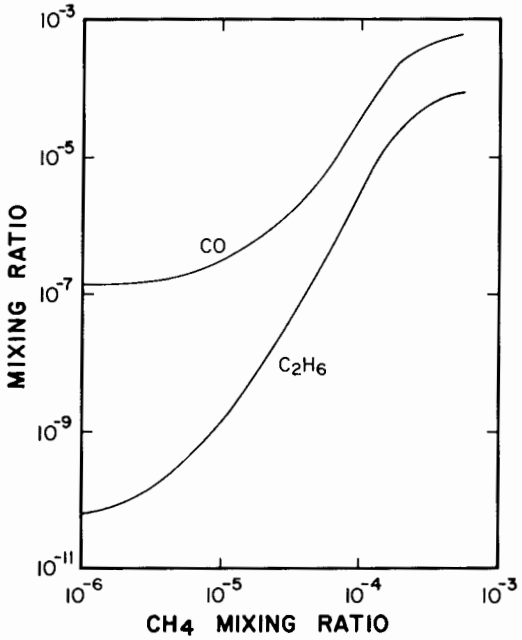

Fig. 4. Variation of CO and C_2H_6 with CH_4 mixing ratio for $f(CO_2) = 1$ PAL and $f(H_2) = 10^{-4}$.

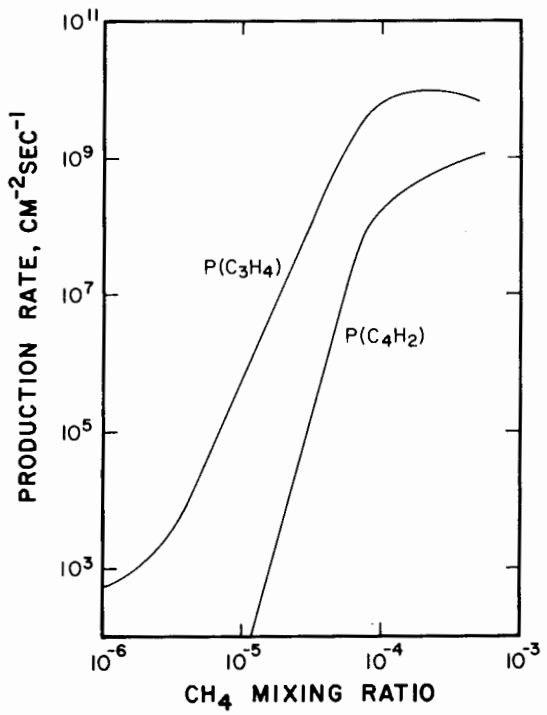

Fig. 5. Column-integrated production rates of C_3H_4 and C_4H_2 as functions of ground-level CH_4 mixing ratio. The assumed H_2 and CO_2 mixing ratios are 10^{-4} and 1 PAL, respectively.

The results presented so far correspond to an amount of CO_2 in the early atmosphere equal to today's value. We suggested earlier, though, that primitive CO_2 levels of 10—100 PAL are entirely possible, perhaps even likely. What effect would enhanced carbon dioxide levels have had upon the photochemistry of atmospheric methane?

Figure 6 shows calculated hydrocarbon mixing ratios for $f(CH_4) = 10^{-5}$, $f(H_2) = 10^{-4}$ and a CO_2 mixing ratio of 10 PAL. Comparison with Fig. 2 shows that hydrocarbon concentrations have increased dramatically: propane and butane have been enhanced by ~5 orders of magnitude, and ethane has become comparable to methane. The other hydrocarbons are similarly affected and, notably, so too is CO.

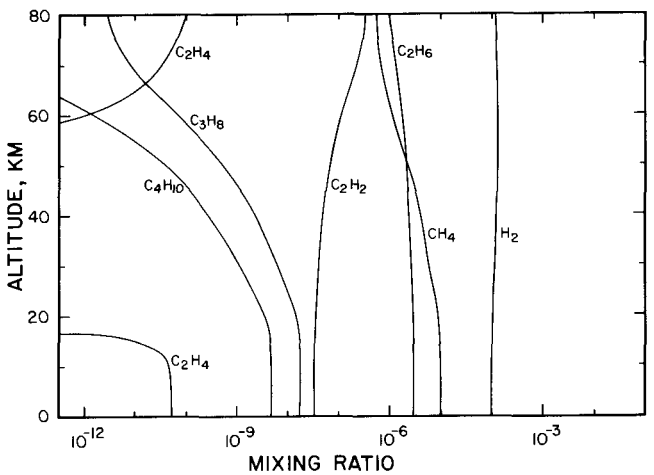

Fig. 6. Mixing ratio profiles of major reduced species at $f(CH_4) = 10^{-5}$, $f(H_2) = 10^{-4}$, and $f(CO_2) = 10$ PAL.

Figure 7 shows calculated hydrocarbon and CO mixing ratios for $f(CH_4) = 10^{-5}$ and $f(H_2) = 10^{-4}$ at 100 PAL of CO_2. The hydrocarbons are all somewhat less abundant than at 10 PAL, but CO now constitutes ~0.1% of the atmosphere.

Figure 8 summarizes these results by showing the effect of varying CO_2 on CO, C_2H_6 and the required methane flux for $f(H_2) = 10^{-4}$ and $f(CH_4) = 10^{-5}$. Although the details are complex, the underlying cause of this behavior is that the increased CO_2 absorbs a larger fraction of the incident photolyzing flux, and does so higher in the atmosphere. Thus, there is more primary production of CO and O by R29, and less of H and OH by R27, and photolysis in the shielded troposphere becomes less important.

As CO_2 is increased from 1 to 10 PAL, the initial effect of reducing the rate of tropospheric water photolysis is to greatly weaken the primary atmospheric sink for CO (R30) and so CO increases. The combined effects of decreased photolytic production and increased catalytic removal by the CO cycle

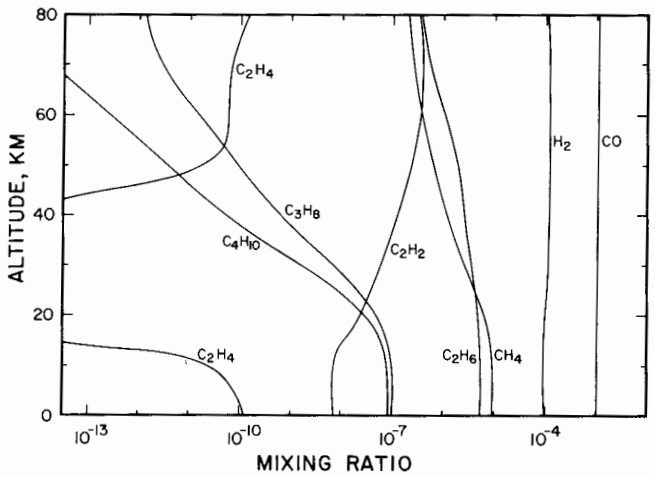

Fig. 7. The same as Fig. 6, except $f(CO_2)$ = 100 PAL.

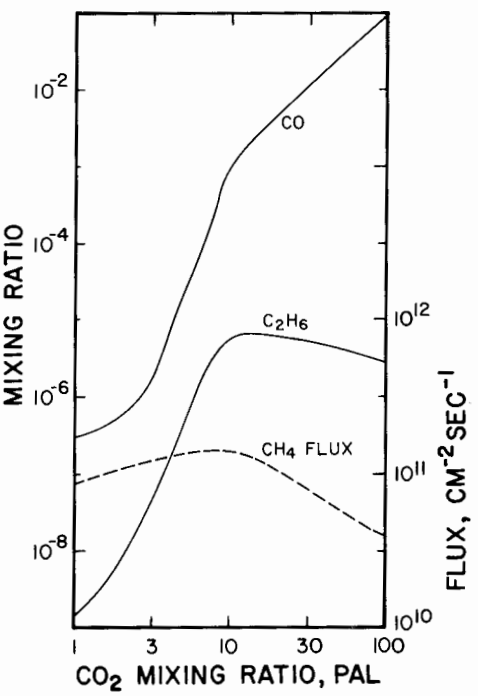

Fig. 8. Dependence on $f(CO_2)$ of $f(CO)$, $f(C_2H_6)$, and the methane flux required to maintain a steady state for $f(H_2) = 10^{-4}$ and $f(CH_4) = 10^{-5}$.

(R32–33) greatly decrease tropospheric H densities. Thus, the reaction of CH_3 with itself (R53) becomes faster than the reaction of CH_3 with H (R50), so the rate of ethane formation is dramatically increased. A quirk in the alkane chemistry further favors the production of polymers. The reported re-

action rates of CH_4 with O and OH (R48 and R47) are approximately equally fast in the troposphere (see discussion of limitations below), but for the higher alkanes, the analogous reaction with O is roughly 100 times slower than the analogous reaction with OH. Hence, as decreasing rates of water photolysis and increasing mixing ratios of CO combine to reduce tropospheric OH densities, the switch to O as the dominant oxidizing radical increases the lifetimes of the higher alkanes while not seriously slowing the methyl formation rate.

At CO_2 mixing ratios above 10 PAL, water photolysis plays an almost negligible role. The basic chemistry of this atmosphere is reduced to the photolysis of CO_2 and its recombination. In the absence of an efficient means of removing CO, the relatively slow direct 3-body recombination (which is inhibited by a significant activation energy)

$CO + O + M \rightarrow CO_2 + M$ (R31)

becomes important below about 20 km. This reduces O densities in the lower atmosphere, slowing the alkane photochemistry, as indicated by the relatively low methane flux required at 100 PAL of CO_2.

A fairly complete set of model experiments was performed at $f(H_2) = 10^{-4}$, including $f(CH_4) = 10^{-6}$ and 10^{-5} at 1—100 PAL CO_2, and $f(CH_4) = 10^{-4}$ at 1—10 PAL CO_2. At 1 PAL, models with $f(CH_4) = 2.5 \times 10^{-4}$ and 5×10^{-4} were run, but these are not able to treat the alkane chemistry properly. The dependence of the required source strength on CH_4 and CO_2 mixing ratios is illustrated explicitly in Fig. 9. The contours represent the base 10 logarithm of the methane source (molecules cm^{-2} s^{-1}) needed to maintain the steady state. Figure 10 is a contour plot of the tropospheric ethane mixing ratio as a function of CH_4 and CO_2 mixing ratios. It illustrates regimes under which CH_4

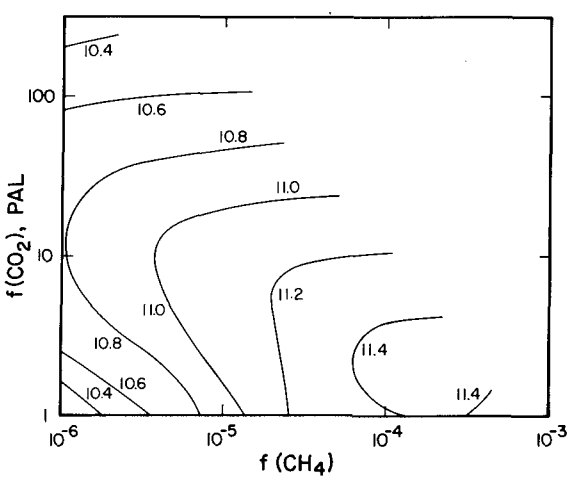

Fig. 9. Calculated ground-level methane fluxes needed to maintain the atmosphere in equilibrium for different CH_4 and CO_2 mixing ratios. Contours represent the base 10 logarithm of the required methane source in CH_4 molecules cm^{-2} s^{-1}. The mixing ratio of $H_2 = 10^{-4}$.

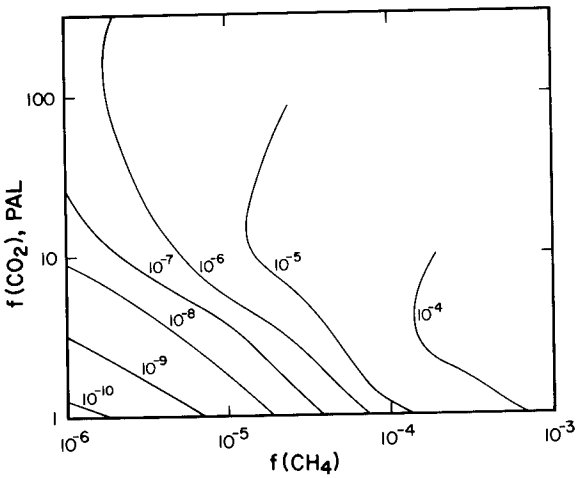

Fig. 10. Mixing ratio of C_2H_6 as a function of the mixing ratios of CO_2 and CH_4 for $f(H_2) = 10^{-4}$.

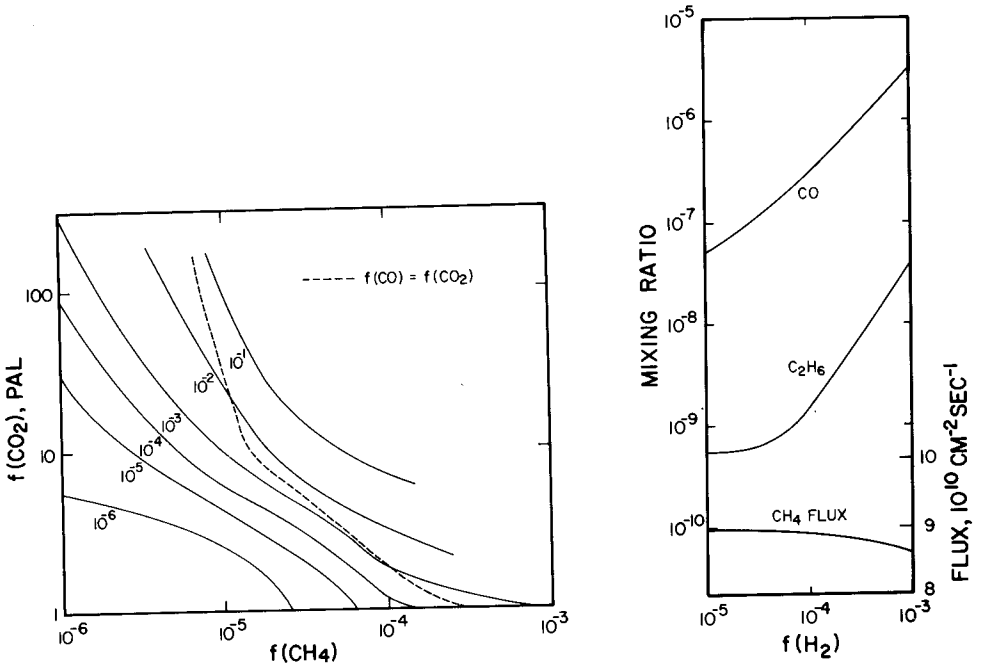

Fig. 11. Mixing ratio of CO as a function of the mixing ratios of CO_2 and CH_4 for $f(H_2) = 10^{-4}$.

Fig. 12. Dependence on $f(H_2)$ of $f(CO)$, $f(C_2H_6)$, and the methane flux required to maintain a steady state for $f(CH_4) = 10^{-5}$ and $f(CO_2) = 1$ PAL.

and CO_2 polymerization may be expected to have been important at $f(H_2) = 10^{-4}$. In order to be effective greenhouse gases, the higher alkanes and associated hydrocarbons, aldehydes, alcohols, etc. would presumably have had to assume mixing ratios $>\sim 10^{-6}$. Thus, a substantial greenhouse effect would not be expected below and to the left of the $f(C_2H_6) = 10^{-6}$ contour.

The dependence of $f(CO)$ upon CH_4 and CO_2 at $f(H_2) = 10^{-4}$ is shown in Fig. 11. The upper right hand region of the plot corresponds to conditions in which CO replaces CO_2 as the more stable carbon oxide. These atmospheres are quite reducing in character. However, at high CO mixing ratios it is possible that otherwise unimportant loss processes for CO (e.g., perhaps surface catalyzed oxidation of CO by H_2O) may act to prevent the dominance of CO. In any event, the question of the stability of CO_2 in the early terrestrial atmosphere requires more consideration.

Figure 12 shows the effect of varying the H_2 mixing ratio from 10^{-5} to 10^{-3} for $f(CH_4) = 10^{-5}$ and CO_2 = 1 PAL. Both CO and C_2H_6 increase with increasing H_2, but neither increases as rapidly or nonlinearly as when CH_4 or CO_2 are varied. The change in the required methane flux is very small indeed.

These effects are relatively easy to understand. Molecular hydrogen reacts with OH

$$H_2 + OH \rightarrow H + H_2O \quad (R4),$$

so increased H_2 decreases OH densities. Since CO is removed by OH

$$CO + OH \rightarrow CO_2 + H \quad (R30),$$

$f(CO)$ should increase linearly with $f(H_2)$, as is the case in Fig. 12.

Ethane presents a more complex problem, since both its production and its loss are affected by changes in H_2 concentrations. The dominant loss process for ethane at all H_2 levels is the reaction with OH

$$C_2H_6 + OH \rightarrow C_2H_5 + H_2O \quad (R54),$$

so it can be expected that C_2H_6 concentrations should vary linearly with $f(H_2)$, all other things being equal. However, the ethane production rate depends on CH_3 concentrations and these, in turn, are affected by the densities of H and OH. At low H_2 levels, CH_3 production stems largely from the reaction of CH_4 with OH (R47). This tends to counteract the OH dependence of the loss rate, with the result that the ethane concentration is nearly independent of $f(H_2)$. At high H_2 levels, the CO catalytic cycle (R32—R33) tends to reduce H densities, which results in a slower rate of destruction of methyl radicals via the reaction of CH_3 with H (R50). The C_2H_6 production rate is enhanced and so the ethane concentration increases faster than linearly with increasing $f(H_2)$.

The required methane flux is almost independent of H_2, because methane is oxidized almost exclusively in the stratosphere, by reactions with atomic oxygen (R48 and R57). The reaction of H_2 with O (R3) is very slow, and does not compete effectively for O atoms at the hydrogen mixing ratios considered here.

Although we have not made a systematic evaluation of the effects of varying H_2 at all CH_4 and CO_2 levels, we expect that at higher CO_2 levels, variations in H_2 would be even less important than they are at 1 PAL, since OH becomes a less important species that is effectively dominated by reaction with abundant CO. For H_2 to have a major effect would require enough H_2 to force reaction with O. This would require both $f(H_2) \gtrsim 10^3 f(CH_4)$ and $f(H_2) \gtrsim 30 f(CO)$ for the C—H—O atmospheres considered here.

LIMITATIONS OF THE MODEL

Obviously, considerable uncertainty arises in this calculation because of incomplete knowledge of hydrocarbon photochemistry. Our results are probably most secure at low methane and CO_2 levels, where the primary photochemical pathway for methane is the relatively well understood process of oxidation to formaldehyde. At higher methane levels one of the chief problems is a poor understanding of the production and loss processes for acetylene. In this model we have minimized the importance of acetylene by including a number of speculative loss processes (R100, R110, R114—116 and R131) and only relatively well-known production processes. Consequently, C_2H_2 concentrations remain relatively low, even at high methane mixing ratios. The result is that the atomic hydrogen catalytic destruction cycle involving C_2H_2 (R112 and R113) is less effective than that involving CO (R32 and R33). Since lowered atomic hydrogen densities result in higher polymerization rates, our model is very sensitive to both of these cycles. An earlier version of this model, which did not include as many loss processes for acetylene, exhibited higher C_2H_2 concentrations and a more rapid onset of polymerization at high methane levels.

In general, uncertainty in an individual reaction rate does not pose a major problem — the exception is

$O + CH_4 \rightarrow CH_3 + OH$ (R48).

A much slower rate for R48 has been reported by Barassin and Combourie (1974). This rate strongly affects the details of the chemistry; in particular (for the case where $f(H_2) = 10^{-4}$, $f(CH_4) = 10^{-5}$, and $f(CO_2) = 1$ PAL), the slower rate causes larger tropospheric O densities, and hence delays the onset of hydrocarbon polymerization as a function of methane mixing ratio. The methane sustaining flux is also reduced by a factor of ~ 2; the flux calculations are much less sensitive to details of the chemistry, since the CH_4 loss rate is largely a function of photon flux.

Another factor which would affect these results would be a change in the eddy diffusion profile. We have used the present-day profile from Hunten (1975), which assumes a very small value for the eddy diffusion coefficient in the lower stratosphere. In the absence of a temperature inversion due to ozone, the early atmosphere may have been more turbulent in this region.

This would result in increased downward transport of C_2H_2 and CO and, consequently, in reduced atomic hydrogen concentrations in the troposphere. Thus, again, the degree of methane polymerization could have been greater than we have calculated here.

Another major problem with this model is the exclusion of alkanes of greater molecular weight than butane. If the rate of the three-body recombination remains unchanged for the higher alkyl radicals, the production of pentane, hexane and still higher alkanes cannot be ignored in atmospheres containing large amounts of CH_4 or CO_2. The situation is difficult to analyze because it is not clear where the polymerization process would stop. In a study of the primitive Martian atmosphere, Yung and Pinto (1978) predicted that alkanes heavier than heptane would condense to liquid form at temperatures expected to prevail on the Martian surface. The warmer surface temperature on the primitive Earth would prevent condensation until much higher molecular weights were attained. It may be that alkane mist would have condensed out of the colder regions of the stratosphere and then evaporated as it descended into the relatively warm troposphere. However, such speculation is probably premature at this time, due to uncertainty concerning the formation rates of the higher hydrocarbon species. Here we can only point out two expected effects of higher alkane formation on our results. First, by providing additional loss processes for C_3H_7 and C_4H_9, such reactions should tend to restore the normal ordering of alkane concentrations, whereby the densities decrease with increasing molecular weight. Second, oxidation and possibly condensation of higher alkanes would have constituted an additional drain on atmospheric methane, so the required methane source strength at high CH_4 and CO_2 levels may have been greater than we have calculated here.

The large CO concentrations predicted by our model at high CH_4 and CO_2 mixing ratios may be unrealistic. Possibly, CO could have been reduced to CH_4 by catalytic processes occurring at the Earth's surface or in oceans. This reaction is favored thermodynamically, but requires a mechanism for breaking the C—O bond. Direct photolysis of CO requires wavelengths shorter than 1100 Å and could only occur high up in the atmosphere, but alternative gas phase pathways may exist. Bar-Nun and Chang (1983) recently reported methane and other hydrocarbons among the products formed by 1849 Å irradiation of a gaseous mixture of CO and H_2O. The mechanism and efficiency of CH_4 formation remains unclear. Additional study of this system would be of interest because of its implications for the composition of the primitive atmosphere.

The steady-state CO/CO_2 ratio is quite sensitive to tropospheric photolysis rates and the assumed water vapor profile. An earlier version of this model that did not include Rayleigh scattering predicted much smaller amounts of CO at high CO_2 and CH_4 mixing ratios, due to a more rapid rate of hydroxyl formation by photolysis of water vapor. The hydrocarbon chemistry considered here may well have produced aerosols similar to those observed on

Titan, so the scattering optical depth of the atmosphere may have been much greater than assumed here.

Finally, due to our neglect of nitrogen chemistry, the present model overlooks the production of hydrogen cyanide — a compound of special interest to biochemists studying the origin of life. Hydrogen cyanide could have been formed at altitudes above 40 km by

$$CH_4 + h\nu \rightarrow CH + H_2 + H$$

followed by

$$CH + N_2 \rightarrow HCN + N$$

About 7% of methane photolysis reactions yield CH radicals (Gorden and Ausloos, 1967), which react with N_2 at a rate of between 7.3×10^{-14} (Braun et al., 1967) and 1×10^{-12} (Bosnali and Perner, 1971). Hydrogen cyanide, like CH_4, photolyzes only at very short wavelengths (Huebner and Carpenter, 1979), so most of the HCN produced at high altitudes could have survived long enough to be transported down into the lower atmosphere. Current studies of HCN in the atmosphere of Titan (Hanel et al., 1981) should shed more light on the photochemistry of this important molecule.

TENTATIVE LIMITS ON METHANE IN THE ARCHEAN ATMOSPHERE

We have shown that methane would have been an ephemeral constituent of an anaerobic primitive atmosphere of the kind considered here and could have remained in the atmosphere for geologically significant periods of time only if there was a continuous supply. Our calculations show that a source strength of about 10^{10} molecules cm^{-2} s^{-1} or larger would have been needed to sustain methane mixing ratios of 10^{-6}, the lowest value likely to be of climatic significance.

The present-day flux of methane to the atmosphere has been estimated as about 10^{14} moles y^{-1} or 3.75×10^{11} molecules cm^{-2} s^{-1} (Koyama, 1963; Baker-Blocker et al., 1977; Ehhalt and Schmidt, 1978; Kasting and Donahue, 1980). This flux is almost entirely of biogenic origin, being a product of methanogenic bacteria that derive energy mainly from the reaction

$$CO_2 + 4H_2 \rightarrow CH_4 + 2H_2O \qquad (1)$$

(Wolfe, 1971; Deuser et al., 1973; Zeikus and Winfrey, 1976; Dacey and Klug, 1979). The hydrogen and carbon dioxide are products of microbial fermentation of organic matter in anaerobic environments (Gray and Gest, 1965)

$$H_2O + CH_2O \rightarrow 2H_2 + CO_2 \qquad (2)$$

Walker (1980a) has pointed out that much of the present day biogenic methane may be oxidized by microorganisms in overlying aerobic waters before reaching the atmosphere; with allowance for this loss, the total source of microbial methane today might be 10^{12} cm^{-2} s^{-1}.

The total rate of photosynthetic fixation of carbon today is 2.6×10^{13} atoms cm^{-2} s^{-1} using the tabulation of Holland (1978), so ~4% of current

productivity is converted into methane (Watson et al., 1978). On the anaerobic Earth, the fraction of organic carbon recycled as methane would presumably have been higher, but the productivity might well have been lower. The present day marine productivity of 1.1×10^{13} atoms cm^{-2} s^{-1} might be a more plausible estimate of productivity during the Archean. A still more plausible estimate might be obtained by excluding open ocean productivity for reasons that have been discussed by Knoll (1979) and Walker (1978). The resulting estimate of a globally averaged carbon flux today of 2.7×10^{12} atoms cm^{-2} s^{-1} is derived from the figures quoted by Koblentz-Mishke et al. (1970) for inshore and neritic waters. Such waters may, of course, have been rare on the Archean Earth.

Undoubted evidence of life extends back to 3.5 Ga ago (Walter et al., 1980), and isotopic evidence for the activity of methanogenic bacteria as long ago as 2.7 Ga has also been reported (Schoell and Wellmer, 1981; Hayes, 1983). Nor is the antiquity of the methanogens in doubt (Woese and Fox, 1977). Therefore, it seems possible that microorganisms on the Archean Earth might have generated a methane flux approaching 10^{12} molecules cm^{-2} s^{-1}, depending on the fraction of fixed carbon converted into methane.

Possibly tighter constraints on the problem can be set by considering the oxidation—reduction balance of the atmosphere and ocean combined. The atmospheres we have described would have been losing hydrogen to space at a rate that can be estimated as

$$F(\mathrm{H}) = 4 \times 10^{13} \; [2f(\mathrm{H_2}) + 2f(\mathrm{H_2O}) + 4f(\mathrm{CH_4})] \text{ atoms cm}^{-2} \text{ s}^{-1} \qquad (3)$$

where $f(H_2O) = 3.8 \times 10^{-6}$ is the mixing ratio of water vapor in the stratosphere, and $f(H_2)$ and $f(CH_4)$ are the mixing ratios of hydrogen and methane at the ground (Hunten, 1973; Hunten and Donahue, 1976; Walker, 1977; Kasting et al., 1979; Kasting and Walker, 1981). This loss of reducing power to space must have at least been balanced by a supply of reducing power to the atmosphere and ocean, or the world would have become aerobic (see discussion below). Evidence for a predominantly reducing atmosphere and ocean in the Archean has been summarized most recently by Walker et al. (1983).

The present-day flux of reduced volcanic and metamorphic gases to the atmosphere has been estimated by Kasting and Walker (1981) as equivalent to 8×10^{8} H atoms cm^{-2} s^{-1}. The potential flux of divalent iron released by terrestrial weathering might be as large as 8×10^{10} Fe atoms cm^{-2} s^{-1} (Kasting and Walker, 1981), equivalent to 8×10^{10} H atoms cm^{-2} s^{-1} by way of the schematic reaction

$$Fe^{++} + 3H_2O \rightarrow Fe(OH)_3 + 2H^+ + H \qquad (4)$$

We are aware of no estimate of the total flux of reduced species provided by submarine weathering today. This flux must be considerably less than the flux of oxygen into the deep sea, for otherwise the deep sea would be anoxic. Using numbers presented by Broecker (1974) we calculate an upper limit on

the submarine weathering flux equivalent to 4×10^{12} H atoms cm^{-2} s^{-1}. These estimates are all highly uncertain and their applicability to the distant past is even more uncertain, but we conclude that methane mixing ratios in the range 10^{-4}—10^{-6} are not obviously inconsistent with the maintenance of anaerobic conditions in the atmosphere and ocean. Such mixing ratios could have been sustained by a sufficiently abundant source of reduced iron in solution and a flourishing microbiota, including photoautotrophs, fermenting heterotrophs and methanogens. Oxidation—reduction balance could have been maintained by oxidation of the iron, either directly by the photoautotrophs (Walker, 1980a) or by reaction with photosynthetic oxygen

$$4Fe^{++} + O_2 + 10H_2O \rightarrow 4Fe(OH)_3 + 8H^+ \quad (5)$$

Figure 13 illustrates a hypothetical biogeochemical cycle of methane and hydrogen under Archean conditions. The methane generated by methanogens was oxidized photochemically in the atmosphere to carbon dioxide and hydrogen. These products then flowed back into the ocean to be converted by biological activity into methane and water. The steady loss of hydrogen from the top of the atmosphere was balanced by the oxidation of a fraction of the flux of reduced minerals passing through the ocean in solution.

Our results, summarized in Fig. 9, allow some estimates to be made of the relative magnitudes of the fluxes and concentrations in this cycle. Suppose, for example, that the methane flux was close to the modern value, $\sim 1.5 \times 10^{11}$ cm^{-2} s^{-1}, and that the CO_2 mixing ratio was about 10 PAL. According to Fig. 9 the methane mixing ratio would have been about 3×10^{-5}. Using the piston velocity approach (Broecker, 1974) we calculate that an average supersaturation of methane in surface seawater by a factor of ~ 3 would have

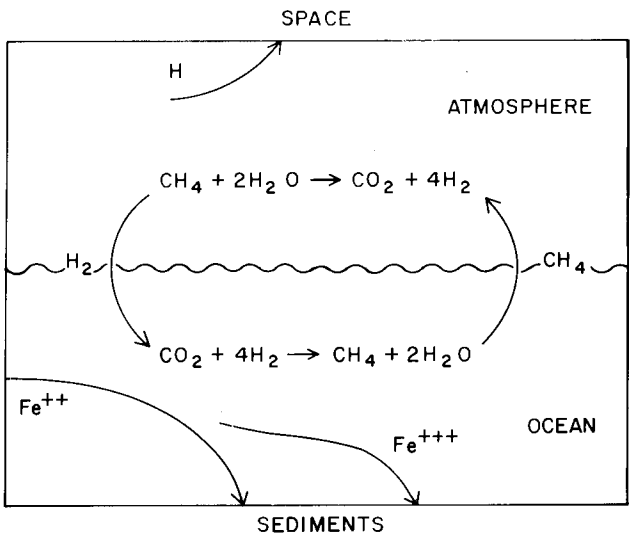

Fig. 13. Possible biogeochemical cycles of methane and hydrogen during the Archean era.

provided the necessary flux. The return flux of hydrogen would have required an atmospheric hydrogen partial pressure larger by 5×10^{-4} atmospheres than the partial pressure in solution equilibrium with surface seawater (Walker, 1980b). Modern methanogens can apparently hold hydrogen partial pressures down to 3×10^{-4} atmospheres (Hungate, 1967; Wolin, 1976) and photosynthetic bacteria can probably lower hydrogen even further (Walker, 1980c), so the atmospheric partial pressure of hydrogen was not likely to have exceeded 8×10^{-4} atmospheres.

With a hydrogen mixing ratio of 8×10^{-4}, a methane mixing ratio of 3×10^{-5}, and a stratospheric water vapor mixing ratio of 3.8×10^{-6}, the hydrogen escape flux would have been 10^{11} atoms cm^{-2} s^{-1} according to eq. 3. This expression probably overestimates the escape flux at high hydrogen partial pressures (Kasting and Walker, 1981) so the required rate of supply of reducing power to atmosphere and ocean would have been smaller than 10^{11} cm^{-2} s^{-1}. From the point of view of biogeochemical cycles we find no obvious defect in the hypothesis that methane mixing ratios exceeding 10^{-6} could have been sustained in the Archean atmosphere by methanogenic bacteria.

We have already noted the possible climatic impact of the greenhouse effect due to this much methane and the hydrocarbon products of its photochemical destruction. Accumulation of abundant free oxygen in the atmosphere in the Early Proterozoic may have lowered the concentrations of methane and other hydrocarbons in the atmosphere, causing a global climatic cooling (Walker et al., 1983). The Early Proterozoic glaciogenic rocks of the Huronian sequence in Canada are underlain by sedimentary rocks that appear to have been deposited under reducing conditions and are overlain by rocks that appear to have been deposited under oxidizing conditions (Roscoe, 1969, 1973).

Turning to the possible abundance of methane in the prebiological atmosphere, abiotic sources of methane are likely to have been quite small (with the possible exception of a CO rich atmosphere, as discussed above) after the initial period of Earth accretion, dissipation of the solar nebula, and differentiation of the Earth into core, mantle and crust. The present oxidation state of the Earth's upper mantle is such that the fraction of total carbon released as methane by volcanoes and metamorphic reactions is much less than that released as carbon dioxide or carbon monoxide. An estimate for the present-day release rate of carbon monoxide is 2×10^{8} molecules cm^{-2} s^{-1} (Kasting and Walker, 1981). Thus, even if the early rate of release of volcanic and metamorphic gases were 10—100 times higher than at present, the amount of methane released is hardly likely to have been enough to maintain a methane mixing ratio as high as 10^{-6}. Since the segregation of the core very probably occurred during the course of Earth accretion (Stevenson, 1983), there is no reason to believe that volcanic and metamorphic gases on the early Earth were richer in methane than they are today (Holland, 1962).

Mid-ocean hot springs provide a potentially important source of abiotic methane, especially in light of evidence for much stronger interaction be-

tween seawater and mantle in the Archean (Veizer, 1976, 1979; Veizer and Jansen, 1979). The present-day rate of supply of methane by mid-ocean ridge hot springs has been estimated at 1.6×10^8 m^3 y^{-1} (Welhan and Craig, 1979; Craig and Lupton, 1980), equivalent to a flux of 3×10^7 molecules cm^{-2} s^{-1}. Unless this mid-ocean source of methane were 1,000 times larger on the Archean Earth it could not have yielded methane mixing ratios in the atmosphere as high as 10^{-6}. As discussed in the previous section, methane may have been generated photochemically in an atmosphere rich in H_2O and CO. The magnitude of the source will remain uncertain until more is known about the reeaction mechanisms involved.

These findings can be summarized in a very tentative history of atmospheric methane. Any primordial methane accumulated during the course of Earth accretion would have been dissipated by photochemical reactions in the atmosphere in a geologically short period of time after the segregation of the core. Abiotic sources of methane are not likely to have been large enough to sustain methane mixing ratios as high as 10^{-6}, the threshold for a possible methane greenhouse, with a CO-rich atmosphere being a possible exception. After the origin of life an increasing biogenic source of methane may have driven methane mixing ratios well above 10^{-6}. The rise of atmospheric oxygen in the early Proterozoic may have led to more rapid photochemical destruction of methane, lowering the methane mixing ratio to approximately its present value of 1.4×10^{-6}. Indeed, the methane mixing ratio may have dropped briefly to much lower values due to rapid photochemical oxidation processes in mildly oxidizing atmospheres (Kasting and Donahue, 1980).

ACKNOWLEDGMENTS

We would like to thank Y.L. Yung and R.E. Dickinson for valuable discussions concerning methane photochemistry and possible greenhouse effects. The National Center for Atmospheric Research is sponsored by the National Science Foundation. This research was supported in part by the National Aeronautics and Space Administration under Grant Number NAGW-176, and by the National Center for Atmospheric Research under project number 6567.

REFERENCES

Allen, M., Pinto. J.P. and Yung, Y.L., 1980. Titan: aerosol photochemistry and variations related to the sunspot cycle. Astrophys. J., 242: L125—L128.

Baker-Blocker, A., Donahue, T.M. and Mancy, K.H., 1977. Methane flux from wetland areas. Tellus, 29: 245—250.

Barassin, J. and Combourie, J., 1974. Etude cinétique des réaction entre l'oxygèn atomique et les dérivés chlorés du méthane. II. Réactions $CH_3CO + O$, $CHCl_3 + O$, $CCl_4 + O$ et $CH_4 + O$; resulthes experimentaux. Bull. Soc. Chim. Fr., p. 1—5.

Bar-Nun, A. and Chang, S., 1981. Photochemical reaction of carbon monoxide and water in the Earth's primitive atmosphere. J. Geophys. Res., in press.

Baulch, D.L., Drysdale, D.D., Duxbury, J. and Grant, S.J., 1976. Evaluated Kinetic Data for High Temperature Reactions. Vol. 3, Butterworth's, London, 433 pp.

Becker, K.H., Haaks, D. and Schürgers, M., 1971. Fluorescence by the vacuum-UV photolysis of acetylene. Z. Naturforsch., 26: 1770—1771.

Bell, J.A., 1971. Methylene reaction rates. Quantum yields in the diazomethane—propane photolysis system: Effects of photolysis time, reactant ratios, and added gases. J. Phys. Chem., 75: 1537—1549.

Benson, S.W., 1964. Some problems of structure and reactivity in free radical and molecule reactions in the gas phase. Adv. Photochem., 2: 1—23.

Benson, S.W. and Haugen, G.R., 1967. The mechanisms of the high temperature reactions between C_2H_2 and hydrogen. J. Phys. Chem., 71: 4404—4411.

Bosnali, M.W. and Perner, D., 1971. Reaktionen von pulsradiolytisch erzeugtem $CH(^2\Pi)$ mit Methan und anderen substanzen. Z. Naturforsch., 26a: 1768—1769.

Braun, W., Bass, A.M. and Pilling, M., 1970. Flash photolysis of ketene and diazomethane: The production and reaction kinetics of triplet and singlet methylene. J. Chem. Phys., 52: 5131—5143.

Braun, W., McNesby, J.R. and Bass, A.M., 1967. Flash photolysis of methane in the vacuum ultraviolet. II. Absolute rate constants for reactions of CH with methane, hydrogen, and nitrogen. J. Chem. Phys., 46: 2071—2080.

Broecker, W.S., 1974. Chemical Oceanography. Harcourt Brace Jovanovich, New York, 214 pp.

Calvert, J.G. and Pitts, J.N., 1966. Photochemistry. Wiley, New York, 899 pp.

Calvert, J.G., Kerr, J.A., Demerjian, K.L. and McQuigg, R.D., 1972. Photolysis of formaldehyde as a hydrogen atom source in the lower atmosphere. Science, 175: 751—752.

Campbell, J.M. and Thrush, B.A., 1967. The association of oxygen atoms and their combination with nitrogen atoms. Proc. R. Soc. London, Ser. A, 296: 222—232.

Cheng, J.T. and Yeh, C., 1977. Pressure dependence of the rate constant of the reaction $H + CH_3 \rightarrow CH_4$. J. Phys. Chem., 81: 1982—1984.

Craig, H. and Lupton, J.E., 1980. Helium-3 and mantle volatiles in the ocean and the oceanic crust. In: The Sea. Vol. 7, The Oceanic Lithosphere. Wiley, New York, 758 pp.

Dacey, J.W.H. and Klug, M.J., 1979. Methane flux from lake sediments through water lilies. Science, 203: 1253—1255.

Demerjian, K.L., Kerr, J.A. and Calvert, J.G., 1974. The mechanism of photochemical smog formation. In: J.N. Pitts and R.L. Metoalf (Editors), Advances in Environmental Science and Technology. Vol. 4, Wiley, New York, 382 pp.

Deuser, W.G., Degens, E.T., Harvey, G.R. and Rubin, M., 1973. Methane in Lake Kivu: new data bearing on its origin. Science, 181: 51—54.

Donner, L. and Ramanathan, V., 1980. Methane and nitrous oxide: their effects on the terrestrial climate. J. Atmos. Sci., 37: 119—124.

Ehhalt, D.H. and Schmidt, U., 1978. Sources and sinks of atmospheric methane. Palaeogeogr. Palaeoclimatol. Palaeoecol., 116: 452—464.

Frakes, L.A., 1979. Climates Throughout Geologic Time. Elsevier, New York, 310 pp.

Gorden, R. and Ausloos, P., 1967. Gas-phase photolysis and radiolysis of methane. Formation of hydrogen and ethylene. J. Chem. Phys., 46: 4823—4834.

Gray, C.T. and Gest, H., 1965. Biological formation of molecular hydrogen. Science, 148: 186—192.

Hack, W., Wagner, H.G. and Hoyermann, K., 1978. Reaktionen von Wasserstoffatomen mit Hydroperoxylradikalen. I. Bestimmung der spezifischen Geschwindigkeitskonstanten der Reaktionskanäle. Ber. Bunsenges. Phys. Chem., 82: 713—719.

Hack, W., Preuss, A.W., Wagner, H.G. and Hoyermann, K., 1979. Reaktionen von Wasserstoffatomen mit Hydroperoxylradikalen. II. Bestimmung der Geschwindigkeitskonstanten der Bruttoreaktion. Ber. Bunsenges. Phys. Chem., 83: 212—217.

Hampson, R.F. and Garvin, D., 1977. Reaction Rate and Photochemical Data for Atmospheric Chemistry — 1977. Natl. Bur. Stand. Spec. Publ. No. 513, 107 pp.

Hanel, R., Conrath, B., Flaser, F.M., Kunde, V., Maguire, W., Pearl, J., Pirraglia, J., Samuelson, R., Herath, L., Allison, M., Cruikshank, D., Gautier, D., Gierasch, P. Horn, L., Koppany, R. and Ponnamperuma, C., 1981. Infrared observations of the Saturnian system from Voyager 1. Science, 212: 192—200.

Hayes, J.M., 1983. Geochemical evidence bearing on the origin of aerobiosis, a speculative interpretation. In: J.W. Schopf (Editor), The Earth's Earliest Biosphere: Its Origin and Evolution. Princeton University Press, Princeton, NJ, 873 pp.

Huebner, W.F. and Carpenter, C.W., 1979. Solar photo rate coefficients. NASA informal report LA-8085-MS, Los Alamos, NM, 97 pp.

Hochanadel, C.J., Sworski, T.J. and Ogren, P.J., 1980. Ultraviolet spectrum and reaction kinetics of the formyl radical. J. Phys. Chem., 84: 231—235.

Holland, H.D., 1962. Model of the evolution of the earth's atmosphere. In: A.E.J. Engle, H.L. James and B.F. Leonard (Editors), Petrologic Studies: A Volume to Honor A.E. Buddington. Geological Society of America, NY, pp. 447—477.

Holland, H.D., 1978. The Chemistry of the Atmosphere and Oceans. Wiley, New York, 351 pp.

Hungate, R.E., 1967. Hydrogen as an intermediate in the rumen fermentation. Arch. Microbiol., 59: 158—164.

Hunten, D.M., 1973. The escape of light gases from planetary atmospheres. J. Atmos. Sci., 30: 1481—1494.

Hunten, D.M., 1975. Vertical transport in atmospheres. In: B.M. McCormac (Editor), Atmospheres of Earth and Planets. D. Reidel, Dordrecht, The Netherlands, pp. 59—72.

Hunten, D.M. and Donahue, T.M., 1976. Hydrogen loss from the terrestrial planets. Annu. Rev. Earth Planet. Sci., 4: 265—292.

Jet Propulsion Laboratory, 1979. Chemical Kinetic and Photochemical Data for Use in Stratospheric Modelling. JPL Publication 79-27, Pasadena, 240 pp.

Kasting, J.F., 1982. Stability of ammonia in the primitive terrestrial atmosphere. J. Geophys. Res, 87: 3091—3098.

Kasting, J.F. and Donahue, T.M., 1980. The evolution of atmospheric ozone. J. Geophys. Res., 85: 3255—3263.

Kasting, J.F. and Walker, J.C.G., 1981. Limits on oxygen concentration in the prebiological atmosphere and the rate of abiotic fixation of nitrogen. J. Geophys. Res., 86: 1147—1158.

Kasting, J.F., Liu, S.C. and Donahue, T.M., 1979. Oxygen levels in the prebiological atmosphere. J. Geophys. Res., 84: 3097—3107.

Knoll, A.H., 1979. Archean photoautotrophy: some alternatives and limits. Origin Life, 9: 313—327.

Koblentz-Mishke, O.J., Volkovinsky, V.V. and Kabanova, J.G., 1970. Plankton primary production of the world ocean. In: W.S. Wooster (Editor), Scientific Exploration of the South Pacific. Natl. Acad. Sci, Washington, DC, 257 pp.

Koyama, T., 1963. Gaseous metabolism in lake sediments and paddy soils and the production of atmospheric methane and hydrogen. J. Geophys. Res., 68: 3971—3973.

Kuhn, W.R. and Atreya, S.K., 1979. Ammonia photolysis and the greenhouse effect in the primordial atmosphere of the Earth. Icarus, 37: 207—213.

Lasaga, A.C., Holland, H.D. and Dwyer, M.J., 1971. Primordial oil slick. Science, 174: 53—55.

Laufer, A.H. and Bass, A.M., 1974. Rate constants for reactions of methylene with carbon monoxide, oxygen, nitric oxide and acetylene. J. Phys. Chem., 78: 1344—1348.

Laufer, A.H. and Bass, A.M., 1979. Photochemistry of acetylene. Bimolecular rate constant for the formation of butadiene and reactions of ethynyl radicals. J. Phys. Chem., 83: 310—313.

Lee, J.T., Michaels, J.V., Payne, W.A. and Stief, L.J., 1978. Absolute rate of the reaction of atomic hydrogen with ethylene from 198 to 320 K at high pressure. J. Chem. Phys., 68: 1817—1820.

Liu, S.C. and Donahue, T.M., 1974. The aeronomy of hydrogen in the atmosphere of the Earth. J. Atmos. Sci., 31: 1118—1136.
Mount, G.H. and Moos, H.W., 1978. Photoabsorption cross sections of methane and ethane, 1380—1600 Å, at T = 295K and T = 200K. Astrophys. J., 224: L35—L38.
Mount, G.H., Warden, E.S. and Moos, H.W., 1977. Photoabsorption cross sections of methane from 1400 to 1850 Å. Astrophys. J., 214: L47—L49.
Nakayama, T. and Watanabe, K., 1964. Absorption and photolysis coefficients of acetylene, propyne and 1-butyne. J. Chem. Phys., 40: 558—561.
Newman, M.J. and Rood, R.T., 1977. Implications of solar evolution for the Earth's early atmosphere. Science, 198: 1035—1037.
Okabe, H. and Becker, D.A., 1963. Vacuum ultraviolet photochemistry. VII. Photolysis of n-butane. J. Chem. Phys., 39: 2549—2555.
Okabe, H. and McNesby, J.R., 1962. Vacuum ultraviolet photochemistry. IV. Photolysis of propane. J. Chem. Phys., 37: 1340—1346.
Owen, T., Cess, R.D. and Ramanathan, V., 1979. Early Earth: an enhanced carbon dioxide greenhouse to compensate for reduced solar luminosity. Nature, 277: 640—642.
Payne, W.A. and Stief, L.J., 1976. Absolute rate constant for the reaction of atomic hydrogen with acetylene over an extended pressure and temperature range. J. Chem. Phys., 64: 1150—1155.
Pilling, M.J. and Robertson, J.A., 1975. A rate constant for $CH_2(^3B_1) + CH_3$. Chem. Phys. Lett., 33: 336—339.
Pinto, J.P., Gladstone, C.R. and Yung, Y.L., 1980. Photochemical production of formaldehyde in the Earth's primitive atmosphere. Science, 210: 183—185.
Reilly, J.P., Clark, J.H., Moore, C.B. and Pimental, G.C., 1978. HCO production, vibrational relaxation, chemical kinetics and spectroscopy following laser photolysis of formaldehyde. J. Chem. Phys., 69: 4381—4394.
Roscoe, S.M., 1969. Huronian rocks and uraniferous conglomerates in the Canadian Shield. Geol. Surv. Can. Pap. 68-40, 205 pp.
Roscoe, S.M., 1973. The Huronian supergroup, a Paleophebian succession showing evidence of atmospheric evolution. Geol. Assoc. Can. Spec. Pap. 12: 31—48.
Russell, R.L. and Rowland, F.S., 1979. Mechanism of product formation during the photolysis of ketene. J. Phys. Chem., 83: 2073—2078.
Sagan, C. and Mullen, G., 1972. Earth and Mars: Evolution of atmospheres and surface temperatures. Science, 177: 52—56.
Schoell, M. and Wellmer, F.W., 1981. Anomalous ^{13}C depletion in early Precambrian graphites from Superior Province, Canada. Nature, 290: 696—699.
Stevenson, D.J., 1983. The nature of the Earth prior to the rock record (The Hadean Earth). In: J.W. Schopf (Editor), The Earth's Earliest Biosphere: Its Origin and Evolution, Princeton University Press, Princeton, NJ, 873 pp.
Stief, L.J., DeCarlo, V.J. and Mataloni, R.J., 1965. Vacuum-ultraviolet photolysis of acetylene. J. Chem. Phys., 42: 3113—3121.
Strobel, D.F., 1973. The photochemistry of hydrocarbons in the Jovian atmosphere. J. Atmos. Sci., 30: 489—498.
Takita, S., Mori, Y. and Tanaka, I., 1968. The acetylene-photosensitized reaction of methane at 1470 Å. J. Phys. Chem., 72: 4360—4365.
Takita, S., Mori, Y. and Tanaka, I., 1969. Acetylene photolysis at 1236 and 1470 Å. J. Phys. Chem., 73: 2929—2934.
Teng, L. and Jones, W.E., 1972. Kinetics of the reactions of hydrogen atoms with ethylene and vinyl fluoride. J. Chem. Soc. Faraday Trans., 1, 68: 1267—1277.
Troe, J., 1977. Theory of thermal unimolecular reactions at low pressures. II. Strong collision rate constants. Applications. J. Chem. Phys., 66: 4758—4775.
Van den Bergh, H.E., 1976. The recombination of methyl radicals in the low pressure limit. Chem. Phys. Lett., 43: 201—204.

Veizer, J., 1976. $^{87}Sr/^{86}Sr$ evolution of seawater during geologic history and its significance as an index of crustal evolution. In: B.F. Windley (Editor), The Early History of the Earth. Wiley, London, pp. 569—578.
Veizer, J., 1979. Secular variations in chemical composition of sediments: a review. In: L.H. Ahrens (Editor), Origin and Distribution of the Elements.. Pergamon, Oxford, pp. 269—278.
Veizer, J. and Jansen, S.L., 1979. Basement and sedimentary recycling and continental evolution. J. Geology, 87: 341—370.
Walker, J.C.G., 1977. Evolution of the Atmosphere. Macmillan, New York, 318 pp.
Walker, J.C.G., 1978. The early history of oxygen and ozone in the atmosphere. Pure Appl. Geophys., 117: 498—512.
Walker, J.C.G., 1980a. The oxygen cycle. In: O. Hutzinger (Editor), The Natural Environment and the Biogeochemical Cycles. Springer-Verlag, Berlin, pp. 87—104.
Walker, J.C.G., 1980b. The influence of life on the evolution of the atmosphere. Life Sci. Space Res., 8: 89—100.
Walker, J.C.G., 1980c. Atmospheric constraints on the evolution of metabolism. Origins Life, 10: 93—104.
Walker, J.C.G., Hays, P.B. and Kasting, J.F., 1981. A negative feedback mechanism for the long-term stabilization of Earth's surface temperature. J. Geophys. Res., 86: 9776—9782.
Walker, J.C.G., Klein, C., Schidlowski, M., Schopf, J.W., Stevenson, D.J. and Walter, M.R., 1983. Environmental evolution of the Archaean—Early Proterozoic Earth. In: J.W. Schopf (Editor), The Earth's Earliest Biosphere: Its Origin and Evolution. Princeton University Press, Princeton, NJ, 873 pp.
Walter, M.R., Buick, R. and Dunlop, J.S.R., 1980. Stromatolites 3,400—3,500 Myr old from the North Pole era, Western Australia. Nature, 284: 443—445.
Watson, A., Lovelock, J.E. and Margulis, L., 1978. Methanogenesis, fires and the regulation of atmospheric oxygen. Biosystems, 10: 293—298.
Welhan, J.A. and Craig, H., 1979. Methane and hydrogen in East Pacific Rise hydrothermal fluids. Geophys. Res. Lett, 6: 829—831.
Woese, C.R. and Fox, G.E., 1977. Phylogenetic structure of the prokaryotic domain: the primary kingdoms. Proc. Natl. Acad. Sci. U.S.A., 74: 5088—5090.
Wolfe, R.S., 1971. Microbial formation of methane. Adv. Microb. Physiol., 6: 107—146.
Wolin, M.J., 1976. Interactions between H_2-producing and methane-producing species. In: H.G. Schlegel, G. Gottschalk and N. Pfennig (Editors), Symposium on Microbiological Production and Utilization of Gases (H_2, CH_4, CO). E. Goltzke KG, Göttingen, pp. 141—150.
Yung, Y.L., 1976. A numerical method for calculating the mean intensity in an inhomogeneous Rayleigh scattering atmosphere. J. Quant. Spectrosc. Radiat. Transfer, 16: 755—761.
Yung, Y.L. and McElroy, M.B., 1979. Fixation of nitrogen in the prebiotic atmosphere. Science, 203: 1002—1004.
Yung, Y.L. and Pinto, J.P., 1978. Primitive atmosphere and implications for the formation of channels on Mars. Nature, 273: 730—732.
Yung, Y.L. and Strobel, D.F., 1980. Hydrocarbon photochemistry and Lyman alpha albedo of Jupiter. Astrophys. J., 239: 395—402.
Zeikus, J.G. and Winfrey, M.R., 1976. Temperature limitation of methanogenesis in aquatic sediments. Appl. Environ. Microbiol., 31: 99—107.
Zelikoff, M. and Watanabe, K., 1953. Absorption coefficients of ethylene in the vacuum ultraviolet. J. Opt. Soc. Am., 43: 756—759.

PROTEROZOIC AEOLIAN QUARTZ ARENITES FROM THE HORNBY BAY GROUP, NORTHWEST TERRITORIES, CANADA: IMPLICATIONS FOR PRECAMBRIAN AEOLIAN PROCESSES

GERALD M. ROSS

Department of Geology, Carleton University, Ottawa, Ontario K1S 5B6 (Canada)

ABSTRACT

Ross, G.M., 1983. Proterozoic aeolian quartz arenites from the Hornby Bay Group, Northwest Territories, Canada: implications for Precambrian aeolian processes. Precambrian Res., 20: 149—160.

The Hornby Bay Group is a Middle Proterozoic 2.5 km-thick succession of terrestrial siliciclastics overlain by marine siliciclastics and carbonates. A sequence of conglomeratic and arenaceous rocks at the base of the group contains more than 500 m of mature hematitic quartz arenite interpreted to have been deposited by migrating aeolian bedforms. Bedforms and facies patterns of modern aeolian deposits provided a basis for recognizing two sequences of aeolian arenite. Both sequences interfinger with alluvial—wadi fan conglomerates and arenites deposited by braided streams. Depositional processes, facies patterns and paleotopographic position of the arenites are consistent with modern sand sea dynamics.

Distal aeolian facies in both sequences are composed of trough crossbed megasets deposited by climbing, sinuous-crested, transverse dunes. Megasets comprise a gradational assemblage of tabular to wedge-planar cosets formed by deflation/reactivation of dune lee slopes and migration of smaller superposed aeolian bedforms (small dunes and wind ripples). Megasets in the proximal facies are thinner, display composite internal stratification and have a tabular-planar geometry which suggests that they were formed by smaller, straight-crested transverse dunes. Most stratification within the crossbeds is inferred to have formed by the downwind climbing of aeolian ripples across the lee slopes of dunes.

Remarkably few Precambrian aeolian deposits have been reported previously. This seems anomalous, because most Precambrian fluvial sediments appear to have been deposited by low sinuosity (braided) streams, the emergent parts of which are prime areas for aeolian deflation. Frequent floods and rapid lateral migration of Precambrian humid climate fluvial systems probably restricted aeolianite deposition to arid paleoclimates. Thus the apparent anomaly may reflect non-recognition and/or non-preservation of aeolianites and/or variations in some aspect of sand sea formation and migration unique to the Precambrian. Reconstruction of the Hornby Bay Group aeolianites using recently developed criteria for their recognition suggests that the latter reason did not exert a strong influence.

INTRODUCTION

This paper is intended as a short note to bring attention to a recently recognized sequence of Middle Proterozoic arenites deposited by aeolian processes,

and to outline the methods by which they were recognized. A detailed account of the sedimentology and stratigraphy of the Hornby Bay Group aeolianites is given elsewhere (Ross, 1983).

Understanding of aeolian processes has advanced considerably in recent years as a result of (1) intensive study of recent dunes (McKee, 1966; Wilson, 1972a,b; Hunter, 1977), (2) interpretation of ancient aeolianites in terms of the dynamics of modern aeolian bedform migration (Brookfield, 1977; Hunter, 1981; Kocurek, 1981a,b; Kocurek and Dott, 1981; Rubin and Hunter, 1982), and (3) the availability of satellite imagery of modern sand seas (Breed and Grow, 1979). An aeolian interpretation for the Hornby Bay Group arenites is based on a comparison of their sedimentary structures and stratification styles with those in recent aeolian environments described by Hunter (1977).

GEOLOGIC SETTING AND DESCRIPTION OF THE ARENITES

The Coppermine Homocline, in the northwest corner of the Canadian Shield (Fig. 1), is a thick (>15 km) sequence of terrestrial and marine siliciclastics, marine carbonates and subaerial plateau basalts deposited in an intracratonic basin (Baragar and Donaldson, 1973; Baragar, 1977; Kerans et al., 1981). Details of the stratigraphy, depositional environments and tectonic history of the Homocline are described by Kerans et al. (1981). The Hornby Bay Group, which forms the basal unit of the Homocline, contains a 1.8 km-thick succession of conglomeratic and arenaceous rocks deposited by a variety of terrestrial processes. This succession has been subdivided into three units, each of which records a different history of deposition by fluvial, and

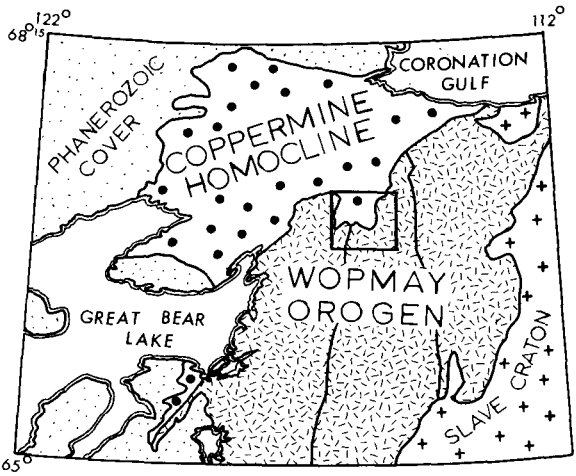

Fig. 1. Principal structural components of the northwestern Canadian Shield. Boxed area shows location of the basin discussed in text.

to a lesser extent aeolian, processes. The Bigbear unit, the oldest and thickest unit of the Hornby Bay Group, was deposited in a closed intermontane basin.

The Bigbear unit is more than 1200 m thick, and is composed mostly of mature to submature hematitic arenite and subordinate polymictic and oligomictic conglomerate. The Bigbear unit is conformably overlain by the youngest fluvial sequence of the Hornby Bay Group (Lady Nye unit) and was deposited in three stages (Fig. 2). Initial infill of rugged basement paleotopography by alluvial and fluvial processes, which culminated in the formation of a 4000 km^2 braidplain (stage I), was succeeded by formation of an aeolian sand sea within the basin (stage II). Deposition in the basin ended during a period of regional normal fault activity and associated change in

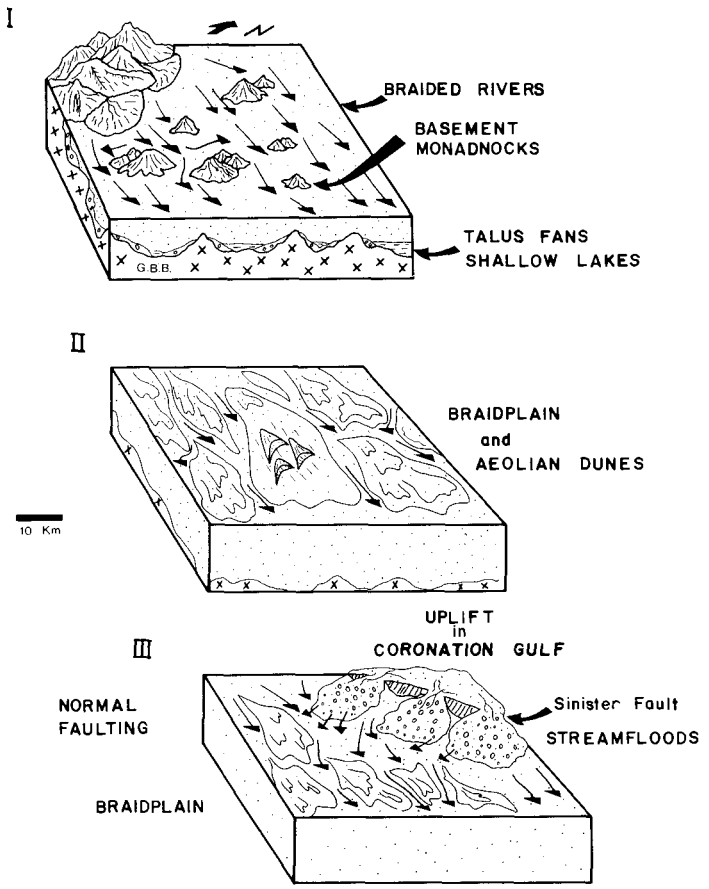

Fig. 2. Schematic diagram of the stages of deposition recorded in the Bigbear unit. Stage I. infill of rugged paleotopography and formation of a braidplain; stage II, formation of aeolian sand sea and associated low energy fluvial facies; and stage III, normal fault activity (for Sinister Fault, the author has followed the terminology of Hoffman, 1980) in response to regional uplift (for location of Coronation Gulf see Fig. 1) and drainage basin reorganization. G.B.B.: Great Bear Batholith (basement).

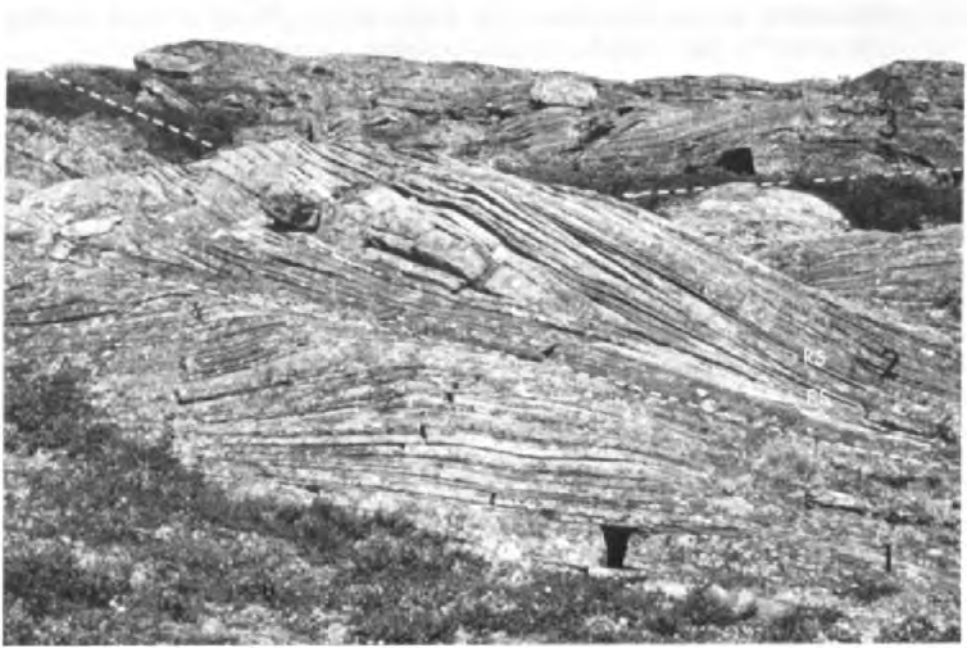

Fig. 3. Trough festoon megasets typical of distal aeolianite facies. Three individual megasets (marked by dashed white lines) are shown. Set 1 forms the limb of a large trough crossbed (cf. set 3), the axis of which is towards the left side, out of the field of view. Set 2 contains at least two reactivation surfaces (RS) which truncate underlying strata at low angles ($< 5°$). Hammer for scale in right center of photo.

paleoslope (stage III), before deposition of the Lady Nye unit conglomerates. Such topographically closed intracratonic basins hold the greatest potential for accumulation and preservation of aeolian sand seas (Fryberger and Ahlbrandt, 1979; Breed et al., 1979; Brookfield, 1980).

Stage II deposits comprise a lower and upper unit approximately 500 m in total thickness. Both units are composed almost entirely of moderate to very well-sorted quartz arenite, and interfinger with alluvial fan conglomerates and fluvial arenites along the western margin of the basin. Large-scale (2—10 m) crossbeds are the dominant sedimentary structures within the arenites. In distal facies, interwoven 2—7 m trough cosets are typical (Fig. 3).

Fig. 4. Detail of stratification in two intrasets that form part of a 2 m tabular planar megaset. Paleocurrent azimuth for the megaset plunges down into the photograph. The intrasets are separated by a reactivation surface (RS). Individual stratal units (SU) formed by the migration of a single wind ripple that deposited a finer-grained saltation population (recessive weathering) and a coarse-grained creep load (resistant laminae). Several of the thicker strata (R) display foreset cross-lamination that indicates ripple migration to the left, across the dune lee slope. Signal flare for scale is 4 cm long.


RS
ISU
R
R

These grade laterally into 1—5 m stacked tabular to wedge-planar cosets of proximal facies. In both facies the large crossbed sets, referred to here as megasets, display a complex internal arrangement of down-current dipping, smaller-scale crossbed intrasets. These intrasets are 20—50 cm thick, ranging from tabular to distinctly wedge-shaped, and are bounded by low-angle planar to gently concave-up erosion surfaces. The intrasets contain very even, 1—2 cm scale, parallel stratification (Fig. 4) that is parallel to inclined (up to 25°) to the lower bounding surface. Individual strata within the intrasets are generally massive or composed of alternated fine- and coarse-grained layers (cf. Fig. 4). In some places individual strata display ripple foreset cross-lamination (Fig. 4). Megaset slipface orientations show a broad unimodal (>90% in one quadrant) transport pattern, whereas intraset orientations show wider dispersion (>90% in two quadrants) and in some cases have an acute (<45° between maxima) bimodal pattern.

INTERPRETATION

One of the most commonly applied criteria for the recognition of aeolian sediments has been the large scale of the crossbed sets (Walker and Middleton, 1977; McKee, 1979). Although the large size of the megasets in this area is suggestive of an aeolian origin, additional criteria are, however, preferable because of the ambiguity surrounding the interpretation of arenites based largely on crossbed scale (e.g., Freeman and Visher, 1975; Picard, 1977; Kocurek and Dott, 1981). The type of stratification shown in Fig. 4 is essentially identical to examples from recent dunes along the coasts of Texas and Oregon, U.S.A., which have been observed to form by the downwind climbing of wind ripples across larger bedforms (Hunter, 1977). Some of the intraset stratification, however, may also have formed by grainfall deposition; it is frequently difficult to distinguish between the two stratification types where individual strata do not have ripple foreset lamination (Hunter, 1981). Intrasets within the megasets and the complex arrangement of bounding surfaces suggest superposition of two scales of bedforms: those that produced the intrasets and those that produced the megasets. Some intrasets probably formed by deflation and reactivation of megaset lee slopes (the parallel stratified sets, that are bounded by 3 order surfaces (Brookfield, 1977)) whereas others may have formed by the migration of small dunes (tabular-planar sets bounded by 2 order (?) surfaces). The superposition of bedforms of different scales, although the result of multiple causes (Allen, 1973, 1974), is typical of modern dunes (Wilson, 1972b) and has been inferred for several ancient examples (e.g., Brookfield, 1977; Kocurek, 1981b; Kocurek and Dott, 1981). By analogy with aqueous bedforms (Harms et al., 1975), the trough crossbeds in distal regions suggest a dune bedform with a fairly sinuous crest, whereas the stacked tabular sets in proximal regions were produced by relatively straightcrested bedforms. Complex, sinuous-crested, transverse aeolian bedforms, referred to as aklé (Wilson, 1972b; Cooke and Warren, 1973), are

common in modern day closed basin ergs (Breed and Grow, 1979). The lack of recognized, laterally-extensive, truncation surfaces between megasets (1 order bounding surface (Brookfield, 1977)) suggests a relatively simple system of superposed dune and ripple bedforms with no development of large complex dunes (draas of Wilson (1972a) and Kocurek (1981b)). The inferred change in bedform morphology across the basin and the associated fluvial facies are shown diagrammatically in Fig. 5. The change in sinuosity across the basin, in a direction parallel to paleowind flow, is interpreted as a natural consequence of bedform—flow interaction, as observed in modern dune fields (Wilson, 1972b).

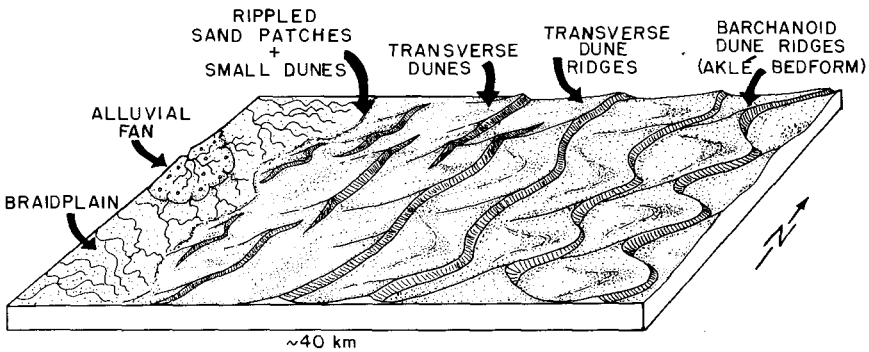

Fig. 5. Reconstruction of aeolian bedforms which produced the megasets and associated fluvial facies for the lower aeolianite unit. See text for discussion. Not to scale.

IMPLICATIONS FOR PROCESSES OF PRECAMBRIAN TERRESTRIAL SEDIMENTATION

There are relatively few published examples of Precambrian aeolianites; examples of aeolian cross-stratification are described from the Proterozoic of South Africa (Clemmey, 1976; Meinster and Tickell, 1976), Australia (Bunting et al., 1978; Goode and Hall, 1981), and in Proterozoic and possibly Archean rocks of the Canadian Shield by Donaldson (personal communication, 1982) and Hyde (1980) respectively. Other studies have suggested textural modification by aeolian processes (cf. Canadian Shield, Donaldson (1967), Ramaekers (1981), Hoffman (personal communication, 1982), Pettijohn et al. (1973) and Donaldson and Ojakangas (1977); India, Chaudhuri (1977), see also Folk, 1968 for additional Late Precambrian to Early Palaeozoic examples). The paucity of documented examples of aeolian arenites in the Precambrian rock record is surprising. Most pre-Devonian fluvial sedimentation was by low sinuosity/braided river systems (Schumm, 1968; Cotter, 1978; Rust, 1979). Such rivers typically display 'flashy' behavior: relatively catastrophic flood events separated by periods of low flow during which parts of the river system, especially the flood-stage bars, become

emergent (Miall, 1977). These emergent regions are prime areas for aeolian deflation of sand and finer grained detritus (cf. Collinson, 1970). Platform cover and intracratonic basin terrestrial to shallow-marine siliciclastic sedimentation has been described from Precambrian rocks, especially those of Proterozoic age (cf. Condie, 1982; Tankard et al., 1982) and it might be expected that aeolian arenites would be a common facies within siliciclastic deposits. The apparent scarcity of such deposits may be due to non-preservation, non-recognition, or different character of the factors that now control sand sea formation (e.g., climate, topography, wind regime, sand supply: Fryberger and Ahlbrandt, 1979).

The factors that affect the formation of sand seas (i.e., climate, topography, wind regime, sand supply) are difficult to quantitatively evaluate throughout geologic time. Walker (1982) for example, finds little evidence, or even theoretical basis, to suggest radically different climates during the Precambrian. Based upon various lines of isotopic and sedimentological evidence (Windley, 1977; Veizer and Jansen, 1977; Lowe, 1980) the suggestion has been made that the Archean Earth (before 2.6 Ga) may have been characterized by continental land masses considerably less in areal extent than the present. This also implies a lower proportion of exposed land relative to ocean area, and has consequences for both the nature of atmospheric circulation and formation of aeolian sand seas.

On a global scale, Walker's (1982; and personal communication, 1982) suggestion of increased latitudinal gradients in temperature during the Archean raises the possibility of a more turbulent ("windy") atmosphere on the early Earth, as wind generation is a consequence of these latitudinal gradients (Warren, 1979). Although such an effect on the early Earth would probably favor the formation of sand seas the availability of depocenters would have been low because of low amounts of stable arenaceous material. Thus, aeolianites should be less common in the Archean.

As mentioned above, intracratonic basin deposits are common in Proterozoic rocks and, therefore, non-preservation of sedimentary sequences likely to contain aeolianites does not appear to be a factor for the lack of Precambrian aeolianites. The character of Precambrian fluvial sedimentation, however, may have influenced development and preservation of sand seas. With the advent of land plants in the Silurian, the character of fluvial sedimentation changed from dominantly braided to meandering (Cotter, 1978). The effect of vegetation on emergent bars and interfluves was, with respect to the development of aeolianites, detrimental in that it decreased sediment availability (stabilization) and increased surface roughness (sediment-trapping of wind-blown particles by vegetation). Thus, post-Silurian Phanerozoic aeolianites would be expected to be developed almost exclusively in arid environments, where growth of vegetation is inhibited, a prediction that is borne out in the rock record (McKee, 1979; Hunter, 1981). It is likely that pre-land-vegetation fluvial systems would be susceptible to deflation and would not have significantly impeded through going sandflow.

However, evaluation of the character of Precambrian humid fluvial systems suggests that they probably inhibited aeolian sand sea formation because of the high rate of lateral migration of river systems and rapid intra-river channel switching and greater flood frequency.

The rates of lateral migration of the Brahmaputra River, (600 m y^{-1}, Coleman, 1969) and the Kosi River, (1000 m y^{-1}, Gole and Chitale, 1966), both humid climate rivers, are rapid and possibly analogous to many Precambrian fluvial systems. Such rates of lateral migration are high relative to the amount of time required for the formation of recent large-scale dunes (draas may require up to 10,000 years to form, Wilson, 1972b) and would tend to impede the build-up of aeolian sand. In addition, rapid channel switching and migration of humid braided river systems renders emergent areas ephemeral on the scale of minutes to days (cf. Smith, 1974; Smith and Minter, 1980, among others). This would tend to inhibit both aeolian sand accumulation and deflation of emergent areas. These effects would be compounded by the greater flood frequency typical of braided river systems in humid climates. Thus, it appears that Precambrian aeolian sedimentation would have taken place in arid environments where the fluvial system would have a lower annual discharge, flood frequency and lateral migration rate, and longer periods of emergence and desiccation.

Reliable criteria for the recognition of aeolian arenites has only been established since 1977. In addition to crossbed scale and sediment texture, interpretations of Phanerozoic aeolianites have relied heavily on biogenic structures (bioturbation, faunal composition, ichnofossils) and infrequently preserved physical structures (raindrop imprints, wind ripplemarks, fulgurites). The work of Hunter (1977, 1981), Brookfield (1977), and Kocurek and Dott (1981) augments the earlier work of Bagnold (1954), McKee and Tibbits (1964), McKee (1966), and Glennie (1970), among others, and provides sedimentologists with a distinctive assemblage of sedimentary structures formed by processes intrinsic to the migration of aeolian bedforms (e.g., downwind climb of aeolian bedforms and bedform superposition). Study of the Hornby Bay Group arenites indicates that these criteria are applicable to rocks as old as 1.5 Ga and probably to many other deposits of Precambrian siliciclastics.

CONCLUSIONS

The Proterozoic Hornby Bay Group contains aeolian arenites that were recognized on the basis of their similarity to recent aeolian sediments and to well-documented ancient aeolianites. In addition, the basinal facies patterns are similar to the modern-day distribution of aeolian bedforms and lateral facies associations of sand seas. It is probable that the character of Precambrian fluvial sedimentation in humid climates restricted aeolianite deposition to arid climates and thus they serve as useful paleoclimate indicators. The apparent lack of Precambrian aeolianites, especially in Proterozoic rocks, is

attributed to their non-recognition rather than to preservational bias of the rock record. Thus, more examples of Precambrian aeolian deposits should be forthcoming through the application of recently published criteria for recognizing aeolian arenites.

ACKNOWLEDGMENTS

This study is part of a Ph.D. project supported in part by the Natural Sciences and Engineering Research Council of Canada (operating grant A5536 to J.A. Donaldson). Field expenses and expediting services of the Department of Indian Affairs and Northern Development, Yellowknife, Northwest Territories, are also gratefully acknowledged. BP Minerals provided logistic support in an otherwise inaccessible region. F.H.A. Campbell provided useful discussions and H.P. Clemmey provided pertinent portions of his thesis on sedimentary rocks of the Zambian Copperbelt. A.J. Tankard, F.H.A. Campbell and J.A. Donaldson are thanked for their efforts in editing and clarifying the manuscript.

REFERENCES

Allen, J.R.L., 1973. Features of cross-stratified units due to random and other changes in bedforms. Sedimentology, 20: 189—202.

Allen, J.R.L., 1974. Reaction, relaxation, and lag in natural sedimentary systems: general principles, examples, and lessons. Earth Sci. Rev., 10: 263—342.

Bagnold, R.A., 1954. The Physics of Blown Sand and Desert Dunes. Methuen, London, 265 pp.

Baragar, W.R.A., 1977. Volcanism of the stable crust. In: W.R.A. Baragar, L.C. Coleman, and J.M. Hall (Editors), Volcanic Regimes in Canada. Geol. Assoc. Can. Spec. Pap., 16: 377—405.

Baragar, W.R.A. and Donaldson, J.A., 1973. Coppermine and Dismal Lakes map-areas. Geol. Surv. Can. Pap., 71-39, 20 pp.

Breed, C.S. and Grow, T., 1979. Morphology and distribution of dunes in sand seas observed by remote sensing. In: E.D. McKee (Editor), A Study of Global Sand Seas. U.S. Geol. Surv. Prof. Pap., 1052: 253—302.

Breed, C.S., Grolier, M.J. and McCauley, J.F., 1979. Morphology and distribution of common 'sand' dunes on Mars: comparison with the Earth. J. Geophys. Res., 84: 5183—5204.

Brookfield, M.E., 1977. The origin of bounding surfaces in ancient aeolian sandstones. Sedimentology, 24: 303—332.

Brookfield, M.E., 1980. Permian intermontane basin sedimentation in southern Scotland. Sediment. Geol., 27: 167—194.

Bunting, J.A., Brakel, A.T. and Commander, D.P., 1978. Explanatory notes on the Nabberu 1:250,000 Geological Sheet, Western Australia. West. Aust. Geol. Surv., Rec. 1978/12.

Chaudhuri, A., 1977. Influence of aeolian processes on Precambrian sandstones of the Godavari Valley, southern India. Precambrian Res., 4: 339—360.

Clemmey, H., 1976. Aspects of stratigraphy, sedimentology, and ore genesis in the Zambian Copperbelt. Unpublished Ph.D. thesis, Department of Earth Sciences, Leeds University, pp. 60—67.

Coleman, J.M., 1969. Brahmaputra River: channel processes and sedimentation: Sediment. Geol., 3: 129—239.

Collinson, J.D., 1970. Bedforms of the Tana River, Norway. Geografiska Annaler, 52-A: 31—56.
Condie, K.C., 1982. Early and middle Proterozoic supracrustal successions and their tectonic settings: Am. J. Sci., 282: 341—357.
Cooke, R.W. and Warren, A., 1973. Geomorphology of Deserts. Batsford, London, 374 pp.
Cotter, E., 1978. The evolution of fluvial style, with special reference to the central Appalachian Paleozoic. In: A.D. Miall (Editor), Fluvial Sedimentology. Can. Soc. Petrol. Geol., Memoir 5: 361—384.
Donaldson, J.A., 1967. Two Proterozoic clastic sequences: a sedimentological comparison. Proc. Geol. Assoc. Can., 18: 33—54.
Donaldson, J.A. and Ojakangas, R.W., 1977. Orthoquartzite pebbles in Archean conglomerate, North Spirit Lake, northwestern Ontario. Can. J. Earth Sci., 14: 1980—1990.
Folk, R.L., 1968. Bimodal supermature sandstones: product of the desert floor. Report of the Twenty-third Session, International Geological Congress, Proceedings of Section 8, pp. 9—32.
Freeman, W.E. and Visher, G.S., 1975. Stratigraphic analysis of Navajo Sandstone. J. Sediment. Petrol., 45: 651—661.
Fryberger, S.G. and Ahlbrandt, T.S., 1979. Mechanisms for the formation of aeolian sand seas. Z. Geomorphol., 23: 440—460.
Glennie, K.W., 1970. Desert Sedimentary Environments. Developments in Sedimentology, 14. Elsevier, New York, 222 pp.
Gole, C.V. and Chitale, S.V., 1966. Inland delta building activity of the Kosi River. Am. Soc. Civil Eng. Proc., J. Hydraul. Div., 92: 111—126.
Goode, A.D.T. and Hall, W.D.M., 1981. The Middle Proterozoic eastern Bangemall Basin, Western Australia. Precambrian Res., 16: 11—29.
Harms, J.C., Southard, J.B., Spearing, D.R. and Walker, R.G., 1975. Depositional environments as interpreted from primary sedimentary structures and stratification sequences. Soc. Econ. Paleontol. Mineral., Short Course, 2, 161 pp.
Hoffman, P.F., 1980. Conjugate transcurrent faults in north-central Wopmay Orogen (Early Proterozoic) and their dip-slip reactivation during post-orogenic extension, Hepburn Lake map-area, District of Mackenzie. In: Current Research, Part A, Geol. Surv. Can. Pap., 80-1A: 183—185.
Hunter, R.E., 1977. Basic types of stratification in small aeolian dunes. Sedimentology, 24: 361—387.
Hunter, R.E., 1981. Stratification styles in aeolian sandstones: some Pennsylvanian to Jurassic examples from the western interior U.S.A. In: F.G. Etheridge and R.M. Flores (Editors), Recent and Ancient Nonmarine Depositional Environments: Models for Exploration. Soc. Econ. Paleontol. Mineral. Spec. Publ., 31: 315—329.
Hyde, R.S., 1980. Sedimentary facies in the Archean Timiskaming Group and their tectonic implications, Abitibi greenstone belt, northeastern Ontario, Canada. Precambrian Res., 12: 161—192.
Kerans, C., Ross, G.M., Donaldson, J.A. and Geldsetzer, H.J., 1981. Tectonism and depositional history of the Helikian Hornby Bay and Dismal Lakes groups, District of Mackenzie. In: F.H.A. Campbell (Editor), Proterozoic Basins in Canada. Geol. Surv. Can. Pap., 81-10: 157—182.
Kocurek, G., 1981a. Erg reconstruction: the Entrada Sandstone (Jurassic) of northern Utah and Colorado. Palaeogeogr. Palaeoclimatol. Palaeoecol., 36: 125—153.
Kocurek, G., 1981b. Significance of interdune deposits and bounding surfaces in aeolian dune sands. Sedimentology, 28: 753—780.
Kocurek, G. and Dott, R.H., Jr., 1981. Distinctions and uses of stratification types in the interpretation of aeolian sand. J. Sediment. Petrol., 51: 579—595.
Lowe, D.R., 1980. Archean sedimentation. Ann. Rev. Earth Planet. Sci., 8: 145—167.

McKee, E.D., 1966. Structures of dunes at White Sands National Monument, New Mexico (and a comparison with structures of dunes from other selected areas). Sedimentology, 7: 1—70.
McKee, E.D., 1979. Ancient sandstones considered to be aeolian. In: E.D. McKee (Editor), A Study of Global Sand Seas. U. S. Geol. Surv. Prof. Pap., 1052: 187—238.
McKee, E.D. and Tibbits, G.C., 1964. Primary structures of a seif dune and associated deposits in Libya. J. Sediment. Petrol., 34: 5—17.
Meinster, B. and Tickell, S.J., 1976. Precambrian aeolian deposits in the Waterburg Supergroup. S. Afr. Geol. Soc. Trans., 78: 191—199.
Miall, A.D., 1977. A review of the braided-river depositional environment. Earth Sci. Rev., 13: 1—62.
Pettijohn, F.J., Potter, P.E. and Siever, R., 1973. Sand and Sandstone. Springer-Verlag, Berlin, 617 pp.
Picard, M.D., 1977. Stratigraphic analysis of the Navajo Sandstone: a discussion. J. Sediment. Petrol., 47: 475—483.
Raemekers, P., 1981. Hudsonian and Helikian basins of the Athabasca region, northern Saskatchewan. In: F.H.A. Campbell (Editor), Proterozoic Basins in Canada. Geol. Surv. Can. Pap., 81-10: 219—233.
Ross, G.M., 1983. Bigbear erg: a Proterozoic aeolian sand sea in the Hornby Bay Group, Northwest Territories, Canada. In: M.E. Brookfield and T. Ahlbrandt (Editors), Eolian Sediments and Processes. International Assoc. of Sedimentologists Symp. (in press).
Rubin, D.M. and Hunter, R.E., 1982. Climbing of large-scale bedforms in theory and in nature. Sedimentology, 29: 121—138.
Rust, B.R., 1979. Coarse alluvial deposits. In: R.G. Walker (Editor), Facies Models. Geosci. Can. Reprint Series, 1: 9—22.
Schumm, S.A., 1968. Speculation concerning paleohydrologic controls of terrestrial sedimentation. Geol. Soc. Am. Bull., 79: 1573—1588.
Smith, N.D., 1974. Sedimentology and bar formation in the upper Kicking Horse River, a braided outwash stream: Journal of Geology, 81: 205—223.
Smith, N.D. and Minter, W.E.L., 1980. Sedimentological controls of gold and uranium in two Witwatersrand paleoplacers. Econ. Geol., 75: 1—14.
Tankard, A.J., Jackson, M.P.A., Eriksson, K.A., Hobday, D.K., Hunter, D.R. and Minter, W.E.L., 1982. Crustal Evolution of Southern Africa: 3.8 Billion Years of Earth History. Springer-Verlag, New York, 523 pp.
Veizer, J. and Jansen, S.L., 1977. Basement and sediment recycling and continental evolution. J. Geol., 87: 341—370.
Walker, J.C.G., 1982. Climatic factors on the Archean Earth. Palaeogeogr. Palaeoclimatol. Palaeoecol., 40: 1—12.
Warren, A., 1979. Aeolian processes. In: C. Embleton and J. Thornes (Editors), Process in Geomorphology. Edward Arnold, London, pp. 325—351.
Wilson, I.G., 1972a. Universal discontinuities in bedforms produced by the wind. J. Sediment. Petrol., 42: 667—669.
Wilson, I.G., 1972b. Aeolian bedforms; their development and origins. Sedimentology, 19: 173—210.
Windley, B.F., 1977. Timing of continental growth and emergence. Nature, 270: 426—427.

PRECAMBRIAN ATMOSPHERIC OXYGEN AND BANDED IRON FORMATIONS: A DELAYED OCEAN MODEL

KENNETH M. TOWE

Department of Paleobiology, Smithsonian Institution, Washington, DC 20560 (U.S.A.)

ABSTRACT

Towe, K.M., 1983. Precambrian atmospheric oxygen and banded iron formations: a delayed ocean model. Precambrian Res., 20: 161—170.

Evidence and arguments increasingly in favor of free oxygen in the Earth's early atmosphere renew the constraints on the environmental significance of Precambrian banded iron formations. An early moist greenhouse atmosphere with a delay in, and gradual growth of, the world oceans offers a mechanism to provide a geochemically and mechanically segregated source of iron and silica for banded iron formation, while simultaneously 'cannibalizing' evidence for early Archean red beds. The model supports the high rates of weathering necessary to remove initially outgassed CO_2 quickly, favors continuity in early biogenic evolution, provides a mechanism for hydrogen and strontium isotope partitioning, and is consistent with iron oxide facies that are devoid of organic carbon or stromatolites that are not encrusted by iron oxide.

INTRODUCTION

As new evidence continues to accumulate, it is increasingly clear that arguments in support of free oxygen in the Earth's early atmosphere must be given serious consideration. The presence or absence of free oxygen is becoming less the subject of debate. Rather, the levels of such oxygen and its sources of supply are becoming the focus of attention.

The presence of photolytically derived oxygen very early in Earth history, and prior to the advent of oxygenic photosynthesis, requires a reconsideration of the conditions surrounding the origin and early evolution of life. As traditional atmospheric sources of primordial organic matter assume less importance in such scenarios, renewed roles for carbonaceous chondrites (Engel and Nagy, 1982) or comets (Lazcano-Araujo and Oró, 1981), and hydrothermal vents (Corliss et al., 1981) come to the fore. The many experimental successes in prebiotic chemistry that emphasize fluctuating wetting and drying conditions serve to re-emphasize the importance of a biologically effective, UV-protective ozone screen to the origin and early evolution of life (Towe, 1981). The view of the primitive Earth as covered with an

oceanic 'primordial soup' beneath a more-or-less reducing atmosphere free of oxygen for billions of years is less certain than ever before.

INFERENCES AND EVIDENCE FOR FREE OXYGEN

A rock record is lacking for the first 700—800 Ma of Earth history. Thus, with the evidence missing, or yet to be found, the nature of the environment at this time has been conjecture, and conjecture supporting the presence of free oxygen in the atmosphere can be assembled. One such argument related to the origin of life concerns the so-called UV-liquid water dilemma (Towe, 1981), in which peptide bonds formed through prebiotic dehydration reactions faced UV-destruction during evaporative exposure, but under continued subaqueous protection faced spontaneous hydrolysis and curtailment of sustained polypeptide chain elongation. Thus, the environments most favorable for the concentration and continued growth of complex prebiotic molecules (proteins and nucleic acids) would be subjected to UV-destruction in the absence of an effective oxygen/ozone screen. Utilization of visible light to promote later experiments with early biological photoenergy conversions leading to photosynthesis would also have been severely inhibited by a simultaneous UV-flux to DNA-based life forms. In short, the continuity of both prebiotic and early biogenetic evolution would be difficult to maintain.

Astronomical data gathered on the high UV-flux emitted by young stars (Gaustad and Vogel, 1982; Canuto et al., 1982) further emphasizes the importance of the UV problem to the early Earth at this time. Model support for the presence of photolytic free oxygen and ozone in this early atmosphere as a result of an enhanced UV-flux has already been produced (Canuto et al., 1982). Greenhouse atmospheres, dictated by the need to prevent a frozen Earth (e.g., Owen et al., 1979) because of a lower stellar luminosity (Newman and Rood, 1977), are thus capable of generating free oxygen through photodissociation with ultimate loss of hydrogen to space. The levels of such oxygen are still open questions. They should be lower than modern levels yet high enough to oxidize ferrous iron and provide a reasonable ozone screen. The Berkner-Marshall level of $<1\%$ present atmospheric level (PAL) seems reasonable.

Even with the beginning of the rock record, the 3.8 Ga Isua deposits in Greenland, the first actual evidence for free oxygen is found. In addition to clastic (or volcanoclastic) sediments, chemical sediments implying free oxygen in a subaqueous medium are found — the first banded iron formations. Later, bedded gypsum deposits in Australian evaporite sequences that are 3.5 Ga-old indicate the presence of oxidized sulfur in the waters from which they precipitated (Groves et al., 1981). Coeval rocks interpreted as stromatolitic (Lowe, 1980; Walter et al., 1980) imply the presence of life, but do not provide unequivocal evidence of oxygenic photosynthesis. The sedimentological evidence for their intermittent dessication does, however, require some sort of UV-protection and suggests the existence of an ozone screen

(Walter et al., 1980). Either oxygenic photosynthesis evolved very early on, and at least by Isua time, or photodissociation was the source of the early oxygen. Although the source of any prebiotic oxygen must have been atmospheric photolysis, later sources may have been augmented by photosynthesis. Some biochemical arguments against an initial role for photosynthesis have been presented (Towe, 1978; Schwartz and Dayhoff, 1978).

Mineralogic and geochemical data from younger Archean and early Proterozoic rocks add to the evidence. There are Archean pillow basalts with oxidized crusts implying the presence of free oxygen during a period of submarine weathering (Dimroth and Lichtblau, 1978). Archean calcites contain levels of Fe^{2+} and Mn^{2+} in their structures that are lower, by orders of magnitude, than expected had these carbonates been formed in anoxic waters (Veizer, 1978). Archean (Shegelski, 1980; Schau and Henderson, 1983) and early Proterozoic (Button, 1979; Gay and Grandstaff, 1980) weathering profiles in Canadian and South African rocks indicate oxidative conditions during a subaerial weathering process.

Geological evidence for reducing conditions cannot prove the general absence of oxygen in past atmospheres, especially if the O_2-levels were lower, because reducing environments are widespread locally today under a clearly oxygenic atmosphere. Thus, the presence of pyrite and uraninite in modern detrital sediments (Simpson and Bowles, 1977), coupled with the kinetic studies on the behavior of such minerals (Grandstaff, 1976) have markedly lowered the significance of these minerals for the interpretation of Precambrian atmospheres (cf., Clemmey and Badham, 1982).

It may be concluded that inferences for the interval before the earliest rock record (pre-3.8 Ga) combined with evidence from the subsequent rock record indicate that free oxygen was not only present in the early environment (in lower than PAL), but occurred generally in the atmosphere and locally in the hydrosphere. As support for free oxygen grows, the origin and significance of the banded iron formations requires re-examination.

THE BANDED IRON FORMATIONS REVISITED

Central to most arguments regarding early Precambrian atmospheric oxygen are the iron-rich bedded chert deposits known collectively as the banded iron formations. The banded iron formations (BIF) are first and foremost, subaqueous oxidized chemical precipitates. They, therefore, differ substantially from their subaerial oxidized analogues, the clastic red beds. It is this distinction, perhaps more than any other, that has placed the BIF into a position of such importance in the interpretation of Precambrian atmospheres. By themselves, the BIF lose much of this importance simply because they occur in rocks of all ages from the earliest Precambrian to the clearly oxygenic atmospheres of the Phanerozoic (Schultz, 1966; Cloud, 1973). Although their abundance in the Precambrian is significant, it is in conjunction with the temporal distribution of red beds and other terrestrial deposits

that the BIF assume their pivotal role in the interpretation of Precambrian atmospheres. This is because of the source of supply of the oxygen used to oxidize the iron.

If there was free oxygen in the hydrosphere but, as is commonly supposed, none (less than $\sim 10^{-13}$ $_pO_2$) in the atmosphere, then BIF are possible, but red beds or other evidence of terrestrial oxidation are not. An algal—cyanobacterial source of free oxygen localized in the hydrosphere, in proximity to and in balance with the supply of ferrous iron could explain both the BIF and the absence of evidence for terrestrial oxidation. In other words, oxygen produced in the water by photosynthesis must be combined with ferrous iron or sulfide so as not to evade into the atmosphere to permit the formation of red beds. This is the essence of the heuristic proposal outlined by Cloud (1973) to explain the major Precambrian BIFs. On the other hand, if there was free oxygen in the atmosphere (regardless of its source and with due allowance for kinetics) then both subaerial and subaqueous oxidations are possible. Therefore, as newer geological evidence continues to emerge showing that terrestrial oxidation has taken place, both prior to and synchronous with the deposition of BIF, the importance of these banded chemical precipitates to the qualitative composition of the atmosphere is devalued. When this newer evidence is added to the other arguments in favor of atmospheric oxygen, as above, the idea of a direct relationship between photosynthetic oxygen and precipitated iron requires reassessment.

A major advance in our understanding of banded iron formations was the quantitative assessment of possible iron sources made by Holland (1973). Using the Hamersley Basin of Australia as a model, he was able to demonstrate that neither subaerial weathering nor volcanic emanations were likely to have been the immediate sources of soluble iron. This left the oceans, and Holland (1973) proposed that the upwelling of bottom waters could have provided the necessary quantities of dissolved iron to explain this deposit, and similar Lake Superior-type accumulations where clastic detritus is notably sparse.

If the direct supply of soluble iron for the major Proterozoic BIF was necessarily the deeper ocean bottom waters then there is an important corollary to the Holland assessment: free oxygen need not be absent from the atmosphere in order to maintain the anoxic surface waters required for the free movement of weathered ferrous iron to the basin. What is required is that the deeper basins remain stagnant and anoxygenic for reasonable lengths of time, a viewpoint expressed by many (Hough, 1958; Govett, 1966; Drever, 1974; Degens and Stoffers, 1976; Veizer, 1983; and others).

Acceptance of the Holland assessment that ocean bottom waters are the only plausible immediate source for the iron in the Superior-type BIF also raises the question of what the indirect source of the iron was. In other words, what were the massive and continuous oceanic sources of supply for iron? Can a choice be made between the two available alternatives: volcanic emanations and chemical weathering? Both were certainly involved, but vol-

canic emanations appear to be insufficient unless more evidence for intensive submarine volcanism at the beginning of the Proterozoic is forthcoming. Holland's (1973) objections to weathering apply very well to local conditions that surround a basin such as the Hamersley, but they do not negate a world-wide weathering source. With the necessity for an anoxic atmosphere softened by the Holland assessment, the weathering process could have taken place under oxygenic conditions.

A DELAYED OCEAN MODEL

The delayed ocean model begins with the environmental conditions hypothesized by Towe (1981) and it is an extension of this speculative proposal. Like other models, it is of course tentative, and offered in the spirit of focussing attention to the problem.

The early Archean environment (pre-3.8 Ga) consisted of an Earth surrounded by a moist greenhouse atmosphere (principally H_2O and CO_2). Derived from an initial, but incomplete outgassing, it was an atmosphere disturbed and augmented by late-stage bombardment impacts into limited liquid water reservoirs. Beneath this wet atmosphere lay a generally mafic lithospheric crust with primarily shallow bodies of water, many near hydrothermal vents. Differentiated 'continental' masses were small, few in number, and of generally low relief. No oceans as such existed at first and the area of land ('oceanic' crust) exposed to the early atmosphere exceeded that covered by liquid water. Terrestrial silicate weathering could therefore proceed rapidly to initiate the necessary removal of CO_2. The moist atmosphere provided the necessary conditions for the photolytic production of oxygen and development of the important UV-protective ozone screen necessary for DNA-based life to begin at the Earth's surface. The abundant land areas provided the important hydration—dehydration locales necessary for the formation and continued growth and experimentation with peptide bonds in protein evolution. The mafic ('oceanic') crust exposed to this early moist atmosphere was subjected to extensive weathering — a mafic laterization. A clay and oxide-rich weathering profile (perhaps analogous to Martian soils?) began to establish itself. Surficial oxidation of iron (and sulfur) served to protect early experimentation with life-forming processes and the $_pO_2$ in the limited hydrosphere was, thus, kept low. Indeed, although the atmosphere was on the oxidizing side of neutral, the limited hydrosphere was more likely to have been generally reducing, and especially so near hydrothermal vents.

The majority of early sedimentary environments were likely shallow water. The general absence of continental relief would preclude major areas of coarse clastics. Such sediments would be local and related at first to impact-generated crater relief and later to volcaniclastic activity, as in the Isua rocks and in Algoma-type BIF. With the subsequent reduction of atmospheric CO_2, first through silicate dissolution during weathering and then through the deposition of carbonates, and with a general tendency for tec-

tonic cooling, more atmospheric water condensed and the oceans began to grow. Continued outgassing (post 3.8 Ga) coupled with increased continental growth and basin development through isostatic readjustment, resulted in a continuous transfer of the initially oxidized weathering products to increasingly deeper basins. Aluminum and trace elements are geochemically partitioned during weathering and erosion. Large amounts of iron and silica would move into the growing oceans where reduction of the iron through interaction with organic matter placed it into solution.

As oceanic circulation patterns developed the Superior-type BIF would tend to replace the Algoma-type. Dissolved iron (and the silica) was brought into the shallow surface waters to interact with atmospheric oxygen causing its precipitation as hydrous ferric oxide. The overall sedimentary environment was one of worldwide transgression because the oceans were steadily growing in size — an overstep leading to the process known as marine replacement (cf. Dunbar and Rodgers, 1957, p. 142). By this process the earlier Precambrian red beds were gradually 'cannibalized' and mostly eliminated as their iron was transferred by erosion to oceanic repositories. With this gradual rise in eustatic sea level, the exposed areas of increasingly larger continents remained generally low in relief and, thus, consistent with the worldwide paucity of clastic sediments so characteristic of many later banded iron formations. By ~ 2.0 Ga-ago the cycle would have been completed and the major episode of banded iron formation come to an end; subsequent BIFs would not be precluded, but would never again be as abundant.

COMPARISONS WITH OTHER MODELS

Most current models begin with an immediately outgassed and condensed ocean system equilibrated with CO_2. With few differentiated continents, the early condensed oceans would cover the land surface to a considerable depth (e.g., Hargraves, 1976). Initially, the outgassed carbon dioxide would have to be dissolved in these oceans at very high concentrations in order to provide the high atmospheric partial pressures (1000 PAL) considered necessary to offset the reduced solar constant and prevent a frozen Earth (Owen et al., 1979).

In the delayed ocean model, a greenhouse is provided by water and CO_2 with the potential for runaway mediated by the more rapid removal of both water and CO_2 in surface weathering reactions and in photolysis. The bulk of the photolytic oxygen is used for early oxidation of weathered iron and sulfur rather than primarily to oxidize atmospheric components such as CH_4 and NH_3 (e.g., Hart, 1978). With little land area exposed above sea level, the dominant geochemical reactions in all instant ocean models would necessarily have been the submarine weathering of mafic silicates. The rates should have been low because submarine reactions are limited by the rate at which fresh rock is exposed at the ocean bottom. Higher rates of silicate weathering remove CO_2 more rapidly where warm temperatures combine

with high runoff (Holland, 1978; Walker et al., 1981). Thus, the conditions expected with a moist greenhouse—delayed ocean model would provide greater potential for runoff at warmer temperatures. Exposed land areas ('oceanic' crust) would have been the sites of very active silicate weathering to provide the abundant clay minerals considered useful for hydration—dehydration experiments in prebiotic organic polymerization reactions.

Although prebiotic reactions at hydrothermal vents (Corliss et al., 1981) are not precluded by either model, it should be noted that for maintaining continuity in prebiotic polymerization chemistry, the addition of numerous dehydration sites to submarine hot spring sources gives the delayed ocean model an advantage. Alone, hot springs can produce one cycle polymerizations, but it seems difficult to maintain continuity for evolutionary development of initial polypeptides in a flowing gradient where the products formed at one temperature are moved to a lower temperature locale (impeding further peptide bond formation).

In comparing models, the hydrogen isotope data are important because they indicate differences between the deuterium composition of mantle water and mean ocean water over geologic time. The argument is as follows: ocean water is isotopically enriched in deuterium (heavier) with respect to mantle water. This implies a partitioning of juvenile (original) water at some time in the distant past. The deuterium composition of juvenile water was fixed by its chondritic origin at planetary formation (Anders and Owen, 1977). Therefore, either ocean water became heavier or mantle water became lighter with respect to original water. As there is no plausible mechanism for the preferential loss of deuterium or enrichment of protium in mantle rocks, it is the oceans that seem to have changed. The most likely mechanism for this fractionation is the preferential gravitational escape of protium following the photodissociation of water vapor in the upper atmosphere. Very limited geological evidence exists to support this (Fig. 10, Knauth and Epstein, 1976).

In the moist atmosphere—delayed ocean model advocated here, the mantle water—ocean water hydrogen isotope reservoirs would have diverged early on and much of the oxygen produced by the photodissociation was used in the weathering of the early mafic crustal materials exposed on land. In other models, the process of photodissociation is considered to be very limited, and what oxygen does form is rapidly recombined with hydrogen to keep the atmosphere anoxic. Little hydrogen escapes; isotopic partitioning between ocean and mantle waters is limited.

Mantle buffering models (e.g., Veizer et al., 1982) require that massive amounts of ocean water be pumped back into the basaltic crust. This would rapidly mix the two reservoirs and thereby also inhibit hydrogen isotopic partitioning between them. On the other hand, the $^{87}Sr/^{86}Sr$ anomaly discussed by Veizer et al. (1982) is equally consistent with a delayed ocean model that specifically allows for the 'continental' weathering of mafic 'oceanic' crust, thereby giving the strontium ratios in Archean carbonates their mantle-like appearance.

Finally, with respect to the Superior-type banded iron formations, two comparisons are worth mentioning:

(1) BIF oxide facies are well-known to be remarkably free of organic carbon. Anoxic atmosphere models require that hydrospheric oxygen produced locally by photosynthesis in the basin waters be used to oxidize iron and, thus, unavailable for oxidation of the algal carbon (Van Valen, 1971; Towe, 1978), which must be accounted for somewhere. For example, in the Hamersley Basin BIF, 6000 billion tons (6×10^{18} gm) of photosynthetic carbon should have been produced to account for the 100,000 billion tons (10^{20} gm) of iron estimated to exist there. The idea (Cloud, 1973) that the magnetite in oxide facies could be diagenetically derived from the reduction of six moles of hematite for every mole of organic carbon is acceptable. However, if the algal communities living in these quiet waters died back following episodes of photosynthetic precipitation of hydrous iron oxides, then most of their organic remains should appear in the iron-poor cherty bands alternating with the iron-rich bands. If so, the organic carbon was not in immediate proximity to the bulk of the hematite it was supposed to have reduced. The use of atmospheric oxygen (from any source) is more readily reconcilable with oxide facies that are so deficient in organic carbon and yet considered deposited in very quiet waters where most of the dead phytoplankton would be expected to have accumulated.

(2) Superior-type BIF are generally clastic-free precipitates notably depleted in aluminum and titanium (Lepp, 1966). A submarine volcanic source of iron and silica would allow for mechanical segregation of clastics, but would make geochemical segregation difficult. An indirect weathering source for iron and silica to deepening ocean basins allows for both. Thus, clastic-free upwelling water, reduced in its aluminum and trace element content, permits the precipitation of hydrous iron oxides on contact with surface atmospheric oxygen in shallow waters, while it also permits the formation of pure Fe-silicates rather than aluminous clay minerals (Govett, 1966; Klein and Bricker, 1977) in the oxygen-poor offshore silicate facies. Shoreward continental platform carbonates need not be iron-rich (Larue, 1981). Stromatolites, if they were formed by oxygenic photosynthesizers, need not be draped with iron oxides, and coeval red beds are permitted, not prohibited. Reduced facies, as they are today, can be expected.

ACKNOWLEDGMENT

I thank R.F. Fudali and anonymous referees for reading early drafts of the manuscript and offering useful suggestions, and I thank numerous colleagues for providing references and valuable discussion.

REFERENCES

Anders, E. and Owen, T., 1977. Mars and Earth: origin and abundance of volatiles. Science, 198: 453–465.

Button, A., 1979. Early Proterozoic weathering profile on the 2200 my old Hekpoort Basalt, Pretoria Group, South Africa: preliminary results. Univ. Witwatersrand Econ. Geol. Res. Unit Inform. Circ. 133.

Canuto, V.M., Levine, J.S., Augustsson, T.R. and Imhoff, C.L., 1982. Ultraviolet radiation from the young Sun and levels of oxygen and ozone in prebiological paleoatmosphere. Nature (London), 296: 816—820.

Clemmey, H. and Badham, N., 1982. Oxygen in the Precambrian atmosphere: an evaluation of the geological evidence. Geology, 10: 141—146.

Cloud, P., 1973. Paleoecological significance of the banded iron-formation. Econ. Geol., 68: 1135—1143.

Corliss, J.B., Baross, J.A. and Hoffman, S.E., 1981. An hypothesis concerning the relationship between submarine hot springs and the origin of life on Earth. Oceanologica Acta, 26: 59—69.

Degens, E.T. and Stoffers, P., 1976. Stratified waters as a key to the past. Nature (London), 263: 22—27.

Dimroth, E. and Lichtblau, A.P., 1978. Oxygen in the Archean ocean: comparison of ferric oxide crusts on Archean and Cainozoic pillow basalts. Neues Jahrb. Mineral., Abh., 133: 1—22.

Drever, J.I., 1974. Geochemical model for the origin of Precambrian banded iron formations. Geol. Soc. Am. Bull., 85: 1099—1106.

Dunbar, C.O. and Rodgers, J., 1957. Principles of Stratigraphy. Wiley, New York, NY, 356 pp.

Engel, M.H. and Nagy, B., 1982. Distribution and enantiometric composition of amino acids in the Murchison meteorite. Nature (London), 296: 837—840.

Gaustad, J.E. and Vogel, S.N., 1982. High energy solar radiation and the origin of life. Origins Life, 12: 3—8.

Gay, A.L. and Grandstaff, D.E., 1980. Chemistry and mineralogy of Precambrian paleosols at Elliot Lake, Ontario, Canada. Precambrian Res., 12: 349—373.

Govett, G.J.S., 1966. Origin of banded iron formations. Geol. Soc. Am. Bull., 77: 1191—1212.

Grandstaff, D.E., 1976. A kinetic study of the dissolution of uraninite. Econ. Geol., 71: 1493—1506.

Groves, D.I., Dunlop, J.S.R. and Buick, R., 1981. An early habitat of life. Sci. Am., 245: 64—73.

Hargraves, R.B., 1976. Precambrian geologic history. Science, 193: 363—371.

Hart, M.H., 1978. The evolution of the atmosphere of the Earth. Icarus, 33: 23—39.

Holland, H.D., 1973. The oceans: a possible source of iron in iron-formations. Econ. Geol., 68: 1169—1172.

Holland, H.D., 1978. The Chemistry of the Atmosphere and Oceans. Wiley, New York, NY, 351 pp.

Hough, J.L., 1958. Fresh-water environment of deposition of Precambrian banded iron formations. J. Sediment. Petrol., 28: 414—430.

Klein, C. and Bricker, O.P., 1977. Some aspects of the sedimentary and diagenetic environment of Proterozoic banded iron-formation. Econ. Geol., 72: 1457—1470.

Knauth, L.P. and Epstein, S., 1976. Hydrogen and oxygen isotope ratios in nodular and bedded cherts. Geochim. Cosmochim. Acta, 40: 1095—1108.

Larue, D.K., 1981. The early Proterozoic pre-iron-formation Menominee Group siliciclastic sediments of the southern Lake Superior region: evidence for sedimentation in platform and basinal settings. J. Sediment. Petrol., 51: 397—414.

Lazcano-Araujo, A. and Oró, J., 1981. Cometary material and the origins of life on Earth. In: C. Ponnamperuma (Editor), Comets and the Origin of Life. Dordrecht, Reidel, pp. 191.

Lepp, H., 1966. Chemical composition of the Biwabik iron formation, Minnesota. Econ. Geol., 61: 243—250.

Lowe, D.R., 1980. Stromatolites 3,400-Myr old from the Archean of Western Australia. Nature (London), 284: 441—443.
Newman, M.J. and Rood, R.T., 1977. Implications of solar evolution for the Earth's atmosphere. Science, 198: 1035—1037.
Owen, T., Cess, R.D. and Ramanathan, V., 1979. Enhanced CO_2 greenhouse to compensate for reduced solar luminosity on early Earth. Nature (London), 277: 640—641.
Schau, M. and Henderson, J.B., 1983. Archean chemical weathering at three localities on the Canadian Shield. Precambrian Res., 20: 189—224.
Schultz, R.W., 1966. Lower Carboniferous cherty ironstones at Tynagh, Ireland. Econ. Geol., 61: 311—342.
Schwartz, R.M. and Dayhoff, M.O., 1978. Origins of prokaryotes, eukaryotes, mitochondria and chloroplasts. Science, 199: 395—403.
Shegelski, R.J., 1980. Archean cratonization, emergence and red bed development, Lake Shebandowan area, Canada. Precambrian Res., 12: 331—347.
Simpson, P.R. and Bowles, J.F.W., 1977. Uranium mineralization of the Witwatersrand and Dominion Reef systems. Philos. Trans. R. Soc. London, Ser. A, 286: 527—548.
Towe, K.M., 1978. Early Precambrian oxygen: a case against photosynthesis. Nature (London), 274: 657—661.
Towe, K.M., 1981. Environmental conditions surrounding the origin and early Archean evolution of life: a hypothesis. Precambrian Res., 16: 1—10.
Van Valen, L., 1971. The history and stability of atmospheric oxygen. Science, 171: 439—443.
Veizer, J., 1978. Secular variations in the composition of sedimentary carbonate rocks, II. Fe, Mn, Ca, Mg, Si and minor constituents. Precambrian Res., 6: 381—413.
Veizer, J., 1983. Geologic evolution of the Archean—Early Proterozoic Earth. In: J.W. Schopf (Editor), Origin and Evolution of Earth's Earliest Biosphere: An Interdisciplinary Study. Chapter 10, Princeton University Press, Princeton, NJ.
Veizer, J., Compston, W., Hoefs, J. and Nielsen, H., 1982. Mantle buffering of the early oceans. Naturwissenschaften, 69: 173—180.
Walker, J.C.G., Hays, P.B. and Kasting, J.F., 1981. A negative feedback mechanism for the long-term stabilization of Earth's surface temperature. J. Geophys. Res., 86: 9776—9782.
Walter, M.R., Buick, R. and Dunlop, J.S.R., 1980. Stromatolites 3400—3500 My old from the North Pole area, Western Australia. Nature (London), 284: 443—445.

TECTONIC SYSTEMS AND THE DEPOSITION OF IRON-FORMATION

GORDON A. GROSS

Geological Survey of Canada, 601 Booth St., Ottawa K1A 0E8 (Canada)

ABSTRACT

Gross, G.A., 1983. Tectonic systems and the deposition of iron-formation. Precambrian Res., 20: 171—187.

The iron-formation group of chemically precipitated cherty iron-rich sediments ranges in age from Early Precambrian to Recent and is composed of a variety of lithological facies. Iron-formations are classified as Lake Superior and Algoma types to emphasize the contrasting conditions in the spectrum of sedimentary—tectonic environments in which they formed. Thick stratigraphic units of Lake Superior type iron-formation, which form the most extensive iron ranges of the world, are part of sedimentary—tectonic systems that developed along the margins of cratons or continental platforms and were deposited over extended periods of time under relatively stable tectonic conditions. The Algoma type iron-formations were deposited with volcanic rocks and greywacke in various tectonic—volcanic systems, formed under more dynamic tectonic conditions, but are otherwise comparable to present day spreading ridges on the ocean floor. The thick sequences of Lake Superior type iron-formation deposited between 2.7 and 2.0 Ga form part of major sedimentary—tectonic systems that extended along the margins of continents. Direct biogenic factors and the composition of the atmosphere probably had only limited influence on the precipitation of these chemical sediments.

INTRODUCTION

Iron-formations are composed of many different lithological facies and their deposition was closely related to specific types of tectonic systems. Although deposition of these chemically precipitated rocks was not restricted to any special period of time, the thicker stratigraphic sequences of iron-formation are more abundant in middle Precambrian than in other periods (Cloud, 1973).

Banded siliceous ferruginous sediments called iron-formation, as distinct from the oolitic chamosite—siderite—clay-ironstones, have been the subject of much research and investigation throughout the world during the past few decades. Important advances have been made in understanding their sedimentary, stratigraphic and tectonic context throughout geological time. They are now generally recognized as a major group of chemically precipitated metalliferous sediments of special metallogenetic significance, rather than localized phenomena important only as sources of iron ore. New data

and the re-assessment of previous data enable concepts on the nature and origin of the iron-formation sediments, the environments in which they form, genetic concepts regarding the sources of iron and silica, tectonic control of their distribution throughout the geological record and their metallogenic significance, to be revised.

LITHOLOGY OF IRON-FORMATION

Iron-formation was defined by James (1954) as a chemical sedimentary rock, typically thin banded and/or finely laminated, containing at least 15% iron of sedimentary origin and commonly, but not necessarily, containing layers of chert. Iron-formation, by this definition, has been generally accepted and widely used as a generic lithological term analogous to limestone (Gross, 1965; Brandt et al., 1972). Iron-formation and the genetically related chemical sediments included in this broadly defined lithological group are distinguished from the clay-ironstone ferruginous sediments by the presence of banded and layered chert and quartz, and a siliceous matrix for the iron minerals, by a lower alumina and titania content, and by characteristic primary sedimentary features (Gross, 1965, 1972).

A variety of lithological types with diversified physical and chemical features are found in the iron-formation group of chemical sediments. Recognition of the principal oxide, silicate, carbonate and sulphide facies by James (1954) was an important step in appreciating genetic relationships between different lithological facies of iron-formation. Distinctive textures, primary sedimentary features, mineralogy, minor element content and the associated rocks indicate the wide range of environmental conditions in which iron-formations were deposited (Gross, 1965, 1968, 1972, 1973, 1980). Thinly laminated quartz-magnetite facies of iron-formation ubiquitously distributed in Precambrian volcanic and sedimentary rock sequences are probably the most commonly recognized, but many different lithological varieties of oxide facies are known. Commonly, one lithological facies is predominant in a single stratigraphic unit, but the association of different facies of iron-formation, primary sedimentary features, and variations in the composition and character of the banding indicate dynamic changes in physical and chemical conditions during precipitation and diagenesis of these siliceous iron-rich sediments. Understanding of the origin and geological significance of the iron-formations requires study of large and small stratigraphic units, their distribution and depositional environments as revealed throughout the geological record, as well as detailed description of the petrography, sedimentary features and tectonic setting of individual occurrences.

SEDIMENTARY ENVIRONMENTS FOR IRON-FORMATION

Iron-formations of the Lake Superior region of the United States were the first to be mined on a large scale for iron ore and to have their geological

setting described in detail. Iron-formations in other parts of the world were compared to the Lake Superior examples and genetic concepts were developed with reference to the sedimentary basins in this classical area. Different geological settings for the iron-formations in the Canadian Shield were referred to in the past as Lake Superior, Keewatin, Temiscaming or Archean types depending on the age of associated rocks. A classification of the iron-formations as Lake Superior and Algoma types was introduced (Gross, 1965) to emphasize differences in the kinds of associated rock in the depositional environments and geological settings for the various occurrences of iron-formation, and to use terms that did not have a time connotation.

The Lake Superior type iron-formations were deposited near shore on continental shelves and are associated with dolomite, quartzite, black shale and minor amounts of tuff or other volcanic rocks. The Algoma type iron-formations are associated with shale, greywacke, turbidite sedimentary beds and volcanic rocks, and formed at or relatively close to volcanic centres. Oxide, silicate, carbonate or sulphide facies are common constituents in both of these major groups of iron-formation and reflect the different environmental conditions under which they formed.

Classification of the iron-formations as Lake Superior or Algoma type has emphasized the contrast in sedimentary environments which range from those in neritic shelf basins to those near volcanic centres in eugeosynclinal basins. These types represent reference points in the broad spectrum of environmental conditions in which iron-formations were deposited. Iron-formations interbedded with dolomite, quartzite, shales and volcanic rocks suggest deposition on continental shelves close to craton margins, and others associated with greywacke sediments and volcanic rocks suggest deposition on deeper parts of the continental slopes closer to volcanic centres. Sedimentary environments for the deposition of iron-formation extended through a broad spectrum from neritic basins to the deeper parts of the continental shelves, to tectonic—volcanic ridges offshore, and to deeper ocean basins (Fig. 1; see Gross, 1980).

The Snake River iron-formation in the Rapitan Group in the Mackenzie Mountains in Canada and the iron-formation in the Jacadigo Series in Brazil and Bolivia (Van N. Dorr, 1973) appear to have formed under different conditions than either the Algoma or Lake Superior types of iron-formation. A thick irregularly banded hematite iron-formation in the Yukon Territory of Canada, more than 100 m thick, and similar iron-formations in the Jacadigo Series in Brazil and Bolivia, up to 300 m thick, are associated with sandstone, siltstone and coarse pebble and boulder conglomerates of late Precambrian or early Paleozoic age. Deposition of the Snake River iron-formation in the Yukon appears to have taken place in a graben or in a fault scarp basin along the margin of a continent or craton (Gross, 1973; Eisbacher, 1978) and the Jacadigo Series was probably deposited under similar basin conditions. The metalliferous sediments being deposited by hydrothermal springs along faults in the deep basins of the rift system in the Red Sea graben

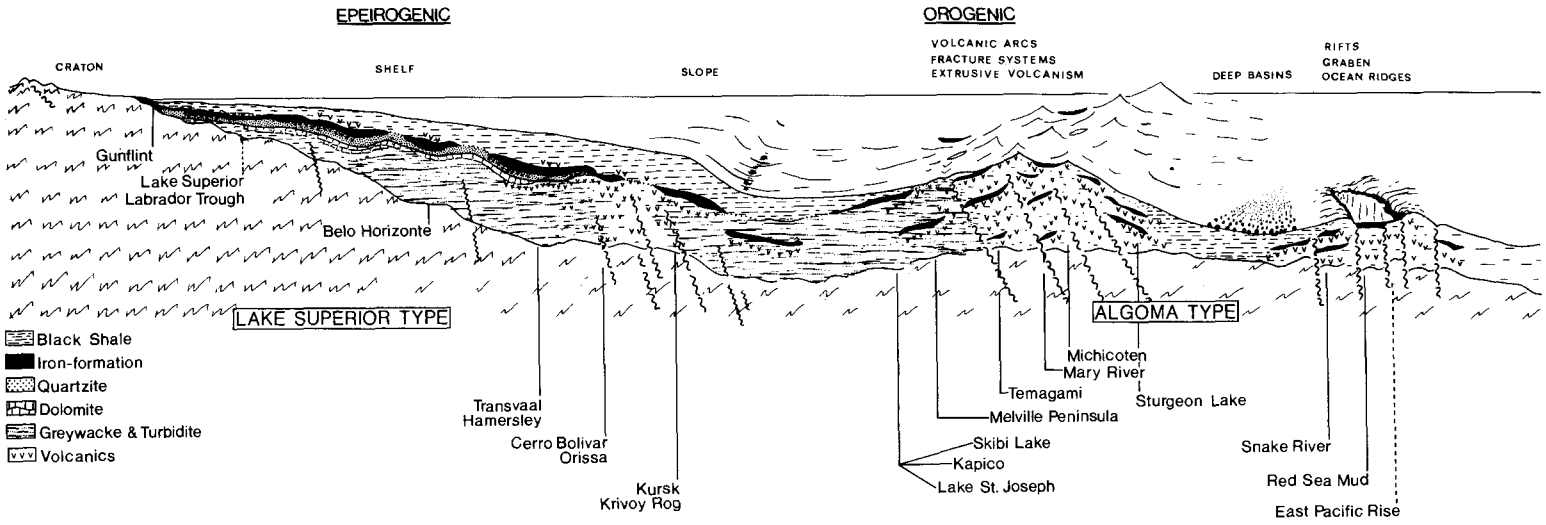

TECTONIC ENVIRONMENTS FOR DEPOSITION OF IRON-FORMATION

Fig. 1. Tectonic environments for deposition of iron-formation (from Gross, 1980).

(Bischoff, 1969; Weber-Diefenbach, 1977), are considered by the writer to be progenitors of siliceous iron-formation; the composition and banding is directly comparable to many facies of Algoma-type iron-formation.

Different environments for the deposition of iron-formation are illustrated in Fig. 1. Lake Superior type iron-formations with granular and oolitic textures that were deposited in relatively shallow water on continental shelves near the craton shoreline are depicted on the left of the diagram and include the Gunflint (Goodwin, 1956), and other iron-formations of the Lake Superior region, those in the Labrador Trough and other basins of the Circum-Ungava belt and the Caue Itabirite of Brazil. Depositional conditions for the iron-formation in the Transvaal Supergroup of South Africa (Beukes, 1973) probably fluctuated from turbulent shallow water environments, in which granular textures formed, to quieter environments that existed down slope on the shelf where microbanding and thin laminations developed in thick sections of iron-formation. Microbanding in the iron-formations and the prominent association of greywackes, pyroclastics and pillow lavas in the Hamersley Basin suggest deposition on deeper parts of the continental shelf where stable basin conditions permitted uniform development of microbanding over a large part of the basin (Trendall, 1973; Trendall and Blockley, 1970).

Sequences of iron-formation on the Russian platform, with total thicknesses of 500—1300 m, extend intermittently from the Azov Sea through Krivoy Rog, Kursk and northward into Karelia. They are associated with quartzite, dolomite, limestone, carbonaceous schist, chlorite—amphibole schist, phyllite, tuff and mafic and ultramafic lavas. The associated rocks, and the predominance of thin layered and microbanded oxide facies iron-formation, indicate deposition in miogeosynclinal conditions in the west and eugeosynclinal conditions in the east (Alexandrov, 1973; Gross, 1967b).

Many iron-formations of considerable thickness and lateral extent, composed mainly of banded quartz—magnetite—hematite or siderite facies, are widely distributed in the Precambrian Shield areas in Canada, in the Baltic Shield, in South America, West Africa, India and China. Metasedimentary and metavolcanic rocks associated with these iron-formations suggest that they may have been deposited offshore on the edge of continental slopes under conditions similar to those in the Kursk—Krivoy Rog geosyncline.

Algoma type iron-formations and their progenitors, which form along fracture systems in volcanic belts, range in age from early Precambrian to the modern metalliferous sediments being deposited along spreading ridges on the ocean floors. They are associated with greywackes, turbidites, fine grained clastic sediments and volcanic rocks ranging in composition from rhyolites to andesites and ultramafics. Stratigraphic units of Algoma type iron-formation are commonly thinner and of local extent compared to the iron-formations deposited on the continental shelves. Occurrences formed at or near volcanic vents and extrusive centres commonly consist of a heterogeneous assemblage of lithological facies with sulphide and carbonate facies

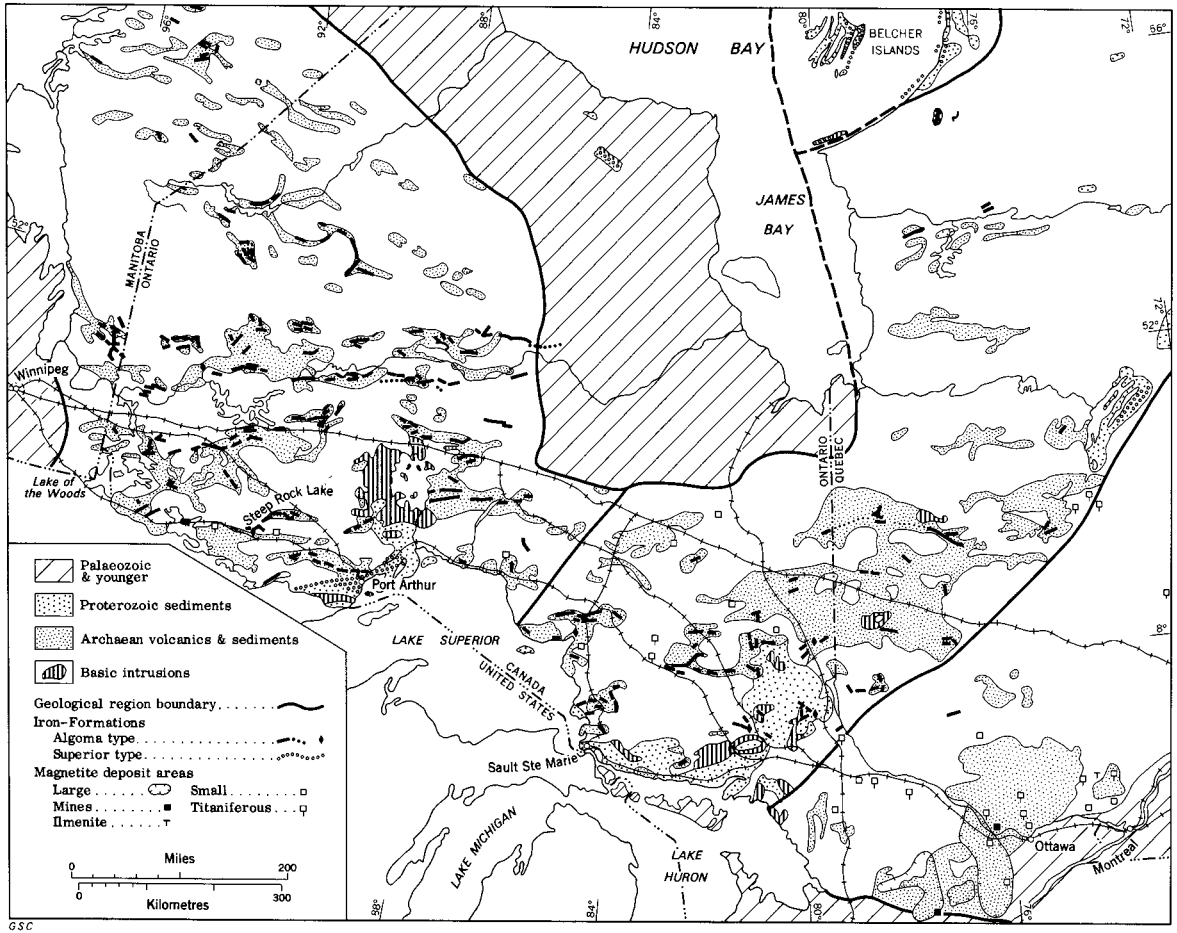

Fig. 2. Distribution of iron-formation in the southern part of the Ungava—Superior craton in Canada.

being most abundant in the vent areas, and oxide facies forming thicker and more extensive units in the greywacke sediments distal from the extrusive centres (Goodwin, 1973; Gross, 1965).

Algoma type iron-formations may have formed at any stage in the development of a volcanic belt starting with deposition around hydrothermal effusive centres, and extending into local basins and depressions amid the lava flows and sedimentary fan complexes. Iron-formations in the Precambrian Shield in Canada (Fig. 2) in the Michipicoten area and at Sturgeon Lake are predominantly carbonate—sulphide facies and formed close to volcanic centres (Goodwin, 1962); those in the Mary River and Timagami areas, and in the Melville Peninsula have less volcanic material associated with them and formed on the flanks of a volcanic belt. Other iron-formations, such as those at Skibi Lake, Bruce Lake and in the Lake St. Joseph area, are mainly associated with greywacke—turbidite rocks and are believed to have formed some distance from the main centres of extrusive volcanism (Goodwin, 1973). Iron and silica in these distal occurrences may have been derived from hydrothermal effusive activity located on fracture systems on the flanks of the main volcanic belt. The distal sediment-hosted iron-formations may have formed on either side of a volcanic belt in basins marginal to a craton slope or on the seaward side. Many sections of thinly laminated or microbanded oxide facies iron-formation are more than 100 m thick and of considerable lateral extent. Iron-formations in the Lake St. Joseph belt are comparable in size (more than 100 m thick), and iron and silica content to lenses of iron-formation deposited in separate basins on the continental shelves (Meyn and Palonen, 1980). The thick accumulations of iron-formation deposited on the continental shelves and platform margins of the Ungava craton are for the most part composites made up of lenticular and sheet-like stratigraphic units that were deposited in a succession of smaller inter-connected linear basins.

TECTONIC SYSTEMS AND THE DEPOSITION OF IRON-FORMATION

The thick stratigraphic units of Lake Superior type iron-formation that form most of the major iron ranges of the world were directly related to tectonic systems located along the margins of Precambrian cratons or continents. Iron-formations were precipitated over various kinds of clastic and carbonate sediments on the continental shelves and slopes, and their deposition coincided with volcanic activity in offshore linear belts that were parallel to the continental margins. These offshore tectonic belts were marked by extensive volcanic activity, deepening of the offshore linear basins or troughs, and the extrusion and intrusion of mafic and ultramafic rocks, usually toward the close of the period of deposition in the basins. Although other sources have been proposed (Holland, 1973), I believe that the iron and silica deposited in abundance in the iron-formation is derived from hydrothermal effusive activity associated with fractures and deep seated faults on the flanks of tectonic ridges.

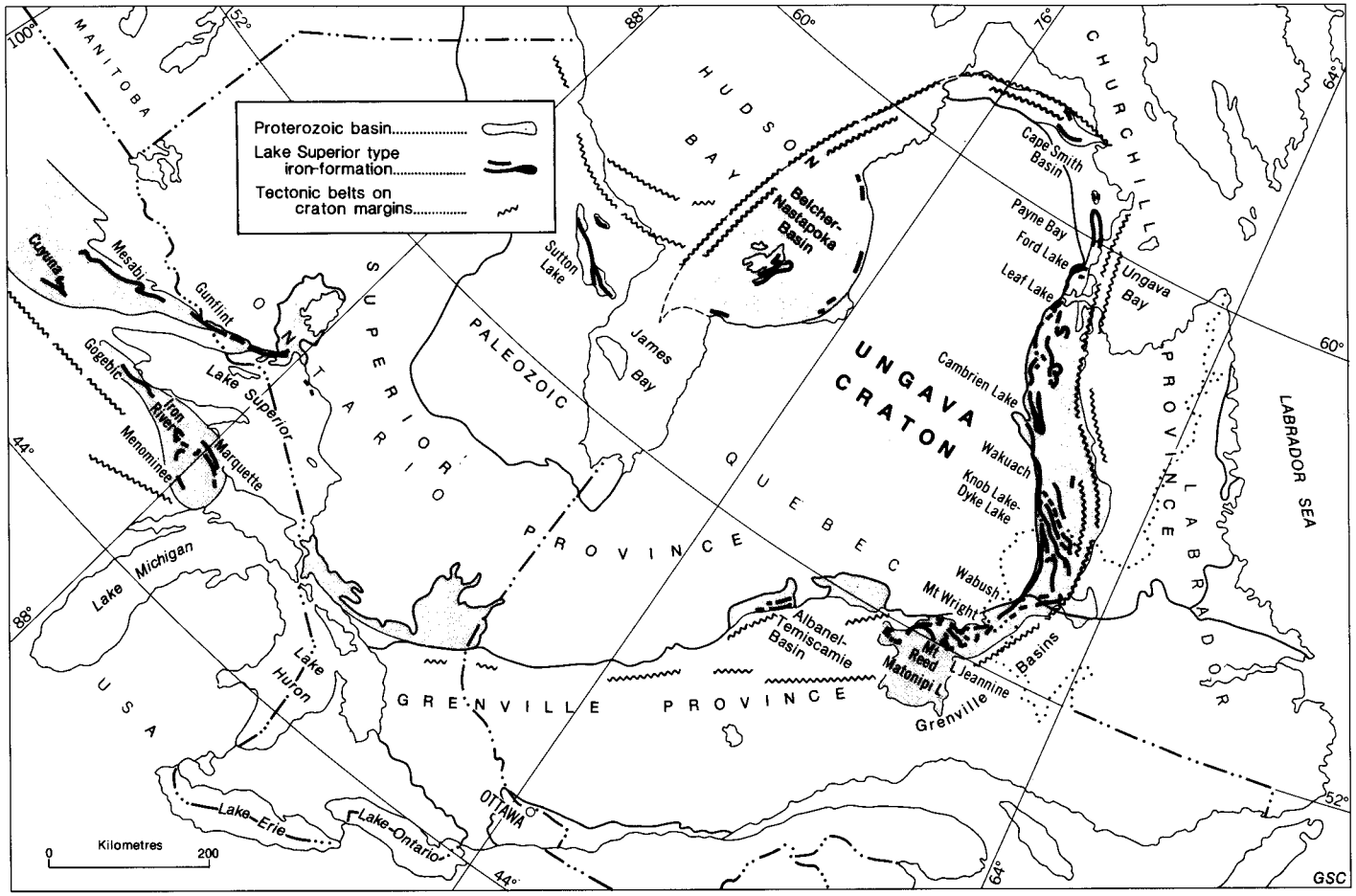

Fig. 3. Distribution of iron-formation in sedimentary—tectonic basins marginal to the Ungava—Superior craton.

The Ungava—Superior craton was surrounded by inter-connected linear basins in which shale, siltstone, dolomite, quartzite, carbonaceous shale, iron-formation, tuff, lava, greywacke and turbidite were deposited in neritic to miogeosynclinal environments on the craton shelf (Fig. 3). Iron-formations of the Lake Superior area are believed to have been deposited on the southwestern edge of this craton, and other iron-formations in northern Manitoba may have been deposited on its northwestern margin. The sedimentary record in the Labrador—Quebec geosyncline and in the Belcher—Nastapoka basin shows a transgression from shallow water depositional environments on the craton margins to deeper water environments, and an increase of volcanic material in the section offshore from the craton. Rocks characteristic of deeper water parts of this transitional series, including mafic and ultramafic extrusive and intrusive rocks, are preserved in the Cape Smith belt on the north margin of the Ungava craton, and the iron-formation and associated rocks along the southeastern margin indicate deposition in a shelf environment. Most rocks in the southeast are too highly metamorphosed for volcanic material to be identified, except for the tuffaceous shale in the Temiscamie basin.

Typical sedimentary—tectonic features on the craton margins are well exposed in the Labrador—Quebec geosyncline (Fig. 4) and have been described in some detail previously (Gross, 1968; Dimroth et al., 1970; Zajac, 1974; Baragar and Scoates, 1981; Gross and Zajac, 1983). The following features are of special significance in this context. The iron-formation is associated with ordinary types of shelf sediments and formed in a series of inter-connected basins; it extends continuously along the craton margin for more than 1000 km. The thicker sections of iron-formation occur adjacent to the thicker sections of volcanic rocks. The iron-formation was deposited on the craton shelf and slopes, but thins out or discontinues with the increasing amounts of clastic sediments and volcanic rock near the extrusive centres. Deposition took place during numerous transgressions and regressions of the sea over the shelf with fluctuation of the depth of water; high energy levels were recorded in oolitic textures and sedimentary features in most of the iron-formations, with some members in the Knob Lake basin showing a transition from oolitic texture to thin banding or microbanding with increasing depth of water. The linear marginal basins were related to the development of the deep seated tectonic system that surrounded the craton. Transverse fault systems, related to the offshore volcanic—tectonic belt, transect the craton margins and appear to have been active throughout the evolution of the marginal basins. The marginal tectonic system appears to have been a continuous deep seated fracture system that surrounded the craton. As sedimentation cycles and the accumulation of volcanic material neared completion the marginal basins were subjected to tectonic stresses that caused tectonic transport of the basin sediments toward the craton, and possibly the subduction of the outer marginal volcanic and sedimentary rocks of the offshore tectonic belt. Analogous conditions appear to have existed in the Lake

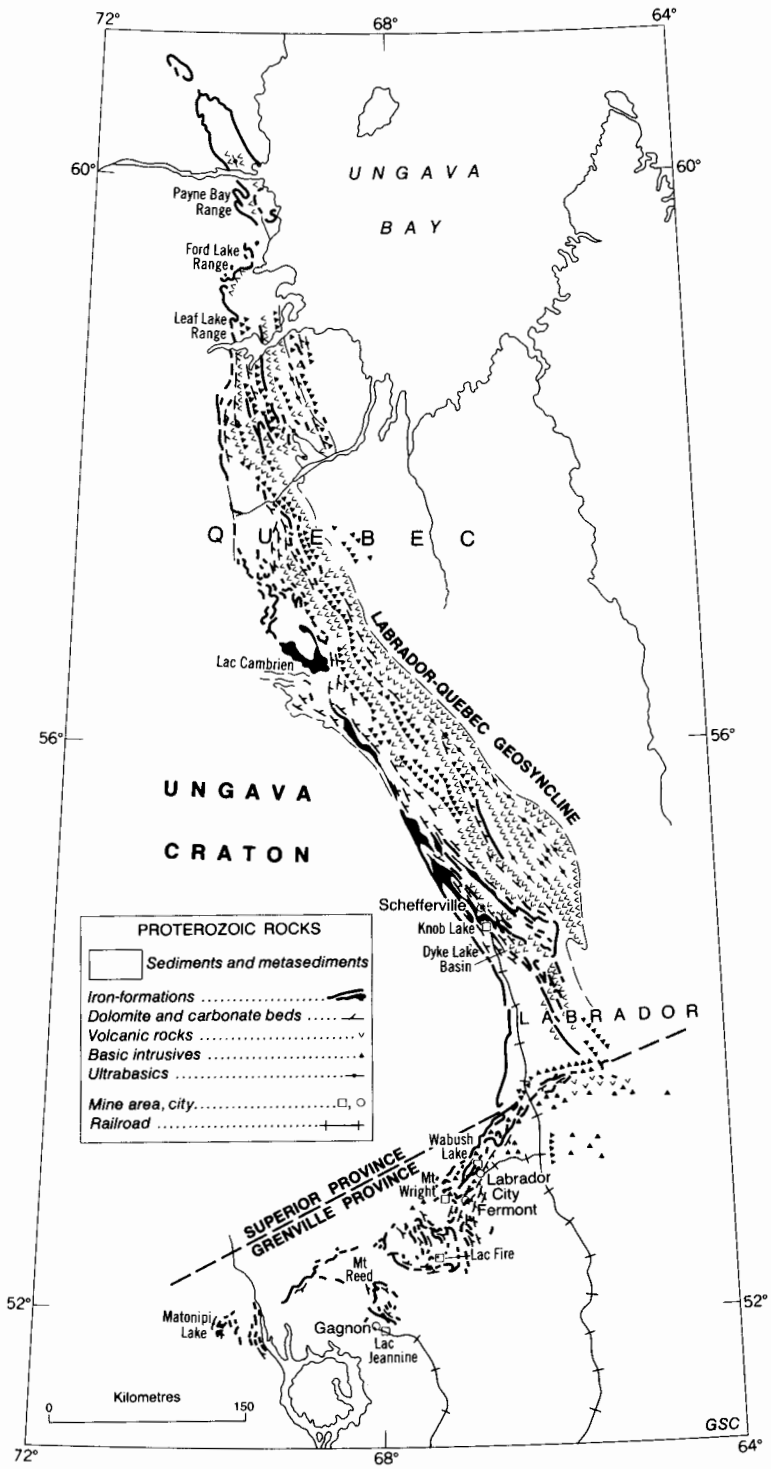

Fig. 4. General geology and distribution of iron-formation in the Labrador—Quebec geosyncline.

Superior region on the southern edge of the craton where thick sections of iron-formation were deposited in a series of linear basins along the margins of the craton (Bayley and James, 1973).

A transgression, from shallow to deeper water sedimentary environments offshore, is found in most of the marginal basins where the major iron-formations of the world are preserved. Most of the iron-formation in basins marginal to the Ungava—Superior craton was deposited in shallow water under high energy conditions, but in the Quadrilatero Ferrifero in Brazil it appears to have been deposited in deeper parts of the shelf where limestone deposition was still abundant. Iron-formations in the Transvaal Supergroup of South Africa are mostly characteristic of deeper shelf conditions and are associated with limestone, dolomite and volcanic material, and microbanding is more common than granular texture in the iron-formation.

The depositional environment in the Nabberu basin in Australia (Hall and Goode, 1978) appears to have been comparable to that in parts of the Labrador—Quebec geosyncline. However, the Hamersley basin, with assemblages of shale, sandstone, greywacke and volcanic rock, suggests a deep shelf environment. Very stable tectonic conditions must have prevailed during the deposition of this iron-formation in order for microbanded sequences to be uniformly developed over hundreds of kilometres (Trendall, 1973). The iron-formations in the Kursk—Krivoy Rog belt transgress from deep shelf environments in the west to eugeosynclinal conditions in the east where mafic to ultramafic volcanic rocks are developed along strong tectonic lineaments. Other thick sequences of iron-formation in Venezuela, West Africa, India and China are associated with greywacke and volcanic rock assemblages, but in most cases these rocks are highly metamorphosed, and the sedimentary—tectonic environment is not clearly defined.

Tectonic environments during the deposition of Algoma type iron-formations varied greatly in detail from one sedimentary—volcanic belt to another. The smaller size and facies variation of these iron-formations is to be expected. They developed under active tectonic conditions during the accumulation of sedimentary—volcanic sequences and basin environments were seldom stable or uniform over extended periods of time. Many iron-formations of this type probably formed in tectonic environments similar to the present day spreading ridges on the ocean floor where less extensive progenitors of some facies of iron-formation are forming today (Rona, 1978). Algoma type iron-formations may be genetically related to any tectonic—volcanic system where deep fractures pass through a higher geothermal gradient in the crust and effusive hydrothermal activity is generated.

The contrast in tectonic settings for Lake Superior and Algoma types of iron-formation provides a basis for explaining the relative differences in size and lateral distribution of the two groups, and the contrast in uniformity and heterogeneity of facies developed. The continental platforms and marginal basins provided relatively stable depositional environments over long periods of time for the accumulation of thick sequences of iron and silica

IRON-FORMATION DEPOSITION THROUGH TIME

(a)

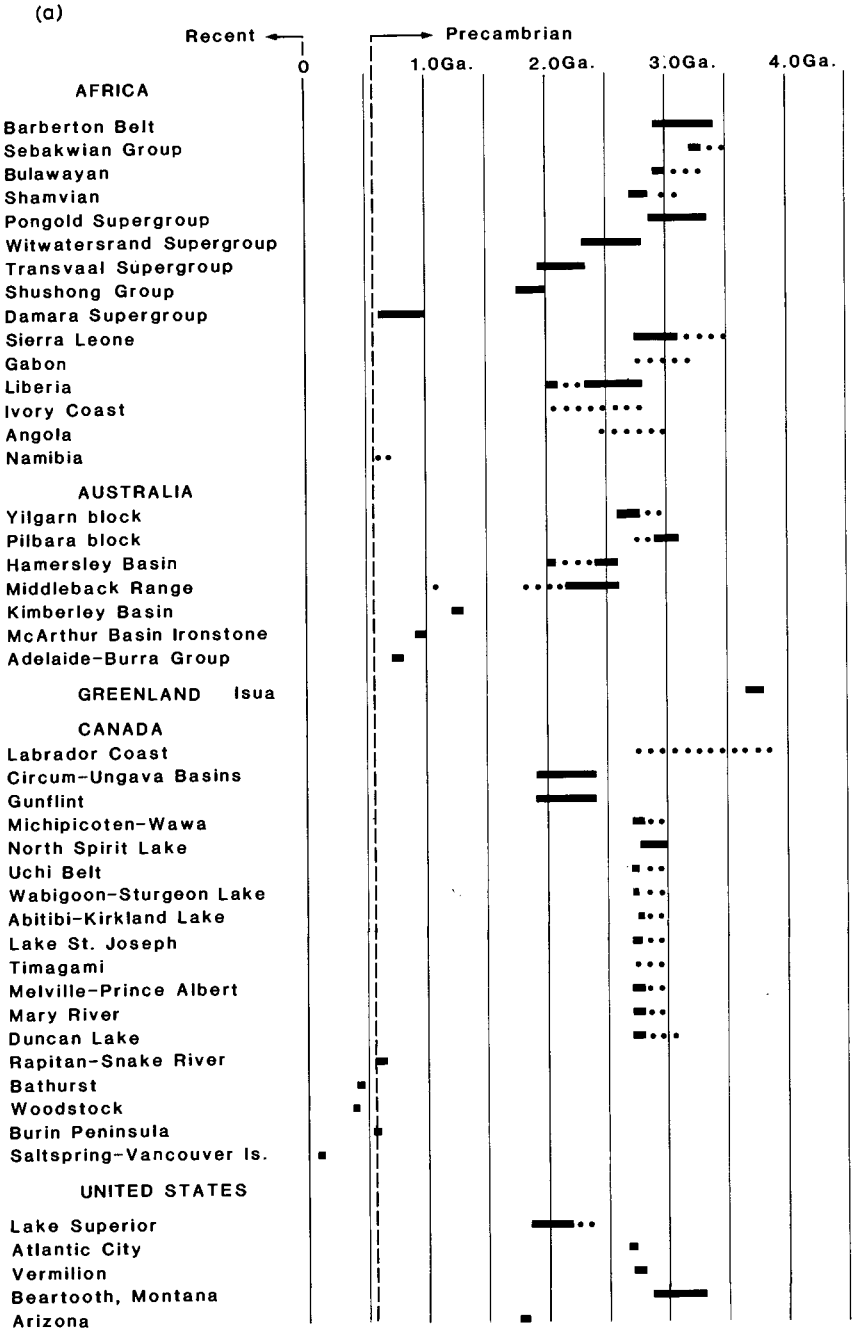

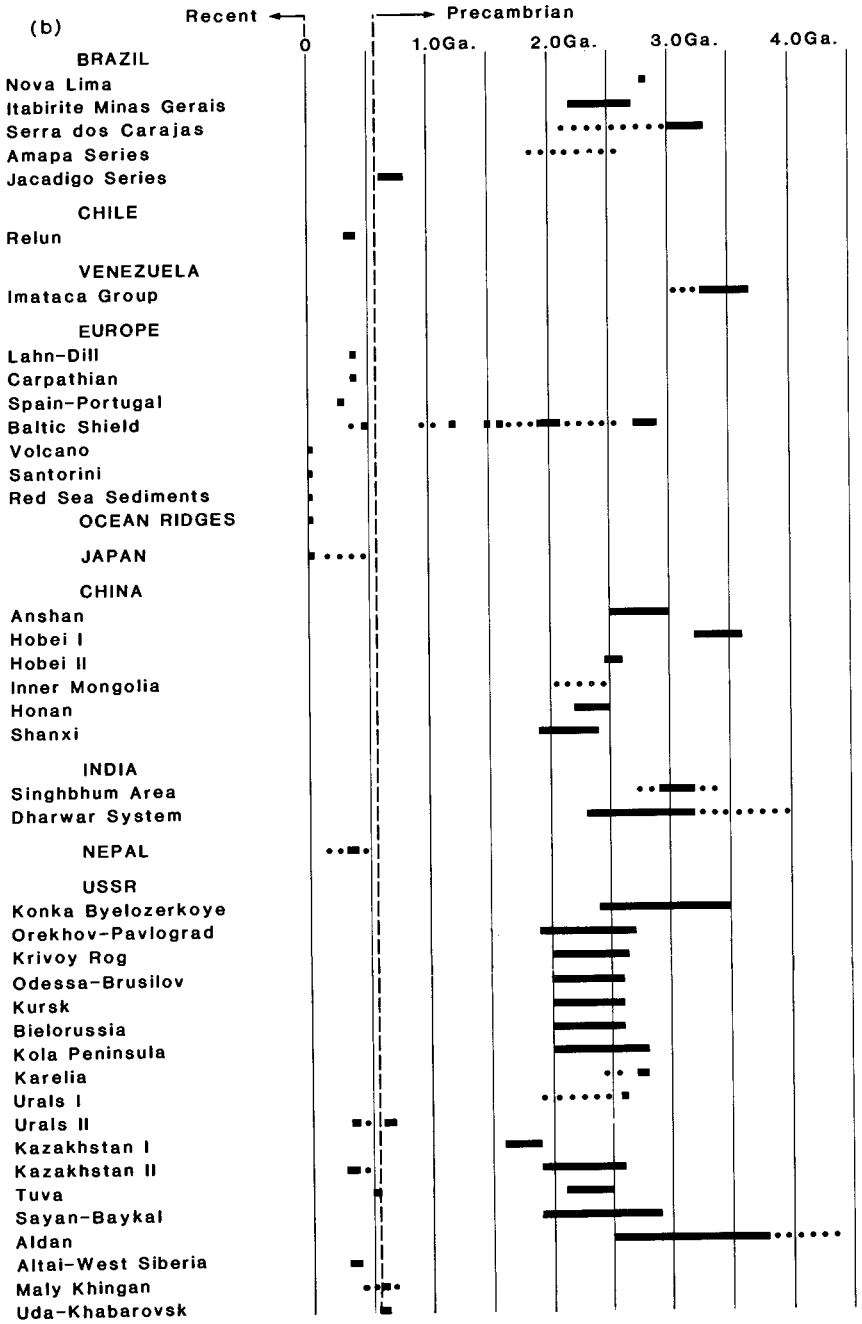

Ages of deposition for a selection of iron-formations based on isotopic dates; bars indicate minimum to maximum age of deposition; dots indicate possible age or extension of depositional periods.

Fig. 5. Possible time of deposition for a selection of iron-formations based on isotopic dates for associated rocks. (Source of data: Frietsch, 1980; Montgomery, 1979; Stockwell, 1982.)

derived from hydrothermal effusive sources. Development of the Circum-Ungava tectonic system, with the accumulation of shelf sediments, iron-formation and volcanic-greywacke rocks in linear basins on the craton margins, could have extended over a period of 500 Ma from 2400 to 1900 Ma-ago. The iron-formations were probably deposited during a relatively short interval within this period and form part of a sedimentary—tectonic system of continental or perhaps global dimension that existed through onetenth of recorded geological history. In contrast, the Algoma type iron-formations were deposited along spreading ridges or volcanic arc systems under more dynamic tectonic conditions during relatively short periods of time, probably from 10,000 to a few million years, and chemical sedimentation was interrupted by frequent extrusion of volcanic material and the deposition of clastic sediments.

DEPOSITION OF IRON-FORMATION THROUGH GEOLOGICAL TIME

Iron-formation is present throughout the geological record (Fig. 5) from the Isua iron-formation in West Greenland, dated at 3.8 Ga, to contemporary deposition of siliceous ferruginous muds in the deep basins of the Red Sea and along the ocean ridges (O'Rourke, 1961; Schultz, 1966; Gross, 1967a; Bischoff, 1969; Goldich, 1973; Rona, 1978; Perry et al., 1978; Leggett and Smith, 1980). Algoma type iron-formation occurrences are reported in all geological periods, but the Lake Superior type or continental margin group are known to occur primarily with rocks dated from ~2.7 to 2.0 Ga. It has been suggested that extensive deposition of iron-formations during this period was related to special factors in the development of the atmosphere and lithosphere involving the origin and evolution of organisms, an increase of oxygen in the atmosphere, the influence of carbon and oxygen in sedimentary environments, and in the transportation and deposition of iron. Genetic models for iron-formation which emphasize these factors have been proposed, especially in recent decades (MacGregor, 1927; Cloud, 1973; Holland, 1973; LaBerge, 1973; Garrels et al., 1973; Drever, 1974). However, I have concluded that the deposition and distribution of iron-formation has been controlled primarily by tectonic factors, and that biogenic factors and the composition of the atmosphere had a lesser, and probably limited influence on the precipitation of these chemical sediments.

Algoma type iron-formations of considerable thickness and lateral extent are widely distributed with volcanic and greywacke rocks that are older than 2.5 Ga (O'Rourke, 1961; Beukes, 1973; Goldich, 1973; Van N. Dorr, 1973). Gole and Klein (1981) point out that recent dating of Precambrian rocks associated with iron-formation, and data on their size and distribution indicate that the relative abundance of iron-formation increased gradually to reach a peak at ~2.4 Ga, and declined in the late Precambrian. Data on the size and distribution of iron-formations through geological time are still limited, and the geological record is incomplete so that firm conclusions con-

cerning the abundance of iron-formation with respect to the time of deposition remain tentative.

The thick sequences of iron-formation formed between 2.7 and 2.0 Ga, which account for a large proportion of the iron contained in iron-formations, were deposited in linear miogeosynclinal and eugeosynclinal basins where tectonic—volcanic systems transect craton margins. Deposition of sedimentary and volcanic rocks in the Kursk—Krivoy Rog geosyncline took place between 2.7 and 2.0 Ga. Deposition of the iron-formations extended from shelf to eugeosynclinal parts of the belt and may have continued intermittently through a large part of this period (Alexandrov, 1973).

Iron-formations in the Hamersley Group in Australia and the Transvaal Supergroup in South Africa are believed to be equivalent in age, and the associated rocks were deposited on continental shelves and slopes over a period extending from 2.5 to 1.9 Ga (Beukes, 1973; Button, 1976). The basins marginal to the Ungava—Superior craton containing extensive iron-formation, shelf sediments and volcanic rocks developed between 2.4 and 1.9 Ga and are believed to be part of a continuous tectonic system that surrounded the craton (Baragar and Scoates, 1981; Gross and Zajac, 1983). Thick members of iron-formation in the Rapitan Group and the Jacadigo Series were deposited in a relatively short period of time at the close of the Precambrian where major fracture systems developed grabens and basins on the margins of continental plates or cratons. Although rift systems and spreading ridges during the Phanerozoic do not appear to have provided depositional environments that were stable over any extended period of time, many small iron-formations were deposited in them. Iron—silica mud in the Red Sea graben is presently being deposited where a rift system cuts a continental plate or craton, and metalliferous sediments along ocean ridges consisting of iron and manganese oxide and sulphide facies may be considered progenitors of iron-formation.

REFERENCES

Alexandrov, E.A., 1973. The Precambrian banded iron-formations of the Soviet Union. In: H.L. James and P.K. Sims (Editors), Precambrian Iron-Formations of the World. Econ. Geol., 68: 1035—1062.

Baragar, W.R.A. and Scoates, R.F.J., 1981. The Circum-Superior belt: a Proterozoic plate margin. In: A. Kroner (Editor), Precambrian Plate Tectonics. Elsevier, Amsterdam, 782 pp.

Bayley, R.W. and James, H.L., 1973. Precambrian iron-formations of the United States. In: H.L. James and P.K. Sims (Editors), Precambrian Iron-formations of the World. Econ. Geol., 68: 934—959.

Beukes, N.J., 1973. Precambrian iron-formations of Southern Africa. In: H.L. James and P.K. Sims (Editors), Precambrian Iron-Formations of the World. Econ. Geol., 68: 960—1004.

Bischoff, J.L., 1969. Red Sea geothermal brine deposits: their mineralogy, chemistry and genesis. In: E.T. Degens and D.A. Ross (Editors), Hot Brines and Recent Heavy Metal Deposits in the Red Sea. Springer-Verlag, New York, pp. 368—406.

Brandt, R.T., Gross, G.A., Gruss, Hans, Semenenko, N.P. and van N. Dorr, J., II, 1972. Problems of nomenclature for banded ferruginous-cherty sedimentary rocks and their metamorphic equivalents. Econ. Geol., 67: 682—684.

Button, A., 1976. Transvaal and Hamersley Basins — review of basin development and mineral deposits. Miner. Sci. Eng., 8: 262—293.

Cloud, P., 1973. Paleoecological significance of the banded iron-formation. In: H.L. James and P.K. Sims (Editors), Precambrian Iron-Formations of the World. Econ. Geol., 68: 1135—1143.

Dimroth, E., Baragar, W.R.A., Bergeron, R. and Jackson, G.D., 1970. The filling of the Circum-Ungava geosyncline. In: A.J. Baer (Editor), Symposium on Basins and Geosynclines of the Canadian Shield. Geol. Surv. Can. Pap., 70-40: 45—157.

Drever, J.I., 1974. Geochemical model for the origin of Precambrian banded iron-formation. Geol. Soc. Am. Bull., 85: 1099—1106.

Eisbacher, G.H., 1978. Re-definition and subdivision of the Rapitan Group, Mackenzie Mountains. Geol. Surv. Can. Pap., 77-35: 21.

Frietsch, R., 1980. The ore deposits of Sweden. Geol. Surv. Finl. Bull., 306: 20.

Garrels, R.M., Perry, E.A., Jr. and Mackenzie, F.T., 1973. Genesis of Precambrian iron-formations and the development of atmospheric oxygen. In: H.L. James and P.K. Sims (Editors), Precambrian Iron-Formations of the World. Econ. Geol., 68: 1173—1179.

Goldich, S.S., 1973. Ages of Precambrian banded iron-formations. In: H.L. James and P.K. Sims (Editors), Precambrian Iron-Formations of the World. Econ. Geol., 68: 1126—1134.

Gole, M.J. and Klein, C., 1981. Banded iron-formations through much of Precambrian time. J. Geol., 89: 169—183.

Goodwin, A.M., 1956. Facies relations in the Gunflint Iron-Formation. Econ. Geol., 51: 565—595.

Goodwin, A.M., 1962. Structure, stratigraphy and origin of iron formation, Michipicoten area, Algoma district, Ontario, Canada. Geol. Soc. Am. Bull., 73: 561—586.

Goodwin, A.M., 1973. Archean iron-formations and tectonic basins of the Canadian Shield. In: H.L. James and P.K. Sims (Editors), Precambrian Iron-Formations of the World. Econ. Geol., 68: 915—933.

Gross, G.A., 1965. Geology of iron deposits in Canada. I. General geology and evaluation of iron deposits. Geol. Surv. Can. Econ. Geol. Rep., 22: 181.

Gross, G.A., 1967a. Geology of iron deposits in Canada. II. Iron deposits in the Appalachian and Grenville Regions of Canada. Geol. Surv. Can. Econ. Geol. Rep., 22: 111.

Gross, G.A., 1967b. Iron deposits of the Soviet Union. Can. Min. Metall. Bull., Dec. 1967: 6.

Gross, G.A., 1968. Geology of iron deposits in Canada, III. Iron ranges of the Labrador geosyncline. Geol. Surv. Can. Econ. Geol. Rep., 22: 179.

Gross, G.A., 1972. Primary features in cherty iron-formation. Sed. Geol., 7: 241—261.

Gross, G.A., 1973. The depositional environment of principal types of Precambrian iron-formation. In: M.P. Semenenko (Editor), Genesis of Precambrian Iron and Manganese Deposits. Proc. Kiev Symp. 1970, Unesco Earth Sci., 9: 15—21.

Gross, G.A., 1980. A classification of iron formations based on depositional environments. Can. Mineral., 18: 215—222.

Gross, G.A. and Zajac, I.S., 1983. Iron-formations in fold belts marginal to the Ungava Craton. In: A.F. Trendall and R.C. Morris (Editors), Banded Iron-Formation. Elsevier, Amsterdam, in press.

Hall, W.D.M. and Goode, A.D.T., 1978. The early Proterozoic Nabberu Basin and associated iron-formations of Western Australia. Precambrian Res., 7: 129—184.

Holland, H.D., 1973. The oceans: a possible source of iron in iron-formations. In: H.L. James and P.K. Sims (Editors), Precambrian Iron-Formations of the World. Econ. Geol., 68: 1169—1172.

James, H.L., 1954. Sedimentary facies of iron-formation. Econ. Geol., 49: 235—293.

LaBerge, G.L., 1973. Possible biological origin of Precambrian iron-formations. In: H.L. James and P.K. Sims (Editors), Precambrian Iron-Formations of the World. Econ. Geol., 68: 1098—1109.

Leggett, J.K. and Smith, T.K., 1980. Fe-rich deposits associated with Ordovician basalts in the southern uplands of Scotland: possible Lower Palaeozoic equivalents of modern active ridge sediments. Earth Planet. Sci. Lett., 47: 431—440.

MacGregor, A.M , 1927. Problems of Precambrian atmosphere. S. Afr. J.Sci., 24:155—172.

Meyn, H.D. and Palonen, P.A., 1980. Stratigraphy of an Archean submarine fan. Precambrian Res., 12: 257—285.

Montgomery, C.W., 1979. Uranium—lead geochronology of the Archean Imataca Series, Venezuelan Guayana Shield. Contrib. Mineral. Petrol., 69: 167—176.

O'Rourke, J.E., 1961. Paleozoic banded iron-formations. Econ. Geol., 56: 331—361.

Perry, E.C., Jr., Ahmad, S.N. and Swulius, T.M., 1978. The oxygen isotope composition of 3,800 M.Y. old metamorphosed chert and iron-formation from Isukasia, West Greenland. J. Geol., 86: 223—239.

Rona, P.A., 1978. Criteria for recognition of hydrothermal mineral deposits in ocean crust. Econ. Geol., 73: 135—160.

Schultz, R.W., 1966. Lower Carboniferous cherty ironstones at Tynagh, Ireland. Econ. Geol., 61: 311—342.

Stockwell, C.H., 1982. Proposals for time classification and correlation of Precambrian rocks and events in Canada and adjacent areas of the Canadian Shield, Part 1; a time classification of Precambrian rocks and events. Geol. Surv. Can. Pap., 80-19: 135.

Trendall, A.F., 1973. Varve cycles in the Weeli Wolli Formation of the Precambrian Hamersley Group, Western Australia. In: H.L. James and P.K. Sims (Editors), Precambrian Iron-Formations of the World. Econ. Geol., 68: 1089—1097.

Trendall, A.F. and Blockley, J.G., 1970. The iron-formations of the Precambrian Hamersley Group, Western Australia. Geol. Surv. West. Aust. Bull., 119: 365.

Van N. Dorr, J., II, 1973. Iron-formation in South America. In: H.L. James and P.K. Sims (Editors), Precambrian Iron-Formations of the World. Econ. Geol., 68: 1005—1022.

Weber-Diefenbach, K., 1977. Geochemistry and diagenesis of recent heavy metal ore deposits at the Atlantis-II-Deep (Red Sea). In: D.D. Klemm and H.-J. Schneider (Editors), Time and Strata-Bound Ore Deposits. Springer-Verlag, Berlin, Heidelberg, New York, pp. 419—436.

Zajac, I.S., 1974. The stratigraphy and mineralogy of the Sokoman Formation in the Knob Lake area, Quebec and Newfoundland. Geol. Surv. Can. Bull., 220: 159.

This Page Intentionally Left Blank

ARCHEAN CHEMICAL WEATHERING AT THREE LOCALITIES ON THE CANADIAN SHIELD

MIKKEL SCHAU and JOHN B. HENDERSON

Geological Survey of Canada, 588 Booth Street, Ottawa, Ontario K1A 0E4 (Canada)

ABSTRACT

Schau, M. and Henderson, J.B., 1983. Archean chemical weathering at three localities on the Canadian Shield. Precambrian Res., 20: 189—224.

Sapropelite developed on a granodiorite basement below the Archean Steeprock Group in the western Superior Structural Province of Canada, weathered materials from a 3.15 Ga granitic basement to the Archean Yellowknife Supergroup in the Slave Structural Province, and weathered detritus from contemporaneous komatiites and gneissic basement of the Archean Prince Albert Group in northern Churchill Structural Province, have been analysed. The deviation of the weakly metamorphosed weathered material from the chemical composition of their precursors is comparable to that seen in more recent weathered profiles from similar source materials. This includes the enhancement of ferric to ferrous iron ratios, and potash to soda, lime and magnesia ratios. There is also an increase in lighter REE and a depletion of heavier REE. Quartz rich sediments immediately above the unconformity, derived from the basement granitoids, may be enriched in aluminum and iron, and yield chloritoid under proper metamorphic conditions. Sediments formed from mixed sources, such as weathered gneissic basement and contemporaneous komatiitic volcanics, yield anomalous resistate sedimentary mixtures such as chromiferous quartzites. Based on the data given here, there is no need to postulate that different weathering and/or ground water systems were operative during the Archean, compared to more recent times. On the other hand the complicated weathering and diagenetic history that altered material undergoes below a subsiding unconformity, relies as much or more on the buffering capacity of the enclosed rock mass as on the atmospheric conditions prevalent at the time of weathering. Hence weathering profiles, old and new, are more a response to local environmental conditions within the rock than the composition of the atmosphere.

INTRODUCTION

Precambrian weathered materials are a tempting source of information regarding atmospheric environmental conditions during the first half of Earth history. Some understanding of these conditions is of great importance when considering such fundamental problems as, among others, the evolution of the atmosphere and the origin of life. It has been suggested that during the Archean, weathering processes differed from those of today (Rubey, 1964;

Roscoe, 1969; Button and Tyler, 1979; Cloud, 1980; Awramik, 1982, p. 315; Schidlowski, 1982, p. 118). To assess this assertion, indeed to examine the original premise that the chemical composition of preserved materials is significantly influenced by the atmospheric conditions they were initially formed under, chemical data from three localities in the Canadian Shield are considered with the hope of providing information towards the understanding and significance of materials weathered during the Archean.

In a profile across a paleo-weathered horizon, the chemical pattern preserved is the combined result of weathering and diagenesis (Loughnan, 1969). The range of local chemical conditions which dictate the nature of a soil or weathered products is a result of vadose waters with varied composition percolating through rock or soil of varied bulk composition and permeability. The greater the available volume of water, the more charged it is with atmospheric gases, the greater its rate of flow through the rock and the longer mineral surfaces are exposed to it, the greater will be the alteration and/or removal of materials from the rock or soil. The net result is the formation of an assemblage of low temperature — low pressure minerals in dynamic equilibrium with pore waters. These minerals will be different in volume, density, surface area, permeability, consolidation and strength from those of the unweathered rock. The differing soil zones on the Earth's surface today are a reflection of the varied influence of precipitation, evaporation and temperature during their formation. For example, these factors strongly influence whether iron is reduced and leached or oxidized and deposited, at what depth carbonate is deposited, and which of the various clay minerals form (Berner, 1971).

In any weathered profile there are two contrasting hydrologic environments; the subsurface zone and the subaqueous zone. The subsurface zone is characterized by circulating and often renewed ground water. Intense chemical weathering occurs nearest the surface, while lower in the zone leaching takes place when the system is wet and precipitation when it is dry. Oxidation and reduction processes are particularly common in the zone of capillary water immediately above the water table. The subaqueous zone on the other hand is characterized by water completely filling all void space. Solutions, precipitates and eluviated particles are added from the overlying subsurface zone. Chemical processes, such as hydration and reduction, are slower here, although diffusion may occur down concentration gradients along well connected pore systems. Oxidation may occur locally in this zone; the martization of ilmenite is one such process (Turner, 1980).

Diagenetic processes have a strong influence on the nature of the final products with the precipitation of cements, the oxidation of iron minerals and the formation of other minerals, although the physical makeup of the starting materials is a strong control. For example, large diagenetic changes are not expected in saprolites since they contain abundant clay and so are not particularly permeable. On the other hand, a well sorted sandstone with 40% porosity and high permeability can be expected to undergo considerable diagenetic alteration.

One feature of Archean weathered profiles and weathered materials is that they have, in general, been subjected to some degree of metamorphism. In all the examples considered in this study the mineralogy of the weathered materials are metamorphic assemblages, not primary weathering products. What influence, if any, has this had on their chemistry? Metamorphism is the mineralogical reconstitution of a material due to changing pressure and temperature. The controlling factor, as to whether or not bulk compositional changes occur, seems to be the water to rock ratio. If there is a high water flux, the system is open and there is opportunity for the transport of various elements into and out of the rock. If there is a low water flux then the chances for the removal and/or addition of elements are greatly reduced (Baragar et al., 1979). In metamorphism, it is the change from greenschist to amphibolite grade where most of the dehydration occurs. However, all localities considered in this study are at or below greenschist grade, that is, below the point of maximum dehydration. The amount of water involved in reactions within the low grade greenschist facies of metamorphism is only a small proportion of the total rock involved; it is almost negligible in comparison to the volume of water involved in normal weathering processes. Thus, metamorphic dehydration probably has little if any effect on the composition of a weathered rock. Of, perhaps, more concern is the potential change in oxidation state during metamorphism due to the presence of organic materials. For example, ferric oxide and other silicates can react with kerogen to form ferrous silicates and CO_2 (Thompson, 1972). This is more of a problem with metamorphosed sedimentary materials and probably has a minimal effect in weathered granitoid profiles such as those studied here.

Thus, instead of being a complicating factor, we argue that metamorphism enhances the preservation of premetamorphic compositional patterns. All metamorphic rocks are metastable with respect to conditions at the Earth's surface. They persist because they have been crystallized and their porosities and permeabilities are considerably reduced so that water no longer has easy access to the mineral surfaces. Indeed, the recognition of a weathering mineral assemblage in an Archean metasaprolite is probably as good an indication as any that the material has undergone further weathering subsequent to its metamorphism.

The rocks considered in this study were exposed at or near the surface where, in contact with the atmosphere—hydrosphere of the day, they underwent weathering, passed at least once from the subsurface to the subaqueous zone of weathering, underwent diagenesis, reached sufficient depths for metamorphism to take place and were finally uplifted to the surface again. The chemical product present in the field today is, therefore, the sum of the effects of the varied stages of weathering and diagenesis (only the first of which directly involves the atmosphere) which have been sealed in the rock with low grade metamorphism and which have remained essentially unaltered since.

GEOLOGICAL SETTING

The data for this study were collected from Archean rocks exposed at three rather different localities on the Canadian Shield (Fig. 1). They consist of: (1) a presumably weathered profile below an unconformity at Steeprock Lake in the western Superior Structural Province, (2) a selection of sedimentary rocks, with weathered boulders above and basement granite below an Archean unconformity at Point Lake in the Slave Structural Province and (3) a suite of sedimentary rocks from the Prince Albert Group at Laughland Lake, northern Churchill Structural Province thought to be derived from an ancient gneiss terrane and the contemporaneous Prince Albert Group komatiitic volcanoes.

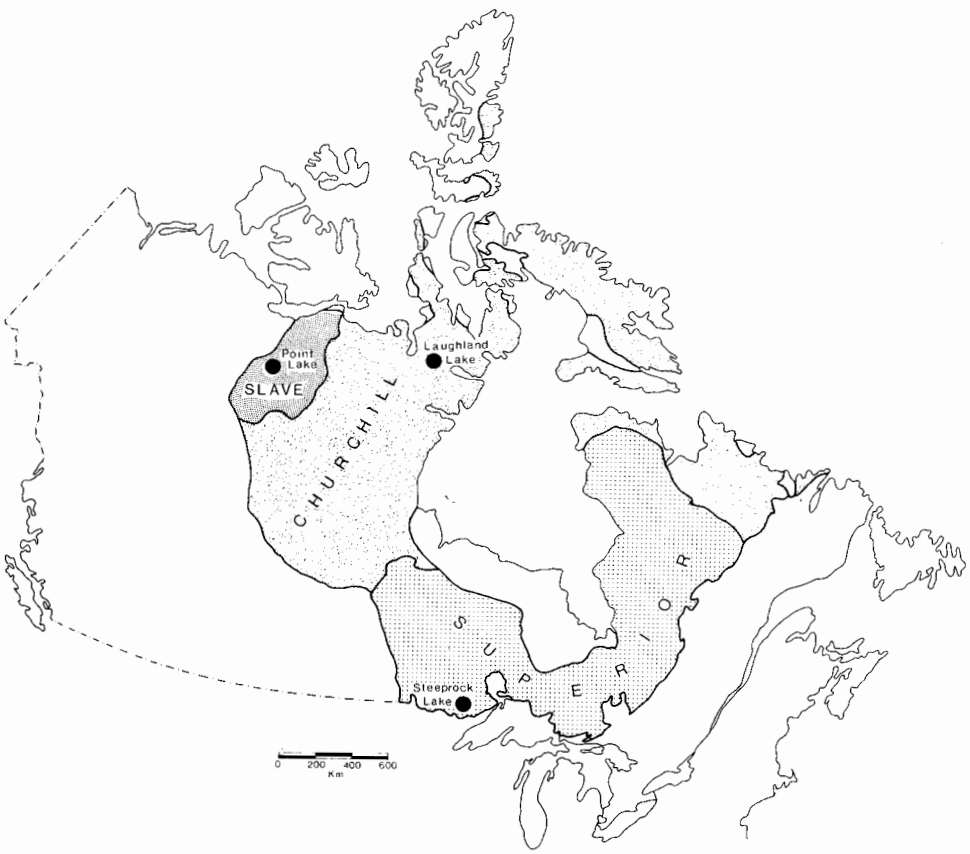

Fig. 1. Samples and site locations for the study include an Archean weathered granitoid profile at Steep Rock Lake in the western Superior Structural Province, a selection of Archean sediments, weathered boulders and basement granites at Point Lake in the Slave Structural Province and a suite of sediments from the Archean Prince Albert Group at Laughland Lake in the northern Churchill Structural Province.

Steep Rock Lake

At Steep Rock Lake in the western Superior Province at the boundary between an extensive metasedimentary and metavolcanic terrane, 200 km west of Thunder Bay, Ontario, is one of the more geologically interesting as well as controversial Archean sequences in the Canadian Shield. The Steeprock Group (Jolliffe, 1966) occurs in a relatively small area and contains important iron deposits which have been a focus for geological study for over 90 years. Jolliffe (1966) has described the geology of the area and has provided a summary of the various interpretations proposed. The area has been mapped at 1:12 000 scale by Shklanka (1972). The following summary is based mainly on the review of Jolliffe (1966).

The relationship of the Steeprock Group to the regional Archean stratigraphy is far from clear. Most investigators agree that the group occurs as a steeply dipping, faulted, homoclinal succession over a strike length of ~12 km with a granitoid terrane on one side and a structurally complex, dominantly mafic volcanic sequence on the other (Fig. 2). Arcuate faults, that are splays off the Quetico Fault system to the south, generally run parallel to stratigraphic units within the Steeprock Group. Almost all agree that the contact

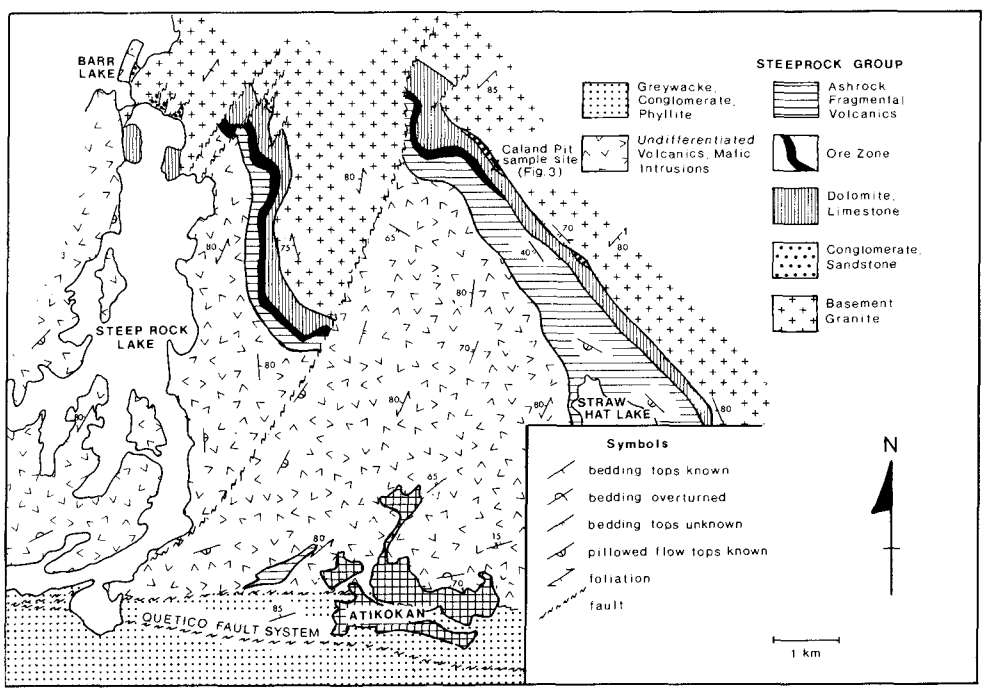

Fig. 2. Geology of the Steep Rock Lake area in the western Superior Province where four units of the Archean Steeprock Group unconformably overlie granitoid basement and have a poorly understood relationship with the volcanics to the west. Material from a weathered profile in the basement was collected at the Caland pit in the northeastern part of the area. Geology modified after Jolliffe (1966) and Shklanka (1972).

between the eastern granitoid terrane and the Steeprock Group is an unconformity (Smyth, 1891; Smith, 1893; McInnes, 1899, Lawson, 1912; Moore, 1940; Roberts and Bartley, 1943; Jolliffe, 1955, 1966). Those who interpret the granitoid terrane as younger include Bartley (1948) Hicks (1950) and Shklanka (1972), while few venture any opinion regarding the relationship between the mafic volcanics and the Steeprock Group. Jolliffe (1966), from the sheared nature of the volcanics and evidence of opposite facing directions from that of the Steeprock homocline, implies a tectonic discordance. Shklanka (1972), on the other hand, in addition to concluding that the granitoid terrane is younger and faulted against the Steeprock Group, suggested that the mafic volcanic rocks occur stratigraphically above and below the Steeprock Group.

The basement granite is compositionally heterogeneous, ranging from biotite granodiorite to biotite hornblende tonalite with some of the more mafic phases gradational into amphibolite. Feldspars are sericitized and the mafic minerals are commonly chloritized. The rock is variably and irregularly gneissic, and is typically medium grained, but finer grained locally. Altered mafic dykes, commonly with chilled margins preserved, are abundant in the complex. Most do not cross into the Steeprock Group and several are terminated at the unconformity (Fig. 3). Mafic inclusions, some recognizeable as

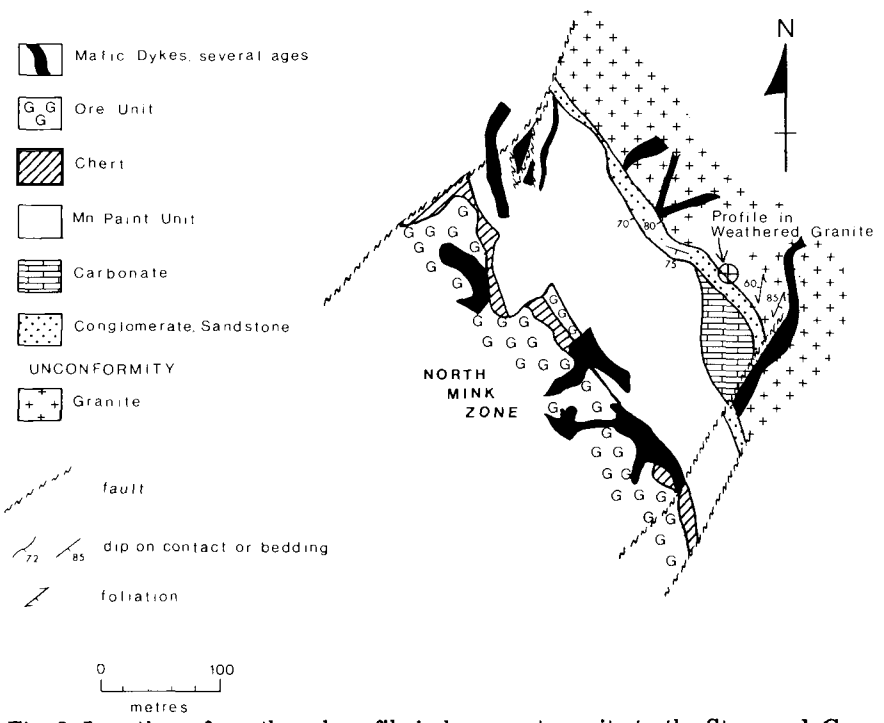

Fig. 3. Location of weathered profile in basement granite to the Steeprock Group. Note the truncation of diabase dykes at the unconformity. After McIntosh (1972).

metavolcanics, are also present. Most workers have concluded that the granite is older than the Steeprock Group based mainly on the fact that an unconformity can be observed; in places there is a gradation from the granite to the limestone unit, passing from massive granite through a schistose zone in which the foliation is at high angle to the contact, to a feldspar rock that increases in carbonate content as it grades into the limestone unit (Smyth, 1891); the contact is conformable with bedding in the adjacent sedimentary rocks (McIntosh, 1972); conglomeratic units next to the granite contain cobbles similar in lithology to that of the granitoid complex; and no contact metamorphic effect and no dykes or veins from the granite have been noted in the immediately adjacent country rocks (Jolliffe, 1966). At one locality in the Caland Ore Company pit the unconformity was well exposed (McIntosh, 1972), with what is interpreted as a weathered horizon developed in the granodiorite below the unconformity (Figs. 2,3). A profile across the weathered zone was sampled for this study.

The Steeprock Group itself consists of 4 units. At the base of the sequence is a conglomerate of varied thickness that fills depressions in the unconformity surface. Clasts in the conglomerate are similar to the granitoid lithologies of the basement complex and the dykes that intrude it, and are contained in a quartz rich matrix. Within the conglomerate are massive lenticular beds of sandstone.

Above the conglomerate or the basement, where the basal conglomerate is missing, are up to 500 m or more of grey, fine grained dolomite and limestone (no iron rich carbonates are present in this unit (Jolliffe, 1955)) in well defined beds of varied thickness with minor interbedded chert. Breccias are present locally and are of tectonic origin. Large stromatolitic domes in excess of 2 m across occur within the unit (Hofmann, 1971, 1981).

The ore zone unit consists of three members. At the base is what is termed the manganiferous paint member, consisting of poorly layered to fragmental material of varied composition ranging from 10—40% iron and 20—60% silica with up to 5% manganese. It is irregular in thickness, from a meter or less to over 300 m, cutting down through the underlying dolomite and locally through to the basement granite which is there altered to a loose sheared kaolinitic granite rubble. Although such an incursion of the granite by the manganiferous paint member has occurred near the location of the sampled profile (Fig. 3) the structural, mineralogical and compositional characteristics of the member do not appear in the samples analysed and so it is not thought to have played a major part in the alteration of the granite in the sampled profile. Jolliffe (1955, 1966) considered the ore zone to be an Archean sedimentary iron deposit. On the other hand Riley (1969) and Shklanka (1972), among others, strongly disagree and suggest the ore zone represents a post Archean alteration of a major siderite—pyrite—chert iron formation within the Steeprock Group. The goethite member, consisting largely of that mineral, but also present with hematite, occurs as a uniform, rarely layered, brecciated unit sharply above the manganiferous paint member and is mostly of

ore grade. The same steeply dipping goethite member, with essentially the same characteristics seen at the surface, has been intersected at a depth of 700 m. The pyrite member at the top of the ore zone unit occurs in conformable lenses consisting of interlayered pyrite rich and aluminous siliceous sediments, with the pyrite typically having colloform texture. These sediments can contain as much as 12.9% carbon (Wright, 1959, cited in Jolliffe, 1966). Jolliffe (1966), on the basis of the highly irregular lower surface of the manganiferous paint member, suggested it represents a karst surface complete with pinnacles and sinkholes with the unit itself representing a residual soil.

The uppermost member of the Steeprock Group is the ashrock formation, which is a massive, iron and magnesium rich, silica poor, fragmental rock consisting almost entirely of poorly sorted, closely packed, rounded to subangular, fine grained, black volcanic clasts < 3 cm in size set in a carbonate matrix. The unit is heterogeneous and many different metamorphic minerals, including pumpelleyite and stilpnomelane, occur within it.

Of concern here is the age of the weathered material below the unconformity. Is it Archean? As mentioned previously the origin and age of the ore unit within the Steeprock Group, above the unconformity, is controversial. If the ore was concentrated due to a post Archean alteration process, then is it not possible that the 'weathered zone' below the unconformity could represent the same or a similar post Archean event? Riley (1969), a proponent of the post Archean age of the ore, argued on the basis of the best data available to him (Schmalz, 1959) that the iron hydroxide minerals claimed by Jolliffe as Archean in age could not have survived metamorphism up to lower greenschist grade (Shklanka, 1972) which accompanied the Archean deformation of the Steeprock Group. Experimental studies have produced a variety of results and have not been able to define the stability field of goethite with regard to hematite, as indeed it has not been possible to reverse the reaction (Schmalz, 1959; Langmuir, 1971; Fischer and Schwertmann, 1975; Threirr-Sorel et al., 1978; Murray, 1979). Similarly the stability under surface and metamorphic conditions of aluminum hydroxide minerals, such as gibbsite (which occurs in the manganese paint unit), is difficult to interpret (Helgeson et al., 1978); in fact Perkins et al. (1979) conclude that thermodynamically the only mineral of this group stable at room temperature is diaspore which, together with kaolinite, will persist up to 360°C at 2 kb. Thus, gibbsite and boehmite, two common minerals in bauxite and laterite, are considered metastable at the Earth's surface! There are, therefore, no thermodynamic reasons against suggesting that the low grade minerals reported by Jolliffe (1966) may not be a low grade metamorphic assemblage. However, there are considerable difficulties if the ore zone formed due to supergene oxidation of a carbonate—pyrite—chert unit by downward percolating meteoric waters in post Archean time, as proposed by Shklanka (1972) and Riley (1969) among others. It is difficult to imagine a process that would completely alter a postulated carbonate—pyrite—chert unit to a

goethite—hematite unit, usually < 100 m thick at a depth of at least 700 m, yet only partially affect the immediately adjacent limestone unit. What was the fate of the sulphate presumably produced during the oxidation of the pyrite? There is no evidence of any sulphate minerals being preserved. In the opinion of the present authors there is considerable doubt as to the existence of a major post Archean alteration event, which is not to say that localized alteration near the surface could not have taken place in post Archean times. Indeed, Tanton (1941) reported the occurrence of Cretaceous plant fossils within a limestone formation breccia near the surface of a formation that he interpreted as the collapse of a near surface cave, formed as a result of Cretaceous karstification. Cretaceous plant material on the surface was incorporated into the collapse breccia.

As far as the altered zone below the granite—Steeprock contact is concerned, it contains the mineral assemblage paragonite—muscovite—chlorite—quartz—opaques. It is evident that this is a metamorphic assemblage and not the primary weathering products. To our knowledge, no one has recognized a post Archean metamorphism in the region. Thus, as has been discussed previously, it is assumed that the composition of this zone, which we interpret as forming due to weathering, was sealed at the time of metamorphism.

The best estimate of the time of metamorphism is 2.7 Ga which is derived from a K—Ar age determination on a dark gray phyllite taken from a drill core in the Steeprock Group about 4 km southeast of the sample locality (Lepp and Goldich, 1964), and is assumed to be an estimate of the age of crystallization of the micas in the phyllite. An Archean age for the weathered zone, as well as for the Steeprock Group, is indicated if this age is considered a minimum estimate for the age of the succession. Similarly, volcanic and sedimentary rocks just west of Steep Rock Lake, thought to be correlative with the Steeprock Group and volcanic rocks east of the lake (Shklanka, 1972), are metamorphosed and intruded by granitic rocks whose biotite has a K—Ar age of 2.56 Ga (Goldich et al., 1961).

Point Lake

The second of the localities under consideration in this study is in the Slave Province in the northwestern part of the Canadian Shield. The Slave Province consists of about 190 000 km^2 of Archean 'granite—greenstone' terrane dominated by metasedimentary rocks that have undergone no major deformation other than faulting in the last 2.5 Ga.

At Point Lake, in the west central part of the province, the relationship between sialic basement rocks and Archean supracrustal rocks of the Yellowknife Supergroup, first recognized by Stockwell (1933), is particularly well preserved and exposed. In the Slave Province, the supracrustal basins are thought to have formed about 2.67 Ga ago in a series of fault bounded rifts that formed in a sialic basement which was in large part at least 3 Ga old (Henderson, 1981). Point Lake is situated across the margin of one of these

rift basins (Fig. 4) (Henderson and Easton, 1977). As in many such fault bounded basins of the province, the margin is marked by a thick sequence of dominantly mafic pillowed and massive volcanic flows. The volcanics thin away from the margin out into the basin where, ~ 15 km from the margin, the volcanics are no longer present and the basement granite and basal conglomerate is overlain by the greywacke—mudstone turbidites that constitute the main fill of the rift basin. Meter-thick layers of oxide, carbonate and/or silicate—sulphide facies of iron formation are locally interbedded with the metasediments. A few beds of limestone and dolomite also occur in the turbidite sequence. A conglomeratic unit, derived in varied proportions from both the sialic basement and the mafic volcanic unit, is also present in the basin margin sequence. Commonly associated with this conglomerate are cross-bedded fluvial sandstones.

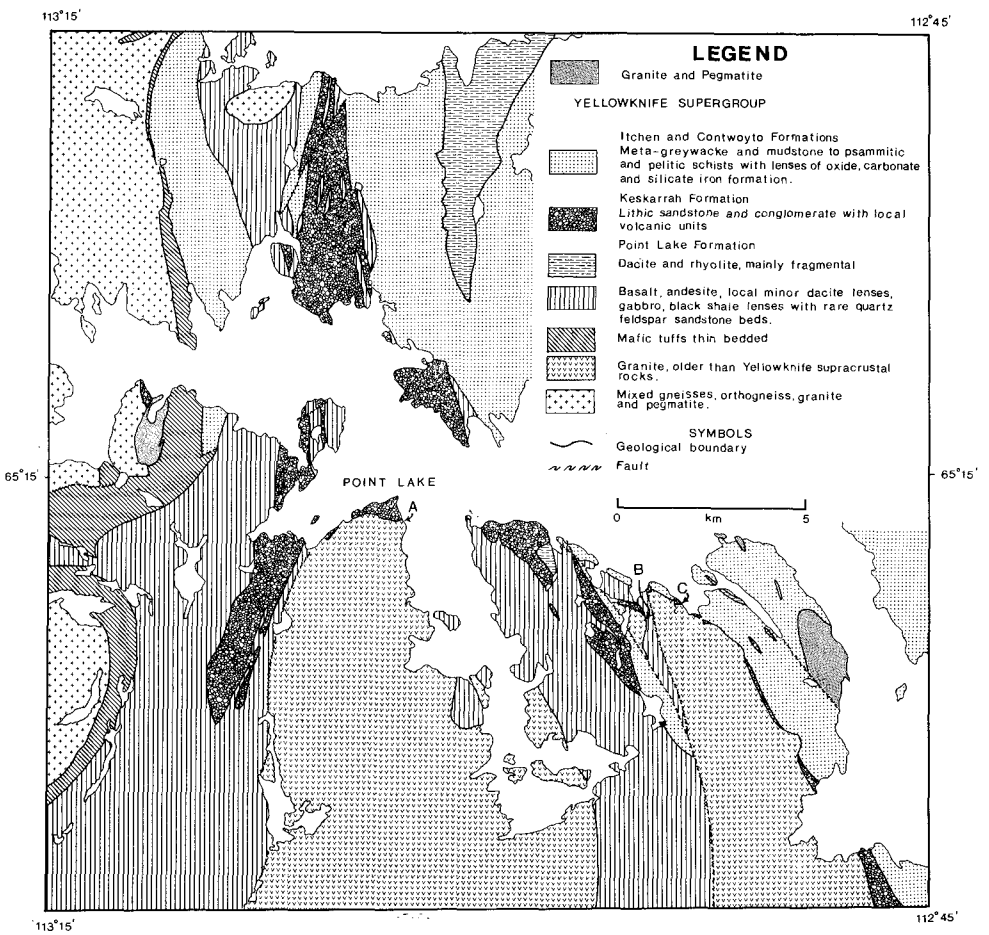

Fig. 4. Geology of the Point Lake area in the west central Slave Province. The area includes part of the margin of an Archean rift basin with Yellowknife supracrustal rocks unconformably overlying granite basement. The basement, the weathered granite and cobbles from the conglomerate above the unconformity were sampled at the localities indicated. Geology after Henderson and Easton (1977).

This basin margin sequence rests unconformably on a granite basement. It is a massive, equigranular, leucocratic granite in which the primary mafic minerals have been altered to chlorite before or in association with the deposition of the supracrustal rocks and prior to being subsequently weakly metamorphosed. This basement granite has a U—Pb concordia intercept age of 3.155 Ga based on 3 zircon fractions from one sample (Krogh and Gibbins, 1978). West of the basin is a complex of tonalitic to granodioritic gneisses that are also believed to be older than the supracrustal rocks (Henderson and Easton, 1977; Bostock, 1980; Easton et al., 1982).

The unconformity between the basement granite and the overlying supracrustal rocks is exposed in several localities and is typically, but not always overlain by conglomerate. At several of these localities, an Archean weathered zone is evident in the granite below the unconformity in which the feldspars are extremely altered although the original granitic texture of the rock is still apparent, mainly preserved by the quartz. At some localities a thin lag deposit of very angular quartz, presumably derived from the weathered zone, occurs immediately above the unconformity. More commonly, however, a conglomerate occurs in which generally rounded cobbles, derived from both the fresh basement and its weathered equivalent, are a major component.

Both the granite and the sedimentary rocks show evidence of having been metamorphosed to the biotite zone of the greenschist grade, with decussate biotite textures in the basement granite and typical mineral assemblages of the biotite zone in the metasediments.

Laughland Lake

The third area under consideration is in the Laughland Lake area in the Committee Block (Heywood and Schau, 1978) of the northern Churchill Province (Fig. 1) where metasedimentary rocks of the Archean Prince Albert Group overlie a gneissic basement. Although relationships are less clear than at Steeprock Lake and Point Lake due to structural complexity, the unusual chemical composition of some of the sediment is indicative of subaerial weathering of distinctive source rocks.

Rocks of the Prince Albert Groups are preserved over a distance of at least 750 km in keels of subparallel subhorizontal north-easterly trending folds within a gneiss terrane (Fig. 5). Zircons from volcanic units on Melville Penninsula have minimum ages of 2.952 Ga (Wanless, 1979) while gneisses derived from Prince Albert Group rocks have zircon ages of 2.605 Ga (Wanless, personal communication, 1980). A minimum age of 2.95 Ga for the Prince Albert Group is indicated, which is significantly older than the presumed age of either the Yellowknife at Point Lake (2.67 Ga) or the Steeprock Group. The metamorphism of these rocks is varied with the highest grades occurring near the centre of the outcrop belt (Schau, 1978). Facies change from a 7 km thick sequence of subaerial to shallow marine volcanic and sedimentary rocks in the northeast (Schau, 1977) to a thinner, more

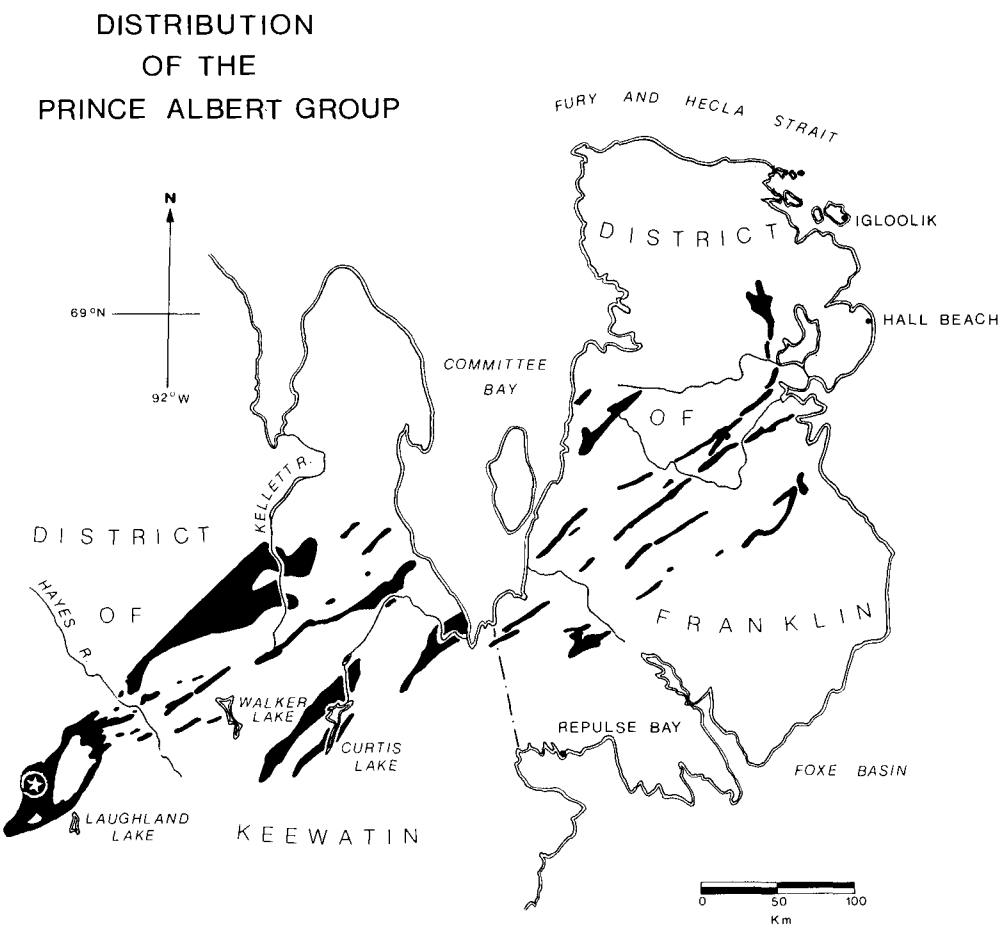

Fig. 5. Distribution of Prince Albert Group as keels of subparallel, subhorizontal, northeasterly trending folds within a gneissic terrane in northern Churchill Province. The Laughland Lake area and location of Fig. 6 is marked by the star.

sediment dominated assemblage, locally subaerially deposited, in the southwest. The present relationship of these rocks to the surrounding gneisses is related to the grade of metamorphism of the supracrustal rocks. At amphibolite grade the contacts are typically tectonic or intrusive. Where the Prince Albert Group is at greenschist grade the contacts are either faults or possible unconformities.

In the Laughland Lake area (Fig. 5) a central dome of tonalite to granodiorite gneisses is, in most places, in fault contact with the greenschist grade (chlorite—chloritoid—kyanite) Prince Albert Group, but at one locality on the east flank of the dome, the granitoid gneisses are structurally overlain at moderate angles by a fragmental unit consisting of lenticular fragments of gneiss in a biotite matrix. This unit is overlain by low grade metasediments in which primary grading and cross bedding are preserved (Schau, 1983).

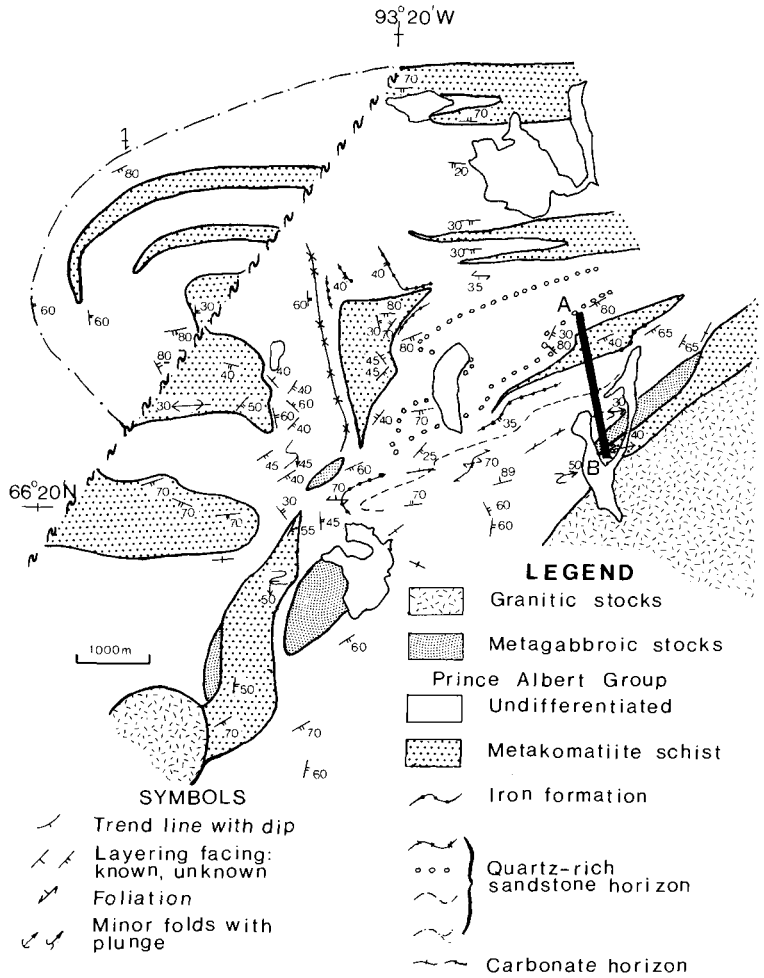

Fig. 6. Location of a representative section in the Prince Albert Group (section B-A) in intricately and complexly folded Prince Albert Group rocks (Table I).

West of the gneiss dome the metasediments are intricately and complexly folded (Fig. 6), and tectonic repetition together with poor exposure make it difficult to determine the complete stratigraphic section. However, in one region (see Fig. 6) it is possible to measure a partial, unrepeated section consisting of phyllitic to schistose quartzite, iron rich sediments, shales, limestones, conglomerate and komatiite interlayered on a decimeter scale (Table I). These sediments are quite different from the more typical sequences of greywacke—mudstone turbidites and their metamorphosed equivalent, which are so common in the granite—greenstone terranes of the Slave and Superior Provinces.

Quartzite and micaceous quartzite units up to several hundred meters thick

TABLE I

Representative section (location shown in Figs. 5 and 6) in the Prince Albert Group, southern part of Laughland Lake map area (numbers in parentheses refer to samples from the unit analysed and reported in Table VI)

Thickness	Description
	Top unknown
15 m	Metakomatiite schist with talc and siderite spots set in chlorite—magnesite—dolomite matrix (6-1) interlayered with iron-rich hornblende horizons
200 m	Sheared gabbro stock
200 m	Chloritic phyllite with actinolite-rich carbonate layers (Garbenschiefer)
100 m	Sheared gabbro apophyses emplaced in layered amphibolite-rich fragmental units with clasts of quartz and chert as a fine grained quartz mosaic set in matrix of actinolite and hornblende
100 m	Calcareous fragmental unit with quartz-rich layers, hornblende porphyroblasts and relict komatiite fragments, now serpentine and carbonate, set in a carbonate matrix
10 m	Garnetiferous pyritic metasiltstones interbedded with a more calcareous and chloritic variety near base; quartzose and quartzofeldspathic fragments, magnetite and poikiloblastic helicitic garnets are set in chlorite—biotite—quartz—amphibole matrix (6-2)
100 m	Mainly covered; phyllite with kyanite laths in microfolded white mica—quartz matrix interbedded with chloritic phyllite with quartz, chlorite, white mica, chloritoid and opaques (6-3)
40 m	Limestone with poorly defined layers and variable amounts of breccia. Some units are well layered on a 10 cm — 1 m scale. Some layers contain both ankerite and calcite
10 m	Calcareous chlorite schist
20 m	Phyllite
10 m	Rusty weathering garnet-rich layer
20 m	Quartzose schist
20 m	Amphibole-rich iron formation with garnetiferous layers (6-4)
15 m	Schistose quartzite with minor white mica—chlorite matrix and accessory garnet, tourmaline and opaques (6-5)
5 m	Grey chloritoid bearing phyllites
5 m	Fine grained amphibolite-rich iron formation with minor carbonate and magnetite (6-6)
150 m	Calcareous chlorite schists with local quartz-rich or quartzofeldspathic layers, and layered amphibole-rich iron formation (6-7)
10 m	Lean oxide iron formation
100 m	Chloritic and biotitic metasiltstone compound of chlorite and biotite set in quartz and quartzofeldspathic matrix (6-8)
15 m	Quartzite with muscovite interbeds and local chromian muscovite along strike
1145 m	

are lenticular and locally crossbedded on a large scale (Fig. 7). The limestones are composed of calcite and less abundant ankerite or tremolite. Many of the units are calcareous, although carbonated relict komatiite flows contain magnesite and dolomite as well as calcite. No siderite has been recognized in the

area. The shale is commonly graphitic and locally pyritic. The peridotitic komatiite unit in the section is schistose with no relict textures, but elsewhere in the region, spinifex textures have been recognized in better preserved peridotitic komatiitic flows (Eckstrand, 1975; Schau, 1977). Iron rich units consist of mixtures of iron—aluminium minerals such as chlorite, chloritoid, garnet and actinolitic hornblende; only a few banded quartz—magnetite units are known. The rare conglomerates commonly contain felsic fragments but irregularly shaped fragments of completely serpentinized komatiite occurs in one of the calcareous units.

In the following section evidence based mainly on chemical data from these rocks will be summarized that suggests the sediments of the Prince Albert Group were derived from the subaerial weathering and erosion of the older gneisses as well as from contemporaneous komatiitic volcanoes (Schau, 1983).

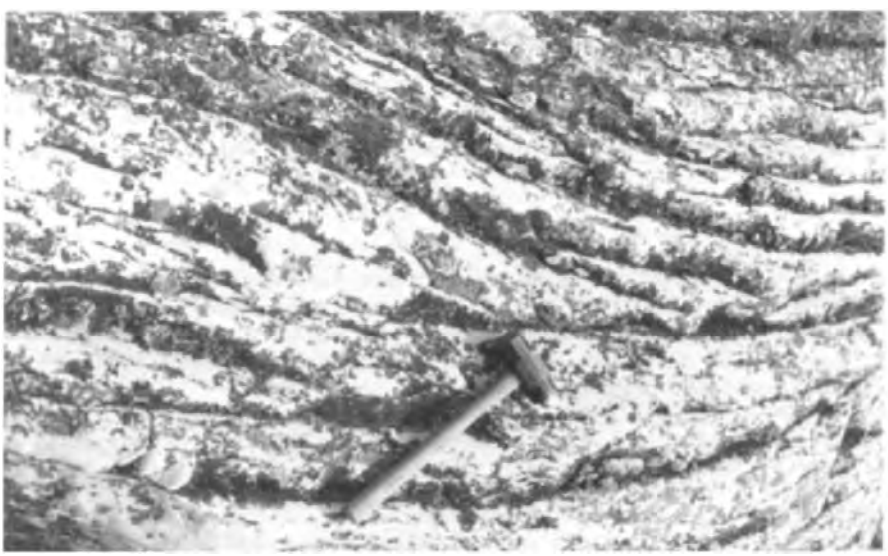

Fig. 7. Quartzite and micaceous quartzite units of the Prince Albert Group up to several hundred metres thick are lenticular and crossbedded on a large scale. Note cross bedding fore sets tangential to bedding plane above hammer (GSC photo 178 407).

ANALYSIS AND RESULTS

Method of analysis

The samples submitted for chemical analyses were hand specimens from which a thin section was made, a slice is usually saved, and the remaining rock is trimmed of weathered material by sawing or grinding. This sample is then crushed to pass through a 250 μm screen. These powders are the materials analysed.

The major elements are analysed by an automated X-ray fluorescence method developed at the Geological Survey of Canada. CO_2 was determined by acid evolution and titration, H_2O by fusion in a Penfield tube and a Karl Fisher titration, FeO by cold acid decomposition and back titration with $K_2Cr_2O_7$ and F and Cl by carbonate fusion and determination by selective ion electrodes. Analyses cited in this report are accurate to within the limits stated in Table II. This table was derived by continuous monitoring of international standards with the method current at the time of analysis.

Trace elements are determined by the Geological Survey of Canada using a semi-automatic optical spectroscopic method. Some of the minor elements were also analysed by XRF. Elements run by both methods yield the same values within the limits cited. Volatile elements are determined by screw rod technique with the atomic absorption method. Some trace elements (As to Nb) were analyzed by Energy Dispersion Spectra utilizing a method currently under development at the GSC (Lachance, personal communication, 1981). Where possible, several methods were used to insure the accuracy of the data. The reliability of these analyses are given in Table IIa.

The rare earths (Sc, Y, and the lanthanides) were analyzed by J.G. Sen Gupta of the GSC Chemical Laboratories. Sc, Dy, Er and Yb were determined by flame absorption spectrometry (Sen Gupta, 1976). Y and Ce were

TABLE IIa

Reliability of chemical analyses: the validity of the results for this study, using the 'productivity oriented methods', have been assessed (versus international reference materials) as shown below, i.e., at the levels reported ~95% of the results should fall within the figure given (G. Lachance, personal communication, 1976, 1980, 1982; Sen Gupta, personal communication, 1982)

SiO_2	± 0.7%	Rb	± 6 ppm	± 5% of value reported	La	± 10 % of value reported
TiO_2	± 0.03%	Sr	± 6 ppm	± 5% of value reported	Ce	± 10 % of value reported
Al_2O_3	± 0.5%	Ba	± 10 ppm	± 15% of value reported	Pr	± 10 % of value reported
Fe_2O_3	± 0.2%	Zr	± 10 ppm	± 7% of value reported	Nd	± 10 % of value reported
FeO	± 0.4%	Cr	± 5 ppm	± 15% of value reported	Sm	± 0.2 ppm
MnO	± 0.02%	Co	± 10 ppm	± 15% of value reported	Eu	± 10 % of value reported
MgO	± 0.4%	Ni	± 10 ppm	± 15% of value reported	Gd	± 0.2 ppm
CaO	± 0.1%	Cu	± 5 ppm	± 15% of value reported	Tb	± 0.2 ppm
Na_2O	± 0.3%	V	± 10 ppm	± 15% of value reported	Dy	± 0.1 ppm
K_2O	± 0.03%	B	± 10 ppm	± 15% of value reported	Ho	± 10 % of value reported
P_2O_5	± 0.03%	Li	± 5 ppm		Er	± 0.1 ppm
CO_2	± 0.1%	Zn	± 20 ppm	± 20% of value reported	Tm	± 10 % of value reported
H_2O	± 0.1%				Yb	± 10 % of value reported
S	± 0.03%				Lu	± 10 % of value reported

TABLE IIb

Comparison of Sen Gupta's methods of REE analyses with USGS reference data (modified from Sen Gupta, 1982)

	Rhyolite (USGS reference RGM-1)		Quartz Latite (USGS reference QLO-1)		Cody Shale (USGS reference SCo-1)	
	Sen Gupta (ppm)	Others (ppm)	Sen Gupta (ppm)	Others (ppm)	Sen Gupta (ppm)	Others (ppm)
La	24	23.1[a], 27[a], 23 ± 0.5[d]	28	26.1[a], 35.9[a], 27 ± 0.5[d]	30	28.4[a], 34.2[a], 28 ± 1[d]
Ce	49	53 ± 6[a], 32 ± 3.2[d], 48 ± 4[e]	60	57 ± 3[a], 59 ± 3[d], 57 ± 5[e]	66	62 ± 6[a], 63.4[b], 65 ± 2[d], 67 ± 7[e]
Pr	5	4.1[a]	6	6.1[a]	7	5.43[a], 7.62[b]
Nd			22	(17—35.3)[a], <20[d]	28	(23.8—29)[a], <20[d]
Sm	4.8	4.3 ± 0.4[a], <5[d]				
Eu	0.7	0.77 ± 0.12[a], 0.62 ± 0.3[d]	1.4	1.55 ± 0.12[a], 1.5 ± 0.15[d]	1.2	1.2 ± 0.2[a], 1.1 ± 0.1[d]
Gd	4	3.1[a], 3.6[c], 3.1 ± 0.3[d]	4.6	5.2 ± 1.4[a], 3.7 ± 0.4[d]	4.7	5 ± 1[a], 4 ± 4[d]
Tb	0.7	0.74[a], 0.66[c]	0.7	0.82 ± 0.08[a]	0.7	0.75 ± 0.04[a]
Dy	4	4.3[a], 5[c]	4	<3.2[a], 5.2[c]	4.3	3.8[a], 3.79[b]
Ho	0.9	<1.0[a]	0.8	<1.0[a]	1	0.93[a]
Er	2.7	<2.2[a]	2.3	<2.2[a]	2.5	2.5[a], 2.39[b]
Tm	0.4	0.37[a]	0.35	0.39[a]	0.4	0.35[a], 0.61[c]
Yb	2.4	2.9 ± 0.2[a], 2.3 ± 0.07[d]	2.3	2.8 ± 0.7[a], 2.3 ± 0.07[d]	2.3	2.6 ± 0.3[a], 2.2 ± 0.07[d]
Lu	0.45	0.42[a]	0.36	0.42[a]	0.32	0.37[a], 0.34[b]

[a] Gladney and Goode (1981); [b] McLennan and Taylor (1980); [c] Rosenberg and Zilliacus (1980); [d] Church (1981); [e] Mazzucotelli and Vannucci (1980).

determined by arc-emission spectroscopy (Sen Gupta, 1977) and La, Pr, Nd, Sm, Eu, Gd, Tb, Ho, Tm, and Lu were determined by a graphite furnace atomic absorption spectrometry method (Sen Gupta, 1981, 1982). Their precision and comparison with standards is given in Table IIb.

Steep Rock Lake

Samples along a 70 cm profile across the weathered granodiorite below the unconformity surface were collected at the Caland pit (Figs. 2,3). The length of the profile was limited by exposure; the weathered zone below the unconformity is $>$ 1 m. Individual samples from the overlying basal units of the Steeprock Group were also analysed.

The altered granodiorite collected is white with pale brownish spots and has a chalky texture. In thin section the rock consists mainly of fine grained, densely matted, white mica and sand sized quartz grains. No voids are evident and the specific gravity on the powdered samples is $\sim$ 2.75, which is somewhat higher than the fresh granodiorite (2.69). On the basis of X-ray diffraction, the well crystallized white mica (in the sense of Kubler, in Frey (1978)) is both paragonite and muscovite. No shifts in diffraction peaks occur with glycolation of clay size separates, indicating that no expandable clay is present. Modal quartz is higher by a third in the altered rock than nearby fresh granodiorite. Clearly, the material collected is metamorphosed with none of the primary weathering mineral assemblage preserved. However, the assemblage paragonite—muscovite is what should be expected in the metamorphosed equivalents of a weathered granodiorite. Garrels and McKenzie (1967) have shown that potassium feldspar and smectite are the usual products in the deeper weathering of granodiorite which, after diagenesis, can be converted to an illite/smectite mixed layer mineral (Hower et al., 1976). The low grade metamorphic equivalent of this mineral is paragonite—muscovite (Frey, 1978), which is the assemblage occurring here.

Individual samples of the basal sandstones in the Steeprock Group, a few tens of centimeters above the unconformity, were also collected and analysed. These sandstones are coarse grained, quartz rich, poorly sorted, wacke. The quartz is polycrystalline, angular and strained. A very minor component is coarse to fine grained amoeboid grains of quartzo-feldspathic material with minor white mica that probably represents highly weathered feldspathic clasts. Similar material forms the matrix of the sandstone.

The chemical data is presented in Table III. A ratio diagram of this data in Fig. 8 shows the relative loss or gain of constituents. Normally, an isovolumetric method (i.e., Gardner et al., 1978) is used in making such comparisons. However, the larger amount of modal quartz in the altered versus fresh rock, the lack of voids and greater specific gravity of the altered rock indicates significant compaction of the weathered material had taken place due to deformation, diagenesis and metamorphism. Following the method of Nesbitt (1979) the assumption is made that Zr is a relatively immobile element, and gains and losses are reported relative to this element.

TABLE III

Chemical analyses — Steep Rock Lake area (NF = not found, ND = not determined)

		Sample No.										
		3-1[a]	3-2[a]	3-3[b]	3-4[b]	3-5[b]	3-6[b]	3-7[b]	3-8[b]	3-9[c]	3-10[c]	3-11[c]
SiO_2	(%)	73.6	70.9	74.9	75.6	71.9	67.6	68.4	66.7	90.3	94.8	91.3
TiO_2	(%)	0.15	0.20	0.23	0.24	0.24	0.31	0.31	0.34	0.34	0.07	0.17
Al_2O_3	(%)	14.8	15.7	16.9	16.1	17.2	22.1	23.2	22.9	4.9	2.3	4.4
Fe_2O_3	(%)	0.4	0.3	1.2	1.1	2.6	0.8	0.3	0.2	1.3	0.6	0.8
FeO	(%)	0.9	1.5	0	0.1	0.6	0	0	0.3	0.3	0	0.1
MnO	(%)	0.01	0.02	0.01	0.01	0.02	0	0	0	0.01	0.04	0.03
MgO	(%)	0.63	0.77	0.47	0.41	0.97	0.33	0.26	0.18	0.37	0.04	0.15
CaO	(%)	0.98	2.02	0	0.07	0.18	0.08	0.05	0.06	0	0	0
Na_2O	(%)	4.4	4.6	0.8	0.8	1.1	2.3	2.6	2.2	0	0.1	0.1
K_2O	(%)	1.54	1.49	2.92	2.83	2.04	2.41	2.49	2.68	0.66	0.30	0.74
P_2O_5	(%)	0.03	0.05	0	0	0	0	0	0	0	0	0
S	(%)	NF	NF	NF	NF	NF	NF	0.03	NF	NF	NF	NF
CO_2	(%)	0.5	0.5	0	0	0	0	0	0	0	0	0
H_2O	(%)	0.9	1.0	0.8	1.0	3.1	3.2	2.5	2.6	0	0.8	0.4
Rb	(ppm)	42	35	66	61	43	52	49	55	25	10	18
Sr	(ppm)	259	377	141	129	187	290	288	279	25	12	34
Ba	(ppm)	328	287	357	320	283	275	226	280	113	46	115
Zr	(ppm)	95	96	118	108	115	147	138	161	111	75	58
Cr	(ppm)	6	<5	<5	<5	<5	<5	<5	<5	8	<5	<5
Co	(ppm)	<10	<10	<10	<10	13	<10	<10	<10	13	<10	<10
Ni	(ppm)	<10	<10	<10	<10	11	13	<10	<10	<10	<10	<10
Cu	(ppm)	14	<5	<5	<5	<5	<5	<5	<5	54	7	14
V	(ppm)	325	266	34	31	41	67	53	63	31	<20	<20
B	(ppm)	55	50	76	66	73	95	93	103	56	56	61
Li	(ppm)	9	8	21	20	40	48	48	46	14	6	6
REE		d		d	d	d				d	d	d
SG		2.70	2.68	2.80	2.73	2.74	2.77	2.77	2.77	ND	2.69	ND

[a] Fresh basement granitoid remote from unconformity.
[b] Samples from profile in weathered granitoid 70, 70, 35, 14, 7 and 3 cm, respectively, below the unconformity surface.
[c] Sandstones derived from granitoid basement 2, 15 and 35 cm, respectively, above the unconformity.
[d] Reported in Table IV.

Alumina, titania and boron show very little change. Lime, strontium, vanadium and soda show a precipitous decrease, and silica a more gentle decline up profile. Potash, rubidium and barium all have a similar distribution although the latter two show a decrease upward through the profile. Potash is enriched low in the profile. Magnesia and ferrous iron appear to be somewhat enriched at −35 cm along with a very large (~525%) increase in the ferric iron content. Lithium is also increased at and above this point of iron enrichment.

A combination of processes leading to this chemical profile is indicated. The breakdown of plagioclase during weathering leads to the diminishment of Ca, Na and Sr, and the breakdown of mafic constituents to the release of vanadium, alumina and boron, trapped in the formation of clay minerals, along with titania in the form of 'leucoxene' remain constant. Potash, rubidium and barium are released with the degradation of potassium feldspar, but in general, is fixed in clay minerals, possibly during diagenesis. An enrichment of ferric iron as seen in the Steeprock profile at the −35 cm level is a well known

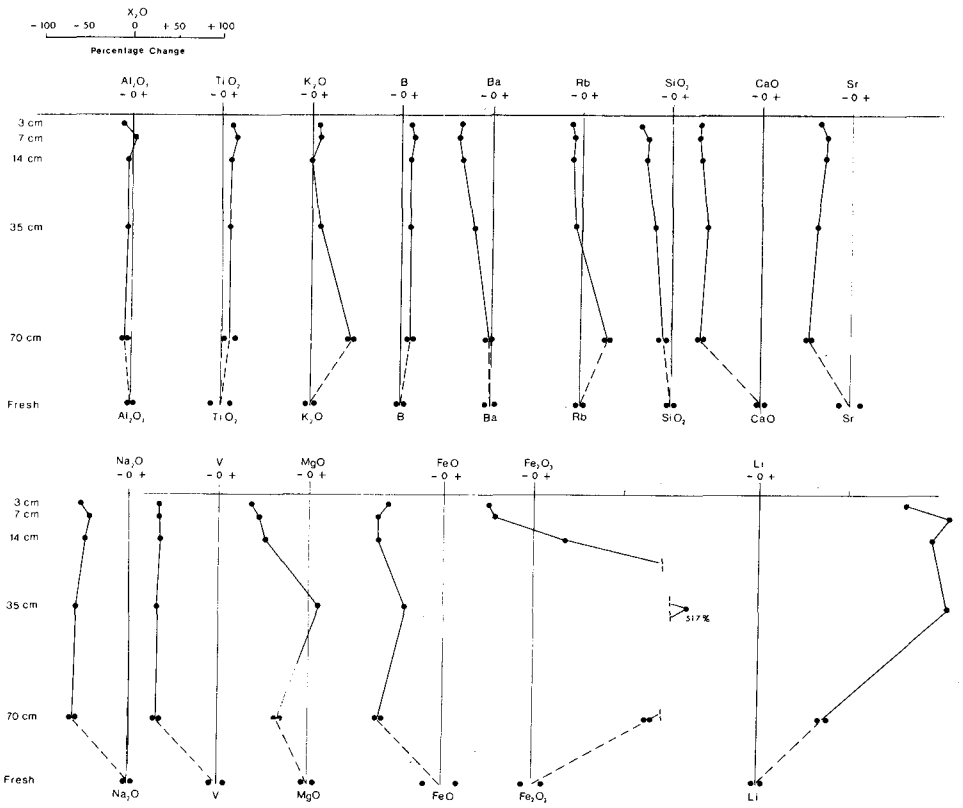

Fig. 8. Ratio diagram of chemical data from the profile in the weathered granite at Steep Rock Lake area. Losses and gains are plotted relative to Zr on the assumption that it is the most immobile of elements.

phenomenon in weathered sequences (Augustithis and Ottermann, 1966) and, following Duddy (1980), is thought to represent a fossil position of the weathering front. The lithium enrichment above this point and the potassium enrichment below may also be a related phenomenon. Ferrous iron, magnesia, cobalt and nickel, which are slightly above the detection limit at this horizon, reflect the formation of chlorite. The increase of soda upward in the profile from its most depleted state at −70 cm is a reflection of an increasing proportion of paragonite.

Lanthanide concentrations were determined in 4 samples from the profile and in 3 of the overlying clastic rocks (Table IV). In Fig. 9 the profile data is plotted in a similar manner as the previously discussed elements by utilizing the ratio method with respect to Zr. The diagram is arranged so that the style of presentation is similar to traditional REE pattern diagrams except that the normalization is with respect to Zr concentration in the sample compared to the same ratio in the unweathered granite. In the weathered profile it is evident that the lighter lanthanoid elements (La, Ce, Pr, Nd)

TABLE IV

REE analyses (ppm) from Steep Rock Lake profile, Point Lake area and Yellowknife, N.W.T. (the number of the analysis corresponds to the major and trace element analyses in other tables, i.e., 3-9 = Table III, analysis 9; ND = not determined)

	3-1	3-4	3-5	3-8	3-9	3-10	3-11	5-9	5-11[d]	5-12[d]	5-13[d]
Sc[a]	1.9	1.8	2.5	4.0	2.7	0.8	2.4	1.7	ND	ND	ND
Y[b]	6	8	6.7	7	10	3.3	6	7	32	16	21
La[c]	6	12	15	28	40	6	11	15	7.9	9.2	22
Ce[d]	16	25	28	53	59	<12	22	30	20	19	46
Pr[c]	1.9	2.7	2.6	5.6	5.5	0.8	2.2	2.5	3	2.1	5.8
Nd[c]	7	9	8	18	18	2	7	8	15	8.5	21
Sm[c]	1.1	1.1	1	3	2.4	0.3	0.9	1	5	2.1	4.4
Eu[c]	0.3	0.3	0.3	0.8	0.7	0.1	0.2	0.3	1	0.7	1.4
Gd[c]	0.9	1.0	1.0	2.0	1.8	0.4	0.7	1.0	4.3	1.8	3.9
Tb[c]	0.15	0.2	0.17	0.22	0.26	0.07	0.12	0.15	ND	ND	ND
Dy[a]	1.0	1.2	1.0	1.0	1.6	0.2	0.9	1.0	4.1	1.2	3.7
Ho[c]	0.18	0.24	0.2	0.2	0.32	0.1	0.2	0.24	ND	ND	ND
Er[a]	0.5	0.6	0.5	0.6	0.9	0.4	0.6	0.6	2.2	0.9	1.9
Tm[c]	0.07	0.08	0.07	0.08	0.12	0.05	0.09	0.1	ND	ND	ND
Yb[a]	0.4	0.4	0.4	0.5	0.7	0.3	0.6	0.6	1.9	0.6	1.8
Lu[c]	<0.1	<0.1	<0.1	<0.1	0.1	<0.1	<0.1	0.1	ND	ND	ND

[a] By flame absorption spectrometry.
[b] By arc emission spectroscopy.
[c] By graphite furnace atomic absorption spectrometry.
[d] Method and data from Jenner et al. (1981).

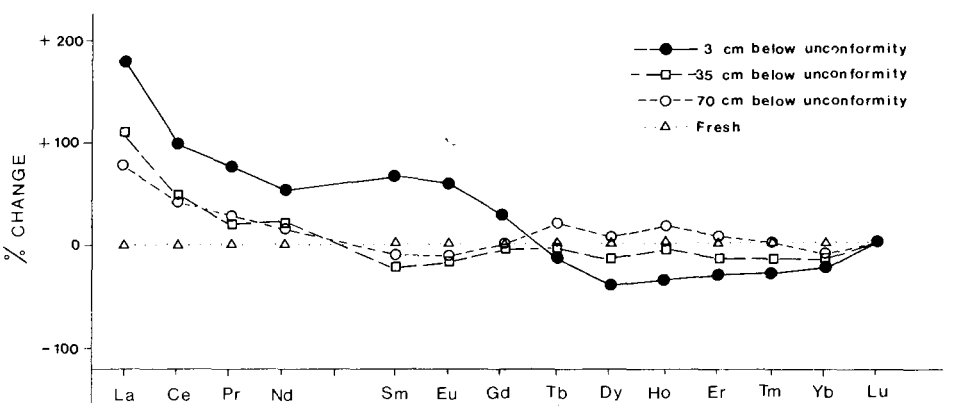

Fig. 9. REE data from the profile in weathered granite basement in Steeprock Lake area plotted with respect to Zr. Note that in the weathered profile the lighter elements have increased in concentration while the heavier ones have decreased.

have increased in concentration while the heavier ones (Tb, Dy, Ho, Er, Tm, Yb) have decreased with respect to the unweathered protolith. The proportion of Sm, Eu and Gd increases in the samples above the iron enrichment point and decreases below it. Chemical differentiation of the lanthanide elements, involving at least two processes, is indicated.

The first process, resulting in the increase of lighter elements and the decrease of heavier ones, affects all the samples. It also involves the change of the La/Y ratio and the linear increase of La with increasing Al_2O_3/SiO_2 and NaO_2 in the profile. Presumably, the site of the La is now, in part, in the paragonite thought to have been derived from the smectite precursor formed during weathering. The La should be more easily fixed in clay than Lu in accordance with the principle that for ions of equal valence, the bond strength between ion and exchanger decreases with decreasing ionic radius (Herrmann, 1969) and the fact that lanthanide element ionic radius decreases with increasing atomic number (Cotton and Wilkinson, 1962; Herrmann, 1969; Burkov and Podborina, 1971).

This shift in lanthanide proportion has been noted by others in both weathering and other contexts. For example, Girin et al. (1979) in a study of Phanerozoic clays in Russia noted the correlation of La with Al_2O_3/SiO_2 and postulated that the La was trapped in clay minerals, whereas the heavier lanthanides were removed in solution. Loubet and Allegre (1977), after examining the after-effects of the natural reactor at Oklo, recognized a noticeable migration of heavy REE occurred after the nuclear reactions had run their course, which suggests that they are more easily complexed and, thus, more mobile during diagenesis. Duddy (1980) has shown the distribution of La within a Cretaceous weathering profile to be highly irregular and suggested that La will only move short distances before being trapped in sheet silicates, while the heavier lanthanide elements are more likely to leave the system. A similar scenario is postulated for the Steeprock profile with the lanthanoids being released as weathering breaks down the silicate minerals. The lighter lanthanoids were trapped more effectively than the heavier lanthanoids in the newly formed clays.

The second process, which involves the enrichment of Sm, Eu and Gd above the iron enrichment level in the profile, is not understood, but indications that such processes involving clays take place elsewhere in younger rocks has been discussed by Christie and Roaldset (1979).

Point Lake

At Point Lake, no detailed profile was sampled. The data is derived from samples from within the basement pluton, the regolith at 3 localities along the unconformity and cobbles from the overlying conglomerate at 2 localities.

Fig. 10. Photomicrograph of relatively fresh and weathered granite from locality B (Fig.4). The fresh basement rock is a massive, fractured, medium grained, even grained, hypersolvus granite in which the quartz (light areas) occurs as blocky grains (Photo A). In the weathered equivalent (Photo B) from just below the unconformity the feldspars are completely altered to a moderately foliated fine grained assemblage of quartz—feldspar—white mica —carbonate. Only the texture and distribution of a quartz (light areas) is retained from the fresh rock. Scale bar is 2 mm long. Chemical analyses of this material can be seen in Table V, analyses 5-4 (A) and 5-5 (B) (GSC photo 203 884-A,B).

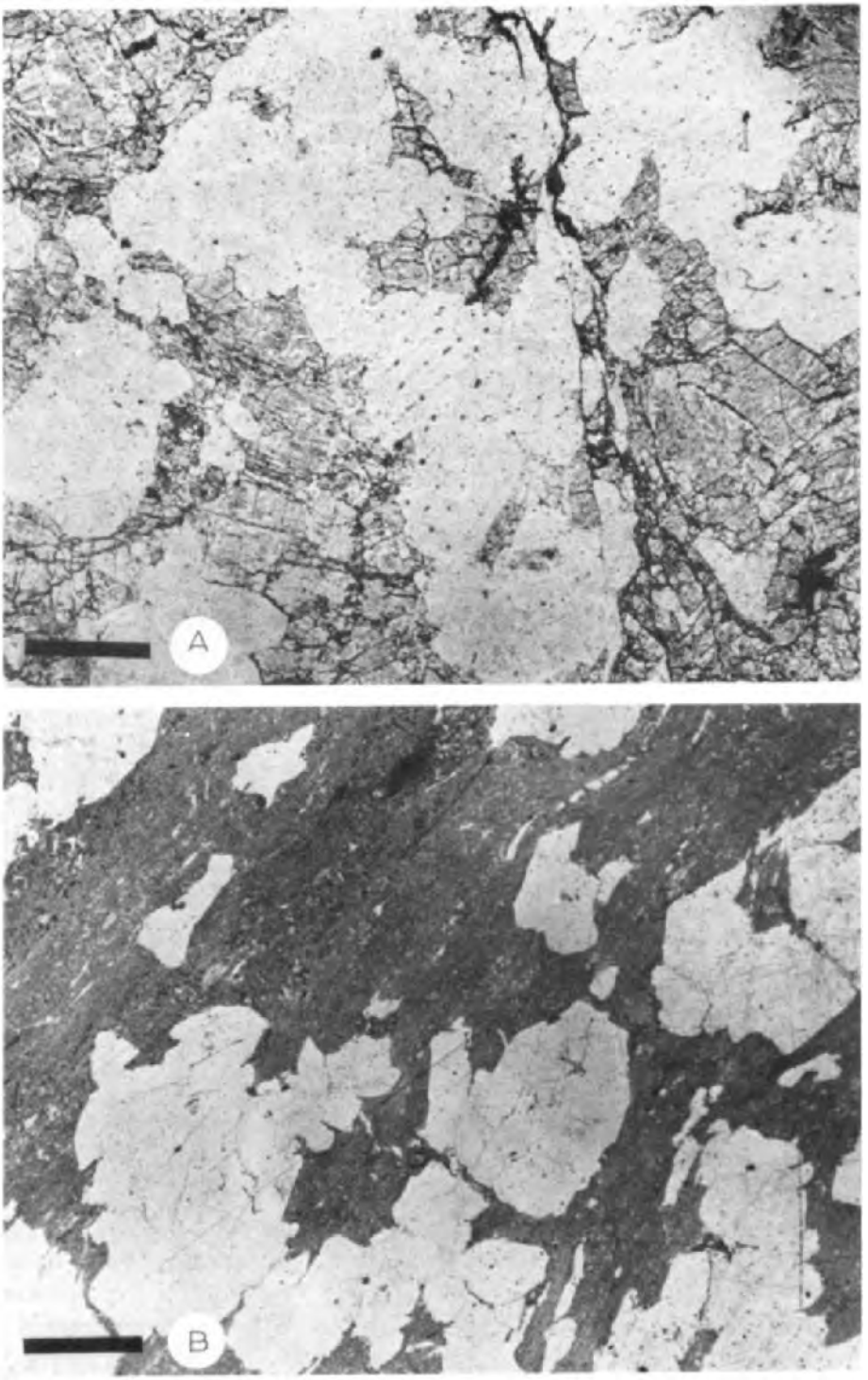
A
B

TABLE V

Chemical analyses — Point Lake area and Yellowknife (NF = not found; ND = not determined)

		Sample No.												
		5-1[a]	5-2[a]	5-3[a]	5-4[b]	5-5[b]	5-6[b]	5-7[c]	5-8[c]	5-9[d]	5-10[d]	5-11[e]	5-12[f]	5-13[g]
SiO_2	(%)	77.7	76.6	74.5	78.2	78.0	77.2	75.7	68.1	91.4	79.8	69.22	70.54	67.98
TiO_2	(%)	0.07	0.07	0.15	0.05	0.06	0.06	0.07	0.29	0.08	0.54	0.47	0.27	0.78
Al_2O_3	(%)	12.0	12.3	11.7	11.4	13.6	12.9	13.9	21.1	4.4	7.7	15.02	13.73	14.85
Fe_2O_3	(%)	0.1	0.8	0.3	0.5	0.3	0.9	0.5	0.8	0.2	0.7	3.65	2.75	6.99
FeO	(%)	0.2	0.2	1.4	0.2	0.7	0	0.4	0	0.6	3.3			
MnO	(%)	0.01	0.03	0.05	0.02	0.03	0.02	0.03	0	0.01	0.03	0.06	0.12	0.03
MgO	(%)	0.2	1.62	0.15	0.48	0.84	0.74	0.7	0.57	0.5	2.53	1.16	1.08	2.38
CaO	(%)	0.13	0.70	1.62	0.40	0.47	0.71	0.42	0	0	0	2.48	1.88	0.70
Na_2O	(%)	3.3	0.15	5.5	3.3	0.1	0	4.2	0.2	0	0	3.52	6	0.50
K_2O	(%)	3.80	3.65	0.33	3.81	3.95	3.91	1.97	6.09	1	1.51	3.60	0.39	1.69
P_2O_5	(%)	0	0	0.01	0	0	0	0.02	0	0	0	0.10	0.02	0.12
S	(%)	NF	NF	NF	NF	NF	NF	NF	NF	NF	0.27			
CO_2	(%)	0.0	1.5	1.3	0.5	0.3	0.6	0.2	0	0.1	0	0.91	2.56	3.96
H_2O	(%)	0.3	1.8	1.8	0.4	1.6	1.8	0.8	2.7	0.4	2.4			
Rb	(ppm)	68	119	12	117	135	134	83	186	35	65	172	6	62
Sr	(ppm)	30	28	123	25	22	19	101	20	<10	13	193	232	103
Ba	(ppm)	204	268	102	115	254	210	715	658	151	247	697	496	345
Zr	(ppm)	120	119	103	117	169	134	82	167	<20	<20	215	115	248
Cr	(ppm)	<5	<5	21	<5	<5	<5	<5	<5	9	463	25	23	219
Co	(ppm)	<10	<10	<10	<10	<10	<10	<10	<10	15	41	ND	ND	ND
Ni	(ppm)	<10	<10	<10	<10	<10	<10	<10	<10	10	253	23	9	71
Cu	(ppm)	<5	7	95	21	8	14	8	8	56	146	17	19	31
V	(ppm)	<20	<20	<20	<20	<20	<20	<20	<20	<20	81	45	34	150
B	(ppm)	<50	<50	<50	<50	<50	<50	<50	<50	51	55	ND	ND	ND
Li	(ppm)	NF	ND	5	ND	ND	ND	8	9	6	22	ND	ND	ND
REE										[h]				

[a] Fresh granite, weathered granite and lithologically distinct, fresh granite cobble from overlying conglomerate at locality A (Fig. 4).
[b] Fresh granite, weathered granite and lithologically similar weathered granite cobble from overlying conglomerate at locality B (Fig. 4). See also photomicrograph in Fig. 10.
[c] Fresh granite and weathered granite at locality C (Fig. 4).
[d] Quartz rich sandstones at unconformity and 60 cm above unconformity, respectively, at locality C (Fig. 4).
[e] Mafic granitoid gneiss 40 km north of Yellowknife (Jenner et al., 1981, sample YK 18).
[f] Granitoid cobble from Jackson Lake Formation at Yellowknife (Jenner et al., 1981, sample YK 16).
[g] Sandstone from Jackson Lake Formation at Yellowknife (Jenner et al., 1981, sample YK 15).
[h] Reported in Table IV.

The basement granite material consists of medium-grained, mafic poor, hypersolvus granite. Quartz has square outlines, feldspars are perthitic and mafic minerals, where present, are large fine grained masses of chlorite or decussate aggregates of biotite, indicating the original biotite has been retrograded and then, with later metamorphism, up-graded to biotite. The rock is characteristically fractured with fillings of mainly white mica, but in some cases chlorite, biotite or carbonate. In the regolith material the feldspar is variably altered to a moderately foliated, fine grained, white mica—quartz—feldspar—minor biotite assemblage in which the largely unaffected quartz is distributed with essentially the same texture as seen in the fresh granite (Fig. 10). In the least altered material, feldspar is better preserved with K-spar being more resistant. In one case the K-spar intergrowths, in what were originally perthite grains, survive in optical continuity although the plagioclase is completely replaced by a white mica, quartzo-feldspathic material and carbonate assemblage. The granite cobbles are more varied with some similar to the fresh granite, others like the regolithic material and still others petrographically distinct with coarse muscovite flakes, coarse chlorite, presumably pseudomorphed after original biotite, and plagioclase in addition to the perthitic feldspars. As at Steep Rock the specific gravity of the altered rocks, at ~ 2.75, is greater than that of the fresh (2.68), indicating that considerable post weathering compression has taken place.

The chemical changes from fresh to weathered granite in general have similar trends to that seen in the profile at Steep Rock Lake. The least altered regolith material (location A, Fig. 4; analyses 1, 2, and 3; Table V), still with perthitic intergrowths evident in the altered feldspars, differs only minimally from the nearby less altered rock. The higher tenor of ferric iron and water, and reduced sodium are indicative of oxidation, hydration and leaching, processes that can be expected during weathering. The increase of calcium, magnesium and carbon dioxide can be explained by the formation of dolomite during diagenesis. The granitoid cobbles in the conglomerate at this locality have a varied composition, reflecting a varied parentage different from the underlying granite as well as weathering effects.

At location B (Fig. 4; analyses 4, 5 and 6; Table V) the regolith and a petrographically very similar cobble from immediately above the unconformity are more altered with the original feldspars replaced by a moderately foliated fine grained matte of white mica, quartz and feldspar (Fig. 10). Chemically, there is a decrease of sodium due to leaching with a concomitant slight increase in aluminum, titanium, zirconium and potassium, and in water due to hydration during weathering. There is also a slight increase in magnesium and iron which may be a similar effect to the abrupt diagenetic increase in ferric iron and magnesium seen at one point in the profile at Steep Rock Lake, although in this case the iron in the regolith is mainly ferrous.

Alteration is most intense at the third locality (C) (Fig. 4; analyses 7 and 8; Table V); even more so than at Steep Rock. Petrographically the regolith

consists of dispersed quartz, with a similar habit as in the nearby relatively fresh granite, in a fine matrix of white mica with little if any quartz and feldspar. The regolith is less foliated at this locality and in some cases the outlines of the original feldspar crystals are visible in the white mica matrix. Chemically, the ferrous iron, magnesium, calcium, strontium and sodium have been leached relative to the less altered granite with a concomitant increase in aluminum, ferric iron, titanium, zirconium and potassium. Water also shows an increase.

The variation in degree of alteration of the regolith is perhaps a reflection of the degree of weathering of the materials preserved at the unconformity. The variation should be expected, as rates of erosion of the weathered rock are likely to vary on a surface with an apparent local relief of as much as 500 m.

At some localities, a lag deposit dominated by coarse angular quartz derived from the erosion of weathered granite (Table V, analyses 9 and 10) occurs immediately above the unconformity. It is similar to rare siliceous debris flow deposits within the volcanic section and the more quartz rich varieties of the crossbedded fluvial sandstones above the volcanics, both of which are thought to be derived in large part from the erosion of the granite regolith. Chemically, this very siliceous deposit is almost identical to similar sandstones above the unconformity at Steeprock profile, both in major oxides and REE content (Table III; analyses 9, 10 and 11). Although the starting materials, a hypersolvus granite at Point Lake and a tonalite at Steep Rock Lake, are compositionally distinct, the similarity of the final product including REE (Table IV; analyses 3-9, 3-10, 3-11 and 5-9) indicates that the processes these materials were exposed to during weathering had a much stronger influence on the composition of the final product than the initial composition of the source materials. In particular, as already discussed with the Steep Rock Lake data, the common assumption that REE proportions are not influenced by the process of weathering should perhaps be re-examined.

In this regard, in a recent study of the geochemistry of the Yellowknife Supergroup near Yellowknife, NWT, 300 km to the south, Jenner et al. (1981) postulate, largely on the basis of rare earth concentrations, that chemically, a fluvial sandstone and conglomerate unit (the Jackson Lake Formation — which is very similar to the conglomerate and sandstone unit of the Keskarrah Formation at Point Lake) form two groups. They suggest that one group (A) was formed from equal amounts of basalt and acid volcanic rocks while the second (B) was derived mainly from felsic volcanics. The basic assumption is that no chemical differentiation of REE occurs during weathering. In the Fig. 11 data (Table V), taken from Jenner et al. (1981), which is derived from a sample of biotite bearing, mafic granitoid gneiss, possibly basement to the Yellowknife Supergroup at Yellowknife (Henderson, 1976), a granitoid cobble and a Jackson Lake sandstone, are presented normalized with respect to the gneiss as though the gneiss were the parent. It can be seen that there is a small enhancement of light rare earths

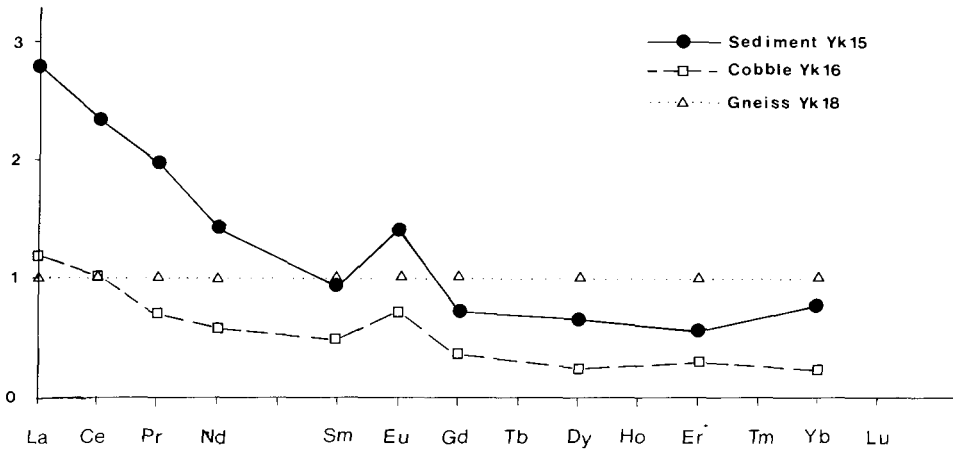

Fig. 11. REE data from a sandstone and granitoid cobble from the Jackson Lake Formation at Yellowknife is normalized against a granitoid mafic gneiss that is thought to be a possible basement to the Yellowknife Supergroup. Note that relative to the possible source rock, the granitoid cobble and the sediment are enriched in the lighter and depleted in the heavier lanthanides. This is similar to the pattern seen in the rare earth data from the profile in the weathered granite below the Steeprock Group. REE data at Yellowknife from Jenner et al. (1981).

and a diminishment of heavy rare earths which is similar to the pattern exhibited by the weathered materials in the profile at Steep Rock Lake (Fig. 9). The major element composition is low in soda and magnesia, and high in alumina, titania, and iron (Table V) which is the trend that would be expected for sediments derived from a deeply weathered granitoid terrane. On examination of the thin sections of the Jackson Lake sandstones (Henderson, 1975) it was noted that most contain abundant chloritoid, a metamorphic mineral which can only occur within a narrow compositional range characterized by large Fe/Mg ratio, high Al, and low K, Na and Ca (Hoschek, 1967). Such compositions are to be expected after weathering or hydrothermal alteration, but since the occurrence of chloritoid is a characteristic of the stratigraphic formation as a whole the weathering origin is preferred. Although predicted by the model of Jenner et al. (1981), no petrographic evidence for the presence of basalt fragments was found. The textures of the metasediments and indeed of the clasts that make up the rock are very much like the sandstones above the unconformity at both Steep Rock Lake and Point Lake. In particular, all contain fine grained clasts of quartz—feldspar—white mica material which has previously been interpreted as being dominantly derived from a felsic volcanic source (Henderson, 1975). This is no doubt true for some of these clasts, particularly those rare examples that have included phenocrysts of quartz or feldspar. However, the textural similarity of this material to the weathered granite below the unconformities at Point Lake and Steep Rock Lake suggests that the input of detritus from a

weathered granitoid terrane may be significant. It is, therefore, suggested that an alternate hypothesis, which incorporates the principle that rare earths are chemically differentiated during weathering and early diagenesis, should perhaps be formulated for these rocks.

Laughland Lake

The occurrence of quartzites, pelites, and aluminous iron rich sediments and chemical sediments in the Prince Albert Group at Laughland Lake illustrate the extreme sedimentary differentiation that has occurred in the region of detritus derived dominantly from the granitoid gneissic basement. Chemical analyses of a suite of metasedimentary rocks collected near the previously described section at Laughland Lake (Table I) are presented in Table VI.

Most of the samples differ from those previously discussed in this paper in that they also contain appreciable amounts of chromium. For example, the quartzite can contain up to 0.24% chrome, which is over a thousand times more than in quartzites from Steep Rock Lake or Point Lake (Table VI, analysis 6-9). Chrome in the iron and aluminum rich, hornblendic and chloritic rocks is 2000 times more abundant than in a somewhat similar silicate iron formation at Point Lake. These very high values of chrome are unusual in rocks of any type other than ultramafics (Shiraki, 1969). In sediments, chrome is usually considered a resistate element as opposed to being introduced by diagenetic solutions. Chrome in igneous rocks is normally present in hundreds of ppm or less and only ultramafics and chromite bearing layered intrusions of tholeiitic parent composition contain the thousands of ppm chrome similar to that seen in these quartzites. It seems reasonable that the bulk of the quartz in the quartzites is the residue after intense weathering of the granitoid gneisses of the Brown River Complex thought to be basement to the group. Contemporaneous weathering of komatiitic flows, ultramafic rocks within the Prince Albert Group itself, would provide an abundant source of chrome (Table VI, analyses 6-10, 6-11).

The aluminous and iron rich sediments are also thought to be influenced by the komatiites, mainly through the input of weathered detritus derived from these unusual rocks. For example, the preserved komatiites show a magnesium to chrome ratio of ~ 130, whereas in these sediments it is as low as 17. This represents a depletion of up to 10 fold of magnesium and suggests chemical weathering of the source rocks took place by freshwaters in a non-marine milieu. Removal, during weathering, of easily dissolved ions, like magnesium, would proportionately increase the more insoluble elements such as chromium, titanium, aluminum and iron. The fact that both the titania/alumina and total iron/alumina ratios remain similar to that in the average komatiite from the Prince Albert Group (although their absolute concentrations have increased markedly) supports the hypothesis that these rocks are in part derived from considerably leached komatiitic detritus.

Chloritoid, which occurs in some of the metasedimentary units suggests a

TABLE VI

Chemical analyses — Laughland Lake area (ND = not determined)

		Sample No.										
		6-1[a]	6-2[a]	6-3[a]	6-4[a]	6-5[a]	6-6[a]	6-7[a]	6-8[a]	6-9[b]	6-10[c]	6-11[d]
SiO_2	(%)	39.00	52.20	80.00	56.70	90.20	54.20	37.60	73.7	96.8	43.30	40.7 ± 8.7
TiO_2	(%)	0.15	0.69	0.42	1.00	0.16	0.68	0.58	0.24	0.03	0.29	0.26± 0.07
Al_2O_3	(%)	2.20	10.00	11.20	11.50	6.36	7.60	9.10	6.8	1.63	6.90	5.6 ± 2.1
Fe_2O_3	(%)	2.60	9.20	0.76	4.30	0.50	4.50	2.9	2.5	0.10	0.35	2.8 ± 1.4
FeO	(%)	7.10	13.30	3.20	12.30	0.47	15.4	9.8	8.7	0.85	7.60	6.4 ± 1.8
MnO	(%)	0.24	0.57	0.07	0.37	0	0.95	0.27	0.02	0.02	0.19	0.19± 0.05
MgO	(%)	27.70	5.20	0.38	3.7	0.42	6.6	7.7	1.9	0.32	26.70	27.6 ± 5.0
CaO	(%)	2.30	0.20	0.34	1.5	0.05	5.5	18.8	0.47	0.06	7.10	5.5 ± 2.5
Na_2O	(%)	0.05	0.04	0.34	0.13	0.20	0.23	0.97	5.2	0.3	0.13	0.13± 1.0
K_2O	(%)	0.01	0.20	1.60	1.7	1.69	0.25	0.19	3.3	0.34	0.04	0.03± 0.05
P_2O_5	(%)	0.03	0.03	0.31	0.04	0.05	0.07	0.07	0.14	0.03	0.04	0.04± 0.01
S	(%)	0.04	1.90	0.03	0.05	0	0.19	0.07	0.04	0	0.02	0.1 ± 0.1
CO_2	(%)	13.00	0.00	0	0	0	0.59	8.3	0	0	5.80	0.02± 0.03
H_2O	(%)	5.00	5.10	1.60	5.1	0.9	2.2	2.4	1.5	0.4	0	6.2 ± 2.3
C	(%)	ND	0.04	0.35	0.11	ND	ND	ND	0.05	ND	ND	ND
Sr	(ppm)	24	<20	440	270	60	74	88	46	<20	21	e
Ba	(ppm)	<20	38	1000	640	120	68	39	390	20	<20	e
Zr	(ppm)	<20	NF	100	ND	60	72	<20	140	<20	<20	ND
Cr	(ppm)	4100	3400	72	4200	350	3100	4300	17	2400	2500	2330 ± 930
Co	(ppm)	94	74	<10	140	<10	130	110	<10	<10	50	80 ± 20
Ni	(ppm)	990	1000	56	1400	<10	1500	47	<10	19	770	1210 ± 560
Cu	(ppm)	36	58	<5	<5	12	80	160	<5	13	90	60 ± 120
V	(ppm)	10	250	110	280	30	240	380	30	64	170	150 ± 60
B	(ppm)	<50	<50	190	100	<50	<50	<50	<50	<50	<50	e
Zn	(ppm)	80	700	41	210	33	250	71	47	<20	66	e
Sc	(ppm)	13	370	11	31	<10	300	31	<10	<10	25	20 ± 10

[a] From units noted in section in Prince Albert Group (Table I).
[b] Quartzite with high chrome content 30 km northeast of section (Figs. 5,6)
[c] Metakomatiite 50 km east of section (Figs. 5,6).
[d] Average of 26 metakomatiites, Prince Albert Group.
[e] Values are lower than detection limit of method used.

weathered or altered protolith since, as was discussed for the example at Yellowknife, the mineral only forms within a restricted compositional range that includes a relatively high Fe/Mg ratio, high Al and low K, Na and Ca (Hoschek, 1967), which are compositions characteristic of weathered materials.

The low ferric/ferrous ratios of the metasediments of the Prince Albert Group should not be taken as a reflection of environmental conditions at the time of deposition. Metamorphic processes commonly have the effect of reducing the iron in sedimentary rocks (Shaw, 1956). Graphitic material still persists in some of the Prince Albert pelites, so it seems likely that the oxidation of originally more abundant graphite during diagenesis and metamorphism (Thompson, 1972) has reduced the iron in the associated aluminous iron rich rocks as well as in the pelites.

The conditions of tectonic stability implied by the abundance of mature quartzite and aluminous iron rich sediments at Laughland Lake differ from the dominantly volcanogenic facies seen at both Steep Rock and Point Lake. Nevertheless, the processes of weathering and later diagenesis in all three areas under consideration were similar. Leaching of magnesium led to the enhancement of chrome, titanium, aluminum and iron while hydration and oxidation led to the development of clay minerals. Subsequent different sedimentational histories in the various areas led to the present variety of rock types.

CONCLUSIONS

The processes of subaerial Archean weathering of granitoid basement rocks and subsequent diagenesis of both the regolith and its eroded and deposited detritus are similar in each of three widely separated localities on the Canadian Shield. The processes involved include leaching, oxidation and hydration of certain elements leading to concomitant increases in the relatively immobile elements.

There is no need to postulate that different weathering and/or ground water systems, were operative during the Archean, compared to more recent times. For example, a comparison of the iron, aluminum and titanium behavior in weathered profiles of various ages shows no large change with decreasing age (Fig. 12). On the other hand the mere presence of ferric iron doesn't necessarily demonstrate an Archean oxygenic atmosphere since oxidation of iron occurs at very low oxygen activity. The complicated weathering and diagenetic history that a subsiding granitoid surface undergoes relies as much or more on the flux of diagenetic waters and the buffering capacity of the enclosing rock mass as on the atmospheric conditions prevalent at the time of weathering. Hence, weathering profiles, old and new, are more a response to local environmental conditions within the weathered system than the composition of the atmosphere.

In general, Archean weathering profiles are represented by metamorphic mineral assemblages that have replaced the weathering and diagenetic miner-

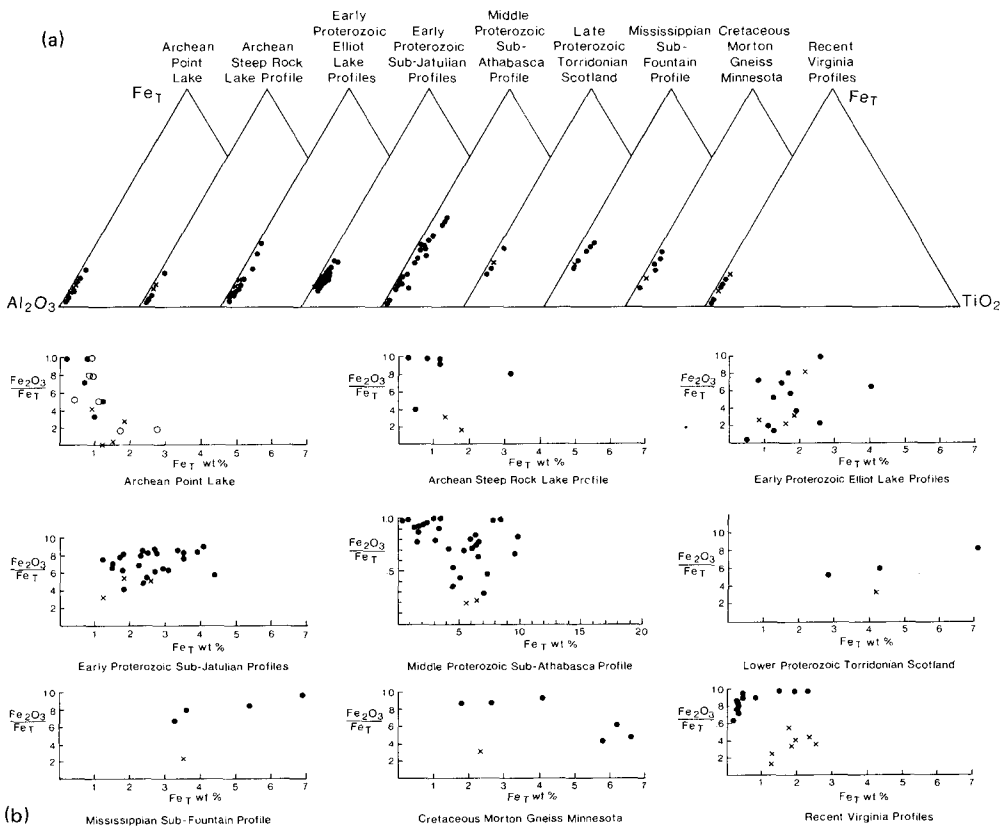

Fig. 12. (a) Comparison of iron—aluminum—titanium behavior in weathered granitic rocks of various ages. Note that there is no apparent change with decreasing age. (b) Comparison of oxidation ratio with total iron in the same rock suites. Source of data as follows: Point Lake (this paper), Steep Rock Lake (this paper), Elliot Lake (Gay and Grandstaff, 1980; Pienaar, 1963; Roscoe, 1969), Jatulian (Koryakin, 1971), Athabaska (Fahrig, personal communication, 1981), Torridonian (Williams, 1968), Fountain (Wahlstrom, 1948), Morton (Goldich, 1938), Virginia (Gardner et al., 1980). Dots indicate weathered materials; x, fresh materials; and circles, boulders of basement in overlying sediments.

alogy such that the composition of the rock at the time of metamorphism is effectively sealed by the crystallization of the metamorphic mineral assemblage. The presence of minerals formed during weathering, such as montmorillonite, in such an assemblage suggests that post metamorphic weathering has taken place.

On the basis of the rare earth data from Steep Rock Lake there has been a shift in the proportion of lanthanoids in the weathered materials compared to fresh rock which is shown by an increase in the lighter elements and a decrease in the heavier ones. This chemical differentiation is similar to that seen elsewhere in a variety of weathering and diagenetic contexts of varied ages.

The sedimentary accumulations are different at each of the three locations, although all have certain features in common. Quartzites or quartz rich rocks are present in each, implying that thorough subaerial chemical weathering has taken place. The presence of carbonate beds in each of the areas which may be calcitic, dolomitic or, more rarely, sideritic implies varied chemical conditions in the sedimentary environment during sedimentation and/or diagenesis. The common occurrence of graphite bearing pelitic rocks might suggest that any reduction in these and adjacent beds was controlled by the oxidation of carbon during metamorphism. Indeed Rankama's (1955) evidence for a reduced atmosphere during the early history of the Earth, based on the lack of evidence for oxidation of diorite cobbles in a graphite rich matrix at Suodenniemi, Finland, may be more a result of the reduction of iron and concomitant oxidation of carbon compounds during the amphibolite grade metamorphism of these rocks.

The occurrence of the metamorphic mineral chloritoid within stratigraphic units at two of the localities discussed may be reflection of strong chemical weathering of the source terrane of the sediments in which the mineral is found. The products of chemical weathering tend to have a high Fe/Mg ratio, and a high Al and low K, Na, and Ca content which are the compositional constraints required for the formation of this mineral (Hoschek, 1967). Other chloritoid bearing metasediments should perhaps be considered with this in mind.

Clasts in meta-sandstones derived from the weathered granitoid terranes commonly consist, in part, of amoeboid grains of fine grained, quartzo-feldspathic material and white mica that represents altered feldspars. These grains bear a strong resemblance to meta-dacitic clasts and are difficult to differentiate without additional criteria, such as included phenocrysts of quartz or feldspar. This should be considered, for example, in the interpretation of some greywacke suites where the relative proportion of granitoid to volcanogenic components may not be appreciated.

ACKNOWLEDGEMENTS

We thank the staff of the Caland Ore Co. Ltd. and Steep Rock Iron Mines Ltd., and we appreciate the guidance of Dr. J.M. Franklin in the Steep Rock Lake area, who also critically read an earlier version of this paper. Discussion with Drs. R.V. Kirkham and S.M. Roscoe during the preparation of this paper helped to focus many of the ideas expressed here.

REFERENCES

Augustithis, S.S. and Ottemann, J., 1966. On diffusion rings and spheroidal weathering. Chem. Geol., 1: 201—204.

Awramik, S.M., 1982. Biogeochemical evolution of the ocean atmosphere system; state of the art report. In: H.D. Holland and M. Schidlowski (Editors), Mineral Deposits and the Evolution of the Biosphere. Dahlem Conferenzen, Berlin, Springer-Verlag, Berlin, pp. 309—320.

Baragar, W.R.A., Plant, A.G., Pringle, G.J. and Schau, M., 1979. Diagenetic and post-diagenetic changes in the composition of an Archean pillow. Can. J. Earth Sci., 16: 2102—2121.

Bartley, M.W., 1948. Steep Rock Iron Mine. In: M.E. Wilson (Editor), Structural Geology of Canadian Ore Deposits. Canadian Institute of Mining and Metallurgy, Montreal, pp. 419—421.

Berner, R.A., 1971. Principles of Chemical Sedimentology. McGraw Hill, Toronto, 240 pp.

Bostock, H.H., 1980. Geology of the Itchen Lake Area, District of Mackenzie. Geol. Surv. Can. Mem. 391, 101 pp.

Burkov, V.V. and Podborina, I.K., 1971. Some geochemical characteristics of rare (trace) elements in weathering crusts. Lithol. Miner. Resour., 6: 437—445.

Button, A. and Tyler, N., 1979. Precambrian paleo-weathering and erosion surfaces in Southern Africa: review of their character and economic significance. Information Circular 135, Econ. Geol. Res. Unit, Univ. Witwatersrand, Johannesburg, 37 pp.

Christie, O.H.J. and Roaldset, E., 1979. Geochemical behavior of lanthanoid elements in some clays and bauxite. Geochem. J., 13: 11—14.

Church, S.E., 1981. Multi-element analysis of fifty-four geochemical reference samples using inductively coupled plasma-atomic emission spectrometry. Geostandards Newsletter, 5: 133—160.

Cloud, P., 1980. Early biogeochemical systems. In: M.R. Trudinger, M.R. Walter and B.J. Ralph (Editors), Biogeochemistry of Ancient and Modern Environments. Springer-Verlag, Berlin, pp. 7—27.

Cotton, F.A. and Wilkinson, G., 1962. Advanced Inorganic Chemistry. Interscience Publishers, New York, 959 pp.

Duddy, I.R., 1980. Redistribution and fractionation of rare-earth and other elements in a weathering profile. Chem. Geol., 30: 363—381.

Easton, R.M., Boodle, R.L. and Zalusky, L., 1982. Evidence for gneissic basement to the Archean Yellowknife Supergroup in the Point Lake Area, Slave Structural Province, District of Mackenzie, N.W.T. In: Current Research, Part B, Geol. Surv. Can. Pap., 82-1B: 33—41.

Eckstrand, O.R., 1975. Nickel potential of the Prince Albert Group N.W.T. In: Report of Activities. Part A, Geol. Surv. Can. Pap., 75-1A: 253—255.

Fisher, W.R. and Schwertmann, U., 1975. The formation of hematite from amorphous iron (II) hydroxide. Clays Clay Miner., 23: 33—37.

Frey, M., 1978. Progressive low-grade metamorphism of a black shale formation, central Swiss Alps, with special reference to pyrophyllite and margarite bearing assemblages. J. Petrol., 19: 93—135.

Gardner, L.R., Kheoruenromne, I. and Chen, H.S., 1978. Isovolumetric geochemical investigation of a buried granite saprolite near Columbia, S.C., U.S.A. Geochim. Cosmochim. Acta, 42: 417—424.

Garrels, R.M. and McKenzie, F.T., 1967. Origin of the chemical compositions of some springs and lakes. In: R.F. Gould (Editor), Equilibrium Concepts in Natural Water Systems. Adv. Chem., 67: 222—242.

Gay, A.L. and Grandstaff, D.E., 1980. Chemistry and mineralogy of Precambrian paleosols at Elliot Lake, Ontario, Canada. Precambrian Res., 12: 349—373.

Girin, Y.V., Balashov, Yu. A. and Bratishko, R.Kh., 1979. Redistribution of the rare earths during diagenesis of humid sediments. Geochem. Int., 11: 438—452.

Gladney, E.S. and Goode, W.E., 1981. Elemental concentrations in eight new United States Geological Survey Rock Standards: a review. Geostandards Newsletter, 5: 31—64.

Goldich, S.S., 1938. A study of rock weathering. J. Geol., 46: 17—23.

Goldich, S.S., Nier, A., Baadsgaard, H., Hoffman, J.H. and Krueger, H.W., 1961. The Precambrian geology and geochronology of Minnesota. Minn. Geol. Surv., Bull. 41, 193 pp.

Helgeson, H.C., Delany, J.M., Nesbitt, H.W. and Bird, D.K., 1978. Summary and critique of the thermodynamic properties of the rock forming minerals. Am. J. Sci., 278-A: 1—229.

Henderson, J.B., 1975. Sedimentology of the Archean Yellowknife Supergroup at Yellowknife, District of Mackenzie. Geol. Surv. Can. Bull. 246, 62 pp.
Henderson, J.B., 1976. Geology of the Yellowknife Map Area, District of Mackenzie. Geol. Surv. Can., Open File 353.
Henderson, J.B., 1981. Archean basin evolution in the Slave Province, Canada. In: A. Kroner (Editor), Precambrian Plate Tectonics. Developments in Precambrian Geology 4. Elsevier, Amsterdam, pp. 213—235.
Henderson, J.B. and Easton, R.M., 1977. Archean supracrustal — basement rock relationships in the Keskarrah Map-area, Slave Structural Province, District of Mackenzie. In: Report of Activities, Part A; Geol. Surv. Can. Pap. 77-1A: 217—221.
Herrmann, A.G., 1969. Yttrium (39) and lanthanides (57-71). In: K.H. Wedepohl (Editor), elements La(57) to U(92). In Handbook of Geochemistry. Vol. II/5, Springer-Verlag, New York.
Heywood, W.W. and Schau, M., 1978. A subdivision of the Northern Churchill Structural Province. In: Current Research. Part A, Geol. Surv. Can. Pap. 78-1A: 139—149.
Hicks, H.S., 1950. Geology of the iron deposits of Steep Rock Iron Mines Limited. The Precambrian, 23: 8—10, 13.
Hofmann, H.J., 1971. Precambrian fossils, pseudofossils and problematica in Canada. Geol. Surv. Can. Bull. 189, 146 pp.
Hofmann, H.J., 1981. Precambrian fossils in Canada — the 1970's in retrospect. In: F.H.A. Campbell (Editor), Proterozoic Basins of Canada. Geol. Surv. Can. Pap., 81-10: 419—444.
Hoschek, G., 1967. Untersuchungen zum Stabilitatsbereich von Chloritoid und Staurolith. Contrib. Mineral. Petrol., 14: 123—162.
Hower, J., Eslinger, E.V., Hower, M. and Perry, E.A., 1976. Mechanism of burial metamorphism of argillaceous sediment: 1. Mineralogical and chemical evidence. Geol. Soc. Am. Bull., 87: 725—737.
Jenner, G.A., Fryer, B.J. and McLennan, S.M., 1981. Geochemistry of the Archean Yellowknife Supergroup. Geochim. Cosmochim. Acta, 45: 1111—1129.
Jolliffe, A.W., 1955. Geology and iron ores of Steep Rock Lake. Econ. Geol., 50: 373—398.
Jolliffe, A.W., 1966. Stratigraphy of the Steeprock Group, Steep Rock Lake, Ontario. In: A.M. Goodwin (Editor), The Relationship of Mineralization to Precambrian Stratigraphy in Certain Mining Areas of Ontario and Quebec. Geol. Assoc. Can. Spec. Pap., 3: 75—98.
Koryakin, A.S., 1971. Results of a study of Proterozoic weathering crusts in Karelia. Int. Geol. Rev., 13: 973—980.
Krogh, T.E. and Gibbins, W., 1978. U—Pb isotopic ages of basement and supracrustal rocks in the Point Lake area of the Slave Structural Province, Canada. Abstr. with Programs, Geol. Assoc. Can., 3: 438.
Langmuir, D., 1971. Particle size effects on the reaction goethite = hematite + water. Am. J. Sci., 271: 147—156.
Lawson, A.C., 1912. Geology of Steep Rock Lake, Ontario. Geol. Surv. Can. Mem. 28, 10 pp.
Lepp, H. and Goldich, S.S., 1964. Origin of Precambrian iron formations. Econ. Geol., 59: 1025—1060.
Loubet, M. and Allegre, C.J., 1977. Behavior of the rare elements in the Oklo Natural Reactor. Geochim. Cosmochim. Acta, 41: 1539—1548.
Loughnan, F.C., 1969. Chemical weathering of the silicate minerals. Elsevier, Amsterdam, 154 pp.
Mazzucotelli, A. and Vannucci, R., 1980. Candoluminescence emission analysis of cerium in thirty-six international geochemical reference samples. Geostandards Newsletter, 4: 149—151.
McInnes, W., 1899. On the geology of the area covered by the Seine River and Lake Shebandowan Map-sheets. Annual Report 1897, Geol. Surv. Can., 10: 1—65.

McIntosh, J.R., 1972. The Caland Ore Company Limited deposit, a geological description. In: Geology of the Steep Rock Lake Area, District of Rainy River. Part 2, Ontario Dept. Mines North. Aff. Geol. Rep. 93: 81—105.

McLennan, S.M. and Taylor, S.R., 1980. Geochemical standards for sedimentary rocks: trace-element data for USGS Standards SCo-1, MAG-1 and SGR-1. Chem. Geol., 29: 333—343.

Moore, E.S., 1940. Geology and ore deposits of the Atikokan area. Ont. Dept. Mines, 48: 1—34.

Murray, J.W., 1979. Iron oxides. In: R.G. Burns (Editor), Marine Minerals. Rev. Mineral., 6: 47—98.

Nesbitt, H.W., 1979. Mobility and fractionation of rare earth elements during weathering of a granodiorite. Nature, 279: 206—210.

Perkins, D., III, Essene, E.J., Westrum, E.F., Jr. and Wall, V.J., 1979. New thermodynamic data for diaspore and their application to the system Al_2O_3—SiO_2—H_2O. Am. Mineral., 64: 1080—1090.

Pienaar, P.J., 1963. Stratigraphy, petrology and genesis of the Elliot Group, Blind River, Ontario, including the uraniferous conglomerate. Geol. Surv. Can. Bull. 83, 140 pp.

Rankama, K., 1955. Geologic evidence of chemical composition of the Precambrian atmosphere. In: A. Poldervaart (Editor), Crust of the Earth (a symposium). Geol. Soc. Am. Spec. Pap., 62: 651—664.

Riley, R.A., 1969. The character and origin of the Steeprock Buckshot. M.Sc. Thesis, Department of Geology, Queen's University, Kingston, Ontario.

Roberts, H.M. and Bartley, M.W., 1943. Replacement hematite deposits, Steep Rock Lake, Ontario. Trans. Can. Inst. Min. Metall., 46: 342—374.

Roscoe, S.M., 1969. Huronian rocks and uraniferous conglomerates. Geol. Surv. Can. Pap. 68-40, 205 pp.

Rosenberg, R.J. and Zilliacus, R., 1980. Instrumental neutron activation determination of 23 elements in 8 new USGS standard rocks. Geostandards Newsletter, 4: 191—198.

Rubey, W.W., 1964. Geologic history of seawater, an attempt to state the problem. In: P.J. Brancazio and A.G.W. Cameron (Editors), The Origins and Evolution of Atmospheres and Oceans. Wiley, New York, pp. 1—63.

Schau, M., 1977. Komatiites and quartzites: the Archean Prince Albert Group. In: W.R.A. Baragar, L. Coleman and J. Hall (Editors), Volcanic Regimes in Canada. Geol. Assoc. Can. Spec. Pap. 16: 341—354.

Schau, M., 1978. Metamorphism of the Prince Albert Group, District of Keewatin. In: J.A. Fraser and W.W. Heywood (Editors), Metamorphism in the Canadian Shield. Geol. Surv. Can. Pap., 78-10: 203—213.

Schau, M., 1983. Geology of the Prince Albert Group in parts of Walker Lake and Laughland Lake, District of Keewatin. Geol. Surv. Can. Bull. 337, 62 pp.

Schidlowski, M., 1982. Content and isotopic composition of reduced carbon in sediments. In: H.D. Holland and M. Schidlowski (Editors), Mineral Deposits and the Evolution of the Biosphere. Dahlem Konferenzen, Berlin, Springer-Verlag, Berlin, pp. 103—122.

Schmalz, R.F., 1959. A note on the system Fe_2O_3—H_2O. J. Geophys. Res., 64: 575—579.

Sen Gupta, J.G., 1976. Determination of lanthanides and yttrium in rocks and minerals by atomic-absorption and flame-emission spectrometry. Talanta, 23: 343—348.

Sen Gupta, J.G., 1977. Determination of traces of rare earth elements, yttrium and thorium in several international geological reference samples and comparison of data with other published values. Geostandards Newsletter, 1: 149—155.

Sen Gupta, J.G., 1981. Determination of yttrium and rare-earth elements in rocks by graphite furnace atomic-absorption spectrometry. Talanta, 28: 31—36.

Sen Gupta, J.G., 1982. Flame and graphite furnace atomic absorption and optical-emission spectroscopic determination of yttrium and rare-earth contents of sixteen international reference samples of rocks and coal. Geostandards Newsletter, 6: 241—248.

Shaw, D.M., 1956. Geochemistry of pelitic rocks, Part III. Major elements and general geochemistry. Geol. Soc. Am. Bull., 61: 191—234.
Shiraki, K., 1969. Chromium (24). In: K.H. Wedepohl (Editor), Elements Cr(24) to Br (35); Handbook of Geochemistry. Vol II/3, Springer-Verlag, New York.
Shklanka, R., 1972. Geology of the Steep Rock Lake area. In: Geology of the Steep Rock Lake Area, District of Rainy River. Part 1, Ont. Dept. Mines North. Aff. Geol. Rep. 93, 80 pp.
Smith, W.H.C., 1893. Archean Rocks west of Lake Superior. Bull. Geol. Soc. Am., 4: 333—348.
Smyth, H.L., 1891. Structural geology of Steep Rock Lake, Ontario. Am. J. Sci., 42: 317—331.
Stockwell, C.H., 1933. Great Slave Lake—Coppermine River area, Northwest Territories. Geol. Surv. Can. Summary Rep. 1932, Part C, pp. 37—63.
Tanton, T.L., 1941. Origin of the hematite deposits at Steep Rock Lake Ontario. Trans. R. Soc. Can., Ser. 3, 35: 131—141.
Thompson, J.B., Jr., 1972. Oxides and sulphides in regional metamorphism of pelitic schists. 24th Int. Geol. Congress, Sect. 10, Montreal, pp. 27—35.
Thrierr-Sorel, A., Larpin, J-P. and Mougin, G., 1978. Étude Cinétique de la Transformation de la Goethite α-FeOOH en Hematite α-Fe_2O_3. Ann. Chim. Français, 3: 305—315.
Turner, P., 1980. Continental Red Beds. Developments in Sedimentology 29. Elsevier, Amsterdam, 562 pp.
Wahlstrom, E.E., 1948. Pre-Fountain and recent weathering on Flagstaff Mountain near Boulder, Colorado. Geol. Soc. Am. Bull., 59: 1173—1190.
Wanless, R.K., 1979. Geochronology of Archean rocks of the Churchill Province. Abstr. with Program, Geol. Assoc. Can., 4: 85.
Williams, G.E., 1968. Torridonian weathering and its bearing on Torridonian Paleoclimate and source. Scott. J. Geol., IV: 164—183.
Wright, C.M., 1959. Pyrite zones in the hanging-wall of the Steeprock Ore Zone. M.Sc. Thesis, Department of Geology, Queen's University, Kingston, Ontario.

PEDOGENETIC AND DIAGENETIC FABRICS IN THE UPPER PROTEROZOIC SARNYÉRÉ FORMATION (GOURMA, MALI)*

JANINE BERTRAND-SARFATI and ALEXIS MOUSSINE-POUCHKINE

Centre Géologique et Géophysique, Place E. Bataillon, U.S.T.L., 34060 Montpellier (France)

ABSTRACT

Bertrand-Sarfati, J. and Moussine-Pouchkine, A., 1983. Pedogenetic and diagenetic fabrics in the Upper Proterozoic Sarnyéré formation (Gourma, Mali). Precambrian Res., 20: 225—242.

Several diagenetic fabrics are described in the uppermost member of the Sarnyéré formation, an Upper Proterozoic dolomite (700—600 Ma). Micronodular micrite, microsparite showing nodulisation processes, orbicular crusts and oncoids are thought to be due to the pedogenetic alteration of an algal (Porostromata) boundstone. Further evolution in a vadose zone creates a network of cavities which are later filled by "cave stromatolites", micropopcorn micrite and multilayered cements. A rhythmical repetition of facies evidences a polyphased pedogenetic history, leading to a 30 m thick highly complex section. Such numerous and diversified structures are rarely preserved, especially in Proterozoic rocks, but each of them have equivalents in recent examples of caliche soil profiles.

INTRODUCTION

During the course of studies carried out on the Upper Proterozoic carbonate sedimentation of the Gourma (northern Mali), evidence was found which suggests that some structures apparent in the carbonate platform deposits of the Sarnyéré formation are of pedogenetic origin, due to subaerial exposure and related vadose processes. Similar profiles, commonly appearing near the surface in recent arid to semi-arid regions are known as caliche or calcareous crusts (Reeves, 1970). Indurated parts of caliche deposits are called "calcrete" and such carbonates are usually developed under a soil cover.

GEOLOGICAL SETTING

The Gourma basin lies to the south of the loop of the River Niger in eastern Mali. It crops out on the south-eastern part of the Taoudenni basin, which is the sedimentary cover of the West African craton. The Gourma is considered nowadays as an aulacogen, located perpendicular to the Pan-African suture (Fig. 1; Moussine-Pouchkine and Bertrand-Sarfati, 1978; Black et

*Contribution C.G.G. No. 83.20.

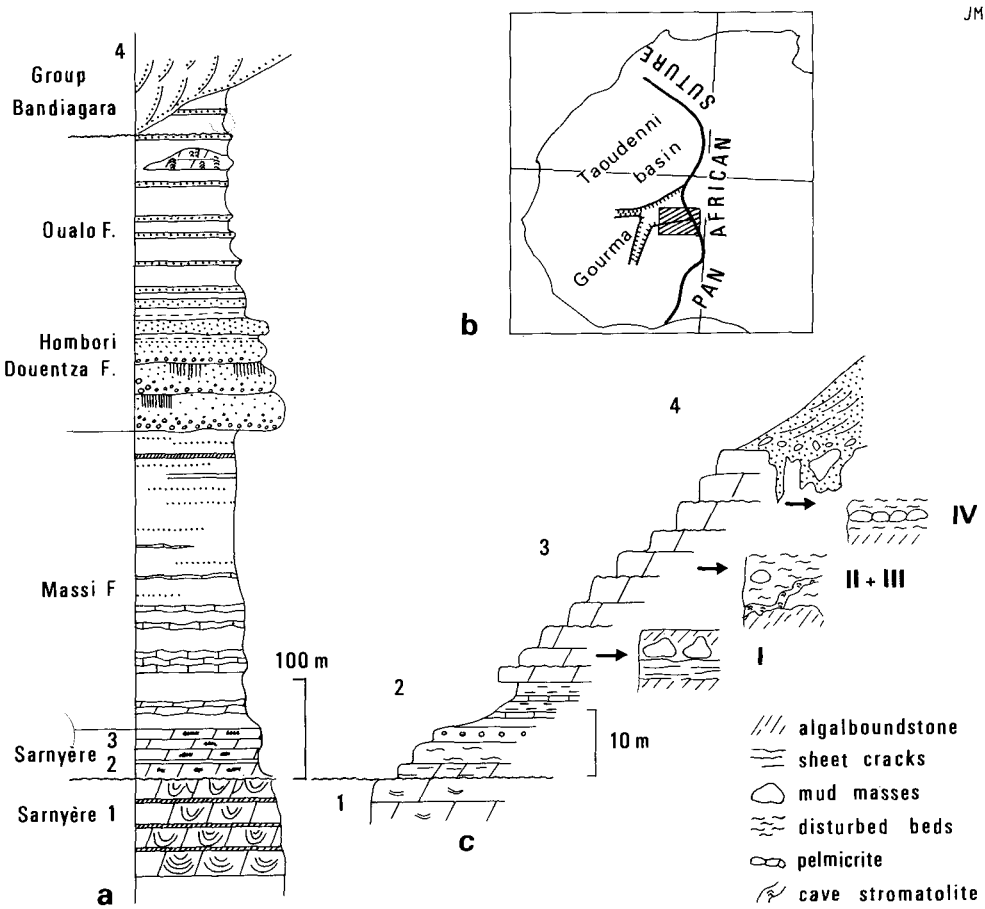

Fig. 1. Geographic location and stratigraphic setting. (a) Synthetic section of the Late Proterozoic (Ediacarian?) sediments on the south edge of Gourma. (b) Structural position of the Gourma basin. (c) Section of the upper part of the Sarnyéré Formation: (1) microbially laminated dolomite ending with subaerially exposed surface; (2) shales and microbial mats; (3) uppermost member studied herein (I to IV are the groups of facies described in the text); (4) Bandiagara sandstones disconformity.

al., 1979; Lesquer and Moussine-Pouchkine, 1980). It has a WSW—ENE direction. The Pan-African orogeny has affected the sediments of the Gourma (600 Ma).

The sedimentary record (8000 m in the central part of the basin) begins with silici-clastic deposits, then carbonates, largely transgressive towards the south, are overlaid by another silici-clastic episode. In the south-west of the basin, the fluviatile sandstones of the Bandiagara group rest unconformably (Fig. 1) over diverse formations of the underlying group (Bertrand-Sarfati and Moussine-Pouchkine, 1978).

The age of the Gourma sedimentary sequence is not known exactly. It is certainly older than 600 Ma, when the Pan-African orogeny ended. It was

usually accepted (Reichelt, 1972) that the Gourma sediments and the base of the sedimentary cover of the Taoudenni basin were contemporaneous (between 1000 and 780 Ma; Clauer, 1976). They are now considered to be late Upper Proterozoic (Ediacarian; Cloud and Glaessner, 1982), based on the fact that they contain calcareous algae unknown in older rocks (Bertrand-Sarfati, 1979). These algae have been found in carbonates in two different areas of the Gourma sediments (Bertrand-Sarfati and Moussine-Pouchkine, 1983).

The Sarnyéré dolomite formation

The Sarnyéré dolomites outcrop on the flank of the Sarnyéré Mountain which is a mesa (or a gara; 900 m high) made up of coarse fluviatile Bandiagara sandstones. Except for this preserved section (150 m high), the formation usually disappears under the recent lateritic cover. The dolomites of the Sarnyéré formation were deposited in a quiet protected tidal environment (Fig. 1). Three types of facies have been described (Bertrand-Sarfati and Moussine-Pouchkine, 1983).

(1) A basal, microbially laminated dolomite (Moussine-Pouchkine and Bertrand-Sarfati, 1980) is deposited in intertidal to supratidal environments with evidence of subaerial exposure (karstic features) and can be recognized over tens of kilometres, parallel to the shoreline. The subaerial exposure is, therefore, a large scale regional event.

(2) A transgressive sequence of microbial mats followed by detrital dolomites and clays.

(3) The uppermost dolomite is composed of an algal boundstone which has been periodically submitted to subaerial exposure, resulting in a cortege of pedogenetic and diagenetic structures. At the Sarnyéré section (Fig. 1), this member is unconformably overlain by the Bandiagara sandstones.

DESCRIPTION OF FACIES

This study is focused on the subaerial fabrics discovered in the uppermost Sarnyéré dolomite. We will describe four different groups of facies:

(1) an algal boundstone with a micrite matrix and micrite masses;

(2) a complex group of facies composed of layered orbicular crusts and oncoids, scattered masses of microsparite, together with relicts of Porostromata boundstones and pelmicrite with microfissures.

(3) large planar cavities filled with "cave stromatolites" and various cements;

(4) pelmicrite with microfissures.

The second and the third groups of facies are found in the same disturbed beds, but they are not contemporaneous. These disturbed beds overlay, without noticeable disconformity (Fig. 2b, c), layers of Porostromata boundstone and they present an uneven complex layered texture, long planar cracks with cement (Fig. 2c), and planar cavities filled with sediment (Fig. 2d,e).

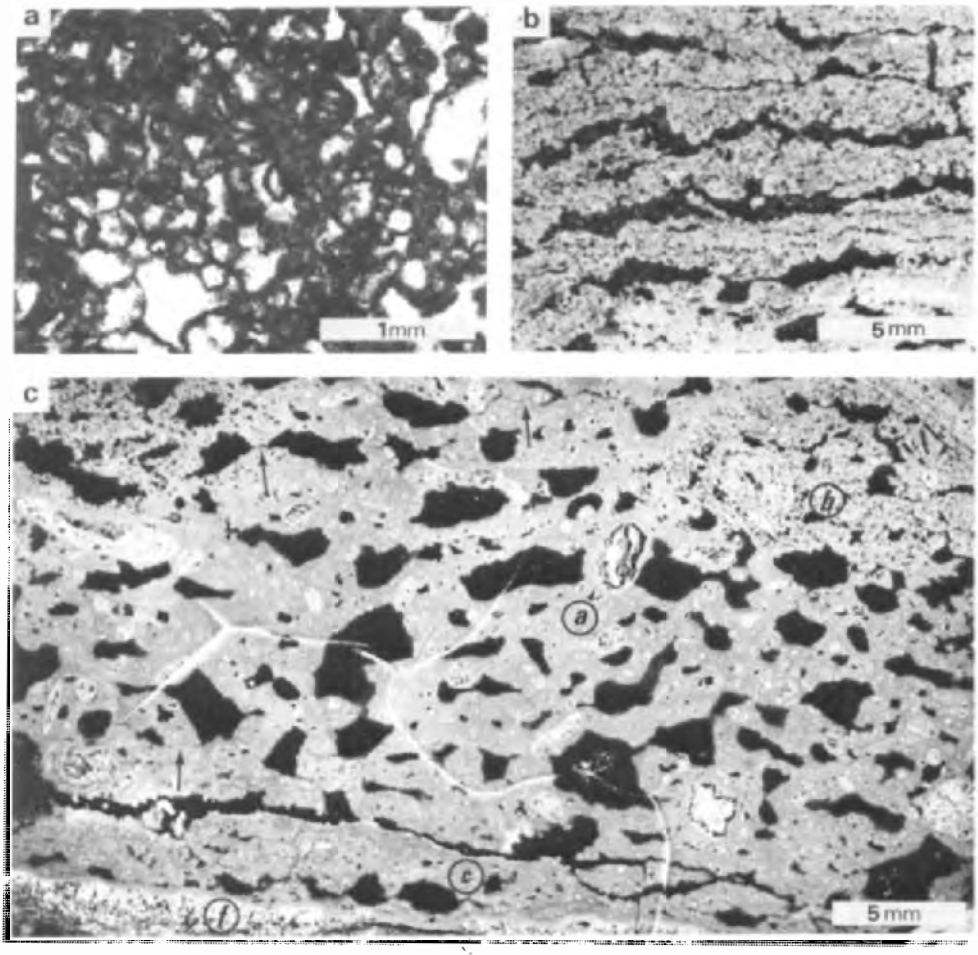

Fig. 2. Porostromata boundstone and micrite masses. (a) Porostromata boundstone with associated micrite showing the primary porosity (thin section). (b) Laminoid voids superimposed on the Porostromata boundstone (negative print). (c) Micrite masse with coated grains: flat and altered surface (*f*) of the underlying Porostromata boundstone (see Fig. 3a), note the micrite coating; numerous coated round grains of different size; micrite coating (*a*) around an altered element, oncoid (*b*) derived from in situ alteration of the overlaying Porostromata; voids of various size and shape (arrow indicates the thin planar connections). The sheet crack (*c*) is secondary in respect to the other voids (negative print).

First group of facies

Algal boundstone and associated micrite

This is a poorly laminated dolomite deposited in a shallow subtidal environment (Bertrand-Sarfati and Moussine-Pouchkine, 1983). In thin section, an abundant micrite matrix is associated with an algal boundstone. The boundstone is composed of an aggregate of cells having micritic walls and,

most of the time, a subcircular section, also showing short elongated sections (30—50 μm). This structure is attributed to interwoven short tubes or cells of algae considered to be Porostromata (Pia, 1927; Monty, 1981a) and is supposed to have borne a calcareous skeleton (Fig. 2a). Tiny fenestrae are interspersed among the boundstone and these are related to biological activity; Porostromata growth (axial voids of the tubes or primary porosity between interlacing tubes), or the decay of colonies of unicells. Their sizes range from 20 to 100 μm. Higher up in the bed, a pseudo-lamination is defined by laminoid voids which may reach tens of centimeters and stay parallel to the bedding (Fig. 2b). They do not present traces of enlargement by vadose solution and they do not usually contain internal sediments.

Micrite masses

Discrete masses of micrite are found in the Porostromata boundstone (Fig. 3a). They have a flat bottom and a roughly globular shape. They rest, on the flat eroded and reddened surface of the underlying dessicated Porostromata boundstone. The discrete masses are made of micrite with numerous angular voids and they contain loose coated clasts (wackestone) of Porostromata boundstone (Fig. 2c) ranging from isolated sub-circular sections of tubes to centimetre-sized compound elements. The coating is an unlaminated dark micrite which rounds off the particles. The micrite contains numerous voids: some are small and round (150—200 μm), and others are large (3—5 mm). Their shapes can be subcircular or angular, with straight or scalloped walls. Thin planar voids connect several of these large voids or simply extend horizontally from their angles.

Interpretation

The abundance of micrite matrix in the boundstone, together with its high primary porosity, reduce its cohesiveness. It suffers from dessication which produces the laminoid voids and leads to the formation of an indurated and altered surface. Some of the coated grains may derive from these dessicated beds and are reworked in the micrite masses, which suggests a sedimentary origin. However, a majority of grains are similar to the enclosing Porostromata boundstone. They increase in abundance and size toward the blurred boundaries of the micrite masses. Therefore, the micrite may be the result of an alteration process. Ooids with such a non-laminated micrite coating are well known from pedogenetic alteration (Freytet and Plaziat, 1979; Hay and Wiggins, 1980; Arakel, 1982).

Second group of facies

Nodular microsparite

This occurs as small patches of microsparite which clearly show a process of "nodulisation" (Freytet, 1973, p. 42). The size of crystals increases along curved lines outlining ooids (Fig. 4) and iron oxide migrates along these

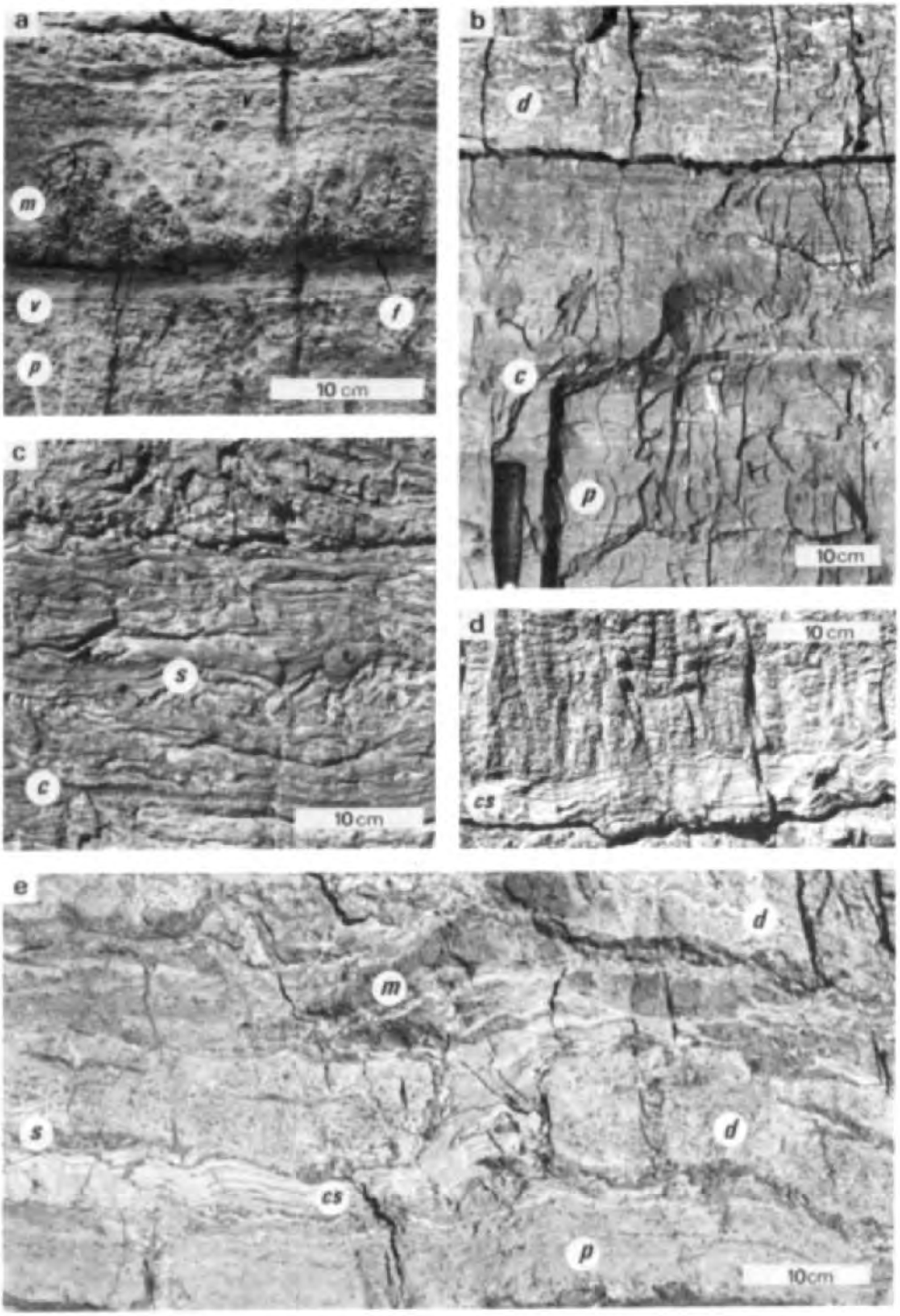
a
m
v
f
p
10 cm
b
d
c
p
10cm
c
s
c
10cm
d
10 cm
cs
e
d
m
s
d
cs
p
10cm

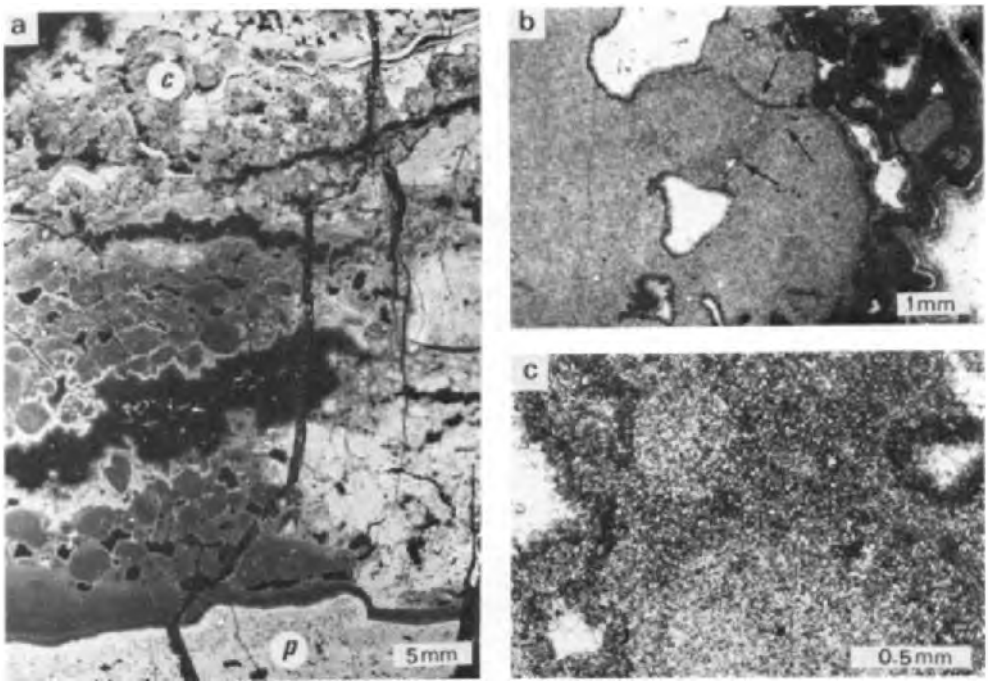

Fig. 4. (a) Nodulisation of microsparite: (*p*) Porostromata boundstone; (*c*) orbicular crust posterior to the microsparite. The large central void is filled by different generations of cement (phreatic?) (negative print). (b) and (c) Details of the nodulisation (ooids); aggrading recrystallization along curved lines (arrow) and migration of iron oxides (thin section).

lines. Further diagenesis, i.e., solution and cementation by sparry dolomite is also guided by these curved lines. The microsparite occurs in patches and might be either an internal sediment (vadose) or a product of an alteration process. The most interesting feature is the nodulisation which is reported from pedogenetically altered carbonates.

Fig. 3. Diagenetic features. (a) First group of facies: (*p*) Porostromata boundstone; (*v*) planar voids; (*f*) flat surface; (*m*) globular micrite masses with flat bottom. (b) Porostromata boundstone (*p*) overlaid by (*d*) disturbed beds (groups of facies 2 and 3) and cut by a long planar cavity (*c*). (c) Disturbed beds: (*c*) sheet cracks; (*s*) internal sediment. (d) Disturbed bed with discontinuous laminoid voids and a long planar cavity filled entirely by a "cave stromatolite" (*cs*). (e) Large horizontal cavity and transverse connection filled by a "cave stromatolite" (*cs*), showing dessication cracks. The cavities cut: the Porostromata boundstone (*p*), the disturbed beds (*d*) and a micrite sediment (*m*). A micrite with elements (*s*) filled the remaining void of the cavity.

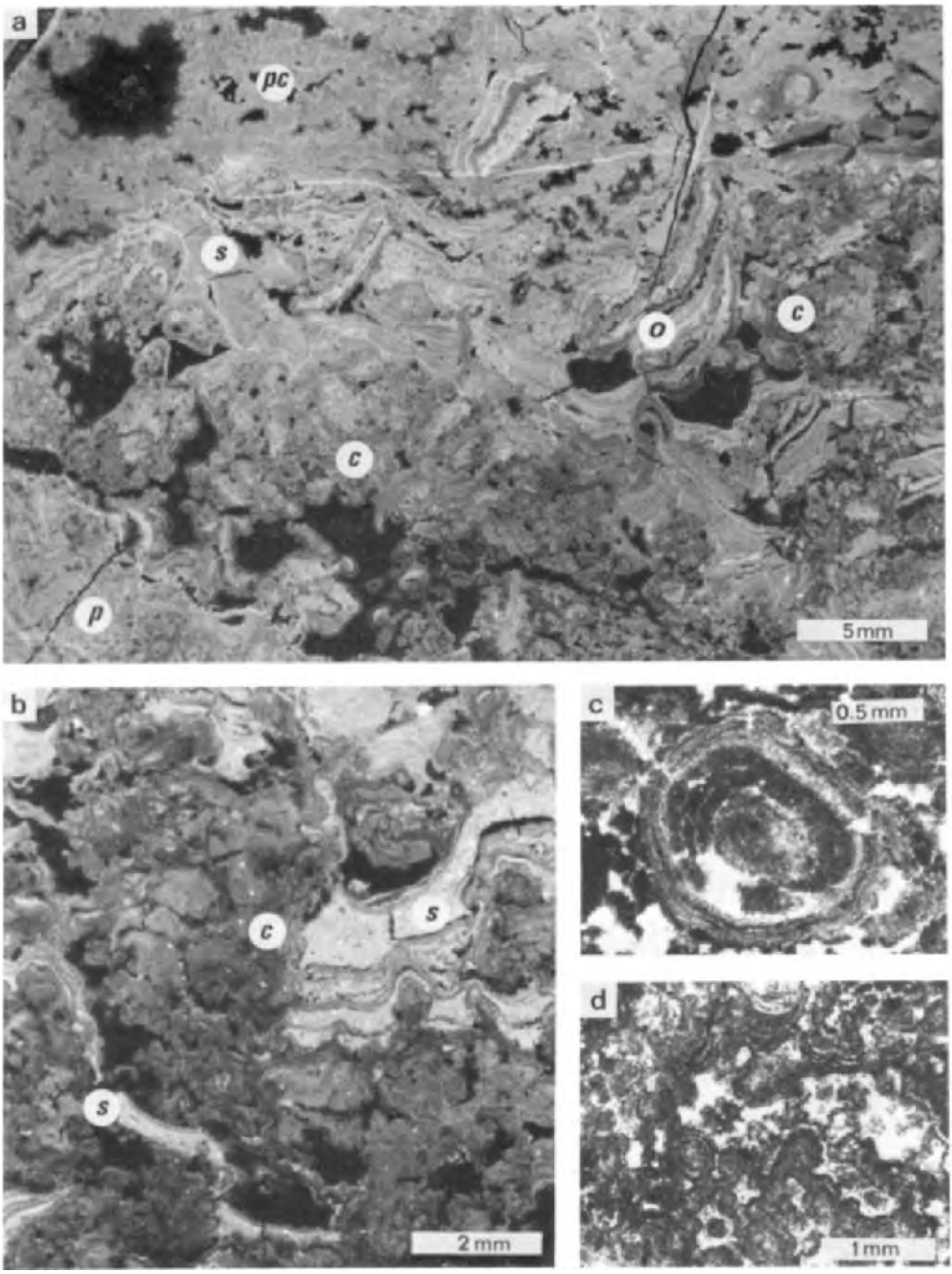

Fig. 5. Orbicular crusts and oncoids. (a) Orbicular crust (*c*) and internal sediment (*s*) associated with oncoids of an unusual shape (*o*) around chips of crust; (*p*) encrusted pelmicrite relicts. The upper part of the figure is a filling of micropopcorn micrite (*pc*) younger than the crust. Note the numerous voids (negative print). (b) Orbicular crust (*c*) and, in voids, laminar crust and vadose sediments (negative print). (c) Oncoid with a bumpy, microdomal, coating (thin section). (d) Orbicular crust growing regardless of gravity (thin section).

Orbicular crusts and oncoids

These complex bodies are formed by microdomal laminations, grading from oncoid to discontinuous orbicular crusts (Fig. 5). These features are developed within a facturated pelmicrite, patches of which still remain (Fig. 5a), and the encrustations are made of alternating dark and clear (microspar) layers. The crusts show microdomes with convexity oriented in all directions without any gravity polarity (Fig. 5c). In the voids, an internal sediment may be included in the crust. The oncoids may be round without a nucleus (Fig. 5c) or they can have a more irregular shape when they encrust chips of crust (Fig. 5a). The history of growth of these crusts is obviously multiphased. Iron oxide usually stains the structures.

The orbicular crust differs from the laminar crust (Multer and Hoffmeister, 1968; James, 1972; Read, 1976) and from the laminar calcrete (Arakel, 1982). Most of the oncoids do not correspond to the definition of vadose pisolite by Dunham (1969). Nevertheless, the lack of evidence for the sedimentary transportation of the oncoids, the absence of a nucleus in the oncoids, the in situ growth shown by spatial relationships and the association with geopetal sediment represent criteria in favour of a concretionary origin for the irregular oncoids and the orbicular crust (Blatt et al., 1972; Friedman and Sanders, 1978).

Third group of facies

Large cavities and cave stromatolites

Large planar horizontal cavities (5 cm thick and one to several meters long) cut through the previous facies (Fig. 3d). They are linked by short transverse connections (Fig. 2e) and, together with the smaller ones, are filled by "cave stromatolite" [compare to Monty's endostromatolites (Monty, 1981b)]. They are laminated, undulated, stromatolite-like structures. The laminations are alternating clear microsparite and dark micrite, which is obviously detrital (Fig. 6). These "cave stromatolites" definitely show a preferential upward growth resulting in pseudocolumns (Fig. 6c). Some laminae show a thickening of the pseudocolumn apex. The laminae succession is very regular and the "cave stromatolites" often fill the entire cavity (Fig. 3c). Post depositional structures affect the laminae, including interlayered and transverse cracks, brecciation and folding of the mud (Fig. 6a), and in situ cementation of the brecciated elements.

The large cavities may be due to solution and/or erosion by unsaturated waters percolating through a more or less indurated sediment. However, true karst cavities are very different from the "cave stromatolites" (d'Argenio, 1967; Carannante et al., 1975) with more irregular (scalloped) walls and filled by flat laminated sediments. Most of the cavities are planar and horizontal in shape, with transverse connections, which may indicate a dessication origin as described by Brewer (1964) for skew planes (see Freytet and Plaziat, 1982, p. 38). In respect of their larger scale they may also be compared to the buckle cracks of the caliches of Texas and New Mexico (Reeves,

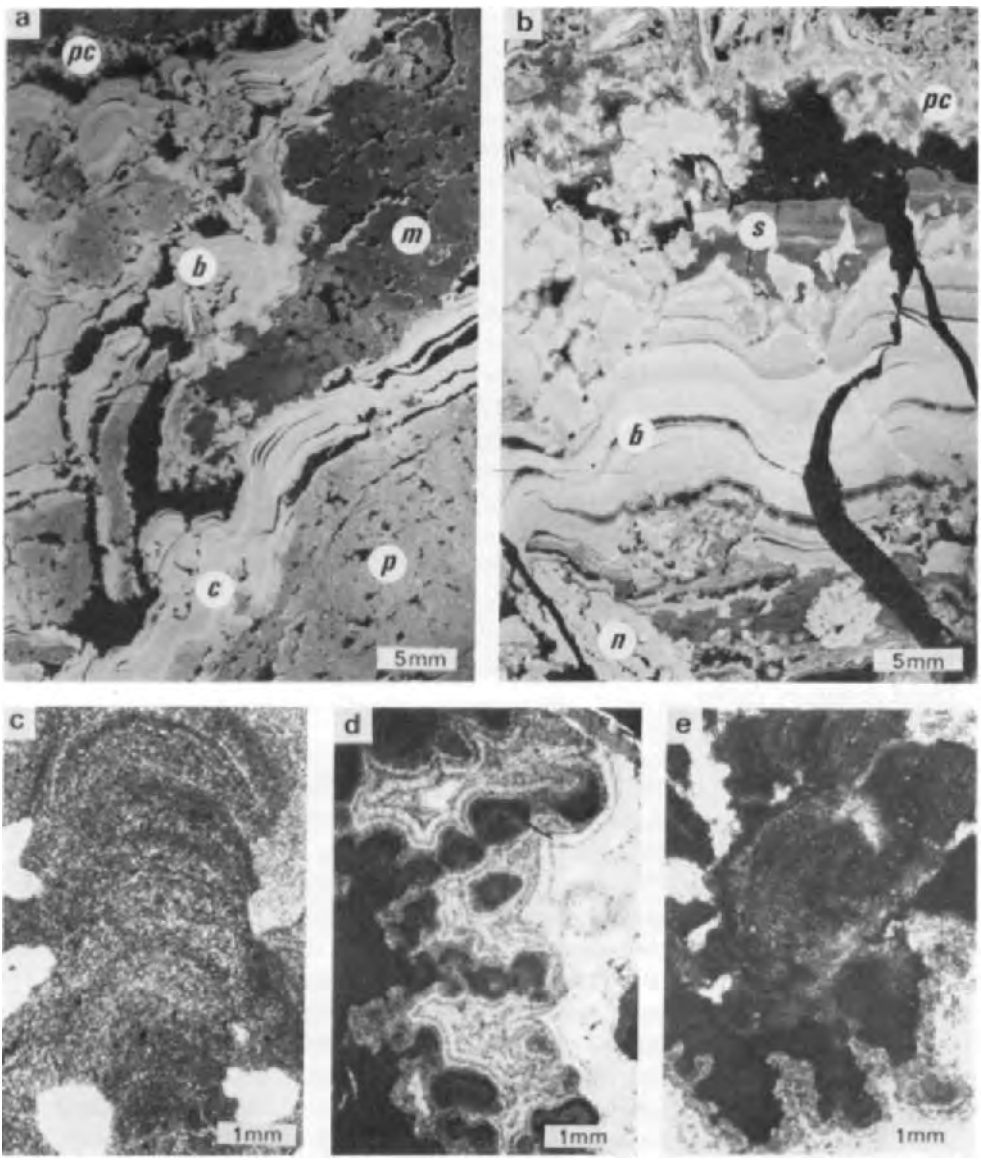

Fig. 6. "Cave stromatolites" and micropopcorn micrite. (a) and (b) "Cave stromatolites" growing in cavities cut in pelmicrite (*p*) and in microsparite with ooids (*m*). Note the micropopcorn fringe (*pc*) Pseudocolumns (*c*) and numerous post depositional cracks and breccia (*b*). In Fig. 6b a vadose sediment (*s*) is visible on the bottom of a solution cavity. The central filling of the cavity is contemporaneous with the cement filling of the latest fracture. There is no multilayered cement on the sediment surface (negative print). (c) Pseudocolumn in a "cave stromatolite". The micrite lamination is due to trapping of mud and shows a thickening of the apex (thin section). (d) Micropopcorn micrite: aborescent micrite concretions coated by a multilayered cement (thin section). (e) Micropopcorn micrite growing on an orbicular crust and partly dissolved (?) before the growth of the cement fringe (thin section).

1970). The sedimentary nature of the mud is obvious when compared to the accretionary laminae of the orbicular crusts, but sediment deposition in a void cannot explain the features observed in the "cave stromatolites" i.e., pseudocolumnar growth. For that reason, we assume that microbial activity has been necessary for binding the mud particles. The thickening upward of the laminae is usually attributed to microbial activity. However, the alternation of laminae cannot be related to an alternation of the microbial activity in response to changes in light. Therefore, the cyclicity of the sediment supply may be the main cause of the lamination. "Cave stromatolite" differs greatly from laminar crusts known from a soil surface or within a pedologic profile (Multer and Hoffmeister, 1968; James, 1972; Blatt et al., 1972; Read, 1976; Arakel, 1982) which are flat laminated, following the irregularities and filling the depressions of the substrate. Other laminated internal structures, named speleothems (Thrailkill, 1976) are accretionary structures and are never formed by mud entrapment.

Micropopcorn micrite

Arborescent encrustments of dark micrite (Fig. 6d,e) occur in cavities which cut through the orbicular crust, and are clearly associated with the cave stromatolites. These encrustations, though composed of dark micrite, like the aforementioned stromatolites, are only faintly laminated and lack detrital components. They differ from the orbicular crusts, on which they grow, by the absence of iron staining and the micritic grain size. They are riddled by solution voids which were formed before the last cementation. The term micropopcorn is proposed by Asseretto and Folk (1981) for somewhat similar micrite encrustations growing in a vadose environment with no regard to gravity. Micropopcorn are contemporaneous or slightly younger than the cave stromatolites.

Latest diagenetic events

Numerous voids remain in all the types of facies described, or are created by further solution processes. They are filled by various cements, the more frequent one being a phreatic cement composed of an isopachous fringe of palissadic crystals followed by a mosaic of equant crystals. A particularly spectacular case (Fig. 7) shows several horizontal cracks in a brecciated pelmicrite which are filled by two fringes of fibrous crystals, one being multilayered. Geopetal sediments are locally deposited between the fringes and may indicate an alternation of phreatic and vadose processes (Plaziat and Freytet, 1978).

Interpretation

Cavities existed before the growth of the "cave stromatolites", which remain located in the vadose zone during their growth and receive sediment carried by percolating waters. The cyclicity of the sediment supply is ruled by the water input and/or the production of sediment. The texture of the

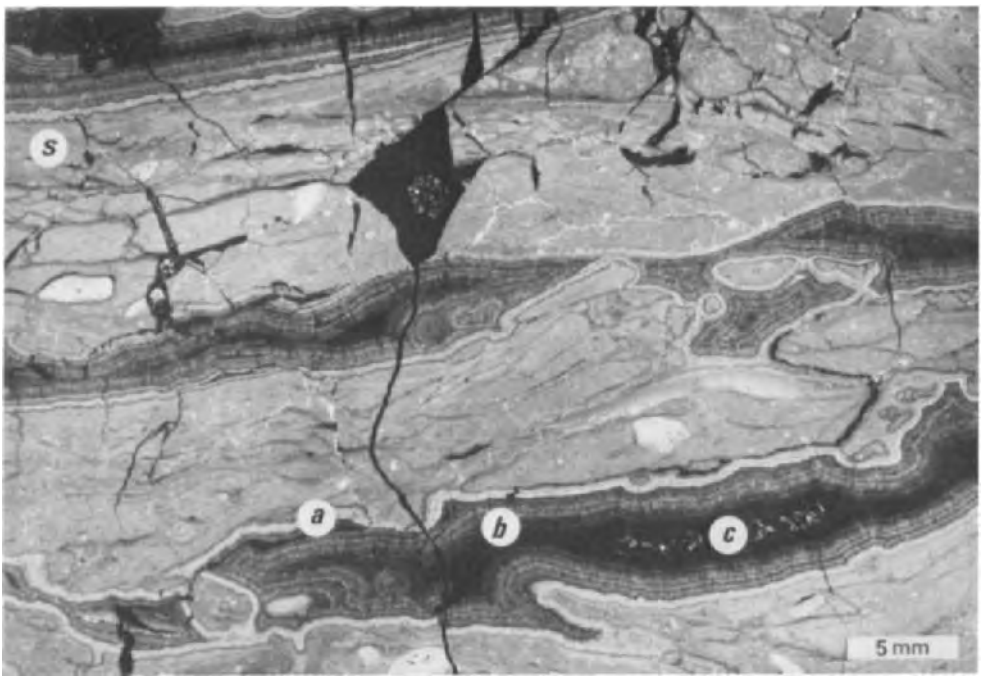

Fig. 7. Latest cements. In a pelmicrite fissured by pedogenetic alteration, dessication creates numerous horizontal voids. They are filled by complex phreatic cements: (*a*) fringe of fibrous crystals, (*b*) multilayered radial fibrous fringe, and (*c*) a central mosaic of equant crystals. In places, an early geopetal sediment (*s*) is visible. Vertical fractures filled by a mosaic of equant crystals are clearly secondary (negative print).

sediment is characterized by grain size (< 10 μm), with the absence of coarser grains suggesting a distal origin, a sieving during long transportation and a lack of local erosion. The total lack of syn-sedimentary dessication involves permanent humid conditions over a time span sufficient for the deposition of hundreds of laminations. A dessication episode ends the stromatolite growth. Later on, cementation, micropopcorn, fringes of crystals etc. and geopetal sedimentation alternate, testifying a succession of vadose and phreatic processes. The geopetal sediments are completely different from the sediment of "cave stromatolites".

Fourth group of facies

Pelmicrite with microfissures

In the upper part of the section, discontinuous layers of micrite sediment are interbedded with the facies of the second and third groups. Locally, these layers display a polygonal network of vertical cracks on their surfaces (Fig. 8a). In thin sections, the unlaminated pelmicrite shows a spongy texture due to small fissures, planar or curved, sometimes enlarged. The elements (mm size)

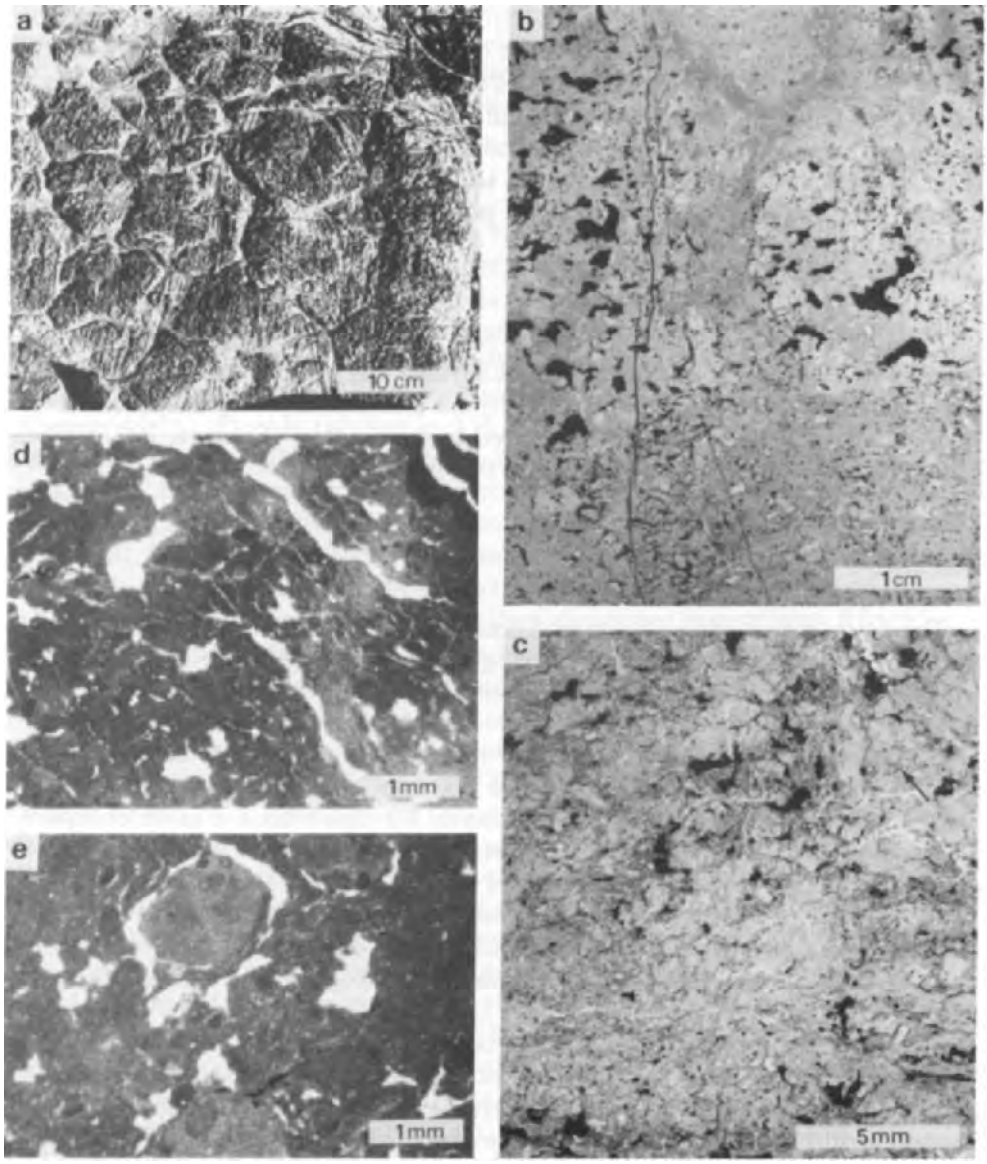

Fig. 8. Pelmicrite with microfissures. (a) Polygonal network produced by the dessication of a micrite. (b) Pelmicrite (micrite matrix with rounded grains) with vertical cracks (see (a)) filled by the same material. Three different stages of fissure are visible (negative print). (c) Pelmicrite showing fissuration network isolating new elements (arrow) (negative print). (d) and (e) Details of (c) network of thin fissures, curved and planar voids, circum granular cracks (see text) (thin section).

are mostly micritic, some of them exhibit recognizable features of Porostromata boundstone. They are supported by a micrite matrix. The smaller microfissures (30—50 μm, Fig. 8d) look like a web and occur throughout the whole sediment. Bigger voids are globular (500 μm) or more or less planar (200 μm thick and 2 to 4 mm long) and are guided by the previous network (Fig. 8d). Curved fissures generated in the inhomogeneous micrite isolate the grains. The vertical cracks which form polygons are filled by the same, but less fissurated pelmicrite (Fig. 8b).

Interpretation

The polygonal cracks are obviously produced by the dessication of a pelletoidal mud and we consider that this surface has been subaerially exposed. The microfissures, planar, curved or circum granular are very common in pedogenetic profiles and are also related to dessication (Freytet, 1973; Steel, 1974; Hubert, 1978; McPhearson, 1979; Freytet and Plaziat, 1979, 1982; Riding and Wright, 1981).

Discussion

The four groups of facies are not equivalent: the first and the last are essentially composed of layers of the original sediment (Porostromata and pelmicrite layers). The second and the third groups are intricated, but they are not contemporaneous and do not represent the same process of formation. The third group is related to a further evolution in the vadose zone while the second one contains, besides its proper features, elements of the original sediments remaining as relicts. It represents for that reason a more complex stage of evolution. The fact that Porostromata boundstone and pelmicrite are found in the three groups of facies implies that the whole section has been primarily deposited as a carbonate mud bounded by algae. In fact the observed facies are very complex and cannot be explained by a simple sedimentary process whereas the hypothesis of a pedogenetic alteration takes into account all the described facies.

The different groups of facies have been described from the base to the top of the section: the Porostromata boundstone at the base and the pelmicrite near the top. Between these relatively simple to interpret facies, the second group of facies exhibits complex intricated structures which can only be explained by the superimposition of different phases of pedogenetic alteration.

Two hypotheses may explain the thickness of the altered sediment (almost 30 m). In one case, the sediment is subaerially exposed only once and the different crusts and other pedogenetic facies are related to a unique paleosol profile; such thick paleosol profiles (between 30 and 50 m) are known in Texas (Brown, 1956, in Read, 1976) and in Algeria (Durand, 1963). In the other case, the peritidal sediments are repeatedly exposed to subaerial weathering, leading to a succession of paleosol profiles involving a poly-

phased evolution of the sediment; a thick succession of paleosols (over 80 m) is described by McPhearson (1979) in Devonian siltstones. The lack of well defined profile surfaces, except the polygons on the pelmicrite surface, restricts evidence favouring either hypothesis.

COMPARISONS AND CONCLUSIONS

The whole set of diagenetic fabrics visible in the field is unusual. Nevertheless, the different diagenetic microfacies described in the upper Proterozoic Sarnyéré dolomite are comparable to various structures recorded from recent examples of soil profiles, i.e., calcrete, caliche, etc. Within the vadose zone of these soil profiles, calcrete, caliche, calcareous crusts have been reported from different localities, such as Barbados (James, 1972); Texas (Reeves, 1970), Florida (Multer and Hoffmeister, 1968); Israël (Yaalon and Singer, 1974); Australia (Read, 1976; Arakel, 1982). The climatic conditions suitable for the appearance of such structures have been evaluated as temperate, semi-arid. The ideal climate would be the alternation of short periods of rainfall, followed by intense evaporation during relatively long periods. Such soils are well known today from both north and south edges of the Sahara desert. With increasing rainfall they disappear in northern Africa (Durand, 1963; Ruellan, 1967) and they are gradually replaced by ferruginous lateritic soils in the tropical humid region, south of the Sahara (Nahon, 1976).

The fossil counterparts of these calcretised soils are difficult to trace in the geological record (Blatt et al., 1972), especially in the Proterozoic rocks, because of the poor preservation potential of caliches. However, many weathering profiles have been recognized in the Proterozoic record (Retallack, 1980), affecting diverse metamorphic or igneous bedrocks, mainly chemically altered. Diverse types of structures related to subaerial exposure have been recognized in the Proterozoic sediments of Canada. Pisolitic beds from the Goulburn group (Campbell and Cecile, 1981) are attributed to vadoses pisolites. These beds also extend to the Athapuscow aulacogen (Hoffman, in Campbell and Cecil, 1981). Other karst features (collapse breccias, cave floor sediments, carbonate speleothems) are reported from a Middle Proterozoic formation in the same area (Kerans et al., 1981). Beach rocks associated with micritic (caliche) crusts (Donaldson and Ricketts, 1979) are reported from the McLeary formation (Lower Proterozoic of Belcher Island area, Canada). Laminated travertines are attributed to cave deposits in the Athapuscow aulacogen (Hoffman, 1978).

None of these structures can be compared to the highly diversified set of facies described here with all the intermediate fabrics preserved, from the undisturbed bedrock to the micronodular micrite and the orbicular crusts, and with such an alternation of processes evident, implying that the relevent conditions endured over a long period of time.

According to James (1972) and Retallack (1980) microbial activity may

have played an important role in pedogenetic processes, either through the disruption of the bedrock or the precipitation of carbonate (Krumbein, 1968; Campbell, 1979; Klappa, 1979a,b). Some of the micro-organisms involved in this precipitation are known from late Proterozoic microbiota (Schopf, 1978) and may have played the same role at that time. This is reinforced by the existence of cave stromatolites assumed to be formed by microbial activity.

In conclusion, it is worth noting that such a complex set of facies has never been described from Proterozoic rocks. The preservation of such a variety of pedologic and diagenetic features is challenging. The succession of events began by a marine deposition of mud, bounded by algae (Porostromata), followed by periods of subaerial exposure and dessication, producing pedogenetic alteration at different levels. This happens in a semi-arid climate. After a change in climate i.e., a more humid period with increasing water-flow, the cavities left by dessication and buckling are filled by "cave stromatolites" corresponding to a seasonal or more regular sediment supply. Thereafter, evolution stopped during alternating periods of dryness and cementation in phreatic conditions.

ACKNOWLEDGEMENTS

This research has been supported by the C.N.R.S. We thank the Direction Nationale de la Géologie et des Mines of Mali, for allowing the field work. Special thanks are offered to J.C. Plaziat for help with the understanding of complex fabrics and their relations with paleosol fabrics. We also thank C. Monty for his constructive criticism of the manuscript.

REFERENCES

Arakel, A.V., 1982. Genesis of calcrete in quaternary soil profiles, Hutt and Leeman lagoons, Western Australia. J. Sed. Petrol., 52: 109—126.

Assereto, R. and Folk, R.L., 1980. Diagenetic fabrics of aragonite calcite and dolomite in an ancient peritidal spelean environment, Triassic calcare rosso, Lombardia, Italy. J. Sed. Petrol., 50: 371—394.

Bertrand-Sarfati, J., 1979. Une algue inhabituelle verte, rouge ou bleue dans une formation dolomitique présumée d'âge Précambrien supérieur. Bull. Cent. Rech. Elf-Aquitaine, 3: 453—461.

Bertrand-Sarfati, J. and Moussine-Pouchkine, A., 1978. Mise en évidence d'une discordance du groupe de Bandiagara sur les formations sédimentaires du Précambrien supérieur (Gourma, Mali). C.R. Somm. Soc. Géol. Fr., 2: 59—61.

Bertrand-Sarfati, J. and Moussine-Pouchkine, A., 1983. Platform to basin facies evolution: the carbonates of late Proterozoic (Vendian), Gourma, Mali. J. Sed. Petrol., 53 (1)

Black, R., Caby, R., Moussine-Pouchkine, A., Bayer, R., Bertrand, J.M., Boullier, A.M., Fabre, J. and Lesquer, A., 1979. Evidence for late Precambrian plate tectonics in West Africa. Nature, 278: 223—227.

Blatt, H., Middleton, G. and Murray, R., 1972. Origin of Sedimentary Rocks. Prentice-Hall, Englewood Cliffs, N.J., 634 pp.

Brewer, R., 1964. Fabric and Mineral Analysis of Soils. Wiley, New York, 470 pp.
Brown, C.N., 1956. The origin of caliche on the northeastern Llano Estacado, Texas. J. Geol., 64: 1—16.
Campbell, S.E., 1979. Soil stabilization by a Prokaryotic desert crust: implications for Precambrian land biota. Origins Life, 9: 335—348.
Campbell, F.H.A. and Cecile, M.P., 1981. Evolution of the early Proterozoic Kilohigok basin, Bathurst inlet, Victoria Island, Northwest Territories. In: F.H.A. Campbell (Editor), Proterozoic Basins of Canada. Geol. Surv. Can. Pap., 81-10: 103—131.
Carannante, G., Ferreri, V. and Simone, L., 1975. Le cavita paleocarsiche cretaciche di Dragoni (Campania). Boll. Soc. Nat. Napoli, 83: 1—12.
Clauer, N., 1976. Géochimie isotopique du strontium des milieux sédimentaires. Application à la géochronologie de la couverture du craton ouest-africain. Sci. Géol., 45: 256 pp.
Cloud, P. and Glaessner, M., 1982. The Ediacarian period and system: Metazoa inherit the Earth. Science, 217: 783—792.
D'Argenio, B., 1967. Geologia del Gruppo de Taburno-Camposauro (Apenino-Campano). Mem. Geomineral. Sicl. Italia Centro Merid. Atti Dell. Ac. de Sc. Fin. Math. 3, 6, Napoli, 218 pp.
Donaldson, J.A. and Ricketts, B., 1979. Beach rock in Proterozoic dolostone of the Belcher Islands, Northwest Territories, Canada. J. Sed. Petrol., 49: 1287—1294.
Dunham, R.J., 1969. Vadose pisolite in the Capitan reef (Permian), New Mexico and Texas. In: G.M. Friedman (Editor), Depositional Environments in Carbonate Rocks. SEPM Spec. Publ., 14: 182—191.
Durand, J.H., 1963. Les croûtes calcaires et gypseuses en Algérie, formation et âge. Bull. Soc. Géol. Fr., Ser. 7, 5: 959—968.
Freytet, P., 1973. Petrography and paleo-environment of continental carbonate deposits with particular reference to the upper Cretaceous and lower Eocene of Languedoc (Southern France). Sed. Géol., 10: 25—60.
Freytet, P. and Plaziat, J.C., 1979. Les ooides calcaires continentaux: diversité des formes, des gisements, des modes de formation. Rech. Geograph. Strasbourg, 12: 69—80.
Freytet, P. and Plaziat, J.C., 1983. Continental Carbonate Sedimentation and Pedogenesis. Late Cretaceous and Early Tertiary of Southern France. Contributions to Sedimentology, 11, Schweizerbart'sche, Stuttgart, 216 pp.
Friedmann, G.M. and Kolesar, P.T., 1971. Fresh water carbonate cements. In: J. Hopkins (Editor), Carbonate Cements: Studies in Geology, No. 19.
Friedmann, G.M. and Sanders, J.E., 1978. Principles of Sedimentology. Wiley, New York, 792 pp.
Gardner, L.R., 1972. Origin of the Mormon Mesa Caliche, Clark county, Nevada. Bull. Géol. Soc. Am., 83: 143—156.
Hay, R.L. and Wiggins, B., 1980. Pellets, ooids, sepiolite and silica in three calcretes of the southwestern United States. Sedimentology, 27: 559—576.
Hoffman, P.F., 1978. Speleothems and evaporite solution collapse in Athapuscow aulacogen (Middle Precambrian), Great Slave Lake, Northwest Territories. Abstr. AAPG-SEPM, Annu. Conv., Oklahoma, p. 74.
Hubert, J.F., 1978. Paleosol caliche in the New Haven arkose, Newark group, Connecticut. Palaeogeogr. Palaeoclimatol. Palaeoecol., 24: 151—168.
James, N.P., 1972. Holocene and Pleistocene calcareous crusts (caliche) profiles criteria for subaerial exposure. J. Sediment. Petrol., 42: 817—836.
Kerans, C., Ross, G.M., Donaldson, J.A. and Geldsetzer, H.J., 1981. Tectonism and depositional history of the Helikian Hornby Bay and Dismal Lake Groups, District of Mackenzie. In: F.H.A. Campbell (Editor), Proterozoic Basins of Canada. Geol. Surv. Can. Pap., 81-10: 157—182.

Klappa, C.F., 1979a. Lichen stromatolites: criterion for subaerial exposure and a mechanism for the formation of laminar calcretes (caliche). J. Sediment. Petrol., 49: 387—400.

Klappa, C.F., 1979b. Calcified filaments in quaternary calcretes: organo mineral interactions in the subaerial vadose environments. J. Sediment. Petrol., 49: 955—968.

Krumbein, W.E., 1968. Geomicrobiology and geochemistry of the "Nari Lime crust" (Israel). In: G. Muller and G.M. Friedmann (Editors), Recent Development in Carbonate Sedimentology in Central Europe. Springer Verlag, New York, pp. 138—147.

Lesquer, A. and Moussine-Pouchkine, A., 1980. Les anomalies gravimétriques de la boucle du Niger. Leur signification dans le cadre de l'orogenèse pan-Africaine. Can. J. Earth Sci., 17: 1538—1545.

McPhearson, W., 1979. Calcrete (caliche) paleosols in fluvial redbeds of the Aztec siltstone (Upper Devonian), Southern Victoria Land, Antarctica. Sediment. Geol., 22: 267—285.

Monty, C., 1981a. Spongiostromate vs Porostromate stromatolites and oncolites. In: C. Monty (Editor), Fossil Algae. Springer Verlag, Berlin, pp. 1—4.

Monty, C., 1981b. The paleontological significance of coelobiotic or endostromatolites in carbonate build ups. Abstr., 5th Australian Geol. Convention.

Moussine-Pouchkine, A. and Bertrand-Sarfati, J., 1978. Le Gourma: un aulacogene du Précambrien supérieur. Bull. Soc. Géol. Fr., 20: 851—856.

Moussine-Pouchkine, A. and Bertrand-Sarfati, J., 1980. Sequences sédimentaires algo-laminaires littorales: les dolomies de Sarnyéré du Protérozoique supérieur (Vendien, Gourma, Mali). Rev. Géogr. Phys. Géol. Dyn., 22: 89—99.

Multer, H.G. and Hoffmeister, J.E., 1968. Subaerial laminated crusts of the Florida Keys Geol. Soc. Am. Bull., 79: 183—192.

Nahon, D., 1976. Cuirasses ferrugineuses et encroûtements calcaires au Sénégal occidental et en Mauritanie: systèmes évolutifs: géochimie, structures, relais et coexistence. Sci. Géol., Univ. L. Pasteur, Strasbourg, Mém. 44, 200 pp.

Pia, J., 1927. Thallophyta. In: M. Hirmer (Editor), Handbuch der Paläobotanik. Oldenburg—Berlin, Abschnit, 1, pp. 31—136.

Plaziat, J.C. and Freytet, P., 1978. Le pseudo-microkarst pédologique: un aspect particulier des paleo-pédogénèses développées sur les dépôts lacustres dans le Tertiaire du Languedoc. C.R. Acad. Sci. Paris, 286: 1661—1664.

Read, J.F., 1976. Calcretes and their distinction from stromatolites. In: M. Walter (Editor), Stromatolites. Development in Sedimentology, 20. Elsevier, Amsterdam, pp. 55—72.

Reeves, C.C., 1970. Origin, classification and geologic history of caliche on the southern high plains, Texas and Eastern Mexico. J. Geol., 78: 352—362.

Reichelt, R., 1972. Géologie du Gourma (Afrique occidentale). Un seuil et un bassin du Précambrien supérieur. Mém. Bur. Rech. Géol. Min. 53: 213 pp.

Retallack, G., 1980. Fossil soils — Indications of ancient terrestrial environments. In: K.J. Niklas (Editor), Paleoecology, Evolution and the Fossil Record. Peangas, New York, pp. 21—54.

Riding, R. and Wright, V.P., 1981. Paleosols and tidal flat/lagoon sequences on a carboniferous carbonate shelf: sedimentary associations of triple disconformities. J. Sediment. Petrol., 51: 1323—1339.

Ruellan, A., 1967. Individualisation et accumulation du calcaire dans les sols et les dépôts quaternaires du Maroc. Cah. O.R.S.T.O.M., Pédologie, 4: 421—462.

Schopf, J.W., 1978. The evolution of the earliest cells. Sci. Am., 239: 110—138.

Steel, R.J., 1974. Cornstone (fossil caliche). Its origin, stratigraphic and sedimentological importance in the new red sandstone, western Scotland. J. Geol., 82: 351—370.

Thrailkill, J., 1976. Speleothems. In: M. Walter (Editor), Stromatolites. Developments in Sedimentology, 20. Elsevier, Amsterdam, pp. 73—86.

Yaalon, D.H. and Singer, S., 1974. Vertical variation in strength and porosity of calcrete (Nari) on chalk, Shefela, Israel and interpretation of its origin. J. Sediment. Petrol., 44: 1016—1023.

RARE EARTH ELEMENTS IN THE EARLY ARCHAEAN ISUA IRON-FORMATION, WEST GREENLAND

PETER W. UITTERDIJK APPEL*

Geological Institute, Oester Voldgade 10, DK 1350, Copenhagen (Denmark)

ABSTRACT

Appel, P.W.U., 1983. Rare earth elements in the early Archaean Isua iron-formation, West Greenland. Precambrian Res., 20: 243—258.

The rare earth element (REE) patterns in the 3.8 Ga-old Isua iron-formation are generally flat, resembling those of some primitive basalts. Samples with positive, negative or no europium anomaly were found. It is shown that diagenesis and metamorphism did not significantly change the REE patterns. The presence or absence of europium anomalies in iron-formations cannot be used as an indicator of the presence or absence of oxygen in the atmosphere during the Archaean and Precambrian. The REE contents cannot be used to distinguish Algoma-type from Superior-type iron-formations. There appears to be a striking similarity between the Archaean submarine exhalations and modern submarine hydrothermal systems. It is considered likely that Archaean and early Precambrian seawater had a chondritic REE pattern with a slight enrichment of light REE.

INTRODUCTION

The Isua supracrustal belt is situated in the central part of an ancient gneiss complex in West Greenland. Radiometric dating of the supracrustal belt has given an age of 3.8 Ga. (Moorbath et al., 1973; Michard-Vitrac et al., 1977). Thus, the Isua supracrustals are the oldest terrestrial rocks known. This old age, however, is the most unique feature of the Isua rocks. The supracrustals do not significantly differ from younger Precambrian supracrustals of similar metamorphic grade. At Isua the common supracrustal belt assemblage consists of basic and acid volcanics, intercalated horizons of chemically precipitated carbonates and iron-formation, ultrabasic intrusives, minor amounts of clastic sediments and strata-bound sulphide mineralizations. The striking similarity of the Isua supracrustals compared to younger Precambrian supracrustal belts shows that the broad scale sedimentary environments in which Archaean and younger Precambrian supracrustals were depo-

*Present address: Geological Survey of Greenland, Oester Voldgade 10, DK 1350, Copenhagen, Denmark.

sited did not change drastically with time. This is important in the evaluation of the geochemical secular trends for major and trace elements through the early Precambrian. An example of a supposed secular trend is the behaviour of rare earth elements (REE), especially europium (Eu). Fryer (1977 a, b) and Laajoki (1975) found that Eu anomalies in Precambrian iron-formations could be used as indicators for the absence of free oxygen in the atmosphere during the Archaean to middle Precambrian.

GEOLOGY OF THE ISUA IRON-FORMATION

A brief description of the geology of the Isua iron-formation is given here (for more information see Appel, 1979, 1980). The Isua supracrustals (Fig. 1), which are enclosed in the younger Amîtsoq gneisses, can be divided into five main sequences. The quartzitic sequence in the northeastern part, consists mainly of quartzites with intercalated horizons of iron-formation, carbonates and amphibolites. The amphibolitic sequence is mainly composed of layered and massive amphibolites, presumably derived from volcanics. Horizons of iron-formation, carbonates and quartzites are interlayered in the amphibolites. Most of the quartzites in these two sequences are metacherts. After deposition, the supracrustals suffered several phases of deformation and were metamorphosed under low to medium grade amphibolite facies conditions.

The Isua iron-formation is found throughout the supracrustal belt, within the quartzitic and amphibolitic sequences. The individual iron-formation horizons range from a few cm to several tens of metres in thickness, and can be traced for up to a few hundred metres along strike. The iron-formation can be divided into different facies according to the concepts of James (1954). There is no clear distribution pattern of the different facies through the supracrustal belt and nowhere has a carbonate—oxide facies transition along strike been observed. There is, however, a tendency for oxide facies to be most abundant in the eastern part of the belt, whereas the more reduced facies tend to be to the west. A brief description of the different facies of iron-formation is given here (for further information see Appel, 1980).

Oxide facies

A major iron ore body in the northeastern part of the belt consists of oxide facies. The horizons of oxide facies in the rest of the belt rarely exceed 10 m in width. This facies is characteristically banded, with quartz-rich bands alternating with magnetite-rich bands. The individual bands range from a fraction of a millimetre to tens of centimetres in thickness; the thicker bands usually show internal layering. The main minerals are quartz (metachert) and magnetite. Small amounts of actinolite and carbonate occur. Pyrite is found in large subhedral scattered grains up to 1 cm.

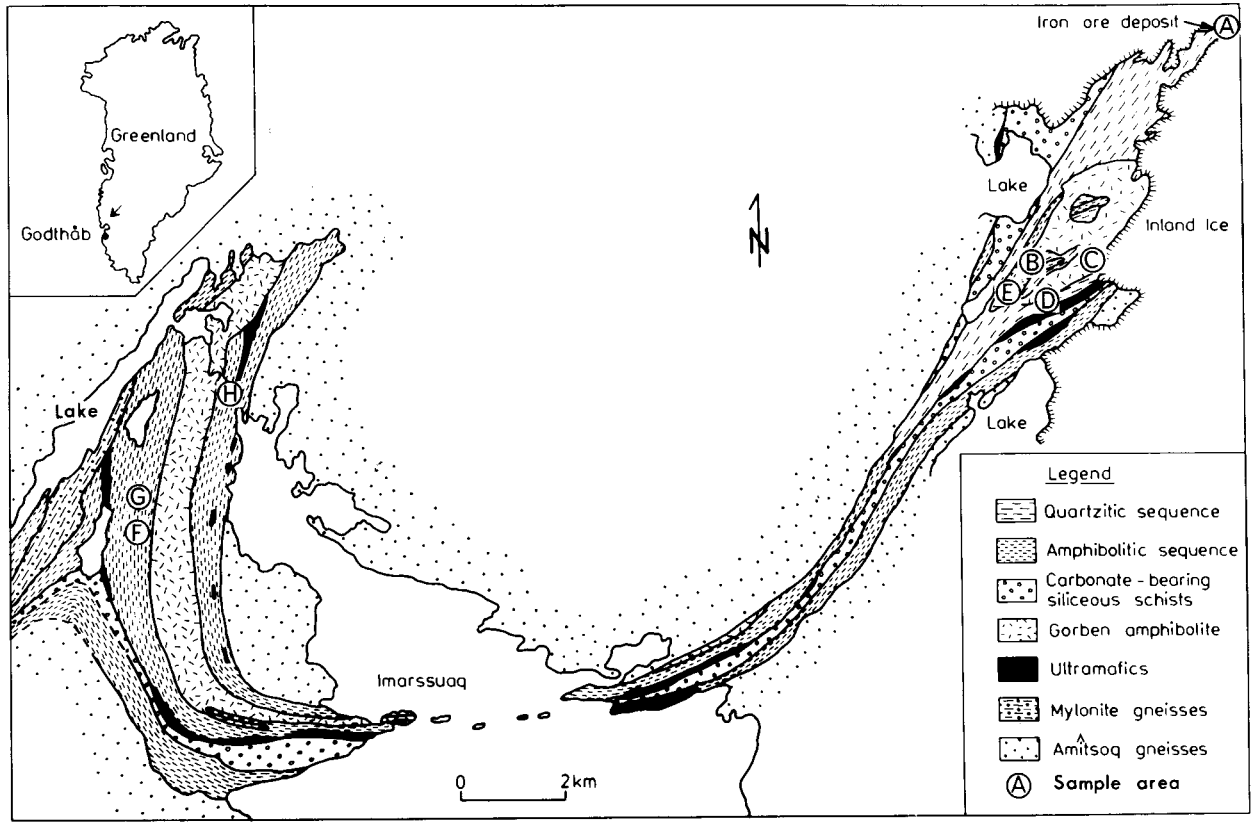

Fig. 1. Simplified geological map of the Isua supracrustal belt. Area A: samples 1—4. Area B: samples 14—16 and 23—27. Area C: sample 17. Area D: samples 19—20 and 28—32. Area E: samples 8 and 13. Area F: samples 5—7 and 9—10. Area G: samples 11—12. Area H: samples 18 and 21—22.

Within the oxide facies, several 10—30 cm thick intraformational breccias occur, consisting of flat angular quartz-rich fragments embedded in a magnetite-rich matrix.

Carbonate facies

These occur in up to 4 m thick horizons, traceable for up to a few hundred metres along strike, mostly in the amphibolitic sequence. This facies is mostly layered with 2—3 cm thick carbonate layers alternating with up to 0.5 cm thick magnetite-rich layers. The carbonate is siderite with a small percentage of magnesium and manganese. Graphite in the form of scattered tiny flakes or spherical aggregates, also makes up a small percentage. Actinolite and grunerite occur locally, whereas quartz is absent or occurs in trace amounts only. A peculiar sub-facies is locally predominant. It is a massive rock, with carbonate forming the major mineral and magnetite occurring in subordinate amounts only. The most peculiar feature of this subfacies is the magnesium content which ranges from ~ 10 to 32% MgO, in contrast to the normal carbonate facies which has an average MgO content of ~ 5%.

Silicate facies

This facies is found throughout the belt in horizons up to several tens of metres thick and can be sub-divided into several sub-facies. The most common consists of centimetre thick alternating magnetite and grunerite layers, with appreciable amounts of quartz present locally. Another type is finely laminated with magnetite and actinolite laminae. The third type is the finely laminated shaly iron-formation, consisting mainly of magnetite with ~15% grunerite and ~5% graphite. Massive horizons of silicate facies iron-formation occur locally, and consist of grunerite with a few scattered subhedral magnetite grains. In silicate facies, pyrrhotite and chalcopyrite are found in small amounts only.

Sulphide facies

A transitional facies occurs between the sulphide and silicate facies, consisting of magnetite, chalcopyrite and pyrrhotite, together with varying amounts of actinolite and hornblende. Sulphide facies occur exclusively as thin horizons in the amphibolitic sequence.

ANALYTICAL TECHNIQUES

The samples for mineral separates were crushed and sieved and fractions between 45 and 74 μm were separated using a hand magnet, Franz isodynamic magnetic separator and heavy liquids. This process provided very pure concentrates of magnetite, quartz, carbonates and iron silicates. The

mineral separates were analysed using neutron activation analysis (NAA) by R. Gwozdz, Risø National Laboratory (RISØ). The samples for whole-rock analysis were crushed and analysed using NAA by B. Spettel, Max-Planck-Institute (MPI). The NAA results for REE are listed in Table I, and their chondrite (Cl) normalised patterns are shown in Figs. 2—5. Chondrite REE contents are from Evenson et al. (1978). The total amounts of REE (ΣREE) are calculated from the chondrite normalised patterns, and listed in Table I.

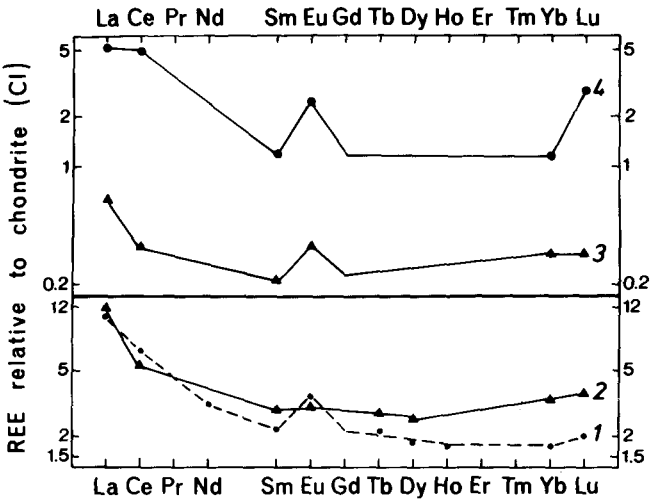

Fig. 2. Rare earth element patterns in oxide facies iron-formation. Sample numbers as in Table I.

It might seem odd to normalise the REE contents in the Isua iron-formation to that of carbonaceous chondrites when other authors have used other standards, e.g., North American Shale (NAS), in their studies of iron-formations. It is not really logical to use either standard in the study of iron-formations. Indeed, the only reason for using NAS is because it is a sedimentary rock, but NAS and iron-formations do not have more in common than present deep-sea ooze and coastal conglomerates. The main reason for using the chondrite (Cl) as a standard is because it contains the primordial REE abundance patterns, and is widely used and recognised by most geochemists.

Samples of iron-formation were anlaysed by both RISØ and MPI in order to check the results. The chondrite normalised results are plotted in Fig. 5, where samples 7 and 18 were analysed by MPI, and samples 7A and 18A were analysed by RISØ. The vertical bars on the RISØ results show the amount of error for each element. The results from the two laboratories agree reasonably well in their overall REE pattern. The RISØ results, however, tend to be slightly lower than those from MPI, especially in the heavy REE.

TABLE I

Rare earth elements and aluminium (%), and yttrium contents (ppm) in different facies of iron-formation. Samples 1 and 2, whole-rock oxide facies. Samples 3 (quartz) and 4 (magnetite), mineral separates from oxide facies. Samples 5—8 and 11—13, whole-rock carbonate facies. Samples 9 (magnetite) and 10 (carbonate), mineral separates from carbonate facies. Samples 14 (cummingtonite), 15 (magnetite) and 16 (actinolite) mineral separates from sulphide-type facies. Samples 17 and 18 whole-rock sulphide facies. Samples 19—25 whole-rock silicate facies. Samples 26 (magnetite) and 27 (cummingtonite) mineral separates from silicate facies. Samples 28 (cummingtonite), 29 (magnetite) and 30 (quartz) mineral separates of silicate facies. Samples 31 (cummingtonite) and 32 (magnetite) mineral separates from silicate facies (n.a. = not analysed)

	La	Ce	Pr	Nd	Sm	Eu	Gd	Tb	Dy	Ho	Er	Tm	Yb	Lu	ΣREE	Y	Al
1	2.58	4.20		1.50	0.34	0.20		0.08	0.46	0.10			0.29	0.050	11.0		1429
2	2.88	3.40			0.43	0.18		0.10	0.65				0.56	0.094	11.8	0.0	212
3	0.15	0.212			0.03	0.02							0.05	0.007	0.8	n.a	n.a.
4	1.23	3.18			0.18	0.14							0.21	0.07	7.3	n.a	n.a.
5	4.19	6.65		4.22	1.09	0.64	1.12	0.18		0.25		0.11	0.69	0.102	22.0	20.4	4605
6	2.88	4.90			1.11	0.48		0.43					1.60	0.26	23.2		4129
7	7.70	14.0		11.0	2.40	1.25		0.64		0.96			3.01	0.46	55.2	16.4	3292
8	6.61	12.5		8.54	2.39	1.98	3.70	0.70		1.09		0.47	3.06	0.451	51.0	58.6	18102
9	3.89	13.30			0.76	0.34							0.32	0.04	25.5	n.a.	n.a.
10	1.96	3.88			0.50	0.23							0.80	0.14	13.1	n.a.	n.a.
11	0.68	1.22		0.73	0.20	0.13		0.04	0.25	0.06		0.03	0.20	0.032	4.2	4.9	582
12	0.57	1.40		1.06	0.34	0.16	0.57	0.10	0.64	0.15		0.07	0.43	0.065	6.2	8.7	159
13	9.26	16.8	2.0	9.1	2.47	1.65		0.66		0.95			2.55	0.39	57.0	32.3	7410
14	0.05				0.20	0.11							0.50	0.09	3.3	n.a.	n.a.
15	1.54	3.44			0.25	0.12										n.a.	n.a.
16	0.38	1.94			2.60	1.67		0.69					2.99	0.42	28.0	n.a.	n.a.
17	2.68	6.60			1.08	0.32			1.1				0.71	0.11	19.8	n.a.	n.a.
18	19.3	36.1		20.0	2.93	0.30		0.58	3.4	0.84			1.57	0.19	96.6	27.0	9422
19	1.15	1.43			0.24	0.21		0.08	0.54				0.37	0.061	6.1	3.3	688
20	0.38	0.90		0.72	0.24	0.22		0.09	0.75	0.22			0.42	0.064	5.3	1.7	793
21	0.28	2.0		1.05	0.35	0.02	1.00	0.19	1.16	0.28	0.75	0.13	0.70	0.106	8.3	7.5	8733
22	10.1	24.6		17.0	4.65	0.29	6.7	1.34	7.6	1.69			3.96	0.52	87.2		9580
23	1.08	2.04	0.26	1.17	0.34	0.38	0.50	0.10	0.65	0.15			0.44	0.067	7.7		318
24	0.99	1.75		1.00	0.25	0.28	0.55	0.10	0.72	0.18			0.46	0.068	7.1	n.a.	476
25	4.25	8.70		5.80	1.23	0.91	1.20	0.21	1.32	0.30			0.81	0.12	27.1	6.0	3917
26	0.61	1.39			0.10	0.11							0.31	0.04	4.1	n.a.	n.a.
27	0.51				0.11	0.12							0.26	0.05	3.6	n.a.	n.a.
28	0.194	0.79			0.05	0.04							0.15	0.03	2.3	n.a.	n.a.
29	0.49				0.05	0.08										n.a.	n.a.
30	1.03	2.21		0.68	0.29	0.16		0.05					0.30	0.05	6.7	n.a.	n.a.
31	0.82	2.05			0.10	0.09										n.a.	n.a.
32	1.47	4.44			0.11	0.16										n.a.	n.a.

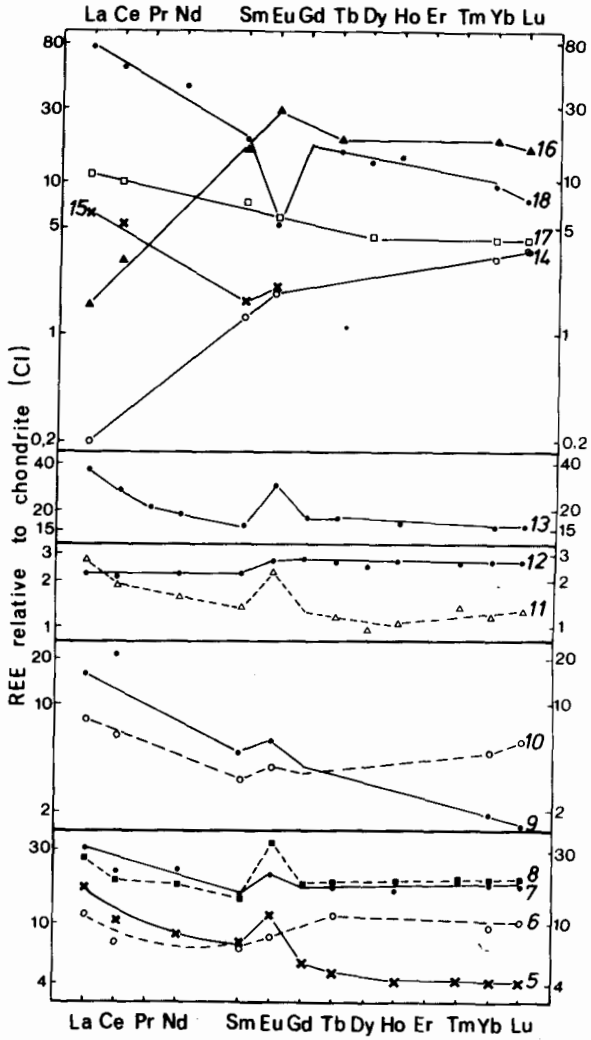

Fig. 3. Rare earth element patterns in carbonate and sulphide facies iron-formation. Sample numbers as in Table I.

The following list gives the degree of error for the MPI analysis in percent for each element, where the first figure is the maximum error and the last figure the most common error. La (5,3), Ce (25, 10), Pr (20, 20), Nd (25, 15), Sm (5, 3), Eu (5, 3), Gd (10, 7), Tb (10, 7), Dy (20, 10), Ho (15, 10), Er (20, 20), Tm (25, 10), Yb (5, 3), Lu (5, 3). Yttrium was analysed by J. Bailey (Geological Institute Copenhagen, Denmark). The detection limit is 0.5 ppm with an error of ~10%. Aluminium has been analysed by XRF and AA, with an average error of ~5%. A description of each of the analysed samples is given in the appendix.

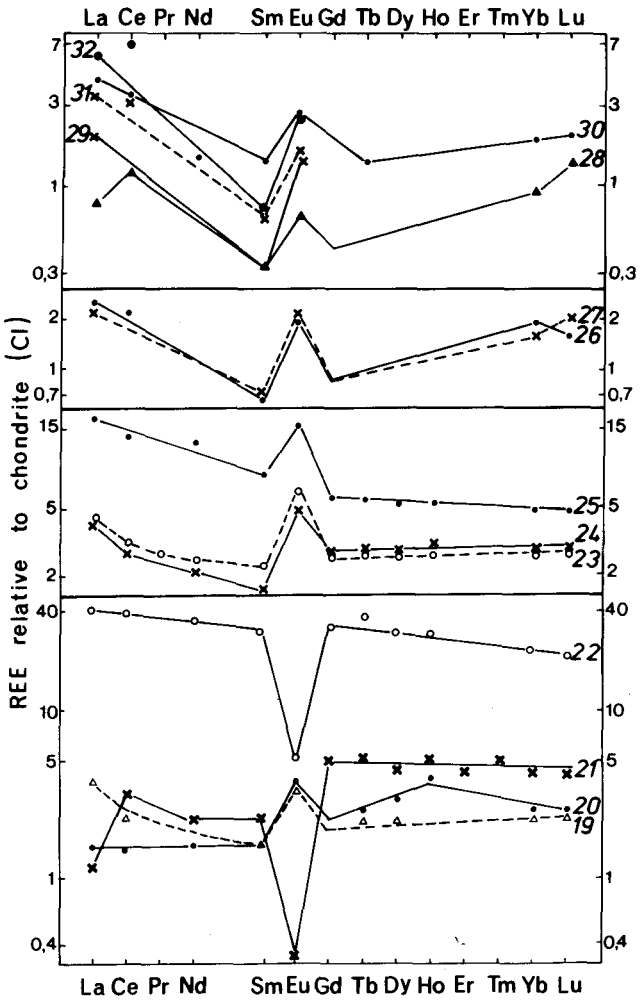

Fig. 4. Rare earth element patterns in silicate facies iron-formation. Sample numbers as in Table I.

CHEMISTRY

The REE are a group of 14 elements characterized by very similar chemical behaviour and they are usually trivalent. Cerium (Ce) and europium (Eu), however, can also occur in tetravalent and divalent states, respectively. Whether Ce is trivalent or tetravalent depends on the redox potential (Eh) of the system. Under highly oxidising conditions, tetravalent Ce will be fractionated from the trivalent REE, and precipitates from oxidising aqueous solutions will thus have strong Ce anomalies. Divalent Eu can likewise be fractionated from the trivalent REE. Hence Eu anomalies in iron-formations

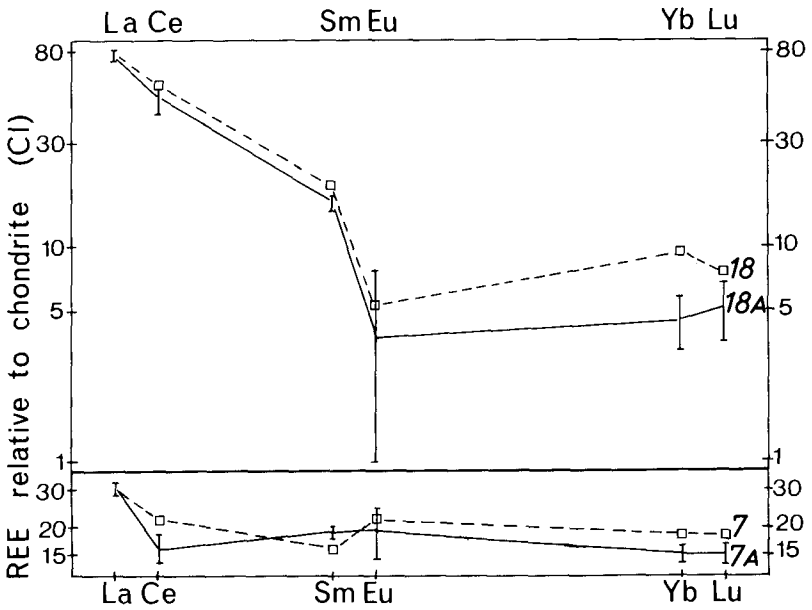

Fig. 5. Rare earth element patterns in duplicate samples of iron-formation. Samples 7 and 18 analysed by MPI. Samples 7A and 18A analysed by RISØ.

have been used as indicators for oxidising v. reducing conditions in the Precambrian atmosphere (Laajoki, 1975; Fryer, 1977 a, b). However, it requires very special conditions for divalent Eu to survive in aqueous solutions. The Eh for the reaction $Eu^{2+} \rightleftharpoons Eu^{3+} + e^-$ is -0.43 volts, and decreases with increasing pH. It will, therefore, require highly reducing conditions to keep appreciable amounts of Eu^{2+} in solution.

In the depositional environment of the iron-formations, abundant Fe^{2+} and Fe^{3+} was present, with a redox potential for the transition $Fe^{2+} \rightleftharpoons Fe^{3+} + e^-$ of + 0.77 volts. The Eh for this reaction decreases with increasing pH, but will always be well above the redox potential for the stability of divalent Eu. Thus, Eu^{2+} cannot exist in the depositional environment where the iron-formations were deposited, Hence Eu in iron-formations cannot have been fractionated on the grounds of redox conditions from the other REE. Therefore, Eu anomalies in iron-formations do not give any indication of the composition of the atmosphere during the Precambrian.

The total amount of REE (ΣREE) in the different facies of the Isua iron-formation varies from ~4 ppm to almost 100 ppm. There is no clear-cut relationship between ΣREE and the facies of iron-formation. There is, however, a tendency for carbonate facies to be high in ΣREE compared to oxide facies, whereas silicate facies cover the whole range from very low ΣREE contents to high ΣREE contents. Within the different mineral phases there is the same absence of clear relationships. In oxide facies quartz is low in REE compared to the coexisting magnetite, whereas the opposite relation-

ship is seen in silicate facies (see samples 3, 4 and 29, 30, respectively). The REE contents in coexisting magnetite and iron silicates are of the same order of magnitude in silicate facies iron-formation (cf. samples 26, 27 and 28, 29 and 31, 32). None of the individual mineral phases have REE contents or REE patterns significantly different from the whole-rock composition. REE patterns from the different facies of the Isua iron-formation show the same general trend. The REE pattern is rather flat, resembling that of Isua basalt (Appel, 1979). The most common deviation from the flat pattern is a slight enrichment in light REE in the iron-formation. A few samples are depleted in lanthanum, e.g. sample 21.

Europium is clearly anomalous in many of the samples. In some samples it is depleted by a factor up to 10; in others it is enriched by a factor up to 3. In several samples, however, there is no europium anomaly at all. There is no obvious relationship between the behaviour of europium and the facies of iron-formation. In oxide and carbonate facies about half the samples have positive Eu anomalies and the rest have no anomalies. In silicate facies two samples have strong negative Eu anomalies, whereas all others have positive Eu anomalies. It is noticeable that the silicate facies with negative Eu anomalies consist of magnetite and actinolite, whereas the silicate facies samples with positive anomalies mainly consist of magnetite and grunerite.

ROLE OF METAMORPHISM

Before evaluating the REE results, the role of metamorphism has to be considered. The REE are a group of elements in the third group of the periodic system, together with elements such as aluminium and yttrium. The group three elements have many chemical similarities and tend to covariate in aqueous solutions. Figure 6 shows the relationship of aluminium and yttrium v. ΣREE in the Isua iron-formation. Both elements show a fairly good correlation with ΣREE. The relationship of aluminium and yttrium v. the individual REE (except Eu) are very similar to the trends in Fig. 6. This was to be expected since the elements were precipitated contemporaneously in an aqueous environment.

During diagenesis many elements are highly mobile, e.g., Rb and Sr. However, aluminium and yttrium are generally immobile during metamorphism. The behaviour of REE during diagenesis and metamorphism is debated, however, the results shown in Fig. 6 strongly indicate that the REE were immobile, like aluminium and yttrium, during diagenesis and metamorphism of the Isua iron-formation. Rare earth elements all behave very similarly, except for europium which is dealt with below. This chemical similarity indicates that even if some metamorphic addition or removal of REE took place, it would not affect the distribution pattern of the REE, but merely push the general level slightly up or down. Is it possible that the Eu anomalies in some of the iron-formation samples are of diagenetic or metamorphic

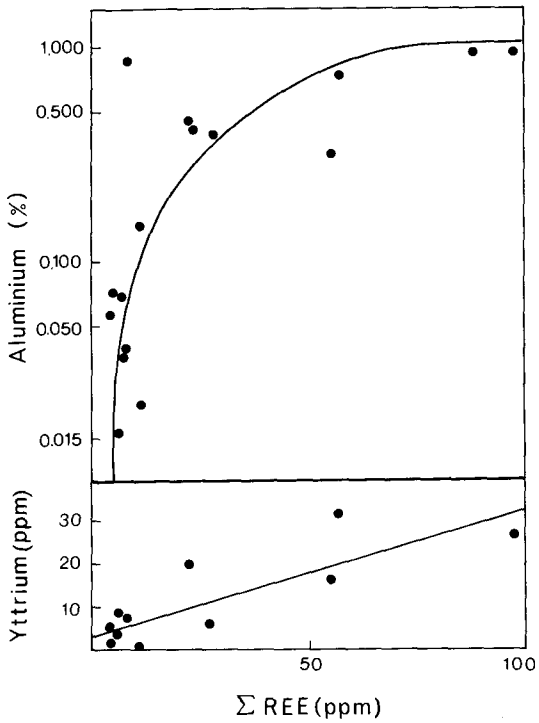

Fig. 6. Aluminium (%) and ytttrium (ppm) v. ΣREE (ppm) in different facies of iron-formation. Sample 8 is not included. The correlation coefficients are Al – ΣREE = 0.79 and Y – ΣREE = 0.81. Note that the scale for aluminium is logarithmic.

origin? This would require very reducing alkaline conditions with no Fe^{3+} or other oxidising ions present. If these conditions were met, which is highly unlikely, then Eu^{3+} would be reduced to the more soluble Eu^{2+} with the result that the soluble Eu^{2+} compounds could be removed from the system, leaving a rock with a negative europium anomaly. The carbonate facies with a high graphite content would be the best candidate for strongly reducing conditions during diagenesis or metamorphism, but none of the carbonate facies samples have negative europium anomalies. Thus, the Eu anomalies are unlikely to be of metamorphic or diagenetic origin. The REE patterns depicted in Figs. 2—4 are, therefore, considered to be pre-diagenetic and pre-metamorphic.

DISCUSSION

Previous investigations of the REE distribution patterns in iron-formations revealed an apparent secular trend of europium anomalies (Laajoki, 1975; Fryer, 1977 a, b). These authors found that the early Precambrian iron-formations had negative Eu anomalies, whereas younger iron-formations

had positive or no Eu anomalies. The suggested explanation was that europium under reducing conditions occurred in the soluble divalent state, thus being fractionated from the trivalent REE (Laajoki, 1975; Fryer, 1977 a, b). The divalent Eu was supposedly accumulated in the oceans as long as the reducing conditions prevailed. When oxygen appeared in the atmosphere, Eu ceased to be anomalous and was precipitated in its trivalent state (Laajoki, 1975; Fryer, 1977 a, b). The first iron-formations to be deposited had therefore positive Eu anomalies, whereas iron-formations deposited later had no Eu anomalies (Laajoki, 1975; Fryer, 1977 a, b).

This theory is clearly inconsistent, not only with the physical chemistry of europium, but also with the REE patterns of the 3.8 Ga-old Isua iron-formation. In the Isua area, the iron-formation shows positive, negative or no Eu anomalies.

Fryer (1977 a, b) and Laajoki's (1975) model was clearly inspired by the behaviour of cerium in sediments. Cerium covariates with the other REE in Precambrian deposits. Present day seawater has a pronounced negative Ce anomaly, corresponding to a positive Ce anomaly in deep sea Mn nodules. The explanation for this behaviour is quite simple. During present day oxidising conditions Ce is oxidised to its tetravalent state and Ce^{4+} compounds are less soluble than trivalent Ce compounds. Therefore, Ce is fractionated in seawater from the trivalent REE. This feature seems to provide a means for investigating the oxygen content in the atmosphere via the presence or absence of Ce anomalies in sea floor deposits. However, in a recent paper, Elderfield and Greaves (1981) report ferromanganese nodules from the Pacific Ocean with negative Ce anomalies. Thus, it can be concluded that neither cerium nor europium anomalies can be used as indicators for the presence or absence of oxygen in the atmosphere.

It has been suggested that the REE patterns could be used to distinguish different types of iron-formations. Graf (1978) suggested that the absolute contents of REE and the type of Eu anomaly could distinguish an Algoma-type iron-formation from a Superior-type iron-formation. This is clearly inconsistent with the REE patterns in the Isua iron-formation, where the general level of REE varies by a factor of 20, and positive, negative or no europium anomalies occur.

The REE content and distribution patterns in coexisting mineral phases in the Isua iron-formation do not show any systematic trends. A likely explanation is that precipitation of the REE was governed by solution chemistry rather than by scavenging.

Is it possible to obtain any information from the REE regarding the genesis of iron-formations? The genesis of iron-formations has been debated during most of this century, but little progress has been made. What is agreed upon, is that iron-formations are chemical sediments, precipitated in a very quiet sedimentary environment, with a general absence of detrital material. It is still an open question where the material, mainly iron and silicon, came from. The most likely origin is hot brines pouring on to the

sea floor. The most plausible source for these brines is either direct magmatic exhalations, or brines which have been circulating in and leaching the oceanic crust. Both processes are observed today, e.g., in the Pacific Ocean. When hot brines of either origin are expelled on the sea floor, they mix with seawater. Most of the material carried in solution by the brines will subsequently precipitate. The chemistry of the precipitates will depend on the degree of mixing, temperature, redox conditions and pH, as well as on the original composition of the brines and the composition of the seawater. The degree of seawater brine mixing depends on the temperature, velocity and density of the brines, as well as the bottom topography. Thus, there are a considerable number of unknowns in this process. Is it possible to elucidate any of these problems by the study of REE patterns of the precipitated sediments?

Modern submarine hydrothermal systems observed at the East Pacific rise have apparently much in common with Archaean submarine exhalations (Corliss et al., 1981). Corliss (personal communication, 1982) has found strong positive Eu anomalies in the hot metal-rich brines exhaled on the sea floor at the East Pacific Rise and he attributes the positive Eu anomalies to highly reducing conditions under which hot circulating water leached sea floor basalts at depth. The presence of methane and carbonaceous matter in the brines indicates such reducing conditions that all the iron must be in divalent form. During the leaching process Eu is reduced to Eu^{2+} which is more soluble than trivalent REE. When the brines ascend and are exhaled at the sea floor, the material carried in solution will precipitate under conditions with higher redox potential than at depth. The Eu carried in solution will be oxidized to Eu^{3+} and precipitated together with the other REE. If only a limited mixing of brine and seawater occur, the precipitates will have strong positive Eu anomalies. With extensive mixing, the REE pattern of precipitate will be modified by the seawater REE pattern. In close proximity to the modern exhalative sea floor vents, metalliferous deposits can be expected to be found with positive Eu anomalies. Further away the deposits will have REE patterns resembling that of seawater.

This model is applicable to the Isua iron-formation. The horizons with positive Eu anomalies were thus precipitated close to the submarine exhalative vents and those horizons with no Eu anomalies were deposited further away from the vents, where extensive brine seawater mixing had taken place and the REE pattern of the brines were modified by the REE pattern of seawater. This leads to the suggestion that the Archaean seawater had a chondritic REE pattern, possibly with a slight enrichment of light REE.

The negative Eu anomalies found in two silicate facies (samples 21 and 22) and one sulphide facies (sample 18) are puzzling. Possible explanations are, that the material in these horizons were leached from rocks which were previously depleted in europium or preferential leaching of mafic minerals in the sea floor basalts occurred.

Leaching of a basaltic pile will remove most of the incompatible elements, e.g., REE from the basalts, and thus the circulating hot water will attain a REE pattern resembling that of basalts (Piper et al., 1975). One exception is Eu, which during crystallization of a basaltic magma is built into plagioclase. A mild leaching, not affecting plagioclase, will produce a brine with a basaltic REE pattern, but with a negative Eu anomaly (Piper et al., 1975). Exhalations from a magma contain high proportions of incompatible elements. Submarine exhalations from a basaltic magma will have a basaltic REE pattern. An exception is if plagioclase in the magma has started to crystallise, thus depleting the magma in Eu. Exhalations from such a magma will have a REE pattern resembling that of the basalt, but with a negative Eu anomaly.

Disregarding europium for the moment, most REE patterns in the Isua iron-formation have the same general trend of a slight enrichment of light REE. This trend resembles that of some primitive basaltic rocks, and the average levels of REE in the Isua iron-formation and in Isua basalts are of the same order of magnitude (Appel, 1979). Therefore, it is considered likely that the brines or exhalations which supplied the material for the iron-formation were of basaltic pedigree, and obtained their metal content through leaching of sea floor basalt and/or directly from basaltic magmas.

The REE patterns in the Isua iron-formation show that local small scale features, such as proximity to hot vents and sea floor topography determined the site and facies type of iron-formation precipitated. This explains why none of the individual horizons of iron-formation can be traced more than a few hundred metres along strike. It also explains the irregular distribution pattern of the different facies of iron-formation, and the lack of transition facies between oxide and carbonate facies.

CONCLUSIONS

The results of this investigation, compared with similar investigations of younger iron-formations and recent submarine hydrothermal systems, have led to the following conclusions:

(1) the REE content and distribution patterns in the Isua iron-formation have not been significantly changed during diagenesis and metamorphism;

(2) the presence or absence of europium anomalies in iron-formations cannot be used as an indicator for the presence or absence of oxygen in the atmosphere during the Archaean and Precambrian;

(3) REE distribution patterns cannot be used to distinguish Algoma-type and Superior-type iron-formations;

(4) the ultimate source of the material in the iron-formations are submarine exhalations from basaltic volcanism and/or leaching of sea floor basalts;

(5) the Archaean and early Precambrian seawater had a chondritic REE pattern, with a slight enrichment of light REE.

ACKNOWLEDGEMENTS

Part of the work was done while the author held a research stipend at the Max-Planck-Institute for Chemistry (MPI), Mainz, W. Germany. The Isua programme at MPI was initiated by M. Schidlowski and C.E. Junge, and performed as part of the Sonderforschungsbereich 73 "Atmospheric Trace Components", partially funded by the Deutsche Forschungsgemeinschaft. Whole rock analysis were made at MPI, Department of Cosmochemistry. The mineral separates were analysed at Risø National Laboratory on a grant provided by the Danish Natural Science Research Council. The XRF analyses were done by John Bailey, Institute of Petrology, University of Copenhagen, Denmark.

APPENDIX

Sample description

Samples 1 and 2: oxide facies iron-formation consisting of mm-thick alternating quartz and magnetite layers, with subordinate amounts of actinolite and trace amounts of carbonate. Average grain size of quartz 0.2 mm and of magnetite 0.002 mm.
Samples 3 and 4: quartz and magnetite mineral separates of oxide facies iron-formation.
Samples 5—8: carbonate facies iron-formation consisting of mm-thick alternating siderite and magnetite rich layers, with up to 10% grunerite and up to 5% graphite. Quartz is characteristically absent or occurs in trace amounts only. Graphite occurs mostly as scattered small flakes or spherical aggregates. In some very thin layers, however, graphite can amount to 75%. Average grain size of carbonate facies is 0.1—0.2 mm.
Samples 9 and 10: magnetite and siderite mineral separates of sample 7.
Samples 11 and 12: massive carbonate facies iron-formation consisting of more than 80% Mg—Fe carbonate and ~15% magnetite as scattered subhedral grains, together with minor amounts of grunerite. This rock type characteristically contains roughly equal amounts of iron and magnesium. Average grain size 0.5 mm.
Sample 13: unusual type of iron-formation. Finely laminated with ~90% magnetite, together with graphite, grunerite and garnet. Average grain size 0.5—1 mm.
Samples 14, 15 and 16: cummingtonite, magnetite and actinolitic hornblende mineral separates of a sulphide-type iron-formation (see below).
Samples 17 and 18: sulphide-type iron-formation. Can be regarded as a transition facies between sulphide facies and silicate facies iron-formation. This facies type consists of chalcopyrite, magnetite and actinolitic hornblende with small amounts of pyrrhotite and normal hornblende.
Samples 19 and 20: silicate facies iron-formation, consisting of mm-thick alternating grunerite and magnetite rich layers, with small amounts of quartz locally. Average grain size 0.5 mm.

Samples 21 and 22: silicate facies iron-formation. Thinly laminated with alternating actinolite and magnetite rich laminae. Average grain size 0.05—0.1 mm.
Samples 23—25: massive silicate facies iron-formation consisting of grunerite with scattered subhedral magnetite grains. Grain size up to a few mm.
Samples 26 and 27: magnetite and grunerite mineral separates from sample 25.
Samples 28, 29 and 30: grunerite, magnetite and quartz mineral separates from sample 19.
Samples 31 and 32: grunerite and magnetite mineral separates from silicate facies iron-formation.

REFERENCES

Appel, P.W.U., 1979. Stratabound copper sulfides in a banded iron-formation and in basaltic tuffs in the early Precambrian Isua supracrustal belt, West Greenland. Econ. Geol., 74: 45—52.

Appel, P.W.U., 1980. On the Early Archaean Isua iron-formation, West Greenland. Precambrian Res., 11: 73—87.

Corliss, J.B., Baross, J.A. and Hoffman, S.E., 1981. An hypothesis concerning the relationship between submarine hot springs and the origin of life on Earth. Proc. 26 Int. Geol. Congr., Geology of Oceans Symposium, Paris, July 7—17, 1980, Oceanologica Acta, pp. 59—69.

Elderfield, H. and Greaves, M.I., 1981. Negative cerium anomalies in the rare earth element patterns of oceanic ferromanganese nodules. Earth Planet. Sci. Lett., 55: 163—170.

Evensen, N.M., Hamilton, P.J. and O'Nions, R.K., 1978. Rare earth abundances in chondritic meteorites. Geochim. Cosmochim. Acta, 42: 1199—1212.

Fryer, B.J., 1977a. Rare earth evidence in iron-formations for changing Precambrian oxidation states. Geochim. Cosmochim. Acta, 41: 361—367.

Fryer, B.J., 1977b. Trace element geochemistry of the Sokoman iron-formation. Can. J. Earth Sci., 14: 1598—1610.

Graf, I.L., 1978. Rare earth elements, iron-formations and seawater. Geochim. Cosmochim. Acta, 42: 1845—1850.

Holland, H.D., 1973. The oceans: a possible source of iron in iron-formations. Econ. Geol., 68: 1169—1172.

James, H.L., 1954. Sedimentary facies of iron-formation. Econ. Geol., 49: 235—293.

Laajoki, K., 1975. Rare earth elements in Precambrian iron formations in Väyrylänkylä, South Puolanka area, Finland. Bull. Geol. Soc. Finl., 47: 93—107.

Michard-Vitrac, A., Lancelot, J., Allegre, C.J. and Moorbath, S., 1977. U—Pb ages on single zircons from the early Precambrian rocks of West Greenland and the Minnesota river valley. Earth Planet. Sci. Lett., 35: 449—453.

Moorbath, S., O'Nions, R.K. and Pankhurst, R.J., 1973. Early Archaean age for the Isua iron-formation, West Greenland. Nature, 270: 43—45.

Piper, D.Z., Veh, H.H., Bertrand, W.G. and Chase, R.L., 1975. An iron-rich deposit from the northeast Pacific. Earth Planet. Sci. Lett., 26: 114—120.

PRIMITIVE EARTH ENVIRONMENTS: ORGANIC SYNTHESES AND THE ORIGIN AND EARLY EVOLUTION OF LIFE

A. LAZCANO

Instituto de Astronomia, Universidad Nacional Autonoma de Mexico, Apartato Postal 70-264, Mexico, D. F. 04510 (Mexico)

J. ORÓ

Department of Biochemical and Biophysical Sciences, University of Houston, Houston, TX 77004 (U.S.A.)

STANLEY L. MILLER

Department of Chemistry, University of California, San Diego, La Jolla, CA 92093 (U.S.A.)

ABSTRACT

Lazcano, A., Oró, J. and Miller, S.L., 1983. Primitive Earth environments: organic syntheses and the origin and early evolution of life. Precambrian Res., 20: 259—282.

The Precambrian is the longest and least understood period in the history of our planet. There is no direct evidence which bears on the primitive Earth environment, the synthesis of organic compounds and the origin of life on our planet, since the geological record only goes back to 3.8 Ga ago. To overcome this deficiency it is necessary to extrapolate backwards from 3.8 Ga ago to the time when the Earth was formed, ~4.6 Ga ago, and also make use of additional scientific approaches. These include models of the solar nebula and planet formation, comparative observations with other cosmic environments, and experimental simulation studies under plausible primitive Earth conditions, particularly in regard to the prebiological synthesis of organic compounds. A large number of interstellar organic molecules have been detected by radioastronomy in the interstellar medium, particularly in places where other solar systems may be in the process of formation. It is remarkable that ~10 of these molecules are known to be the precursors of the most important biochemical monomers. Furthermore, some of these monomers, e.g., amino acids, purines and pyrimidines, have also been detected in carbonaceous chondrites, which were presumably synthesized on the parent bodies of the meteorites or possibly in the solar nebula. Comparative studies on the terrestrial planets indicate that their primitive atmospheres resulted primarily from outgassing of CO_2 and other partially oxidized (CO, N_2) and reduced (H_2, CH_4, NH_3, H_2S) volatiles. Furthermore, comets and meteorites are thought to have made a significant contribution to the reduced carbon precursors for the prebiological synthesis of biochemical compounds. A brief review of the experiments carried out in the laboratory under possible primitive Earth conditions shows that amino acids, purines, pyrimidines, monosaccharides, fatty acids and other compounds are readily obtained using different energy sources. However, the formation of oligopeptides, oligonucleotides and phospholipids requires more restrictive conditions. They have been synthesized by means of condensing agents, such as cyanamide, as well as by heating under relatively dry conditions of less than 100° C. Experiments have been carried out on the formation of liposomes from prebiotically synthesized phospholipids. Also, using 2-methylimidazolide derivatives of

nucleotides, the template directed synthesis of polynucleotides has been demonstrated. In the latter experiments a high fidelity of complementary base pairing has been observed, which if further improved would approach that of enzyme catalyzed replication. However, it is not known how the prebiologically synthesized polymers became organized into a self-replicating system. At any rate the first living systems were probably very rudimentary heterotrophic micro-organisms which used organic compounds from the environment for both cell components and energy. They were probably followed by fermenters and eventually by autotrophic CO_2 reducing micro-organisms similar to the methanogenic and photosynthetic bacteria.

INTRODUCTION

Of all the terrestrial planets in the solar system perhaps none is as complex as the Earth, a body whose atmosphere, hydrosphere and lithosphere have been profoundly altered in the course of the evolutionary history of the biosphere by biological activity. Much of this change took place during the Precambrian which constitutes the longest, but least understood period of the history of our planet.

The purpose of this paper is to review and bring together some of the dispersed and limited evidence that gives an insight to the cosmic and primitive Earth environments, particularly those in which life is thought to have originated. To do so, we first discuss the extraterrestrial organic syntheses in interstellar clouds, comets and meteorites. This is followed by a discussion of the early evolution of the atmosphere, together with the prebiotic formation of organic molecules essential to life. Finally, the processes that led to the appearance of the first cells in the Archaean Earth and the early evolution of biological systems are briefly considered.

EXTRATERRESTRIAL ORGANIC SYNTHESES

Although the existence of simple combinations (C_2, CN, CH, CO) in the atmosphere of relatively cool stars has been known for a long time, it was not until 1969 that microwave radioastronomical techniques led to the detection of ammonia, water and the first organic molecule, formaldehyde (Snyder et al., 1969). This was quickly followed by the identification of many organic compounds, including acetaldehyde, hydrogen cyanide, cyanamide and the relatively complex linear cyano-oligoacetylenes, such as HC_3N, HC_5N, HC_7N, HC_9N (cf. Turner, 1980), and the largest organic molecule identified so far, $HC_{11}N$ (Bell et al., 1982). The latter molecule was found in the circumstellar envelope of the cool carbon star IRC+10° 216, providing evidence that one source of these complex interstellar molecules are cool carbon stars which, by means of different processes, eject material into the interstellar medium. A similar mechanism was suggested some time ago for the formation of interstellar molecules (Oró, 1972).

Quite remarkably, among the identified interstellar compounds are many

that have been used previously in prebiotic organic synthesis to obtain most of the biochemical monomers found in contemporary living systems (Table I). However, as of June, 1982, no interstellar biochemical monomer has been reported. The search for interstellar heterocyclic furan and imidazole (Dezafra et al., 1971), and for pyrimidines and pyridines (Simon and Simon, 1973) has yielded negative results. Glycine, which is a major product of most abiotic syntheses and one of the most abundant amino acids in meteorites, has been looked for unsuccessfully in several galactic molecular clouds (Brown et al., 1979). More recently, Hollis et al. (1980) have detected a single emission line in the Sgr B2 complex that is coincident with a rotational transition of this amino acid, but this is inadequate for definitive identification.

Moreover, a large number of interstellar emission lines in the 3—6 mm wavelength region remain to be identified, and it is possible that some of them could correspond to biochemical compounds. This possibility is made plausible by the results of several laboratory simulations of the interstellar environment

TABLE I

Biochemical monomers and properties which can be derived from molecules found in space[a]

Space molecules	Formulae	Biochemical monomers and properties
Hydrogen	H_2	Reducing agent, protonation
Water	H_2O	Universal solvent, hydroxylation
Ammonia	NH_3	Base catalysis, amination
Carbon monoxide (+ hydrogen)	CO	Fatty acids and hydrocarbons
Formaldehyde	CH_2O	Monosaccharides (ribose) and glycerol
Acetaldehyde (+ formaldehyde)	CH_3CHO	Deoxypentoses (deoxyribose)
Aldehyde (+ hydrogen cyanide)	RCHO	Amino acids
Thioformaldehyde (+ other molecules)	CH_2S	Cysteine
Methylmercaptan (+ other molecules)	CH_3SH	Methionine
Hydrogen cyanide	HCN	Purines (adenine, guanine) and amino acids
Cyanoacetylene	HC_2CN	Pyrimidines (cytosine, uracil, thymine)
Cyanamide	H_2NCN	Condensation of monomers to polypeptides, polynucleotides and lipids
Phosphine (Jupiter and Saturn) or Phosphates (meteorites)	PH_3 PO_4	Conversion to organic phosphates

[a] After Oró et al. (1978).

With the exception of phosphine and phosphate, which so far have only been detected in the giant planets or meteorites, all the other molecules have been found in interstellar space. These molecules either directly or through a sequence of chemical processes in aqueous solution involving other simple molecules can lead to the formation of the most important biochemical compounds.

in which icy-mixtures of H_2O, CH_4, CO_2, N_2, NH_3 and other simple molecules are irradiated by ionizing radiation (cf. Oró, 1963, Lazcano-Araujo and Oró, 1981) and ultraviolet light (cf. Greenberg, 1981). These experiments have yielded significant amounts of non-volatile organic polymers and monomeric water soluble biochemical compounds.

Since most of the interstellar organic compounds have been detected in dense cool interstellar clouds where star formation is taking place, it is reasonable to assume that the primordial solar nebula had a similar molecular composition. Indirectly this assumption is supported by the detection of a number of organic molecules and radicals (C_2, C, CH, CO, CS, HCN, CH_3CN) and other simple chemical species (NH, NH_3, OH, H_2O) in cometary spectra. Comets are relatively minor bodies with diameters of a few kilometers, consisting of ices (CO_2, NH_3, H_2O, etc.) and clathrates of simple compounds. They appear to be the most pristine bodies in the solar system (Whipple, 1950; Delsemme, 1977; Lazcano-Araujo and Oró, 1981; Donn, 1982).

Moreover, the presence of organic molecules in the solar nebula is further indicated by the large array of amino acids, carboxylic acids, purines, pyrimidines and hydrocarbons which have been found in carbonaceous chondrites. The earlier evidence has been reviewed by Hayes (1967) and Nagy (1975), the interesting results on extraterrestrial D and L amino acids were published by Kvenvolden et al. (1970, 1971) and Oró et al. (1971a, b), and data on nucleic acid bases (Stoks and Schwartz, 1981) and amino acids (Cronin et al., 1980, 1981; Cronin, 1982) have recently been presented. These compounds are presumed to be condensation and hydrolytic products of several of the interstellar molecules (see Table I). This suggests that some of these organic compounds were a part of the material from which the planets were formed.

There is a relatively close correspondence between the amino acid content of the Murchison CII carbonaceous chondrite and the products of electric discharge experiments with a CH_4—NH_3—N_2—H_2O atmosphere. A suggested interpretation is that the amino acids in the meteorite were synthesized on its parent body by similar processes (Wolman et al., 1972; Miller et al., 1976). Such a possibility is in part supported by the presence of veins of magnesium sulfate and dolomite in type I carbonaceous chondrites, which in turn has been interpreted by some to indicate exposure to fluid water (DuFresne and Anders, 1962; Nagy et al., 1963; Richardson, 1978; Kerridge and Bunch, 1979). Furthermore, it has also been claimed that the meteoritic organic compounds were abiotically formed at the pressures and temperatures of the solar nebula by a Fischer—Tropsch-type catalytic synthesis (Hayatsu et al., 1971). But, as Cronin et al. (1981) have pointed out, neither model system produces an amino acid suite completely comparable to that found in the Murchison meteorite. However, a complete correspondence of the model experiments and the meteorite amino acids would not be expected since the meteorite organic compounds have probably undergone considerable alteration since their synthesis. In particular, there are indications of considerable thermal decomposition. At any rate it is quite likely that several processes have been involved in

the synthesis of the amino acids (or their precursors) in carbonaceous chondrites. These include electric discharges, HCN condensation reactions, catalysis by the alumino-silicates of carbonaceous chondrites, and metal catalyzed Fischer–Tropsch-type reactions (cf. Oró, 1965; Hayatsu et al. 1968, 1971; Miller et al., 1976; Cronin et al., 1980).

The recent report by Engel and Nagy (1982) of partially racemized alanine, aspartic acid, proline, leucine and glutamic acid with a predominance of the L-stereoisomers in samples of the Murchison meteorite has once more raised the question of the abiotic origin of chirality and the problem of contamination. Although care was taken to prevent contamination during analysis, it is very difficult to control the contamination present in the meteorite sample before analysis. The possibility of bacterial intrusion is not negligible and was demonstrated for other meteorites (Oró and Tornabene, 1965). Furthermore, some of the first results on the separation of amino acid enantiomers from the Orgueil, Mokoia and Murray carbonaceous meteorites (Nakaparksin, 1969; Oró et al., 1971b), suggested that non-racemic meteoritic mixtures were due to terrestrial biological contamination prior to laboratory analysis. In support of this concept is the fact that the excess of L-enantiomeric forms found in the above study (Engel and Nagy, 1982) were only observed among some of the amino acids commonly present in proteins or bacterial cell walls, whereas only racemic mixtures were found in amino acids that are unlikely to be contaminants (e.g., α-aminobutyric, isovaline) (Bada et al., 1983).

THE ORIGIN OF THE TERRESTRIAL ATMOSPHERE

In attempting to understand the origin and evolution of Archaean environments, one of the major problems immediately faced is that of the origin and detailed chemical composition of the early terrestrial atmosphere. Since it is generally accepted that the solar system was formed ~4.6 Ga ago as a result of the condensation of the solar nebula, whose elementary abundances and molecular composition were essentially similar to those of the dense gas and dust regions found in the direction of the Milky Way, it would be tempting to assume that the early Earth inherited not only simple organic compounds from the solar nebula, but also relatively complex biochemical monomers such as those that are known to form from the irradiation of frozen mixtures of H_2, H_2O, CH_4, CO, CO_2, N_2, NH_3 and other molecules, as indicated earlier.

There are at least two reasons, however, that make it unlikely that the organic molecules from which the first living systems were formed were derived directly from the solar nebula. First, many of the theoretical models developed to explain the formation of the terrestrial planets predict a molten early Earth (Wetherill, 1980), which would lead to an extensive pyrolysis of primordial organic compounds whose products would form an equilibrium gaseous mixture of CO_2, CO, CH_4, H_2, N_2, NH_3 and H_2O (Miller, 1982).

Secondly, the amount of interstellar gaseous material trapped by the prebiotic Earth was very small, since the well-known terrestrial depletion of noble

gases relative to solar abundances (Brown, 1952; Suess and Urey, 1956; Rasool, 1972; Cameron, 1980) shows that the primordial atmosphere was almost completely lost and the Earth acquired most of its secondary atmosphere from the release of internal volatiles (cf. Walker, 1977). From the contemporary abundances of ^{20}Ne, a non-radiogenic isotope that is not incorporated into rocks (Canalas et al., 1968), Walker (1977) believes that the mass of the primordial terrestrial atmosphere must have been $< 10^{19}$ g ($< 0.2\%$ of the present atmosphere) with relative abundances of hydrogen, carbon and nitrogen given by $H/C \sim 6.28 \times 10^{-3}$ and $N/O \sim 2.09 \times 10^{-1}$, of which only very minor amounts were in the form of higher hydrocarbons and other organic compounds.

According to Greenberg (1981) and Johansson (1981), it is possible that relatively complex organic compounds abiotically synthesized in the interstellar medium may have been accreted by our planet during its encounters with interstellar clouds as the solar system travels around the galactic center. It is possible that such collisions were not rare in the past. Talbot and Newman (1977) have shown that the Sun has collided, during its life as a main-sequence star, with ~150 clouds with $>10^2$ hydrogen atoms per cm^3 and with ~15 clouds with $>10^3$ hydrogen atoms per cm^3. However, as Butler et al. (1978) have shown, during such encounters $\sim 1.5 \times 10^{15}$ g of carbon would have been accreted by the Earth, suggesting that they have been a relatively small source of primordial volatiles, comparable perhaps to the contribution made by solar wind atoms trapped by the early Earth (Lazcano-Araujo and Oró, 1981). This would represent a concentration of much less than 1 ppb of dissolved organic matter in the primeval sea.

As it is generally believed, the most likely source of the terrestrial secondary atmospheric gases was the release of volatiles from the Earth's interior (Walker, 1977; Pollack and Yung, 1980), although it is possible that very significant contributions were made by accreted chondritic material (Anders and Owen, 1977), cometary nuclei (Oró, 1961; Oró et al., 1980; Whipple, 1976; Chang, 1979; Lazcano-Araujò and Oró, 1981) and related volatile-rich interplanetary material (Wetherill, 1980).

Assuming that the probability of minor-body collisions with the Earth is approximately the same as for Venus, if cometary collisions were the major sources of terrestrial volatiles then the noble gas abundances and the N/C values should be the same for both planets (Pollack and Black, 1979). Since the Pioneer Venus spacecraft results have shown that this is not the case, Pollack and Black (1979) have argued that the atmosphere of Mars, Venus and the Earth were formed essentially by degassing, although McElroy and Prather (1981) have suggested that the abundances of primordial noble gases were enhanced in the pre-planetary material from which Venus was formed by the implantation of solar wind particles.

However, independent calculations based on dynamical considerations and lunar cratering rates (Oró et al., 1980; Pollack and Yung, 1980) and solar system chemical abundances (Chang, 1979) show that the early Earth must have accreted approximately 10^{22-23} g of cometary material over at least 1

Ga years. It is probable that a substantial fraction of the organic molecules present in cometary nuclei were destroyed due to the high temperatures and shock wave energy generated during the collision with the Earth. However, under the anoxic conditions generally thought to prevail in the prebiotic atmosphere, the post-collisional formation of large numbers of excited molecules and radicals may have led to the formation of more complex organic compounds of biochemical significance.

It should also be pointed out that recently published observations on the deuterium/hydrogen abundance ratio by the Venus pioneer orbiter and probe show that Venus is more than 100 times as deuterium-rich as the Earth (Donahue et al., 1982). This deuterium enrichment is presumed to be the result of the preferential escape of hydrogen from the upper atmosphere. Since this hydrogen and deuterium is ultimately derived from water, it implies that the primitive Venus had much more water than at present; at least a 10 m layer of liquid water covering its surface. Indeed, in 4.6 Ga years there is enough time for the hydrogen escape to have exhausted the equivalent of a terrestrial ocean of water from Venus. It would be of interest to perform similar measurements on the atmosphere of Mars to answer this and other related questions (Owen, 1979). We hope that with a more detailed study of the above and newly obtained data we will be able to eventually obtain a more complete assessment of the origin of the primitive atmospheres of the terrestrial planets.

THE CHEMICAL COMPOSITION OF THE ARCHAEAN PALEOATMOSPHERE

In the three decades that have gone by since the first successful synthesis of organic compounds was achieved under the highly reducing conditions of a CH_4—NH_3—H_2O—H_2 model atmosphere (Miller, 1953), one of the major questions in the understanding of the origin of life has been the detailed chemical composition of the Earth's early atmosphere. In a sense, the debate over the oxidation state of the gases of the prebiotic Earth is as old as the original hypothesis on chemical evolution put forward by the founding fathers of the field, since it is worth remembering that Oparin (1924, 1972) favored a CH_4—NH_3 primitive atmosphere, while Haldane (1929) assumed a CO_2-rich one.

Although it is possible that if intense degassing took place during the accretional phase of our planet then the primitive Earth could have had a highly reducing atmosphere (Pollack and Yung, 1980). The presence of the ~3.8 Ga-old carbonate-rich metasedimentary rocks in Isua, West Greenland (Moorbath et al., 1973) shows that even if methane was the dominant form in the primitive atmosphere, a substantial amount of CO_2 had to be present in the atmosphere 800 Ma after the Earth condensed (Schidlowski, 1978; Lazcano-Araujo and Oró, 1981). There was probably some CO_2 on the Earth at all times during the Archaean era even if methane was the predominant carbon-containing gas. This is similar to the situation in CI carbonaceous

chondrites, which contain carbonates (cf. Nagy, 1975, Richardson, 1978) and in cometary nuclei which contain CO_2 (Delsemme, 1977), even though these bodies as a whole are quite reducing.

Paleontological and geochemical evidence of early carbon dioxide is also provided by the presence of carbonate-rich 3.5 Ga-old fossil stromatolites from Western Australia (Lowe, 1980; Walters et al., 1980) and by the abundant amounts of reduced carbon in Archaean and early-Proterozoic sediments, which is generally accepted as evidence of extensive primary prokaryotic photosynthetic production (Reimer et al., 1979). Furthermore, there are various carbon dioxide fixation pathways that are found not only in aerobic and anaerobic photosynthetic prokaryotes, but also in more primitive methanogenic archaebacteria and some *Clostridia* (Broda, 1975; Margulis, 1981). This indicates that the early metabolic processes used the CO_2 in the environment, since such pathways would not be developed in the absence of CO_2. However, it is possible that the CO_2 was present in a localized environment produced by anaerobic fermentative micro-organisms rather than in the whole atmosphere.

Thus, it would appear in a first approach to the problem that the CH_4—NH_3—H_2 atmosphere proposed by Oparin (1924, 1972) and Urey (1952) was not very long lived. In fact, Walker (1977) has argued that the prebiotic atmosphere was dominated by CO_2 and H_2O with minor amounts of N_2 and only trace amounts of H_2 (~1%) and CO. The presence of Archaean atmospheric oxygen has also been proposed (Dimroth and Kimberly, 1976; Blake and Carver, 1977; Towe, 1981; Carver, 1981), a supposition that is supported by the work of Canuto et al. (1982), who have shown that since UV-observations of young T-Tauri stars suggest that the early Sun was emitting $\sim 10^4$ times more UV than at present, the photolytic dissociation of H_2O and CO_2 would lead to a prebiotic O_2 surface mixing ratio of 10^{-9} to 10^{-11}. This represents, however, a very small amount of oxygen which would quickly be removed by reaction with the Fe^{2+} of the surface minerals.

However, as the student of prebiological chemistry is painfully aware, when the non-reducing atmospheres discussed above are used in laboratory simulations, only negligible amounts of a few organic compounds are produced (Abelson, 1965). Theoretical calculations by Pinto et al. (1979) suggest that significant amounts of H_2CO can be produced from a weakly reducing atmosphere (CO_2 + H_2). Also, high partial pressures of H_2 appear to inhibit the synthesis of partially dehydrogenated compounds like purines, pyrimidines (Ponnamperuma et al., 1963; Bar-Nun et al., 1981) and nitriles (Bossard et al., 1982). But, as Miller (1982) has emphasized, electric discharge experiments with a CO_2—N_2—H_2O atmosphere with no added H_2 give only extremely small yields of amino acids (10^{-3}%), formaldehyde and hydrogen cyanide. These results are supported by Chameides and Walker's (1981) theoretical analysis that has shown that in a prebiotic atmosphere where C/O <1, shock processes from lightning and impacting bodies would yield very small

amounts of HCN, which is known to be a key intermediate in the prebiotic synthesis of amino acids and purines (Oró and Lazcano-Araujo, 1981).

In order to overcome these problems, it has been suggested that the prebiotic starting material was actually derived from cometary nuclei and carbonaceous chondrites accreted by the early Earth (Blake and Carver, 1977; Towe, 1981). The large number of impact craters which have been identified in the Moon, Mercury and Mars, and in several of the satellites of the outer planets, show that collisional processes with small interplanetary bodies probably played a major role in shaping the surface of the early Earth (Goodwin, 1976, 1981; Lazcano-Araujo and Oró, 1981). Thus, it is quite likely that important amounts of extraterrestrial organic material were brought to the Earth by such bodies. However, under the slightly-oxidizing conditions proposed by Blake and Carver (1977) and by Towe (1981) a partial photolytic degradation and oxidation of the organic compounds would be expected, as appears to have happened in Mars. In fact, the absence of indigenous organic compounds at the two Viking Lander sites on Mars (Biemann et al., 1976, 1977) can be explained as the result of the UV-degradation and oxidation of the organic molecules to CO_2, as has been demonstrated in the laboratory (Oró and Holzer, 1979a, b).

It seems likely to us that the accretion of cometary nuclei and related volatile-rich minor bodies by the primitive Earth were an important supply of reduced gases. Such collisions would in themselves produce organic compounds as a result of pyrolysis reactions caused by shock waves (cf. Oró et al., 1980; Lazcano-Araujo and Oró, 1981).

In addition to comets, reducing gases would have been produced by volcanoes as well as by mid-ocean spreading centers, if the latter had been present on the primitive Earth. These processes probably helped to provide the necessary precursors and to generate the aqueous and reducing environmental conditions required for the synthesis of organic compounds of biological significance.

SYNTHESIS OF BIOCHEMICAL MONOMERS

The wide variety of energy sources (Table II) and chemical precursors that have been used in experiments of prebiological organic synthesis are reviewed elsewhere (Miller et al., 1976; Oró and Lazcano-Araujo, 1981). It is true that some of these prebiotic model experiments have been performed under extreme concentrations or high inputs of energy (Miller and Van Trump, 1981; Chang, 1981) or, as in the case of the Fischer—Tropsch synthesis of fatty acids, under conditions of pressure and temperature that, although they may have been present in the solar nebula, are more difficult to envisage on the primitive Earth (Miller et al., 1976).

On the other hand, it is generally accepted that, at least in principle, the results of the laboratory abiotic synthesis of organic molecules indicates that

TABLE II

Present sources of energy averaged over Earth[a]

Source	Energy (cal cm^{-2} y^{-1})
Total radiation from Sun	260,000
Ultraviolet light	
3,000 A	3,400
2,500 A	563
2,000 A	41
1,500 A	1.7
Electric discharges[b]	4
Cosmic rays	0.0015
Radioactivity (to 1.0 km depth)	0.8
Volcanoes	0.13
Shock waves[b]	1.1
Solar wind	0.2

[a] From Miller et al. (1976).
[b] Due to the collisional events occurring during Earth's late accretion phase, the amounts of energy available as shock waves and electrical discharges may have been higher than the values listed here.

in the early Earth comparable processes took place and led eventually to an accumulation of a complex heterogeneous mixture of monomeric and polymeric organic compounds. For example, the sparking of a gaseous mixture of methane, nitrogen, ammonia and water produces protein and non-protein amino acids (Miller, 1953), although if a similar gaseous mixture is irradiated with ultraviolet light the yields are very low (Groth and Weyssenhoff, 1960). It should also be pointed out that significant amounts of amino acids, as well as ammonia, can be derived from the hydrolysis of HCN condensation products or oligomers (Oró and Kamat, 1961; Ferris et al., 1978). Also a number of protein amino acids may be produced non-enzymatically starting with formaldehyde and hydroxylamine (Oró et al., 1959; Ochiai et al., 1978).

Furthermore, possible prebiotic routes for the formation of all the components of nucleic acids have been established. Sugars are readily formed when formaldehyde polymerizes under alkaline conditions (Butlerow, 1861). Adenine, a purine that plays a central role in genetic processes and energy utilization, can be obtained together with guanine from the condensation of HCN under ammoniacal conditions (Oró, 1960; Oró and Kimball, 1961, 1962). Adenine was also synthesized from aqueous solutions of HCN via the photolysis of diaminomaleonitrile to 4-aminoimidazole–5-carbonitrile (Sanchez et al., 1966). It has also been shown that Fischer–Tropsch-like reactions using ammonia in addition to CO and H_2 yield purines, pyrimidines and other nitrogenous products (Yoshino et al., 1971; Yang and Oró, 1971). Cytosine is obtained from cyanacetylene (Sanchez et al., 1966), which on deamina-

tion yields uracil (Ferris et al., 1968) and thymine can be formed from the condensation of uracil with formaldehyde under reducing conditions (Stephen-Sherwood et al., 1971). Moreover, it has recently been shown by Ferris et al. (1978) that the hydrolysis of HCN oligomers releases significant amounts of pyrimidines and some of their biological precursors, together with several protein and non-protein amino acids and adenine.

In the presence of linear and cyclic phosphates the phosphorylated forms of the nucleosides of these bases (nucleotides) can be produced non-enzymatically. However, the nucleosides themselves are difficult to synthesize and additional studies are required to demonstrate their prebiotic synthesis. Fatty acids may be formed from CO and H_2 in the presence of meteoritic nickel-iron and other catalysts (Nooner et al., 1976; Nooner and Oró, 1979) and glycerol, a component of fats, can be readily formed by the reduction of glyceraldehyde, which is a product of the base-catalyzed condensation of H_2CO (Oró, 1965).

The major prebiotic pathways that may have led to non-enzymatic syntheses in primitive terrestrial environments of the most important biochemical monomers are shown in Table III. It should be emphasized, however, that the schematic reactions summarized in Table III are the result of a process of

TABLE III

Major prebiotic reaction pathways

1. CO H_2	FTT Catalysis	→	Hydrocarbons Fatty acids
2. CH_2O	Base catalysis	→	Ribose (glycerol)
3. CH_3CHO CH_2O	Base catalysis	→	Deoxyribose
4. RHCO HCN NH_3	Strecker synthesis	→	Amino acids Hydroxy acids
5. As 4 above CHL_2S or CH_3SH	Strecker synthesis (+ condensation)	→	Cysteine, methionine
6. HCN	Base catalysis	→	Adenine, guanine
7. HC_3N Urea	Condensation	→	Uracil, cytosine
8. As 7 above CH_2O	Hydrazine or H_2S	→	Thymine
9. Amino acids	Condensation	→	Oligopeptides
10. Mononucleotides	Condensation	→	Oligonucleotides
11. Isoprene	Condensation	→	Polyisoprenoids
12. Fatty acids Glycerols Phosphate Bases	Condensation	→	Neutral lipids Phospholipids

After Lazcano-Araujo and Oró (1981).
Simplified prebiotic pathways for the formation of monomers by reaction of simple molecules (1—8), and for the synthesis of oligomers and lipids by condensation of their building blocks (9—12) as they may have occurred by different condensing agents.

selection and simplification that reflects to a certain extent our personal preferences, since it is obvious that neither a single process nor a single set of precursors would account for all the organic matter produced in the prebiotic Earth (Oró et al., 1977).

OLIGOMER FORMATION AND THE EMERGENCE OF LIFE

As a recapitulation and further development of what has been said so far, there were at least three major steps in the synthesis and evolution of organic matter on the primitive Earth before the emergence of life, which may be briefly summarized as follows (Oró et al., 1978).

First, as a result of the action of various kinds of energy and catalysts, the simple organic molecules from the atmosphere, hydrosphere and lithosphere reacted to form a wide variety of low molecular weight biochemical compounds, including amino acids, purines, pyrimidines, sugars and fatty acids which were dissolved in bodies of water on the surface of the Earth.

Second, with the accumulation of these biochemical monomers in the lakes and other shallow bodies of water of the primitive Earth's surface, further condensation and polymerization reactions occurred yielding higher molecular weight compounds and oligomeric products, principally oligopeptides, oligonucleotides and lipids.

Several mechanisms for the condensation of amino acids and nucleotides have been studied under abiotic conditions (Oró and Stephen-Sherwood, 1974). These include coupling reactions using activated derivatives, condensation reactions using polyphosphates, and condensation reactions using organic condensing agents derived from HCN, such as cyanamide (Oró and Lazcano-Araujo, 1981). Cyanamide, which has been detected in the interstellar medium and was presumably synthesized on the primitive Earth from HCN is one of the best condensing agents. The evaporating pond model provides a geologically plausible and realistic model by means of which cyclic changes in humidity and temperature in the presence of cyanamide may have yielded significant amounts of oligopeptides (Hawker and Oró, 1981), oligonucleotides (Odom et al., 1982) and phospholipids (Rao et al., 1982). The prebiotic synthesis of acylglycerols (Eichberg et al., 1977), phosphatidic acids (Epps et al., 1978) and other lipids (Hargreaves et al., 1977) has also been accomplished recently. For reviews see Oró et al. (1978) and Hargreaves and Deamer (1978).

A number of recent experiments by L.E. Orgel (1982) and his associates have shown the catalytic role of Zn^{2+} in non-enzymatic template-directed syntheses of activated nucleotides (Lohrmann et al., 1980), in which a rather high fidelity in the incorporation of complementary bases was observed (Bridson et al., 1981). More recent experiments with an activated nucleotide with 2-methyl imidazole in the absence of metal ions have shown that the process of template-directed replication on a poly(C) template gives rise to over 90% of 3′—5′-linked oligo(G) nucleotides with chain lengths from 2 to ~40 (Orgel, 1982).

Third, the selective interactions and associations of these oligomers are presumed to have led to the emergence of replication, to the formation of liposomes, and to the appearance of cooperative association processes (Oró, 1980; Oró and Lazcano-Araujo, 1981) prior to the appearance of the first living systems.

Some investigators favor the process by which rudimentary transcriptional and translational processes evolved from the absorption of oligonucleotides and oligopeptides on clay mineral surfaces. Others favor a process in which the prebiologically synthesized oligomers reacted in aqueous solution or in liposome structures, i.e., within bilayer lipid membranes. Liposomes are known to be capable of selective absorption and concentration of ions and weak bases (Deamer and Oró, 1980) as well as of encapsulation of macromolecular compounds (Deamer and Barchfeld, 1982) within their self-sealing membrane structures. Presumably, this eventually led to systems of increased structural and functional complexity in which biocatalytic oligopeptides, informational replicating oligonucleotides and other biochemical molecules were established within liposomal structures until the first living system emerged.

A number of suggestions have been made in the past concerning the origin of life in the interstellar medium, comets, meteorites, the atmospheres of the giant planets, the atmosphere of the Earth and in submarine thermal springs. However, none of these environments appear to fulfill the conditions necessary for the accumulation of monomers, condensation of monomers into linear oligomers, elongation of monomers, replication of oligonucleotides, formation of liposomes and macromolecular encapsulation processes, which are provided by the aqueous evaporating pond model described above, through cyclic changes of humidity and temperature. It seems that only the primitive Earth surface, or a similar planetary surface with evaporating bodies of aqueous solutions of organic compounds, can provide an almost unique environment with the highly restrictive conditions necessary for the emergence of early forms of life. The panspermia theory suggests the continuous universal distribution of life, but transfers the problem of the origin of life to other unknown planets or environments. Since it does not deal directly with the real problem of biopoiesis it cannot be considered as a theory of the origin of life.

EARLY EVOLUTION OF LIFE

It must be admitted that the study of the early phases of biological evolution is still highly speculative (Miller and Orgel, 1974). This situation exists in spite of the fact that the problem can be approached by various techniques, including micropaleontology and comparative studies of the complexity of metabolic pathways, as well as by studies on macromolecular sequence data of proteins, DNA, and 16S r RNA, the so-called "molecular living fossils". The discussion that follows is, therefore, tentative and is meant only to briefly illustrate some of the possibilities in this field, and indicate some recent developments, including carbon isotopic measurements of the Precambrian

and studies on methanogenic bacteria, which, as has been suggested recently (Hayes, 1983), were probably present in the Precambrian.

At the outset there seems to be a general consensus that the very first organisms on the primitive Earth must have grown and reproduced at the expense of the prebiotic soup. They must have been relatively simple anaerobic heterotrophic organisms which depended on the prebiotically synthesized organic matter, both as a source of carbon and energy. It is possible that the prebiotic synthetic processes overlapped for some time with the existence of early life. However, sooner or later the demand for essential components from the prebiotic soup must have exceeded the supply. This constituted the first material and energy crisis that life experienced on this Earth. When this happened the further expansion of life depended on the ability of organisms to find ways of synthesizing their own constituents. They may have used as starting materials simple organic compounds that remained abundant in their aqueous environment (primitive metabolism) or components of the atmosphere (chemolithotrophism and primitive photosynthesis). Modern biosynthetic pathways have presumably developed by the elaboration of these primitive processes.

In a parallel way, the earliest organisms must have used energy-rich organic molecules formed abiotically in their surroundings to accomplish protein synthesis and nucleic acid replication. Here, too, the supply of energy-rich molecules must soon have proved inadequate to support the rapid expansion of life. At this point, other available chemical and physical sources of energy must have been utilized. This probably included, on one hand, substrate phosphorylation resulting from fermentative processes, as well as from reactions of reduced compounds (H_2, H_2S, etc.) with CO_2 (chemoautotrophic reactions). Moreover, the most important source of energy, radiation from the sun, must have also been harnessed in a process analogous to photosynthetic phosphorylation. Indeed, this represents a permanent solution to the first energy crisis experienced by life, so that it could continue to exist and evolve on Earth until the present time.

In relation to the utilization of solar radiation it is clear that the early development of adequate ultraviolet protection mechanisms (Rambler and Margulis, 1980), of metabolic pathways for the biological fixation of atmospheric CO_2 and N_2 and the biosynthesis of cytochromes, magnesium porphyrins and other compounds, must have preceded the appearance of photosynthetic organisms (Margulis, 1982; Margulis and Lazcano-Araujo, 1982). However, it is not possible to establish the time of appearance of prokaryotic photosynthesis, nor can it be said that the fossil evidence for life in the 3.5 Ga-old stromatolites from Western Australia (Lowe, 1980; Walters et al., 1980) is that of photosynthetic organisms. These may have been built up by cyanobacteria, photosynthetic bacteria, or other type of prokaryotes (Awramik, 1982; Margulis et al., 1980).

Isotopic measurements of the kerogen carbon from rocks of the Fortescue group of Western Australia, about 2.75 Ga-old, give $\delta^{13}C$ fractionation values of about −50 per million (Hayes et al., 1983). These highly negative values

appear to be widely spread not only in Australia, but also in the Lake Superior area of the North American continent as found by other investigators (−43 per million) (cf. Hayes et al., 1983). The high degree of fractionation has been interpreted to suggest the extensive presence of methanogenic bacteria at that time in the Precambrian (Hayes, 1983). Presumably some of these methane producing bacteria were associated with other micro-organisms which used methane, and the organic compounds with lighter carbon isotopes were eventually converted into kerogen. This continuous recycling of the carbon isotopes would have led to a larger fractionation than the one produced by the ribulodiphosphate carboxylase of modern photosynthetic organisms. In this respect it would be of interest to measure the $\delta^{13}C$ values of the bacterial association known as *Methanobacillus omelianski.* This is not a single organism, but rather the symbiotic partnership of two organisms, one producing CO_2 and H_2 and the other a methanogen that fixes the CO_2 and the H_2 into methane (Bryant et al., 1967; Reddy et al., 1972). It is possible that similar symbiotic associations may have existed in the Precambrian.

Furthermore, the $\delta^{13}C$ values of the carbon from sedimentary rocks 2.8—3.5 Ga-old, which are typically −35 per million, do not exclude the participation of methanogens, although photosynthetic and other bacteria may also have contributed to the fractionation process. In fact, $\delta^{13}C$ values of −35 per million are considered typical of marine chemoautotrophic bacteria (cf. Degens, 1979), which metabolically belong to the same class as methanogens. The $\delta^{13}C$ values of the graphitic carbon in the ~3.8 Ga-old Isua metasediments reflect an Archaean photoautotrophic carbon fixation (Schidlowski et al., 1979), but neither do they exclude other interpretations of the data, including chemoautotropic CO_2 fixation processes.

METHANOGENIC AND OTHER BACTERIA

Recent findings in the nucleotide sequence of the 16S r RNA of several species of methanogenic bacteria (Fox et al., 1977, 1980) suggest that these organisms, which are distantly related to typical bacteria by several criteria, diverged from their common prokaryotic ancestors at least after the development of the genetic system and the biosynthesis of ferrodoxins and isoprenoids (Margulis, 1981). It is likely that the chemoautotrophy of methanogens may have predated bacterial photosynthesis, although a parallel evolution for these two groups of organisms cannot be ruled out.

Methanogens, which belong to a new class of bacteria designated as archaebacteria (Woese and Fox, 1977), are a unique group of obligate anaerobes that produce CH_4 from CO_2 and H_2, although different species can use formate, ethanol and other compounds as electron donors for the CO_2 reduction (Zeikus, 1977). They are also known to possess a unique set of coenzymes, such as mercaptoethanesulfonic acid, involved in the formation of methane (McBride and Wolfe, 1971), and to have a relatively smaller genome than other bacteria.

The distinguishing features of archaebacteria involve major properties of

cellular organization and include (1) the primary sequence homologies seen by 16S rRNA cataloging (Fox et al., 1980); (2) cell walls (when present) which lack peptidoglycan and do not contain muramic acid (Kandler and König, 1978); (3) membranes whose major component is a branched chain (phytanyl or biphytanyl) ether linked lipid in contrast to the usual ester lipids of fatty acids which are universal among eubacteria (Tornabene et al., 1978; Tornabene and Langworthy, 1979; Oró et al., 1981); (4) the presence of squalene and related isoprenoid hydrocarbons among the neutral lipids which are not widely found among eubacteria (Tornabene et al., 1978, 1979; Holzer et al., 1979); and (5) RNA polymerases that are insensitive to rifampicin and streptolydigin, and which do not observe the sub-unit pattern of eubacterial RNA polymerases (Zillig et al., 1978).

In addition to these distinguishing features the archaebacteria also show a phenotypic diversity which is comparable to that of eubacteria. This is what would be expected if these organisms constituted a separate kingdom from prokaryotes and eukaryotes. Even though the name archaebacteria was chosen to indicate that some of its members seem to be ancient, this does not mean that it should apply to all of the individual genera. Thus, it is reasonable to suppose that some phenotypes of this kingdom may be old and others may be of more recent origin. In fact, the S_{ab} values of Table IV (Fox, 1981) indicate that the extreme halophiles are of much more recent origin than the methanogens. This table summarizes the S_{ab} values obtained by analysis of the 16S rRNA catalog sequences of different bacterial phenotypes. Lower

TABLE IV

Phenotypic diversity from 16S rRNA cataloging data[a]

Phenotype	Comments	Lower S_{ab} limit
Bioluminescent bacteria	Luciferase gene expressed	0.65
Enteric/vibrio	*Escherichia coli* and relatives	0.52
Bacillus	Aerobic, endospores	0.49
Extreme halophiles	Aerobic, 12% NaCl	0.44
Actinomyces/relatives	*Nocardia, Micrococcus,* etc.	0.40
Cyanobacteria	Oxygenic photosynthesis	0.36
Purple non-sulfur bacteria	Photoheterotrophs	0.32
Clostridia	Anaerobes, endospores	0.28
Methanogens	$CO_2 + H_2 \rightarrow CH_4$ anaerobes	0.20

[a]From Fox (1981).

The lower S_{ab} limit is a measure of the similarity of the 16S rRNAs from the ribosomes of various species (e.g., 15 different methanogens and 20 clostridia) (Fox et al., 1980). If the phenotypic traits chosen are evolutionarily significant and if the organisms actually cataloged are representative of the phenotype then the lower S_{ab} limit would be expected to be indicative of the relative age of that phenotype. Lower values are indicative of greater diversity in the phenotype, and are thus suggestive of earlier evolutionary divergence.

S_{ab} values are indicative of greater diversity in the phenotype and are thus suggestive of earlier evolutionary divergence (Fox et al., 1980). This comparison also shows that the methanogens and the *Clostridia* are probably some of the most ancient extant organisms since they have the lowest S_{ab} values, a conclusion which is not incompatible with DNA sequence data (Barnabas et al., 1982).

CONCLUSION

It appears that the most effective way for ultimately unraveling the nature of the earliest living organisms on Earth will not be obtained by the sole application of microfossil and carbon isotopic methods, or by comparative geological, geochemical and biological studies. So far, these studies have only led to a conclusion that the earliest known bacterial communities are similar to those living in stromatolites (Margulis et al., 1980). Of course a complete answer may never be obtained because many evolutionary links are probably extinct. Therefore, the only hope of advance in this field is by a multiple pronged attack, including primarily the study of the macromolecular living fossils of extant organisms, namely, the sequences of DNA, RNA and proteins.

However, a special emphasis should be placed on the genetic and structural analysis of the microbial and organelle genomes, and their correlation with the enzymes which are responsible for the different metabolic pathways and their evolution in the course of time. Only by knowing the details of the organization of the microbial genome and of how it is transcribed and translated, and by comparing this information with other pertinent data, will it be possible to establish the philogenetic relationships among different microorganisms and eventually to determine the most primitive representatives. Thus, the crucial data is to be found in the genome's organization. Such data should also be eventually correlated with the gross morphological features of the most ancient microfossils and with any available structural and chemical composition data about the organic remains of these fossils. Hopefully, the development of new high resolution techniques for the ion microprobe analysis of such microfossils may provide the required complementary information.

ACKNOWLEDGMENTS

This work was supported in part by grants from the National Aeronautics and Space Administration, Grant NGR 44-005-002 to J. Oró, and NAGW 20 to S.L. Miller. A. Lazcano is indebted to the NASA Summer Program on Planetary Biology and Microbial Ecology, the First European Summer School on the Origins and Early Evolution of Life, and to the 1981 NATO Advanced Study Institute on Cosmochemistry and the Origin of Life.

REFERENCES

Abelson, P.H., 1965. Abiogenic synthesis in the Martian environment. Proc. Natl. Acad. Sci. U.S.A., 54: 1490—1494.

Anders, E. and Owen, T., 1977. Mars and Earth: origin and abundance of volatiles. Science, 198: 453—465.

Awramik, S.M., 1982. The Pre-Phanerozoic fossil record. In: H.D. Holland and M. Schidlowski (Editors), Mineral Deposits and the Evolution of the Biosphere. Springer-Verlag, Berlin, pp. 67—81.

Bada, J.L., Cronin, J.R., Ho, M.-S., Kvenvolden, K.A., Lawless, J.G., Miller, S.L., Oro, J. and Steinberg, S., 1983. On the reported optical activity of amino acids in the Murchison meteorite. Nature, 301: 494—496.

Bar-Nun, A., Lazcano-Araujo, A. and Oró, J., 1981. Could life have evolved in cometary nuclei? Origins Life, 11: 387—394.

Barnabas, J., Schwartz, R.M. and Dayhoff, M., 1982. Evolution of major metabolic innovations in the Precambrian. Origins Life, 12: 81—91.

Bell, M.B., Feldman, P.A., Kwok, S. and Matthews, H.E., 1982. Detection of $HC_{11}N$ in IRC+10° 216. Nature, 295: 389—391.

Biemann, K., Oró, J., Toulmin III, P., Orgel, L.E., Nier, A.O., Anderson, D.M., Simmonds, P.B., Flory, D., Diaz, A.V., Rushneck, D.R. and Biller, J.E., 1976. Search for organic and volatile inorganic compounds in two surface samples from the Chryse Planitia region of Mars. Science, 194: 72—76.

Biemann, K., Oró, J., Toulmin III, P., Orgel, L.E., Nier, A.O., Anderson, D.M., Simmonds, P.B., Flory, D., Diaz, A.V., Rushneck, D.P., Biller, J.E. and Lafleur, A.L., 1977. The search for organic substances and inorganic volatile compounds in the surface of Mars. J. Geophys. Res., 82: 4641—4658.

Blake, A.J. and Carver, J.H., 1977. The evolutionary role of atmospheric ozone. J. Atmos. Sci., 34: 720—728.

Bossard, A., Mourey, D. and Raulin, F., 1982. The escape of molecular hydrogen and the synthesis of organic nitriles in planetary atmospheres. Abstracts of the 24th COSPAR Plenary Meeting, Ottawa, 16 May—2 June, 1982, Cospar, Paris.

Bridson, P.K., Fakhrai, H., Lohrmann, R., Orgel, L.E. and van Roode, M., 1981. Template-directed synthesis of oligoguanylic acids: Metal ion catalyses. In: Y. Wolman (Editor), Origin of Life. Reidel, Dordrecht, pp. 233—239.

Broda, E., 1975. The Evolution of the Bioenergetic Processes. Pergamon, Oxford, 211 pp.

Brown, H., 1952. Rare gases and the formation of the Earth's atmosphere. In: G.P. Kuiper (Editor), The Atmospheres of the Earth and Planets, 2nd Ed. University Chicago Press, Chicago, pp. 258—266.

Brown, R.D., Godfrey, P.D., Storey, J.W.V., Bassez, M.P., Robinson, B.J., Batchelor, R.A., McCulloch, M.G., Rydbeck, O.E.H. and Hjalmarson, A.G., 1979. A search for interstellar glycine. Mon. Not. R. Astron. Soc., 186: 5P—8P.

Bryant, M.P., Wolin, E.A., Wolin, M.J. and Wolfe, R.S., 1967. *Methanobacillus omelianski*, a symbiotic association of two species of bacteria. Arch. Mikrobiol., 59: 20—31.

Butler, D.M., Newman, M.J. and Talbot, R.J., 1978. Interstellar cloud material: contribution to planetary atmospheres. Science, 201: 522—525.

Butlerow, A., 1861. Formation synthetique d'une substance sucree. C.R. Acad. Sci., 53: 145—147.

Cameron, A.G.W., 1980. A new table of abundances of the elements in the Solar System. In: L.A. Ahrens (Editor), Origin and Distribution of the Elements. Pergamon, New York, pp. 125—143.

Canalas, R.A., Alexander, E.C. and Manuel, O.K., 1968. Terrestrial abundance of noble gases. J. Geophys. Res., 73: 3331—3334.

Canuto, V.M., Levine, J.S., Augustsson, T.R. and Imhoff, C.L., 1982. UV radiation from the young Sun and oxygen and ozone levels in the prebiological paleoatmosphere. Nature, 296: 816—820.

Carver, J.H., 1981. Prebiotic oxygen atmospheric levels. Nature, 292: 136—138.
Chameides, W.L. and Walker, J.C.G., 1981. Rates of fixation by lightning of carbon and nitrogen in possible primitive atmospheres. Origins Life, 11: 291—302.
Chang, S., 1979. Comets: cosmic connections with carbonaceous chondrites, interstellar molecules and the origin of life. In: M. Neugebauer, D.K. Yeomans, J.C. Brandt and R.W. Hobbs (Editors), Space Missions to Comets. NASA CP-2089, Washington, D.C., pp. 59—111.
Chang, S., 1981. Organic chemical evolution. In: J. Billingham (Editor), Life in the Universe. MIT Press, Cambridge, pp. 21—46.
Cronin, J.T., 1982. Amino acids in meteorites. Abstracts of the 24th COSPAR Plenary Meeting, Ottawa, 16 May—2 June, 1982, Cospar, Paris, 510 pp.
Cronin, J.R., Gandy, W.E. and Pizzarello, S., 1980. Amino acids in the Murchison meteorite. In: P.E. Hare and K. King (Editors), The Biogeochemistry of Amino Acids. Wiley, New York, pp. 153.
Cronin, J.R., Gandy, W.E. and Pizzarello, S., 1981. Amino acids of the Murchison meteorite: I. Six carbon acyclic primary α-aminoalkanoic acids. J. Mol. Evol., 17: 265—272.
Deamer, D.W. and Barchfeld, G.L., 1982. Encapsulation of macromolecules by lipid vesicles under simulated prebiotic conditions. J. Mol. Evol., 18: 203—206.
Deamer, D.W. and Oró, J., 1980. Role of lipids in prebiotic structures. Biosystems, 12: 167—175.
Degens, E.T., 1969. Biogeochemistry of stable carbon isotopes. In: G. Eglinton and M.T.G. Murphy (Editors), Organic Geochemistry. Springer, New York, pp. 304—329.
Delsemme, A.H., 1977. The pristine nature of comets. In: A.H. Delsemme (Editor), Comets, Asteroids, Meteorites. University Toledo Press, Toledo, Ohio, pp. 3—13.
Dezafra, R.L., Thaddeus, P., Kutner, M., Scoville, N., Solomon, P.M., Weaver, H. and Williams, D.R.W., 1971. Search for interstellar furan and imidazole. Astrophys. Lett., 10: 1—3.
Dimroth, E. and Kimberley, M.M., 1976. Precambrian atmospheric oxygen: evidence in the sedimentary distribution of carbon, sulfur, uranium and iron. Can. J. Earth. Sci., 13: 1161—1185.
Donahue, T.M., Hoffman, J.H., Hodges, R.R. Jr. and Watson, A.J., 1982. Venus was wet: a measurement of the ratio of deuterium to hydrogen. Science, 126: 630—633.
Donn, B., 1982. Comets: Chemistry and chemical evolution. J. Mol. Evol., 18: 157—160.
DuFresne, E.R. and Anders, E., 1962. On the chemical evolution of carbonaceous chondrites. Geochim. Cosmochim. Acta, 26: 1085—1114.
Eichberg, J., Sherwood, E., Epps, D.E. and Oró, J., 1977. Cyanamide mediated syntheses under plausible primitive Earth conditions. IV. The synthesis of acylglycerols. J. Mol. Evol., 10: 221—230.
Engel, M.H. and Nagy, B., 1982. Distribution and enantiomeric composition of amino acids in the Murchison meteorite. Nature, 296: 837—840.
Epps, D.E., Sherwood, E., Eichberg, J. and Oró, J., 1978. Cyanamide mediated synthesis under plausible primitive Earth conditions. V. The synthesis of phosphatidic acids. J. Mol. Evol., 11: 279—292.
Ferris, J.R., Joshi, P.C., Edelson, E. and Lawless, J.G., 1978. HCN: a plausible source of purines, pyrimidines and amino acids on the primitive Earth. J. Mol. Evol., 11: 293—311.
Ferris, J.R., Sanchez, R.A. and Orgel, L.E., 1968. Studies in prebiotic synthesis. 3. Synthesis of pyrimidines from cyanoacetylene and cyanate. J. Mol. Biol., 33: 693—704.
Fox, G., 1981. Archaebacteria, ribosomes and the origin of eukaryotic cells. In: G.G.E. Scudder and J.L. Reveal (Editors), Evolution Today. Proceedings of the Second International Congress of Systematic and Evolutionary Biology, Carnegie-Mellon Univ. Press, Pittsburgh, PA, pp. 235—244.
Fox, G.E., Magrum, L.J., Balch, W.E., Wolfe, R.S. and Woese, C.R., 1977. Classification of methanogenic bacteria by 16S ribosomal RNA characterization. Proc. Natl. Acad. Sci. U.S.A., 74: 4537—4541.

Fox, G.E., Stackebrandt, E., Hespell, R.B., Gibson, J., Maniloff, J., Dyer, T., Wolfe, R.S., Balch, W., Tanner, R., Magrum, L., Zablen, L.B., Blakemore, R., Gupta, R., Bonen, K.R., Luehrsen, K.R., Lewis, R.J., Chen, K.N. and Woese, C., 1980. The phylogeny of procaryotes. Science, 209: 457—463.

Goodwin, A.M., 1976. Giant impacting and the development of continental crust. In: B.F. Windley (Editor), The Early History of the Earth. Wiley, New York, pp. 77—95.

Goodwin, A.M., 1981. Precambrian perspectives. Science, 213: 55—76.

Greenberg, J.M., 1981. Chemical evolution of interstellar dust. A source of prebiotic material? In: C. Ponnamperuma (Editor), Comets and the Origin of Life. Reidel, Dordrecht, pp. 111—127.

Groth, W. and von Weyssenhoff, H., 1960. Photochemical formation of organic compounds from mixtures of simple gases. Planet. Space Sci., 2: 79—85.

Haldane, J.B.S., 1929. The Origin of Life. Rationalist Annu., 148: 3—10. Reprinted in J.D. Barnal, 1967, The Origin of Life. World, Cleveland, OH, pp. 242—249.

Hargreaves, W.R., Mulvihill, S. and Deamer, D.W., 1977. Synthesis of phospholipids and membranes in prebiotic conditions. Nature, 266: 355—357.

Hargreaves, W.R. and Deamer, D.W., 1978. Liposomes from ionic, single chain amphiphiles. Biochemistry, 17: 3759—3768.

Hawker, J.R. and Oró, J., 1981. Cyanamide mediated synthesis of Leu, Ala, Phe peptides under plausible primitive Earth conditions. In: Y. Wolman (Editor), Origin of Life. Reidel, Dordrecht, pp. 225—232.

Hayatsu, R., Studier, M.H. and Anders, E., 1971. Origin of organic matter in the early Solar System. IV. Amino acids: confirmation of catalytic synthesis by mass spectrometry. Geochim. Cosmochim. Acta, 35: 939—951.

Hayatsu, R., Studier, M.H., Oda, A., Fuse, K. and Anders, E., 1968. Origin of organic matter in early Solar System. 2. Nitrogen compounds. Geochim. Cosmochim. Acta, 32: 175—190.

Hayes, J.M., 1967. Organic constituents of meteorites — a review. Geochim. Cosmochim. Acta, 31: 1395—1440.

Hayes, J.M., 1983. Geochemical evidence bearing on the origin of aerobiosis, speculative interpretation. In: J.W. Schopf, (Editor), The Earth's Earliest Biosphere: Its Origin and Evolution. Princeton University Press, Princeton, N.J., Chapter 12 (in press).

Hayes, J.M., Kaplan, I.R. and Wedeking, K.W., 1983. Precambrian organic geochemistry, preservation of the record. In: J.W. Schopf, (Editor), The Earth's Earliest Biosphere: Its Origin and Evolution. Princeton University Press, Princeton, N.J., Chapter 5 (in press).

Hollis, J.M., Snyder, L.E., Suenram, R.D. and Lovas, F.J., 1980. A search for the lowest energy conformer of interstellar glycine. Astrophys. J., 241: 1001—1006.

Holzer, G., Oró, J. and Tornabene, T.G., 1979. Gas chromatographic—mass spectrometric analysis of neutral lipids from methanogenic and thermoacidophylic bacteria. J. Chromatogr., 186: 873—887.

Johansson, K.L.V., 1981. On the origin of organic molecules in interstellar space and some of its consequences. In: Y. Wolman (Editor), Origin of Life. Reidel, Dordrecht, pp. 19—25.

Kandler, O. and König, H., 1978. Chemical composition of the peptidoglycan-free cell walls of methanogenic bacteria. Arch. Microbiol., 118: 141—152.

Kerridge, J.G. and Bunch, T.E., 1979. Aqueous activity on asteroids. Evidence from carbonaceous meteorites, In: T. Gehrels (Editor), Asteroids. University Arizona Press, pp. 745—764.

Kvenvolden, K.A., Lawless, J.G. and Ponnamperuma, C., 1971. Nonprotein amino acids in the Murchison meteorite. Proc. Natl. Acad. Sci. U.S.A., 68: 486—490.

Kvenvolden, K.A., Lawless, J.G., Perking, K., Peterson, E., Flores, J., Ponnamperuma, C., Kaplan, I.R. and Moore, C., 1970. Evidence for extraterrestrial amino acids and hydrocarbons in the Murchison meteorite. Nature, 228: 923—926.

Lazcano-Araujo, A. and Oró, J., 1981. Cometary material and the origins of life on Earth. In: C. Ponnamperuma (Editor), Comets and the Origin of Life. Reidel, Dordrecht, pp. 191—225.

Lohrmann, R., Bridson, P.K. and Orgel, L.E., 1980. Efficient metal-ion catalyzed template-directed oligonucleotide synthesis. Science, 208: 1464—1465.
Lowe, D.R., 1980. Stromatolites 3,400 M.Y. old from the Archean of Western Australia. Nature, 284: 441—443.
Margulis, L., 1981. Symbiosis in Cell Evolution. Freeman, San Francisco, 419 pp.
Margulis, L., 1982. Early Life. Science Books International, Boston, 160 pp.
Margulis, L. and Lazcano-Araujo, A., 1983. Evolución Celular (in preparation).
Margulis, L. and Lovelock, J., 1978. The biota as ancient and modern modulator of the Earth's atmosphere. Pure Appl. Geophys., 116: 239—243.
Margulis, L., Barghoorn, E.S., Banerjee, S., Giovannoni, S., Francis, S., Ashendorf, D., Chase, D. and Stolz, J., 1980. The microbial community in the layered banded sediments in Laguna Figueroa, Baja California, Mexico: does it have Precambrian analogues? Precambrian Res., 11: 93—123.
McBride, B.C. and Wolfe, R.S., 1971. A new coenzyme of methyl transfer, coenzyme M. Biochemistry, 10: 2317—2324.
McElroy, M.B. and Prather, M.J., 1981. Noble gases in the terrestrial planets. Nature, 293: 535—539.
Miller, S.L., 1953. A production of amino acids under possible primitive Earth conditions. Science, 117: 528—529.
Miller, S.L., 1982. Prebiotic syntheses of organic compounds. In: H.D. Holland and M. Schidlowski (Editors), Mineral Deposits and the Evolution of the Biosphere. Dahlem Konferenzen, Springer-Verlag, Berlin, pp. 155—176.
Miller, S.L. and Orgel, L.E., 1974. The Origins of Life on Earth. Prentice-Hall, Englewood Cliffs, 229 pp.
Miller, S.L. and Van Trump, J.E., 1981. The Strecker synthesis in the primitive ocean. In: Y. Wolman (Editor), Origin of Life. Reidel, Dordrecht, pp. 135—141.
Miller, S.L., Urey, H.C. and Oró, J., 1976. Origin of organic compounds on the primitive Earth and in meteorites. J. Mol. Evol., 9: 59—72.
Moorbath, S., O'Nions, R.K. and Pankhurst, F.J., 1973. Early Archean age for the Isua Iron-formation, West Greenland. Nature, 245: 138—139.
Nakaparksin, S., 1969. Separation of amino acid enantiomers by gas chromatography on optically active stationary phases and applications to organic geochemistry. Ph.D. Thesis, University of Houston.
Nagy, B., 1975. Carbonaceous Meteorites. Elsevier, Amsterdam, 747 pp.
Nagy, B., Meinschein, W.G. and Hennesy, G.G., 1963. Aqueous low-temperature environment of the Orgueil meteorite parent body. Ann. N.Y. Acad. Sci., 93: 25—35.
Nooner, D.W. and Oró, J., 1979. Synthesis of fatty acids by a closed system Fischer—Tropsch process. In: E.L. Kugler and F.W. Steffgen (Editors), Advances in Chemistry Series, No. 178: Hydrocarbon Synthesis from Carbon Monoxide and Hydrogen. American Chemical Society, Washington, DC, pp. 159—171.
Nooner, D.W., Gibert, J.M., Gelpi, E. and Oró, J., 1976. Closed system Fischer—Tropsch synthesis over meteoritic iron, iron ore and nickel-iron alloy. Geochim. Cosmochim. Acta., 40: 915—924.
Ochiai, T., Hatanaka, H., Ventilla, M., Yanagawa, H., Ogawa, Y. and Egami, F., 1978. Experimental approach to the chemical evolution in the primeval sea: I. Formation of amino acids and amino acid polymers in modified sea mediums. In: H. Noda (Editor), Origin of Life. Proceedings of Second ISSOL Meeting and Fifth ICOL Meeting, Center for Academic Publications, Japan Scientific Societies Press, Tokyo, pp. 135—139.
Odum, D.B., Yamrom, T. and Orô, J., 1982. Oligonucleotide synthesis in a cycling system at low temperature by cyanomide or a water soluble carbodiimide. Abstracts of the 24th COSPAR Plenary Meeting, Ottawa, 16 May—2 June, 1982. Cospar, Paris, p. 511.
Oparin, A.I., 1924. Proiskhozdenie Zhizni, Moskovkii Rabotchii, Moscow (in Russian). Translation reprinted in J.D. Bernal, 1967. The Origin of Life. World, Cleveland, OH, pp. 199—241.

Oparin, A.I., 1972. The appearance of life in the universe. In: C. Ponnamperuma (Editor), Exobiology. North-Holland, Amsterdam, pp. 1—15.
Orgel, L.E., 1982. An RNA polymerase model. Abstracts of the 24th COSPAR Plenary Meeting, Ottawa, 16 May—2 June, 1982, Cospar, Paris, p. 513.
Oró, J., 1960. Synthesis of adenine from ammonium cyanide. Biochim. Biochem. Res. Comm., 2: 407—412.
Oró, J., 1961. Comets and the formation of biochemical compounds on the primitive Earth. Nature, 190: 389—390.
Oró, J., 1963. Synthesis of organic compounds by high energy electrons. Nature, 197: 971—974.
Oró, J., 1965. Stages and mechanisms of prebiological organic synthesis. In: S.W. Fox (Editor), The Origins of Prebiological Systems. Academic Press, New York, pp. 137—162.
Oró, J., 1980. Prebiological organic synthesis and the origin of life. In: H.O. Halvorson and K. van Holde (Editors), The Origins of Life and Evolution. Alar R. Liss, New York, pp. 47—63.
Oró, J. and Holzer, G., 1979a. The effects of ultraviolet light on the degradation of organic compounds: a possible explanation for the absence of organic matter on Mars. In: R. Holmquist (Editor), COSPAR: Life Sciences and Space Research, Vol. XVII. Pergamon Press, Oxford, pp. 77—86.
Oró, J. and Holzer, G., 1979b. The photolytic degradation and oxidation of organic compounds under simulated Martian conditions. J. Mol. Evol., 14: 153—160.
Oró, J. and Kamat, S.S., 1961. Amino acid synthesis from hydrogen cyanide under possible primitive Earth conditions. Nature, 190: 442—443.
Oró, J. and Kimball, A.P., 1961. Synthesis of purines under primitive earth conditions. I. Adenine from hydrogen cyanide. Arch. Biochem. Biophys., 34: 217—227.
Oró, J. and Kimball, A.P., 1962. Synthesis of purines under possible primitive Earth conditions. II. Purine intermediates from hydrogen cyanide. Arch. Biochem. Biophys., 96: 293.
Oró, J. and Lazcano-Araujo, A., 1981. The role of HCN and its derivatives in prebiotic evolution. In: B. Vennesland, E.E. Conn, C.J. Knowles, J. Westley and F. Wissing (Editors), Cyanide in Biology, Academic Press, London, pp. 517—541.
Oró, J. and Stephen-Sherwood, E., 1974. The prebiotic synthesis of oligonucleotides. In: J. Oró, S.L. Miller, C. Ponnamperuma and R. Young (Editors), Cosmochemical Evolution and the Origins of Life, Vol. I. Reidel, Dordrecht, pp. 159—172.
Oró, J. and Tornabene, T.G., 1965. Bacterial contamination of some carbonaceous chondrites. Science, 150: 1046—1048.
Oró, J., Holzer, G. and Lazcano-Araujo, A., 1980. The contribution of cometary volatiles to the primitive Earth. In: R. Holmquist (Editor), COSPAR: Life Sciences and Space Research, vol. XVIII. Pergamon Press, Oxford, pp. 67—82.
Oró, J., Holzer, G., Rao, M. and Tornabene, T.F., 1981. Membrane lipids and the origin of life. In: Y. Wolman (Editor), Origin of Life. Reidel, Dordrecht, pp. 313—322.
Oró, J., Gibert, J., Lichtenstein, H., Wikstrom, S. and Flory, D.A., 1971a. Amino acids, aliphatic and aromatic hydrocarbons in the Murchison meteorite. Nature, 230: 105—106.
Oró, J., Kimball, A.P., Fritz, P. and Master, F., 1959. Amino acid synthesis from formaldehyde and hydroxylamine. Arch. Biochem. Biophys., 85: 115—130.
Oró, J., Miller, S.L. and Urey, H.C., 1977. Energy conversion in the context of the origin of life. In: R. Buvet, M.J. Allen and J.P. Massue (Editors), Living Systems as Energy Converters. North-Holland, Amsterdam, pp. 7—19.
Oró, J., Nakaparksin, S., Lichtenstein, H. and Gil-Av, E., 1971b. Configuration of amino acids in carbonaceous chondrites and a Precambrian chert. Nature, 230: 107—108.
Oró, J., Sherwood, E., Eichberg, J. and Epps, D.E., 1978. Formation of phospholipids under primitive Earth conditions and the role of membranes in prebiological evolution. In: D.W. Deamer (Editor), Light Transducing Membranes. Academic Press, New York, pp. 1—21.

Owen, T., 1979. The Martian atmosphere: some unanswered questions. J. Mol. Evol., 14: 5—12.
Pinto, J.P., Gladstone, R.G. and Yung, Y.L., 1979. Photochemical production of formaldehyde in the Earth's primitive atmosphere. Science, 209: 42—44.
Pollack, J.B. and Black, D.C., 1979. Inplications of the gas compositional measurements of Pioneer Venus for the origin of planetary atmospheres. Science, 205: 56—59.
Pollack, J.B. and Yung, Y.L., 1980. Origin and evolution of planetary atmospheres. Ann. Rev. Earth Planet. Sci., 8: 425—487.
Ponnamperuma, C., Lemmon, R.M., Mariner, R. and Calvin, M., 1963. Formation of adenine by electron irradiation of methane, ammonia and water. Proc. Natl. Acad. Sci. U.S.A., 49: 737—740.
Rambler, M.G. and Margulis, L., 1980. Bacterial resistance to ultraviolet irradiation under anaerobiosis: implications for Pre-Phanerozoic evolution. Science, 210: 638—640.
Rao, M., Eichberg, J. and Oró, J., 1982. Synthesis of phophatidylcholine under possible primitive Earth conditions. J. Mol. Evol., 18: 196—202.
Rasool, S.I., 1972. Planetary atmospheres. In: C. Ponnamperuma (Editor), Exobiology. North-Holland, Amsterdam, pp. 369—399.
Reddy, C.A., Bryant, M.P. and Wolin, M.J., 1972. Characteristics of the 16S organism isolated from *Methanobacillus omelianski*. J. Bacteriol., 109: 539—545.
Reimer, T.O., Barghoorn, E.S. and Margulis, L., 1979. Primary productivity in an early Archean microbial ecosystem. Precambrian Res., 9: 93—104.
Richardson, S.M., 1978. Vein formation in the CI carbonaceous chondrites. Meteoritics, 13: 141—159.
Sanchez, R.A., Ferris, J.P. and Orgel, L.E., 1966. Cyanoacetylene in prebiotic synthesis. Science, 154: 784—786.
Schidlowski, M., 1978. Evolution of the Earth's atmosphere: current state and exploratory concepts. In: H. Noda (Editor), Origin of Life. Center for Academic Publications, Tokyo, pp. 3—20.
Schidlowski, M., Appel, P.W.V., Eichmann, R. and Junge, C.E., 1979. Carbon isotope geochemistry of the 3.7 × 10^4-yr-old Isua sediments, West Greenland: implications for the Archean carbon and oxygen cycles. Geochim. Cosmochim. Acta, 43: 189—199.
Simon, M.N. and Simon, M., 1973. A search for interstellar acrylonitrile, pyrimidines and pyridines. Astrophys. J., 194: 757—761.
Snyder, L.E., Buhl, D., Zuckerman, B. and Palmer, P., 1969. Microwave detection of interstellar formaldehyde. Phys. Rev. Lett., 22: 679—681.
Stephen-Sherwood, E., Oró, J. and Kimball, A.P., 1971. Thymine: a possible prebiotic synthesis. Science, 173: 446—447.
Stoks, P.G. and Schwartz, A.W., 1981. Nitrogen-heterocyclic compounds in meteorites: significance and mechanisms of formation. Geochim. Cosmochim. Acta, 45: 563—569.
Suess, H. and Urey, H.C., 1956. Abundances of the elements. Rev. Mod. Phys., 28: 53—62.
Talbot, R.J. and Newman, M.J., 1977. Encounters between stars and dense interstellar clouds. Astrophys. J. Suppl. Ser., 34: 295—308.
Tornabene, T.G. and Langworthy, T.A., 1979. Diphytanyl and dibiphytanyl glycerol ether lipids of methanogenic archaebacteria. Science, 204: 51—53.
Tornabene, T.G., Langworthy, T.A., Holzer, G. and Oró, J., 1979. Squalenes, phytanes and other isoprenoids as major neutral lipids of methanogenic and thermoacidophylic "Archaebacteria". J. Mol. Evol., 13: 73—83.
Tornabene, T.G., Wolfe, R.S., Balch, W.E., Holzer, G., Fox, G.E. and Oró, J., 1978. Phytanyl-glycerol ethers and squalenes in the Archaebacterium *Methanobacterium thermoautotrophicum*. J. Mol. Evol., 11: 259—266.
Towe, K.M., 1981. Environmental conditions surrounding the origin and early Archean evolution of life: a hypothesis. Precambrian Res., 16: 1—10.
Turner, B.E., 1980. Interstellar molecules. J. Mol. Evol., 15: 79—101.
Urey, H.C., 1952. On the early chemical history of the Earth and the origin of life. Proc. Natl. Acad. Sci. U.S.A., 38: 351—363.

Walker, J.G.C., 1977. Evolution of the Atmosphere. Macmillan, New York, 318 pp.
Walters, M.R., Buick, R. and Dunlop, J.S.R., 1980. Stromatolites 3.4—3.5 billion years old from the North Pole area, Pilbara Block, Western Australia. Nature, 284: 443—445.
Wetherill, G.C., 1980. Formation of the terrestrial planets. Ann. Rev. Astron. Astrophys., 18: 77—113.
Whipple, F.L., 1950. A comet model. I. The acceleration of Comet Encke. Astrophys. J., 111: 375—394.
Whipple, F.L., 1976. A speculation about comets and the Earth. Mem. Soc. R. Sci. Liege, Serie 6e, IX: 101—111.
Woese, C.R. and Fox, G.E., 1977. Phylogenetic structure of the prokaryotic domain: the primary kingdoms. Proc. Natl. Acad. Sci. U.S.A., 77: 5088—5090.
Wolman, Y., Haverland, W.H. and Miller, S.L., 1972. Non-protein amino acids from spark discharges and their comparison with the Murchison meteorite amino acids. Proc. Natl. Acad. Sci. U.S.A., 69: 809—811.
Yang, C.C. and Oró, J., 1971. Synthesis of adenine, guanine, cytosine and other nitrogen organic compounds by a Fischer—Tropsch-like process. In: R. Buvet and C. Ponnamperuma (Editors), Molecular Evolution. I. Chemical evolution and the Origin of Life. North Holland, Amsterdam, pp. 155—170.
Yoshino, D., Hayatsu, R. and Anders, E., 1971. Origin of organic matter in the early Solar System, 3. Amino acids: catalytic synthesis. Geochim. Cosmochim. Acta, 35: 927—938.
Zeikus, J.G., 1977. The biology of methanogenic bacteria. Bacteriol. Rev., 41: 514—541.
Zillig, W., Stetter, K.O. and Tobien, M., 1978. DNA dependent RNA polymerase from *Halobacterium halobium*. Eur. J. Biochem., 91: 193—199.

NATURAL NUCLEAR REACTORS AND IONIZING RADIATION IN THE PRECAMBRIAN

I.G. DRAGANIĆ and Z.D. DRAGANIĆ

Centro de Estudios Nucleares, Universidad Nacional Autónoma de México, Delegación Coyoacán, 04510-México,D.F. (México)

D. ALTIPARMAKOV

Boris Kidrič Institute of Nuclear Sciences, P.O. Box 522, 11001 Beograd (Yugoslavia)

ABSTRACT

Draganić, I.G., Draganić, Z.D. and Altiparmakov, D., 1983. Natural nuclear reactors and ionizing radiation in the Precambrian. Precambrian Res., 20: 283—298.

The natural nuclear reactors were geological arrangements of uranium and water where, like the 2 Ga-old uranium deposits discovered in Oklo (Gabon, Africa), uranium chain fission processes took place. Ten years after its discovery the phenomenon of Oklo is still neglected in Precambrian evolutionary studies. We consider some probable reasons for this and show that natural reactors might have been important, specific, localized sources of ionizing radiation during both the criticality and shut-down periods. Some of the long-lived fission products which migrated from the reactor core could also have been effective radiation energy sources after fixation in the environment or upon uptake by the earliest forms of living matter. The results presented here concern the examination of conditions for nuclear criticality on the Precambrian Earth, the dose-rates of ionizing radiation available and the estimate of the number of natural nuclear reactors that could have been active in the past.

INTRODUCTION

Natural nuclear reactors were geological arrangements of uranium and water which led to a fission chain in the uranium on Precambrian Earth, as was the case at the fossil reactor site discovered in Oklo (Gabon, Africa) by Bodu et al. (1972) and Neuilly et al. (1972). The basic aspects of the Oklo phenomenon seem to be well understood (Anonymous, 1975; Anonymous, 1978). Among various conclusions reached regarding its nature there are two of particular interest for the present work: none of the geological and geochemical characteristics of the Oklo deposit appear unique (Maurette, 1976) and the nuclear reactor site at Oklo could not have been a singular occurrence on the Precambrian Earth (Cowan, 1975; Maurette, 1976; Apt et al., 1978).

The evolutionary processes in the Precambrian are concerned with chemi-

cal evolution and the evolution of early life. They could only have started after the crust—oceans—atmosphere system was established and the planet's surface became hospitable for organic compounds, i.e., somewhere between 4.1 and 3.9 Ga-ago (Holland, 1976; Schaw, 1976; Walker, 1976, 1977; Jahn and Nyquist, 1976; Siever, 1977). Although chemical evolution preceeded biological evolution, there are some reasons to believe that they continued simultaneously until the abundance of life made the environment hostile to primordial organic synthesis.

Ionizing radiation is often considered to be a minor partner in the group of energy sources for evolutionary processes and only the radioactivity dispersed in the rocks is taken into account (Miller et al., 1976). In spite of various achievements in radiation chemistry and biology which are of potential interest to evolutionary studies, the natural nuclear reactors are still neglected as localized sources of ionizing radiation energy ten years after their discovery.

One of the probable reasons is that the Oklo phenomenon is still little known in the Precambrian-science community. Other reasons, of no lesser importance, are that:

(1) with one exception the Oklo reactor site appears to be an isolated phenomenon in the history of the Earth, especially since a search for other fossil reactors was unsuccessful (Apt et al., 1978);

(2) there is uncertainty regarding the feasibility of uranium concentration processes, providing a locally high enough concentration of uranium for nuclear criticality on the early Earth, when the presence of oxygen in the atmosphere and biota in the hydrosphere is doubtful, or negligible;

(3) a general belief that nuclear reactor radiations are invariably at high dose-rates and large doses and hence, being destructive, are of little relevance to chemical and biological evolution;

(4) the role of long-lived fissiogenic nuclides which can migrate from the reactor core is neglected.

In this study we examine these aspects, taking into account the known facts about the Oklo phenomenon and some recent achievements in Precambrian research.

THE CHAIN FISSION OF URANIUM IN NATURE

The fissile ^{235}U has a half-life of 0.71 Ga. Its present atomic concentration in natural uranium is only 0.7%, and the chain fission cannot even start in the richest uranium deposits. On the early Earth its concentration was up to 40 times higher and, as suggested by Kuroda (1956) long before the discovery of the Oklo phenomenon, could have led to the chain fission process in nature. As the Oklo fossil reactors show, it did indeed.

The natural nuclear reactor site at Oklo is quite well understood. There are six reactor cores within four distinct reaction zones which are spread out for 150 m in the general direction of sedimentation (Naudet, 1978a). The lens

shaped reactors are about 1 m thick and 10—20 m long (Boyer et al., 1975). The concentration of uranium in the matrix varies between 0.2 and 0.5%, while in the reactor zones it ranges from 20 to 60% (Naudet et al., 1975). It is a sedimentary deposit, of sandstone, 4—10 m thick (Chauvet, 1975) and its age is similar to that of chain fission processes, i.e., 2.05(±0.03) Ga (Gancarz, 1978) and 2.0(±0.1) Ga (Ruffenach et al., 1976).

The total energy liberated during the lifetime of the Oklo phenomenon is estimated, by establishing the balance of missing ^{235}U, at 500×10^9 megajoules (Naudet, 1978a). It has been suggested that the operation time of individual reactors was between 0.6 and 0.8 Ma, while the duration of the composite Oklo phenomenon was considerably longer, i.e., up to several million years (Naudet, 1978e).

The Oklo sediments with uranium-rich lenses were buried at great depth, probably several thousands of meters beneath sea level, and the water which served as both coolant and moderator was supercritical (Naudet, 1978e). Several linked reactors were involved in the initiation and the propagation of the fission chains. These were maintained by the destruction of neutron poisons in the ore, and were controlled by the water temperature (Naudet, 1978c).

THE CONDITIONS FOR NUCLEAR CRITICALITY IN THE PRECAMBRIAN

According to nuclear reactor theory the condition for maintaining a fission chain is that on average, at least one neutron created in a fission event causes another fission. It has been shown that classical methods of nuclear reactor theory can be applied to the Oklo phenomenon and, therefore, used in examining the conditions for criticality in the Precambrian (Naudet and Filip, 1975a,b).

In these computations five parameters have to be taken into account: the age of the deposit, its content of natural uranium, the volume of the reaction zone, the neutron capture in the gangue and the amount of water associated with the uranium. Sophisticated computations were performed for the Upper and Middle Precambrian (Naudet, 1978b). They show that 1.1 Ga-ago is the lowest age limit for reaching the nuclear criticality. In this case, the requirements for moderation and tolerable amounts of nuclear impurities seem to be reasonable for a deposit already containing 50% of UO_2. The required minimum amount of uranium decreases rapidly further into the Earth's past: 30% of UO_2 for 1.8 Ga-ago and 10% for 3 Ga-ago. In these calculations the thickness of the uranium-rich ore was up to 1 m. We have used a simplified approach to examining the conditions for criticality also in the early Precambrian (Appendix). The bare sphere model was taken as the geometrical configuration and the computations provided the critical radius of the sphere and its dependence on the age of the uranium, its concentration in the deposit, the amount of water associated with uranium and the amount of nuclear impurities. The chemical composition of the uranium deposit was assumed to be the same as that of the Oklo deposit (Naudet and Filip, 1975a). The results show that

critical conditions could have been reached in a sphere of 2—3 m in radius, even in deposit with a modest uranium content. Between 6 and 3.5% of UO_2 in the deposit would have been enough to trigger the fission chain process between 3.2 and 4.1 Ga-ago (see Figs. 1 and 2 in Appendix).

URANIUM FOR NATURAL NUCLEAR REACTORS

Various accumulation processes could have supplied the lower-grade ores (<6% UO_2) required for the Early Precambrian, and higher-grade material (10—50% UO_2) needed for the Middle and Upper Precambrian.

An oxidizing—reducing cycle is usually considered to be the process that has produced all major, presently known, uranium deposits (Adler, 1974; Simov, 1979). This process involved the oxidation of U^{4+} compounds to the water soluble U^{6+} compounds which were then transported easily to the reducing zones, with high concentrations of organic materials (or the inorganic reductants such as sulfides), where uranium was reduced and precipitated as uraninite.

An abundance of oxygen in the atmosphere and organic materials in the crust are considered to be of primary importance for high-grade ore formation, and the occurrence of the oxidizing—reducing cycle is usually limited to ~2 Ga-ago. Nevertheless, this process could also have occurred in the Earth's more remote past: although not rich in organic matter and oxygen, the Middle and Early Precambrian were not entirely devoid of them.

Organic material of abiotic origin could have appeared on the primitive Earth (~4 Ga-ago) as the result of chemical reactions in the atmosphere caused by ultraviolet light and electrical discharges (Miller and Orgel, 1974b), as well as from collisions of the Earth with comets (Lazcano-Araujo and Oró, 1981).

Organic material of biological origin may have began to accumulate on the Earth considerably earlier than it is still usually assumed. One piece of supporting evidence is the enrichment of ^{12}C already observed in the oldest known rocks on Earth (Schidlowski et al., 1979) as well as in numerous Precambrian sediments (Eichman and Schidlowski, 1975). This isotopic anomaly is known to be inherent in the process of formation of living matter, due particularly to the kinetic fractionation in photosynthetic carbon fixation. Some recent findings (Lowe, 1980; Orpen and Wilson, 1981) show the presence of complex microbiota ~3.5 Ga-ago.

There is accumulating evidence that some oxygen was present in the atmosphere throughout the span of recorded geological history. This is supported by the sedimentary distribution of uranium, iron, sulfur and carbon in old, well preserved, sedimentary rocks of various ages (Dimroth and Kimberley, 1976). Of particular interest is the observed increase of the thorium—uranium ratio throughout geological time, from 3.1 for samples 3.8 Ga-old (Gothab, Akilia association, Greenland), to ~6 for 0.3 Ga-old samples (Perth, Australia) (McLennan and Taylor, 1980). This offers strong

supporting evidence for uranium migration during the formation of the oldest sedimentary rocks. Both uranium and thorium appear, with several other lithophile refractory elements, very early in the upper mantle and crust, possibly as early as 100 Ma after core formation (Murthy, 1976). Since intensive weathering and sedimentation are considered to be characteristic of the primitive Earth (Siever, 1977), the above finding suggests that uranium must have already been selectively lost at an early date during repeated cycles of weathering. A satisfactory explanation based on the known chemical behavior of uranium and thorium requires the presence of O_2 in the atmosphere. This oxidized the U^{4+}, and the water soluble U^{6+} compounds were removed, while the thorium oxidation state did not change and its compounds remained relatively insoluble (see note added in proof).

There is also reason to believe that, because of intensive weathering, uranium accumulation on the primitive Earth could have taken place in the absence of oxygen, or in an O_2 poor environment. Many sediments which are presently of economic significance for their content of gold and/or uranium were laid down in an oxygen-poor atmosphere by exogenic processes. They may have been deposited under local reducing conditions, or have failed to have reached equilibrium with the atmosphere at the time of sedimentation (Miller and Orgel, 1974a). A cycle in which only U^{4+} (as UO_2) was involved, comprising weathering—erosion—transportation—sedimentation steps, has been suggested (Rutten, 1971). The tentative ages of these gold—uranium deposits are between 3 and 1.8 Ga (Rutten, 1971; Miller and Orgel, 1974b; Simov, 1979) and their existence has a more general significance. They indicate that such a mode of uranium accumulation could also have taken place in the Early Precambrian, after the core, mantle and crust had differentiated. It may be worthwhile noting that the oldest well-dated rocks on the Earth (3.8 Ga-old) are water deposited sediments (Moorbath et al., 1973).

Both chemical and mechanical weathering were effective on the early Earth because of acid gases in the primitive atmosphere and of land surfaces unbound by any vegetation (Siever, 1977). They could also have provided a way to supply uranium for natural nuclear reactors between 4.1 and 3.2 Ga-ago. To supply enough uranium for a critical sphere of 2 m radius during the Early Precambrian, a 10 cm thick layer would need to have been eroded from a uranium-poor surface (0.4 ppm UO_2) over not more than 40 km^2. This could have happened in a few tens of years.

GENERAL ASPECTS OF A NATURAL NUCLEAR REACTOR

Operating conditions

The principal constituents for the reactor were up to several tons of UO_2 as the fuel, and water as a moderator and coolant. The minimum content of uranium in the deposit required to trigger and maintain the fission chain varied between 50 (1.1 Ga-ago) and 3.5% (4.1 Ga-ago). A mass ratio for

water—uranium of 0.5 was mainly adequate, but could be lower (down to 0.1) or higher (up to 1.5) depending on the deposit's content of natural uranium, of its fissile isotope and the nuclear impurities due to the gangue (see Appendix). In deriving these data we have assumed that the reactor core was a sphere with a radius between 2 and 3 m, with larger diameters being required for the lower-grade uranium ores.

The temperature and the pressure within the reactor core would depend on the geophysical conditions of the reactor site. If the reactor was situated beneath shallow water and/or in porous sediments, these conditions could not have been much different from ambient conditions. With a rise in temperature the density of the water would decrease leading to a less efficient slowing down of the neutrons and eventually to termination of the chain process. The fission chain could recommence only after sufficient cooling of the water and increase in water density. At greater depths and/or in less porous sediments, higher temperatures and pressures could have developed and critical conditions for the water might have been reached. Supercritical water has T_{cr} = 647.2 K and P_{cr} = 213.5 bars, as was present in the Oklo deposit.

The fact that natural nuclear reactors were controlled by the water temperature suggests that they could operate only at low powers: from several watts in the case of a simmering water critical unit, buried beneath shallow water, up to multikilowatt peaks for supercritical water at greater depths. It seems reasonable to consider 1 kW as an average power for a typical natural nuclear reactor. For comparison, the average power in the Oklo case was ~3 kW. It is true that the total amount of energy liberated was enormous, but these hundreds of billions of megajoules have to be spread out over about a million years of operation of each of six reactors. Large powers might be possible in a natural cavity, but the heat dissipation would eventually limit the power. We do not consider that occassional multikilowatt power peaks were of particular significance for general operating conditions.

Radiation doses and conditions for irradiations

Nuclear reactor dosimetry (Draganić, 1971) enables reliable estimates to be made of the dose rates within the core of a natural nuclear reactor. If the case of a critical unit 3.2 Ga-ago is considered, with a 2 m diameter and operating at 1 kW power, the following dose rates (in krad h^{-1}) are found within the reactor core: 3.65 due to fission fragments, 0.11 due to prompt neutrons, 0.14 due to prompt gamma rays, 0.14 due to the gamma rays from fission product decay, 0.17 from fission product decay-beta radiation and 0.13 due to the neutron capture gamma rays.

Dose rates of krad h^{-1} or less are similar to those available in present day laboratory facilities. Nevertheless, the extent of radiation-induced chemical changes could have been quite significant even with modest radiation-chemical yields. If the radiation chemical yield of only 1 molecule formed per 100 eV absorbed is considered, then 330 kg of a product of molecular weight 100

could have been synthesized during 1 year of operation, at 1 kW, in the water moderator within a 3.2 Ga-old reactor.

Variations of the reactor power would also cause variations of the dose rate, but from what is known about dose rate effects in aqueous media, they could not have been important for radiation-induced changes. The corresponding changes in temperature and pressure, however, could have been important, especially when a supercritical water regime was established. The radiation-induced chemical changes at higher temperatures and pressures, such as under a supercritical water regime, do not seem to be of particular interest to evolutionary processes. Nevertheless, the supercritical water regime might have been rather exceptional as it required, as in the Oklo case, the simultaneous occurrence of a very rich UO_2 deposit and a great depth of burial.

Besides irradiations within the reactor core, there were other possibilities. Some of the more penetrating radiations could reach the peripheral area, depositing their energy in the water above the reactor. The specific mode of radiant energy deposition in condensed media makes its use very effective. It is localized along the radiation path and only there are the chemically reactive free-radicals and radical-ions formed. They produce new compounds by reacting among themselves and/or with neighboring molecules while they diffuse away from their place of origin. In addition, it should be noted that the radiolytically produced molecules diffuse away into the bulk of the water and escape degradation due to the continued irradiation. Their amounts could have been considerable, in spite of low dose-rates in the peripheral reactor area, because of the long periods of criticality.

Underground water drains also offer a possibility for irradiation during both reactor criticality and shut-down periods. It has been noted on the Oklo site that convection was an important way for heat removal from the reactor core. Larger amounts of heat liberated during the fission chain process could have initiated a true thermal siphon (Weber, 1978) and cause a gradual, slow (Naudet, 1978d), replacement of water in the reactor core, thus leading to circulation of materials through the irradiation source.

Fissiogenic radionuclides

During 1 year of criticality at 1 kW power, 2.3×10^{21} fission product atoms appear in the reactor core. Of these ~14% have half-lives longer than 1 year and could provide radiation during the shut-down periods, when the pressure and temperature conditions could have been suitable for synthesis of organic compounds. Among them were: ^{147}Pm, 2.6 y (0.25%); ^{154}Eu, 8.6 y (0.10%); ^{151}Sm, 90 y (0.10%); ^{93}Zr, 9×10^5 y (2.7%); ^{99}Tc, 2×10^5 y (2.9%) and ^{107}Pd, 7×10^6 y (0.74%). The last figure is the percentage of all fission product atoms forming the designated isotope (%-g-atom) (Cohen, 1977).

Of no lesser importance were the fission products that migrated from the reactor core and these could have represented up to 7% of all the fission pro-

duct atoms. Even in the Oklo case, where most of the materials remained in situ after 2 Ga, an extensive loss of Xe, Kr and I was observed, along with the migration of alkaline earths, halides and some chalcophile elements (Brookins et al., 1975; Brookins, 1978). After fixation in the environment or uptake by early forms of living matter, they were specific and effective internal radiation sources for centuries, as was the case for ^{90}Sr, 29 y (2%) and ^{137}Cs, 30 y (3%), or millions of years for ^{129}I, 1.6×10^7 y (0.61%) and ^{135}Cs, 2×10^6 y (0.18%). The total amounts of energy liberated in these cases are important, e.g., 2.3×10^{11} rad from ^{137}Cs, although the dose-rates were still very modest. The reason for low dose-rates is not only the long delivery time, ~300 y for ^{137}Cs, but also the larger volumes over which the radionuclides were deposited following their various geochemical fates.

NATURAL BACKGROUND OF IONIZING RADIATION AND NATURAL NUCLEAR REACTORS IN THE PRECAMBRIAN

The identification of a fossil reactor site is based on isotopic anomalies such as the depletion of fissionable ^{235}U and the enrichment of stable isotopes which are the end products of the decay of fission products. This means that for a successful search some severe requirements have to be fulfilled: the geological configuration of the fossil reactor must have survived from Precambrian times; redistribution of material within the ore body must have been absent or minimal in order to avoid dilution of isotopic anomalies and the samples for analyses have to be taken from the right locations. The most promising locations for a search are high-grade uranium deposits (>20%) which are older than 0.7 Ga and are in massive deposit zones with volumes of 1 m^3 or larger. However, the approach to such places depends on the willingness of the uranium-exploring companies to communicate confidential characteristics of the deposits, as well as to supply the data on both the frequent analyses of uranium isotopic abundance and the identification of local hot spots of sufficient size within these deposits (Maurette, 1976). Also, the reliable identifications of a fossil reactor requires an investment of considerable time and money, as shown by the thousands of analyses which had to be performed to characterize only one natural nuclear reactor at the Oklo site. This might explain why very little has been done to find other fossil reactor sites.

Several Precambrian uranium ores (0.45—1.88 Ga-old) from world-wide locations (Canada, South America, Africa, Australia) were tested for isotopic variations in the uranium, neodymium, samarium and ruthenium. The locations were carefully selected, but only 42 samples, from as many locations, were analyzed. No isotopic anomalies were detected and the conclusion was drawn that critical conditions had not been reached at the sample sites. However, these samples represent only a small part of the potential reactor zones which were exposed during mining, hence, the possibility cannot be ruled out that the remains of critical assemblies will still be found (or have not been ex-

humed) even at these locations (Apt et al., 1978). Some encouraging anomalies were reported for Oklebondo, a uranium deposit close to the site of the Oklo fossil reactors (Cesario et al., 1978). Unfortunately, this location is buried at 300 m depth and does not appear, at present, to be accessible to further detailed investigations.

The search for fossil reactors cannot go very far beyond 2.1 Ga which is the age of the oldest known important uranium deposits. The oldest well-dated uranium bearing sedimentary rocks appear to be ~ 2.5 Ga-old (Simov, 1979), although the careful examination of lead compositions of galenas from Witwatersrand and Orange Free State shows that the most probable age of crystallisation of their parent uraninites is 3 Ga, which agrees with independent observations on uraninites from the Dominion Reef (Burger et al., 1962). It should also be remembered that relatively few rocks have been preserved on the Earth for more than ~2.8 Ga (Wetherill and Drake, 1980) and that only some tens of those reliably dated are from the Early Precambrian (Moorbath, 1976; Jahn and Nyquist, 1976). An increased interest in the Early Precambrian may well result in new findings, but there are some strong reasons why the geological evidence will always remain insufficient. Lunar studies clearly show that the absence of primordial rocks on Earth is due to very extensive magmatic and geological activity of internal origin, combined with massive external impact generated metamorphism of all primordial surfaces (Wetherill and Drake, 1980). It is known that there is little likelihood of many more traces of the early crust being found because of intense bombardment, prolonged weathering and metamorphism in a water rich environment (Smith, 1976).

There are other reasons why the lack of known uranium deposits older than 2 Ga cannot be used to argue against the presence of natural nuclear reactors on Precambrian Earth earlier than 2 Ga-ago. It is true that there is a clustering of the age of the known, oldest, high-grade uranium ores at around 2 Ga, but a satisfactory explanation for this remains to be found. It is usually attributed to the appearance of abundant oxygen in the atmosphere and biota in the hydrosphere at that time, but this simplified answer cannot easily be accepted if present knowledge about the atmospheric oxygen and life at the end of the Middle Precambrian is taken into account. This clustering also represents a geological anomaly (Simov, 1979), and is in contrast with the formation of ore deposits of other mobile metals (Mo, Pb, etc.). It has been suggested that, because of its peculiar crystal chemistry, the uranium was driven upwards to the Earth's crust during the early evolution of the planet. It appeared in early Archean rocks, which were enriched in uranium but were later redistributed during subsequent orogenesis (Simov, 1979).

Another explanation for the absence of uranium ores older than 2 Ga could be their destruction during criticality, i.e., in natural reactors (Kuroda, 1956). This cannot be easily ruled out: it is evident that uranium appeared very early in the geological history of the Earth and processes were available for its accumulation which did not necessarily lead to high grade ores be-

cause of the larger abundance of the fissile isotope. A burst of criticality, followed by high geological activity, could easily destroy the reactor core, i.e., accumulation of several m^3 of deposit where the fission chain occurred and to "dilute" both the uranium content and the isotopic anomalies.

Nevertheless, there is the possibility of making a rough estimate of the amount of terrestrial uranium that has taken part in natural nuclear reactors. It has been pointed out, by Cowan (1975) and Cowan and Addler (1976), that the measured ratio $^{235}U/^{238}U$ from various uranium deposits on the Earth appears constant up to $1-2 \times 10^{-3}$, and this suggests that only $1-2 \times 10^{-3}$ of the total amount of terrestrial uranium could have been used as fuel in natural nuclear reactors. If only 1/1000 of the total uranium mass was involved in chain fissions in a 1 km thick layer of the crust, with a uranium abundance of 3 ppm and a ratio of $^{235}U/(^{235}U + ^{238}U) = 0.1$, then, in the history of the Earth, $\sim 10^8$ reactor sites of the Oklo-type could have been active between 4.1 and 1.1 Ga-ago. When the same criteria are applied to the amount of uranium (5×10^6 tons) in ores with $\geqslant 1000$ ppm of UO_2 which are presently considered to be the world's accessible uranium inventory, then ~1300 natural nuclear reactors were operating at 1 kW power each, for a million years or more. The total energy that they released was lower by several orders of magnitude than the total natural background of ionizing radiations, which was up to ~ 2.8 cal cm^{-2} y^{-1} (Miller et al., 1976). Therefore, their significance was in providing specific rather than abundant energy sources. They were also very effective through the free-radial processes that could have been initiated.

EVOLUTIONARY PROCESSES AND NATURAL NUCLEAR REACTORS AS LOCALIZED SOURCES OF IONIZING RADIATIONS IN PRECAMBRIAN

The occurrence of natural nuclear reactors in the Earth's history must have been a natural phenomenon. The information available on the Oklo fossil reactors, together with present calculations and recent achievements in Precambrian research, suggest that enough uranium could have been accumulated to trigger and maintain fission chain processes on the early Earth. Their number was not large and their contribution to the total amount of energy available for evolutionary processes was small. However, the specific action on the environment even of a thousand natural nuclear reactors, each of them providing a localized source of ionizing radiations for up to a million years, should not be neglected in evolutionary studies. This will be certainly more true for a much larger number of reactor sites, than the present conservative evaluation suggests.

The achievements in radiation chemistry, in particular the abundant studies of biologically important molecules, as well as findings in radiation biology, offer numerous facts of potential interest to Precambrian evolutionary studies that still wait to be exploited. Systematic investigations of radiation-induced chemical changes of interest to chemical evolution are scarce and concern mainly aqueous solutions of simple cyanides and nitriles (Draganić

and Draganić, 1980). It has been found that in prebiotic conditions the free-radical reactions can lead to the formation of a great variety of biologically important molecules, like aldehydes, amines, carboxylic acids, amino acids, urea, as well as different oligomeric materials with molecular weights up to 20 000 Daltons. (Draganić et al., 1980a; Draganić et al., 1980b; Niketić et al., 1982; Jovanovich et al., 1982; Negrón-Mendoza et al., 1983, Niketić et al., 1983). Among them are some oligomers whose fragments have the peptidic structure. They release amino acids on hydrolysis, give positive tests for the peptide bond (Draganić et al., 1977) and some of them can be digested by enzymes of broader specificity (Niketić et al., 1982). A fairly large yield of arginine was observed in irradiated aqueous solutions of cyanamide (Draganić et al., 1978). It might be worth noting that its concentration, like the concentrations of all other radiolytic products, are proportional to the energy of radiation absorbed.

There are no published data on the potential role of ionizing radiation in the evolution of the earliest, simple, microscopic forms of life. An examination of major events in Precambrian biological evolution shows that the main evolutionary changes of prokariotic life, between 3 and 1.8 Ga-ago, resulted from biochemical and metabolic rather than morphological innovations (Schopf, 1978). By initiating free-radical processes, the ionizing radiation could have also been an effective source of energy, hence one more mutagenic agent in the large inventory available in Precambrian.

It is important to note that the natural nuclear reactors were weak energy sources compared with man-made commercial nuclear reactors which often have powers as large as hundreds of thousands of kilowatts. They were operating at powers of only ~1 kW, similar to present-day critical units in research laboratories. The radiation doses within the reactor cores were of the order of krad h^{-1} (tens of Gy h^{-1}) which were very convenient for radiation-induced free-radical processes, and for the efficient production of chemical and biological changes. Higher temperatures and pressures that could have developed under conditions such as a nonporous sediment and/or greater burial depths of a deposit very rich in uranium, would not prevent the free-radical reactions, but only limit their usefulness for evolutionary processes (unstable aqueous solutions and organic materials). In such cases the underground water drains may have been of some help.

The presence of long-lived fission products ensured that the reactor site was a place of localized radiations for long periods of time (hundreds of years and more) after the critical period was over. Some of them would migrate and continue to irradiate after fixation in the environment or after uptake by Precambrian life. The low dose-rates combined with the possibility of irradiation during a very large time period (centuries and millenia) could have been particularly effective in producing evolutionary changes in Precambrian biota.

NOTE ADDED IN PROOF

It has been pointed out recently (V. Canuto et al., Nature, 296 (1982) 816) that the prebiological palaeoatmosphere contained oxygen in quantities several orders of magnitude greater than is generally accepted. This was the result of increased emission of UV radiation (up to 10^4 times) from the young Sun.

ACKNOWLEDGEMENT

The authors are indebted to Dr. Lawrence Grossman (Department of Nuclear Engineering, University of California, Berkeley, U.S.A.) for reading the manuscript and to Dr. Alfred G. Maddock (Chemical Laboratory, Cambridge University, U.K.) for discussion of the text and useful suggestions.

APPENDIX

The bare sphere model and critical conditions for the Early Precambrian

In the computation the bare sphere model was taken as a geometrical configuration. The radius of the critical sphere was calculated by using the neutron

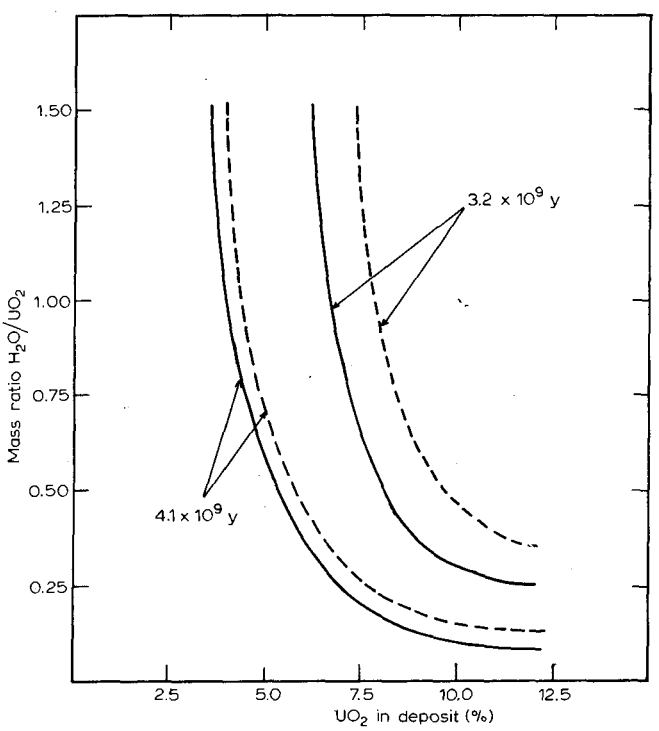

Fig. 1. The critical requirements for uranium deposit on the early Earth. The reactor core is a sphere with constant radius, R_{cr}: 2 m (– – –) or 3 m (——).

multiplication factor, K_{eff}, and the Regula Falsi iterative procedure; larger amounts of ^{235}U required stricter treatment of neutron energy transport (Bondarenko, 1975; Krilov et al., 1977). Attention has been paid to the resonant selfshielding due to the presence of various types of nuclei (Zizin, 1978); the transport correction of scattering cross section was also taken into account. Figures 1 and 2 summarize the results of the computations.

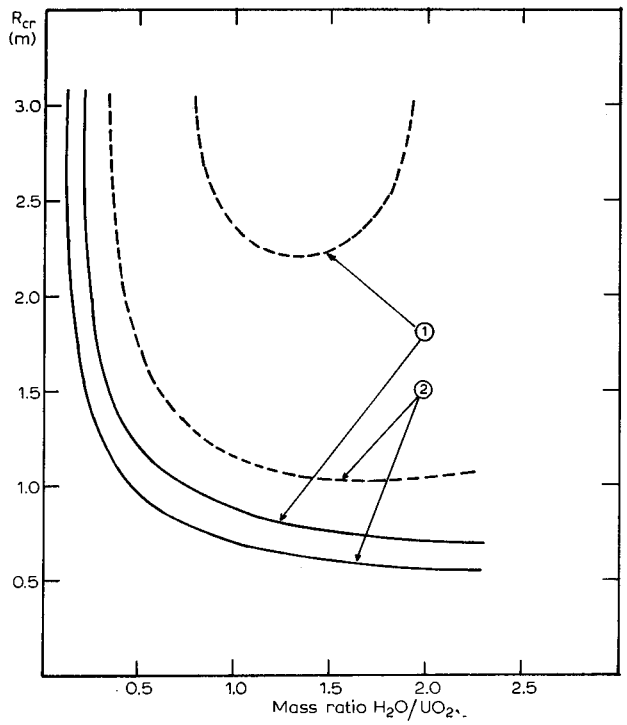

Fig. 2. The influence of various factors on the radius of the critical sphere (R_{cr}) for a natural nuclear reactor. $^{235}U/(^{235}U + ^{238}U)$ = 0.2. The UO_2 content in the deposit: ① 10% and ② 7.5%. The dotted line is used when 50 ppm of ^{10}B are also present in the deposit.

REFERENCES

Adler, H.H., 1974. In: Formation of Uranium Ore Deposits. I.A.E.A., pp. 141—156.

Anonymous, 1975. The Oklo phenomenon. International Atomic Energy Agency, Vienna, 647 pp.

Anonymous, 1978. Natural Fission Reactors. International Atomic Energy Agency, Vienna, 754 pp.

Apt, K.E., Balagana, J.P., Bryant, E.A., Cowan, G.A., Daniels, W.R., Vidale, R.J. and Brookins, D.G., 1978. Search for other sites. In: Natural Fission Reactors. I.A.E.A., Vienna, pp. 677—689.

Bodu, R., Bouzigues, H., Morin, N. and Pfiffelman, J.P., 1972. Sur l'existence d'anomalies isotopiques rencontrées dans l'uranium du Gabon. C.R. Acad. Sc., 275 D: 1731—1733.

Bondarenko, I.I., 1975. Group Constants for Nuclear Reactor Calculations. Consultants Bureau Enterprises, New York.

Boyer, R.L., Naudet, R. and Pfiffelmann, J.P., 1975. Exploration des foyers de reaction. In: The Oklo Phenomenon. I.A.E.A., Vienna, pp. 67—81.

Brookins, D.G., 1978. Application of Eh—pH diagrams to problems of retention and/or migration of fissiogenic elements at Oklo. In: Natural Fission Reactors. I.A.E.A., Vienna, pp. 243—265.

Brookins, D.G., Lee, M.J., Mukhopadhyay, B. and Bolivar, S.L., 1975. Search for fission-produced Rb, Sr, Cs and Ba at Oklo. In: The Oklo Phenomenon. I.A.E.A., Vienna, pp. 401—413.

Burger, A.J., Nicolaysen, L.O. and Villiers, J.W.I., 1962. Lead isotopic composition of galenas from the Witwatersrand and Orange Free State, and their relation to the Witwatersrand and Dominion Reef uraninites. Geochim. Cosmochim. Acta, 26: 25—59.

Cesario, J., Poupard, D. and Naudet, R., 1978. Nouvelles analyses de terres rares dans les échantillons d'Oklo. In: Natural Fission Reactors. I.A.E.A., Vienna, pp. 473—492.

Chauvet, R.J., 1975. Description du gisemenent d'uranium d'Oklo. In: The Oklo Phenomenon. I.A.E.A., Vienna, pp. 53—65.

Cohen, B.L., 1977. High-level radioactive waste from light-water reactors. Rev. Mod. Phys., 49: 1—20.

Cowan, G.A., 1975. Discussion. In: The Oklo Phenomenon. I.A.E.A., Vienna, pp. 498 and 630.

Cowan, G.A. and Addler, H.H., 1976. The variability of the natural abundance of ^{235}U. Geochim. Cosmochim. Acta, 40: 1487—1490.

Dimroth, E. and Kimberley, M.M., 1976. Precambrian atmospheric oxygen: evidence in the sedimentary distribution of carbon, sulfur, uranium and iron. Can. J. Earth Sci., 13: 1161—1185.

Draganić, I.G., 1971. The chemical dosimetry. In: Determination of Absorbed Doses in Reactors. I.A.E.A., pp. 197—221.

Draganić, I.G. and Draganić, Z.D., 1980. Radiation—chemical aspects of chemical evolution and radiation chemistry of simple cyano compounds. Radiat. Phys. Chem., 15: 195—201.

Draganić, I.G., Draganić, Z.D., Jovanović, S.V. and Ribnikar, S.V., 1977. Infrared spectral characterization of peptidic material produced by ionizing radiation in aqueous cyanides. J. Mol. Evol., 10: 103—109.

Draganić, Z.D., Draganić, I.G. and Jovanović, S.V., 1978. The radiation chemistry of aqueous solutions of cyanamide. Radiat. Res., 75: 508—518.

Draganić, Z.D., Niketić, V., Jovanović, S. and Draganić, I.G., 1980a. The radiolysis of aqueous ammonium cyanide: compounds of interest to chemical evolution studies. J. Mol. Evol., 15: 239—260.

Draganić, I.G., Jovanović, S., Niketić, V. and Draganić, Z.D., 1980b. The radiolysis of aqueous acetonitrile: compounds of interest to chemical evolution studies. J. Mol. Evol., 15: 261—275.

Eichmann, R. and Schidlowski, M., 1975. Isotopic fractionation between coexisting organic carbon—carbonate pairs in Precambrian sediments. Geochim. Cosmochim. Acta, 39: 585—595.

Gancarz, A.J., 1978. U—Pb age (2.05×10^9 years) of the Oklo uranium deposit. In: Natural Fission Reactors. I.A.E.A., Vienna, pp. 513—520.

Holland, H.D., 1976. The evolution of seawater. In: B.F. Windley (Editor), The Early History of the Earth. Wiley, New York, pp. 559—667.

Jahn, B.M. and Nyquist, L.E., 1976. Crustal evolution in the early Earth—Moon system: constraints from Rb—Sr studies. In: B.F. Windley (Editor), The Early History of the Earth. Wiley, New York, pp. 55—76.

Jovanović, S., Nešković, S., Spririć, V., Draganić, Z.D. and Draganić, I.G., 1982. The radiolysis of aqueous propionitrile: compounds of interest to chemical evolution studies. J. Mol. Evol., 18: 337—343.

Krilov, V.I., Bobkov, V.V. and Monastirskii, P.I., 1977. Vitchislitenie Metodi. Vol. 2, Chapter 8, Nauka, Moskva.

Kuroda, P.K., 1956. On the nuclear stability of the uranium minerals. J. Chem. Phys., 25: 781—782.

Lazcano-Araujo, A. and Oró, J., 1981. Cometary material and the origins of life on Earth. In: C. Ponnamperuma (Editor), Comets and the Origin of Life. Reidel, Dordrecht, pp. 191—225.

Lowe, D.R., 1980. Stromatolites 3,400 Myr old from the Archean of Western Australia. Nature, 284: 441—443.

Maurette, M., 1976. Fossil nuclear reactors. Annu. Rev. Nucl. Sci., 26: 319—350.

McLennan, S.M. and Taylor, S.R., 1980. Th and U in sedimentary rocks: crustal evolution and sedimentary recycling. Nature, 285: 621—624.

Miller, S.L. and Orgel, L.E., 1974. The Origins of Life on the Earth. Prentice-Hall, Englewood Cliffs, (a) pp. 49—52 and (b) pp. 83—92.

Miller, S.L., Urey, H.C. and Oró, J., 1976. Origin of organic compounds on the primitive Earth and in meteorites. J. Mol. Evol., 9: 59—72.

Moorbath, S., O'Nions, R.K. and Pankhurst, R.J., 1973. Early archaean age for the Isua iron formation, West Greenland. Nature, 245: 138—139.

Moorbath, S., 1976. Age and isotope constraints for the evolution of Archaean crust. In: B.F. Windley (Editor), The Early History of the Earth. Wiley, New York, pp. 351—360.

Murthy, R.V., 1976. Composition of the core and the early chemical history of the Earth. In: B.F. Windley (Editor), The Early History of the Earth. Wiley, New York, pp. 21—31.

Naudet, R., 1978a. Les reacteurs d'Oklo: cinque ans d'exploration du site. In: Natural Fission Reactors. I.A.E.A., Vienna, pp. 3—18.

Naudet, R., 1978b. Etude parametrique de la criticité des reacteurs naturels. In: Natural Fission Reactors. I.A.E.A., Vienna, pp. 589—599.

Naudet, R., 1978c. Prise en compte des effects thermiques dans l'étude du contrôle et de la propagation des reactions nucléaires. In: Natural Fission Reactors. I.A.E.A., Vienna, pp. 601—608.

Naudet, R., 1978d. Stabilité géochimique des réacteurs. In: Natural Fission Reactors. I.A.E.A., Vienna, pp. 643—673.

Naudet, R., 1978e. Conclusions sur le déroulement du phénomène. In: Natural Fission Reactors. I.A.E.A., Vienna, pp. 715—734.

Naudet, R. and Filip, A., 1975a. Etude du bilan neutronique des réacteurs naturels d' Oklo. In: The Oklo Phenomenon. I.A.E.A., Vienna, pp. 527—540.

Naudet, R. and Filip, A., 1975b. Interprétation neutronique des distributions des taux de réactions dans les réacteurs d'Oklo. In: The Oklo Phenomenon. I.A.E.A., Vienna, pp. 557—564.

Naudet, R., Filip, A. and Renson, C., 1975. Distribution détaillée du l'uranium à l'intérieur des amas. In: The Oklo Phenomenon. I.A.E.A., Vienna, pp. 83—97.

Negrón-Mendoza, A., Draganić, Z.D., Navarro-Gonzáles, R. and Draganić, I.G., 1983. Aldehydes, ketones and carboxylic acids fromed radiolytically in aqueous solutions of cyanides and simple nitriles. Radiation Res., in press.

Neuilly, M., Bussac, J., Frejacques, C., Nief, G., Vendryes, G. and Yvon, J., 1972. Sur l'existence dans un passé reculé d'une réaction en chaîne naturelle de fissions, dans le gisement d'uranium d'Oklo. C.R. Acad. Sci., 275 D: 1847—1849.

Niketić, V., Draganić, Z.D., Nešković, S. and Draganić, I.G., 1982. Enzymatic characterization of peptidic materials isolated from aqueous solutions of ammonium cyanide (pH 9) and hydrocyanic acid (pH 6) exposed to ionizing radiation. J. Mol. Evol., 18: 130—136.

Niketić, V., Draganić, Z.D., Nešković, S., Jovanović, S. and Draganić, I.G., 1983. The radiolysis of aqueous solutions of hydrogen cyanide (pH 6): compounds of interest in chemical evolution studies. J. Mol. Evol., in press.

Orpen, J.L. and Wilson, J.F., 1981. Stromatolites at 3,500 Myr and a greenstone—granite unconformity in the Zimbabwean Archaean. Nature, 291: 218—220.

Ruffenach, J.C., Menes, J., Devillers, C., Lucas, M. and Hageman, R., 1976. Etudes chimiques et isotopiques de l'uranium, du plomb et de plusieurs produits de fission dans un échantillon de minerai du réacteur naturel d'Oklo. Earth Planet. Sci. Lett., 30: 94—108.

Rutten, M.G., 1971. The Origins of Life by Natural Causes. Elsevier, Amsterdam, pp. 253—296.

Schaw, D.M., 1976. Development of the early continental crust, Part 2: Prearchean, Protoarchean and later eras. In: B.F. Windley (Editor), The Early History of the Earth. Wiley, New York, pp. 33—53.

Shidlowski, M., Appel, P.W.U., Eichmann, R. and Junge, C.F., 1979. Carbon isotope geochemistry of the 3.7 × 10^9 y old Isua sediments, West Greenland: implications for the Archaean carbon and oxygen cycles. Geochim. Cosmochim. Acta, 43: 189—199.

Schopf, J.W., 1978. The evolution of the earliest cells. Sci. Am., 239: 110—138.

Siever, R., 1977. Early Precambrian weathering and sedimentation: an impressionistic view. In: C. Ponnamperuma (Editor), Chemical Evolution of the Early Precambrian. Academic Press, New York, pp. 13—23.

Simov, S.D., 1979. Uranium epochs. In: Uranium Deposits in Africa: Geology and Exploration. I.A.E.A., Vienna, pp. 191—204.

Smith, J.V., 1976. Development of the Earth—Moon system with implications for the geology of the early Earth. In: B.F. Windley (Editor), The Early History of the Earth. Wiley, New York, pp. 3—19.

Walker, J.C.G., 1976. Implication for atmospheric evolution of the inhomogeneous accretion model of the origin of the Earth. In: B.F. Windley (Editor), The Early History of the Earth. Wiley, New York, pp. 537—546.

Walker, J.C.G., 1977. Origin of the atmosphere: history of the release of volatiles from the solid Earth. In: C. Ponnamperuma (Editor), Chemical Evolution of the Early Precambrian. Academic Press, New York, pp. 1—11.

Weber, F., 1978. Discussion générale. In: Natural Fission Reactors. I.A.E.A., Vienna, p. 639.

Wetherill, G.W. and Drake, C.L., 1980. The Earth and planetary sciences. Science, 209: 96—104.

Zizin, M.N., 1978. Rastchiot Neitrono—Fizicheskikh Kharakteristik Reaktorov na Bistrikh Neitronakh. Atomizdat, Moskva, pp. 45—62.

EVOLUTIONARY CONNECTIONS OF BIOLOGICAL KINGDOMS BASED ON PROTEIN AND NUCLEIC ACID SEQUENCE EVIDENCE

MARGARET O. DAYHOFF*

National Biomedical Research Foundation, Georgetown University Medical Center, 3900 Reservoir Road N.W., Washington, DC 20007 (U.S.A.)

ABSTRACT

Dayhoff, M.O., 1983. Evolutionary connections of biological kingdoms based on protein and nucleic acid sequence evidence. Precambrian Res., 20: 299—318.

Evolutionary trees are derived based on nucleic acid and protein sequences and the methods of numerical taxonomy. From 5S ribosomal RNA sequences, molecules that participate in protein synthesis, the order of branching of many prokaryote species and the nuclear and organellar components of eukaryote species are inferred. All oxygen-evolving forms, including the chloroplasts and blue-green algae, are to be found on a single branch; the mitochondria are found with the Rhodospirillaceae, nonsulfur photosynthetic bacteria; and the eukaryote cytoplasmic components are found with the archaebacteria, including *Thermoplasma* and *Sulfolobus*. This tree clearly supports the symbiotic origin of the eukaryote organelles. There is much redundant information available from c-type cytochromes, cytochromes c′, 4Fe—4S ferredoxins and 5.8S rRNA molecules. A gene duplication of ferredoxin, probably predating all of the species divergences, permitted us to infer an ancestral molecule that can be placed on the tree to give the base. The heterotrophic anaerobes have a sequence most resembling the ancestral sequence, suggesting that the ancestor may have been a heterotroph. Ten prokaryote species occur on both the c-type and the c′-type cytochrome trees. There is only one inconsistency in the topologies of the two trees, which may reflect a gene transfer among prokaryotes confirming that, for these genes of fundamental importance, gene transfer followed by acceptance is rare. The eukaryote trees derived from 5S and 5.8S rRNA suggest that the earliest eukaryotes were unicellular and that the multicellular forms of plants, animals, fungi and slime molds arose independently.

INTRODUCTION

Many proteins and nucleic acids are "living fossils" in the sense that their structures have been dynamically conserved by evolution over billions of years: recognizably related sequences are found in eukaryotes and prokaryotes. These related forms are believed to be of common evolutionary origin, having evolved by substitutions, insertions and deletions in the limited number of monomers comprising them. The sequences of over 250,000 amino acids in over 1800 proteins (more than 5% different) have been

*Dr. Margaret O. Dayhoff deceased, February 5, 1983.

elucidated during the last 30 years, and the order of more than 600,000 nucleotides in nucleic acids is now known. The rate of nucleic acid sequence analysis has reached an explosive stage, with the output at least doubling each year, due to the recent breakthrough in nucleic acid sequencing techniques (Maxam and Gilbert, 1977; Sanger et al., 1977). Five years ago there were finally sufficient sequence data to propose a comprehensive evolutionary tree, including the position of the base, derived objectively from comparison of sequences (Schwartz and Dayhoff, 1978). This tree, derived by superimposing trees from sequences of c-type cytochromes, ferredoxins, and 5S ribosomal RNA (rRNA) molecules, is remarkably consistent with newer sequence data. In this paper, a comprehensive evolutionary history is derived from a single kind of molecule, 5S ribosomal RNA. This tree includes many bacteria, blue-green algae (or cyanophytes), eukaryotes and eukaryote organelles. Other molecules now supply redundant data, particularly the cytochrome c′, c-type cytochrome, and 4Fe—4S and 2Fe—2S ferredoxin sequences from prokaryotes, and 5.8S rRNA sequences from eukaryotes. A great many people have done the experimental sequence determinations on which our work is based. References to the early work, and alignments of these sequences, are given in Dayhoff (1972, 1973, 1976, 1979). References to the more recent work are indicated in the figure captions. Up-to-date protein and nucleic acid databases, which include all sequences used here, are available (Dayhoff et al., 1982a, 1982b).

The information used in deriving the trees comes from the chemical structures of the sequences. The derivation of the best tree uses the mathematical methods of numerical taxonomy. This line of reasoning is independent of derivations based on biological traits, metabolic capacities, or fossil evidence, but should be consistent with them. The order of divergence is obtained most clearly from the sequences, because of the great amount of information inherent in them. This feature is concentrated upon here, although a description of the biological and metabolic traits of the ancestral organisms requires, in addition to the constraints of the divergence pattern, much additional information that is barely touched upon. In eukaryotes, an approximate time scale can be based on the mutation clock, the changes observed in the molecules, on the assumption that the risk of mutation in a given molecule is constant over time. Such a time scale is of little value for prokaryotes, so time estimates mainly depend on fossil or geological evidence.

Here, the working hypothesis is that for those sequences that perform basic metabolic functions, genetic transfer between major types of bacteria followed by permanent acceptance in evolution is very infrequent. All such basic sequences within an organism share the same phylogenetic history and any one of them can be used to infer its course. If this is not at least approximately true, then consistency of phylogenetic results from different molecules would not be seen. From the considerable amount of redundant data now available, a few exceptions have been identified.

Evolutionary history is conveniently represented by a tree. Each point on

the tree corresponds to a time, a macromolecular sequence and a species within which the sequence functioned. There is one point that corresponds to the earliest time, and to the ancestral organism and sequence, which is referred to as the base of the tree. Time advances on all branches emanating from this point. The topology of the branches gives the relative order of events. During evolution, sequences in different species have gradually and independently accumulated changes yielding the sequences found today in the various organisms represented at the ends of the branches. For the trees in this paper, the lengths of the branches were drawn proportional to the estimated amount of evolutionary change in the sequences. The topological connections between the sequences were determined by the least-squares matrix method described below.

The results of evolution acting on the amino acid or nucleotide sequences are sufficiently well understood that the usefulness of any proposed method for reconstructing phylogeny can be tested. Sequences connected by a known history of divergence and amount of evolutionary change can be constructed by simulating the evolutionary change using random numbers. A computer model that is simple yet adequate for this purpose has been described (Dayhoff et al., 1979). By considering many groups of simulated sequences with each group related by the same evolutionary history, but generated with different random numbers, a measure of the accuracy of a given method can be assessed and different methods can be compared. We have found the least-squares matrix method to be more reliable than acestral sequence methods for distantly related sequences. Sequences are aligned to reflect the genetic changes accepted in evolution. A matrix of percentage difference between them is calculated and corrected for inferred superimposed mutations to yield the "observed" matrix of accepted point mutations per 100 residues (PAMs). This observed matrix is used to construct the best tree, for which a double minimization is required. For a predetermined order of connection or topology of the sequences, the computer program MATTOP determines the branch lengths that give a weighted least-squares best fit of the reconstructed matrix to the observed matrix. Weights were chosen that were inversely proportional to the square of the observed matrix element to compensate for the larger errors to be expected in the larger values. The sum of the absolute values of the branch lengths, the tree size, is used to characterize the many topologies generated. That topology having the smallest tree size is chosen as the best estimate of the true history.

Typically, the best estimate is to be found among the solutions with all positive branch lengths. In putting together a tree of seven branches there are 945 topologies. For one or a few of them, all branches will have positive lengths. Some connections are the same on all of the trees of shortest length and the order of only one or two divergences is in question. Such places are shown with dotted circles on the figures. The data from one molecule may be misleading because of back and parallel mutations. Alternative computational methods will produce the same answer, which may be slightly in

error. Additional sequences for a given tree or information from another molecule will eventually identify such places.

The least-squares matrix method makes no assumptions about rates of change on the various branches in a tree and does not use information concerning the location of the base of the tree. It is not valid to assume equality of rates, especially for the major prokaryote groups shown in the figures, for which there has frequently been twice as much and sometimes ten times as much change in one line as in another during the same time interval.

BACTERIAL FERREDOXINS

The bacterial ferredoxins are found in a broad spectrum of organisms and participate in such fundamental biochemical processes as photosynthesis, reductive carboxylation reactions, nitrogen fixation and dissimilatory sulfate reduction. The active centers are 4Fe—4S clusters. The tree shown in Fig. 1 is derived from these sequences. A gene-doubling is shared by all of the sequences and, therefore, most probably occurred prior to all of the species divergences shown here. From an alignment of the first and second halves of these sequences, we inferred an ancestral half-chain sequence. This sequence, doubled, was included in the computations of the evolutionary tree. The position of the doubled sequence identifies the base of the tree and, by inference, provides a time orientation in the other trees presented here. Several lines diverged near the base from the ancestral stock that is labelled the "early ancestor". *Clostridium*, *Megasphaera* and *Peptococcus* are all anaerobic, heterotrophic bacteria whose sequences are still very similar to the extremely ancient protein that duplicated. It has long been thought that of the extant bacteria, these species most closely reflect the metabolic capacities of the earliest species. Broda (1975), using metabolic data, has argued persuasively to this effect. Unfortunately, only the bacterial ferredoxins have so far been found to have a well-conserved gene duplication that probably occurred early in bacterial evolution. Confirmatory evidence from other sequences would be reassuring.

Two other lines, in which there has been a great deal of evolutionary change, also arose from the early ancestor. One leads to *Chromatium* and *Chlorobium*, which are anaerobic bacteria capable of photosynthesis using H_2S as an exogenous electron donor. The other leads to the "late bacterial ancestor", the common ancestor of *Bacillus stearothermophilus*, *Desulfovibrio gigas*, *Pseudomonas putida* and *Mycobacterium smegmatis*. *Pseudomonas putida* and *M. smegmatis* are aerobes and *B. stearothermophilus* is a facultative aerobe, whereas *D. gigas* is a sulfate-reducing bacterium that respires anaerobically using sulfate as the terminal electron acceptor.

Unfortunately, there is no blue-green alga or archaebacterium on this tree; therefore, the early ancestor cannot be linked precisely to a position on the other trees derived here.

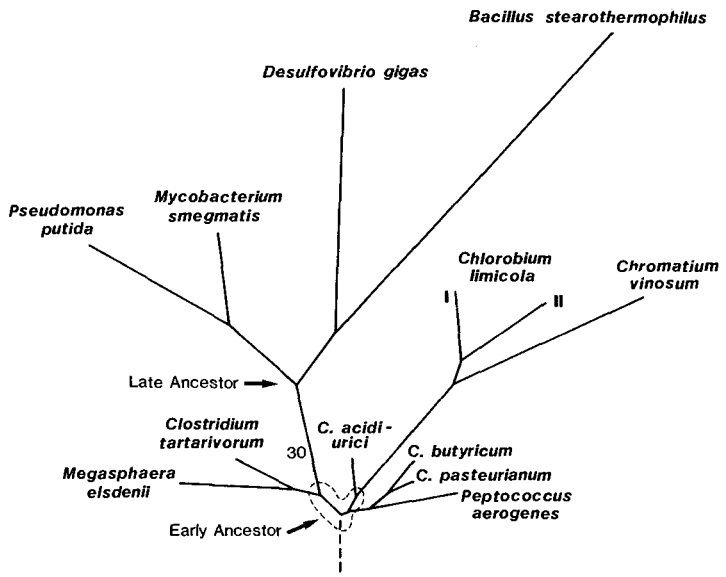

Fig. 1. Evolutionary tree derived from 4Fe—4S ferredoxins. The dotted line indicates that the exact order of branching at the bottom of the tree cannot be derived from these short molecules. The early ancestor is quite distinct from later branching including the late ancestor on the *Pseudomonas* line and the later divergences in the other lines. The branch lengths are drawn proportional to the estimated number of mutations per 100 residues. References for the sequences are as follows: *Bacillus stearothermophilus*, Hase et al. (1976); *Chlorobium limicola* I, Tanaka et al. (1974); *Ch. limicola* II, Tanaka et al. (1975); *Chromatium vinosum*, Hase et al. (1977); *Clostridium acidi-urici*, Rall et al. (1969); *C. butyricum*, Benson et al. (1966); *C. pasteurianum*, Tanaka et al. (1966); *C. tartarivorum*, Tanaka et al. (1971); *Desulfovibrio gigas*, Bruschi (1979); *Megasphaera elsdenii*, Azari et al. (1973); *Mycobacterium smegmatis*, Hase et al. (1979); *Peptococcus aerogenes*, Tsunoda et al. (1968); *Pseudomonas putida*, Hase et al. (1978).

5S RIBOSOMAL RNA

The 5S ribosomal RNA molecules, among the most highly conserved sequences of living organisms, are relatively short, about 120 nucleotides long. They are associated with the large ribosomal sub-unit and may be involved in non-specific transfer RNA binding during protein synthesis. Figure 2 depicts the evolutionary tree based on the bacterial 5S rRNA sequences. The base of the tree, corresponding to the early ancestor, has been placed among anaerobes in approximate conformance with the tree derived from the bacterial ferredoxins. Four branches of the tree are particularly noteworthy. Diverging early is the line to the two oxygen-evolving forms, the blue-green alga *Anacystis nidulans* and the tobacco chloroplast. A number of other chloroplast sequences from higher plants are known, all of which are almost identical with the tobacco sequence. All of the prokaryotes or eukaryote organelles capable of oxygen-evolving photosynthesis are found on this branch.

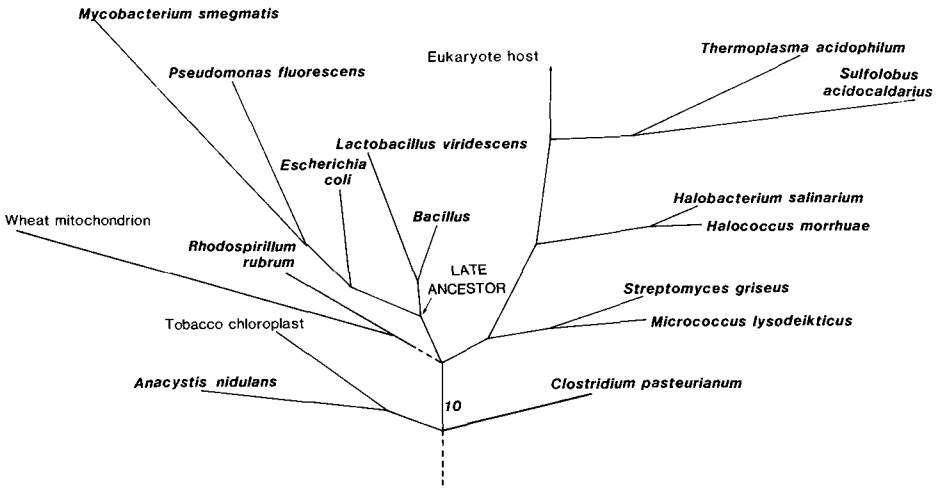

Fig. 2. Evolutionary tree derived from prokaryote 55rRNA sequences. A consensus sequence was used to place the eukaryote host branch. The base has been placed in the anaerobic section of the tree. It may correspond to the same ancestral organism as depicted at the base of the ferredoxin tree. The late ancestor corresponds to the one on the ferredoxin tree, where lines to *Clostridium*, *Bacillus* and *Pseudomonas* come together. References for the sequences are as follows: *Anacystis nidulans*, Corry et al. (1974); *Clostridium pasteurianum*, Pribula et al. (1976); *Escherichia coli*, Brownlee et al. (1968); *Halobacterium salinarium*, Nazar et al. (1978); *Halococcus morrhuae*, Luehrsen et al. (1981b); *Lactobacillus viridescens*, Alexander and Stewart (1980); *Micrococcus lysodeikticus*, Hori et al. (1980b); *Mycobacterium smegmatis*, Jagadeeswaran and Cherayil (1978); *Pseudomonas fluorescens*, Dubuy and Weissman (1971); *Rhodospirillum rubrum*, Sankoff et al. (1982); *Streptomyces griseus*, Simoncsits (1980); *Sulfolobus acidocaldarius*, Stahl et al. (1981); *Thermoplasma acidophilum*, Luehrsen et al. (1981a); tobacco, Takaiwa and Sugiura (1980); wheat, Spencer et al. (1981). Three *Bacillus* sequences were averaged, *B. licheniformis* forms 1 (Raue et al., 1975) and 2 (Raue et al., 1976) and *B. megaterium* (Woese et al., 1976). The *B. stearothermophilus* (Marotta et al., 1976) groups with the other *Bacillus* sequences; however, its sequence is not completely determined.

Slightly later, the branch to the archaebacteria and the eukaryote cytoplasmic constituents (eukaryote host) diverges. This line leads to a number of aerobic bacterial species including, near the base, *Micrococcus lysodeikticus* and *Streptomyces griseus*. More recently, the archaebacteria *Halobacterium salinarium* and *Halococcus morrhuae*, which live at high salt concentrations, *Thermoplasma acidophilum*, with an optimum temperature for growth of 59°C and an optimum pH of 1—2, and *Sulfolobus acidocaldarius*, with an optimum growth temperature of ~72°C, diverge from the eukaryote line. No sequences have been reported for other archaebacteria.

Of particular interest, because of the similarity of its cytochrome c_2 to the mitochondrial cytochrome c, is *Rhodospirillum rubrum*, a purple nonsulfur bacterium. It diverges from the main stem at about the same time as the branch to the archaebacteria. Although its exact position cannot be

determined from these short sequences, it is certainly clear that it does not fit with the archaebacteria and eukaryote host or on the chloroplast branch, but comes off quite separately. The position of the plant mitochondrion sequence seems established on the *R. rubrum* line, even though there has been a great deal of change in the sequence. The wheat mitochondrial 5S rRNA is actually encoded in the mitochondrial genome.

Finally, the late bacterial ancestor is represented, leading to *Pseudomonas fluorescens*, *Mycobacterium smegmatis* and *Bacillus stearothermophilus.* This late ancestor gives rise here to additional species of interest, including *Escherichia coli* and *Lactobacillus viridescens. Desulfovibrio* would be expected to diverge from the *Bacillus—Lactobacillus* line, as seen on the ferredoxin tree.

The mycoplasmas have been candidates for the most primitve organisms because of their very small genomes. *Mycoplasma capricolum* appears to branch from the line to the late ancestor at about the same time as *Rhodospirillum.*

SYMBIOTIC ORIGIN OF EUKARYOTE ORGANELLES

There are two schools of thought concerning the origin of eukaryote DNA-containing organelles: one is that they arose by the compartmentalization of the DNA within the cytoplasm of an evolving protoeukaryote (Raff and Mahler, 1972; Uzzell and Spolsky, 1974); the other is that they arose from free-living forms that invaded a host and established symbiotic relationships with it (Margulis, 1981). Figure 3 illustrates the kind of trees that would be expected for each theory. In the nonsymbiotic theory, all genes arose within the organism; homologous forms, such as the coding apparatus, in both the nucleus and the organelles arose by gene duplication. Organelles formed in this way need not be capable of independent existence outside of the cell and their continued competitive extracellular existence in evolution would be most unlikely. Mitochondria and higher plant chloroplasts have less genetic material than free-living prokaryotes and are incapable of prolonged extracellular existence. Therefore, this theory would predict that there would be no prokaryote branches emanating from the chloroplast or mitochondrial lines after these had diverged from the host, as shown in the upper figure.

The symbiotic theory, on the other hand, proposes that the chloroplast was originally a free-living blue-green alga and that the mitochondrion was originally a free-living aerobic (possibly photosynthetic) bacterium. Their current status as organelles would have gradually evolved from symbioses. In this theory, mitochondrial, chloroplast and host genes are expected to show evidence of recent common ancestry with separate types of contemporary free-living prokaryote forms, as shown in the lower figure. The 5S rRNA tree clearly supports the symbiotic theory for the origin of mitochondria and chloroplasts.

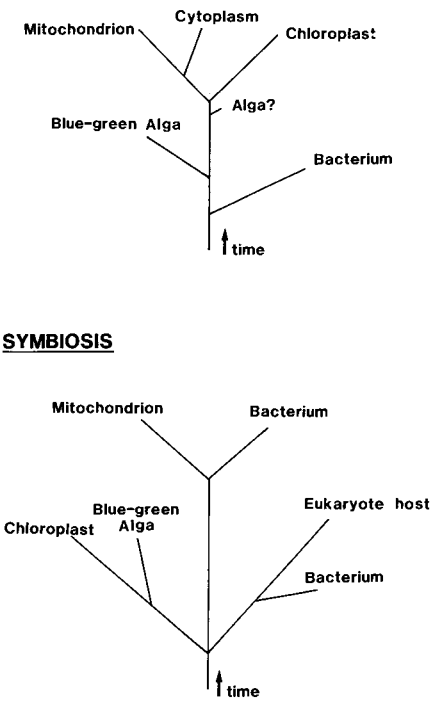

Fig. 3. Phylogenetic trees predicted for the compartmentalization and symbiotic theories of the evolution of eukaryotic mitochondria and chloroplasts.

C-TYPE CYTOCHROMES

The only molecules now available whose sequences give a detailed picture of the origin of mitochondria are the c-type cytochromes. The phylogenetic tree derived from these molecules is shown in Fig. 4. The base is drawn among the anaerobic photosynthetic bacteria as suggested by the ferredoxin tree. The entire lower portion of the tree represents anaerobic organisms and the base could be anywhere there.

On the subtree of mitochondria and Rhodospirillaceae, the bacteria are shown as single solid lines, whereas the mitochondria are shown as parallel lines. The three arrows indicate approximately where endosymbiosis may have occurred, giving rise to the eukaryote organelles. The branches to the mitochondrial sequences of ciliates, flagellates, and the plants, animals and fungi share recent common ancestry with the *Rhodopseudomonas* (*R.*) *globiformis* line and a somewhat more distant ancestry to *Rhodospirillum* (*Rs.*) *rubrum* and *Pseudomonas*.

The *R. globiformis* sequence clearly diverges from the *Euglena* and *Crithidia* branches close to the point of their divergence from one another.

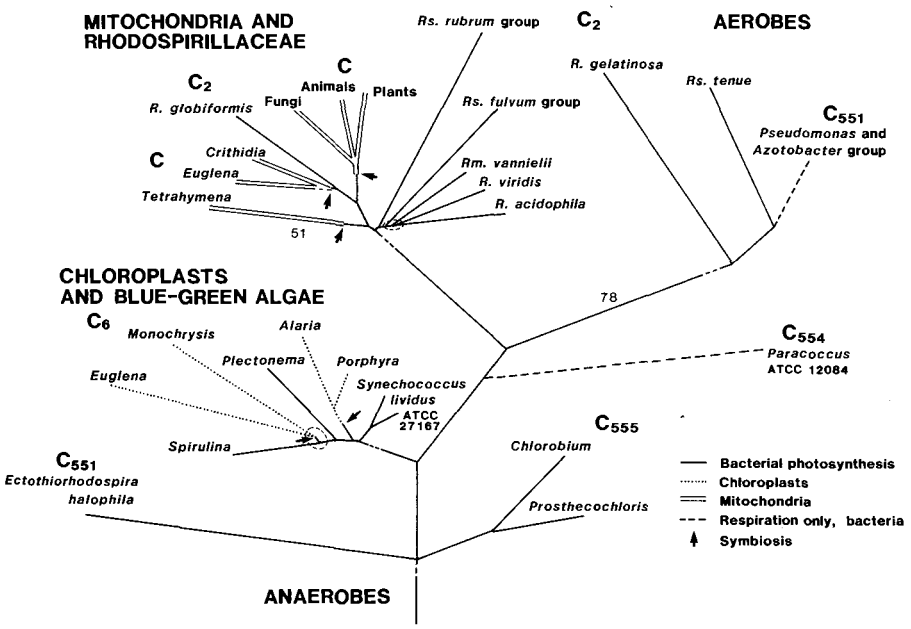

Fig. 4. Evolutionary tree derived from c-type cytochromes. The species used and references to the original work are as follows: *Alaria esculenta*, Laycock (1975); *Azotobacter vinelandii*, Ambler (1973b); *Chlorobium limicola* f.sp. thiosulfatophilum, Van Beeumen et al. (1976); *Crithidia fasciculata*, Hill and Pettigrew (1975); *Cr. oncopelti*, Pettigrew et al. (1975); *Ectothiorhodospira halophila* (R.P. Ambler, personal communication, 1979); *Euglena gracilis* cytochrome c, Pettigrew et al. (1975); *E. gracilis* cytochrome c_6, Pettigrew (1974); *Monochrysis lutheri*, Laycock (1972); *Paracoccus* ATCC 12084, Ambler (1977); *Plectonema boryanum*, Aitken (1977); *Porphyra tenera* (R.P. Ambler, T.E. Meyer and R.G. Bartsch, personal communication, 1973); *Prosthecochloris aestuarii*, Van Beeumen et al. (1976); *Rhodomicrobium* (*Rm.*) *vannielii*, Ambler et al. (1976); *Rhodopseudomonas acidophila*, Ambler et al. (1978); *R. gelatinosa*, (R.P. Ambler, personal communication, 1977); *R. globiformis*, Ambler (1979); *R. viridis*, Ambler et al. (1976 and personal communication, 1977); *Rhodospirillum fulvum* iso-1, Ambler et al. (1978); *Rs. fulvum* iso-2, Ambler et al. (1979a); *Rs. rubrum*, Dus et al. (1968); *Rs. tenue* (R.P. Ambler, personal communication, 1977); *Spirulina maxima*, Ambler and Bartsch (1975); *Synechococcus* ATCC 27167, Aitken (1979); *S. lividus* (D. Borden and E. Margoliash, personal communication, 1979); *Tetrahymena pyriformis*, Tarr and Fitch (1976). Matrix elements for *Pseudomonas aeruginosa* (Ambler, 1963); *P. denitrificans* (Ambler, 1973b); and *P. fluorescens*, *P. mendocina* and *P. stutzeri* (Ambler and Wynn, 1973) were averaged. References for animal, plant and fungal sequences are given in Dayhoff (1972, 1973, 1976, 1979).

At the *R. globiformis* divergence, the ancestral cytochrome occurred in a free-living form. Very soon thereafter, an endosymbiosis occurred to form the mitochondrion. The occurrence of a separate symbiosis among flagellates is consistent with the lack of mitochondria in the Trichomonadida, an anaerobic flagellate group. This group either diverged before the endosymbiosis or else the symbiosis was so newly established that the mitochondrion

could easily be discarded in an anaerobic niche. A second symbiosis could then have occurred and persisted.

It seems likely that, in the species shown, there were at least two other symbioses established, to account for the *Tetrahymena* mitochondrion and that of the multicellular forms. A single origin for the mitochondrion would involve a symbiosis at the bottom of the eukaryote subtree. *Rhodopseudomonas globiformis*, a free-living photosynthetic bacterium, would then be descended from a eukaryote cell, a course of events that seems extremely unlikely.

Cytochrome c_6 is found in the blue-green algae and chloroplasts. It is an electron transport protein that has been shown to substitute for plastocyanin in the electron transport chain between photosystems 1 and 2, depending on the availability of copper. All of the c_6 sequences and the species involved in oxygen-evolving photosynthesis are to be found on one main branch. The detailed topology of the chloroplast—blue-green algal subtree was determined separately. Blue-green algae are shown by solid lines and chloroplasts are shown by dotted lines. No matter where the base of the subtree is placed, at least two symbiotic events must be assumed to explain the origin of the related chloroplast sequences. One possibility is indicated by the arrows. Multiple symbiotic events are similarly predicted in the tree deduced from plant 2Fe—2S ferredoxin molecules (Schwartz and Dayhoff, 1981), where a gene duplication establishes the position of the base of the tree. The base of the cytochrome c_6 subtree was placed to conform with the plant ferredoxin tree, with the branch to *Synechococcus* coming off first.

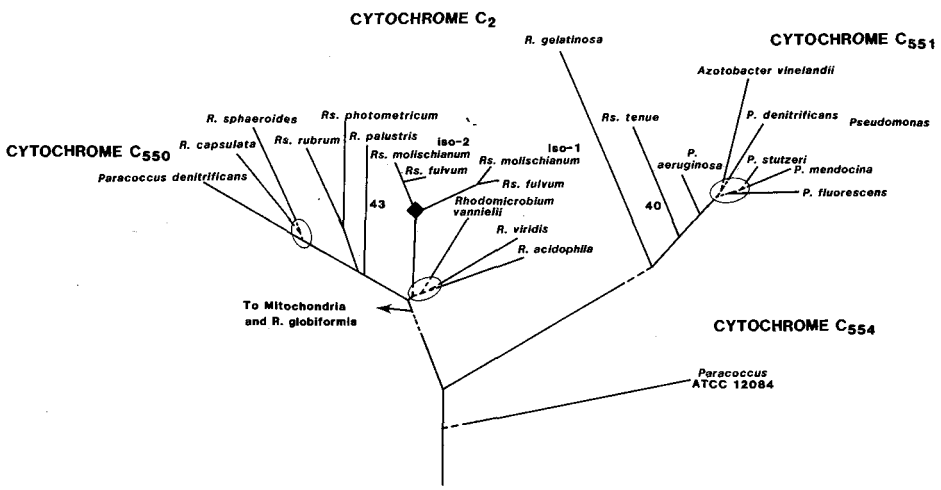

Fig. 5. Evolutionary tree derived from the 12 orders of Rhodospirillaceae. References to the additional sequences are: *Paracoccus denitrificans*, Ambler et al. (1981b) and Timkovich et al. (1976); *Rhodopseudomonas capsulata* and *R. palustris*, Ambler et al. (1979a); *R. sphaeroides* (R.P. Ambler and T.E. Meyer, personal communication, 1974); *Rhodospirillum molischianum*, Ambler et al. (1978); *Rs. photometricum*, Hermoso et al. (1978).

The details of the bacterial branches in the upper part of Fig. 4 are shown in Fig. 5. All twelve species of purple, nonsulfur, photosynthetic bacteria, the Rhodospirillaceae, that are described in Bergey's Manual of Determinative Bacteriology (Buchanan and Gibbons, 1974) are represented. Apparently, morphology is not an accurate guide to the evolution of these bacteria. Sequences from all three genera of Rhodospirillaceae are found intermixed on the tree.

Of concern is the need to know to what extent trees derived from different molecules show the same evolutionary history for the species represented. To shed light on this problem, Richard Ambler and co-workers (1981a) have recently elucidated cytochrome c′ sequences from a number of species. This heme-binding molecule functions in electron transport. The evolutionary tree derived from this molecule is shown in Fig. 6 and the base is placed on the *Chromatium* line. Ten of the species also appear on the c-type cyto-

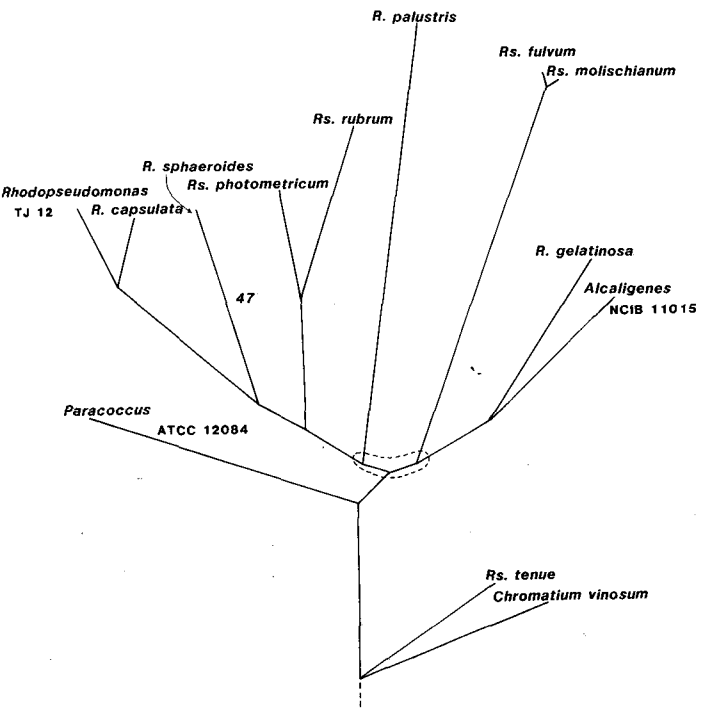

Fig. 6. Evolutionary tree derived from cytochrome c′. References for the sequences are as follows: *Alcaligenes* NCIB 11015, Ambler (1973a); *Chromatium vinosum*, Ambler et al. (1979b); *Paracoccus* ATCC 12084 and *Rhodopseudomonas capsulata*, Ambler et al. (1981a); *R. gelatinosa*, Ambler et al. (1979c); *R. palustris, sphaeroides* and TJ12, and *Rhodospirillum photometricum*, Ambler et al. (1981a); *Rs. fulvum* and *molischianum*, Ambler (1979); *Rs. rubrum*, Meyer et al. (1975); *Rs. tenue*, Ambler et al. (1979c).

chrome tree of Fig. 5. The detailed topology is remarkably consistent with that of the cytochrome c_2 tree. There is only one inconsistency, which is quite beyond the lack of precision of the data or method (Ambler et al., 1981a). We would expect *Rs. tenue* to be close to *R. gelatinosa* rather than to be on the *Paracoccus* branch, close to an anaerobe. This inconsistency may reflect a gene transfer, possibly in the *Rs. tenue* line. An alternative but unlikely possibility would assume an early gene duplication with elimination or suppression of one of the genes in every species. At least five separate events would be required.

EUKARYOTES

Figure 7 shows the tree derived from the cytoplasmic 5S rRNAs of the eukaryote species. The base of this tree fits onto the line to eukaryotes of Fig. 2. All of these species have a nuclear membrane, which must have evolved in the ancestral line. There was a radiation of unicellular forms, followed by the development of multicellular forms in some lines (indicated by heavy lines on the figure). These have evolved independently of one another, consistent with the different forms of organization in the multicellular

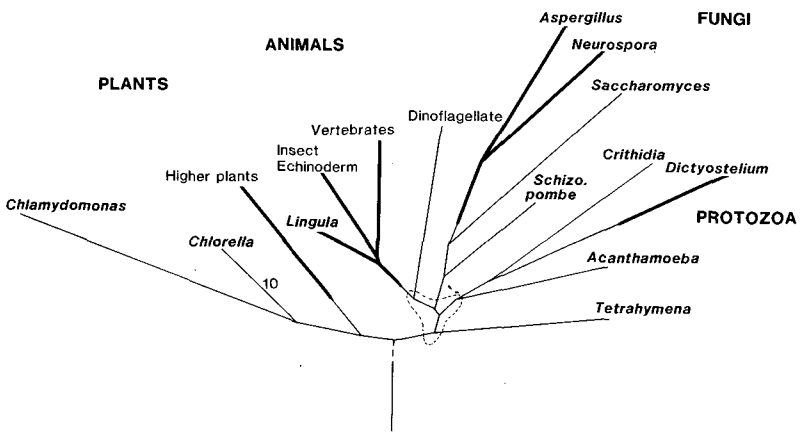

Fig. 7. Phylogenetic tree derived from the cytoplasmic 5S rRNA molecules of eukaryotes. References for the sequences are as follows: *Acanthamoeba castellanii,* MacKay and Doolittle (1981); *Aspergillus nidulans* and *Neurospora crassa,* Piechulla et al. (1981); *Chlamydomonas reinhardii* forms 1 and 2, Darlix (1981); *Chlorella* ATCC 11469, Luehrsen and Fox (1981); *Crithidia fasciculata,* MacKay et al. (1980a); *Dictyostelium discoideum,* Hori et al. (1980a); *Lingula anatina,* Komiya et al. (1980); *Saccharomyces cerevisiae,* Valenzuela et al. (1977); *Schizosaccharomyces pombe,* Komiya et al. (1981); *Tetrahymena thermophila,* Luehrsen et al. (1980). Higher plants included rye (Payne and Dyer, 1976), wheat (Gerlach and Dyer, 1980; MacKay et al., 1980b) and broad bean (Payne et al., 1973). Vertebrates included loach (Mashkova et al., 1981); South African toad (Brownlee et al., 1972); and human (Forget and Weissman, 1967). The insect was fruit fly (Tschudi and Pirrotta, 1980); the echinoderm was sea urchin (*Lytechinus variegatus*) (Lu et al., 1980); and the dinoflagellate was *Crypthecodinium cohnii* (Hinnebusch et al., 1981).

plants, animals, fungi and slime mold. Unicellular forms occur early in all of these groups. The slime mold, *Dictyostelium*, is much closer to *Crithidia* than to the fungi, just as Kudo (1971) suggests in his classification of protozoa. It should be noted that the echinoderm is with the insects, not with the vertebrates, a point of some disagreement among systematists but consistent with the tree derived from cytochrome c sequences (Schwartz and Dayhoff, 1979). *Lingula*, a brachiopod, seems to have come off early. There is a long branch to the animals from which a number of invertebrates probably diverged and it is possible that the dinoflagellate diverged early on this line. The unicellular chlorophyte *Chlorella* and the phytomonad *Chlamydomonas* are clearly on the plant branch.

5.8S RIBOSOMAL RNA TREE

A second opportunity to compare the phylogenetic scheme deduced from two different molecules is given by the 5.8S rRNAs. These molecules are found only in eukaryotes, located 5′ to the 25S rRNA coding region but separated by an intervening sequence that is not incorporated in the functional molecules. The 5.8S rRNAs are homologous to the 5′ end of the large rRNA sequence of prokaryotes. In the evolutionary tree derived from the 5.8S rRNAs (see Fig. 8), the three major groups, plants, fungi

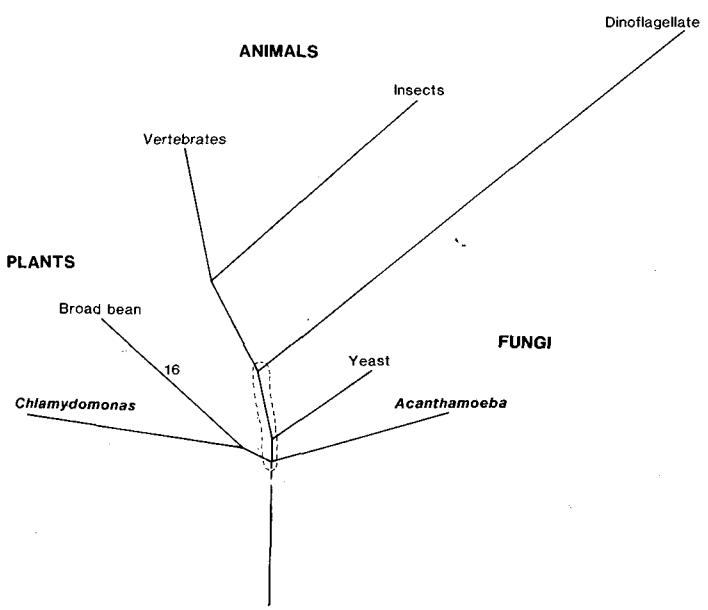

Fig. 8. Evolutionary tree derived from the 5.8S rRNA sequences of eukaryotes. Vertebrates included rat (Nazar et al., 1975), South African toad (Hall and Maden, 1980) and trout (Nazar and Roy, 1978). Insects included gnat (Jordan et al., 1980) and fruit fly (Pavlakis et al., 1979). Yeasts included *Saccharomyces* (Rubin, 1973) and *Thermomyces lanuginosus* (Wildeman and Nazar, 1981). The broad bean (*Vicia faba*) sequence was determined by Tanaka et al. (1980).

and animals are again seen diverging from one another very early. The protozoa are to be found on branches from many early parts of the tree. The invertebrates and vertebrates appear together, with the dinoflagellate branching off early on this line. *Chlamydomonas* is again found on the plant line.

COMPOSITE TREE

Figure 9 shows the entire tree derived from 5S rRNA. The eukaryote line shows a great deal of change, consistent with a large amount of evolution in the whole group of rRNA molecules concerned with the translation of proteins. It is clear from this one tree that the chloroplast of the higher plants, the mitochondrion and the cytoplasmic constituents have very different lineages.

By reference to the trees derived from other molecules, other species can be positioned approximately. These species are shown in parentheses. The ferredoxin tree shows the *Chlorobium* and *Chromatium* sequences diverging from the early ancestor. These may form an entirely separate branch, or they may coincide with the early part of the blue-green branch. The ferredoxin tree shows *Desulfovibrio* branching from the *Bacillus* branch subsequent to the time of the late ancestor.

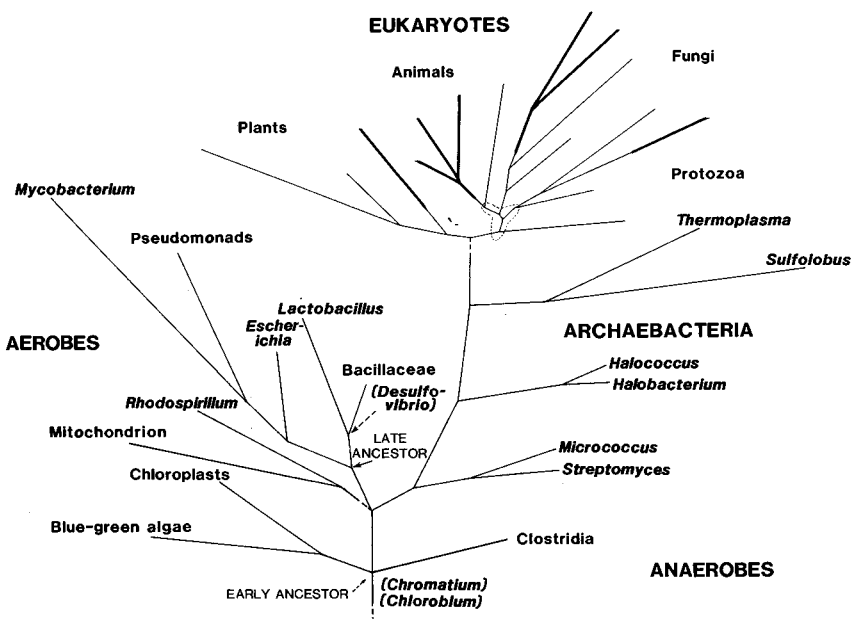

Fig. 9. Complete phylogenetic tree derived from the 5S rRNA sequences. The *Sulfolobus* and *Thermoplasma* sequences were included in the computation of the eukaryote tree and the length of the connecting branch calculated. Species found on other trees are indicated here in parentheses.

The c-type cytochrome tree would position most of the Rhodospirillaceae and the mitochondrial sequences on the *R. rubrum* line. *Rhodopseudomonas gelatinosa* and *Rs. tenue* would diverge from the line to the late ancestor or from one of its descendent lines.

The composite tree describes early evolution starting with the anaerobic heterotrophic bacteria at the base. These species contain a ferredoxin most similar to the primitive form and possibly their metabolism most closely resembles that of the earliest ancestor. Photosynthesis using chlorophyll developed early. Three families of photosynthetic bacteria are represented: Chromatiaceae, Chlorobiaceae and Rhodospirillaceae. All of the forms capable of oxygen-releasing photosynthesis, the prokaryote blue-green algae and the chloroplasts, are to be found on a single branch, and the available sequence data point to this capacity having evolved only once. Respiration must have developed contemporaneously with the development of an oxygen atmosphere. The time of divergence of the archaebacteria, the Rhodospirillaceae, and *Bacillus* (and *Desulfovibrio*) probably marks the presence of major components of this adaptation. The final elements were evolved separately because these groups differ in their terminal electron acceptors in respiration.

It is very possible that sulfate respiration developed on the *Desulfovibrio* branch, after its divergence from *Bacillus*. The dating of presumed products of the reaction (Schidlowski, 1979) at 2.8—3.0 Ga ago would place the time of the late bacterial ancestor prior to this date.

The mainstream of early evolution was very probably carried by species that performed bacterial photosynthesis, contrary to most classifications of bacteria. Bacterial photosynthesis was independently lost in a number of lines including those to the late ancestor, the archaebacteria and eukaryote host, *Paracoccus denitrificans*, and the mitochondria.

At the outset, we assumed no exchange between prokaryote species of the genes for the basic metabolic structures. So far there has proved to be an identifiable exception in the eukaryotes. These species developed the capacity to engulf and form lasting relationships, even extending through the reproductive cycle, with certain prokaryotes that are now identifiable as organelles within them. During the formation of the symbiotic associations, a good deal of the genetic information of the organelles was incorporated into the nucleus. The human mitochondrial genome contains fewer than 17,000 bases and encodes only a few proteins and ribosomal nucleic acids.

There was a great radiation of eukaryote forms closely following the establishment of the nuclear membrane, which is distinctive of all eukaryotes. Characteristically, the individual cells of organisms on these lines are much larger than prokaryotes and could be recognized if found in the fossil record. Schopf and Oehler (1976) have suggested that such an increase is seen at about 1.4 Ga ago, a figure not inconsistent with the eukaryote mutational clock based on the fish—mammalian divergence at 400 Ma ago.

CONCLUSIONS

The eukaryote mitochondria and chloroplasts as well as the cytoplasmic components, or host, are descended from free-living prokaryotes that formed symbiotic associations. More than one symbiotic event occurred for each of these organelles. The mitochondria derive from the Rhodospirillaceae. The chloroplasts derive from the blue-green algae, and the eukaryote host has most recently diverged from the archaebacteria, especially *Thermoplasma acidophilum* and *Sulfolobus acidocaldarius* of the species investigated.

Eukaryote cells are typically much larger than those of prokaryotes. This increase in size could be recognized in the fossil record. Schopf and Oehler (1976) have suggested that such cells are recognizable in formations 1.4 Ga old. Multi cellularity in animals, plants, fungi and slime molds has developed independently. Unicellular forms are found in all of these lines.

The only molecular evidence useful for locating the base of the evolutionary tree is given by the ferredoxin molecule. A gene duplication probably predating the species divergences permits us to infer ancestral molecule, which can be placed on the tree. The heterotrophic anaerobes have a sequence most resembling the ancestral sequence, suggesting that the ancestor may have been a heterotroph. Clearly, confirmatory evidence from other molecules on this important point is needed.

All oxygen-evolving photosynthetic forms are to be found on a single line, and evidently this capacity evolved only once. The tree places no stringent time restriction on this event and it could have occurred very early. However, a full adaptation to the aerobic conditions had not occurred by the time of the late bacterial ancestor, as different descending lines have different terminal acceptors in their respiratory chains.

The archaebacteria investigated, particularly the salt-loving and high-temperature forms, all occur on a single line. No sequences are available as yet from the methanogens.

The late bacterial ancestor, identified on the 5S rRNA and ferredoxin trees, preceded the divergence of *Desulfovibrio* from *Bacillus*. The reduction of sulfate is thought to have evolved in the *Desulfovibrio* line, at about 2.7 Ga ago. If so, the late ancestor would have lived before this time. The important lines to blue-green algae, to most Rhodospirillaceae and to eukaryotes would already have diverged even earlier from one another.

The order of divergence of nine species to be found on both c-type cytochrome and the cytochrome c′ trees is consistent. One instance of gene transfer between prokaryotes is identifiable, probably involving *Rs. tenue.*

There is still much left to be done. Perhaps most important to the question of the nature of the first organisms is additional evidence from sequences regarding the position of the base of the tree. The identification of other early gene duplications is essential for this. Additional information is necessary in order to sort out the order of the divergences in the anaerobic region of the tree, near the early ancestor. Sequences that would be helpful include

Chlorobium and *Chromatium* 5S rRNAs, a 4Fe—4S ferredoxin from a blue-green alga and an archaebacterium, a c-type cytochrome from *Chromatium*, or a cytochrome c′ from *Chlorobium* or a blue-green alga. Additional sequences from forms that diverged early on the eukaryote branch or late on the archaebacterial branch are needed. No methanogen sequences are published. Particularly important are the forms that provide a fossil record that can be dated. From the divergence order as well as morphological, developmental and metabolic information combined with the fossil record, a well-rounded picture of evolutionary history should be possible.

ACKNOWLEDGMENTS

I thank G.C. Johnson for her assistance in making the computations, C. Zovko for drawing the figures, M.C. Blomquist for her assistance in preparing the manuscript, and Drs. W.C. Barker and L.T. Hunt for reading the manuscript and for helpful discussions. This work was supported by Contract NASW3317 from the National Aeronautics and Space Administration and grant GM-08710 from the National Institute of General Medical Sciences of the National Institutes of Health.

REFERENCES

Aitken, A., 1977. Eur. J. Biochem., 78: 273—279.
Aitken, A., 1979. Eur. J. Biochem., 101: 297—308.
Alexander, L.J. and Stewart, T.S., 1980. Nucleic Acids Res., 8: 979—987.
Ambler, R.P., 1963. Biochem. J., 89: 349—378.
Ambler, R.P., 1973a. Biochem. J., 135: 751—758.
Ambler, R.P., 1973b. Syst. Zool., 22: 554—565.
Ambler, R.P., 1977. In: G.J. Leigh (Editor), The Evolution of Metalloenzymes, Metalloproteins and Related Materials. Symposium Press, London, pp. 100—118.
Ambler, R.P., 1979. In: J.M. Nichols (Editor), Abstr. Third Int. Symp. Photosynthetic Prokaryotes (Oxford). Abstr. E17, Univ. Liverpool.
Ambler, R.P. and Bartsch, R.G., 1975. Nature, 253: 285—288.
Ambler, R.P. and Wynn, M., 1973. Biochem. J., 131: 485—498.
Ambler, R.P., Bartsch, R.G., Daniel, M., Kamen, M.D., McLellan, L., Meyer, T.E. and Van Beeumen, J., 1981a. Proc. Natl. Acad. Sci. U.S.A., 78: 6854—6857.
Ambler, R.P., Daniel, M., Hermoso, J., Meyer, T.E., Bartsch, R.G. and Kamen, M.D., 1979a. Nature, 278: 659—660.
Ambler, R.P., Daniel, M., Meyer, T.E., Bartsch, R.G. and Kamen, M.D., 1979b. Biochem. J., 177: 819—823.
Ambler, R.P., Meyer, T.E., Bartsch, R.G. and Kamen, M.D., 1978. Unpublished results, cited by R.P. Ambler. In: H. Matsubara and T. Yamanaka (Editors), Evolution of Protein Molecules. Japan Sci. Soc. Press/Center for Acad. Publ. Japan, Tokyo, pp. 311—322.
Ambler, R.P., Meyer, T.E. and Kamen, M.D., 1976. Proc. Natl. Acad. Sci. U.S.A., 73: 472—475.
Ambler, R.P., Meyer, T.E. and Kamen, M.D., 1979c. Nature, 278: 661—662.
Ambler, R.P., Meyer, T.E., Kamen, M.D., Schichman, S.A. and Sawyer, L., 1981b. J. Mol. Biol., 147: 351—356.

Azari, P., Glantz, M., Tsunoda, J. and Yasunobu, K.T., 1973. Unpublished results, cited by K.T. Yasunobu and M. Tanaka. Syst. Zool., 22: 570—589.
Benson, A.M., Mower, H.F. and Yasunobu, K.T., 1966. Proc. Natl. Acad. Sci. U.S.A., 55: 1532—1535.
Broda, E., 1975. The Evolution of the Bioenergetic Process. Pergamon, Oxford.
Brownlee, G.G., Cartwright, E., McShane, T. and Williamson, R., 1972. FEBS Lett., 25: 8—12.
Brownlee, G.G., Sanger, F. and Barrell, B.G., 1968. J. Mol. Biol., 34: 379—412.
Bruschi, M., 1979. Biochem. Biophys. Res. Commun., 91: 623—628.
Buchanan, R.E. and Gibbons, N.E. (Editors), 1974. Bergey's Manual of Determinative Bacteriology. 8th Edn., Williams and Wilkins, Baltimore, MD.
Corry, M.J., Payne, P.I. and Dyer, T.A., 1974. FEBS Lett., 46: 63—66.
Darlix, J.-L. and Rochaix, J.-D., 1981. Nucleic Acids Res., 9: 1291—1299.
Dayhoff, M.O. (Editor), 1972. Atlas of Protein Sequence and Structure. Vol. 5, Natl. Biomed. Res. Found., Washington, DC.
Dayhoff, M.O. (Editor), 1973. Atlas of Protein Sequence and Structure. Vol. 5, Suppl. 1, Natl. Biomed. Res. Found., Washington, DC.
Dayhoff, M.O. (Editor), 1976. Atlas of Protein Sequence and Structure. Vol. 5, Suppl. 2, Natl. Biomed. Res. Found., Washington, DC.
Dayhoff, M.O. (Editor), 1979. Atlas of Protein Sequence and Structure. Vol. 5, Suppl. 3, Natl. Biomed. Res. Found., Washington, DC.
Dayhoff, M.O., Chen, H.R., Hunt, L.T., Barker, W.C., Yeh, L.-S., George, D.G. and Orcutt, B.C., 1982a. Nucleic Acid Sequence Database. Natl. Biomed. Res. Found., Washington, DC.
Dayhoff, M.O., Hunt, L.T., Barker, W.C., Orcutt, B.C., Yeh, L.-S., Chen, H.R., George, D.G., Blomquist, M.C., Fredrickson, J.A. and Johnson, G.C., 1982b. Protein Sequence Database. Natl. Biomed. Res. Found., Washington, DC.
Dayhoff, M.O., Schwartz, R.M. and Orcutt, B.C., 1979. In: M.O. Dayhoff (Editor), Atlas of Protein Sequence and Structure. Vol. 5, Suppl. 3, Natl. Biomed. Res. Found., Washington, DC, pp. 345—352.
Dubuy, B. and Weissman, S.M., 1971. J. Biol. Chem., 246: 747—761.
Dus, K., Sletten, K. and Kamen, M.D., 1968. J. Biol. Chem., 243: 5507—5518.
Forget, B.G. and Weissman, S.M., 1967. Science, 158: 1695—1699.
Gerlach, W.L. and Dyer, T.A., 1980. Nucleic Acids Res., 8: 4851—4865.
Hall, L.M.C. and Maden, B.E.H., 1980. Nucleic Acids Res., 8: 5993—6005.
Hase, T., Matsubara, H. and Evans, M.C.W., 1977. J. Biochem., 81: 1745—1749.
Hase, T., Ohmiya, N., Matsubara, H., Mullinger, R.N., Rao, K.K. and Hall, D.O., 1976. Biochem. J., 159: 55—63.
Hase, T., Wakabayashi, S., Matsubara, H., Imai, T., Matsumoto, T. and Tobari, J., 1979. FEBS Lett., 103: 224—228.
Hase, T., Wakabayashi, S., Matsubara, H., Ohmori, D. and Suzuki, K., 1978. FEBS Lett., 91: 315—319.
Hermoso, J., Pettigrew, G.W. and Kamen, M.D., 1978. Unpublished results, cited by R.P. Ambler. In: H. Matsubara and T. Yamanaka (Editors), Evolution of Protein Molecules. Japan. Sci. Soc. Press/Center for Acad. Publ. Japan, Tokyo, pp. 311—322.
Hill, G.C. and Pettigrew, G.W., 1975. Eur. J. Biochem., 57: 265—271.
Hinnebusch, A.G., Klotz, L.C., Blanken, R.L. and Loeblich, A.R., III, 1981. J. Mol. Evol., 17: 334—347.
Hori, H., Osawa, S. and Iwabuchi, M., 1980a. Nucleic Acids Res., 8: 5535—5539.
Hori, H., Osawa, S., Murao, K. and Ishikura, H., 1980b. Nucleic Acids Res., 8: 5423—5426.
Jagadeeswaran, P. and Cherayil, J.D., 1978. Proc. Indian Acad. Sci., 87: 213—224.
Jordan, B.R., Latil-Damotte, M. and Jourdan, R., 1980. Nucleic Acids Res., 8: 3565—3573.

Komiya, H., Miyazaki, M. and Takemura, S., 1981. J. Biochem., 89: 1663—1666.
Komiya, H., Shimizu, N., Kawakami, M. and Takemura, S., 1980. J. Biochem., 88: 1449—1456.
Kudo, R.R., 1971. Protozoology. 5th Edn., C.C. Thomas, Springfield, IL.
Laycock, M.V., 1972. Can. J. Biochem., 50: 1311—1325.
Laycock, M.V., 1975. Biochem. J., 149: 271—279.
Lu, A.-L., Steege, D.A. and Stafford, D.W., 1980. Nucleic Acids Res., 8: 1839—1853.
Luehrsen, K.R. and Fox, G.E., 1981. Proc. Natl. Acad. Sci. U.S.A., 78: 2150—2154.
Luehrsen, K.R., Fox, G.E., Kilpatrick, M.W., Walker, R.T., Domdey, H., Krupp, G. and Gross, H.J., 1981a. Nucleic Acids Res., 9: 965—970.
Luehrsen, K.R., Fox, G.E. and Woese, C.R., 1980. Curr. Microbiol., 4: 123—126.
Luehrsen, K.R., Nicholson, D.E., Eubanks, D.C. and Fox, G.E., 1981b. Nature, 293: 755—756.
MacKay, R.M. and Doolittle, W.F., 1981. Nucleic Acids Res., 9: 3321—3334.
MacKay, R.M., Gray, M.W. and Doolittle, W.F., 1980a. Nucleic Acids Res., 8: 4911—4917.
MacKay, R.M., Spencer, D.F., Doolittle, W.F. and Gary, M.W., 1980b. Eur. J. Biochem., 112: 561—576.
Margulis, L., 1981. Symbiosis in Cell Evolution. W.H. Freeman, San Francisco.
Marotta, C.A., Varricchio, F., Smith, I., Weissman, S.M., Sogin, M.L. and Pace, N.R., 1976. J. Biol. Chem., 251: 3122—3127.
Mashkova, T.D., Serenkova, T.I., Mazo, A.M., Avdonina, T.A., Timofeyeva, M.Y. and Kisselev, L.L., 1981. Nucleic Acids Res., 9: 2141—2151.
Maxam, A.M. and Gilbert, W., 1977. Proc. Natl. Acad. Sci. U.S.A., 74: 560—574.
Meyer, T.E., Ambler, R.P., Bartsch, R.G. and Kamen, M.D., 1975. J. Biol. Chem., 250: 8416—8421.
Nazar, R.N. and Roy, K.L., 1978. J. Biol. Chem., 253: 395—399.
Nazar, R.N., Matheson, A.T. and Bellemare, G., 1978. J. Biol. Chem., 253: 5464—5469.
Nazar, R.N., Sitz, T.O. and Busch, H.J., 1975. Biol. Chem., 250: 8591—8597.
Pavlakis, G.N., Jordan, B.R., Wurst, R.M. and Vournakis, J.N., 1979. Nucleic Acids Res., 7: 2213—2238.
Payne, P.I. and Dyer, T.A., 1976. Eur. J. Biochem., 71: 33—38.
Payne, P.I., Corry, M.J. and Dyer, T.A., 1973. Biochem. J., 135: 845—851.
Pettigrew, G.W., 1974. Biochem. J., 139: 449—459.
Pettigrew, G.W., Leaver, J.L., Meyer, T.E. and Ryle, A.P., 1975. Biochem. J., 147: 291—302.
Piechulla, B., Hahn, U., McLaughlin, L.W. and Kuntzel, H., 1981. Nucleic Acids Res., 9: 1445—1450.
Pribula, C.D., Fox, G.E. and Woese, C.R., 1976. FEBS Lett., 64: 350—352.
Raff, R.A. and Mahler, H.R., 1972. Science, 177: 575—582.
Rall, S.C., Bolinger, R.E. and Cole, R.D., 1969. Biochemistry, 8: 2486—2496.
Raue, H.A., Heerschap, A. and Planta, R.J., 1976. Eur. J. Biochem., 68: 169—176.
Raue, H.A., Stoof, T.J. and Planta, R.J., 1975. Eur J. Biochem., 59: 35—42.
Rubin, G.M., 1973. J. Biol. Chem., 248: 3860—3875.
Sanger, F., Nicklen, S. and Coulson, A.R., 1977. Proc. Natl. Acad. Sci. U.S.A., 74: 5463—5467.
Sankoff, D., Cedergren, R.J. and McKay, W., 1982. Nucleic Acids Res., 10: 421—431.
Schidlowski, M., 1979. Origins Life, 9: 299—311.
Schopf, J.W. and Oehler, D.Z., 1976. Science, 193: 47—49.
Schwartz, R.M. and Dayhoff, M.O., 1978. Science, 199: 395—403.
Schwartz, R.M. and Dayhoff, M.O., 1979. In: M.O. Dayhoff (Editor), Atlas of Protein Sequence and Structure. Vol. 5, Suppl. 3, Natl. Biomed. Res. Found., Washington, DC, p. 31.

Schwartz, R.M. and Dayhoff, M.O., 1981. Ann. N.Y. Acad. Sci., 361: 260—272.
Simoncsits, A., 1980. Nucleic Acids Res., 8: 4111—4124.
Spencer, D.F., Bonen, L. and Gray, M.W., 1981. Biochemistry, 20: 4022—4029.
Stahl, D.A., Luehrsen, K.R., Woese, C.R. and Pace, N.R., 1981. Nucleic Acids Res., 9: 6129—6137.
Takaiwa, F. and Sugiura, M., 1980. Mol. Gen. Genet., 180: 1—4.
Tanaka, M., Haniu, M., Matsueda, G., Yasunobu, K.T., Himes, R.H., Akagi, J.M., Barnes, E.M. and Devanathan, T., 1971. J. Biol. Chem., 246: 3953—3960.
Tanaka, M., Haniu, M., Yasunobu, K.T., Evans, M.C.W. and Rao, K.K., 1974. Biochemistry, 13: 2953—2959.
Tanaka, M., Haniu, M., Yasunobu, K.T., Evans, M.C.W. and Rao, K.K., 1975. Biochemistry, 14: 1938—1943.
Tanaka, M., Nakashima, T., Benson, A.M., Mower, H.F. and Yasunobu, K.T., 1966. Biochemistry, 5: 1666—1680.
Tanaka, Y., Dyer, T.A. and Brownlee, G.G., 1980. Nucleic Acids Res., 8: 1259—1272.
Tarr, G.E. and Fitch, W.M., 1976. Biochem. J., 159: 193—199.
Timkovich, R., Dickerson, R.E. and Margoliash, E., 1976. J. Biol. Chem., 251: 2197—2206.
Tschudi, C. and Pirrotta, V., 1980. Nucleic Acids Res., 8: 441—451.
Tsunoda, J.N., Yasunobu, K.T. and Whiteley, H.R., 1968. J. Biol. Chem., 243: 6262—6272.
Uzzell, T. and Spolsky, C., 1974. Am. Sci., 62: 334—343.
Valenzuela, P., Bell, G.I., Venegas, A., Sewell, E.T., Masiarz, F.R., DeGennaro, L.J., Weinberg, F. and Rutter, W.J., 1977. J. Biol. Chem., 252: 8126—8135.
Van Beeumen, J., Ambler, R.P., Meyer, T.E., Kamen, M.D., Olson, J.M. and Shaw, E.K., 1976. Biochem. J., 159: 757—774.
Wildeman, A.G. and Nazar, R.N., 1981. J. Biol. Chem., 256: 5675—5682.
Woese, C.R., Luehrsen, K.R., Pribula, C.D. and Fox, G.E., 1976. J. Mol. Evol., 8: 143—153.

EVOLUTION OF PHOTOAUTOTROPHY AND EARLY ATMOSPHERIC OXYGEN LEVELS

MANFRED SCHIDLOWSKI

Max-Planck-Institut für Chemie, Saarstrasse 23, D-6500 Mainz (West Germany)

ABSTRACT

Schidlowski, M., 1983. Evolution of photoautotrophy and early atmospheric oxygen levels. Precambrian Res., 20: 319—335.

Current photochemical models suggest that oxygen levels in the prebiological atmosphere were extremely low, most probably remaining in the range 10^{-8}—10^{-14} PAL (present atmospheric level). It is, therefore, reasonable to assume that only life processes were able to overwhelm these minor O_2-pressures, with free oxygen resulting from the reduction of carbon dioxide to the carbohydrate level during photoautotrophic carbon fixation using water as an electron donor ($2H_2O^* + CO_2 \xrightarrow{h\nu} CH_2O + H_2O + O_2^*$). It is by now well established that reduced (organic) carbon is a common constituent of sedimentary rocks from the very start of the geological record 3.8 Ga ago. Both direct assays and inferences derived from a carbon isotope mass balance suggest that the C_{org}-content of Archaean sediments was not basically different from that of geologically younger rocks. This poses the problem of the existence 3.5 Ga ago of an oxidation equivalent of such a formidable ancient C_{org}-reservoir which, depending on the model adopted for the growth of the sedimentary mass through time, might have amounted to between ~ 20 and ~ 100% of the present one. Low atmospheric oxygen pressures in the Early Precambrian that are inferred from retarded oxidation reactions, notably in the ancient continental weathering cycle, are likely, therefore, to indicate extremely rapid processes of oxygen consumption in other parts of the system (e.g., hydrosphere) rather than the general absence of photosynthetic oxidation equivalents during this time.

INTRODUCTION

There is no doubt that the appearance of life on Earth had a paramount modulating effect on the terrestrial environment and, in particular, on the reactions proceeding at the interface between atmosphere, hydrosphere and lithosphere, which initiate chemical transformations in the exogenic cycle. Primarily, this effect derives from the accumulation of negative entropy by living systems which forces a thermodynamic gradient upon terrestrial near-surface environments, most obviously in the form of a pronounced redox imbalance. This imbalance results from the reduction of primary oxidized carbon compounds (CO_2, HCO_3^-) to the carbohydrate

level during photosynthetic and chemosynthetic carbon fixation. These processes evolve large quantities of oxidized species such as O_2, SO_4^{2-} and S (depending on whether H_2O or H_2S is being used as a reductant). The redox gradient thus established is, in turn, the driving force for a number of environmentally relevant geochemical reactions. In fact, the geochemical cycles of carbon, sulfur and oxygen appear to be largely governed by the terrestrial biota since almost from the start of the geological record.

For gauging the magnitude of any biologically induced redox perturbance, information on the "base level" oxidation state of the prebiological environment is necessary. This statement addresses, in essence, the partial pressure of oxygen in the Earth's ancestral atmosphere. It is by now well recognized that, prior to the advent of photosynthesis, the principal abiotic source of molecular oxygen would have been photodissociation of water vapour by solar UV radiation with subsequent escape of hydrogen. Recently calculated O_2-density profiles for such an atmosphere, based on a one-dimensional photochemical model that utilizes assumed values for other atmospheric constituents and current estimates for potential oxygen sinks (Kasting et al., 1979; Kasting and Walker, 1981), predict negligible tropospheric oxygen pressures in the order of 10^{-12}—10^{-14} PAL (present atmospheric level). With the escape rate of hydrogen limited by upward transport rather than by the rate of photodissociation, these values are strongly dependent on the H_2O mixing ratio in the stratosphere (presently 3.8 ppm) which is, in turn, controlled by the temperature of the tropopause "cold trap". Allowing for uncertainties in the limiting flux due to potential changes in tropopause temperature, Carver (1981) has argued for the possibility of substantially higher stationary abiotic P_{O_2}-levels (between 10^{-2} and 10^{-3} PAL). Irrespective of the high degree of model-dependence of the figures hitherto proposed it is, however, safe to say that oxygen partial pressures due to inorganic photolysis of water vapour are generally low, hardly exceeding maximum values of 10^{-2}—10^{-3} PAL and most probably staying many orders of magnitude below this range. The highest atmospheric oxygen partial pressure hitherto encountered on a lifeless planet is that observed on Mars (0.13%, Owen et al., 1977). However, this planet represents an exceptional case, having no appreciable contemporary outgassing (that might yield reduced volatiles to scavenge O_2) and no liquid water to enhance surficial oxidation processes.

Accordingly, it may reasonably be assumed that only biological processes were able to overwhelm the small oxygen levels sustained on the inorganic Earth, thus giving rise to the great redox gradient between the atmosphere and lithosphere typical of the contemporary environment. This oxygen ultimately stems from the reduction of carbon dioxide to carbohydrates during biological (photoautotrophic) carbon fixation using water as an electron donor, i.e.,

$$2\,H_2O^* + CO_2 \xrightarrow{h\nu} CH_2O + H_2O + O_2^*$$

Since the most conspicuous impact of life on the terrestrial atmosphere derives from this process, it is appropriate to briefly review the evidence bearing on the antiquity of photosynthetic carbon fixation in the widest sense.

ANTIQUITY OF AUTOTROPHIC CARBON FIXATION

Based on several independent lines of evidence it may be fairly confidently stated that organisms capable of autotrophic carbon fixation must have appeared very early in the Earth's history. The most convincing palaeontological support for this assumption comes from the widespread occurrence during the Archaean of laminated biosedimentary structures (stromatolites) which are generally attributed to the matting behaviour of prokaryotes (mostly photosynthetic bacteria including O_2-releasing cyanobacteria). Stromatolitic microbial ecosystems make their appearance in rocks as old as ~ 3.5 Ga (Dunlop et al., 1978; Lowe, 1980; Walter et al., 1980; Orpen and Wilson, 1981) and this age gives a temporal boundary for the unmetamorphosed sedimentary record. Though these most ancient stromatolites constitute evidence for the presence of prokaryotic ecosystems in the widest sense, rather than specifically for photosynthetic prokaryotes, there are indications that the principal Archaean mat-builders were capable of photic responses in general and of photoautotrophy in particular (Walter, 1983). In any case, Archaean stromatolites do not seem to differ significantly from geologically younger ones. Hence, whatever processes are invoked for the origin of the latter should also apply to the formation of the former. In view of the occurrence of such biosedimentary structures as far back as 3.5 Ga, it is a reasonable conjecture that the ancestral lines of the prokaryotic mat-builders should extend to Isua times (and possibly beyond).

More debatable than the biogenicity of the oldest stromatolites are the morphologies of presumed microfossils of the same age (Dunlop et al., 1978), or the exact stratigraphic relationships within the Archaean sequence of their respective host-rocks (Awramik et al., 1983). Likewise, putative microfossils described by Pflug and Jaeschke-Boyer (1979) from the still older (~ 3.8 Ga) meta-sediments from Isua, West Greenland are objects of a current controversy (Roedder, 1981; Bridgwater et al., 1981). However, with stromatolite-type microbial ecosystems unquestionably extant during Early Archaean times, even the faint evidence of coeval microfossils cannot be readily dismissed and certainly calls for further scrutiny.

The palaeontological evidence is fully supported by the isotope age curve for sedimentary carbon (Fig. 1) which displays a fairly constant average fractionation between carbonate and organic carbon (kerogen) through time. This can be best explained as a signature of biological (photoautotrophic) carbon fixation. Since the prime responsibility for the characteristic enrichment of ^{12}C observed in ancient kerogens rests with the process

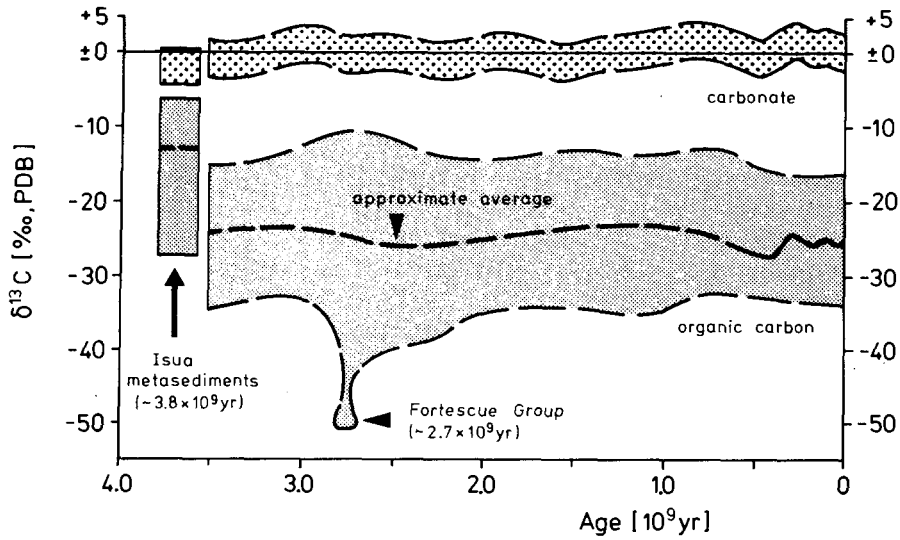

Fig. 1. Isotopic composition of organic carbon and carbonate carbon as a function of geological time. The relatively small standard deviations for carbonate ($\delta^{13}C_{carb}$ = +0.4 ± 2.6‰; cf. Schidlowski et al., 1975; Veizer et al., 1980) are in marked contrast with the wide scatter of $\delta^{13}C_{org}$ values, the bulk of which seem to fall into the range -27 ± 7‰ (the envelope shown for organic carbon covers the data presented in detail by Schidlowski et al., 1983). The shifts displayed by the Isua rocks can be best explained by the amphibolite-grade reconstitution of this suite, entailing an isotopic re-equilibration of both carbon species. Occasional negative spikes imposed on the $\delta^{13}C_{org}$ record (e.g., Fortescue Group) suggest the involvement of methanotrophic pathways in the formation of the respective kerogen precursors.

that gave rise to the biological precursor materials, it will be hard to escape the conclusion that the entire organic carbon record gives a remarkably consistent isotopic signal of biological activity on Earth from 3.5 Ga ago at least. The mainstream of the scatter band for the $\delta^{13}C_{org}$ values is, in fact, the geochemical manifestation of the activities of the key enzyme of the Calvin cycle (ribulose bisphosphate carboxylase), the pathway which is responsible for the bulk of the carbon transfer from the inorganic to the organic world. Since a good case can be made for the isotope shifts displayed by both carbon species in the Isua sediments being due to the amphibolite-grade reconstitution of these rocks, the primary biological signature has, in all probability, originally extended to 3.8 Ga ago (Schidlowski et al., 1983).

It is consistent with these conclusions that variations in the reduced carbon content of Precambrian sediments (including the Isua suite) lie well within the range of geologically younger rocks, approximating mean values between 0.2 and 0.7% (cf. Dungworth and Schwartz, 1974; Moore et al., 1974; Nagy et al., 1974; Reimer et al., 1979; Cameron and Garrels, 1980; Schidlowski, 1982). Such findings are a necessary corollary of the constancy

of the isotope age functions since the $^{13}C/^{12}C$ ratios of both sedimentary carbon species are coupled to their relative proportions by an isotope mass balance. Moreover, the kerogen constituents of Precambrian rocks are likely to constitute, per se, evidence of biological carbon fixation since, in fact, no other process has as yet been shown to introduce sizable quantities of reduced carbon into sediments. (Production of kerogenous substances by photochemical reactions in CH_4-rich atmospheres remains a theoretical possibility, but an actual involvement in the formation of ancient kerogens has never been demonstrated.) In view of the findings by Cohen et al. (1980) that present-day communities of benthic prokaryotes are able to sustain very high rates of primary production in the order of 8 g C m^{-2} day^{-1}, the surprisingly "modern" C_{org} content of Archaean and Early Proterozoic rocks does not seem particularly impressive. It may reasonably be assumed that the early Earth was populated by prokaryotic ecosystems of both the benthic and planktonic type whose sizable rates of productivity suggest that photosynthesis may have gained little in quantitative importance during subsequent evolution. (With no direct evidence available for the existence of planktonic life in the Archaean, parts of the above statement may seem contentious. However, I would be hesitant to view the benthic environment as the cradle of early life rather than as bridgehead in the eventual conquest of the continental surface. This would imply the contemporaneous existence of planktonic communities whenever we encounter benthic ones. Naturally, much more evidence will be needed to release these arguments from the theoretical twilight.)

Therefore, a reasonable case can be made that autotrophy — and notably photoautotrophy as quantitatively the most important process of biological carbon fixation — was achieved very early in the evolution of life on Earth, being extant as both a biochemical process and as a geochemical agent since 3.5 Ga (if not 3.8 Ga) ago at least.

ARCHAEAN PHOTOAUTOTROPHY AND PHOTOSYNTHETIC OXYGEN

Once photosynthesis was in operation, the stage was set for overriding the small oxygen levels of the prebiological atmosphere. Accordingly, the occurrence of biologically derived reduced carbon in the Earth's oldest sediments has crucial implications for the redox state of the ancient environment, since these kerogenous materials (and their metamorphosed derivatives) constitute proof of a contemporaneous release of photosynthetic oxidation products in compliance with the stoichiometry of the photosynthesis reaction. The only debatable point in this context is whether these oxidation products were molecules of free oxygen (as in the case of water-splitting photosynthesis), or other oxidized species, such as evolved by the different forms of bacterial photosynthesis relying on reductants like H_2S or H_2 (cf. Table I). The identification of the specific oxidation equivalent remains a major problem since any differentiation between or-

ganic carbon derived from H_2O-splitting, or from bacterial, photosynthesis has to be based on independent evidence. Hence, the "modern" C_{org} content of ancient sediments, as such, only testifies to the contemporaneous operation of the photosynthesis reaction in its most general version according to which 4 electrons are traded by a reductant per CH_2O (carbohydrate) unit synthesized, with the donor itself emerging in oxidized form from the reaction (Table I).

TABLE I

Biologically mediated reduction of carbon dioxide to the carbohydrate level (CH_2O) by the most common inorganic reducing agents. Reaction 1 would proceed of its own accord (chemosynthesis), while 2—4 have to be powered by light energy (photosynthesis). Note that the energy demand of oxygen-releasing (water-splitting) photosynthesis operated by cyanobacteria and green plants (4) is much higher than in bacterial photosynthesis (2 and 3). Standard free energy changes recalculated from Broda (1975, p.75).

$2\ H_2 + CO_2 \longrightarrow CH_2O + H_2O$	$\Delta G'_0 = -4.2$ kJ	(1)
$0.5\ H_2S + H_2O + CO_2 \xrightarrow{h\nu} CH_2O + H^+ + 0.5\ SO_4^{2-}$	$\Delta G'_0 = +117.2$ kJ	(2)
$2\ H_2S + CO_2 \xrightarrow{h\nu} CH_2O + H_2O + 2\ S$	$\Delta G'_0 = +50.2$ kJ	(3)
$2\ H_2O^* + CO_2 \xrightarrow{h\nu} CH_2O + H_2O + O_2^*$	$\Delta G'_0 = +470.7$ kJ	(4)

In any case, it is safe to assume that bacterial photosynthesis has preceded the oxygen-releasing (water-splitting) process in the evolution of photoautotrophy. Therefore, oxidation products other than free oxygen, notably sulfate, are likely to have been released in much larger quantities in the Archaean than during later times. This might have accounted, among other causes, for a stabilization of atmospheric oxygen pressures at the low levels generally envisioned for the Early Precambrian. It is consistent with the postulated major role of bacterial photosynthesis during the Archaean that there is ample evidence of sulfate evaporites in sediments as old as 3.5 Ga (cf. Heinrichs and Reimer, 1977; Lowe and Knauth, 1977; Barley et al., 1979; and others). This would constitute proof that sulfate was sufficiently abundant in the ancient oceans to allow the formation of evaporite deposits in suitable sedimentary environments. Since SO_4^{2-} may form directly as a result of photosynthetic oxidation of reduced sulfur compounds (Table I, No. 3), free oxygen was not necessarily a prerequisite for the accumulation of the sulfate burden of the Archaean seas. Hence, sulfate as a mild oxidant could have appeared in the environment long before the buildup of appreciable oxygen levels in the atmosphere (cf. Broda, 1975, p. 78, Schidlowski, 1979). It should be noted, furthermore, that H_2S- and H_2-scavenging assimilatory reactions (Table I, Nos. 1—3) which preceded oxygenic photosynthesis had exercised a first modulating effect on the ancient environment

by eliminating some of the most conspicuous reducing gaseous species from the ancestral atmosphere.

It has been argued that, prior to the utilization of water as an electron donor for the process of photoautotrophic carbon fixation, proliferation of life was probably limited by a shortage of available reducing power (Broda, 1975, p. 78; Schidlowski, 1978). In any case, the fact that life ultimately resorted to the water-splitting reaction (Table I, No. 4) characterized by an energy requirement much in excess of the other assimilatory pathways seems to be sufficient proof that there was a strong incentive for overcoming this energy barrier by the introduction of an additional light reaction (photosystem II). There is no doubt that the utilization of water for the reduction of CO_2 was a necessary prerequisite for any major increase of biomass on Earth, as it allowed the exploitation of a ubiquitous and virtually inexhaustible source of reducing power. With this reductant, life was apt to proliferate until the encounter of other limits, notably the exhaustion of critical nutrients such as phosphorus.

EVOLUTION OF PHOTOSYNTHETIC OXYGEN AND ITS OXIDATION EQUIVALENTS THROUGH TIME

Utilizing the stoichiometry of the unified version of the photosynthesis reaction, i.e.,

$$2\,H_2X + CO_2 \xrightarrow{h\nu} CH_2O + H_2O + 2\,X,$$

the accumulation of photosynthetic oxidation products (X) may be quantified through time by tracing the growth of the sedimentary reservoir of organic carbon over the Earth's history. This reservoir stores the bulk of all biologically-derived carbon in the form of kerogen and related substances. With an average C_{org} content of sediments between 0.5 and 0.6% (Ronov, 1980) and a stationary sedimentary mass of $\sim 2.4 \times 10^{24}$ g (Garrels and Lerman, 1977), the C_{org} reservoir of the present sedimentary shell is in the order of 10^{22} g which is $\sim 10^4$ times in excess of the carbon content of the contemporary standing biomass. Therefore, if the stationary reservoir of sedimentary or- the C_{org} reservoir of the present sedimentary shell is in the order of 10^{22} g which is $\sim 10^4$ times in excess of the carbon content of the contemporary standing biomass. Therefore, if the stationary reservoir of sedimentary organic carbon could be traced through geological time, the stoichiometric equivalent of photosynthetic oxidation products might be readily calculated. This would not necessarily give the amount of free oxygen evolved, since oxygen is only one of several oxidation products released as a by-product of biological carbon fixation. However, by introducing additional constraints, tentative limits may also be defined for the accumulation of photosynthetic oxygen.

Utilizing (1) a carbon isotope mass balance and (2) current models for the accumulation of the sedimentary mass as a function of time, a reasonable approximation may be derived for the growth of the sedimentary C_{org}

reservoir through time. As for (1), an interpretation of the data base summarized in Fig. 1 in terms of an isotope mass balance (see Schidlowski et al., 1975; Schidlowski, 1982), would lead to the conclusion that the relative proportions of both sedimentary carbon species (C_{org} and C_{carb}) did not change very much through time, with organic carbon having always accounted for ~20% of total sedimentary carbon from 3.5 Ga ago (or even 3.8 Ga ago, if it is accepted that the values for Isua are reset by metamorphism). Since, according to the "principle of geochemical uniformitarianism" (Garrels and Mackenzie, 1971, p. 276), the total carbon content of the sedimentary shell had always been fixed at ~3%, the results of the isotope mass balance would be consistent with the observation that the average C_{org} content of sedimentary rocks is largely time-invariant (Schidlowski, 1982). Hence, the basic unknown in current attempts to assess the accumulation of the sedimentary C_{org} reservoir through time is the quantitative evolution of the stationary sedimentary mass as a whole, of which organic carbon has made up 0.5–0.6% from the very start of the record.

Since sediments are formed by the reaction of primary igneous rocks with acid volatiles discharged from the Earth's interior, it has become customary to view the increase of the sedimentary mass through time in terms of two limiting models which are based on corresponding limits for the terrestrial degassing process (cf. Garrels and Mackenzie, 1971, p. 255; Li, 1972). These are known as the constant mass model and the linear accumulation model (Fig. 2). In the case of the former, a virtually modern-size sedimentary mass had been formed, as a result of early catastrophic degassing, at the very beginning of the Earth's history, and has subsequently persevered through time as a stationary quantity irrespective of eventual additions and subtractions. The second model is characterized by a linear growth of the sedimentary mass based, in turn, on a linear supply of the sediment-forming degassing products. According to this model, the sedimentary mass would have approached its present size in the recent geological past, with the last 10% added during the Phanerozoic.

These models clearly represent extremes, and there is little doubt that the actual growth curve of the Earth's sedimentary shell has followed a path somewhere between the constant mass and linear accumulation models. In fact, a good case can be made for a terrestrial degassing process characterized by exponentially decreasing degassing rates (cf. Li, 1972). Therefore, a probable growth curve may be assumed which is functionally similar to that defined by the asymptotic accumulation model (Fig. 2). Here, the bulk of the sedimentary mass (~80%) would have formed during the first 1.5 Ga of the Earth's history, the remainder being subsequently added in the form of progressively smaller increments, with the growth curve asymptotically approaching the value for the present mass.

The implications for the accumulation of the sedimentary C_{org} reservoir seem rather straightforward. Irrespective of the particular model adopted, it is obvious that the stationary sedimentary mass could not have been <20%

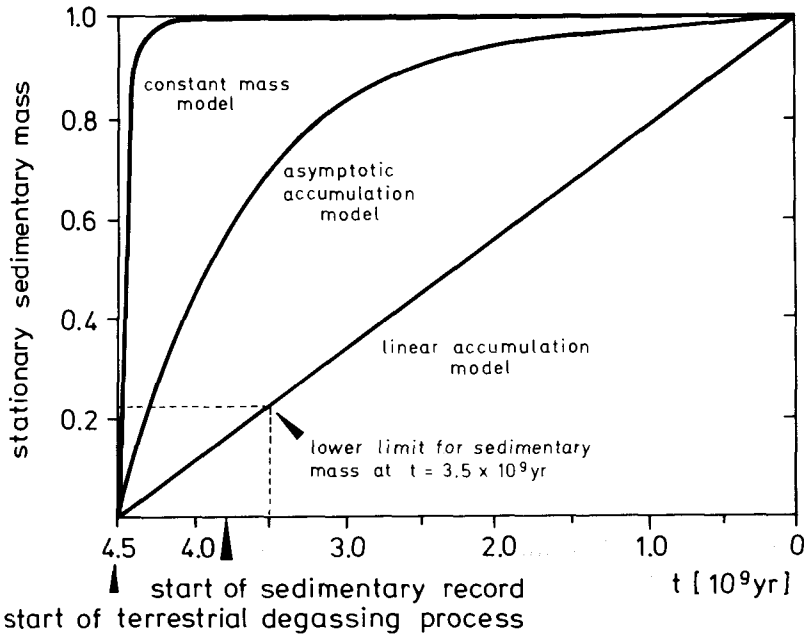

Fig. 2. Graphic synopsis of current models for the evolution of the stationary sedimentary mass as a function of the terrestrial degassing process (present mass = 1). Since the maximum mass is determined in each case by the quantity of acid volatiles available for sediment-forming processes, early catastrophic degassing and linear degassing define limits for the increase of the sedimentary shell through time, and are reflected by the constant mass and linear accumulation models, respectively. The actual growth curve may be expected to lie between these limits (asymptotic accumulation model), and is probably closer to the constant mass than to the linear model. The asymptotic function depicted here is based on a value of $1.16 \times 10^{-9}\,y^{-1}$ which is currently the best approximation for the time-averaged terrestrial degassing constant (Li, 1972).

of the present sedimentary mass as from 1 Ga after the start of the degassing process (i.e., 3.5 Ga ago on the geological time scale, cf. Fig. 2). With both mass balance calculations and direct assays indicating that a fixed percentage (0.5—0.6%) of this quantity was organic carbon, the minimum size of the sedimentary C_{org} reservoir at this time should also have been at least 20% of the present size. As the linear accumulation model only defines a lower limit, it may safely be assumed that the actual increase of the C_{org} reservoir followed the asymptotic function depicted in Fig. 2, or maybe even approached the constant mass model. Therefore, it is a reasonable conjecture that the quantity of organic carbon in the sedimentary shell has stayed approximately within the same order of magnitude ($\sim 10^{22}$ g) during the last 3.5 Ga of the Earth's history.

The storage in the Earth's early sedimentary shell of such large amounts of organic carbon would imply the contemporaneous existence of a correspondingly modern reservoir of photosynthetic oxidation products. On the other hand, the mere existence of C_{org} does not, unfortunately, allow a differentiation among the various oxidized species released by the dif-

ferent pathways of autotrophic carbon fixation. To obtain a clue to early photosynthetic oxygen, additional information is needed on the relative proportions in which the total oxidation equivalent of the ancient reservoir of organic carbon was partitioned among the main photosynthetic oxidation products.

A crucial question in this context is whether the buildup of a sedimentary C_{org} reservoir approaching the magnitude of the present one could have been achieved without photosynthetic carbon fixation resorting to the water-splitting process. As is obvious from the assimilatory reactions listed in Table I, any increase in biomass is ultimately contingent on a supply of reducing power, i.e., electrons for the reduction of carbon dioxide which are provided by a limited number of primary inorganic donors (H_2, H_2S, H_2O). Once the geochemically more rare reducing species (hydrogen and hydrogen sulfide) were approaching exhaustion, biosynthesis of organic matter had to rely principally on water. In fact, water constitutes the most abundant source of electrons available for assimilatory reactions and, as can be inferred from the successful evolution of the plant kingdom during the early history of the Earth, tapping of this reservoir for photoreduction of CO_2 was a paramount evolutionary adaption, constituting the non-plus-ultra in bioenergetic independence (Broda, 1975, p. 78).

With reductants like H_2 and H_2S far less abundant than H_2O among the Earth's primary degassing products, this may also be assumed valid for their relative concentrations in the ancient environment. The buildup of a C_{org} reservoir in the order of 10^{22} g was almost certainly contingent on the utilization of H_2O as the principal electron donor for the primary production of organic matter, because only the use of water as a source of electrons could have met the quantitative requirements for the large-scale production and accumulation of the living and fossil biomass (cf. Schidlowski, 1978). If such reasoning is correct, the water-splitting and oxygen-releasing reaction, as operated by cyanobacteria, eukaryotic algae and green plants, must have been an early achievement in the evolution of photoautotrophy. Naturally, its reliance on current theoretical concepts for the growth of the sedimentary mass (cf. Fig. 2) renders this argument model-dependent, but various lines of evidence seem to point in the same direction. Inter alia, the stromatolitic structures preserved in the early sedimentary record may be attributed to cyanobacteria (which were the first to superimpose "photosystem II" on the first light reaction operated by primitive prokaryotes), and Cloud (1976) has interpreted the very existence of the Isua banded iron-formation as presumptive evidence of cyanobacterial (oxygen-releasing) photosynthesis.

IMPLICATIONS FOR THE TERRESTRIAL OXYGEN CYCLE AND THE RISE OF ATMOSPHERIC OXYGEN

It may be concluded from the foregoing considerations that a very large reservoir of photosynthetic oxidation products including molecular oxygen

(equivalent to the reservoir of sedimentary organic carbon) might have existed from about the start of the sedimentary record 3.8 Ga ago. Since, of all primary carbon-fixing reactions listed in Table I, the water-splitting process (as the top achievement of phototrophic life) has brought about the oxygenation of the atmosphere, it is ultimately this process that was responsible for the most important impact of life on the terrestrial environment.

With organic carbon accounting for ~0.5—0.6% of the present sedimentary mass of 2.4×10^{24} g, a figure between 1.2 and 1.4×10^{22} g can be derived for the amount of C_{org} stored in the sedimentary shell. Accepting the lower limit and expressing the corresponding oxidation equivalents in terms of free oxygen, a figure of 3.2×10^{22} g is obtained for the total budget of photosynthetic oxygen. For comparison, the net gain of oxygen due to "Jeans escape" of hydrogen following inorganic photolysis of water vapour in the upper atmosphere amounts to $\sim 2 \times 10^{11}$ g y^{-1} (cf. Hunten and Strobel, 1974; Walker, 1978). Since the escape rate of hydrogen is ultimately controlled by upward diffusion of water vapour which is, within broad limits, independent of atmospheric background parameters, the above figure should also be basically valid for the geological past. Integration of the inorganic oxygen source over the 4.5 Ga of the Earth's history would give 9×10^{20} g O_2 which is <3% of the photosynthetic oxygen budget.

This budget is graphically represented by the column depicted in Fig. 3 in which the oxygen reservoir is subdivided into the partial reservoirs of iron-bound, sulfate-bound and free oxygen. It is obvious from this graph

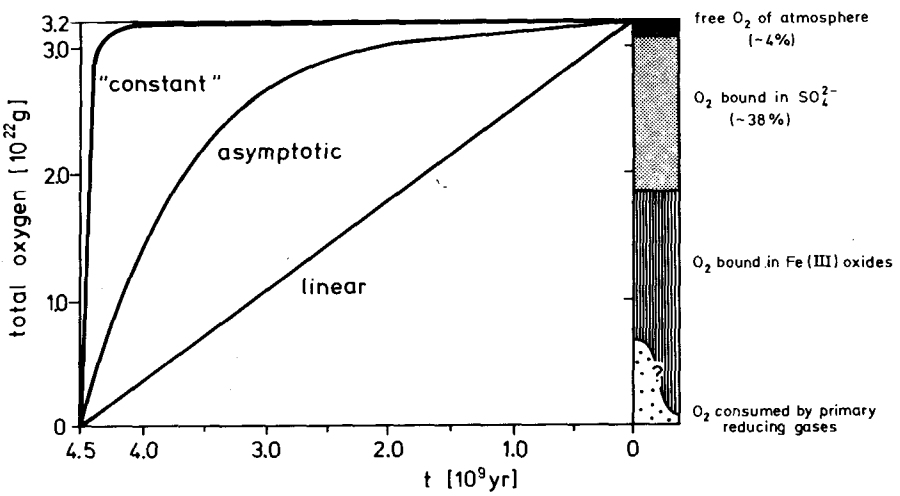

Fig. 3. Growth of the photosynthetic oxidation equivalent of organic carbon (expressed as oxygen) according to alternative models for the evolution of the sedimentary C_{org} reservoir. The 3.2×10^{22} g O_2 of the present reservoir, represented by the budget column, are the stoichiometric equivalent of 1.2×10^{22} g of organic carbon stored in the contemporary sedimentary shell. The oxygen of the atmosphere only makes up ~4% of this budget. While the fraction of sulfate-bound oxygen is amenable to independent calculation (Schidlowski et al., 1977), the iron-bound reservoir has been determined by difference. The amount of oxygen consumed in the oxidation of primary reducing gases (H_2, CH_4, NH_3, CO, etc.) remains a major source of uncertainty in this budget.

that the 1.2×10^{21} g of molecular oxygen presently residing in the atmosphere only constitute the "tip of the iceberg", accounting for just ~4% of the total. This is, inter alia, a vivid illustration of the fact that molecular oxygen is only transient in the oxygen cycle and, after an ephemeral existence in the atmosphere, it is apt to end up in the bound state as a constituent of the Earth's crust. In fact, the very existence of free oxygen is a grave infringement of equilibrium chemistry. There is, accordingly, little doubt that the atmospheric O_2 reservoir as a whole results from the failure of thermodynamics to exercise strict control over the redox balance of the atmosphere—hydrosphere— lithosphere system or, in other words, from the sluggishness of oxygen-consuming reactions.

Since the budget column of Fig. 3 represents the total oxidation equivalent of sedimentary organic carbon, its growth through time must necessarily be coupled to the evolution of the C_{org} reservoir of the crust. Hence, the potential growth curves should be replicas of current models for the accumulation of the sedimentary shell, and notably its organic carbon fraction, with functions resembling the constant mass and linear accumulation models (cf. Fig. 2) as plausible boundary conditions. If the essentials of the model for the increase of sedimentary organic carbon, as outlined in the previous section, are acceptable then the quantitative evolution of the corresponding oxidation products will follow the pathways (most probably the asymptotic one) depicted in Fig. 3 (a disturbance might be introduced only by an excessive operation of reaction (1) listed in Table I). However, a crucial reservation to be made is that this evolution must be viewed in terms of an increase of photosynthetic oxidation equivalents in the widest sense, rather than of free oxygen alone (which is but one of several oxidized species released as by-products of photosynthetic carbon fixation).

However, as pointed out earlier, it seems impossible that the accumulation in the Archaean ($t > 2.5$ Ga) of an organic carbon reservoir of almost modern magnitude could have been achieved with photosynthesis relying exclusively on the limited stock of reductants such as H_2 and H_2S. With the water-splitting reaction having almost certainly contributed to the buildup of the sizable ancient C_{org} reservoirs suggested by current models, the contemporaneous oxidation equivalents of this carbon should, of necessity, have included molecular oxygen. Accordingly, it may be expected that the ancient reservoirs of photosynthetic oxidation products, as defined by the functions of Fig. 3, have contained sizable amounts of oxygen.

Such inferences are apparently at odds with concepts envisioning a basically anoxic, though not necessarily reducing, environment on the Archaean—Early Proterozoic Earth until ~2.0—2.3 Ga ago (Cloud, 1976, 1980; Schidlowski, 1978; Walker et al., 1983; and others). Although sometimes disputed (cf. Dimroth and Kimberley, 1976), the bulk of the geological evidence from this time interval is generally believed to indicate very small atmospheric oxygen levels which, in particular, proved incapable of sustaining

oxygenic weathering conditions on the continents. This is apparently attested to by the general absence from the early record of continental red beds and by the unoxidized condition of minerals like pyrite and uraninite in ancient placer deposits (cf. Schidlowski, 1970, 1981; Grandstaff, 1980). Moreover, anoxygenic weathering on the continents would be a necessary prerequisite for the solubilization of the very large quantities of iron assumed to have finally ended up in Precambrian banded iron-formation (MacGregor, 1927; Cloud, 1973). However, the formation of these sedimentary iron deposits must have hinged on an effective oxygen supply from a marine source capable of maintaining large turnover rates in this particular compartment. Naturally, such division of the cycle (contrasting an oxygenated hydrosphere with a basically anoxic atmosphere) could be stabilized only if the oxygen generated in the marine environment was instantaneously absorbed by an effective acceptor that allowed negligible quantities of the element to escape into the atmosphere.

It is obvious from the budget column depicted in Fig. 3 that storage of free oxygen in the atmosphere is a minor facet of the overall accumulation of photosynthetic oxidation equivalents. After temporary residence in the atmospheric reservoir, which is short in terms of the geological time scale (~ 4 Ma, cf. Holland, 1978, p. 284), this oxygen will be tied up by reducing constituents of the lithosphere (C_{org}, sulfide, bivalent iron), with the resulting sulfate and iron oxides eventually piling up in the sedimentary shell. Although primarily generated by photosynthesis, the long-term source of atmospheric oxygen is the burial of organic matter in sediments, which follows cogently from a comparison of the relative sizes of the reservoirs involved (the stoichiometric O_2 equivalent of the $\sim 10^{18}$ g C_{org} fixed in the contemporary biomass only accounts for a small percentage of the present atmospheric reservoir of 1.2×10^{21} g O_2).

The atmospheric oxygen reservoir is principally stabilized by the condition for steady state

$$Q\,(M) - S(M) = O \qquad (1)$$

where Q = source, S = sink and M = amount of O_2 present in the reservoir. The source ($Q(M)$) and sink ($S(M)$) functions indicate a functional dependence of both Q and S on M (i.e., the higher the partial pressure of O_2 (M), the lower is the burial rate of C_{org} (determining Q) and the higher the oxidation rate (S) responsible for the removal of free oxygen from the reservoir). In the contemporary exogenic cycle, sources and sinks of oxygen are apparently balanced at the present reservoir size (M) of 1.2×10^{21} g.

It is not beyond the imagination to envisage modes of operation for the combined exogenic cycles of C, O, Fe and S (which are coupled by geochemically important redox reactions) in which the amount of oxygen in the molecular reservoir is distinctly different from the present level due to changes in Q or S (or both). Notably, with a set of very effective oxygen-consuming reactions, modern turnover rates in the oxygen cycle might be

sustained with only trace amounts of free oxygen around, since the equilibrium concentration of O_2 in the free reservoir is determined by kinetics rather than by thermodynamics. In principle, the 4% of the total O_2 budget currently residing in the atmosphere (cf. Fig. 3) could be readily eliminated by abundant carriers of reducing power present in both the environment and the accessible parts of the lithosphere, if it were not for a kinetic lag in the geochemically relevant O_2 consuming reactions dominating the present cycle.

It has been always tempting to view the deposition of sedimentary banded iron-formation (BIF) characteristic of Archaean and Early Proterozoic times ($t > 2$ Ga) as such an oxygen-eliminating reaction of high efficiency (MacGregor, 1927; Cloud, 1973; and others). Under conditions of an anoxygenic continental weathering cycle, bivalent iron should have made up a sizable fraction of the weathering load, with the ancient oceans consequently serving as iron accumulators. The hydrated ferrous ions would have acted as ideal oxygen acceptors when O_2-releasing autotrophs discharged their metabolic by-product into the marine environment. With the bulk of the ancient biotopes submerged below ocean levels, and dissolved iron ubiquitous in marine waters, any molecular oxygen released would have been instantaneously sequestered by the abundant Fe^{2+}_{aq}-ions and precipitated as ferric oxides. Only after the ancient oceans had been effectively swept free from ferrous iron during successive periods of BIF deposition, did molecular oxygen have a chance to escape to, and subsequently accumulate in, the atmosphere. From then, oxidation of iron took place in the form of oxidation weathering on the continents, thus drying up the flux of soluble Fe^{2+}_{aq} to the seas and giving rise to extended formations of terrigenous red beds. The sluggishness of subaerial oxidation processes (in contrast with the rapid scavenging of oxygen previously achieved in the marine environment) meant that atmospheric P_{O_2} was apt to rise until sources and sinks had attained equilibrium at a markedly increased atmospheric oxygen level.

Since accumulation of free oxygen in the atmosphere is only a relatively minor side-issue in the global redox cycle, the rise of oxygenic conditions on Earth must be regarded as an integral part of the general release through time, and subsequent differential sequestering by the various geochemical reservoirs, of oxidized molecular species which evolved as a result of biological carbon fixation. If the model, envisaged above, for the origin of Precambrian banded iron-formation stands the test of time (for dissent, see Holland, 1973), then the rise of free oxygen in the atmosphere was not primarily linked to the process of photosynthetic oxygen production as such (which had apparently started long before the build up of an atmospheric reservoir), but was rather a problem of the partitioning of oxygen between the principal geochemical reservoirs. In the absence of a kinetic lag between O_2-production and O_2-consumption, a modern-size reservoir of total photosynthetic oxygen could have been readily coupled with extremely low partial pressures of oxygen in the atmosphere, resulting in a marked dispropor-

tionation between the "bound" and "free" reservoirs compared to contemporary standards.

Hence, though the overall oxidation state of the atmosphere—hydrosphere—lithosphere system has probably not changed since Archaean times, this does not necessarily entail the presence of a stationary reservoir of free oxygen of about modern size during the Earth's early history. If the turnover of oxygen in the ancient exogenic cycle were sufficiently fast, the build up of an atmospheric reservoir could have been delayed which, in turn, would have heavily retarded subaerial oxidation weathering. With this concept of an early anoxygenic continental weathering cycle sometimes challenged (e.g., Schau and Henderson, 1983, this issue), further scrutiny of the oldest sedimentary record seems to be necessary.

ACKNOWLEDGEMENTS

Work leading to the views expressed in this paper was carried out as part of the program of Sonderforschungsbereich 73 ("Atmospheric Trace Components"), receiving partial funding from the Deutsche Forschungsgemeinschaft. Helpful criticism by J.F. Kasting, J.C.G. Walker and two anonymous reviewers on an earlier draft of this paper is gratefully acknowledged.

REFERENCES

Awramik, S.M., Schopf, J.W. and Walter, M.R., 1983. Filamentous fossil bacteria 3.5 Ga-old from the Archaean of Western Australia. Precambrian Res., 20: 357—374.

Barley, M.E., Dunlop, J.S.R., Glover, J.E. and Groves, D.I., 1979. Sedimentary evidence for an Archaean shallow-water volcanic—sedimentary facies, eastern Pilbara Block, Western Australia. Earth Planet. Sci. Lett., 43: 74—84.

Bridgwater, D., Allaart, J.H., Schopf, J.W., Klein, C., Walter, M.R., Barghoorn, E.S., Strother, P., Knoll, A.H. and Gorman, B.E., 1981. Microfossil-like objects from the Archaean of Greenland: a cautionary note. Nature, 289: 51—53.

Broda, E., 1975. The Evolution of the Bioenergetic Processes. Pergamon, Oxford, 220 pp.

Cameron, E.M. and Garrels, R.M., 1980. Geochemical compositions of some Precambrian shales from the Canadian Shield. Chem. Geol., 28: 181—197.

Carver, J.H., 1981. Prebiotic atmospheric oxygen levels. Nature, 292: 136—138.

Cloud, P.E., 1973. Paleoecological significances of the banded iron formation. Econ. Geol., 68: 1135—1143.

Cloud, P.E., 1976. Beginnings of biospheric evolution and their biogeochemical consequences. Paleobiology, 2: 351—387.

Cloud, P.E., 1980. Early biogeochemical systems. In: J.B. Ralph, P.A. Trudinger and M.R. Walter (Editors), Biogeochemistry of Ancient and Modern Environments. Springer, Berlin, pp. 7—27.

Cohen, Y., Aizenshtat, Z., Stoler, A. and Jørgensen, B.B., 1980. The microbial geochemistry of Solar Lake, Sinai. In: J.B. Ralph, P.A. Trudinger and M.R. Walter (Editors), Biogeochemistry of Ancient and Modern Environments. Springer, Berlin, pp. 167—172.

Dimroth, E. and Kimberley, M.M., 1976. Precambrian atmospheric oxygen: evidence in the sedimentary distribution of carbon, sulfur, uranium and iron. Can. J. Earth Sci., 13: 1161—1185.

Dungworth, G. and Schwartz, A.W., 1974. Organic matter and trace elements in Precambrian rocks from South Africa. Chem. Geol., 14: 167—172.

Dunlop, J.S.R., Muir, M.D., Milne, V.A. and Groves, D.I., 1978. A new microfossil assemblage from the Archaean of Western Australia. Nature, 274: 676—678.

Garrels, R.M. and Lerman, A., 1977. The exogenic cycle: reservoirs, fluxes and problems. In: W. Stumm (Editor), Global Chemical Cycles and their Alteration by Man. Abakon, Berlin, pp. 23—31.

Garrels, R.M. and Mackenzie, F.T., 1971. Evolution of Sedimentary Rocks. Norton, New York, 397 pp.

Grandstaff, D.E., 1980. Origin of uraniferous conglomerates at Elliot Lake, Canada and Witwatersrand, South Africa: implications for oxygen in the Precambrian atmosphere. Precambrian Res., 13: 1—26.

Heinrichs, T.K. and Reimer, T.O., 1977. A sedimentary barite deposit from the Archaean Fig Tree Group of the Barberton Mountain Land (South Africa). Econ. Geol., 72: 1426—1441.

Holland, H.D., 1973. The oceans: a possible source of iron in iron-formations. Econ. Geol., 68: 1169—1172.

Holland, H.D., 1978. The Chemistry of the Atmosphere and Oceans. Wiley, New York, 351 pp.

Hunten, D.M. and Strobel, D.F., 1974. Production and escape of terrestrial hydrogen. J. Atmos. Sci., 31: 305—317.

Kasting, J.F. and Walker, J.C.G., 1981. Limits on oxygen concentration in the prebiological atmosphere and the rate of abiotic fixation of nitrogen. J. Geophys. Res., 86: 1147—1158.

Kasting, J.F., Liu, S.C. and Donahue, T.M., 1979. Oxygen levels in the prebiological atmosphere. J. Geophys. Res., 84: 3097—3107.

Li, Y.H., 1972. Geochemical mass balance among lithosphere, hydrosphere and atmosphere. Am. J. Sci., 272: 119—137.

Lowe, D.R., 1980. Stromatolites 3.400-Myr old from the Archean of Western Australia. Nature, 284: 441—443.

Lowe, D.R. and Knauth, L.P., 1977. Sedimentology of the Onverwacht Group (3.4 billion years), Transvaal, South Africa, and its bearing on the characteristics and evolution of the early Earth. J. Geol., 85: 699—723.

MacGregor, A.M., 1927. The problem of the Precambrian atmosphere. S. Afr. J. Sci., 24: 155—172.

Moore, C.B., Lewis, C.F. and Kvenvolden, K.A., 1974. Carbon and sulfur in the Swaziland sequence. Precambrian Res., 1: 49—54.

Nagy, B., Kunen, S.M., Zumberge, J.E., Long, A., Moore, C.B., Lewis, C.F., Anhaeusser, C.R. and Pretorius, D.A., 1974. Carbon content and carbonate ^{13}C abundances in the Early Precambrian Swaziland sediments of South Africa. Precambrian Res., 1: 43—48.

Orpen, J.L. and Wilson, J.F., 1981. Stromatolites at ~3.500 Myr and a greenstone—granite unconformity in the Zimbabwean Archaean. Nature, 291: 218—220.

Owen, T., Biemann, K., Rushneck, D.R., Biller, J.E., Howarth, D.W. and Lafleur, A.L., 1977. The composition of the atmosphere at the surface of Mars. J. Geophys. Res., 82:4635—4639.

Pflug, H.D. and Jaeschke-Boyer, H., 1979. Combined structural and chemical analysis of 3.800-Myr-old microfossils. Nature, 280: 483—486.

Reimer, T.O., Barghoorn, E.S. and Margulis, L., 1979. Primary productivity in an Early Archean microbial ecosystem. Precambrian Res., 9: 93—104.

Roedder, E., 1981. Are the 3.800-Myr-old Isua objects microfossils, limonite-stained fluid inclusions, or neither? Nature, 293: 459—462.

Ronov, A.B., 1980. Osadotchnaya Obolotchka Zemli (20th Vernadsky Lecture). Izdatel'stvo Nauka, Moscow.

Schau, M. and Henderson, J.B., 1983. Archean weathering at three localities on the Canadian Shield. Precambrian Res., 20: 189—224.

Schidlowski, M., 1970. Untersuchungen zur Metallogenese im südwestlichen Witwatersrand-Becken (Oranje-Freistaat-Goldfeld, Südafrika). Beih. Geol. Jb. 85: 80 pp., 23 plates.

Schidlowski, M., 1978. Evolution of the Earth's atmosphere: current state and exploratory concepts. In: H. Noda (Editor), Origin of Life. Center Acad. Publ. Japan, Tokyo, pp. 3—20.

Schidlowski, M., 1979. Antiquity and evolutionary status of bacterial sulfate reduction: sulfur isotope evidence. Origins Life, 9: 299—311.

Schidlowski, M., 1981. Uraniferous constituents of the Witwatersrand conglomerates: ore-microscopic observations and implications for the Witwatersrand metallogeny. In: F. Armstrong (Editor), Genesis of Uranium- and Gold-Bearing Precambrian Quartz-Pebble Conglomerates. U.S. Geol. Surv. Prof. Pap., 1161: N1—N29.

Schidlowski, M., 1982. Content and isotopic composition of reduced carbon in sediments. In: H.D. Holland and M. Schidlowski (Editors), Mineral Deposits and the Evolution of the Biosphere. Springer, Berlin, pp. 103—122.

Schidlowski, M., Eichmann, R. and Junge, C.E., 1975. Precambrian sedimentary carbonates: carbon and oxygen isotope geochemistry and implications for the terrestrial oxygen budget. Precambrian Res., 2: 1—69.

Schidlowski, M., Junge, C.E. and Pietrek, H., 1977. Sulfur isotope variations in marine sulfate evaporites and the Phanerozoic oxygen budget. J. Geophys. Res., 82: 2557—2565.

Schidlowski, M., Hayes, J.M. and Kaplan, I.R., 1983. Isotopic inferences of ancient biochemistries: carbon, sulfur, hydrogen and nitrogen. In: J.W. Schopf (Editor), The Earth's Earliest Biosphere: Its Origin and Evolution. Princeton University Press, Princeton, N.J. (in press).

Veizer, J., Holser, W.T. and Wilgus, C.K., 1980. Correlation of $^{13}C/^{12}C$ and $^{34}S/^{32}S$ secular variations. Geochim. Cosmochim. Acta, 44: 579—587.

Walker, J.C.G., 1978. Oxygen and hydrogen in the primitive atmosphere. Pure Appl. Geophys., 116: 222—231.

Walker, J.C.G., Klein, C., Schidlowski, M., Schopf, J.W., Stevenson, D.J. and Walter, M.R., 1983. Environmental evolution of the Archaean — Early Proterozoic Earth. In: J.W. Schopf (Editor), The Earth's Earliest Biosphere: Its Origin and Evolution. Princeton University Press, Princeton, N.J. (in press).

Walter, M.R., 1983. Archean stromatolites: evidence of the Earth's earliest benthos. In: J.W. Schopf (Editor), The Earth's Earliest Biosphere: Its Origin and Evolution. Princeton University Press, Princeton, N.J. (in press).

Walter, M.R., Buick, R. and Dunlop, J.S.R., 1980. Stromatolites 3.400—3.500 Myr old from the North Pole area, Western Australia. Nature, 284: 443—445.

This Page Intentionally Left Blank

FURTHER SULFUR AND CARBON ISOTOPE STUDIES OF LATE ARCHEAN IRON-FORMATIONS OF THE CANADIAN SHIELD AND THE RISE OF SULFATE REDUCING BACTERIA*

H.G. THODE

Department of Chemistry, McMaster University, Hamilton, Ontario L8S 4K1 (Canada)

A.M. GOODWIN

Department of Geology, University of Toronto, Toronto, Ontario M5S 1A1 (Canada)

ABSTRACT

Thode, H.G. and Goodwin, A.M., 1983. Further sulfur and carbon isotope studies of late Archean iron-formations of the Canadian shield and the rise of sulfate reducing bacteria. Precambrian Res., 20: 337—356.

Sulfur and carbon contents and isotope ratios are reported for five Archean iron-formations, Helen, Nakina and Finlayson, Lumby and Bending Lake areas, distributed across 850 km of the Canadian shield all ~2.7 Ga-old.

A $\delta^{34}S$ profile through a complete stratigraphic column (oxide facies excluded) of the Helen iron-formation shows a $\delta^{34}S$ range of 30.2‰, mean $\delta^{34}S$ value of 2.5‰ and a standard deviation (σ_i) of 7.3‰. In sharp contrast to the sulfide and siderite facies, the oxide facies in the column shows a uniform $\delta^{34}S$ value close to zero. The $\delta^{34}S$ values obtained for the other four iron-formations are again wide ranging, highly variable in the sulfide and pyrite—siderite facies, but uniform and close to zero for the oxide facies.

The carbon in the oxide, siderite, chert facies has $\delta^{13}C$ values of +2.3 to −1.1‰ in the range of Phanerozoic marine carbonates. However, the carbonates in the graphite rich sulfide facies have $\delta^{13}C$ values as low as −7.6‰. The mixing of reduced carbon with marine carbonate is suggested to explain the light carbonate values. The reduced carbon associated with the light carbonate is also relatively light at up to $\delta^{13}C_{org} = 33.5‰$, but is in the range of other Precambrian values. Distal, high temperature, abiogenic sulfate reduction as a source of highly fractionated sulfides in the Archean iron-formations is ruled out on the basis of both isotopic and geologic evidence. It is concluded that only the bacterial reduction of sulfate at low temperatures could produce the wide ranging, highly variable $\delta^{34}S$ values exhibited by these sulfides over large areas.

INTRODUCTION

Fractionation of the sulfur isotopes may occur in uni-directional and or/in equilibrium processes involving the various oxidation states of sulfur, such as

*Contribution number 132 of the McMaster Isotopic, Nuclear and Geochemical Studies Group.

may occur in volcanic emanations and in hydrothermal fluids at elevated temperatures. However, by far the most important process for sulfur isotope fractionation is the low temperature dissimilatory reduction of sulfate to H_2S by anaerobic bacteria. This process together with the activity of sulfur oxidizing bacteria account for the bulk of the contemporary turnover rates of sulfur in the biosphere (Postgate, 1968). In the bacterial reduction process the H_2S produced is light or depleted in ^{34}S by 0 to $\sim 60^0/_{00}$ with respect to the source sulfate pool, the magnitude of this effect depending on conditions of temperature nutrient concentrations, reducing conditions and in general decreases with increasing metabolic rate (Harrison and Thode, 1958; Kaplan and Rittenberg, 1964). In contrast to "sulfate reducers" (photosynthetic), S-oxidizing bacteria in the opposite part of the biological cycle produce little isotope fractionation (Kaplan and Rittenberg, 1964).

A number of models have been proposed to explain the experimental results (obtained with *Desulfovibrio desulfuricans*). Each of these involve a sequence of enzyme catalysed steps which may be wholly, or in part, rate controlling (Harrison and Thode, 1958; Kemp and Thode, 1968; Rees, 1969). Large sulfur isotope effects ($\sim 25\%$) are associated with each of the two steps involving the breaking of sulfur oxygen bonds. At very slow metabolic rates, these two isotope effects become additive. However, at very rapid metabolic rates or very low sulfate concentrations, where the forward reactions proceed as fast as sulfur is supplied, the overall isotope effect approaches zero or essentially that in the first forward step, the uptake of sulfate. Thus, the overall isotope effect will vary widely depending on the operating conditions of the bacterium.

In natural environments, such as marine sediments, the $\delta^{34}S$ values for biogenic sulfides will also depend on whether the sulfate is reduced in an open system in equilibrium with a large pool of sulfate such as the ocean where the $\delta^{34}S$ of the sulfate remains constant during reduction, or in a closed system such as a restricted sulfate pool where the residual SO_4^{2-} becomes progressively heavier ($\delta^{34}S$ becomes more positive) with increased extent of reaction as in a Rayleigh process. Finally, the $\delta^{34}S$ of the sulfides will depend on whether the H_2S formed is accumulating, or is fixed in the sediments, as sulfides as fast as it is formed. Clearly a wide ranging highly variable $\delta^{34}S$ distribution pattern, both on a micro and macro scale within sedimentary rock formations, will provide strong evidence for the existence of sulfate reducing bacteria at the time of sediment depositions.

According to current theories "sulfate reducers" evolved from primitive photosynthetic sulfur oxidizing bacteria (purple sulfur bacteria), although functioning in an opposite direction, the enzymatic equipment of the bacteria involved in the sulfur transformations are found to be similar. It has been assumed that this anaerobic ecosystem of "sulfureta" was most abundant prior to the accumulation of free oxygen in the atmosphere (Broda, 1975).

The availability of sufficient quantities of SO_4^{2-} is naturally a prerequisite

of dissimilatory SO_4^{2-} reduction. With oxygenic weathering largely absent during the Earth's early history, it has been proposed that the phototrophic (green and purple) sulfur oxidizing bacteria (possible ancestors of the sulfate reducers) have probably supplied the bulk of sulfate stored in the Archean oceans (Peck, 1974). In this regard, significant Archean bedded sulfate deposits have been described from the Pilbara Block (Western Australia), the Barberton Mountain Land of South Africa, and Southern India (Perry et al., 1971, 1973; Hickman, 1973; Heinricks and Reimer, 1977; Lambert et al., 1978). Although these are all barite deposits there is petrographic evidence suggesting replacement of an original evaporitic gypsum in the case of the North Pole (Pilbara) deposits, indicating relatively high concentrations of SO_4^{2-}, at least locally, in Archean seas (Lambert et al., 1978).

In recent years several efforts have been made to determine the time of emergence of dissimilatory "sulfate reduction" by tracing back in the Precambrian record the isotopic composition of the sedimentary sulfur (Goodwin, 1975; Goodwin et al., 1976; Shegelski, 1978; Donnelly et al., 1978; Fripp et al., 1979; Monster et al., 1979; Ripley and Nicol, 1981). For the most part banded iron-formations (B.I.Fs.) have been selected for isotope studies because of their (1) wide distribution in Archean and Proterozoic rocks, (2) varied lithologies and (3) often low grade regional metamorphism. The sheer volume and areal extent of many of these low grade metamorphic rocks make it unlikely that gross chemical or isotopic modifications have taken place since their deposition.

The late Archean B.I.Fs. of the Michipicoten and Woman areas (2.75 Ga-old), investigated isotopically by Goodwin et al. (1976) are typical examples of well preserved low temperature Archean iron-formations of the Canadian shield. James (1954) described these Algoma type deposits and was the first to suggest bacterial reduction of SO_4^{2-} as the main source of sulfur in the sulfide facies of these iron-formations. The wide variations in sulfur isotope ratios ($\delta^{34}S^0/_{00}$), $\sim 20^0/_{00}$ reported by Goodwin et al. (1976) for the sulfides in the sulfide, siderite and chert facies provided strong evidence in favour of this suggestion. On the basis of isotopic and geological evidence they ruled out various possible inorganic fractionation processes and proposed a bacterial model of sulfate reduction as the main source of sulfur in these Archean sediments. Shegelski (1978) reported $\delta^{34}S_{(S^{2-})}$ variations of up to $12^0/_{00}$ in equivalent Archean iron-formations in the Savant and Sturgeon Lake areas of Ontario; Ripley and Nicol (1981) reported similar $\delta^{34}S_{(S^{2-})}$ variations in the Archean Deer sediments in Minnesota; and Goodwin (1975) reported $\delta^{34}S$ variations up to $15^0/_{00}$ in sulfide zones of volcanic rocks of Pashkokogan, Ontario. Mainly on the basis of geological evidence they proposed a bacterial source for at least part of the sulfides in these sediments.

However, isotope studies of iron-sulfide bearing sedimentary rocks from other Archean shields have not shown these large variations in $\delta^{34}S$ values and the Canadian shield data has been seen as an exception or anomaly (Trudinger and Cloud, 1981). For example Donnelly et al. (1978) concluded

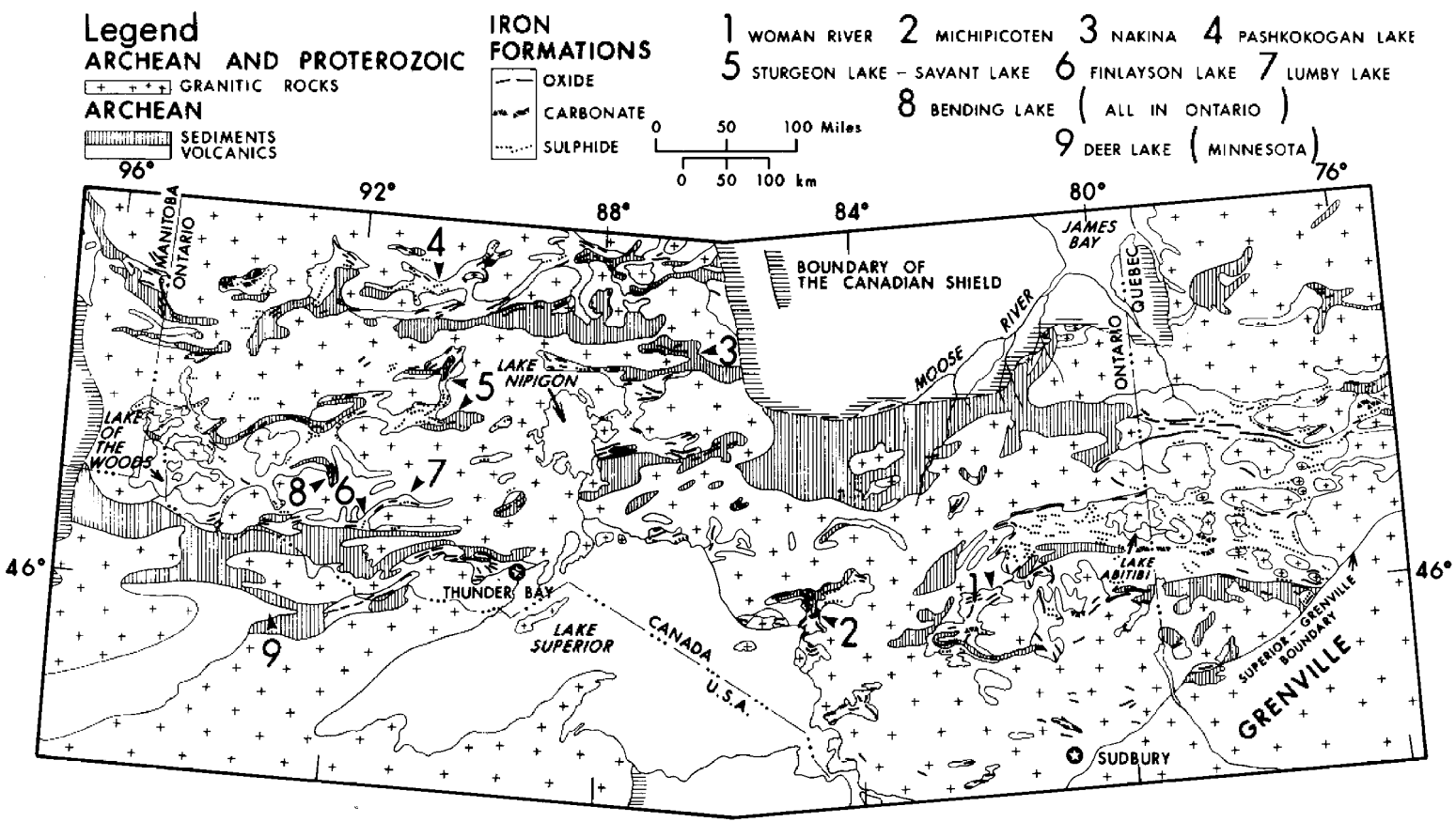

Fig. 1. Site map showing various study areas.

from their isotopic studies that the sulfides in black shales and cherts from the greenstone belts in the Yilgarn Block of Western Australia, also ~ 2.7 Ga-old, formed from solutions containing essentially magmatically derived sulfur. They found no clear evidence of widespread bacterial or abiological sulfate reduction. Their conclusions were based on the very narrow range of near zero $\delta^{34}S$ values for the majority of their Archean sedimentary sulfides. Mean $\delta^{34}S$ value = $1.6^{0}/_{00}$ and standard deviation of distribution (σ_i) = $2.5^{0}/_{00}$.

Also Fripp et al. (1979) concluded that the stratabound and stratiform sulfides within B.I.Fs. in the Archean greenstone belts of Zimbabwe were magmatically derived. Again their conclusion was based on the narrow range of $\delta^{34}S$ values close to zero for these sulfides. Mean $\delta^{34}S^{0}/_{00} = -0.6^{0}/_{00}$; $\sigma_i = 2.0^{0}/_{00}$.

A further study of the sulfur and carbon isotope ratios in Algoma type iron-formations of the Canadian shield has been carried out to obtain further evidence of bacterial sulfate reduction as a source of sulfur in these sediments, and to provide further information concerning the source of mineralization and the nature of the paleoenvironment in which they were deposited.

Measurements of the sulfur and carbon concentrations and isotope ratios have been determined for samples taken from along a single 425 m drill core section of iron-formation, Helen Mine, Michipicoten area, extending from the basal felsic rock through the various iron facies to the overlying mafic rocks. Major and trace element analysis and organic geochemical studies carried out on adjacent samples are the subject of another paper (Goodwin et al., 1982).

Similar isotopic measurements have been made on samples from equivalent Archean iron-formations some 300—900 km to the west and northwest of Michipicoten, at Nakina, Bending Lake, Lumby Lake and Finlayson Lake, Ontario (see site map Fig. 1).

GEOLOGICAL SETTINGS

New data are reported from five Algoma type iron-formations of Archean age (Helen, Nakina and Finlayson, Lumby and Bending Lake areas). These iron-formations are distributed across 850 km of south central Superior Province of the Canadian shield (see site map Fig. 1). All iron-formations are ~ 2.7 Ga-old (Gross, 1965, 1972; Goldich, 1973).

Michipicoten (Helen) iron-formation

This displays a regional distribution pattern of oxide, carbonate and sulfide facies of iron-formation based on the dominant iron minerals present. The three iron facies are broadly transitional across the area, in that order, from west to east. The carbonate facies iron-formation in the central part contains major siderite masses, including the operating Macleod mine on the

Helen iron range. The Helen iron-formation overlies felsic pyroclastic pillowed volcanics and includes, in descending conformable succession: (1) a banded chert member, up to 3000 m thick, typically composed of well-to-poorly banded granular chert with pyrite and minor magnetite, pyrrhotite, dolomite and silicates (chlorite), which are arranged in ascending siderite, sulfide-carbonaceous and "oxide" subdivisions; (2) a pyrite member, < 10 m thick, composed of granular to dense, massive to finely layered pyrite, mixed with more or less chert, siderite, minor pyrrhotite and magnetite; (3) a siderite member. The data reported here has been obtained from a diamond drill intersection at the west end of the Helen range which has provided a continuous core intersection of the complete iron-formation 475 m long (D.D.J.-U-2-647).

Nakina iron-formation

This large oxide facies iron-formation, 75 km north of Nakina, is part of the east-trending Melchett—Percy Lakes metasedimentary belt. The main iron-formation zone is at least 50 km long and is composed megascopically of alternate bands of quartz and fine grained magnetite up to 179 m thick (Swenson, 1960).

Finlayson Lake iron-formation

This cherty iron-formation (with units up to 12 m thick) extends northward from Steep Rock Lake at Antikoken. It is composed of layers of recrystallized chert separated by thin bands (1—2 cm) of minnesotaite and thick bands of pyrite, pyrrhotite, magnetite and siderite (only minor magnetite). The predominance of sulfides over magnetite and the occurrence of graphite suggests a strongly reducing (depositional) environment (James, 1954). The sulfide—siderite facies of iron-formation occurs as follows: in the form of disseminated pyrite in black carbonaceous shale; as pyrite and pyrrhotite mixed with siderite in banded chert; as distinct pyrite and pyrrhotite beds with minor siderite (Gross, 1965, p. 88). Analysis of the sulfide—siderite facies samples are reported here.

Lumby Lake iron-formation

The main sedimentary band, 100—120 m thick, contains distinctive phases including cherty magnetite, silica-siderite, massive siderite, massive sulfides and crystalline limestone. Sulfide—siderite graphite zones up to 50 m thick and 4 km long lie within and at a contact of adjoining argillite.

Bending Lake iron-formation

The Bending Lake iron deposit of Algoma Steel Corp. Ltd. is located 80 km northwest of Antikoken. The iron-bearing rock is part of a thick

sequence of fine grained metasediments. The iron-formation contains a large reserve of concentrating-type magnetite and is mainly composed of quartz, magnetite and amphiboles.

ANALYTICAL PROCEDURES

In general, sulfate and elemental sulfur are rare in the Archean iron-formations of the Canadian shield, e.g., Michipicoten (Goodwin et al., 1976). The sulfides are made up of essentially pyrite and pyrrhotite, being relatively free of Cu, Ni, Zn and other sulfides.

Acid soluble sulfide sulfur (pyrrhotite) is extracted from weighed aliquots of crushed and ground B.I.F. samples by treatment with dilute HCl. The H_2S released is converted in successive steps to CdS to Ag_2S to SO_2, the latter compound being the gas used for isotopic analysis. The concentration of pyrrhotite sulfur is determined gravimetrically at the Ag_2S step.

The pyrite sulfur is extracted from the residue of the pyrrhotite extraction, by treatment with a mixture of nitric acid and bromine, insoluble material is separated, and iron is removed as $Fe(OH)_3$. The sulfate isolated is precipitated as $BaSO_4$, reduced to H_2S with HI—H_3PO_2—HCl mixture and converted to Ag_2S and SO_2. The pyrite sulfur content is again determined at the Ag_2S step.

In cases where sulfide is finely dispersed in magnetite, ground samples of iron-formation are reacted with aqua-regia. Insoluble material is filtered off and filtrate iron is removed by extraction with isopropyl ether as described by Morrison and Freiser (1957). The final sulfate is precipitated as $BaSO_4$ and processed as described above to H_2S, to Ag_2S and SO_2. This method gives the sulfur content and isotope ratio for the total sulfides in the sample (in the absence of sulfates). The aqua-regia extraction method also leads to a residue of graphitic carbon (kerogen), silica and silicates from which the carbon can easily be separated by digesting with HF and HCl. Carbon so isolated can be burnt in a stream of oxygen.

Carbonate carbon (siderite) is reacted with 100% H_3PO_4, applying some heating to facilitate the carbonate decomposition (McCrea, 1950; Becker and Clayton, 1972).

Mass spectrometry

Isotopic analysis of CO_2, SO_2 and SF_6 gas samples is performed using a high precision isotope ratio mass spectrometer described by Thode et al. (1961) and modified by Beaver (1973). SF_6 is used as the working gas for sulfur isotope analysis for samples containing >2—3 mg of sulfur. The SF_6 is prepared by the fluorination of the Ag_2S. Sulfur and carbon isotope ratios are also expressed in terms of the δ notation

$$\text{where } \delta^{13}C^{0}/_{00} = \left[\frac{(^{13}C/^{12}C)\text{sample}}{(^{13}C/^{12}C)\text{standard}} - 1\right] \times 1000$$

Here the P.D.B. standard is used

$$\text{and} \quad \delta^{34}S^{0}/_{00} = \left[\frac{(^{34}S/^{32}S)\text{sample}}{(^{32}S/^{32}S)\text{standard}} - 1\right] \times 1000$$

The standard ratio is that for troilite sulfur of the Canyon Diablo meteorite. There is now considerable evidence to show that the meteoritic ratio $\delta^{34}S = 0$ on the above scale is close to the primordial ratio for the solar system. Primary sulfur, magmatic sulfur, sulfur in basic sills from sources deep in the earth have δ values essentially equal to zero.

RESULTS

Michipicoten area

The percent sulfur and sulfur isotope ratios for the acid soluble sulfur, pyrrhotite (Po) and the pyrite (Py) components for samples from the Helen iron-formation drill core section, Michipicoten area, are given in Table I. The sequence of units or zones in this single sedimentary cycle from which samples are taken at various depths are indicated in column 1. The carbonate content (% CO_2) and carbonate carbon isotope ratios for the samples are given in columns 7 and 8.

The sulfur isotope data of Table I, is illustrated in Fig. 2 as a $\delta^{34}S$ profile ($\delta^{34}S$ v. depth) through the iron-formation stratigraphic column, and in Fig. 3 as $\delta^{34}S$ histograms for the various facies or units. The data for this Archean iron-formation shows a wider range of $\delta^{34}S$ values, $\sim 30^{0}/_{00}$ as compared to $\sim 20^{0}/_{00}$ obtained previously, a higher positive $\delta^{34}S$ value up to $+19^{0}/_{00}$ and a much higher standard deviation of the distribution (σ_i) = $7.3^{0}/_{00}$ (oxide facies excluded).

This range and variability of $\delta^{34}S$, characteristic of biogenic sulfides in low temperature diagenetic sediments, deposited under changing conditions, is clearly illustrated on both a "macro" and "micro" time scale. Figure 2 shows the wide variations in $\delta^{34}S$ from sample to sample taken every 4—15 m in depth, and Table I shows the very significant differences in $\delta^{34}S$ for the pyrite and pyrrhotite sulfur in the same samples. It should be noted that there is no systematic difference between $\delta^{34}S_{(py)}$ and $\delta^{34}S_{(po)}$. The proportion of the two minerals varies markedly through the sedimentary column, probably depending on environmental conditions and the relative concentrations of ferrous iron and sulfide (H_2S) at the time of formation.

In contrast to the sulfide, and pyrite—siderite facies, the cherty-magnetite or oxide facies at the top of the stratigraphic column (see Table I, Figs. 2 and 3) has a uniform $\delta^{34}S$ value close to zero.

TABLE I

Sulfur and carbon contents and isotope ratios of Archean B.I.F. samples of various iron facies from a vertically transitional Helen Mine drill core (U-2-647), Michipicoten, Ontario

Zone (top)	Mafic / felsic	Depth (m)	S (%)		$\delta^{34}S^{0}/_{00}$		CO_2 $\delta^{13}C^{0}/_{00}$ (%)	
			Po	Py	Po	Py	Carbonate	
B_3	Oxide facies: cherty magnetite (qtz.—sid.)	422.1	<0.01	14.2	—	1.4	13.7	0.4
		420.6	<0.01	4.26	—	−0.4	29.1	−1.3
		417.6	<0.01	0.11	—	2.39	4.8	−0.7
		400.8	0.24	<0.01	—	—	10	−1.1
		391.7	<0.01	0.08	—	0.36	—	0.0
		381.0	<0.01	0.07	—	0.85	3.6	+0.1
		362.7	<0.01	0.12	—	2.96	—	−0.1
		350.5	<0.01	0.06	—	0.79	19.3	+0.1
		326.1	<0.01	<0.01	—	—	8.9	−0.9
		295.6	<0.01	0.05	—	1.74	21.9	−0.2
B_2	Sulfide Facies: black carbonaceous slatey chert	254.5	14.21	3.77	−3.2	−3.1	30.3	−5.8
		251.6	<0.01	7.39	—	−4.9	—	—
		228.6	4.9	0.27	−4.5	−3.9	9.7	−7.1
		204.2	1.06	0.15	−11.6	−5.3	17.0	−3.3
		187.4	7.42	0.71	−5.4	−4.3	35	−3.8
		173.7	0.06	0.96	−3.9	−4.6	1.5	−2.4
		172.0	<0.01	23.0	—	5.0	0.4	−1.3
		163.0	0.02	0.13	−4.2	−3.43	—	—
		158.5	<0.01	6.4	—	4.3	14.3	—
		144.8	<0.01	21.6	4.16	5.8	—	—
B_1	Siderite (qtz.)	128.3	<0.01	0.1	—	—	10.4	−2.5
		113.1	<0.01	0.03	—	−0.14	27	−2.9
A_4	Pyrite—siderite	81.1	28.8	3.54	−2.1	−2.8	—	—
		69.5	0.39	25.76	2.7	4.0	13	−1.1
		66.4	0.03	23.1	6.8	7.8	20	0.5
		63.4	<0.01	15.49	—	10.0	30	1.9
		60.4	<0.01	0.09	—	—	32	1.0
A_3	Siderite—pyrite (Po)	57.3	2.71	23.46	11.4	13.2	14	−0.1
		51.2	0.01	3.95	—	15.2	34	−0.2
		48.6	0.02	0.82	—	19.0	34	1.2
		42.0	4.9	0.84	−3.1	−3.4	33	0.1
A_2	Quartz (sid.)	37.5	0.21	0.11	1.7	2.7	5	1.1
A_1	Siderite (qtz.)	20.7	<0.01	0.29	—	13.5	30	2.3
Mean $\delta^{34}S^{0}/_{00}$					−0.9	+2.5[a]		
Standard deviation of distribution (σ_i)					6.0	7.3[a]		

Total $\delta^{34}S$ range = $30.2^{0}/_{00}$.
[a]Oxide facies excluded.

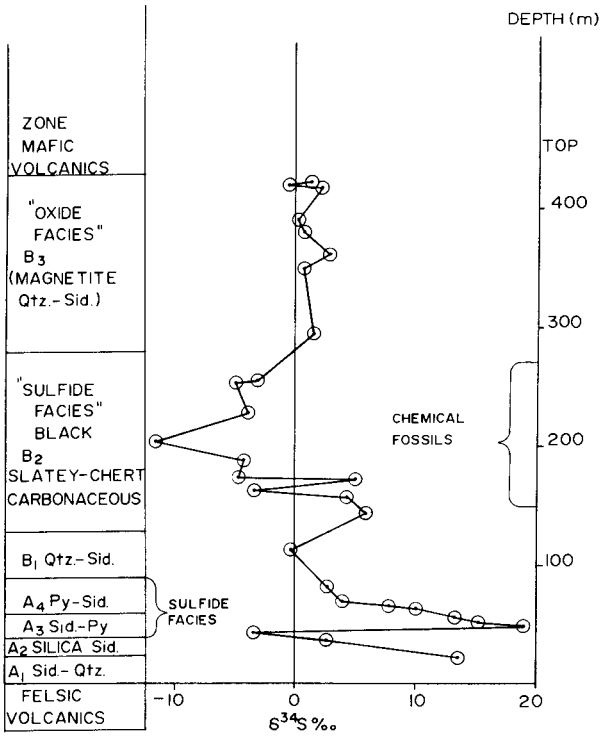

Fig. 2. $\delta^{34}S$ profile ($\delta^{34}S$ v. depth) for continuous core intersection of complete iron-formation 475 m long. Helen Mine, Michipicoten area (D.D.J. U-2-647).

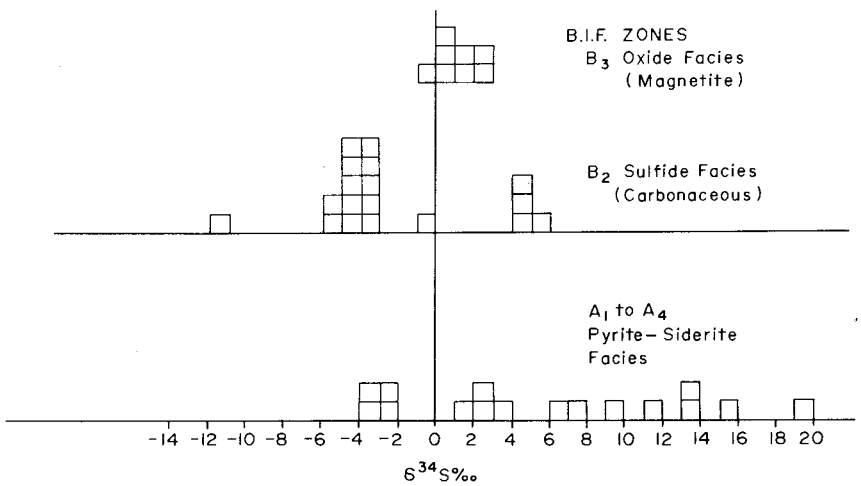

Fig. 3. $\delta^{34}S$ histograms for the various iron facies or units in Helen Mine iron-formation column (Michipicoten).

Nakina and Antikoken areas

Table II gives the sulfur content and sulfur isotope ratios for the acid soluble sulfides (Po) and total sulfides (Po + Py) for samples collected from sulfide—siderite facies in the Archean iron-formations at Lumby Lake and Finlayson Lake, Ontario (see site map Fig. 1). Carbon isotope ratios for kerogen and carbonate carbon are also given for some of these samples. Table III gives the sulfur content and isotope ratios for samples taken at various depths along drill core sections of cherty-magnetite, oxide facies of the iron-formations at Nakina and Bending Lake. The $\delta^{34}S$ distribution patterns obtained for both the oxide, sulfide—siderite facies of these iron-formations are illustrated in Fig. 3.

TABLE II

Sulfur content, sulfur and carbon isotope ratios of Archean B.I.F. samples of sulfide—siderite facies, Lumby Lake, Ontario

Sample no[a]	S (%)		$\delta^{34}S^{0}/_{00}$		$\delta^{13}C^{0}/_{00}$	
	Po	(Py + Po)	Po	Py + Po	Organic	Carbonate
1a	4.6		3.0			
1b		5.3		2.1	−28.14	
2a	0.2		1.0			
2b		4.16		1.8		
3		0.25		4.8	-14.4	
4a	0.27		9.7			
4b		0.56		9.1		
5		0.56		2.9	-25.7	
6a	0.27		14.4			
6b		0.94		13.6		
7a	6.7		1.4			
7b		4.32		0.8		
Sulfide-siderite facies, Finlayson Lake, Ontario						
1a	23.9		−2.1			
1b		11.3		−1.8	−28.5	
2		11.85		−1.7	−28.2	−3.5
3		4.92		−4.2	−33.5	−7.6
5		4.40		1.5	−23.7	−7.5
6		5.13		−3.2	−24.3	−1.5
7		0.92		5.2		−4.6

Total $\delta^{34}S$ range ($-4.2^{0}/_{00}$ to $14.4^{0}/_{00} = 18.6^{0}/_{00}$).
Mean $\delta^{34}S = 3.0^{0}/_{00}$.
Standard deviation of distribution (σ_i) $= 5.3^{0}/_{00}$.
Standard deviation of individual measurement (σ) $= 0.23^{0}/_{00}$.
[a] a and b samples are separate pieces of the same specimen.

TABLE III

Sulfur content and isotope ratios of Archean B.I.F. samples

Zone	Depth (m)	S (%)[a]	$\delta^{34}S^{o}/_{oo}$
Oxide facies (magnetite), Bending Lake, Ontario			
Banded Magnetite	228.6	0.39	1.1
Chert — 20—25% Fe	230.4	0.41	1.4
Interbanded cherty-magnetic	240.8	0.33	1.8
(25—30% Fe)	243.8	0.18	−0.3
	310.9	0.10	0.0
	312.4	0.08	1.0
	341.4	0.12	0.3
	350.8	2.38	0.4
	353.6	0.38	0.9
	356.6	0.35	0.8
Bands of cherty-magnetite	359.7	1.34	0.8
(15—20% Fe)	363.0	0.43	1.9
	366.4	0.41	2.0
	368.2	0.93	1.3
	387.1	0.14	0.2
Mean			0.66
Oxide facies (magnetite), Nakina, Ontario			
Banded chert-magnetite; calcite	65.2	0.259	0.1
identified	72.2	0.198	−0.2
	110.9	0.277	−0.4
	144.8	0.392	−0.6
Mean			−0.27

Standard deviation of individual measurement (σ) = $0.23^{o}/_{oo}$.
Standard deviation of distribution (σ_i) = $0.8^{o}/_{oo}$.
[a]Total sulfides, sulfate largely negligible.

The $\delta^{34}S$ distribution patterns obtained for the Michipicoten (Helen) iron-formation are repeated in the iron-formations at Lumby Lake and Finlayson Lake some 900 km west and north west. The sulfide and sulfide—siderite facies (Table II, Fig. 4) again show wide ranging, highly variable $\delta^{34}S$ values for the sulfides. Thus, evidence for large scale sulfur isotope fractionation is widespread in the Archean iron-formations of the Canadian shield.

In contrast again, the oxide facies (magnetite) iron-formations at Bending Lake and Nakina have uniform $\delta^{34}S$ values close to zero.

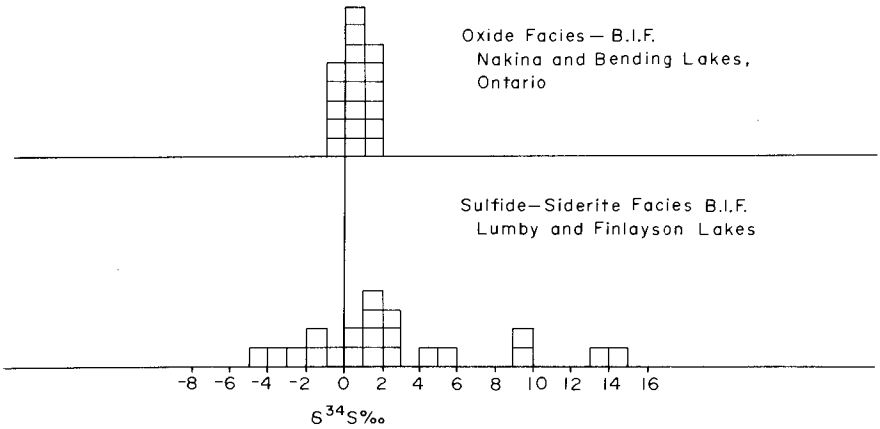

Fig. 4. $\delta^{34}S$ histograms for oxide facies iron-formation Nakina and Bending Lake, and for sulfide and siderite facies iron-formation Lumby and Finlayson Lake.

Oxide facies

Clearly there is little or no evidence of sulfur isotope fractionation due to biogenic or abiogenic sulfate reduction in the environment or under the conditions in which iron oxide was formed. This is consistent with the relatively low concentration of sulfides and almost complete absence of organically derived carbon in the oxide facies. The oxide facies results suggest a thoroughly homogenized direct source of juvenile sulfur (volcanic exhalations) or assimilatory reduction of Archean seawater sulfate at a $\delta^{34}S$ level of ~ zero. Assimilatory reduction of seawater sulfate, e.g., plant metabolism, does not lead to sulfur isotope fractionation (Ishii, 1953; Goldhaber and Kaplan, 1974).

Archean seawater sulfate

There is now considerable isotopic evidence to support a $\delta^{34}S_{(SO_4^{2-})}$ level of ~0 for the Archean ocean. First, the Archean bedded sulfates (barite) from the Pilbara Block, Western Australia, and from the Barberton Mountain Land in South Africa (Perry et al., 1971; Lambert et al., 1978) give mean δ values of $\sim 3^0/_{00}$. Second, the Archean stratabound and stratiform sulfides of the Australian, Zimbabwen and Canadian shields, involving volcanogenic mineralization with some interaction with seawater sulfate, have $\delta^{34}S$ values close to zero, whereas similar younger base metal deposits, such as the Homestake deposits in the United States (Rye and Rye, 1974) and the Kuroko deposits in Japan (Rye and Ohmoto, 1974), have distinctively positive $\delta^{34}S$ values reflecting the build up of ^{34}S enrichment in the younger seas and its incorporation into ore forming solutions by high temperature reduction and exchange (Lambert, 1978). Finally, the mean $\delta^{34}S$ for the highly

fractionated sulfides in the Archean iron-formations of the Canadian shield is close to zero (~200 samples). This is consistent with the bacterial model of sulfate reduction and a contemporaneous source at $\delta^{34}S=0$. Regardless of the extent of sulfur isotope fractionation during sulfate reduction, a material balance requires that the mean $\delta^{34}S$ of the ocean sulfate into the basin must be equal to the mean $\delta^{34}S$ of the sulfide flux into the sediments over a long time period (in the absence of sulfate deposits). There is, therefore, little or no evidence of a build up of ^{34}S enrichment in late Archean oceans on a world scale.

Carbon isotope ratios

Typical of the Michipicoten sediments with relatively high siderite concentrations is the uniform isotope composition of the carbonate-carbon in the range of Phanerozoic marine carbonates, $\delta^{13}C = -0.1 \pm 2.6‰$ (Keith and Weber, 1964). The samples in Table I from the oxide facies zone B_3 and the pyrite—siderite—chert facies zones A_1—A_4 follow this pattern and have a mean $\delta^{13}C$ value of $0.22‰$ and standard deviation of the distribution (σ_i) of $0.8‰$. Marine carbonates as old as 3.3 Ga have been found to have fairly constant $\delta^{13}C$ values in this range (Eichmann and Schildlowski, 1975; and others). This constancy in $\delta^{13}C_{carb}$ is taken as evidence of a steady state balance between organic and inorganic carbon in the shell of the Earth since Archean times. However, the carbonates in the organic carbon rich sulfide facies zone B_2 samples (see Tables I, II) show a departure from this uniformity with $\delta^{13}C$ values as low as $-7.1‰$. Such negative $\delta^{13}C$ values for carbonates in B.I.F. sediments rich in light organically derived carbon are not uncommon (Becker and Clayton, 1972; Perry et al., 1973). Becker and Clayton (1972) have proposed the mixing of carbonate of organic origin with marine carbonate during a period of basin emergence and isolation to explain the light carbonates in the B.I.Fs. of the Hamersley basin area of Western Australia (Proterozoic). They point out that in the absence of dilution by a large oceanic reservoir the input of light CO_2 in reasonable amounts, most likely from the recycling of organic matter by micro-organisms, could cause the $\delta^{13}C_{carb}$ shifts found.

The carbonate carbon in the organic rich sulfide—siderite facies at Finlayson Lake, see Table II, is also isotopically light and has $\delta^{13}C_{carb}$ values of -1.5 to $-7.6‰$. These variable negative $\delta^{13}C_{carb}$ values in the organic rich sulfide—siderite facies suggest high biological activity in a closed basin (at times stagnant) with intermittent sea transgression during their deposition.

Coexisting organic carbon in the sulfide facies of the Finlayson Lake (B.I.Fs.) has $\delta^{13}C_{org}$ values of 23.7 to $-33.5‰$. The mean of these values ($-27.7‰$), taken together with the mean of the coexisting $\delta^{13}C_{carb}$ value ($-4.9‰$), gives a $\Delta\delta^{13}C = \delta^{13}C_{org} - \delta^{13}C_{carb} = 22.8‰$. However, when taken together with the $\delta^{13}C_{carb}$ values of the Michipicoten samples of high siderite concentration, considered to be the contemporaneous marine values, $\Delta\delta^{13}C =$

$-27.9^0/_{00}$. Both these values, with their respective ranges, are in accord with the mean $\delta^{13}C$ value of $-25.7^0/_{00}$ reported for the whole of the Precambrian (Eichmann and Schidlowski, 1975).

Some isotope analyses of Precambrian reduced carbon which is strongly depleted in the heavier ^{13}C isotope have been reported by Schoell and Wellmer (1981). Similar ^{13}C depleted organic carbon is found in the Archean iron-formations of the Canadian shield. $\delta^{13}C_{org}$ values of $-33.5^0/_{00}$ are reported in Table II for Finlayson Lake samples and values as low as $-44.8^0/_{00}$ are reported by Shegelski (1978) for equivalent Savant Lake samples (Fig. 1). The apparent correlation between the light carbonate carbon and light organic in the sulfide facies iron-formation is not one to one and may be fortuitous. It has been argued that the light carbonates result mainly from diagenetic mixing processes (Becker and Clayton, 1972) and that the organic carbon might be anomalously light as a result of multi-step fractionations, perhaps involving the methane cycle in localized stagnant basins (Schoell and Wellmer, 1982). The presence or absence of methane producing and methane oxidizing bacteria could explain the highly variable, often anomalous $\delta^{13}C_{org}$ values, in the Precambrian. In any case, the carbon isotope fractionation between HCO_3^- and organisms ranging from -22 to $-35^0/_{00}$ obtained for marine plankton depending on the species and on local conditions (Eichmann and Schidlowski, 1975) easily explains the range of $\delta^{13}C$ values obtained for the Finlayson Lake iron-formation.

DISCUSSION

It has been suggested that deep circulation of seawater over hot basaltic rocks at a distance from the basin might have provided a source of highly fractionated H_2S to the Archean basin. Mottl (1976) and Mottl et al. (1979) have shown that seawater sulfate is reduced to H_2S by interaction with basaltic rocks at $\sim 250°C$, possibly by ferrous iron leached from the rocks. At these high temperatures isotopic exchange between the H_2S product and the residual SO_4^{2-} is reduced, then the H_2S will have the same $\delta^{34}S$ value as that of the initial seawater SO_4^{2-} and at the other extreme if only a small portion of SO_4^{2-} is reduced then the H_2S will be isotopically light by $\sim 23^0/_{09}$ with respect to the initial SO_4^{2-}. Thus, the $\delta^{34}S$ of the sulfide produced in this high temperature exchange process cannot be more positive than the initial seawater sulfate and the total range of values cannot be greater than the exchange isotope effect of $\sim 23^0/_{00}$.

In areas of the world where this process is believed to have occurred, such as hot springs in the deep pools of the Red Sea (Atlantis II Deep) and the Galapagos spreading center in the Pacific, the total variation in $\delta^{34}S$, in the deposited sulfides is, at $\sim 12^0/_{00}$, insufficient to account for the $30^0/_{00}$ variations observed for the Archean B.I.Fs. (Kaplan et al., 1969; Hekinian et al.,

1980; Shanks et al., 1981). Furthermore, the maximum $\delta^{34}S$ values of the sulfides is always less than that of the contemporaneous seawater SO_4^{2-}. To account for the maximum δ value of $+19^0/_{00}$ obtained for the Archean B.I.Fs. would require ^{34}S enrichment of Archean seawater sulfate of at least $+19^0/_{00}$, contrary to isotopic evidence.

This kind of distal high temperature inorganic reduction can also be ruled out on the basis of geologic evidence. Deposition from hydrothermal fluids would be relatively rapid and would be expected to produce sulfidic bands, and at least locally massive sulfide zones. Such features are absent in the Michipicoten B.I.Fs. Further, the sulfide facies iron-formations are relatively barren of Cu, Pb, Zn and have no lateral or stratigraphical association with the massive base metal deposits of hydrothermal origin, such as occur in the Archean basins of Canada with δ values $\simeq 0$. Finally, such hydrothermal deposits usually cover relatively small areas around hot springs and volcanic centers in contrast to the large volume and areal extent of the B.I.Fs. of the Canadian shield. There are also difficulties in explaining the transport of sulfides to and precipitation in the basins over large areas.

Recent hydrothermal experiments of basalt—seawater interaction and observations of recently discovered hot vents and sulfide deposits on the east Pacific rise (Hekinian et al., 1980) have led to better understanding of these high temperature reaction systems. According to the results of Shanks et al. (1981), exchange sulfur isotope fractionation is not a factor in these systems and sulfur isotope values of sulfide related to natural basalt—seawater systems can be explained using a dual sulfur source, total sulfate reduction model. The key factor of their model is SO_4^{2-} precipitation as anhydrite, which occurs at all temperatures above 150°C and allows only a small fraction of seawater to enter the hotter portions of the geothermal systems. This sulfate is quantitatively reduced to sulfide by interaction with ferrous iron bearing minerals. The result is a homogeneous mixture of sulfide leached directly from the basaltic rock at $\delta^{34}S=0$ and sulfate reduced sulfide at the $\delta^{34}S$ level of $+20^0/_{00}$ for present day seawater sulfate. Sulfides deposited from these solutions would have δ values between 0 and $+20^0/_{00}$ depending on the proportion of each source or the water/rock ratios. In Archean times, before extensive build up of ^{34}S in the oceans, the sulfides deposited from such hydrothermal systems would be expected the have δ values in a very narrow range close to zero. The sulfur isotope data for current and Archean hydrothermal deposits seem to support these conclusions. The only known large scale process for sulfur isotope fractionation is the bacterial reduction of sulfate involving the breaking of S—O bonds in rate controlling steps at low temperatures.

The $\delta^{34}S$ distribution patterns obtained for the carbonaceous sulfide facies iron-formations of the late Archean are characteristic of sulfides formed by sulfate reducers in a restricted marine basin under changing conditions. If bacterial reduction takes place in the basin then the $\delta^{34}S$ of the residual SO_4^{2-} will increase with fraction reduced, until fresh SO_4^{2-} is introduced.

Therefore, ranges in $\delta^{34}S$, dependent on batch process enrichment, are controlled by flow rates of fresh seawater SO_4^{2-} into the basin. The banded nature of the iron-formations possibly results from intermittent flow of ferrous iron into the basin. In the absence of ferrous iron H_2S could build up in the deeper anoxic waters during high biological activity. This cycle of H_2S accumulation and the precipitation would reduce the amplitude of the $\delta^{34}S$ swings.

Finally, the carbonaceous sulfide facies of these Archean iron-formations which exhibit the large $\delta^{34}S$ variations are not unlike those of younger rocks of marine origin. For example, in the Savant and Sturgeon Lakes areas they are found to have carbon/pyrite ratios and sulfur/selenium ratios similar to those of modern marine sediments in which sulfide reduction has occurred (Nielson, 1974; Shegelski, 1978). The pyrite of these sulfide facies is, therefore, considered to be syngenetic and to have formed in a low temperature marine sedimentary environment.

The oldest sediments for which sulfur isotope data are available are the 3.7 Ga-old B.I.Fs. of the Isua area of West Greenland (Moorbath et al., 1973). $\delta^{34}S$ distribution patterns are reported for all iron facies of the Isua sediments (Monster et al., 1979). The most striking features displayed by the $\delta^{34}S$ values of the Isua sediments are the small variation in $\delta^{34}S$, $\pm 0.5^0/_{00}$, and the small displacements of the mean from zero $+0.5^0/_{00}$.

The complete lack of evidence of 'sulfate reducers' in the Isua B.I.F. and the strong evidence both from isotopic and geochemical considerations for their presence in the B.I.Fs. of the late Archean Canadian shield places early and late limits on the time of their beginning.

Sulfur isotope data obtained to date shows some incipient differentiation of the S isotopes before Michipicoten time. The modest variations in $\delta^{34}S(S^{=})$ in Archean sediments older than 3.2 Ga (Fig Tree series of South Africa and Iengra series of the Alden shield, Perry et al. (1971) and Vinogradov et al. (1976)) indicate perhaps a beginning of what was to become a thriving population of sulfate reducers in late Archean times.

Although isotopic and geologic evidence for bacterial sulfate reduction is widespread in the B.I.Fs. of the Canadian shield, such evidence is still limited in other greenstone belts of the world. Characteristic of the iron-formations of the Canadian shield is the prominence of the sulfide and sulfide—siderite facies, which have provided the evidence for sulfur isotope fractionation and bacterial sulfate reduction. In some cases these facies are actually mined for iron in addition to the much more prominent oxide facies. It may be that the rise of 'sulfate reducers' began in restricted marine basins, such as existed in the Canadian shield, where sulfide and sulfide—siderite facies were deposited under special conditions. The lack of significant evidence of ^{34}S enrichment in the late Archean oceans is consistent with the rise of 'sulfate reducers' in limited areas at that time.

ACKNOWLEDGEMENTS

We wish to thank the Natural Sciences and Engineering Research Council of Canada and the Department of Energy, Mines and Resources of Canada, for grants in aid of this research, the Algoma Steel Corporation Ltd. for well documented drill core samples from the Helen and Bending Lake areas of Ontario and C.M. Carmichael for samples from the Nakina area, Ontario. B. Baliat helped in the preparation and isotopic analysis of many of the samples, and J. Monster and C.E. Rees supervised much of the analytic work.

REFERENCES

Beaver, E.M., 1973. An automatic ratio readout system for a double collection mass spectrometer. Mass Spectrom., 21: 37—44.

Becker, R.H. and Clayton, R.N., 1972. Carbon isotopic evidence for the origin of a banded iron-formation in Western Australia. Geochim. Cosmochim. Acta, 36: 577—595.

Broda, E., 1975. The Evolution of the Bioenergetic Processes. Pergamon, Oxford, 220 pp.

Donnelly, T.H., Lambert, I.B., Oehler, D.Z., Hallberg, J.A., Hudson, D.R., Smith, J.W., Bavinton, O.A. and Golding, L.Y., 1978. A reconnaissance study of stable isotope ratios in Archean rocks from the Yilgarn Block, Western Australia. J. Geol. Soc. Aust., 24: 409—420.

Eichmann, R. and Schidlowski, M., 1975. Isotopic fractionation between coexisting organic carbon—carbonate pairs in Precambrian sediments. Geochim. Cosmochim. Acta, 39: 585—595.

Fripp, R.E.P., Donnelly, T.H. and Lambert, I.B., 1979. Sulfur isotope results for Archean banded iron-formations, Rhodesia. Spec. Publ. Geol. Soc. S. Africa, 5: 205—208.

Goldhaber, M.B. and Kaplan, I.R., 1974. The sedimentary sulfur cycle. In: E.D. Goldberg (Editor), The Sea, 5, Marine Chemistry. Wiley, New York, pp. 569—655.

Goldich, S.S., 1973. Ages of Precambrian iron-formations. Econ. Geol., 68: 1126—1134.

Goodwin, A.M., 1975. Sulfur isotope abundances in volcanic rocks of the Pashkokogan River area, Ontario. Proc. of Superior Geotraverse Symp., 38-1 to 38-7. Univ. Toronto, March 1975.

Goodwin, A.M., Monster, J. and Thode, H.G., 1976. Carbon and sulfur isotope abundances in Archean iron-formations and early Precambrian life. Econ. Geol., 71: 870—891.

Goodwin, A.M., Thode, H.G., Chou, C.L. and Karkhanis, S.N., 1982. Stratigraphy, lithology and geochemistry of the Archean iron-formations, Michipicoten area, Canada. (In preparation).

Gross, G.A., 1965. Geology of iron deposits in Canada. V. 1, General geology and evaluation of iron deposits. Geol. Surv. Can. Econ. Geol. Rep., 22: 1—181.

Gross, G.A., 1972. Primary features in cherty iron-formations. Sediment Geol., 7: 241—261.

Harrison, A.G. and Thode, H.G., 1958. Mechanism of the bacterial reduction of sulphate from isotope fractionation studies. Trans. Faraday Soc., 54: 84—92.

Heinricks, T.K. and Reimer, T.O., 1977. A sedimentary barite deposit from the Archean Fig Tree Group of the Barberton Mountain Land (South Africa). Econ. Geol., 72: 1426—1441.

Hekinian, R., Fervier, M., Bischoff, J.L., Picot, P. and Shanks, W.C., III, 1980. Sulfide deposits from the East Pacific Rise near 21°N: a mineralogical and geochemical study. Science, 207: 1433—1444.

Hickman, A.H., 1973. The North Pole barite deposits, Pilbara Goldfield. Ann. Rep. Geol. Surv. West. Austr., 1972: 57—60.
Ishii, M.M., 1953. The fractionation of sulphur isotopes in the plant metabolism of sulphates. M.Sc. Thesis, McMaster Univ., Hamilton, Ontario.
James, H.L., 1954. Sedimentary facies of iron-formation. Econ. Geol., 49: 235—293.
Kaplan, I.R. and Rittenberg, S.C., 1964. Microbiological fractionation of sulfur isotopes. J. Gen. Microbiol., 34: 195—212.
Kaplan, I.R., Sweeney, R.E. and Nissenbaum, A., 1969. Sulfur isotope studies on Red Sea geothermal brines and sediments. In: T. Degens and D.A. Ross (Editors), Hot Brines and Recent Heavy Metal Deposits. Springer-Verlag, New York, pp. 474—498.
Keith, M.L. and Weber, J.N., 1964. Carbon and oxygen isotopic composition of selected limestones and fossils. Geochim. Cosmochim. Acta, 28: 1787—1816.
Kemp, A.L.W. and Thode, H.G., 1968. The mechanism of the bacterial reduction of sulphate and of sulphide from isotope fractionation studies. Geochim. Cosmochim. Acta, 32: 71—91.
Lambert, I.B., 1978. Sulfur isotope investigations of Archean mineralization and some implications concerning geobiological evolution. J.E. Glover and D.I. Groves (Editors). Publ. Geol. Dept. of Ext. Services, Univ. West. Austr. 2, 45 pp.
Lambert, I.B., Donnelly, T.H., Dunlop, J.S.R. and Groves, D.I., 1978. Stable isotopic compositions of early Archean sulphate deposits of probable evaporitic and volcangenic origins. Nature, 276: 808—811.
McCrea, J.M., 1950. On the isotopic chemistry of carbonate and a paleotemperature scale. J. Chem. Phys., 18: 849—857.
Monster, J., Appel, P.W.U., Thode, H.G., Schidlowski, M., Carmichael, C.M. and Bridgwater, D., 1979. Sulphur isotope ratios in late and early Precambrian sediments and their implications regarding early environments and early life. Origins Life, 10: 127—136.
Moorbath, S., O'Nions, R.K. and Pankhurst, R.J., 1973. Early Archean age for the Isua iron-formation, West Greenland. Nature, 245: 138—139.
Morrison, G.H. and Freiser, H., 1957. Solvent Extraction in Analytical Chemistry, 62, 63, Wiley, New York, pp. 212—214.
Mottl, M.J., 1976. Chemical exchange between seawater and basalt during hydrothermal alteration of the oceanic crust. Ph.D. Thesis, Harvard Univ.
Mottl, M.J., Holland, H.D. and Corr, R.F., 1979. Chemical exchange during hydrothermal alteration of basalt by seawater — II. Experimental results for Fe, Mn and sulfur species. Geochim. Cosmochim. Acta, 43: 869—884.
Nielsen, P.E., 1974. The geochemistry of the Lyon Lake—Claw Lake sulphide bearing graphitic shale, Sturgeon Lake Area, Ontario. Hon. B.Sc. Thesis (unpubl.), Lakehead Univ., Ontario.
Peck, H.D., 1974. The evolutionary significance of inorganic sulfur metabolism. In: Carlile and Skehel (Editors), Symp. Soc. Gen. Microbiol., 24: 241—262.
Perry, E.C., Jr., Monster, J. and Reimer, T., 1971. Sulfur isotopes in Swaziland system barites and the evolution of the Earth's atmosphere. Science, 171: 1015—1016.
Perry, E.C., Jr., Tan, F.C. and Morey, G.B., 1973. Geology and stable isotope geochemistry of the Biwabik iron-formation, Northern Minnesota. Econ. Geol., 68: 1110—1125.
Postgate, J.R., 1968. The sulfur cycle. In: G. Nickless (Editor), Inorganic Sulfur Chemistry. Elsevier, Amsterdam, pp. 259—279.
Rees, C.E., 1969. Fractionation effects in the measurement of molybdenum isotope abundance ratios. Int. J. Mass Spectrom. Ion Phys., 3: 71—80.
Ripley, E.M. and Nicol, D.L., 1981. Sulfur isotopic studies of Archean slate and graywacke from Northern Minnesota: evidence for the existence of sulfate reducing bacteria. Geochim. Cosmochim. Acta, 45: 839—846.
Rye, R.O. and Ohmoto, H., 1974. Sulfur and carbon isotopes and ore genesis: a review. Econ. Geol., 69: 824—843.

Rye, D.M. and Rye, R.O., 1974. Homestake gold mine, South Dakota: 1. Stable isotope studies. Econ. Geol., 69: 293—317.

Schoell, M. and Wellner, F.W., 1981. Anomalous ^{13}C depletion in early Precambrian graphites from Superior Province, Canada. Nature, 290: 696—699.

Schoell, M. and Wellmer, F.W., 1982. Anomalous ^{13}C depletion in Precambrian organic carbon. Nature, 295: 172.

Shanks, W.C., III and Bischoff, J.L., 1980. Geochemistry, sulfur isotope composition and accumulation rates of Red Sea geothermal deposits. Econ. Geol., 74: 445—459.

Shanks, W.C., III, Bischoff, J.L. and Rosenbauer, R.J., 1981. Seawater sulfate reduction and sulfur isotope fractionation in basaltic systems: interaction of seawater with fayalite and magnetite at 200 to 350°C. Geochim. Cosmochim. Acta, 45: 1977—1995.

Shegelski, R., 1978. Stratigraphy and geochemistry of Archean iron-formations in the Sturgeon Lake—Savant Lake greenstone terrain, N.W. Ontario. Ph.D. Thesis, Univ. of Toronto, Ontario.

Swenson, W.T., 1960. Geology of the Nakina iron property Ontario. Am. Inst. Mining Eng., 217: 451—458.

Thode, H.G., Monster, J. and Dunford, H.B., 1961. Sulfur isotope geochemistry. Geochim. Cosmochim. Acta, 25: 159—174.

Trudinger, P.A. and Cloud, P.E., 1981. Report on Conference. Nature, 292: 494—495.

Vinogradov, V.I., Reimer, T., Leites, A.M. and Smelov, S.B., 1976. The oldest sulfates in Archean formations of the South African and Aldan Shields and the evolution of the Earth's oxygenic atmosphere. Litol. Polezn. Iskop., 11: 12—27 (in Russian).

FILAMENTOUS FOSSIL BACTERIA FROM THE ARCHEAN OF WESTERN AUSTRALIA

S.M. AWRAMIK

Department of Geological Sciences, Preston Cloud Research Laboratory, University of California, Santa Barbara, California 93106 (U.S.A.)

J.W. SCHOPF and M.R. WALTER*

Precambrian Paleobiology Research Group, Department of Earth and Space Sciences and the Institute of Geophysics and Planetary Physics, University of California, Los Angeles, California 90024 (U.S.A.)

ABSTRACT

Awramik, S.M., Schopf, J.W. and Walter, M.R., 1983. Filamentous fossil bacteria from the Archean of Western Australia. Precambrian Res., 20: 357—374.

Four morphotypes of structurally preserved, filamentous fossil bacteria have been discovered in petrographic thin sections of laminated, carbonaceous cherts from the ~3500 Ma-old Warrawoona Group of northwestern Australia. These tubular and septate microfossils are interpreted here as being syngenetic with Warrawoona sedimentation; as such, they are apparently the oldest such fossils now known in the geological record. The diversity of this assemblage, and the evident complexity of its individual components, suggest that the beginnings of life on Earth may have appreciably pre-dated the deposition of the Warrawoona sediments.

INTRODUCTION

Two important papers have appeared reporting the discovery of finely laminated, mound-shaped stromatolites in ~3500 Ma-old metasediments of the Warrawoona Group of the eastern Pilbara region of northwestern Australia (Lowe, 1980; Walter et al., 1980). These distinctive megascopic structures, the most ancient stromatolitic sediments yet reported, have been interpreted as being "the oldest firmly established biogenic deposits now known from the geologic record" (Walter et al., 1980). However, because of the apparent scarcity of stromatolites in Archean terranes, the great age of the Warrawoona structures, and the absence from these stromatolites of cellularly

*Present address: Baas Becking Geobiological Laboratory, P.O. Box 378, Canberra, ACT 2601, Australia.

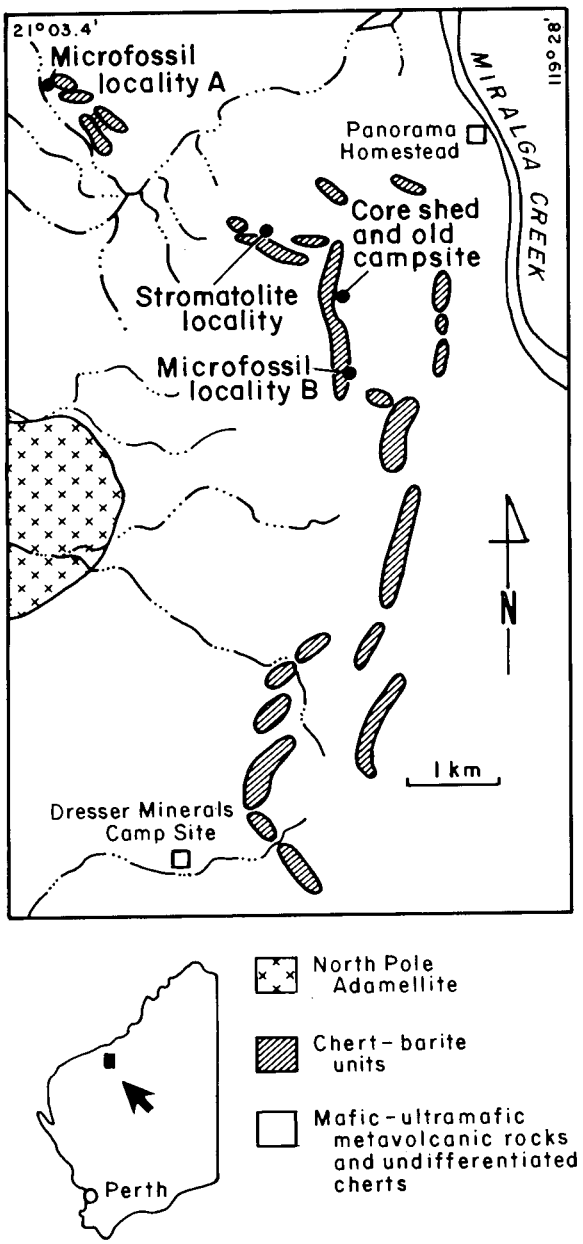

Fig. 1. Map of northeastern part of North Pole Dome, eastern Pilbara Block, Western Australia, showing localities from which cherts containing microfossils and possible microfossils were collected. Also shown is the stromatolite locality noted in Walter et al. (1980).

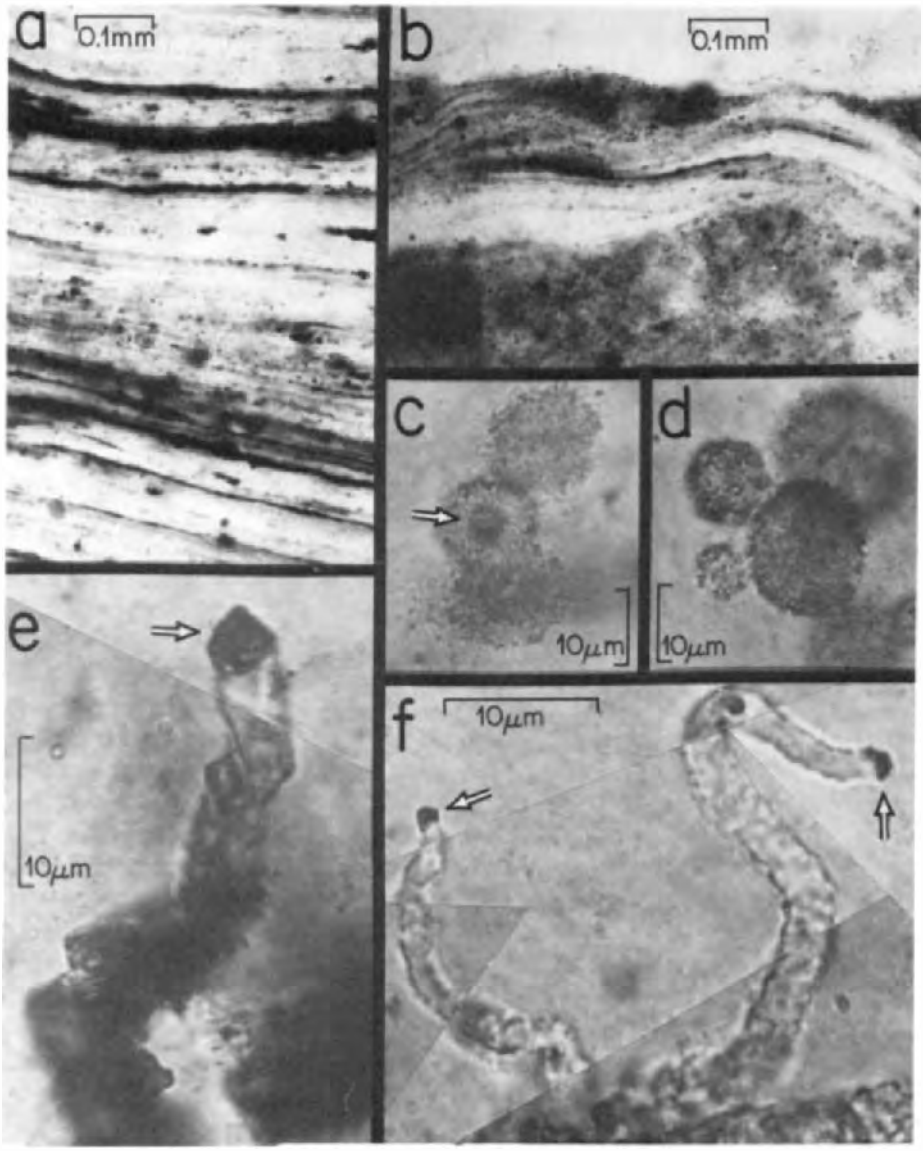

Fig. 2. Optical photomicrographs showing organic-rich, evidently stromatolitic laminae (a, b), spheroidal, mineralic, micropseudofossils (c, d), and filamentous, inorganic micropseudofossils (e, f), in petrographic thin sections of black cherts of the Archean Warrawoona Group of Western Australia; parts e and f are photomontages. (a) Thin section 517-1-A, stage coordinates 51.2 × 103.2, CPC no. 20208; (b) 002-1-A, 34.6 × 104.8, CPC no. 20209; (c, d) SMA 298, 37.6 × 95.5, CPC no. 20210; (e) SMA 298, 41.0 × 107.2, CPC no. 20211; (f) SMA 298, 41.0 × 106.9, CPC no. 20212. Arrow in part c points to center of nucleation about which mineralic material has accumulated to produce the spheroidal pseudofossil; arrows in parts e and f point to hematitic pseudomorphs after pyrite at the ends of the trails produced by "ambient pyrite grains".

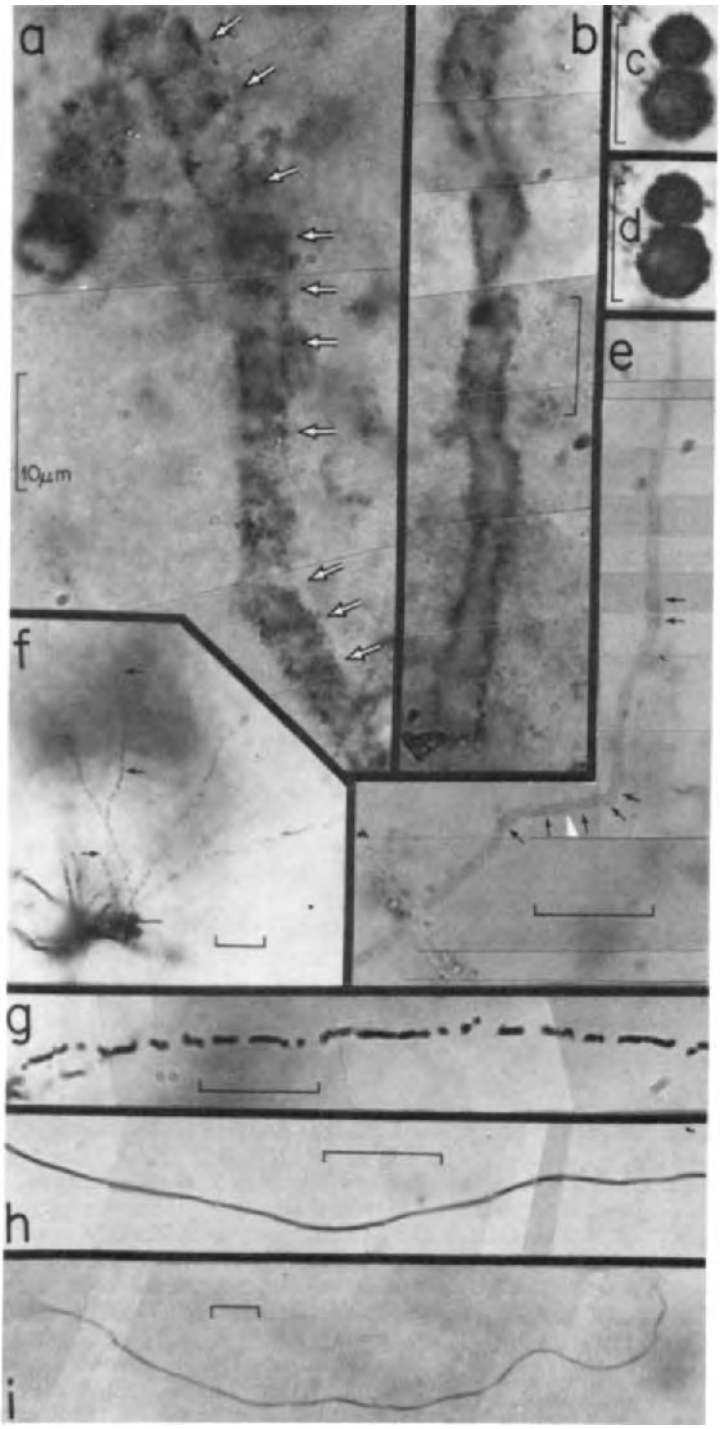
a
b
c
d
e
10µm
f
g
h
i

preserved remnants of the microorganisms presumed to be responsible for their construction, it has been suggested that the Warrawoona structures should be regarded with caution when used as evidence for early life (Nisbet, 1980; Buick et al., 1981; Groves et al., 1981). Subsequent to published descriptions of the Warrawoona stromatolites, several papers have made reference to the discovery of cellularly preserved, diverse, predominantly filamentous microfossils in laminated black cherts from this same sequence of Western Australian rocks (Awramik, 1981, 1982; Nisbet and Pillinger, 1981), with certain of these reports raising questions of the syngenicity, and thus the age, of the reported fossil microbes (Buick et al., 1981; Groves et al., 1981). Here we describe this assemblage in some detail and summarize the data that lead us to regard these fossil microorganisms as comprising firm evidence of Archean life.

THE WARRAWOONA GROUP

The Warrawoona Group, the lowest group of the Pilbara Supergroup, is a 14 km-thick sequence of dominantly ultramafic to mafic metavolcanic rocks containing regionally extensive, interstratified, cherty sedimentary units <50 m thick (Barley et al., 1979; Hickman, 1980). Portions of the sequence, including the carbonaceous cherts from which microfossils are here reported (Fig. 1) and the cherts and chert—barite from which stromatolites have previously been described (Lowe, 1980; Walter et al., 1980; Buick et al., 1981), were deposited in shallow subaqueous to intermittently subaerially exposed settings. Regionally, the metamorphic grade is within the greenschist facies, although locally it is lower, having reached only the prehnite—pumpellyite facies (~250—300°C, 2—4 kb) (Hickman and Lipple, 1978). In the cherts studied here, the quality of organic preservation as evidenced by both optical microscopy (Figs. 2a, b, 3a, b, e, h, i) and by x-ray diffraction studies of isolated kerogen (Hayes et al., 1983) is consistent with metamorphism in the prehnite—pumpellyite facies.

The age of the Warrawoona Group of ~3500 Ma is well established: volcanics from the lower third of the sequence have been dated by the Sm—Nd method at 3556 ± 32 Ma (Hamilton et al., 1980); lavas from the Duffer For-

---

Fig. 3. Optical photomicrographs showing microfossils (a, b, e, h, i) and "possible microfossils" (c, d, f, g) in petrographic thin sections of black carbonaceous cherts of the ~ 3500 Ma-old Warrawoona Group of Western Australia; line for scale in each figure represents 10 μm; parts a, b, e, g—i are photomontages; see text for details regarding source of figured specimens. (a) *Primaevifilum septatum*, n. gen., n. sp.; arrows point to septa. (b) *Siphonophycus antiquus*, n. sp. (c, d) Paired, "unicell-like" organic spheroids, referred here to *Archaeosphaeroides pilbarensis*, n. "sp.", showing granular surface texture (c) and equatorial cross sections (d). (e) *Eoleptonema australicum*, n. gen., n. sp.; arrows point to indistinct possible septations. (f, g) Filamentous "possible microfossils" referred here to *Warrawoonella radia*, n. "gen.", n. "sp."; arrows (f) point to a single long filament radiating from a "holdfast-like" base. (h, i) A single specimen of *Archaeotrichion contortum* (i), the medial portion of which is shown at higher magnification in h.

mation, occurring near the middle of the sequence, have yielded a U—Pb date on zircons of 3452 ± 16 Ma (Pidgeon, 1978) and a model lead age on galena of ~3500 Ma (Sangster and Brook, 1977), while galena in a barite vein cutting the fossiliferous sequence has yielded a model lead age of ~ 3400 Ma (J. Richards, quoted in Walter et al., 1980); and the Pilbara Supergroup as a whole was deformed by a post-depositional event ~3100) 2900 Ma ago (DeLaeter and Blockley, 1972; Oversby, 1976). Thus, the Warrawoona Group is among the oldest, well-dated, relatively well-preserved rock sequences now known in the geological record.

MICROFOSSILIFEROUS CHERTS

Microfossils and possible microfossils have been detected in carbonaceous, laminated cherts of the Warrawoona Group collected at two localities, A and B, 4.7 km apart, both within the North Pole Dome area of the Pilbara Block (Fig. 1). Chert from locality A is apparently from a unit low in the northeast flank sequence (although the precise layer from which the fossiliferous samples were collected in 1977 by S.M.Awramik has not been relocated and thus, its detailed stratigraphic relations are unknown); chert from locality B is from the lowest stratiform chert horizon of the Group. At both localities, the outcrops form resistant ridges of banded chert commonly exhibiting a blocky fracture pattern and a reddish-brown, limonite-stained, weathered surface. The cherts are composed dominantly of an interlocking mosaic of microcrystalline quartz, with pyrite and rhombs of dolomite (30—150 μm in size) as common subsidiary components. Although macroscopic stromatolites have not been detected at either locality A or B, cherts from both localities exhibit stromatolitic lamination (Fig. 2a, b) with dark, relatively thin (5—8 μm), organic-rich laminae alternating with light, thicker (10—500 μm), kerogen-free layers; in especially well-preserved areas, dark—light pairs are ~ 5—20 μm thick. The laminated fabric of the rock parallels the bedding. Both modern (Gebelein, 1969) and ancient (Awramik and Semikhatov, 1979) stromatolites exhibit these light/thicker and dark/thinner laminar relationships. Quartz grain size, ranging from ~ 5 μm in the kerogen-rich laminae to 40 μm or more in organic-free regions, is inversely correlated with organic content. In thin sections, chert specimens from A show multiple fracturing. Most of the fractures cut the laminae at various angles, but a few parallel the laminae for several millimeters before cutting across to the adjacent lamina. In chert from both localities, lenses of chalcedony occur rather commonly in kerogen-free areas, apparently as a result of mineral-infilling of former voids. Lamination in the chert grades from relatively planar and regularly banded, in one sample from A (Fig. 2a), to undulatory and lenticular, from both A and B (Fig. 2b), which is a stromatolitic microstructure of the "distinct, wavy, striated" type (Walter, 1972). Diffuse boundaries between light and dark laminae, a characteristic of biogenic stromatolites, are common in cherts from both A and B (Fig. 2b). Abrupt boundaries between

laminae are more characteristic of non-biogenic stromatolite-like structures (Walter, 1976). The stromatolitic layers are interlaminated with layers of intraclast grainstone, a feature common in many stromatolites. Many of the microfossils described here, but especially the tubular fossils described below as *Siphonophycus antiquus*, are found within dark laminae and are parallel or subparallel to the lamination. Thus, we conclude from the evidence that these chert samples contain stromatolitic laminae.

Geological evidence and facies relationships (where discernable) indicate that both of the chert beds were deposited in shallow water; at B, possibly intermittently exposed lagoonal environments well within the photic zone prevailed (Buick et al., 1981; Groves et al., 1981). Thus, in mineralogy, petrology, laminated organization and general paleoecological setting, these Warrawoona cherts seem quite similar to fossiliferous stromatolitic cherts of Proterozoic, such as those of the Gunflint Iron (Barghoorn and Tyler, 1965) and Bitter Springs (Schopf, 1968) Formations.

THE BIOGENICITY AND SYNGENICITY OF THE WARRAWOONA MICROFOSSILS

Reports of the occurrence of microfossils in Archean rocks merit close scrutiny because of their implications regarding the antiquity and earliest evolution of life on Earth. For such reports to be acceptable, it must be established that: (1) the rocks in question are in fact of Archean age; (2) the microfossil-like objects are actually biogenic; and (3) the microfossils were emplaced in the deposit at the time of original sedimentation. Although numerous putative microfossils have been reported from Archean sediments since 1965, critical appraisal has shown that many of the reports have fallen short with regard to one or another of these three criteria (Schopf and Walter, 1980; Bridgwater et al., 1981). Indeed, of the 29 classes of such microstructures so far reported (Schopf and Walter, 1980), only the carbonaceous spheroids reported from several horizons of the ~ 3500 Ma-old Swaziland Supergroup of South Africa (Muir and Grant, 1976; Knoll and Barghoorn, 1977; Strother and Barghoorn, 1980) seem plausibly biogenic. However, because of their simple morphology and (apparently) their relatively poor preservation, the biological origin of even these relatively convincing examples has been questioned (Schopf, 1976; Cloud and Morrison, 1979). Spheroids from the Warrawoona cherts (described here as *Archaeosphaeroides pilbarensis*) well illustrate the problem (Dunlop et al., 1978). Although paired carbonaceous spheroids occur in the cherts (Fig. 3c, d) and are virtually identical to Archean microstructures regarded by other workers as assuredly biogenic (Muir and Grant, 1976), we also find "microfossil-like" mineralic, non-biogenic spheroids (Fig. 2c, d). At present, evidence is insufficient to indicate whether simple carbonaceous spheroids of the type occurring in the Warrawoona and other Archean cherts are definitely biogenic or whether they might actually be of non-biological origin.

However, filamentous fossil-like microstructures, especially if they are of relatively complex morphology and are comparable to structures of estab-

lished biogenicity, can be interpreted with a greater degree of confidence. Although filamentous micropseudofossils are known from numerous Precambrian cherts (Schopf, 1975; Cloud, 1976a), including those from the Warrawoona Group studied here (Fig. 2e, f), artifacts of this type can usually be readily distinguished from bona fide microfossils by their angular, crystalline morphology, their inorganic (rather than carbonaceous) composition, and, in the case of trails left by "ambient pyrite grains" (Tyler and Barghoorn, 1963; Knoll and Barghoorn, 1974), by their striated, tubular appearance and the presence of euhedral pyrite grains (or mineralogic pseudomorphs after pyrite) at one end of the structures (Fig. 2e, f).

In addition to micropseudofossils of inorganic origin (Fig. 2c—f), and filamentous aggregates (Fig. 3f, g) and organic spheroids (Fig. 3c, d) of possible, but uncertain biogenicity, the Warrawoona cherts contain several types of bona fide filamentous microfossils (Fig. 3a, b, e, h, i). With regard to the first of the criteria noted above, the Archean age of the fossiliferous cherts seems amply demonstrated by the available geological data discussed above. As for the second criterion, the biogenicity of these filaments seems evident: such filaments (Fig. 3a, b, e, h, i) are of organic, carbonaceous composition (as evidenced by their texture, dark brown to black color and other optical characteristics and by the fact that they can be freed from their encompassing mineral matrix by palynological techniques); they are similar in size, form and level of complexity to filamentous microorganisms known from other Precambrian stromatolitic cherts (Barghoorn and Tyler, 1965; Schopf, 1968), and from comparable modern mat-building microbial communities (Monty, 1967; Walter et al., 1973; Javor and Castenholz, 1981); and like the microbes comprising such younger microbial communities, the Warrawoona filaments occur within, and are commonly oriented parallel to, the organic-rich stromatolitic laminae (see Awramik, 1981, pp. 90—91, Fig. 2a, b). Moreover, they are numerous, ranging from $\sim 625 \pm 75$ filaments cm^{-3} for *Archaeotrichion contortum* (Fig. 3h, i), the most abundant morphotype of the assemblage, to $\sim 65 \pm 20$ filaments cm^{-3} for *Siphonophycus antiquus* (Fig. 3b), one of the less commonly occurring components; they are of diverse form, comprising four distinct morphological classes, each of which is comparable to specific living microbial taxa; and some aspects of the preserved fossils are interpretable in terms of such uniquely biological features as cell division (inferred from the occurrence of septate, uniseriate filaments; Fig. 3a), coloniality (also evidenced by the septate filaments) and, apparently, gliding motility (suggested by the presence of tubular, evidently discarded empty sheaths; Fig. 3b).

Finally, with regard to the third criterion: Are the microfossils syngenetic with deposition of the Warrawoona sediments? The microfossils are demonstrably present in petrographic thin sections of the cherts (Fig. 3a, b, e, h, i); they are commonly oriented parallel to, and in part comprising, kerogenous stromatolitic laminae; and they have been organically preserved by permineralization in fine-grained quartz, in a manner identical to that of other Pre-

cambrian microbiotas, with the boundaries of the chemically precipitated quartz grains passing through, but not disrupting, the delicate microorganisms.

Secondarily emplaced dikes, veins and veinlets of carbonaceous chert are common in the North Pole region. One such dike occurs within 5 m of locality B. Thus, the possibility has been alluded to (Groves et al., 1981; Buick et al., 1981) that the laminar fabric of the chert at locality B may have resulted from sheet crack formation (Ramsay, 1980) during the intrusion of this dike, rather than being microbially produced stromatolitic laminae, and that kerogen and the associated filaments (viz., *Warrawoonella radia*) may have been emplaced during this intrusive episode. By analogy, this possibility might also be suggested for the cherts from locality A, but at that locality the microfossil-bearing layer has not been relocated, hence the detailed field relations of the fossiliferous chert are unknown. In addition, in petrographic thin sections from locality A, several generations of silica can be recognized, including that in secondarily infilled veinlets. The possibility has thus been raised that the microfossils and kerogen at this locality may have been emplaced during weathering rather than being syngenetic with primary sedimentation (Buick et al., 1981).

Neither of these possibilities appears supported by available evidence. The dike—sheet crack hypothesis is inconsistent with: (1) the micromorphology of the microfossiliferous chert laminae which are indistinguishable in all salient characteristics from laminae of fossil and modern stratiform stromatolites (including their intimate interlamination with intraclast grainstone), but which differ significantly from the sheet cracks described by Ramsay (1980) (e.g., they lack any sign of disruption or displacement such as the occurrence of fractured grains with serrated margins); (2) the absence of microfossils from secondary, silica-infilled voids, veinlets and fracture filling which are readily distinguishable from early or first generation chert on the basis of their distribution, and the size and shape of their component grains; and (3) the distribution and orientation of the broad filaments of the assemblage (Fig. 3a, b) which, like the filamentous members of extant and fossil stromatolitic biocoenoses, are commonly aligned parallel or subparallel to the organic-rich laminae. Moreover, to the best of our knowledge, it has never been demonstrated that microfossils can be introduced into sedimentary rocks by this proposed mechanism. Similarly, the possibility that the microfossils at locality A may have been emplaced during weathering is inconsistent with petrographic evidence (indicating that the fossils occur only in the earliest formed chert and are absent from all secondarily emplaced mineral phases) and with available micropaleontological data (e.g., the dark color and degraded nature of the kerogenous microfossils from both localities). In addition, although not available from locality A, organic geochemical evidence (e.g., x-ray diffraction, $\delta^{13}C$ and H/C measurements) from the numerous other localities so far investigated (Hayes et al., 1983) support interpretation of the Warrawoona kerogen as being geologically old and metamor-

phically altered rather than being a result of Tertiary or modern contamination. Further, the entire assemblage distinctly differs from all other Precambrian and younger microbial assemblages now known and is unlike described chasmolithic or endothic assemblages of either Recent or older age (Golubic, 1973; Golubic et al., 1975; Friedmann, 1982).

MODERN MICROBIAL COMPARISONS

In general morphology, these filamentous microfossils (which for purposes of reference are formally described below) are comparable to a rather broad spectrum of modern prokaryotic microbes, including pigmented and colorless gliding bacteria, green sulfur bacteria, sheathed bacteria, and small diameter oscillatoriacean cyanobacteria. The spheroidal "possible microfossils" (viz., *Archaeosphaeroides pilbarensis*, described below) seem especially similar to unicellular cyanobacteria; they also resemble spheroidal gliding bacteria, purple non-sulfur bacteria, purple sulfur bacteria, and methanogenic bacteria. The filamentous "possible microfossils" (described below as *Warrawoonella radia*) are at least roughly similar to such rosette-forming modern colonial bacteria as *Thiothrix* and *Leucothrix*.

These modern morphological analogues are metabolically diverse, including obligately aerobic chemoorganotrophs; aerobic or microaerophilic or facultative photoautotrophs; and obligately anaerobic chemolithotrophs and mixotrophs. Moreover, it is conceivable that the fossil taxa described here may have been members of now extinct lineages, forms that were only distantly related to, and perhaps physiologically different from, their modern morphological counterparts.

Although morphology alone provides limited insight into the possible metabolic characteristics of the Warrawoona microorganisms, their mode of occurrence is somewhat more suggestive. Specifically, the presence of these microfossils in laminar, stromatolitic deposits that formed at the sediment—water interface, an organization of a type that in younger sediments is known to have been produced principally as a result of the light-dependent growth of filamentous microbes (Monty, 1967; Javor and Castenholz, 1981), suggests that at least some of the filamentous taxa were probably photoresponsive. This possibility is consistent with the occurrence of naked (unsheathed) trichomes (Fig. 3a) and of empty tubular sheaths (Fig. 3b) which, together with the common orientation of these fossils parallel to the mat-like laminae, suggests that some of the filaments may have been capable of gliding, possibly phototactic, motility (Golubic and Barghoorn, 1977). However, the empty sheaths and trichomes may represent degradational remnants of originally sheathed trichomes. In addition, and by comparison with modern-mat building microbial communities in which aerobes and microaerophiles are dominant only within the top few millimeters or less of sediment, it seems likely that at least some of the Warrawoona organisms were

anaerobic (if the atmosphere at this time was essentially anoxic, as has commonly been postulated (Cloud, 1979), it is possible that the biota was entirely devoid of oxygen-utilizing microbes).

Carbon isotopic abundances measured in organic matter from the cherts at locality B suggest that some members of the community may have been capable of autotrophic CO_2-fixation, and the total organic carbon content of these sediments, similar to that of stromatolitic cherts of younger geologic age, may indicate that heterotrophic recycling of organic carbon occurred within the Warrawoona microbial mats. Analyses at the University of California, Los Angeles (UCLA) of carbon in two Warrawoona chert specimens from Precambrian Paleobiology Research Group (PPRG) sample no. 002 from locality B have yielded $\delta^{13}C_{PDB}$ values of $-35.1‰$ (total organic carbon (TOC) = 0.67 mg g^{-1} of rock) and $-35.7‰$ (TOC = 0.53 mg g^{-1}). Comparable measurements of organic matter in fossiliferous cherts from the ~ 2000 Ma-old Gunflint Iron Formation have yielded values of $-32.0‰$ (TOC = 0.43 mg g^{-1}) and $-31.5‰$ (TOC = 0.39 mg g^{-1}), and for the ~ 850 Ma-old Bitter Springs Formation, $-23.0‰$ (TOC = 0.57 mg g^{-1}) and $-22.7‰$ (TOC = 0.40 mg g^{-1}). Details regarding these measurements will be published by Hayes et al. (1983).

Thus, as a first approximation, it seems probable that the Warrawoona biota included both heterotrophs and autotrophs, that at least some of the microorganisms were anaerobes, and that the major mat-building organisms were filamentous and phototactic. However, available data do not indicate whether the presumed phototactic forms were in fact photosynthetic autotrophs (rather than being photoheterotrophs, for example) or, if actually photoautotrophs, whether they were aerobic, anaerobic or facultative photosynthesizers.

The microbial fossils reported here from the ~ 3500 Ma-old Warrawoona cherts are significant for the following reasons.

(1) For the reasons noted above, we regard the fossils described here as being syngenetic with Warrawoona sedimentation; as such they are apparently among the oldest cellularly preserved filamentous fossil microorganisms now known from the geological record.

(2) In morphology, in mode of occurrence within the finely laminated Warrawoona cherts, and in prokaryotic affinities, the microorganisms are comparable to microfossils known from many stromatolitic deposits of younger Precambrian age. Their presence is thus consistent with, and seems supportive of, the biological interpretation of non-microfossiliferous stromatolites reported from the same region (Lowe, 1980; Walter et al., 1980).

(3) The microbiota described here appears to establish that diverse, multi-component communities of benthonic, prokaryotic microbes, possibly including anaerobes, phototactic filaments, and both heterotrophs and autotrophs, were extant as early as 3500 Ma ago. The diversity of this assemblage and the biological complexity of individual components would imply that either the beginnings of life on Earth must have appreciably pre-dated the

time of deposition of the Warrawoona cherts or that once life appeared, the evolution of several major metabolic pathways proceeded rapidly.

(4) The paleoecology of the fossiliferous cherts, together with that previously adduced for the Warrawoona stromatolites (Lowe, 1980; Walter et al., 1980) and stromatolite-like structures (Buick et al., 1981), indicates that shallow water and intermittently exposed environments were habitable by microorganisms some 3500 Ma ago. Thus, it is probable that effective mechanisms for coping with high intensity visible light and UV-radiation (Awramik et al., 1976; Rambler and Margulis, 1980) had already evolved, and it is also possible that a biologically effective UV-absorbent ozone screen had been established. It follows, that in addition to shallow aqueous settings, land surfaces and open oceanic water may also have been habitable.

(5) Finally, and in the context of many contributions made by other workers over the past decade in the search for evidence of very ancient life (e.g., Muir and Grant, 1976; Knoll and Barghoorn, 1977) these microfossils firmly establish the paleobiological potential of Archean-age deposits.

SYSTEMATIC PALEONTOLOGY

Localities

Locality A (Fig. 1) is on the west side of a 50 m high east—west trending bedded chert ridge, 400 m due east of the intersection of the Dresser Minerals haulage road (from the occupied mine site of June, 1980) and the road to Panorama Homestead; grid reference 504683.5, North Shaw 1:100 000 topographic sheet. This is Awramik's locality for sample number A4 of 9/10/77 (which was collected from outcrop) and the source of thin sections SMA 298 and 299; this same locality is the source of PPRG sample no. 517 from which thin section 517-1-A was prepared.

Locality B (Fig. 1) is 1 m below the top of an outcrop occurring at the entrance to a small gorge on the south side of the gorge beside a track at grid reference 536648, North Shaw 1:100 000 topographic sheet. This is the source of PPRG sample no. 002 (thin sections 002-1-A, 002-1-B); oriented samples were collected from the outcrop in June, 1979, by a field party consisting of M.R. Walter, R. Buick, J.S.R. Dunlop, D.I. Groves, J.M. Hayes and H.J. Hofmann.

Location and repository of figured specimens

Stage coordinates of specimens shown in Figs. 2 and 3 are given for a Leitz microscope with the thin section oriented with the slide label toward the left and an 'x' marked with a diamond scribe on the left front corner of the microscope slide. Coordinates for the 'x' on each slide are as follows: thin section SMA 298, coordinates 67.0 × 111.1; SMA 299, 66.1 × 111.6; 517-1-A, 71.9 × 134.6; 002-1-A, 74.3 × 113.8; 002-1-B, 73.3 × 113.7. All

figured specimens are deposited in the Commonwealth Palaeontological Collections (CPC), Bureau of Mineral Resources, Canberra, Australia.

Description of detected microfossils

Kingdom Procaryotae Murray, 1968, *Incertae Sedis.*

Genus *Primaevifilum* Schopf, n. gen.

Type species: *Primaevifilum septatum* Schopf, n. sp.

Diagnosis: trichomes uniseriate, unbranched and cylindrical, not at all, to slightly constricted at septa, apparently somewhat tapering toward apices; cross walls distinct and granular, or indistinct; trichomes solitary, commonly slightly curved, bent or disrupted, up to 120 μm long (incomplete specimen); cells approximately isodiametric to 1½ times as long as wide, commonly 4.0—6.0 μm wide and 4.5—7.0 μm long (10 individuals); reproduction apparently by fragmentation of trichomes; terminal cells, specialized intercalary cells (e.g., heterocysts, etc.) and encompassing sheaths not observed.

Etymology: with reference to geologic age *(primaevus*, L., early, young) and threadlike form *(filum*, L., thread).

Species *Primaevifilum septatum* Schopf, n. sp. (Fig. 3a).

Diagnosis: as for the genus.

Etymology: with reference to the presence of septa *(septum*, L., partition).

Type locality: locality A.

Type specimen: trichome shown in Fig. 3a (thin section SMA 299, stage coordinates 45.1 X 98.4, CPC no. 20201).

Remarks: *P. septatum* has been detected in cherts only from locality A. In general form, this taxon is similar to the Proterozoic taxon *Gunflintia grandis* Barghoorn, from the ~ 2000 Ma-old Gunflint Iron Formation in Canada (Barghoorn and Tyler, 1965); it differs from this taxon in cell size and in its apparent tendency to taper toward apices.

Genus *Siphonophycus* em. Schopf, 1968

Type species: *Siphonophycus kestron* Schopf, 1968.

Diagnosis (emended): filaments cylindrical, unbranched, tubular (non-septate); partially flattened, circular to elliptical in cross sections; commonly solitary and quite long with granular to finely rugose surface texture.

Species *Siphonophycus antiquus* Schopf, n. sp. Fig. 3b.

Diagnosis: as for the genus (emended). Filaments tubular to flattened, ranging from ~ 3.0 to 9.5 μm in diameter and up to 600 μm long (180 individuals).

Etymology: with reference to great geological age *(antiquus*, L., old, ancient).

Type locality: locality A.

Type specimen: filament shown in Fig. 3b (thin section SMA 299, stage coordinates 46.7 X 103.0, CPC no. 20202).

Remarks: *S. antiquus* has been detected in cherts only from locality A. Filaments referred to the one previously described species of this genus, *S. kestron* from the ~ 850 Ma-old Bitter Springs Formation of central Australia (Schopf, 1968), range from ~ 8 to 15 μm in diameter; thus, *S. antiquus* differs in diameter from this taxon. It also differs from members of the similarly tubular Proterozoic genus *Eomycetopsis* Schopf (1968) as recently emended by Knoll and Golubic (1979), both in its range of diameter and in its predominantly solitary habit.

Genus *Eoleptonema* Schopf, n. gen.

Type species: *Eoleptonema australicum* Schopf, n. sp.

Diagnosis: filaments slender, long, unbranched; possibly septate (apparently composed of uniseriate, isodiametric to somewhat elongate cells); 0.8—1.1 μm in diameter and up to 340 μm long (260 individuals); solitary or in groups of a few intertwined individuals.

Etymology: with reference to geological age *(eos*, Gr., dawn, early) and narrow, threadlike habit *(leptos*, Gr., thin, delicate, plus *nema*, Gr., thread).

Species *Eoleptonema australicum* Schopf, n. sp. (Fig. 3e).

Diagnosis: as for the genus.

Etymology: with reference to type locality in northwestern Australia.

Type locality: locality A.

Type specimen: filament shown in Fig. 3e (thin section SMA 299, stage coordinates 51.1 X 103.7, CPC no. 20204).

Remarks: *E. australicum* has been detected in cherts only from locality A. Among previously described Precambrian taxa, *E. australicum* is perhaps most similar to *Tenuofilum septatum* Schopf of the Late Proterozoic Bitter Springs Formation of central Australia (Schopf, 1968); *T. septatum*, however, is broader (1.1—1.5 μm, with an average diameter of 1.3 μm), and is more evidently septate, than *E. australicum*.

Genus *Archaeotrichion* Schopf, 1968.

Type species: *Archaeotrichion contortum* Schopf, 1968.

Remarks: In the Warrawoona Group, *A. contortum* has only been detected in cherts from locality A. As originally described from the ~ 850 Ma-old Bitter Springs Formation (Schopf, 1968), this taxon was established to include solitary or irregularly entangled, unbranched, non-septate, nontapering, threadlike filaments < 1 μm in diameter (commonly 0.5—0.7 μm broad) and up to 110 μm long. Except for their slightly smaller diameter (commonly as narrow as 0.3 μm) and their somewhat greater length (with individuals ranging up to 180 μm long) specimens (1200 individuals) of the type shown here in Fig. 3h, i, from the Waarawoona cherts meet all of these criteria (locality A, thin section SMA 299, stage coordinates 51.7 X 100.9, CPC no. 20207). Thus, in the absence of significant distinguishing characteristics, and despite the great difference in geological age of the Bitter Springs and North Pole deposits, the Archean fossils are referred here to this Late Proterozoic taxon.

Possible microfossils

"Genus" *Archaeosphaeroides* Schopf and Barghoorn, 1967.

Type "species": *Archaeosphaeroides barbertonesis* Schopf and Barghoorn, 1967.

"Species" *Archaeosphaeroides pilbarensis* Schopf, n. "sp." (Fig. 3c, d).

Diagnosis: hollow, isolated or paired organic spheroids, 4.0 to ~ 14 μm in diameter (average diameter = 6.5 μm); wall thin, of somewhat variable thickness, commonly coarsely and irregularly granular.

Etymology: with reference to the type locality in the Pilbara Block of northwestern Australia.

Type locality: locality A.

Type specimen: the larger of the two spheroids shown in Fig. 3c, d (thin section SMA 299, stage coordinates 48.5 × 96.9, CPC no. 20203).

Remarks: *A. pilbarensis* has been detected in cherts only from locality A. "Unicell-like" organic spheroids of this type have been reported from several Archean deposits, the most comparable such forms being those of the ~3500 Ma-old Swaziland Supergroup of South Africa (Muir and Grant, 1976; Knoll and Barghoorn, 1977; Strother and Barghoorn, 1980). As has been discussed in several publications (Schopf, 1975; Cloud, 1976a; Cloud and Morrison, 1979), however, these bodies are of such simple form that their biogenicity is difficult to establish on the basis of morphology alone. Recognizing this problem, the Warrawoona spheroids are regarded here as only "possible microfossils"; for purposes of reference, they are referred to the "genus" *Archaeosphaeroides*, the one previously described "species" of which, *A. barbertonesis* (from the Swaziland Supergroup; Schopf and Barghoorn, 1967) ranges in diameter from ~ 15 to 24 μm; *A. pilbarensis* thus differs in size from the previously described form.

"Genus" *Warrawoonella* Schopf, n. "gen."

Type "species": *Warrawoonella radia* Schopf, n. "sp."

Diagnosis: narrow, unbranched, cylindrical, sinuous to more-or-less straight, apparently non-septate filaments occurring singly or more commonly in clusters of variable number (2—30) radiating irregularly from a "holdfast-like" base and forming loosely-packed, hemispheroidal groups; filaments 0.5—0.75 μm in diameter, up to 135 μm long; filaments commonly appear mineral-encrusted (with iron- or manganese-oxides?) and disrupted into a uniseriate row of short, rod-like segments. Seventy clusters detected.

Etymology: with reference to the type locality in the Archean-age Warrawoona Group of northwestern Australia.

"Species" *Warrawoonella radia* Schopf, n. "sp." (Fig. 3f, g).

Diagnosis: as for the "genus".

Etymology: with reference to the common radiating organization *(radius*, L., ray, rod, spoke).

Type locality: locality B.

Type specimen: cluster of filaments shown in Fig. 3f (thin section 002-1-A, stage coordinates 18.9 X 100.5, CPC no. 20205; the specimen shown in Fig. 3g is from thin section 002-1-B, stage coordinates 48.4 X 99.4, CPC no. 20206).

Remarks: *W. radia* has been detected in cherts only from locality B. Although in some respects this morphotype is similar to *Eoastrion simplex* Barghoorn, first described from cherts of the ~ 2000 Ma-old Gunflint Iron Formation (Barghoorn and Tyler, 1965), it differs from this taxon in filament diameter and length, and in the orientation of the radiating filaments. Moreover, although many of the filaments are gently curved or sinuous (Fig. 3f), others are linear and essentially straight (Fig. 3f, g); all of the filaments are composed of short coccoid to rod-shaped segments that, although of constant diameter, are of varied length (Fig. 3g); and in none of the filaments have structures interpretable as cells (or as reproductive or other definitively biogenic structures) been detected. Based on these observations, and the fact that assuredly biogenic filamentous clusters of this type have not previously been reported from the geological record, *W. radia* filaments are regarded here as only "possible microfossils"; they may be remnants of a previously undescribed Precambrian taxon, or they may be of solely non-biological inorganic origin.

ACKNOWLEDGEMENTS

We thank J.M. Hayes, I.R. Kaplan and K.W. Wedeking for geochemical analyses; the Bureau of Mineral Resources, Canberra and the Geological Survey of Western Australia, Perth, for field assistance; and R. Buick and J.S.R. Dunlop for unpublished information on the Warrawoona Group and assistance in the field work of June, 1980. The constructive comments of R. Buick, P. Cloud and D. Pierce are appreciated.

This work was supported by NSF Grant INT77-10537 to SMA and by NSF Grants 77-22518 and 79-21777 and NASA Grants NGR 05-007-407 and NSG 7489 to JWS. Contribution no. 107 of the Preston Cloud Research Laboratory, UCSB.

REFERENCES

Awramik, S.M., 1981. The pre-Phanerozoic biosphere—three billion years of crises and opportunities. In: M.H. Nitecki (Editor), Biotic Crises in Ecological and Evolutionary Time. Academic Press, New York, pp. 83—102.

Awramik, S.M., 1982. The pre-Phanerozoic fossil record. In: H.D. Holland and M. Schidlowski (Editors), Mineral Deposits and the Evolution of the Biosphere. Dahlem Konferenzen, Springer-Verlag, Berlin, pp. 67—82.

Awramik, S.M. and Semikhatov, M.A., 1979. The relationship between morphology, microstructure and microbiota in three vertically intergrading stromatolites from the Gunflint Iron Formation. Can. J. Earth Sci., 16: 484—495.

Awramik, S.M., Margulis, L. and Barghoorn, E.S., 1976. Evolutionary processes in the formation of stromatolites. In: M.R. Walter (Editor), Stromatolites. Elsevier, Amsterdam, pp. 149—162.

Barghoorn, E.S. and Tyler, S.A., 1965. Microorganisms from the Gunflint chert. Science, 147: 563—577.

Barley, M.E., Dunlop, J.S.R., Glover, J.E. and Groves, D.I., 1979. Sedimentary evidence for a shallow-water volcanic—sedimentary facies, eastern Pilbara Block, Western Australia. Earth Planet. Sci. Lett., 43: 78—84.

Bridgwater, D., Allaart, J.H., Schopf, J.W., Klein, C., Walter, M.R., Barghoorn, E.S., Strother, P., Knoll, A.H. and Gorman, B.E., 1981. Microfossil-like objects from the Archaean of Greenland: a cautionary note. Nature, 289: 51—53.

Buick, R., Dunlop, J.S.R. and Groves, D.I., 1981. Stromatolite recognition in ancient rocks: an appraisal of irregularly laminated structures in an Early Archaean chert—barite unit from North Pole, Western Australia. Alcheringa, 5: 161—181.

Cloud, P., 1976a. Beginnings of biospheric evolution and their biogeochemical consequences. Paleobiology, 2: 351—387.

Cloud, P., 1976b. Major features of crustal evolution. Geol. Soc. S. Afr. Annexure Vol. 79, pp. 1—32.

Cloud, P. and Morrison, K., 1979. On microbial contaminants, micropseudofossils, and the oldest records of life. Precambrian Res., 9: 81—91.

DeLaeter, J.R. and Blockley, J.G., 1972. Granite ages within the Archaean Pilbara Block, Western Australia. J. Geol. Soc. Aust., 19: 363—370.

Dunlop, J.S.R., Muir, M.D., Milne, V.A. and Groves, D.I., 1978. A new microfossil assemblage from the Archaean of Western Australia. Nature, 274: 676—678.

Friedmann, E.I., 1982. Endolithic microorganisms in the Antarctic cold desert. Science, 215: 1045—1053.

Gebelein, C.D., 1969. Distribution, morphology and accretion rate of Recent subtidal algal stromatolites, Bermuda. J. Sediment. Petrol., 39: 49—69.

Golubic, S., 1973. The relationship between blue-green algae and carbonate deposits. In: N. Carr and B.A. Whitton (Editors), The Biology of Blue-Green Algae. Blackwell, London, pp. 434—472.

Golubic, S. and Barghoorn, E.S., 1977. Interpretation of microbial fossils with special reference to the Precambrian. In: E. Flügel (Editor), Fossil Algae. Springer-Verlag, Berlin, pp. 1—14.

Golubic, S., Perkins, R.D. and Lukas, K.J., 1975. Boring microorganisms and microborings in carbonate substrates. In: R.W. Frey (Editor), The Study of Trace Fossils. Springer-Verlag, New York, pp. 229—259.

Groves, D.I., Dunlop, J.S.R. and Buick, R., 1981. An early habitat of life. Sci. Am., 245: 64—73.

Hamilton, P.J., Evensen, N.M., O'Nions, R.K. and Glikson, A.Y., 1980. Sm—Nd dating of the Talga-Talga Subgroup, Warrawoona Group, Pilbara Block, Western Australia. In: J.E. Glover and D.I. Groves (Editors), Extended Abstracts, Second International Archaean Symposium, Perth, Australia. Geol. Soc. Aust. and Int. Geol. Correlation Project, Perth, Australia, pp. 11—12.

Hayes, J.M., Kaplan, I.R. and Wedeking, K.W., 1983. Precambrian organic geochemistry, preservation of the record. In: J.W. Schopf (Editor), Origin and Evolution of Earth's Earliest Biosphere: An Interdisciplincary Study. Princeton Univ. Press, Princeton, NJ, in press.

Hickman, A.H., 1980. Excursion Guide, Archaean Geology of the Pilbara Block. Second International Archaean Symposium, Perth, Australia. Geol. Soc. Aust., Perth, 55 pp.

Hickman, A.H. and Lipple, S.L., 1978. 1:250 000 Geological Series — Explanatory Notes, Marble Bar, Western Australia. Geol. Surv. W. Aust., Perth, 24 pp.

Javor, B.J. and Castenholz, R.W., 1981. Laminated microbial mats, Laguna Guerrero Negro, Mexico. Geomicrobiology J., 2: 237—273.

Knoll, A.H. and Barghoorn, E.S., 1974. Ambient pyrite in Precambrian chert: new evidence and a theory. Proc. Natl. Acad. Sci. U.S.A., 71: 2329—2331.
Knoll, A.H. and Barghoorn, E.S., 1977. Archean microfossils showing cell division from the Swaziland System of South Africa. Science, 198: 396—398.
Knoll, A.H. and Golubic, S., 1979. Anatomy and taphonomy of a Precambrian stromatolite. Precambrian Res., 10: 115—151.
Lowe, D.R., 1980. Stromatolites 3400 m.y.r. old from the Archaean of Western Australia. Nature, 284: 441—443.
Monty, C.L.V., 1967. Distribution and structure of Recent algal mats, eastern Andros Island, Bahamas. Ann. Soc. Geol. Belg., 90: 55—100.
Muir, M.D. and Grant, P.R., 1976. Micropalaeontological evidence from the Onverwacht Group, South Africa. In: B.F. Windley (Editor), The Early History of the Earth. Wiley, New York, pp. 595—604.
Nisbet, E.G., 1980. Archaean stromatolites and the search for the earliest life. Nature, 284: 395—396.
Nisbet, E.G. and Pillinger, C.T., 1981. In the beginning. Nature, 289: 11—12.
Oversby, V.M., 1976. Isotopic ages and geochemistry of Archaean acid igneous rocks from the Pilbara, Western Australia. Geochim. Cosmochim. Acta, 40: 817—829.
Pidgeon, R.T., 1978. 3450 m.y. old volcanics in the Archaean layered greenstone succession of the Pilbara Block, Western Australia. Earth Planet. Sci. Lett., 37: 421—428.
Rambler, M.B. and Margulis, L., 1980. Bacterial resistance to ultraviolet irradiation under anaerobiosis: implications for pre-Phanerozoic evolution. Science, 210: 638—640.
Ramsay, J.G., 1980. The crack-seal mechanism of rock deformation. Nature, 284: 135—139.
Sangster, D.F. and Brook, W.A., 1977. Primitive lead in an Australian Zn—Pb—Ba deposit. Nature, 270: 423.
Schopf, J.W., 1968. Microflora of the Bitter Springs Formation, Late Precambrian, central Australia. J. Paleontol., 42: 651—688.
Schopf, J.W., 1975. Precambrian paleobiology: problems and perspectives. Annu. Rev. Earth Planet. Sci., 3: 213—249.
Schopf, J.W., 1976. Are the oldest "fossils", fossils? Origins Life, 7: 19—36.
Schopf, J.W. and Barghoorn, E.S., 1967. Alga-like fossils from the early Precambrian of South Africa. Science, 156: 508—512.
Schopf, J.W. and Walter, M.R., 1980. Archaean microfossils and "microfossil-like" objects — a critical appraisal. In: J.E. Glover and D.I. Groves (Editors), Extended Abstracts, Second International Archaean Symposium, Perth, Australia. Geol. Soc. Aust. and Int. Geol. Correlation Project, Perth, Australia, pp. 23—24.
Strother, P.K. and Barghoorn, E.S., 1980. Microspheres from the Swartkoppie Formation: a review. In: H.O. Halvorson and K.E. Van Holde (Editors), The Origins of Life and Evolution. A.R. Liss, New York, pp. 1—18.
Tyler, S.A. and Barghoorn, E.S., 1963. Ambient pyrite grains in Precambrian cherts. Am. J. Sci., 261: 424—432.
Walter, M.R., 1972. Stromatolites and biostratigraphy of the Australian Precambrian and Cambrian. Palaeontol. Assoc. Spec. Paper 11, London, 190 pp.
Walter, M.R., 1976. Geyserites of Yellowstone National Park: an example of abiogenic "stromatolites". In: M.R. Walter (Editor), Stromatolites. Elsevier, Amsterdam, pp. 87—112.
Walter, M.R., Buick, R. and Dunlop, J.S.R., 1980. Stromatolites 3400—3500 m.y. old from the North Pole area, Western Australia. Nature, 284: 443—445.
Walter, M.R., Golubic, S. and Preiss, W.V., 1973. Recent stromatolites from hydromagnesite and aragonite depositing lakes near the Coorong Lagoon, South Australia. J. Sediment. Petrol., 43: 1021—1030.

PSEUDO-OOLITES IN ROCKS OF THE ULUNDI FORMATION, LOWER PART OF THE ARCHAEAN FIG TREE GROUP (SOUTH AFRICA)

THOMAS O. REIMER

Dyckerhoff Engineering GmbH, P.O. Box 2247, Wiesbaden (West Germany)

Dedicated to Professor K. Krejci-Graf on the occasion of his 85th birthday.

ABSTRACT

Reimer, T.O., 1983. Pseudo-oolites in rocks of the Ulundi Formation, lower part of the Archaean Fig Tree Group (South Africa). Precambrian Res., 20: 375—390.

The Ulundi Formation of the lowermost Fig Tree Group in the type area in the Barberton Mountain Land consists of a sequence of quartz—sericite schists, banded cherts and tuffaceous rocks up to 40 m thick. It overlies talc—carbonate schists assigned to the upper part of the Onverwacht Group. In the cherts, which in parts represent the sulfide facies of a banded-iron formation, silicified spheroids have been observed which appear to be diagenetically altered, locally zeolitized accretionary lapilli. Portions of the cherts formed through silicification of fine-grained felsic tuffs and contain abundant stylolite seams along which ~ 4% of the rock thickness has been removed by intrastratal solution during deformation.

A supposedly organogenic spheroidal structure, Ramsaysphera, has been previously described from the upper part of the Ulundi Formation. The spheroids, with diameters of up to 8 mm, occur in a distinct bed of up to at least 1.6 m thickness and can be traced in outcrop over an area which originally covered ~ 17 × 30 km. The bed was deposited in fairly still water of several 100 m depth. The spheroids accumulated with only little finer-grained detrital material, the interstices between them being filled by cherty silica and minor amounts of dolomite. Up to ~ 65% of the spheroids consist of tectonically elongated, originally round fragments of a micro-felsitic groundmass with remnants of phenocrysts. The majority of the remaining spheroids consists of concentrically banded bodies of siliceous material with minor amounts of chlorite and sericite, as well as small dolomite crystals. These spheroids represent highly altered granules of volcanic glass deposited from volcanic ash clouds through a body of water. The prototype of Ramsaysphera also belongs to this group of spheroids, and there is little microscopic or macroscopic evidence for its explanation as an organic structure.

INTRODUCTION

The importance of the rocks of the lower part of the ~ 3.35 Ga-old Fig Tree Group of the Swaziland Supergroup in the Barberton Mountain Land of South Africa (Fig. 1) is related to the number of microfossils and organic chemical compounds which have been described from them over the years. The first microfossils from this part of the stratigraphy were reported by Barghoorn and Schopf (1966) as Eobacterium isolatum from cherts of the

Daylight Mine, and by Pflug (1966) from the Sheba Mine. These microfossils usually consist of microspheres of 0.3—0.8 μm diameter. Other microfossils were later described by Schopf and Barghoorn (1967) and by Knoll and Barghoorn (1977). Organic chemical compounds were first identified in these rocks by Oró and Nooner (1967). For further data on observations of these compounds in Fig Tree rocks reference is made to a compilation by Reimer (1975a) and Knoll and Barghoorn (1977).

Ramsay (1963) drew attention to the similarity of spheroids from the lowermost part of the Fig Tree Group to "primitive algae (calcisphera)". Pflug (1976) investigated these structures in detail and interpreted them as biogenic, representing "asporogenous yeasts" for which he introduced the phylogenetic name "Ramsaysphera n.g. n.sp. Pflug 1976". In this context it is interesting to note that such an important zone of rocks should actually lack proper stratigraphic formalization and it is against this background that it was considered necessary to present a description of the rocks in question, as well as of their stratigraphic position and paleo-environmental significance. Data is also presented on the probable origin of Ramsaysphera and certain other spheroidal rocks from the base of the Fig Tree Group.

STRATIGRAPHY

Despite the extensive stratigraphic investigations carried out in the Mountain Land, there is as yet no agreement on the relationship between the Fig Tree Group and the underlying Onverwacht Group. The rocks underlying the greywackes and shales of the Sheba Formation of the Fig Tree Group, as formalized by Condie et al. (1970), have been classed together as the "Zwartkoppie Zone" by Visser (1956). These rocks have then been correlated by Viljoen and Viljoen (1969) with their "Zwartkoppie Formation" in the southern part of the Mountain Land, which is supposed to comprise the uppermost formation of the Onverwacht Group.

However, detailed investigations by Heinrichs (1969) had already shown that a characteristic marker horizon of accretionary lapilli, at the base of the Fig Tree Group in the so-called southern facies, lies directly on a stratigraphically persistent serpentinite/meta-peridotite zone of the Kromberg Formation of the Onverwacht Group. There is no reason to maintain the "Zwartkoppie Formation" as the topmost part of the Onverwacht Group as is still done by Anhaeusser (1980). It is more likely that it represents a sheared and partially metamorphosed equivalent of the Kromberg Formation which is overlain conformably by the lower part of the Fig Tree Group.

Based on the investigations of Heinrichs (1969, 1980), Reimer (1975a), and Heinrichs and Reimer (1977) it is possible to distinguish two separate facies domains within the Fig Tree Group (Fig. 1). The northern one consists mainly of greywackes and shales, and appears to be of deeper water origin. A volcanic horizon occurs at the top. The southern facies contains a highly varied lithology of shales, jaspilites, cherts, dolomites, tuffs, conglomerates, barites, etc.

deposited in a more proximal, partly still-water environment. The two facies are separated from each other by the Inyoka Zone along the central axis of the Mountain Land, along which intraformational erosion has taken place during the deposition of the lower part of the Fig Tree Group.

Due to structural complications, the stratigraphic position of the rocks underlying the Fig Tree Group in the northern facies cannot be unequivocally ascertained. However, in the northern facies a serpentinite/talc—carbonate schist horizon underlies the Fig Tree Group and is tentatively correlated here with a similar zone at the top of the Onverwacht Group in the southern facies. The results of detailed investigations of this contact zone have been compiled by Van Vuuren (1964) in an unpublished report. The following represents a summary of these data and observations. The term "Ulundi Formation" is proposed here for the basal rocks of the Fig Tree Group, named after the area of best development around the Ulundi Syncline (Fig. 1). It is defined as comprising all rocks occurring at the base of the Fig Tree Group in the northern facies, between the serpentinites and talc—carbonate schist assigned to the upper part of the Onverwacht Group and the lowermost greywackes and shales of the Sheba Formation of the Fig Tree Group. Due to strong lateral facies variations no real type locality can be given.

Along the northern rim of the Ulundi Syncline the formation occurs in a number of echelon-folded and what appear to be partly sheared asymmetric anticlines in the Sheba area. The anticlines on the surface vary in width from 5—100 m. Stratigraphically they are succeeded, usually with a sharp contact, by up to 30 m of dark green to light green quartz—sericite schists, which are locally referred to as "green schists". In places they are absent or only very thin, possibly due to shearing. Bands and lenses of black chert are widespread in these schists. Based on a comparison of their zircon population with that of the Sheba greywackes, Koen (1947) concluded that they are sheared equivalents of the latter. This interpretation was basically upheld by Van Vuuren (1964). Although local shearing of the greywackes also produces green quartz—sericite schists, the stratigraphic persistence of the schists and the notable differences in the chemical composition between these two types of rocks (Table I) suggests that they have been derived from different source materials, most likely from silicified felsic tuffs. There is also little chemical similarity between the schists and shales of the Sheba Formation. However, there is a strong similarity to an accretionary lapilli bed from the Onverwacht Group which has been slightly silicified (Table I). Thus, it is more likely that the quartz—sericite schists of the Ulundi Formation represent sheared, originally felsic tuff horizons with interlaying black chert and local lenses of accretionary lapilli, which are described below.

The schists are overlain by up to 6 m of banded cherts in which stringers of finely laminated black chert (Fig. 2) alternate with coarser, less banded, grey portions. The latter frequently contain abundant light-grey angular chert fragments and silicified debris (Fig. 2). The grains float in fine-grained chert and graded bedding was observed in a number of drill core samples from the Sheba

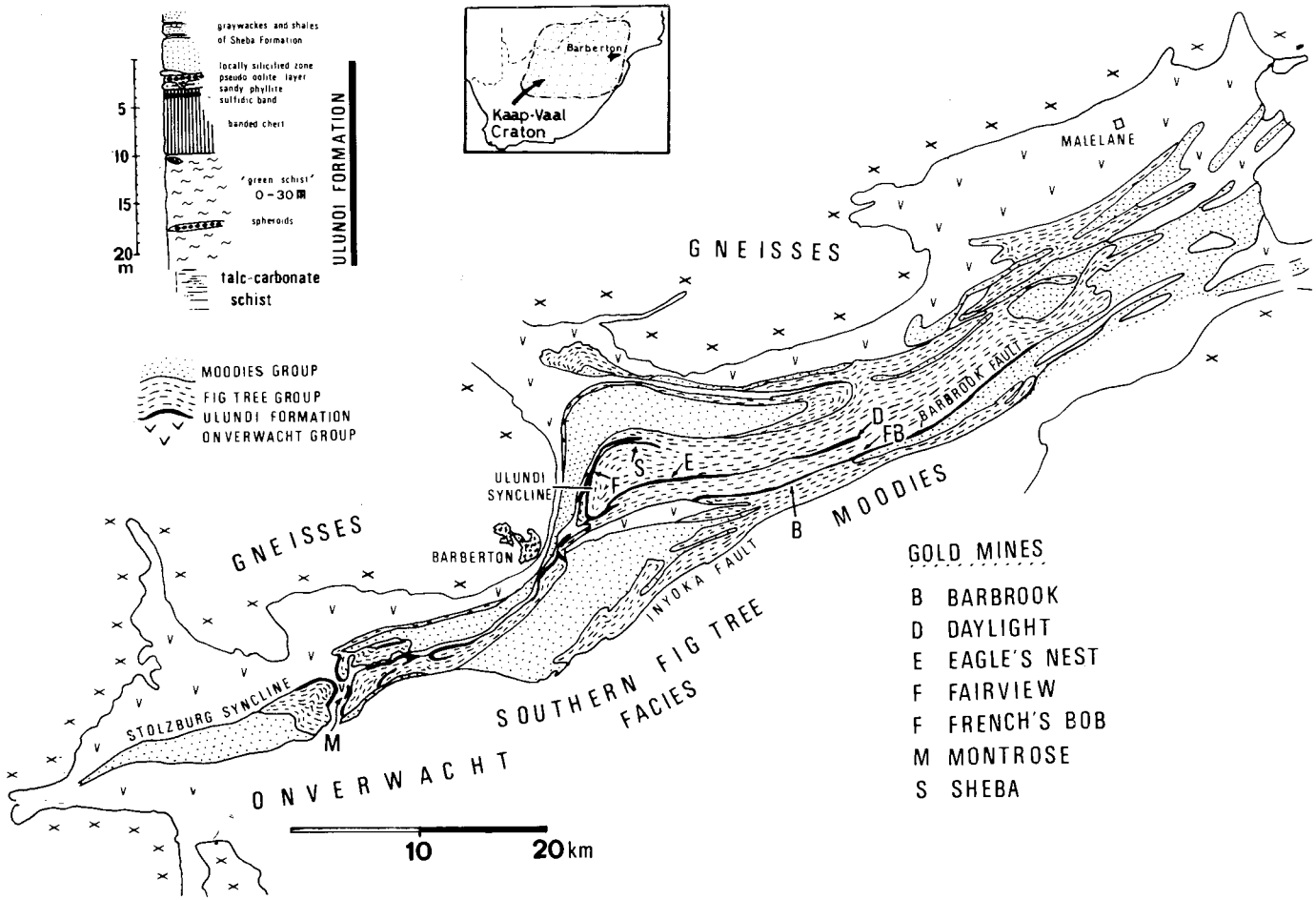

Fig. 1. Geological map of northern part of Barberton Mountain Land, showing distribution of Ulundi Formation.

TABLE I

Chemical composition of rocks from the Ulundi Syncline

	1	2	3	4	5	6	7
SiO_2	76.30	66.17	57.29	81.79	55.91	69.40	57.70
TiO_2	0.36	0.50	0.66	0.43	1.01	0.97	1.35
Al_2O_3	9.61	10.39	14.38	9.12	27.46	14.18	19.76
Fe_2O_3	1.41	7.23	11.61	1.62	1.24	4.13	5.76
MgO	2.09	4.44	5.25	0.57	1.02	1.37	1.91
CaO	2.49	1.85	0.75	0.87	0.07	0.40	0.56
Na_2O	0.20	1.64	0.99	0.20	0.15	0.07	0.10
K_2O	2.04	1.44	2.49	2.48	8.48	4.90	6.83
S	nd	0.05	0.05	0.04	0.01	0.49	0.68
l.o.i.	4.56	5.07	5.48	2.36	4.20	3.18	4.43

1 = quartz-sericite schist (green schist) from Sheba Mine, after Koen (1947)
2 = greywackes of Sheba Formation (average of 22 samples)
3 = shales of Sheba Formation (average of 13 samples)
4 = accretionary lapilli bed from Middle Marker of middle part of the Onverwacht Group
5 = aluminous tuff from Daylight Mine (average of 2 samples)
6 = "pseudo-oolite" from Sheba Mine (average of 2 samples)
7 = (as 6), calculated composition after deduction of 28% SiO_2 included in cherty matrix
l.o.i. = loss on ignition.

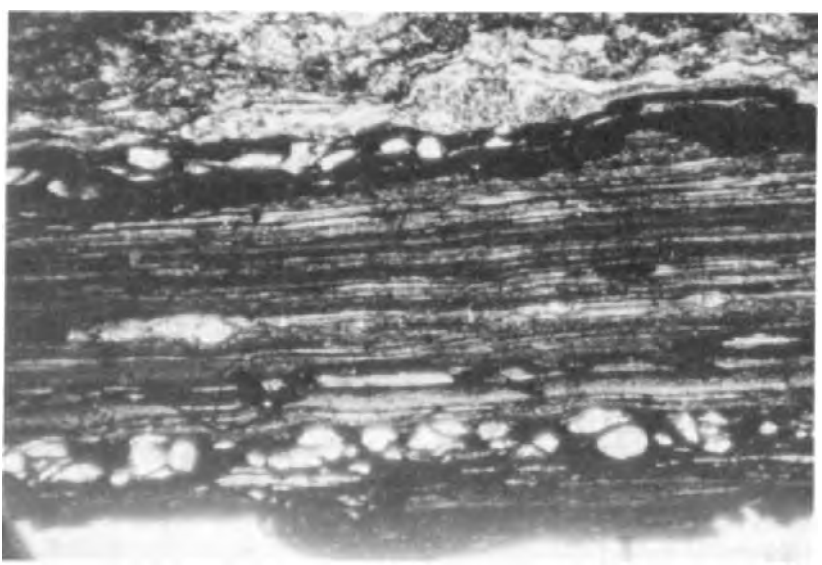

Fig. 2. Photomicrograph of banded chert from Sheba Mine: finely laminated black chert with stringers of volcaniclastic (?) material, width ~1 mm.

Mine. These units are usually 1—2 cm thick, and on rare occasions can be up to 30 cm. Maximum grain size of their clastic particles is ~ 5 mm. In a few samples angular chert slabs of up to 3 cm length have been noted.

The cherts frequently contain thin stringers enriched in small dolomite rhombs. In a number of specimens, it was found that the core of a dolomite rhomb consists of a round dolomite particle rich in carbonaceous matter, surrounded by clear dolomite forming a perfect rhomb. Where silicified, the core is made up of very fine-grained chert while the rim consists of a few larger clear quartz crystals.

Pyrite is a regular constituent of the cherts and occurs in scattered crystals of up to 5 mm length, as disseminated "dust" in certain enriched layers and in massive stringers several mm thick. Locally some arsenopyrite was observed associated with the pyrites.

A particularly persistent, up to 3 cm thick band of massive pyrites or of scattered pyrite crystals (the so-called "sulfidic band"), was recognized by Van Vuuren (1964) in the uppermost part of the chert in the Sheba Mine and also ~ 12 km to the southeast in the Barbrook Mine (Fig. 1). Similar layers are known to occur in cherts of the Ulundi Formation in various gold mines stretching from at least French's Bob in the east to Montrose in the west (Fig. 1), and notably in those along the Barbrook fault zone.

This prominent sulfide content distinguishes the Ulundi cherts from those of the Onverwacht Group and of the southern Fig Tree facies which contain very little sulfide. While some of the sulfides in the Ulundi Formation were introduced into the cherts during the hydrothermal activity which led to the widespread gold mineralization, the majority, however, may be of syngenetic origin, at times having been deposited over larger areas penecontemporaneously.

Some of the black colour of the cherts can be ascribed to finely dispersed sulfides, the majority most probably is caused by disseminated carbonaceous matter which can account for up to 0.43% (Reimer et al., 1979). Cherts with a high content of carbonaceous matter are usually notably finer-grained than those with a low content. It is in these fine-grained cherts that the microfossils and organic chemical compounds have been found.

The cherts are characterized by the ubiquitous presence of stylolite seams. An older irregular network-type system of seams with low amplitude can be distinguished from a younger one, which is mostly parallel to the bedding and most probably structurally controlled. Amplitudes of up to 14 mm have been noted in the younger system (Fig. 3). The extent of silica removal along the stylolites has been estimated in the Sheba Mine. In a composite of 14 m of drill core it was found that ~ 4% of the original rock has been removed along the seams of the younger system, with an average of ~ 1.5 mm per seam. This amounts to ~ 24 cm lost over the average thickness of 6 m for the Ulundi chert.

The cherts represent, to a large extent, silicified volcaniclastic material deposited from ash clouds, together with some coarser material which was

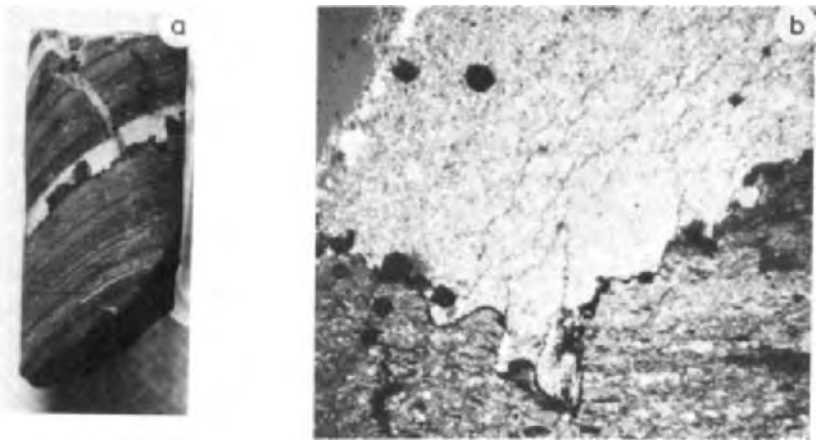

Fig. 3. Stylolites in banded chert from Sheba Mine: (a) core sample (width 25 mm); (b) photomicrograph of core sample, width 2 mm.

brought in by lateral transport through turbidity currents. Some of the cherts could also have formed from primary silica deposited during periods of reduced supply of detrital material, as suggested by Lowe and Knauth (1977). Above the chert a thin, though sometimes up to 1.5 m thick, layer of carbonate-bearing "sandy phyllite" has been noted by Hearn (1942) and Van Vuuren (1964). Locally, thin stringers of this material have been observed in the upper parts of the Ulundi chert. The band consists of a locally sheared, fine-grained matrix of chlorite and sericite with minor disseminated carbonate, and is characterized by rounded to angular unstrained quartz grains ~ 0.1—0.2 mm in size.

Graded bedding is developed near the base in places and cherty lenses occur throughout. The rock is of interest chemically, as it contains a high proportion of alumina (Table I) which has also been noted in a number of tuffaceous rocks of the Fig Tree Group. The rock has been traced by Van Vuuren (1964) from Sheba to the Barbrook Mine and was observed by the author at the Daylight Mine also (Fig. 1). It has not yet been reported from the area to the southwest of the Ulundi Syncline.

Van Vuuren (1964) interpreted the rock as a sheared, unusual clay-rich greywacke. However, it is more likely that it represents a fine-grained, probably felsic tuff with abundant quartz phenocrysts which has been subjected to subaqueous weathering.

The "sandy phyllite" is usually overlain by the "pseudo-oolite" which was described in detail from the Sheba Mine by Van Vuuren (1964). He traced it in intermittent outcrops along the strike of the Ulundi Formation between Eagle's Nest and the Barbrook Mine over ~ 10 km (Fig. 1). It is also known to occur in the Fairview Mine ∿ 5 km southwest of Sheba. It originally covered an area of ~ 17 × 30 km (Fig. 4). It is overlain with a sharp contact by the shales and greywackes of the Sheba Formation, a thin silicified contact zone being developed in places. According to Van Vuuren (1964), the bed is 0.3—

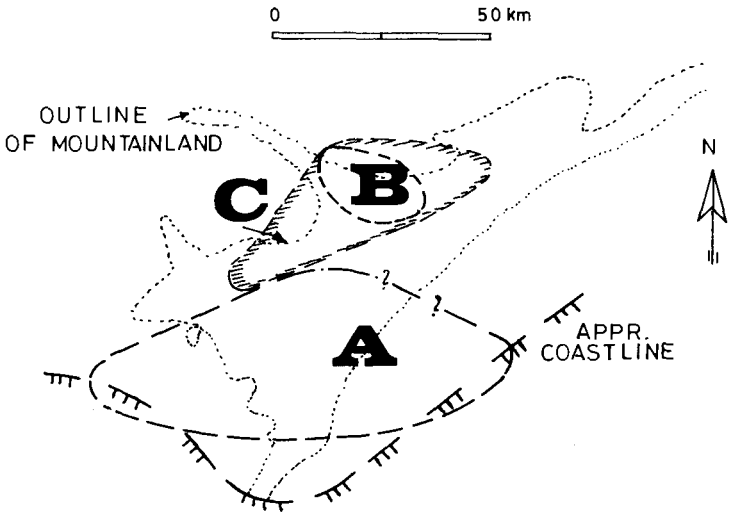

Fig. 4. Distribution of members of Ulundi Formation (A) Msauli accretionary lapilli member of base of Fig Tree Group in southern facies (after Reimer 1975b); (B) "pseudo-oolite" layer of Ulundi Formation (after Reimer, 1983); (C) quartz-sericite schists (green schists) of Ulundi Formation, poorly developed in western portion.

0.6 m thick. From a borehole intersection in the Sheba Mine a true thickness of 1.6 m was calculated and E. Winter (personal communication, 1968) described the outcrops of the bed south of the Eagle's Nest gold mine as "thick", presumably 2—3 m. The bed is dark grey-green with some yellowish-brown sheared bands. It contains small lenses and thin stringers of chert at various levels and localities, some of which show thin laminae of disseminated or massive pyrites.

The lower contact of the chert and pyrite layers is usually sharp, while the upper contact is diffuse in places. The chert layers contain isolated spheroids and Van Vuuren (1964) observed spheroids "scattered for a few inches from the contact in the dark massive underlying chert", suggesting that in places the chert was only slightly solidified at the time of deposition of the spheroid bed. The observations also indicate that deposition of the bed apparently took place over a longer time span, interrupted by the deposition of chert and pyrites. The bed was deposited in deep, still-water as indicated by the directly overlying greywackes and shales of the Sheba Formation, for which Reimer (1975a) reconstructed a depositional depth of several 100 m. Details of the spheroids and their probable mode of origin are described below.

Away from the northern limb of the Ulundi Syncline, further to the southwest, the formation tends to become more ferruginous and north of the Montrose Mine (Fig. 1) a thick, intensely folded, possibly > 150 m thick sequence of banded ferruginous cherts interlayered with some banded black chert layers, is developed at the base of the Fig Tree Group (Herget, 1966).

Still further west, on the northern limb of the Stolzburg Syncline, it changes westwards from ~ 50 m of banded ferruginous cherts into ~ 100 m of ferruginous shales, over ~3 km (Reimer, 1967). Furthermore, a strong ferruginous, also partly shaley component is developed in the Ulundi Formation along the Barbrook Fault (Fig. 1) and on the southwestern limb of the Ulundi Syncline. Further to the northeast, at the Daylight Mine, it consists of ~ 150 m of carbonaceous shales and cherts (Van Vuuren, 1964). Individual chert bands are up to 50 m thick in this area. The latter component decreases in importance to the northeast of Daylight Mine, and southeast of Malelane (Fig. 1) the basal rocks of the Fig Tree Group consist essentially of carbonaceous shales (R. Lindsay, personal communication, 1981). A band similar to the "pseudo-oolite" band has been recognized within these shales (Reimer, 1983). Whether the two horizons can be correlated is not yet known.

The Ulundi Syncline may be a banded-iron formation, with the oxide-, sulfide-, and possibly silicate-facies being developed contemporaneously, and grading laterally and vertically into each other. In some parts of the basin the deposition of this potential banded-iron formation continued at a reduced rate for some time during the deposition of the greywackes and shales, and even in the higher parts of the Sheba Formation some banded, partly ferruginous cherts are developed. Furthermore, the shales of the Sheba Formation are slightly enriched in silica compared with Precambrian shales from greywacke formations (Table I, Reimer, 1975a).

The basal rocks of the Fig Tree Group in the northern facies are mostly of deep water origin, with those more to the west, south, and southeast showing influences of shallower water deposition. In contrast to this, the basal Fig Tree rocks in the southern facies have been deposited in a shallow-water, possibly locally tidal environment (Lowe and Knauth, 1977, 1978). It has been suggested that the accretionary lapilli layer described in detail by Lowe and Knauth (1978) from the base of the Fig Tree Group in the south could be correlated with the "pseudo-oolite layer" in the north (Heinrichs, 1980). However, the differences in origin between the two types of spheroidal rocks militate against such correlation (Reimer, 1983). It is more likely that the quartz—sericite schists of the Ulundi Formation with their black chert lenses and local spheroid occurrences, which are described below, correlate with the Msauli accretionary lapilli bed in the south. The reconstructed extent of the latter is shown in Fig. 4 in relation to the extent of the quartz—sericite schists. The correlation of the higher Fig Tree formations between the two facies realms is presently being investigated.

SPHEROID OCCURRENCES

Spheroids, in what now constitutes the Ulundi Formation, were first described by Hearn (1942) from the underground workings of the Sheba Mine. In a thick chert band within the quartz—sericite schists he observed ".. round and flattened spots up to ½ mm in diameter in which the chert grain is abnor-

mally fine, and in which the proportion of minute dark inclusions is unusually high". Such bodies were also observed by Koen (1947). Their origin is uncertain, they either represent coagulated silica bodies or very small silicified accretionary lapilli. Similar bodies, with sizes of up to 5 mm, in black cherts in the basal rocks of the Fig Tree Group of the southern facies have been interpreted as accretionary lapilli by Reimer (1983).

In the same chert band in the quartz—sericite schists Hearn (1942) also observed several sharply defined layers containing white concentric spheroids with diameters of up to 1.5 mm. They consisted mainly of radiating masses of zeolites with zoisite in places. The method of identification of the zeolites has not been stated and no details on them are available. Many of these bodies contained round chert nuclei while a nucleus of a small radiating fibrous quartz spheroid was found in some. A few of the bodies consisted of alternating shells of finer and coarser cherty quartz with intervening rings of zeolites. The zeolites appeared to have replaced some other mineral and their growth started from the margin as well as from the nucleus when present. Zeolitized accretionary lapilli have been described by Moore and Peck (1962) from Tertiary strata in the western part of the United States.

Koen (1947) described similar spheroids from the Sheba Mine in a lens of 0.5—0.9 m length in the lower part of the Ulundi chert. These spheroids are irregularly distributed in the chert and are also found in the adjoining quartz—sericite schists. Their sizes vary between 1 and 10 mm and they consist mostly of chert with smaller crystal sizes than that of the enclosing material. Others show concentric layering around a core of chert, not necessarily in the centre of the spheroid. Some of the cores consist of quartz or labradorite ($An_{50—54}$), in which case the outer rim is made up of what have been described as zeolites (Koen, 1974). Spheroids consisting entirely of zeolites have also been observed. Some of them contain a round cherty core surrounded by a rim of irregular to sometimes radially arranged intergrowths of micaceous minerals (Fig. 5).

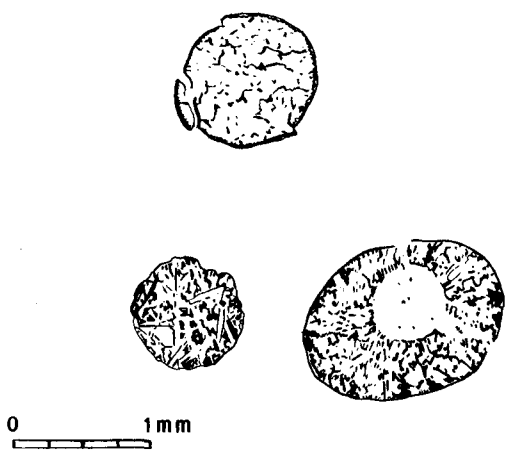

Fig. 5. Spheroids from chert band in "green schist", upper left specimen consists of "zeolite" (redrawn from Koen, 1947).

The occurrence of such large spheroids in the finely laminated cherts deposited in deep still-water militates against their having been brought in by lateral sedimentary transport. Deposition from a volcanic ash cloud would be more feasible. Thus, they could represent intensely silicified and zeolitized accretionary lapilli. The spheroids in the cherts in the quartz–sericite schists could have been preserved due to the comparatively resistant nature of the enclosing material.

The most prominent spheroid band in the Ulundi Formation is the "pseudo-oolite" layer of Van Vuuren (1964) which was described in its stratigraphic context above. The bed consists of rather uniformly sized spheroids with an average diameter of ~ 1.7 mm, ranging from 0.5 to 5 mm. They are usually well-sorted (Fig. 6). The bed shows a grain-supported texture with the small amount of intergranular detrital matrix, mostly quartz grains, replaced by chert. The rock consists of 71% spheroids, 28% matrix and 1% pyrite, the latter occurring within the matrix and the spheroids alike, and being of diagenetic

Fig. 6. Spheroids from "pseudo-oolite" layer.

origin. The above value for the matrix compares with a porosity of 25.9% for the tightest rhombohedral packing of equidimensional grains. The spheroids are usually flattened and elongated in the plane of cleavage, except for those enclosed in the intercalated chert bands. Ramsay (1963) observed elongation with axial ratios of up to 0.74 : 1.0 : 2.1, but flattening, with ratios of up to 0.25 : 1.0 : 2.0, is more frequently developed. Shearing is locally concentrated in certain thin laminae where the spheroids are almost completely obliterated.

The matrix shows feint agate-like microbanding, the parts around the spheroids usually being more cherty, while the tricuspate interstices between the chert laminae are richer in dolomite, which can account for up to 2% of the rock. Pyrite is frequently developed in microcrystalline size in isolated drawn-out lenses consisting of aggregates of chlorite and sericite which appear to represent highly deformed spheroids.

The chemical composition of the spheroid layer is presented in Table I as an average of two closely similar analyses. In Table I, the calculated composition of the bed after deduction of the 28% cherty silica of the matrix is also shown. In this calculated composition the major element composition of rock is similar to that of the "sandy phyllite" from the Daylight Mine for which a tuffaceous origin has been postulated.

Two major types of spheroids have been recognized: the first one, which accounts for up to 65% of the spheroids, macroscopically consists of greenish-grey to translucent microcrystalline material, with some specimens showing thin greyish-white rims. These spheroids are usually elongated and although the majority appear to have been spherical to subspherical, a few irregular grains were also present. The consist of a microfelsitic groundmass with well-developed flow-texture, containing few phenocrysts of quartz with extensively replaced margins and what appear to have been feldspars displaying zonal growth (Fig. 7). The flow-texture is a primary feature as it is also present in the spheroids at right angles to the younger shearing referred to above. Some fragments of highly altered originally ophitic rocks were also observed, as well as fragments of spherulitic growth of quartz and feldspar, the latter being partly replaced by siliceous material.

The second type make-up 30—35% of the spheroids and consist of rings of siliceous material with local enrichment of dolomite (Fig. 8). These spheroids are usually less flattened than the first type. They possess a siliceous core surrounded by a mixture of siliceous material with microcrystalline chlorite and sericite, and subhedral to euhedral dolomite crystals. The core zone of some of these spheroids is rich in dolomite while the rim consists of siliceous material, partly containing thin laminae of rutile and opaque minerals (Van Vuuren, 1964). Double cores were observed in a few spheroids and also multiple rings. The core is not always in the centre. Radial growth is developed locally in the rings and chalcedonic spherulites were observed in the centre of a few spheroids which are partly recrystallized to coarser-grained cherty quartz. Growth of radially diverging bundles of needles or blades of micaceous minerals and possibly zeolites from the margin of spheroid into its centre ap-

Fig. 7. Micro-felsitic fragment in "pseudo-oolite" layer (length of grain 1.6 mm).

pears to be a replacement feature, the siliceous core representing unaffected remnants of the original material, possibly of volcanic glass.

A large number of these spheroids are pervaded by an irregular network of linear-arranged microcrystalline opaque minerals. The fractures do not extend beyond the respective spheroid and they appear to represent deformed perlitic fractures in volcanic glass. Such cracks have been observed by the author (Reimer, 1983) in spheroids from a horizon in the lower part of the Fig Tree Group in the southern facies. This second type of spheroid shows a great similarity to altered hyaloclastic granules which form through the alteration of volcanic glass. However, in hyaloclastic tuffs the granules are not usually as spherical as the spheroids described here and are, furthermore, normally interspersed with finer-grained material. Thus, although these spheroids appear to be of a similar origin, a different mode of deposition has to be sought. Their spherical nature is a primary feature and they appear to have possessed perlitic cracks. They most probably formed as spheres of glass during tuff eruptions associated with low-viscosity lavas. During the fall from the resulting ash cloud they and other particles were coated with fine ash like accretionary lapilli. When they were deposited in water, segregation according to size occurred

Fig. 8. Altered volcanic glass granule with dolomite rhombs (length of grain 1.8 mm).

and they formed layers with only little finer-grained volcaniclastic material. Such segregation has been observed by Lowe and Knauth (1978) in the Msauli accretionary lapilli bed at the base of the Fig Tree Group in the southern facies. The virtual absence of finer material from the bed described here supports deposition from an ash cloud through a body of water rather than lateral sedimentary transport. Some subsequent redistribution might have occurred. Thus, the spheroids in the "pseudo-oolite" layer of the Ulundi Formation could represent a special type of accretionary lapilli with only little coating.

It is in this type of spheroid that the kerogen observed by Pflug (1976, personal communication, 1981) occurs. Inorganic dendritic growth of minerals similar to the structures described as organic by Pflug (1976) was noted in one specimen.

The remaining 1—5% of the spheroids contain round pyrite cores or consist of light-green chloritic aggregates which are usually highly flattened and in places contain enrichments of fine-crystalline pyrites. Some irregular fragments of dark chert were also observed.

From the preserved outcrops, an original extent of at least ~ 17 × 30 km can be reconstructed. Assuming an average thickness of 0.3 m over this area, a

volume of 0.15 km^3 is obtained, corresponding to ~ 0.11 km^3 if the porosity is deducted. Despite the large areal extent this volume would only represent the result of a rather small eruption. After deposition the rock was subjected to subaqueous alteration accompanied by silicification and local enrichment of dolomite. The organic material observed within some of the spheroids could have been introduced during these processes. The accompanying black cherts are rich in such components and could have acted as a source. Thus, there is little evidence for an organic origin of the spheroids described as Ramsaysphera. They are inorganic structures derived from volcanic activity and were deposited in deeper water as the last member of the so-called banded-iron formation, accompanied by felsic volcanic activity. The directly overlying greywackes and shales are evidence of extensive uplift and erosion to the south of the deposit, heralding a new phase in the development of the deposition of the Swaziland Supergroup.

ACKNOWLEDGEMENTS

Presentation of this paper at the Mexico Meeting of IGCP 160 in January 1982 was made possible through financial assistance of the Deutsche Forschungsgemeinschaft (DFG), Bad Godesberg, and is gratefully acknowledged here.

REFERENCES

Anhaeusser, C.R.A., 1980. Barberton Excursion Guide Book: Archaean Geology of the Barberton Mountain Land. Geol. Soc. S. Afr., Johannesburg, 78 pp.

Barghoorn, E. and Schopf, J.W., 1966. Micro-organisms three billion years old from the Precambrian of South Africa. Science, 152: 758—768.

Condie, K.C., Macke, J.E. and Reimer, T.O., 1970. Petrology and geochemistry of early Precambrian greywackes from the Fig Tree Group, South Africa. Geol. Soc. Am. Bull., 81: 2759—2776.

Hearn, M.G., 1942. A study of the working properties of the chief gold producer of the Barberton District, Eastern Transvaal. Unpubl. Ph.D. thesis, Witwatersrand University, Johannesburg.

Heinrichs, T.K., 1969. Report on mapping carried out in search of crysotile asbestos in part of the Barberton Mountain Land between Geluk and Skokohla. Unpubl. report, ETC Mines, Barberton.

Heinrichs, T.K., 1980. Lithostratigraphische Untersuchungen in der Fig Tree Gruppe des Barberton Greenstone Belt im Gebiet zwischen Umsoli und Lomati. Göttinger Arb. Geol. Paläont., 22, 118 pp.

Heinrichs, T.K. and Reimer, T.O., 1977. A sedimentary barite deposit from the Archaean Fig Tree Group of the Barberton Mountain Land (South Africa). Econ. Geol., 72: 1426—1441.

Herget, G., 1966. Archaische Sedimente und Eruptiva im Barberton Bergland (Transvaal—Südafrika). N. Jb. Mineral., Abh., 105: 161—182.

Knoll, A.H. and Barghoorn, E.S., 1977. Archaean microfossils showing cell division from the Swaziland System, South Africa. Science, 198: 396—398.

Koen, G.M., 1947. Die geologie van die Sheba Gebied in die Barbertonse Distrik. Unpubl. M.Sc. thesis, Pretoria University, Pretoria.

Lowe, D.R. and Knauth, P.R., 1977. Sedimentology of the Onverwacht Group (3.4 billion years), Transvaal, South Africa, and its bearing on the characteristics and evolution of the early Earth. J. Geol., 85: 699—723.

Lowe, D.R. and Knauth, P.R., 1978. The oldest marine carbonate ooids reinterpreted as volcanic accretionary lapilli, Onverwacht Group, South Africa. J. Sediment. Petrol., 48: 709—722.

Moore, J.G. and Peck, D.L., 1962. Accretionary lapilli in the western continental United States. J. Geol., 70: 182—193.

Oró, J. and Nooner, D.W., 1967. Aliphatic hydrocarbons in Precambrian rocks. Nature, 213: 1082—1085.

Pflug, H., 1966. Structured organic remains from the Fig Tree Series of the Barberton Mountain Land. Econ. Geol. Res. Unit, Inf. Circ., 17, Witwatersrand University, Johannesburg, 14 pp.

Pflug, H., 1976. Ramsaysphera ramses n.gen. n.sp. aus den Onverwacht Schichten (Archaikum) von Südafrika. Paleontographica Abt. B, 158: 130—168.

Ramsay, J.R., 1963. Structural investigations in the Barberton Mountain Land, Eastern Transvaal. Trans. Geol. Soc. S. Afr., 66: 353—401.

Reimer, T.O., 1967. Die Geologie der Stolzburg Synklinale im Barberton Bergland (Transvaal—Südafrika). Unpubl. Dipl. thesis, J.W. Goethe-Universität, Frankfurt/Main.

Reimer, T.O., 1975a. Untersuchungen über Abtragung, Sedimentation und Diagenese im frühen Präkambrium am Beispiel der Sheba Formation, Südafrika. Geol. Jb., Reihe B: 17, 108 pp.

Reimer T.O., 1975b. Palaeographic significance of the oldest known oolite pebbles in the Archaean Swaziland Supergroup (South Africa). Sediment. Geol., 14: 123—133.

Reimer, T.O., 1983. Accretionary lapilli and other spheroidal rocks from the Swaziland Supergroup of the Barberton Mountain Land, South Africa. In: T. Peryt (Editor), Coated Grains. Springer Verlag, Berlin, pp. 619—634.

Reimer, T.O., Barghoorn, E.S. and Margulis, L., 1979. Primary productivity of an Early Archaean microbial ecosystem. Precambrian Res., 9: 93—104.

Schopf, J.W. and Barghoorn, E.S., 1967. Alga-like fossils from the early Precambrian of South Africa. Science, 156: 508—512.

Van Vuuren, C.J., 1964. The geology of a portion of the Ulundi Syncline between Hislop's Creek and Fig Tree Creek, Barberton Mountain Land. Unpubl. Report, Econ. Geol. Res. Unit, Witwatersrand University, Johannesburg.

Viljoen, M.J. and Viljoen, R.P., 1969. An introduction to the geology of the Barberton granite—greenstone terrain. Geol. Soc. S. Afr., Spec. Publ., 2: 9—28.

Visser, D.J.L., 1956. The geology of the Barberton Area. Geol. Surv. S. Afr., Spec. Publ. 15: 224 pp.

SEDIMENTARY GEOLOGY AND STROMATOLITES OF THE MIDDLE PROTEROZOIC BELT SUPERGROUP, GLACIER NATIONAL PARK, MONTANA

ROBERT J. HORODYSKI

Department of Geology, Tulane University, New Orleans, LA 70118 (U.S.A.)

ABSTRACT

Horodyski, R.J., 1983. Sedimentary geology and stromatolites of the Middle Proterozoic Belt Supergroup, Glacier National Park, Montana. Precambrian Res., 20: 391—425.

The Belt Supergroup is a thick, dominantly fine-grained sequence of Middle Proterozoic strata occurring in western Montana, northern Idaho, and parts of Washington state, Alberta, and British Columbia. The sequence in Glacier National Park is located along the northeastern part of present exposures of the Belt Supergroup; it is ~ 2.9 km thick, extremely well exposed, and for the most part structurally simple. Although it was subjected to lowermost greenschist-facies metamorphism, primary sedimentary structures are exceptionally well preserved.

Subtidal, intertidal, alluvial and possibly deltaic depositional environments appear to be represented in the Belt sequence in Glacier National Park. The lowermost unit, the Altyn Limestone, is not entirely exposed in the park. A partial section, ~ 150 m thick, consists of impure dolostones deposited largely in shallow subtidal and intertidal settings. This carbonate unit is overlain by terrigenous strata of the Appekunny and Grinnell Argillites. The Appekunny Argillite is ~ 700 m thick, consists largely of green-colored, fine-grained terrigenous material and appears to have been deposited predominantly in offshore and/or deltaic settings. The overlying Grinnell Argillite is 605 m thick and consists of red-colored terrigenous material deposited largely on an alluvial plain. The overlying Siyeh Limestone is 780 m thick and consists largely of impure dolostones and dolomitic limestones deposited in shallow subtidal and intertidal settings. Overlying the Siyeh Limestone is the 385 m thick Snowslip Formation, which consists of slightly dolomitic, predominantly fine-grained terrigenous strata deposited largely in intertidal settings. The overlying Shepard Formation is not exposed in its entirety in the central part of Glacier National Park. A 270 m thick section, which excludes the uppermost part of the formation, consists of impure dolostones and argillites, and appears to have been deposited in subtidal and intertidal settings.

Stromatolites are abundant, diverse and well preserved in Glacier National Park, with mound-shaped forms and columnar forms of the group *Baicalia* occurring in the Altyn Limestone and Siyeh Limestone, and mound-shaped stromatolite-like structures occurring in the Snowslip and Shepard Formations. Particularly prominent is a 24—32 m thick stromatolite unit in the upper Siyeh Limestone, which contains *Baicalia* and *Conophyton* and appears to represent a prograding stromatolite reef, with *Baicalia* originating in a moderate-energy reef-front setting, and *Conophyton* originating in a lower energy back-reef setting. Individual units in these cycles can be correlated for 90 km. Many of the *Conophyton* in these cycles are inclined, probably as a result of gentle wave action, and the direction of inclination is relatively constant for 90 km, with the axes trending SW—SSW and plunging 30—60° SW.

INTRODUCTION

The Belt Supergroup, occurring over an area of about 200,000 km^2 in the northwestern United States and adjacent parts of Canada (Fig. 1), is the most extensive Precambrian sedimentary unit exposed in the United States.

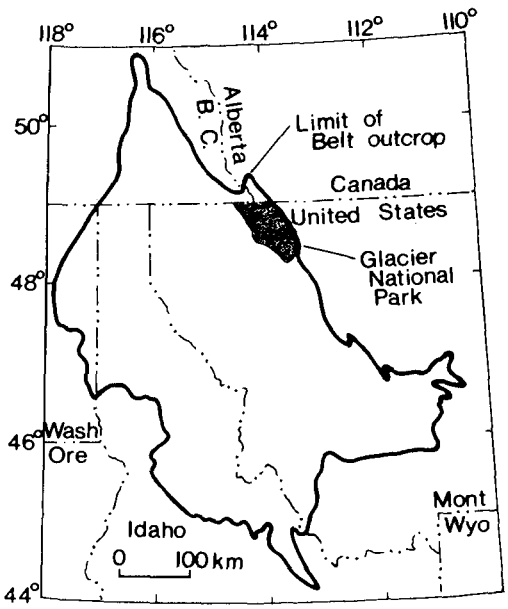

Fig. 1. Approximate distribution of the Belt Supergroup in the northwestern United States and Canada (after Harrison, 1972).

It consists largely of argillaceous, arenaceous and calcareous strata, with coarser grained lithologies being of limited extent (McMannis, 1963). Significant advances have been made recently in understanding the geology of the Belt Supergroup (e.g., Harrison, 1972; Idaho Bureau of Mines and Geology, 1973, 1974); however, many aspects of its geologic history remain poorly known. This can be attributed to several factors: (1) virtually the entire Belt Supergroup is allochthonous, having been thrust substantial distances during the Cretaceous and Early Tertiary (Mudge, 1970; Harrison et al., 1974), and it is difficult to place individual thrust sheets into their relative pre-thrust positions; (2) small- and medium-scale thrusts are difficult to recognize in areas below timberline in the generally monotonous Belt strata, accurate measured sections are difficult to obtain in many areas and the thickness of some measured sections may be overestimated due to structural duplication; (3) age control for the Belt Supergroup is relatively poor and the time intervals represented by different Belt rock-stratigraphic units is not known (Harrison, 1974), nor is it known how diachronous the differ-

ent units are; and (4) the Belt Supergroup has a large areal extent and access to many regions is difficult; thus, the data base of detailed sedimentologic information and thoroughly measured sections is deficient for many areas. The purpose of this report is to provide a summary of the sedimentary geology and stromatolites of an extremely well-exposed section of the Belt Supergroup in the Lewis Range, Glacier National Park, Montana.

GENERAL GEOLOGY

Glacier National Park is located along the northeastern margin of present-day exposures of the Belt Supergroup (Fig. 1). In the central and northeastern part of the park, the site of most of the writer's field studies, a partial section of the Belt Supergroup is about 2 900 m thick, with the base being in fault contact with underlying Cretaceous strata and the top having been removed by erosion (Fig. 2). The strata in the Lewis Range in the eastern and central part of Glacier National Park are exceptionally well ex-

top not exposed

MISSOULA GROUP	SHEPARD FORMATION	> 270 m	Greenish-gray to gray dolomitic argillite, dolomitic muddy sandstone, and muddy dolostone	Mound-shaped dolomitic stromatolites are uncommon
	SNOWSLIP FORMATION	385 m	Red and green argillite and muddy sandstone; greenish-gray to gray dolomitic argillite and dolomitic muddy sandstone	Mound-shaped calcitic and dolomitic stromatolites are common
PIEGAN GROUP	SIYEH LIMESTONE (Helena Dolomite)	780 m	Gray, muddy and sandy dolomitic limestone, dolomitic and calcareous argillite and muddy sandstone; minor oolitic limestone	Mound-shaped calcitic stromatolites are common. Calcitic Baicalia and Conophyton form a prominent 25-30 m thick unit about 200 m below the top of the formation. Silicified stromatolites are common 100-180 m above the base of the formation
RAVALLI GROUP	GRINNELL ARGILLITE (Spokane and Empire Formations)	605 m	Red argillite and sandy argillite; subordinate green argillite, sandy argillite, and quartzose sandstone	Mound-shaped dolomitic stromatolites are very rare 30 m above the base of the formation
	APPEKUNNY ARGILLITE	ca. 700 m	Green argillite and sandy argillite; quartzose sandstone locally prominent; minor black mudstone	No stromatolites are present
PR*	ALTYN LIMESTONE	>150 m	Gray silty and sandy dolostone	Dolomitic Baicalia are common

base not exposed

3,000
2,000
1,000
0 m

Fig. 2. Generalized stratigraphy, lithology, and stromatolites of the Belt Supergroup in the central and northeastern part of Glacier National Park, Montana. Stratigraphic units are after Ross (1959) and Childers (1963), and correlatives to the south (after Harrison, 1972) are given in parentheses. PR* refers to Pre-Ravalli, an informal lithostratigraphic unit encompassing Belt rocks that underlie the Ravalli Group (Harrison, 1972).

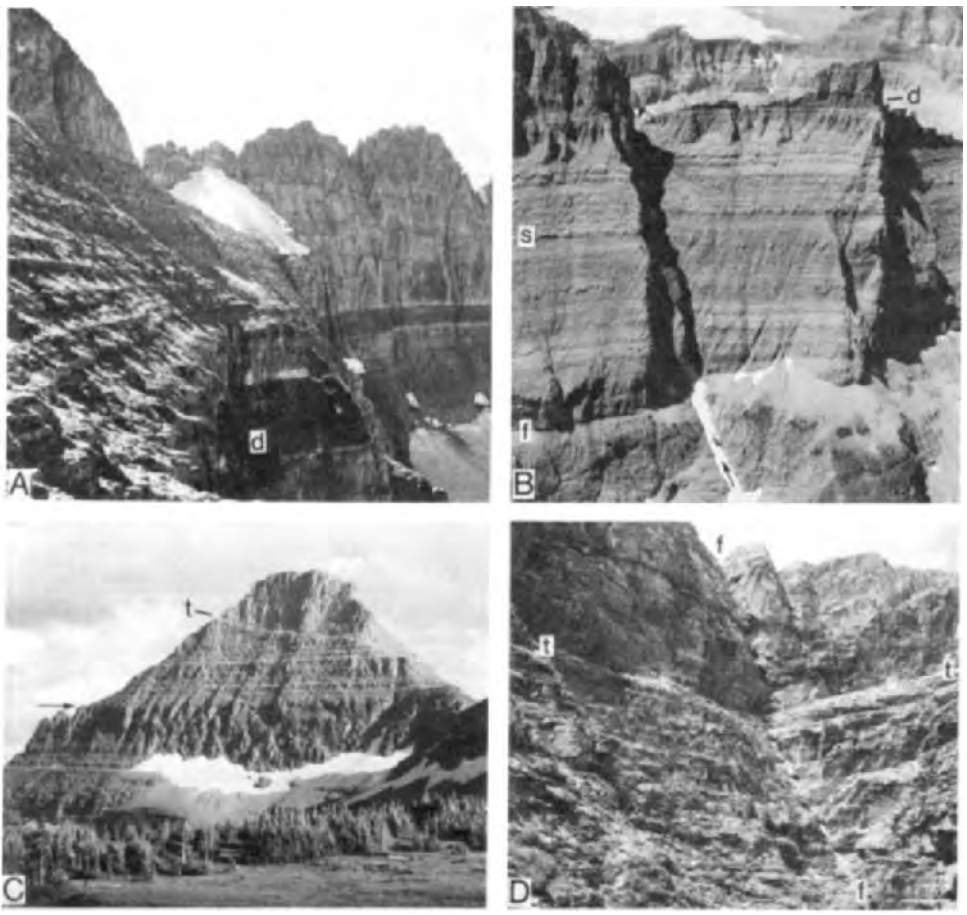

Fig. 3. Structure of the Belt Supergroup in Glacier National Park, Montana. A. North side of Mt. Gould showing nearly horizontal strata of the Siyeh Limestone and Snowslip Formation. The dark band is a ca. 1 100 Ma-old diabasic sill (d) intrusive into the Siyeh Limestone. B. South side of Iceberg Notch showing a diabasic sill (d) intrusive into the lower Snowslip Formation. Most of the exposed strata are of the Siyeh Limestone. The *Baicalia—Conophyton* stromatolites cycles are 24 m thick and form an erosionally resistant unit (s). A diabasic dike dipping 82° cuts the Siyeh Limestone and has been preferentially eroded to form a steeply inclined chute (arrows). This dike is ~ 6 m thick at the top of the arete and it extends for more than 6 km with a strike of N78W. Faulting, probably of normal sense, is indicated by ~ 3 m of stratigraphic separation across the dike. A low-angle fault (f) cuts the lower Siyeh Limestone. C. Thrust fault (t) cutting strata of the Shepard Formation on the north side of Reynolds Mountain. Measurements of stratigraphic separation and the orientation of drag folds indicate that ~ 25 m slip occurred in a northeasterly direction. The arrow marks the contact between the Shepard Formation and underlying Snowslip Formation. D. High-angle fault (f) cut by a thrust fault (t) in the Shepard Formation on the east side of Clements Mountain. The nearly horizontal strata exhibit 30—100 cm stratigraphic separation across the high-angle fault and the high-angle fault exhibits 2.4 m horizontal separation where offset by the thrust fault.

posed, particularly in areas above timberline (Fig. 3). Although these strata were subjected to lowermost greenschist-facies metamorphism (Maxwell, 1974), details of sedimentary structures and fine sedimentary laminae are well preserved, and when studying macroscopic sedimentary features these strata can be considered to be essentially unmetamorphosed. Although the Belt strata in Glacier National Park are allochthonous, having been thrust several tens of kilometers during the Early Tertiary, much of the sequence in the Lewis Range is gently inclined with the major structural complexity being thrust faults (Figs. 3B, C, D), which were probably contemporaneous with the major thrust, the Lewis overthrust. In the northeastern corner of the park and adjacent parts of Alberta, these subsidiary thrusts have relatively large displacements resulting in significant stratigraphic repetition (Douglas, 1952). However, in the area studied by the writer the displacements are relatively small even though the faults extend for several kilometers. For example, the thrust illustrated in Fig. 3B does not appreciably offset a presumably Proterozoic dike, the thrust shown in Fig. 3C has a displacement of ~ 25 m, and the thrust fault in Fig. 4C offsets a high-angle fault ~ 2.4 m. Considering the nature of these outcrops, these thrusts are readily recognized and stratigraphic repetition can be eliminated from measured sections.

A diabasic sill intrudes the Siyeh Limestone and Snowslip Formation (Figs. 3A, B) and was probably contemporaneous with the Purcell Lava which occurs in the Missoula Group. This sill has a Potassium—Argon age of ca. 1 100 Ma (Hunt, 1962), thereby providing an age for part of the Missoula Group. The Purcell Lava is not present in the central part of Glacier National Park, where examined on the east side of Swiftcurrent Mountain it is about 31 m thick with its base being 17 m above the base of the Shepard Formation, and it thickens to the northwest. Thin, but laterally extensive, steeply inclined dikes cut Belt strata, and beds across some of these dikes are offset several meters in an apparently normal sense (Fig. 3B). If these dikes are contemporaneous with the Purcell Lava, they may provide evidence for a ca. 1 100 Ma-old tensional event. Altered glass shards, in which the characteristic Y-shaped cross section is preserved, have been detected in impure dolomitic limestones 60 m below the top of the Siyeh Limestone on Piegan Mountain, indicating a nearby volcanic event that predates the Purcell Lava.

Except for the lower Shepard Formation, strata of the Belt Supergroup in Glacier National Park are poorly dated. The Belt strata are definitely younger than the 1 700 Ma-old crystalline basement that locally underlies the Belt Supergroup, and a reasonable estimate for the age of the lowermost Belt unit in Glacier National Park is ~ 1 400 Ma (Harrison, 1972).

SEDIMENTARY GEOLOGY AND STROMATOLITES

Glacier National Park, having the best exposed and most complete sections of the Belt Supergroup, has been the site for many of the early strati-

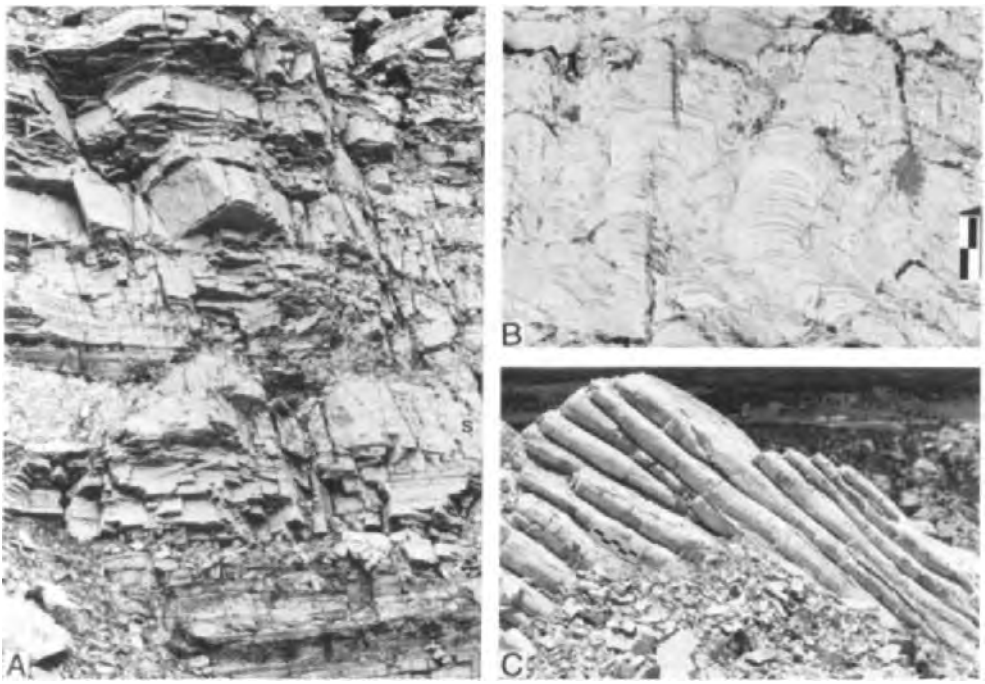

Fig. 4. Outcrops and stromatolites of the Altyn Limestone near Appekunny Falls, Glacier National Park, Montana. A. An 18 m thick exposure of sandy, silty, and argillaceous dolarenites and dololutites containing a 1.5—1.8 m thick unit (s) comprised of closely crowded dolomitic *Baicalia* columns (these are illustrated in Fig. 5C). The bases of well-developed fining and thinning upward sequences are indicated by arrowheads. B. Dolomitic elongate columnar stromatolites shown on a joint surface oriented perpendicular to bedding and perpendicular to the direction of elongation of the columns. Scale is in 5 cm divisions. C. Dolomitic elongate columnar stromatolites shown on a surface parallel to bedding. A cross-sectional view through these stromatolites is shown in Fig. 5D. Scale is in 5 cm divisions. Photograph from Horodyski (1976a, p. 592).

graphic studies of this unit. Major studies were conducted by Willis (1902) and Fenton and Fenton (1937), and later by Ross (1959) who compiled much of the earlier stratigraphic data along with new field observations in a United States Geological Survey Professional Paper. An important study along the southern boundary of Glacier National Park was conducted later by Childers (1963). Glacier National Park was the site of some of the early studies of Proterozoic stromatolites in the United States because of the abundance and diversity of stromatolites in this region. These include the classic studies of Walcott (1914), Fenton and Fenton (1931, 1933, 1937) and Rezak (1957).

The main purpose of this report is to provide a summary of the sedimentary geology and stromatolites of the Belt Supergroup in Glacier National Park. The following discussion is based upon twelve field seasons in Glacier

National Park, with most of this effort being concentrated in the Lewis Range in the central and northeastern part of the park.

Neither the base nor the top of the Belt Supergroup is present in Glacier National Park. The base of the Belt section is in fault contact with Cretaceous strata (Ross, 1959), with the lowest Belt unit being the Altyn Limestone (Fig. 2). In Alberta, however, the underlying Waterton Formation is present (Douglas, 1952). The uppermost Belt unit exposed in the central part of the Lewis Range is the Shepard Formation (Fig. 2); overlying Belt strata are present in the southern (Childers, 1963) and northwestern part of the park.

Altyn Limestone

The lowermost Belt unit exposed in Glacier National Park, the Altyn Limestone, forms a narrow outcrop band along the eastern side of the Lewis Range where it is in fault contact with underlying Cretaceous strata (Ross, 1959). An excellently exposed, structurally simple section of part of the Altyn Limestone is located on the southeast side of Appekunny Mountain near Appekunny Falls in the northeastern part of Glacier National Park. At this locality the Altyn Limestone is ~ 150 m thick and consists predominantly of sandy dolarenite and silty and clayey dololutite. These lithologies commonly form cycles (Fig. 4A), which are a few meters thick and consist of: (1) a slightly undulatory to irregular erosional base having several centimeters to one decimeter relief; (2) a lower medium-bedded sandy dolarenite with sparse centimeter-sized dolostone intraclasts near its base and locally displaying poorly developed low-angle, planar cross-stratification; and (3) an upper unit of thinly bedded, rippled sandy dolarenite interbedded with non-rippled silty dololutite to form the "wavy bedding" of Reineck and Wunderlich (1968). These cycles fine and thin upward, and they might have originated by deposition in laterally migrating tidal channels incised into a tidal flat or by progradation of shallow subtidal and intertidal deposits.

Stromatolites are common, locally, in the Altyn Limestone, and they are particularly well exposed near Appekunny Falls where they generally occur in the lower part of the fining-upward sequences (Horodyski, 1976a). The stromatolites include subcircular, branched columns referable to the group *Baicalia* (Figs. 5A—C) and highly elongate columns (Figs. 4B—C, 5D—E). The elongate columns are typically inclined, very closely spaced to contiguous, and smoothly laminated. The elongation of these columns can be attributed to the streamlining effects of unidirectional currents or possibly bipolar tidal currents. In thin section, both the subcircular and elongate columnar stromatolites are seen to consist of coarser and finer grained laminae (Horodyski, 1976a, p. 588, Figs. 2A—B). The coarser grained stromatolitic laminae contain submillimeter-sized dolostone intraclasts as well as terrigenous material, suggesting that they formed largely by the stabilization of sedimentary particles. In contrast, the finer grained laminae are deficient in terrigenous material relative to that of adjacent texturally equivalent strata,

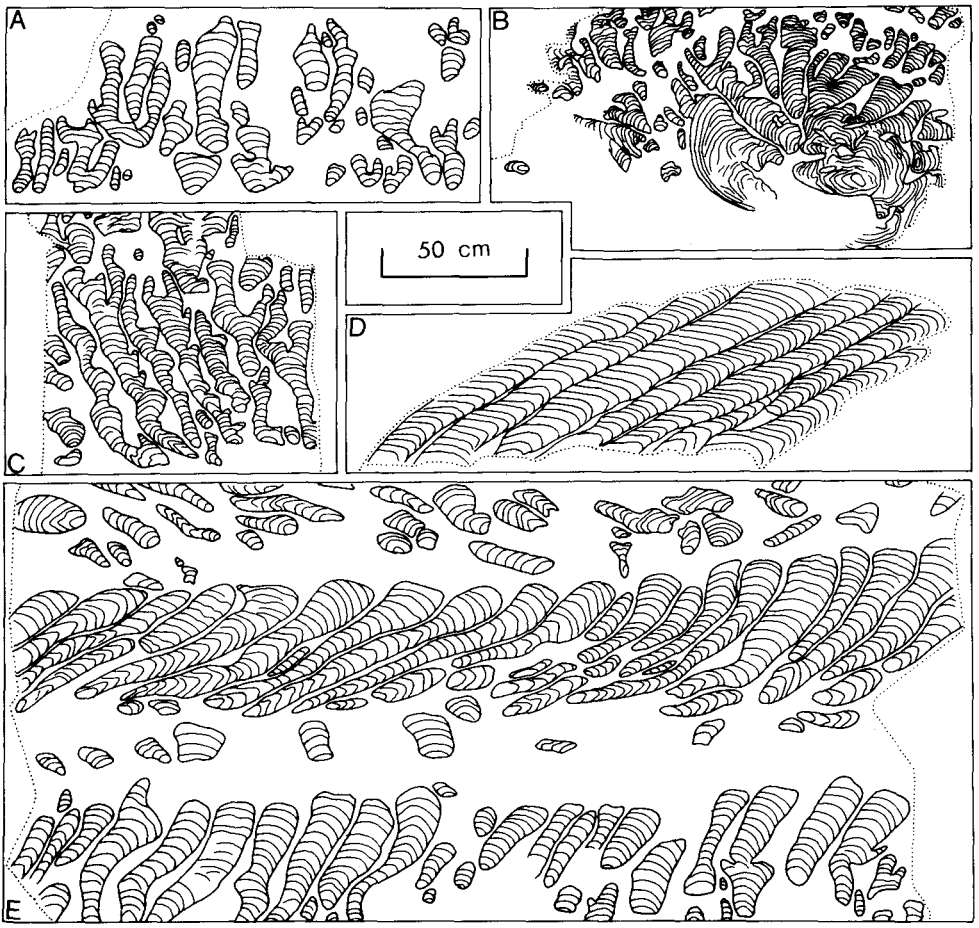

Fig. 5. Stromatolites of the Altyn Limestone near Appekunny Falls, Glacier National Park, Montana. These figures represent tracings from photographs of outcrops oriented perpendicular to bedding in which stromatolite columns and selected laminae were outlined using felt-tip pens. Dotted lines represent outcrop borders. All stromatolites are dolomitic and occur in a dolarenite matrix. The columns in A—C are subcircular and can be assigned to the group *Baicalia*. The columns in D and E are highly elongate and are shown on a joint surface oriented perpendicular to the direction of elongation.

suggesting that these finer grained laminae originated, at least in part, by in situ carbonate precipitation. The fabric of these precipitated laminae is similar to that of many of the millimeter- and submillimeter-sized dolostone intraclasts occurring in the Altyn dolarenites, suggesting that much of the carbonate in these strata was derived from erosion of calcareous material precipitated in microbial mats. Filamentous microfossils of apparent cyanophycean affinity have been described from cherts from the Altyn Limestone near Appekunny Falls (White, 1974).

The Altyn Limestone section is more complete to the north where other lithofacies are present. For example, a distinctive dolomitic limestone unit and other units are present on Chief Mountain, 14 km north of Appekunny Falls; however, these strata have not been intensively studied and will not be discussed in this report.

Appekunny Argillite

The Appekunny Argillite is an ~ 700 m thick, predominantly green-colored, fine-grained terrigenous unit which overlies the Altyn Limestone. The lower part of the Appekunny Argillite is gradational with peritidal impure dolostones of the Altyn Limestone. The main part of the Appekunny Argillite consists of finely laminated to thinly bedded argillite, sandy argillite, siltite and muddy very fine-grained sandstone. Subordinate muddy very fine- to medium-grained sandstone forms prominent units several meters to a few decameters thick. The upper Appekunny Argillite consists, in part, of coarsening-upward and shallowing-upward sequences, which are several decameters thick. The lower part of these sequences, consisting of parallel-laminated argillite, siltite and muddy very fine-grained sandstone, was deposited below effective wave base. The upper part of these sequences, consisting of ripple cross-laminated sandy layers intercalated with silty and pelitic layers, was deposited above effective wave base and was locally subaerially exposed. In places, these sequences are capped by massive sandstone units several decimeters to a few meters thick.

In a significant portion of the Appekunny Argillite, desiccation cracks and megaripple cross-stratification are absent and ripple cross-lamination is uncommon, suggesting that deposition occurred in an offshore setting below effective wave base. Thus, the Appekunny Argillite differs from the other Belt formations in Glacier National Park, which were deposited wholly in shallow subtidal, intertidal and terrestrial settings. Portions of the Appekunny Argillite may represent prograding deltaic deposits or sediment deposited offshore of alluvial plains; however, additional studies are needed before precise depositional settings can be delineated. Those parts of the Appekunny Argillite that are gradational with the underlying Altyn Limestone and overlying Grinnell Argillite appear to have been deposited in peritidal settings.

Stromatolites are not known from the Appekunny Argillite. Sphaeromorphs have been detected in dark gray mudstones from the lower part of the formation, but they have been extensively degraded during lowermost greenschist-facies burial metamorphism (Horodyski, 1981). Problematic bedding-plane markings (Fig. 6), which resemble isolated strings of highly flattened beads, occur in green sandy and argillaceous strata in the lower part of the formation (Horodyski, 1982). These markings range from 1—7 cm long and consist of three to ~30 beads. They resemble the Phanerozoic ichnofossils *Hormosiroidea* and *Neonereites*; however, this

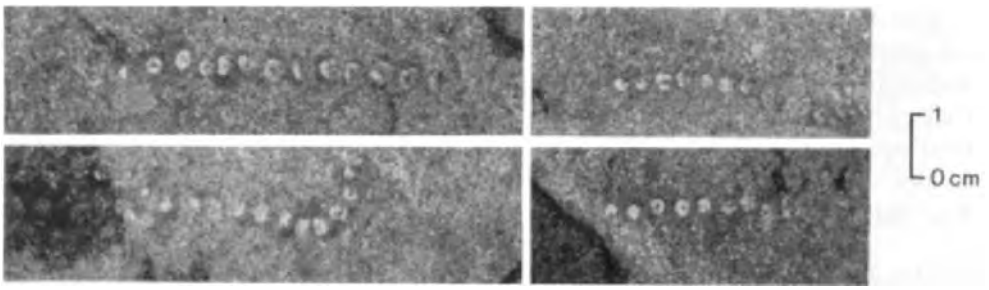

Fig. 6. Problematic bedding-plane markings from the lower Appekunny Argillite, Appekunny Mountain, Glacier National Park, Montana. All specimens figured occur along a bedding plane of a muddy, very fine grained sandstone. These specimens were photographed immersed in ethyl alcohol and are deposited at the Department of Paleobiology, National Museum of Natural History, Smithsonian Institution, Washington, D.C. under catalog number USNM-311320.

resemblance is superficial as the Appekunny Argillite markings consist of highly flattened beads, whereas *Hormosiroidea* and *Neonereites* have substantial relief (Häntzschel, 1975). The Appekunny markings are best regarded, at present, as dubiofossils.

Grinnell Argillite

The Grinnell Argillite is a terrigenous unit of argillite, sandy argillite, very fine- to fine-grained muddy sandstone and fine- to very coarse-grained quartzose sandstone. It is predominantly red colored, although green-colored strata are present locally. On Mt. Henkel in the northeastern part of Glacier National Park the Grinnell Argillite is ~ 605 m thick and it can be subdivided into six informal lithologic units: (1) a basal green argillite unit; (2) a lower red and green argillite unit; (3) a middle red argillite unit; (4) a middle green and red argillite unit; (5) an upper sandy unit; and (6) an upper unit transitional with the Siyeh Limestone (Fig. 7).

One of these units, the upper sandy unit, appears to be particularly important for developing an understanding of the deposition of the Grinnell Argillite. This unit is 148 m thick on Mt. Henkel and is composed of white, medium- to coarse- and locally very coarse-grained quartzose sandstone interbedded with red argillite, sandy argillite and very fine- to fine-grained muddy sandstone. The white quartzose sandstone beds are 1—25 cm thick and they occur as isolated beds within argillite units a few to several decimeters thick, and as tabular cosets which are several centimeters to more than one meter thick and have very sharp contacts with adjacent muddy strata. Commonly intercalated with the sandstone beds in these cosets are muddy laminae a few millimeters thick. Small-scale planar cross-bedding and undulatory crested ripples with wavelengths ranging from 10—50 cm are common, but megaripples or cross-stratification originating from migrating megaripples

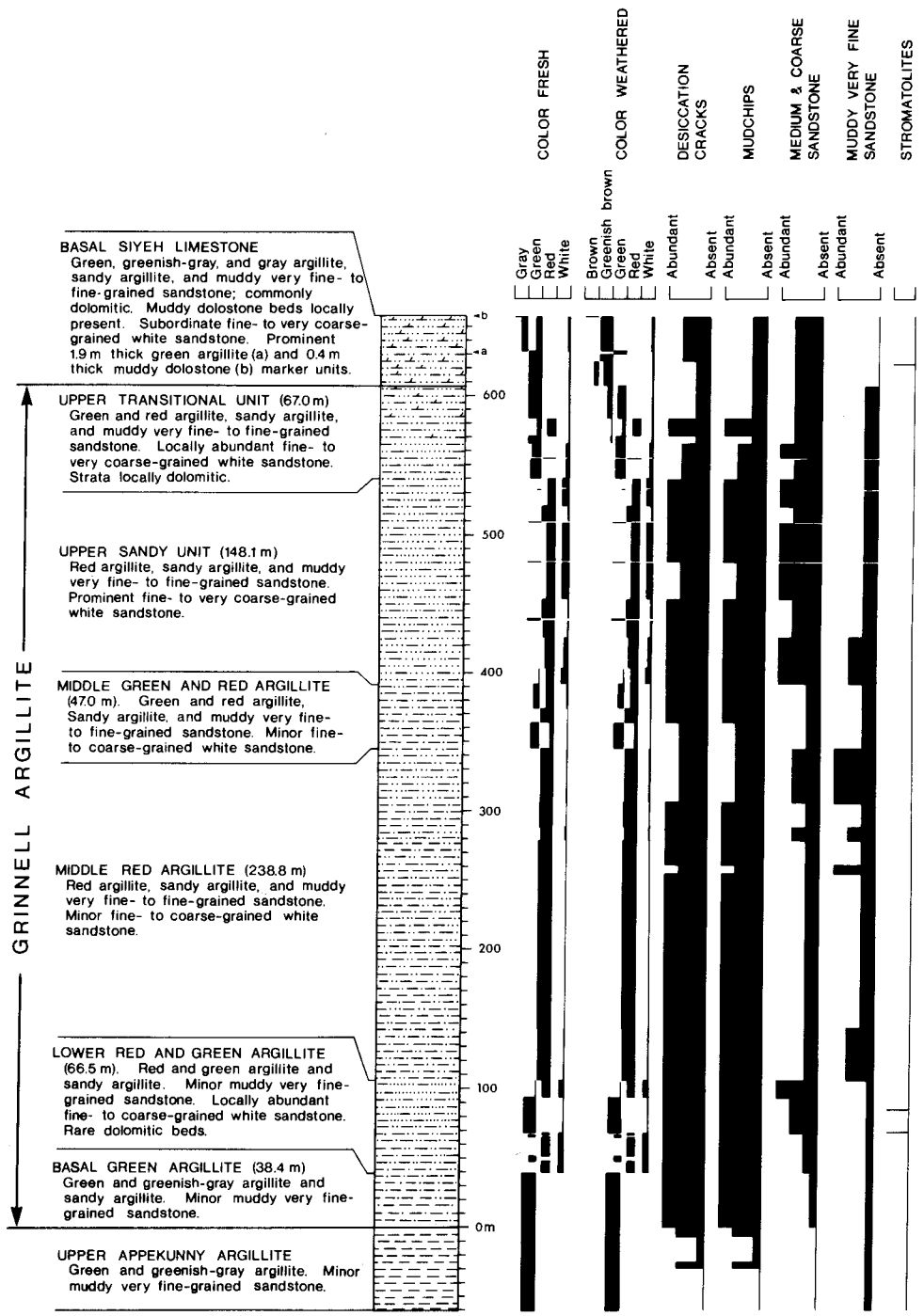

Fig. 7. Section of the Grinnell Argillite measured using a Jacob staff on the south side of Mt. Henkel, northeastern Glacier National Park, Montana.

have not been detected. Well-developed desiccation cracks and desiccation-crack-derived mudchips are abundant throughout this unit. A depositional model for the upper sandy unit of the Grinnell Argillite must account for the following: (1) abundant evidence of subaerial exposure, even within the sandy cosets; (2) very fine interbedding of relatively coarse-grained sandy layers with muddy layers and sharp contacts between these layers; (3) sandstone bed thickness generally 1—10 cm and rarely a maximum of 25 cm; (4) continuity of some sandstone beds for more than 100 m with little change in thickness; (5) an absence of either coarsening- or fining-upward sequences; (6) an absence of uneven scour deeper than a few centimeters beneath the sandstone beds; and (7) an absence of sedimentary-structure associations of the type commonly present in tidal deposits (Klein, 1977).

Upon cursory examination, the attributes enumerated above (particularly the interbedded nature of sandstones and mudstones, continuity of many sandstone beds and abundance of desiccation structures) is suggestive of overbank deposits of a major meandering river, with the sandy layers representing crevasse-splay sands. However, such a model can be ruled out because point-bar sequences and channel-fill deposits have not been detected in nearby strata, the sandstone beds do not fine upward in the manner characteristic of crevasse-splay sands, and the sandstones are coarser than those typical of crevasse-splay sands. An alternative model, based upon braided-stream and possibly sheet-flood deposition, is not appealing initially because recent braided streams typically contain little muddy sediment (Walker and Cant, 1979). However, fluvial deposition may have been substantially different prior to the appearance of an extensive terrestrial plant cover (Schumm, 1968). An alluvial-plain model for parts of the Grinnell Argillite, similar to Winston's (1973) model for younger Belt strata, is proposed. In this model the upper sandy unit of the Grinnell Argillite was deposited on an alluvial plain, which was transected by braided or anastomosing streams. These streams were ephemeral and transported sand-sized material as bedload and finer grained material as suspended load during flooding episodes. Sand may also have been transported and deposited in interchannel areas by sheet floods. Variable discharge and shifting channels would account for the apparently random intercalation of texturally different lithologies, and the episodic nature of flooding events would account for the abundance of desiccation structures. In such a depositional model the middle red argillite unit of the Grinnell Argillite would represent a more distal or peripheral facies than the upper sandy unit, and the other units might represent marginal facies developed where the alluvial plain merged with a presumably marine body of water.

Mound-shaped dolomitic stromatolites 5—20 cm high and 10—50 cm wide are known from a single horizon in the lower Grinnell Argillite along Going-to-the-Sun Road (Rezak, 1957) and from two horizons on Mt. Henkel (Fig. 7). A high rate of terrigenous sedimentation probably accounts for the scarcity of stromatolites in the marginal-marine facies of the Grinnell Argillite.

Siyeh Limestone

The Siyeh Limestone gradationally overlies the Grinnell Argillite, and it consists largely of muddy and sandy dolostone, muddy and sandy dolomitic limestone, muddy and sandy limestone, dolomitic and calcitic argillite, dolomitic and calcitic sandy argillite, and dolomitic and calcitic sandstone. Most strata contain an appreciable amount of terrigenous material, and relatively pure carbonate beds are uncommon. This prominent carbonate unit is 780 m thick in the central part of Glacier National Park, and along with its correlatives, the Helena Dolomite and Wallace Formation, it provides a distinctive unit useful for intrabasinal lithostratigraphic correlation (Harrison, 1972).

The Siyeh Limestone can be divided into seven informal lithologic units (Fig. 8) based upon carbonate content, presence or absence of "molar-tooth" structure (Fig. 9B), presence or absence of oolitic limestone and the type of stromatolites present. In Glacier National Park the Siyeh Limestone appears to be predominantly a peritidal deposit. Desiccation cracks are common in the lower part of the formation and a significant proportion of these strata are probably intertidal. However, shallow-subtidal deposits appear to predominate throughout most of the formation. In the upper 175 m of the Siyeh Limestone, a unit more thoroughly studied by the writer (Horodyski, 1976b), evidence for tidal deposition includes the occurrence of herringbone cross-stratification (Fig. 9C), reactivation surfaces (Fig. 9D), flaser bedding, wavy bedding and lenticular bedding. Desiccation cracks and structures produced during emergence are not common in this part of the Siyeh Limestone, suggesting predominantly subtidal sedimentation. Cyclicity is apparent in parts of the Siyeh Limestone. For example, strata exposed along the headwall on the west side of Grinnell Glacier clearly exhibit cycles consisting of dark gray mudstone and dolomitic mudstone overlain by brown-weathering impure dolostone. These cycles are interpreted as a generally transgressive mudstone unit overlain by a regressive dolostone unit. Other apparently largely regressive carbonate cycles, which contain an abundance of "molar-tooth" structure in the upper part of the cycles, occur in the middle Siyeh Limestone. Halite casts, some as large as 3 cm, have been detected in several beds 250—370 m above the base of the Siyeh Limestone on Mt. Henkel (Fig. 9A) and smaller halite casts have been detected 450 m above the base of the formation on Mt. Grinnell; however, they are absent from most of the formation in Glacier National Park.

Of all of the Belt strata in Glacier National Park, stromatolites are most abundant in the Siyeh Limestone. Silicified stromatolites are common in the interval 110—180 m above the base of the formation and they are particularly well exposed at Grinnell Glacier (Fig. 10). The chert layers comprising these stromatolites commonly extend continuously for several meters to tens of meters and range from 0.5 to 5 cm thick, although locally thicknesses exceed 10 cm. These stromatolitic layers are thicker around the periphery of

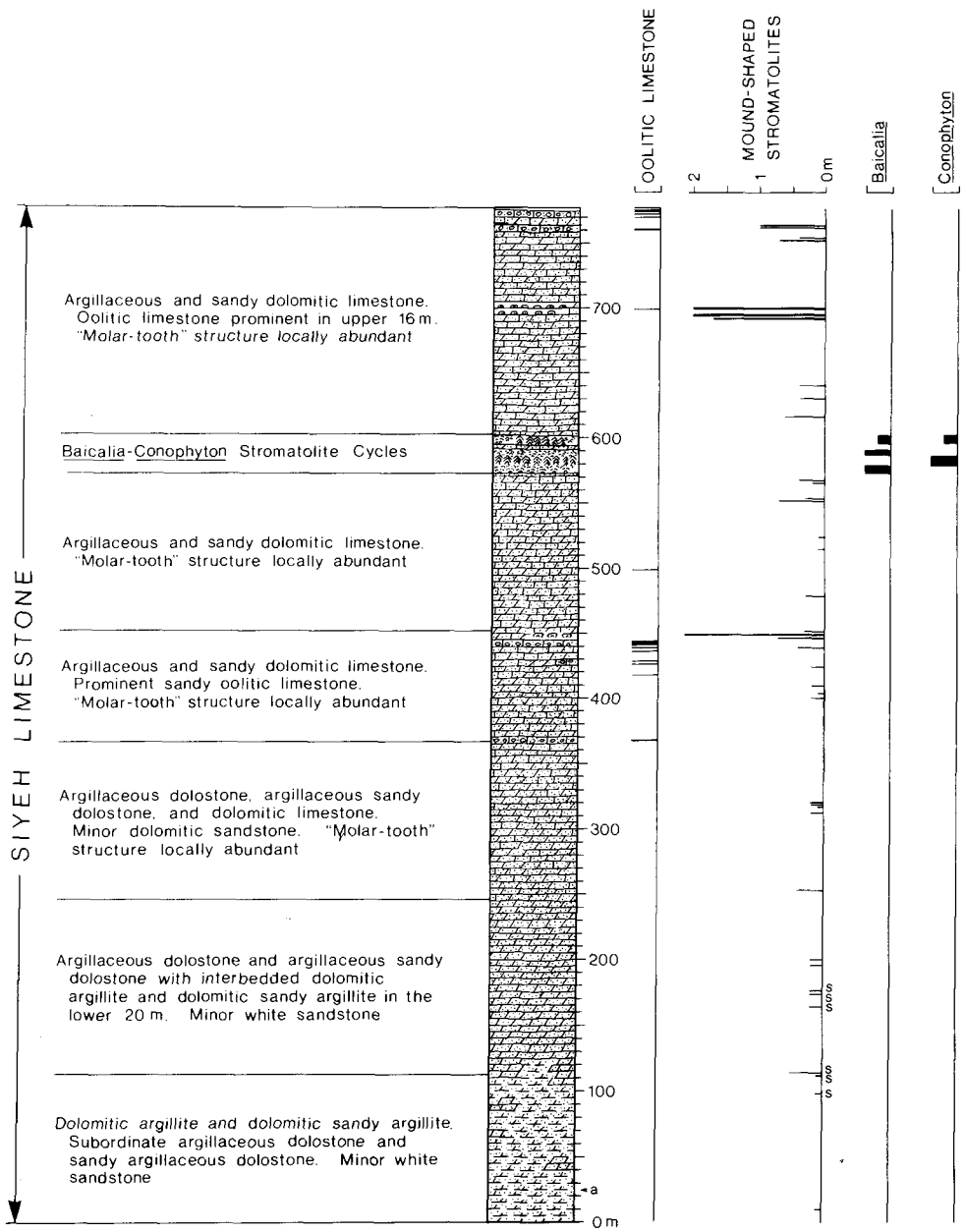

Fig. 8. Composite section of the Siyeh Limestone measured using a Jacob staff. The upper 205 m was measured on the northeast side of Piegan Mountain and the lower and middle part was measured on the southeast side of Mt. Grinnell. The occurrence of oolitic limestone beds, occurrence and height of mound-shaped stromatolites, and occurrence of *Baicalia* and *Conophyton* is indicated. (a) Marks the location of a 2.3 m thick green argillite marker unit correlative with the green argillite marker unit on Mt. Henkel (Fig. 7) and (s) indicates stromatolites that are silicified or partially silicified.

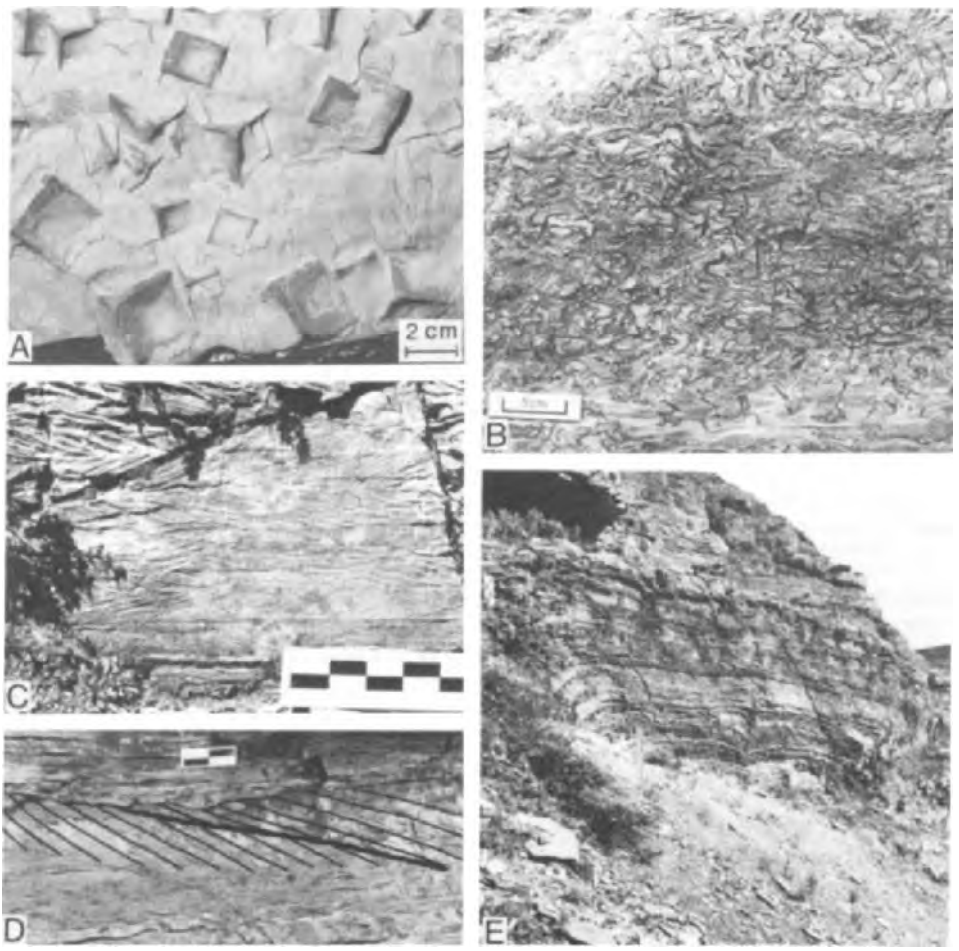

Fig. 9. Sedimentary structures and stromatolites of the Siyeh Limestone, Glacier National Park, Montana. A. Casts of halite hopper crystals on the base of a dolomitic, muddy, very fine grained sandstone bed located ~ 300 m above the base of the Siyeh Limestone on Mt. Henkel. B. "Molar-tooth" structure from the upper Siyeh Limestone. "Molar-tooth" structure is common in parts of the Siyeh Limestone and consists of millimeter-wide vertical and horizontal cracks and pods filled with 5—20 μm diameter, equant calcite crystals. They appear to have originated by early diagenetic precipitation of calcium carbonate in a variety of open-space structures, including syneresis cracks, desiccation cracks, and liquid- and gas-filled voids formed by decay of organic layers and gas produced during decomposition of organic material (Horodyski, 1976b). The crumpling shown in this figure is the result of the "molar-tooth" structures being competent at the time of compaction of the surrounding sediment (Smith, 1968). C. Herringbone cross-stratification in a sandy oolitic limestone in the upper Siyeh Limestone. Scale is in 5 cm divisions. D. Reactivation surface in a cross-stratified sandy oolitic limestone bed in the upper Siyeh Limestone. Selected laminae and the reactivation surface (heavy line) are traced in this photograph. Scale is in 5 cm divisions. E. Mound-shaped stromatolite ~ 7 m across and 2 m high in the upper Siyeh Limestone, Pollock Mtn. Scale in upper left is in 5 cm divisions.

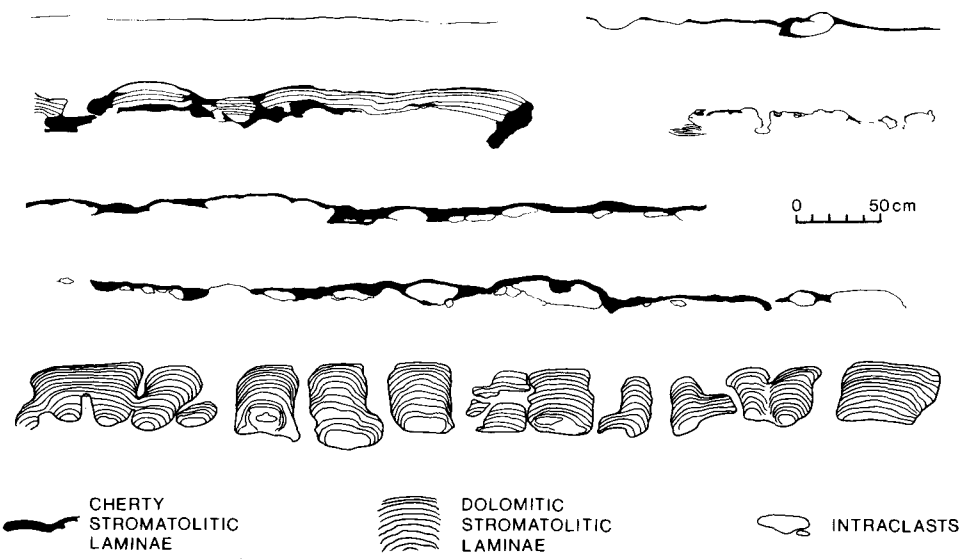

Fig. 10. Silicified and dolomitic stromatolites from the lower Siyeh Limestone, Grinnell Glacier, Glacier National Park, Montana. These stromatolites occur in a sandy and silty dolostone ~ 180 m above the base of the Siyeh Limestone. These sketches were obtained by tracing photographs of seven stromatolite horizons exposed on joint surfaces oriented perpendicular to bedding.

erosional topographic highs, having a few centimeters to about three decimeters relief. This difference in thickness of stromatolitic layers could be the result of accretion in a nearly emergent setting in which a microbial mat developed preferentially along the submerged or moist margins of small channels rather than upon the more frequently exposed topographic highs. These cherts appear to represent a silicified microbial mat, which contained a substantial carbonate component. Microfossils have not been detected in these cherts, and are probably absent because the organic material was extensively degraded prior to silicification. Factors that can lead to poor or non-preservation of microfossils in cherts include: (1) a substantial time lag between death of a microorganism and time of silicification; (2) the absence of anoxic and/or hypersaline conditions that would temporarily preserve organic matter prior to mineralization (Knoll and Golubic, 1979); and (3) aggrading neomorphism of admixed carbonate prior to silicification (Horodyski and Donaldson, 1980). Dolomitic mound-shaped stromatolites ranging from a few centimeters to a few decimeters in height and width occur with and stratigraphically above these cherty stromatolites (Figs. 8, 10).

Mound- and dome-shaped calcitic and calcitic—dolomitic stromatolites are common in the middle and upper Siyeh Limestone (Horodyski, 1976b). These stromatolites range from a few centimeters to ~ 2 m in height (Fig. 9E) and appear to have formed by a combination of in situ carbonate

precipitation and sediment stabilization. Branched columnar morphologies are rare in the Siyeh Limestone outside of the *Baicalia—Conophyton* cycles, which are discussed in the succeeding section. The prevalence of simple mound- and dome-shaped morphologies and scarcity of branched columnar forms may be the result of detrital sedimentation rates on the stromatolitic growth surface being high relative to microbial accretion rates, thereby inhibiting the development and maintenance of columns by smoothing over developing growth irregularities (Horodyski, 1976b, 1977).

Baicalia—Conophyton stromatolite cycles

A very prominent, erosionally resistant unit composed of branched columnar and conical stromatolites is present ~ 200 m below the top of the Siyeh Limestone in Glacier National Park and vicinity (Fig. 3B). This stromatolite unit ranges from ~ 24 to 32 m thick, and it is herein referred to as the *Baicalia—Conophyton* Cycles because of the occurrence of these two groups of stromatolites. Being composed of nearly pure calcite, outcrops of this unit are highly susceptible to dissolution, which obscures details of stromatolitic lamination. Several localities, however, yield clean outcrop surfaces. One such locality is at the northeast margin of South Swiftcurrent Glacier in northeastern Glacier National Park, where a 300 m long, virtually unweathered outcrop has been recently exposed by glacier retreat. The following description of the *Baicalia—Conophyton* Cycles is based upon observations made within a 40 km^2 area, which includes the Swiftcurrent Glacier locality. In this area the *Baicalia—Conophyton* Cycles can be divided into six units (Fig. 11): a Lower *Baicalia* Unit (4.3—6.6 m thick); a Lower Small-Diameter *Conophyton* Unit (2.7—4.0 m thick); a Lower Large-Diameter *Conophyton* Unit (3.3—4.6 m thick); a Middle *Baicalia* Unit (3.9—6.0 m thick); a Middle Sedimentary Unit (2.7—4.3 m thick); and an Upper Mixed Stromatolite Unit (4.3—6.6 m thick). The following description and discussion is based upon work in progress. These stromatolites are not treated systematically in this report because laboratory studies are incomplete.

The Lower *Baicalia* Unit is 6.0 m thick at South Swiftcurrent Glacier and is characterized by the occurrence of branched columnar stromatolites. The lower half of this unit consists of 3—15 cm diameter *Baicalia* columns, which form 1—2 m diameter, closely spaced to contiguous colonies (Fig. 12B and lower part of Fig. 12D). The degree of divergence of branching in these columns is related to the spacing of colonies and the shape of the growth surface, with relatively more divergent branching occurring where the colonies are separated and where the colonies have convex growth profiles. Interbedded with the branched columnar stromatolites, and comprising 20—60% of the lower part of this unit, are thinly bedded silty and sandy dolomitic limestone, micritic limestone and eroded stromatolite-lamina debris beds. In the upper part of the Lower *Baicalia* Unit the stromatolite columns become broader (10—30 cm) and more closely spaced, they branch

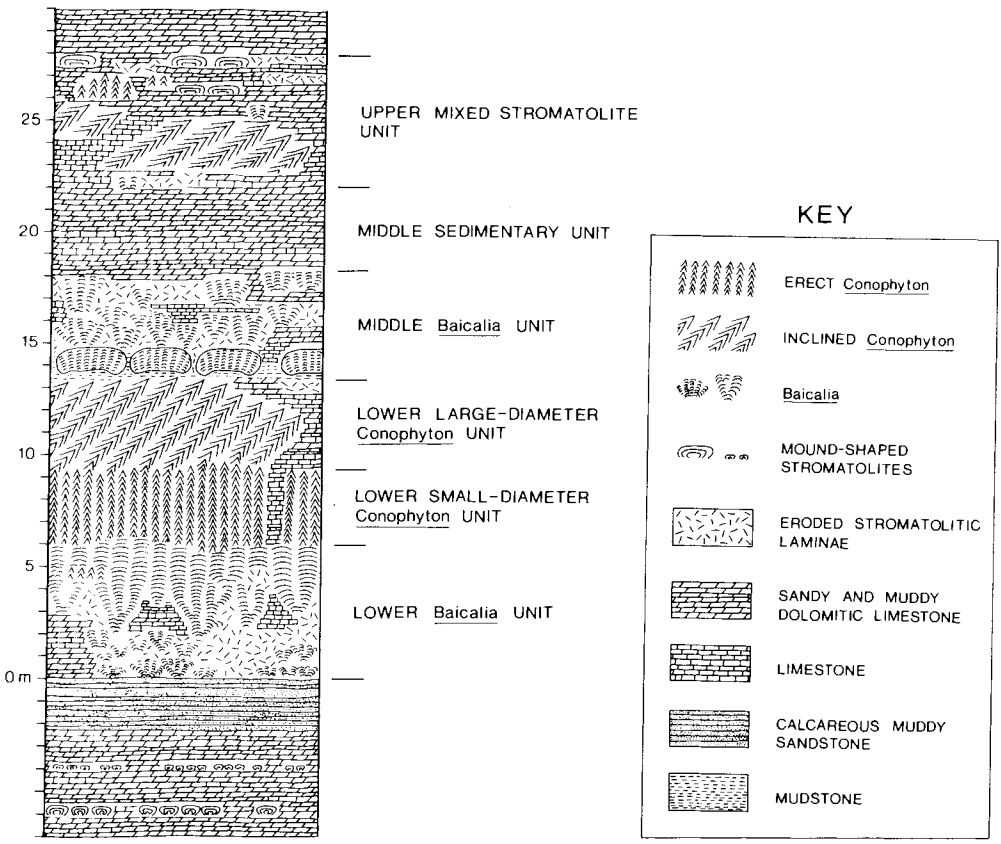

Fig. 11. Diagrammatic representation of the *Baicalia—Conophyton* Cycles in the Siyeh Limestone, South Swiftcurrent Glacier, Glacier National Park, Montana.

less frequently and the laminae become less convex (Fig. 12A and the upper part of Fig. 12D). Interbedded sediment constitutes 5—10% of this unit, and consists largely of eroded stromatolite-lamina debris and subordinate micritic limestone. Poorly developed *Conophyton*-like stromatolites are present locally in the upper part of this unit. They are generally ~ 5 cm in diameter and 5—20 cm high (Fig. 12C), and they form 0.5—2 m wide, 10—40 cm thick units entirely surrounded by gently convex-laminated columnar stromatolites. These conically laminated stromatolites and adjacent convex-laminated stromatolites have similar lamination, and individual laminae can be traced from one morphology into the other.

The lower *Conophyton*-bearing horizon of the *Baicalia—Conophyton* Cycles is very prominent in Glacier National Park and it can be divided into two units — a lower unit consisting of small-diameter, erect *Conophyton* overlain by a unit consisting of larger diameter, inclined *Conophyton* (Fig. 11). At South Swiftcurrent Glacier the Lower Small-Diameter *Cono-*

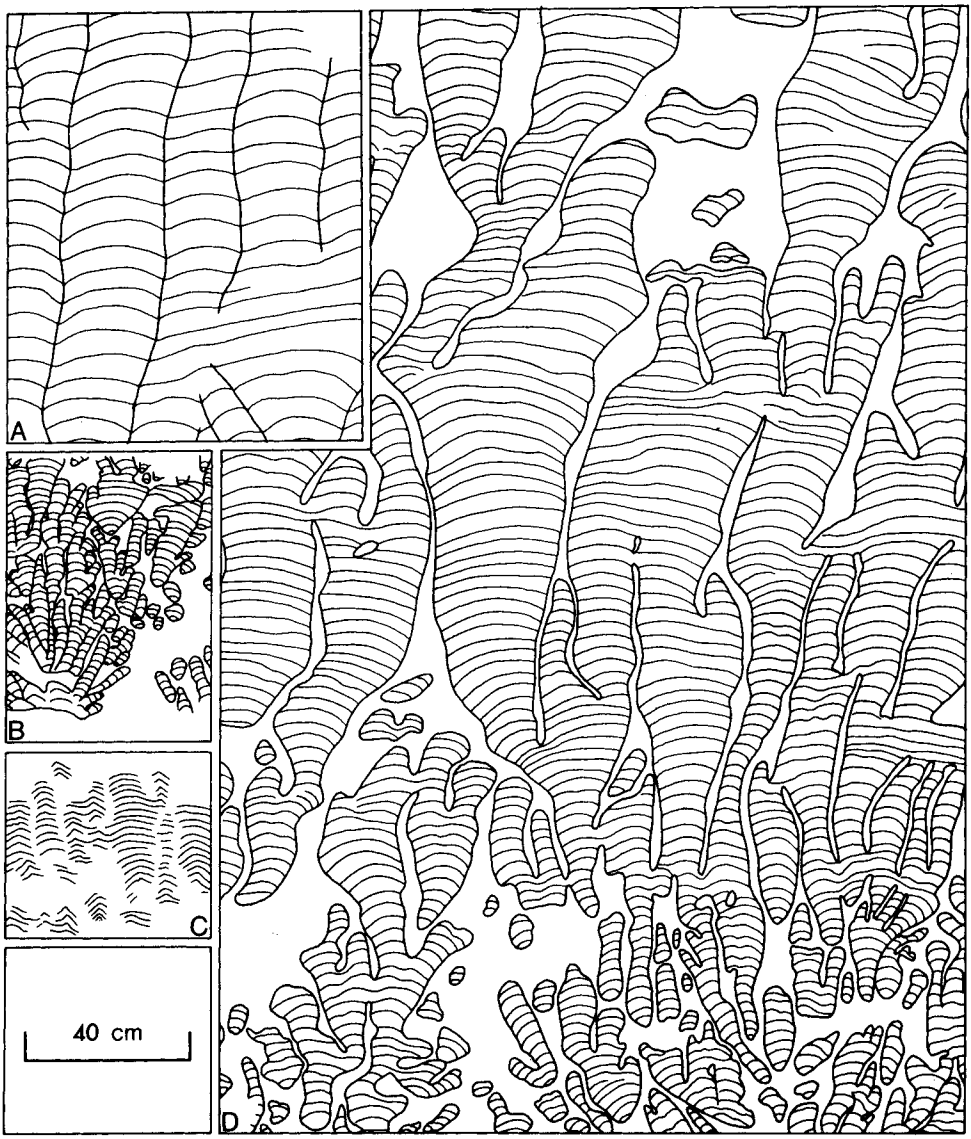

Fig. 12. Stromatolites of the Lower *Baicalia* Unit of the *Baicalia—Conophytón* Cycles, Siyeh Limestone, Glacier National Park, Montana. These figures were obtained by tracing photographs of outcrops oriented perpendicular to bedding in which stromatolite columns and selected laminae were outlined using felt-tip pens. A. Upper part of the Lower *Baicalia* Unit, Hole-in-the-Wall. B. Base of the Lower *Baicalia* Unit, between Lunch Creek and Reynolds Creek. C. Incipient conical lamination 1 m below the top of the Lower *Baicalia* Unit, South Swifcurrent Glacier. D. Middle part of the Lower *Baicalia* Unit, southwest side of Piegan Mountain.

phyton Unit is 3.4 m thick and is characterized by the occurrence of 3—15 cm diameter *Conophyton* columns. No other stromatolites occur in this unit. The *Conophyton* columns are typically erect and, very rarely, are inclined up to 30° from the vertical. Individual columns range from circular to lanceolate, sphenate and stellate in transverse section (Figs. 13D, 14B). Columns are unlinked to intermittently linked (Fig. 14C) and laminae may encircle adjacent columns (Fig. 14B). Columns 1 m long have been observed, but column length can rarely be ascertained in the field due to the irregular nature of most outcrop surfaces. Intercolumn sediment consists of micritic limestone containing small fragments of stromatolitic laminae and irregular centimeter-sized masses of silty dolomitic limestone. Eroded stromatolite-debris beds, common in the underlying Lower *Baicalia* Unit, are absent from this unit. The contact with the underlying Lower *Baicalia* Unit is generally an irregular surface having 5—15 cm relief (Fig. 14A) and the laminae comprising the *Conophyton* in the lower part of this unit is similar to that comprising the gently convexly laminated stromatolites occurring at the top of the Lower *Baicalia* Unit. The *Conophyton* columns in this unit commonly form 5—20 m diameter bioherms separated by 1—2 m.

The Lower Small-Diameter *Conophyton* Unit grades vertically into the Lower Large-Diameter *Conophyton* Unit. This unit is 4.0 m thick at South Swiftcurrent Glacier and is characterized by the occurrence of 10—60 cm diameter *Conophyton* columns with axes inclined 30—60° from the vertical (Figs. 13A, C, 14F). Columns 2 m long have been observed at several localities; however, in most outcrops it is impossible to determine the length of the columns and slabbed samples commonly exhibit growth discontinuities not apparent in outcrop. Individual columns range from circular to lanceolate, sphenate and irregular stellate in cross section (Figs. 13B, 14D). Projections or "ribs" most commonly occur on the lower part of these inclined columns (Fig. 14E), with the ribs generally projecting downward or into spaces between adjacent columns. Ribs occurring on the upper part of inclined columns commonly point toward adjacent columns. These *Conophyton* columns are typically partially linked (Fig. 14F). The inclined *Conophyton* are generally asymmetric. This asymmetry is well displayed on outcrop surfaces oriented perpendicular to bedding where it is manifested by differences in lamina thickness and in the distribution of ribs (Fig. 14E). Biohermal organization is more apparent in this unit than in the underlying unit. These bioherms range from 3—20 m in diameter, are composed of closely packed, inclined *Conophyton* columns, have 0.5—2.0 m synoptic relief, and are separated by 1—2 m and, locally, as much as 10 m of thinly interbedded micritic limestone and silty and sandy dolomitic limestone. Although some bioherms are only 1.5 m thick, others extend through the entire unit and are ~ 4 m thick. Stromatolites other than *Conophyton* do not occur in this unit. Stromatolite-lamina debris beds do not occur in this unit, except for local discontinuous 2—10 cm thick beds that are interbedded with interbiohermal micritic limestone at the top of this unit.

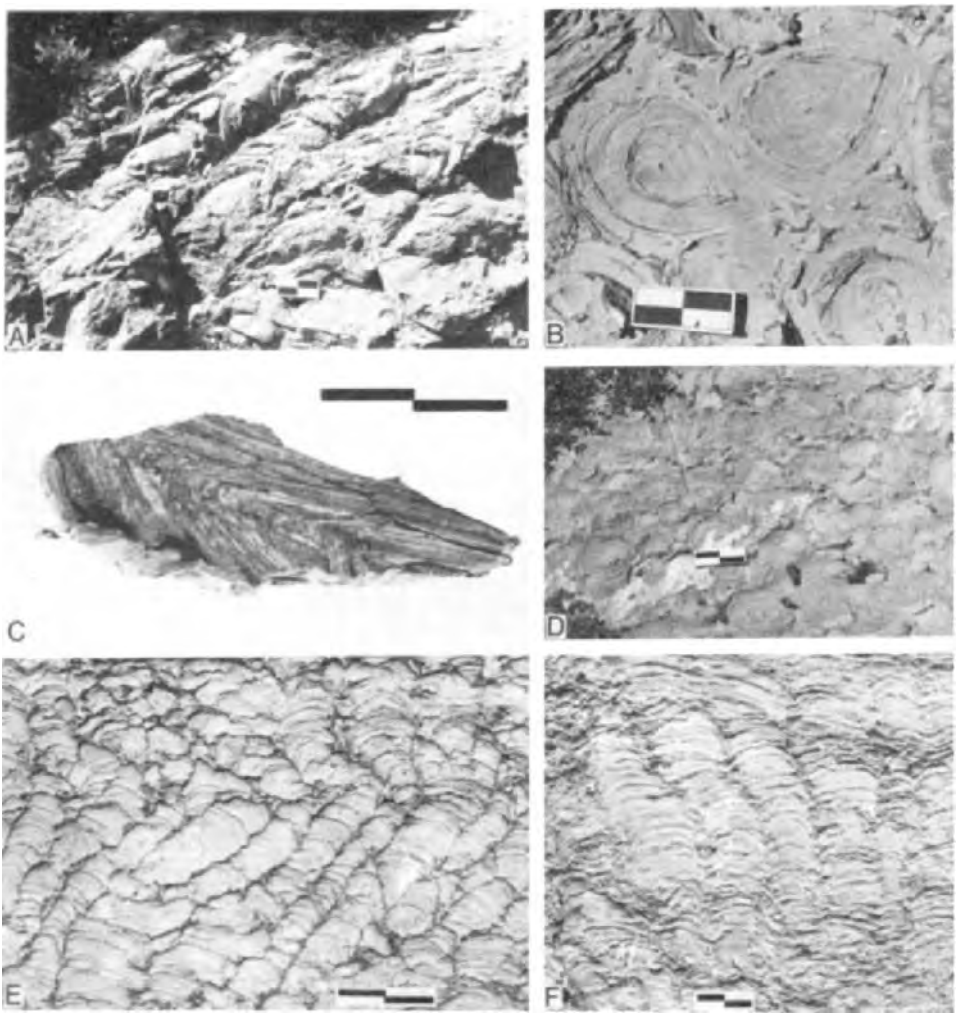

Fig. 13. Stromatolites from the *Baicalia—Conophyton* Cycles, Siyeh Limestone, Glacier National Park, Montana. Scale is in 5 cm divisions in all figures. A. Outcrop showing inclined *Conophyton* from the Lower Large-Diameter *Conophyton* Unit, Swiftcurrent Mountain. B. Outcrop surface parallel to bedding showing inclined *Conophyton* columns from the Lower Large-Diameter *Conophyton* Unit, near Lunch Creek. The sharp inflections in lamination are on the lower side of the inclined columns. C. Slabbed section of an inclined *Conophyton* column from the Lower Large-Diameter *Conophyton* Unit, near Lunch Creek. The axis of this column is inclined ~ 60° from the vertical. D. Outcrop surface parallel to bedding showing *Conophyton* columns from the Lower Small-Diameter *Conophyton* Unit, near Lunch Creek. E. Joint surface oriented perpendicular to bedding showing columnar stromatolites near the base of the Middle *Baicalia* Unit, South Swiftcurrent Glacier. F. Joint surface oriented perpendicular to bedding showing columnar stromatolites from the middle of the Middle *Baicalia* Unit, South Swiftcurrent Glacier.

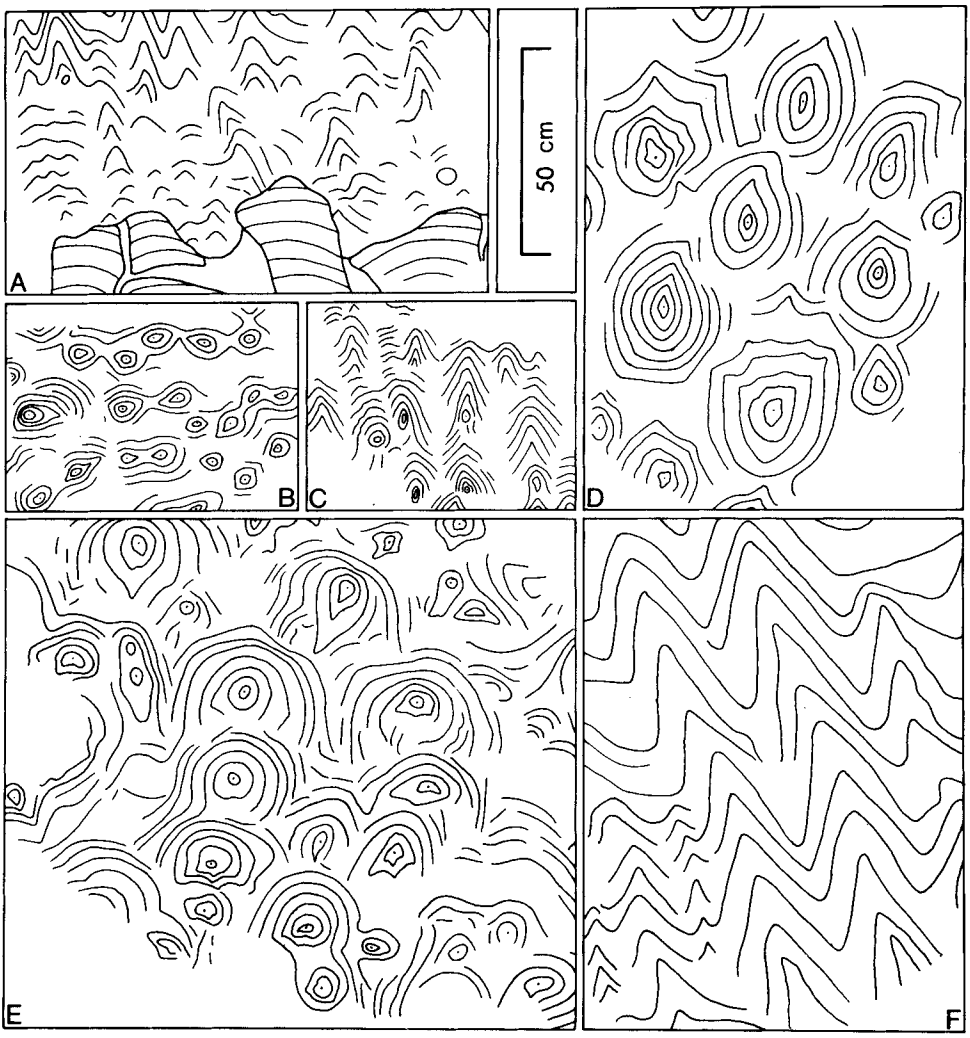

Fig. 14. Stromatolites of the Lower Small-Diameter *Conophyton* Unit (A—C) and Lower Large-Diameter *Conophyton* Unit (D—F) of the *Baicalia—Conophyton* Cycles, Siyeh Limestone, Glacier National Park, Montana. These figures were obtained by tracing photographs of outcrops in which selected stromatolitic laminae were outlined using felt-tip pens. A. Contact between the Lower *Baicalia* Unit and the overlying Lower Small-Diameter *Conophyton* Unit, shown on a joint surface oriented perpendicular to bedding, Haystack Butte. B. Small-diameter *Conophyton* shown on a joint surface oriented parallel to bedding, Hole-in-the-Wall. C. Small-diameter *Conophyton* shown on a joint surface oriented perpendicular to bedding, South Swiftcurrent Glacier. D. Large-diameter, inclined *Conophyton* shown on a joint surface oriented parallel to bedding, Lunch Creek. The sharp inflections in lamination are on the lower side of the inclined columns. E. Large-diameter, inclined *Conophyton* shown on a joint surface oriented perpendicular to bedding, South Swiftcurrent Glacier. F. Large-diameter, inclined *Conophyton* shown on a surface oriented oblique to the trend of the plunging axes, South Swiftcurrent Glacier.

The Middle *Baicalia* Unit, 4.9 m thick at South Swiftcurrent Glacier, is composed largely of branched columnar stromatolites of the group *Baicalia*. Bioherms at the base of this unit are distinctive: they are well-developed flat-topped mounds 1.0—1.5 m high, 2—8 m wide and composed of very closely crowded, 3—10 cm diameter, generally unbranched or parallel-branched columns (Figs. 13E, 15A, lower part of 15B). Interbiohermal sediment consists of black calcareous mudstone, micritic limestone thinly interbedded with silty and sandy dolomitic limestone, and eroded stromatolite laminae. Underlying these bioherms is 10—50 cm of black calcareous mudstone. The remainder of this unit consists of *Baicalia* bioherms, mound-shaped stroma-

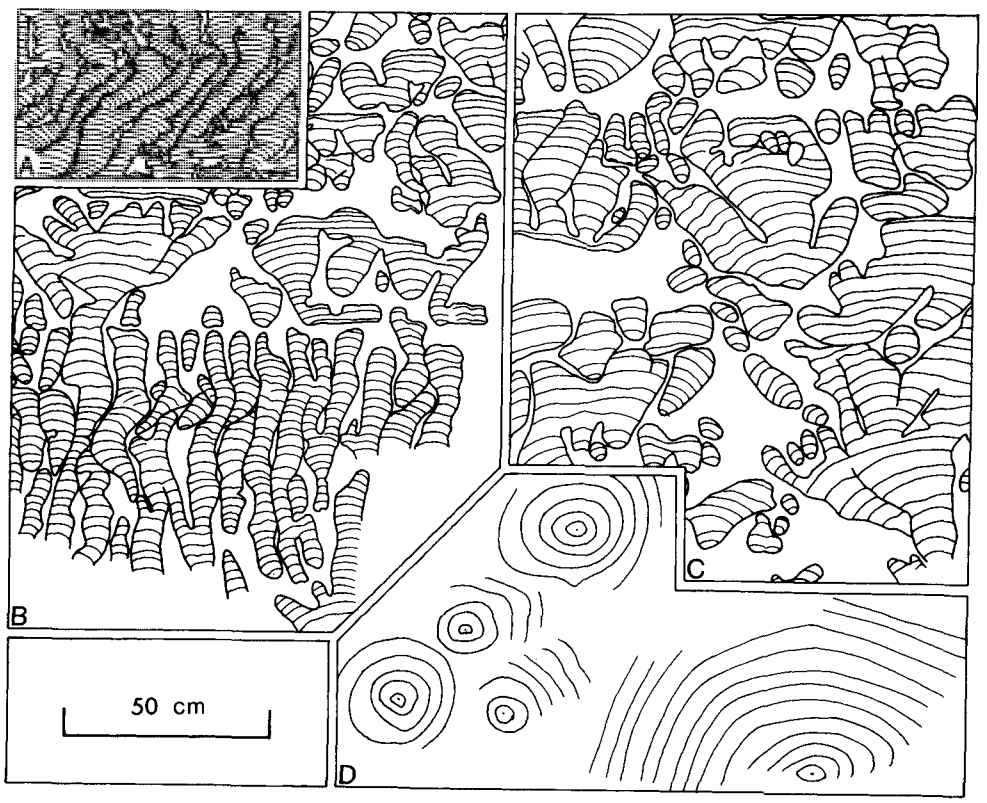

Fig. 15. Stromatolites of the Middle *Baicalia* Unit (A—C) and Upper Mixed Stromatolite Unit (D) of the *Baicalia—Conophyton* Cycles, Siyeh Limestone, Glacier National Park, Montana. These figures were obtained by tracing photographs of outcrops in which stromatolite columns and selected laminae were outlined using felt-tip pens. A. Lower part of the Middle *Baicalia* Unit shown on a joint surface oriented perpendicular to bedding, South Swiftcurrent Glacier. B. Lower part of the Middle *Baicalia* Unit shown on a joint surface oriented perpendicular to bedding, South Swiftcurrent Glacier. C. Middle part of the Middle *Baicalia* Unit shown on a joint surface oriented perpendicular to bedding, South Swiftcurrent Glacier. D. Inclined *Conophyton* shown on a surface oriented perpendicular to their axes, northeast side of Heavens Peak.

tolites and interbedded sediment. The *Baicalia* columns range from 3—60 cm in diameter (Figs. 13F, 15C, and the upper part of 15B), and they form bioherms 0.5—6 m wide and several decimeters to ~ 3 m high. The mound-shaped stromatolites are generally a few to several decimeters high and several decimeters to 1 m wide. Interbedded sediment constitutes 15—30% of this unit above the basal *Baicalia* bioherms and consists of micritic limestone, silty and sandy dolomitic limestone, and eroded stromatolite laminae.

The Middle Sedimentary Unit is 3.8 m thick at South Swiftcurrent Glacier, and consists largely of silty and sandy dolomitic limestone and micritic limestone. "Molar-tooth" structure is common in the lower half of this unit and probable desiccation cracks occur in the middle part of this unit. Mound-shaped stromatolites a few decimeters high are present.

The Upper Mixed Stromatolite Unit is 5.9 m thick at South Swiftcurrent Glacier and it exhibits greater lateral variability than do the other units of the *Baicalia-Conophyton* Cycles. *Conophyton*, *Baicalia* and mound-shaped stromatolites occur in this unit along with intercalated sediment. *Conophyton* is the most prominent stromatolite: columns range from 5—50 cm in diameter, and they generally form prominent bioherms 1—2.5 m high, 2—10 m and locally 20 m wide, and are separated by < 1—> 5 m. These bioherms commonly overlap one another. Columns in these bioherms are closely crowded and highly inclined with their axes oriented 45—75° from the vertical. These *Conophyton* are similar to those in the Lower Large-Diameter *Conophyton* Unit; however, the larger diameter columns in the Upper Mixed Stromatolite Unit (Fig. 15D) are commonly more circular and less ribbed than those in the underlying unit. Small- and medium-diameter *Conophyton* are commonly ribbed with their ribs generally oriented downward. Stromatolites other than *Conophyton* do not occur in these bioherms. Erect *Conophyton* are relatively uncommon in this unit. They tend to be 5—15 cm wide, a few decimeters long and generally form poorly defined meter-sized masses in the upper part of the unit. Branched columnar stromatolites of the group *Baicalia* that occur in this unit range from 5—20 cm in diameter and form bioherms a few decimeters to ~ 2 m high. Mound-shaped stromatolites one to several decimeters high are common in the upper part of this unit. Thinly interbedded micritic limestone, and silty and sandy dolomitic limestone is prominent as interbiohermal sediment between *Conophyton* bioherms. Silty and sandy dolomitic limestone and micritic limestone occurs between the other stromatolite beds. Eroded stromatolite-lamina debris is common laterally adjacent to the mound-shaped stromatolites and *Baicalia* bioherms, and it locally occurs above and below *Conophyton* bioherms. However, such material does not occur within or between *Conophyton* bioherms.

Units comprising the *Baicalia—Conophyton* Cycles are laterally persistent in a northwest—souteast direction in Glacier National Park (Fig. 16). It appears likely, however, that this direction may be subparallel to depositional strike. Lateral changes are more marked in a northeast—southwest direction,

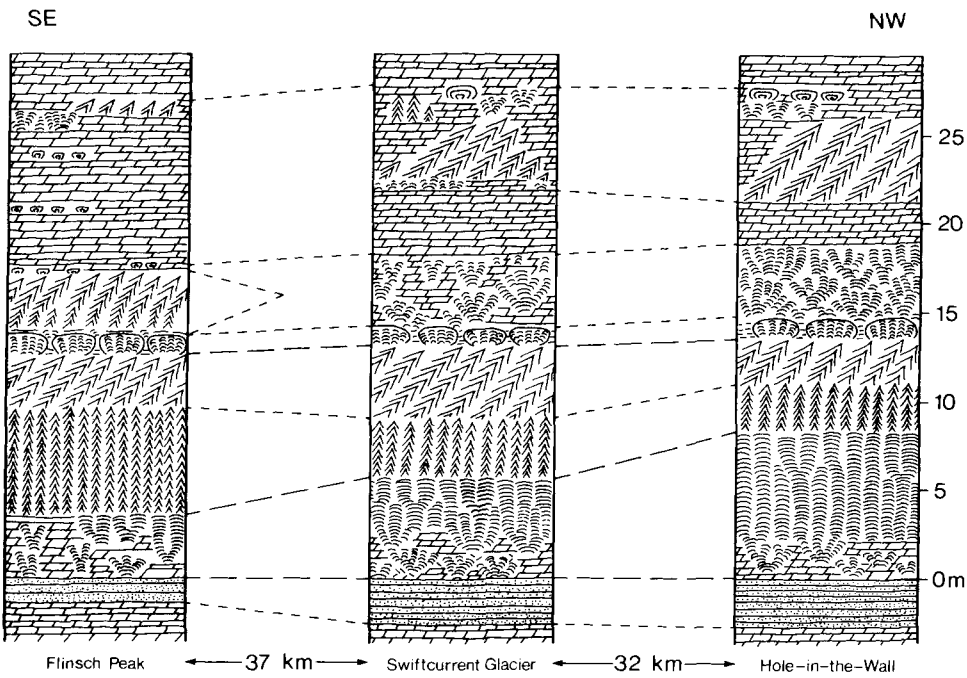

Fig. 16. Correlation of units comprising the *Baicalia—Conophyton* Stromatolite Cycles of the Siyeh Limestone from the northwestern to south-central part of Glacier National Park.

with one of the changes being the disappearance of *Conophyton* to the southwest. A prominent stromatolite unit consisting of a 5.2 m thick and a 3.5 m thick horizon of *Baicalia*-like stromatolites is exposed at Somers, Montana and may be the lithostratigraphic correlative of the *Baicalia—Conophyton* Cycles. This exposure is located 55 km southwest of the southernmost exposure of the cycles in Glacier National Park and it may have a greater palinspastic separation.

The inclined *Conophyton* occurring in the Lower Large-Diameter *Conophyton* Unit and Upper Mixed Stromatolite Unit exhibit a preferred orientation, with columns within a single outcrop tending to be inclined in the same direction (Fig. 17A). The same preferred orientation, with axes trending in a southerly—southwesterly direction, is maintained for a distance of 90 km in Glacier National Park (Fig. 17B).

Although laboratory studies have not yet been completed on stromatolites from the *Baicalia-Conophyton* Cycles, it is possible to make several conclusions based upon available data.

(1) Branched columnar stromatolites of the group *Baicalia* and conical stromatolites of the group *Conophyton* largely comprise the 24—32 m thick *Baicalia-Conophyton* Cycles of the Siyeh Limestone. Branched columnar stromatolites are very rare and conical stromatolites are absent in the re-

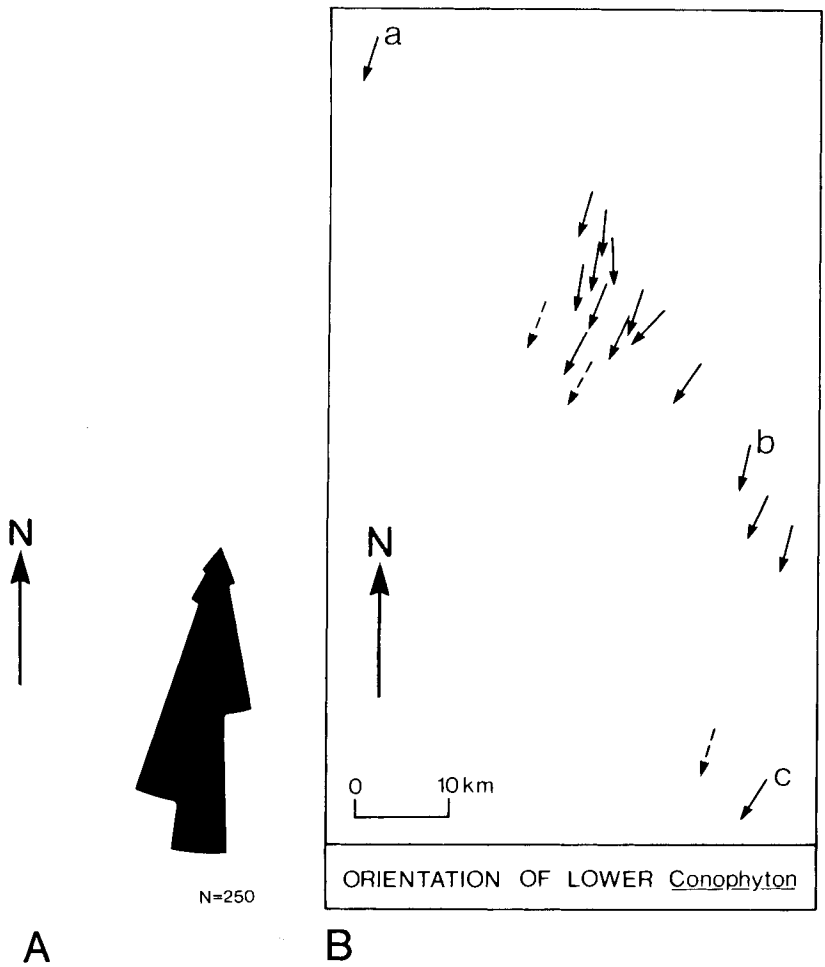

Fig. 17. Orientation of inclined *Conophyton* columns from the Lower Large-Diameter *Conophyton* Unit of the *Baicalia-Conophyton* Cycles, Siyeh Limestone, Glacier National Park, Montana. A. Rose diagram showing the trend of the axes of 250 inclined *Conophyton* columns at South Swiftcurrent Glacier. B. Plot showing the trends of the axes of inclined *Conophyton* columns in Glacier National Park. Solid arrows represent the average trend of 50 columns, broken arrows the average of < 50 columns. The arrowhead points in the direction in which the axes are plunging; thus, the apices of the conical laminae are pointing in a northeasterly direction. Localities are provided for reference: (a) Hole-in-the-Wall in the northern part of Glacier National Park; (b) Norris Mountain; and (c) Snowslip Mountain near the southern boundary of Glacier National Park.

mainder of the 780 m thick Siyeh Limestone. Concentration of these stromatolites within a relatively thin unit reflects environmental conditions particularly conducive to the formation of columnar stromatolites. A critical condition may be a low sedimentation rate of detrital material relative to the growth rate of a microbial mat.

(2) The high carbonate content and low terrigenous content of stromatolites in these cycles relative to that of adjacent strata indicate that these stromatolites formed largely by in situ carbonate precipitation rather than by sediment stabilization.

(3) The abundance of disrupted stromatolite-lamina debris in the *Baicalia* units and the scarcity of such material in the *Conophyton* units indicate that these *Baicalia* formed in settings subject to higher energy events than did *Conophyton*. This is further supported by observations on Heavens Peak on the west side of the study area where *Conophyton* is poorly developed in the Lower Small-Diameter *Conophyton* and Lower Large-Diameter *Conophyton* Units, and is replaced by disrupted stromatolite-lamina debris, mound-shaped stromatolites and *Baicalia*.

(4) The irregular nature of the contact of the Lower Small-Diameter *Conophyton* Unit with the underlying Lower *Baicalia* Unit and the disrupted nature of some laminae along this contact is suggestive of erosion, and may reflect a reef-crest setting. If correct, the Lower *Baicalia* Unit may have originated in a moderate-energy reef-front setting and the Lower *Conophyton* Units in a low-energy back-reef setting. The Lower *Baicalia*—Lower *Conophyton* cycle could have formed by progradation, possibly accompanied by subsidence or eustatic sea level rise.

(5) The *Conophyton* in these particular cycles formed in shallower water than did most or all of the *Baicalia*. They appear, however, to have formed in a subtidal setting as indications of subaerial exposure, such as desiccation cracks and desiccation-crack-derived mudchips, are lacking. Furthermore, *Conophyton* is absent in western exposures where the Siyeh Limestone has a deeper water appearance.

(6) The absence of *Baicalia* and other stromatolites from the massive *Conophyton* units indicates that *Conophyton* either formed under different environmental conditions, was produced by a different microbial community, or was characterized by different microbial activity than *Baicalia*.

(7) The microstructural similarities exhibited between *Conophyton* in the Lower Small-Diameter *Conophyton* Unit and the gently convexly laminated columnar stromatolites near the top of the Lower *Baicalia* Unit suggest that very similar microbial communities produced these morphologically different stromatolites. This is also indicated by the incipient *Conophyton* forming within the upper part of the Lower *Baicalia* Unit. As proposed by Walter et al. (1976), the conical morphology of *Conophyton* is largely due to the presence of actively motile elements in the stromatolite-building community. The transition from gently convexly laminated, branched columnar stromatolites to conically laminated stromatolites in these cycles might be the result of several factors including the addition of a highly motile element to the stromatolite-building community, a change in the activity of a relatively unvarying microbial community, or changing environmental conditions. As an example of the latter, relatively turbulent conditions might inhibit the growth of projecting conical forms and favor the growth of

smoothly laminated forms, whereas relatively quiescent conditions might permit motile filaments to construct a sharp-pointed conical mat.

(8) The ribs that occur in some *Conophyton* columns and the sharp-crested ridges that commonly connect adjacent *Conophyton* columns are probably the result of the same biologic processes that produced the conical growth profile of *Conophyton*, namely the motility of filamentous microorganisms.

(9) The preferred orientation of the inclined *Conophyton* columns was probably produced in response to gentle current or wave activity. The rather uniform orientation of these inclined columns over a large area, combined with the shallow-water setting of this unit and a probable northwest—southeast depositional strike, suggests that waves played a major role in orienting these stromatolites. The apices of the inclined *Conophyton* point toward the inferred shoreline as deduced from facies relationships in the Siyeh Limestone.

(10) The *Baicalia—Conophyton* Cycles may provide a useful lithostratigraphic unit for analyzing the eastern portion of the Belt Supergroup; however, it must not be used as a chronostratigraphic unit.

Snowslip and Shepard Formations

The Snowslip and Shepard Formations are the uppermost Belt units exposed in the central part of Glacier National Park, although overlying Belt strata are present in the northwestern and southern part of the park. The lower unit, the Snowslip Formation, is a 385 m thick, dominantly terrigenous sequence of green and red argillite, dolomitic argillite, and muddy sandstone (Fig. 18). Throughout this unit ripple cross-laminated muddy laminae alternate with pelitic laminae to form wavy and lenticular bedding (Reineck and Wunderlich, 1968), and clay foreset drapes are common in ripple cross-laminated muddy sandstone beds, indicating frequent fluctuations in depositional energy. Desiccation cracks (Fig. 18), mudchip conglomerates, and wave and wave-modified current ripples are ubiquitous, and indicate alternating periods of subaerial exposure and submergence. Runzelmarks and rare raindrop impressions also indicate subaerial exposure. Double-crested ripples, flat-topped ripples and ladder ripples (Fig. 18) are present, and indicate fluctuating water level and emergence runoff (Klein, 1977). Sedimentary cycles are not readily discerned in the Snowslip Formation and in much of the formation there appears to be an almost random intercalation of lithologies. However, a poorly developed and irregular cyclicity consisting of fining-upward cycles ~ 1—2 m thick is apparent locally. The presence of structures indicating frequent alternation of periods of subaerial exposure and emergence, alternating periods of tractional transport and fallout from suspension, and fluctuating water level and emergence suggest that a substantial portion of the Snowslip Formation was deposited in an intertidal setting. Initially it appears unlikely that a thick sequence of

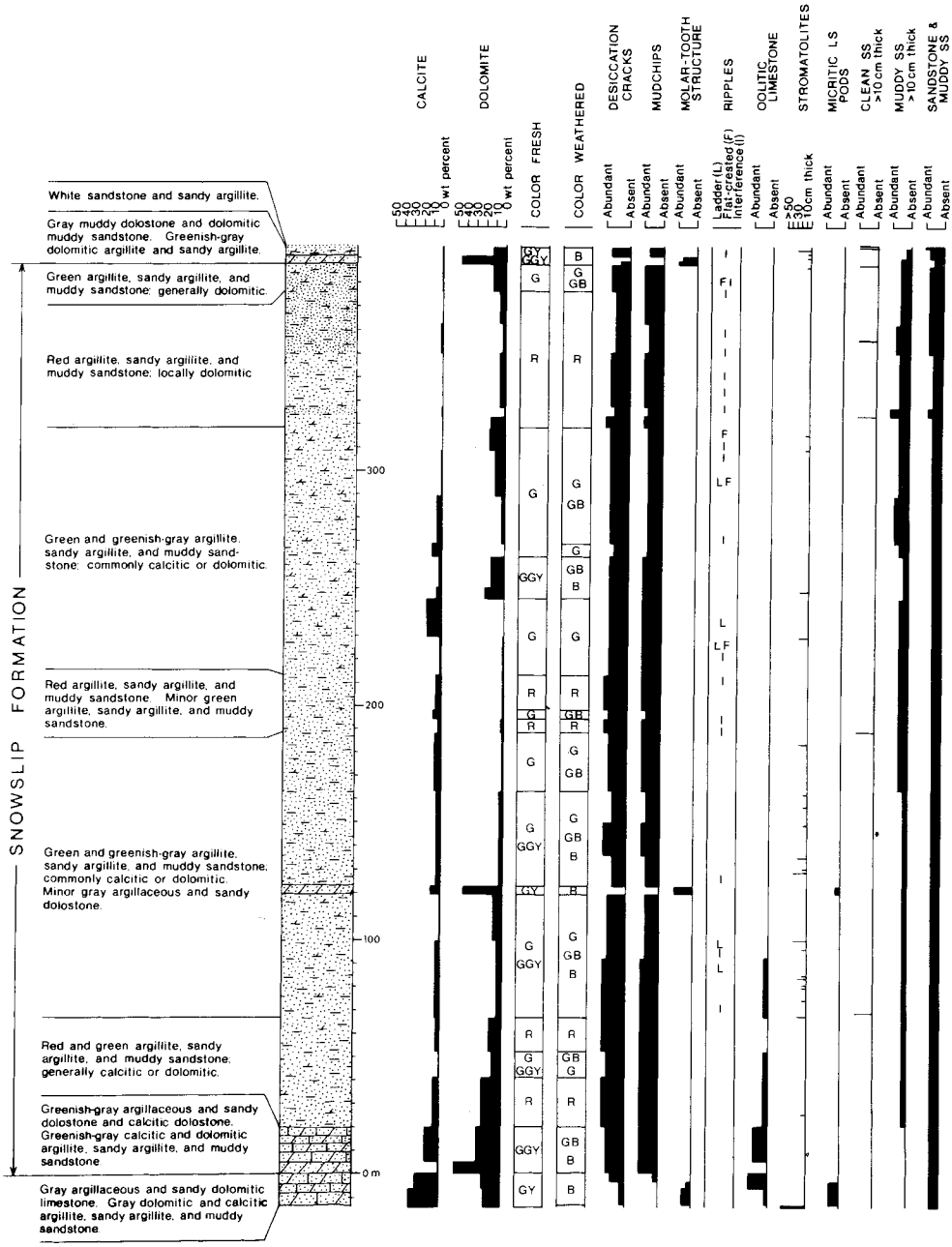

Fig. 18. Section of the Snowslip Formation measured using a Jacob staff on the southwest side of Piegan Mountain, central Glacier National Park, Montana. Total carbonate content and calcite–dolomite ratios were determined by acid dissolution and X-ray diffractometry of powdered chip samples. Abbreviations of colors are as follows: G — green; R — red; B — brown; GY — gray; GB — greenish brown; GGY — greenish gray.

dominantly intertidal sediments would be deposited at a particular locality, as this would appear to require a very precise balance between subsidence and sedimentation. This problem may be resolved if an excess of sediment were transported by longshore drift into a tidal flat in an area that was subsiding at a rate lower than the potential sedimentation rate. In such a setting, sedimentation could keep up with subsidence resulting in a predominance of intertidal deposits, relative scarcity of subtidal deposits and, if wind and wave processes are subordinate, a scarcity or absence of eolian deposits. A possible depositional setting for the Snowslip Formation would be in proximity to a major delta along a moderately low-energy coast. Alternatively, an excess of sediment could have been supplied by an alluvial plain merging with the sea, and the Snowslip Formation might have been a longshore deposit in such a setting (see Winston, 1973).

The overlying Shepard Formation consists of green and greenish-gray argillite, dolomitic argillite, muddy sandstone and muddy dolostone (Fig. 19). It is similar to the Snowslip Formation except that desiccation cracks and mudchip conglomerates are less abundant and dolomitic sediments are more prominent. Shallow subtidal and intertidal deposits appear to be about evenly represented in the Shepard Formation. Irregular cycles one to several meters thick are locally developed in the Shepard Formation. These cycles, generally poorly developed, are best defined 70—150 m above the base of the formation where they consist of an erosional base having a few centimeters relief, a lower fine-grained sandstone or dolomitic sandstone unit several decimeters thick, and an upper unit consisting of several decimeters to several meters of dolomitic argillite, dolomitic sandy argillite, muddy dolostone and sandy dolostone. "Molar-tooth" structure is most abundant near the top of these cycles, and eroded "molar-tooth" debris beds a few centimeters to decimeters thick locally cap the cycles and represent erosional lag deposits. These cycles appear to be dominantly regressive. The top of the Shepard Formation is not exposed in the central part of Glacier National Park, having been removed by erosion.

Stromatolites or stromatoloids (abiogenic stromatolite-like structures (Oehler, 1972)) are relatively common in the Snowslip Formation with 21 horizons occurring in a measured section on Piegan Mountain and are less common in the Shepard Formation with only 3 horizons occurring in a measured section on Reynolds Mountain (Figs. 18, 19). As most horizons are discontinuous, the actual number of horizons present is somewhat greater. The Snowslip structures (Figs. 20B, C, D, H) have a simple mound-shaped morphology, range from 2—80 cm in diameter, and have a lamina thickness of a few millimeters to 30 cm. They generally occur in isolation or form bioherms a few decimeters to a few meters in diameter. Growth was commonly initiated upon irregularities projecting 1—10 cm above the depositional surface, which provided an elevated substrate less subject to sediment scour. These substrate highs are generally of erosional origin, with erosionally modified shrinkage polygons being particularly common. Stromatolites (or

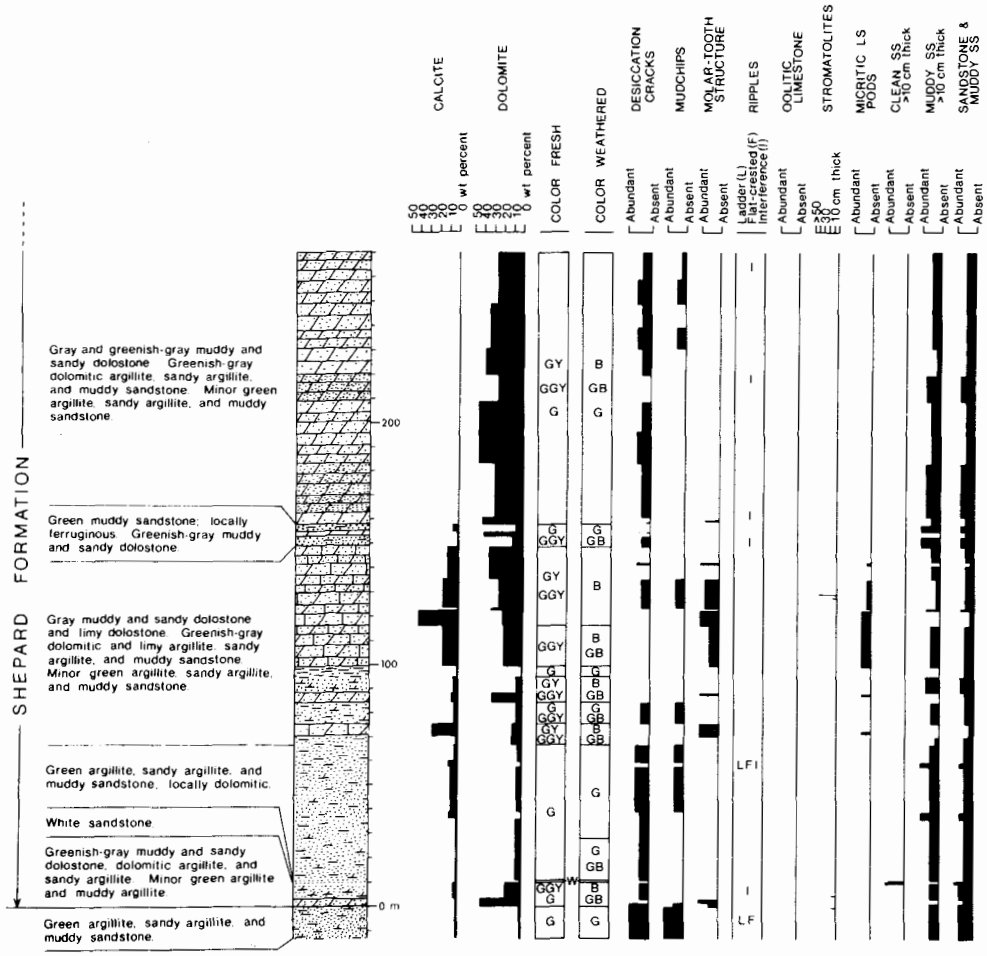

Fig. 19. Section of part of the Shepard Formation measured using a Jacob staff on the east side of Reynolds Mountain, central Glacier National Park, Montana. Total carbonate content and calcite-dolomite ratios were determined by acid dissolution and X-ray diffractometry of powdered chip samples. Abbreviations of colors are as follows: G — green; B — brown; W — white; GY — gray; GGY — greenish gray; GB — greenish brown. Note that the uppermost Shepard Formation is not exposed at this locality.

stromatoloids) in the lower part of the Snowslip Formation are generally calcitic (Horodyski, 1975), whereas both calcitic and dolomitic stromatolites occur in the middle and upper part of the formation. As these structures occur in a predominantly terrigenous sequence that lacks pure calcareous beds and as the laminae are highly deficient in terrigenous material, it is clear that these laminae originated almost entirely by in situ carbonate precipitation. This precipitation could have been the result of the photosynthetic removal of carbon dioxide by a cyanophycean mat, in which case the structures would be true stromatolites. Alternatively, precipitation could have

been the result of a physio-chemical process, such as evaporation or warming of water saturated with respect to calcium carbonate, perhaps in a tidal pool. If this were the case, the resultant structures would not strictly be stromatolites according to the commonly used definition of stromatolite as "organo-sedimentary structures produced by sediment trapping, binding and/or precipitation as a result of the growth and metabolic activity of micro-organisms, principally cyanophytes" (Walter, 1976). This cautious approach to the Snowslip and Shepard stromatolite-like structures is brought about by the resemblance of some of these calcareous laminae, particularly the very smooth, even laminae composed of radial-fibrous calcite (Fig. 20H), to supposedly inorganically precipitated calcite in caves. Filamentous microfossils have been detected from a stromatolite (or stromatoloid) in the lower part of the Snowslip Formation. They have the form of hematized, 0.5—10 μm diameter cylinders (Figs. 20E—G) and may represent the outlines of oscillatoriacean cyanophyte sheaths (Horodyski, 1975). However, their presence does not prove that the calcareous laminae of these structures resulted from microbial rather than physio-chemical processes.

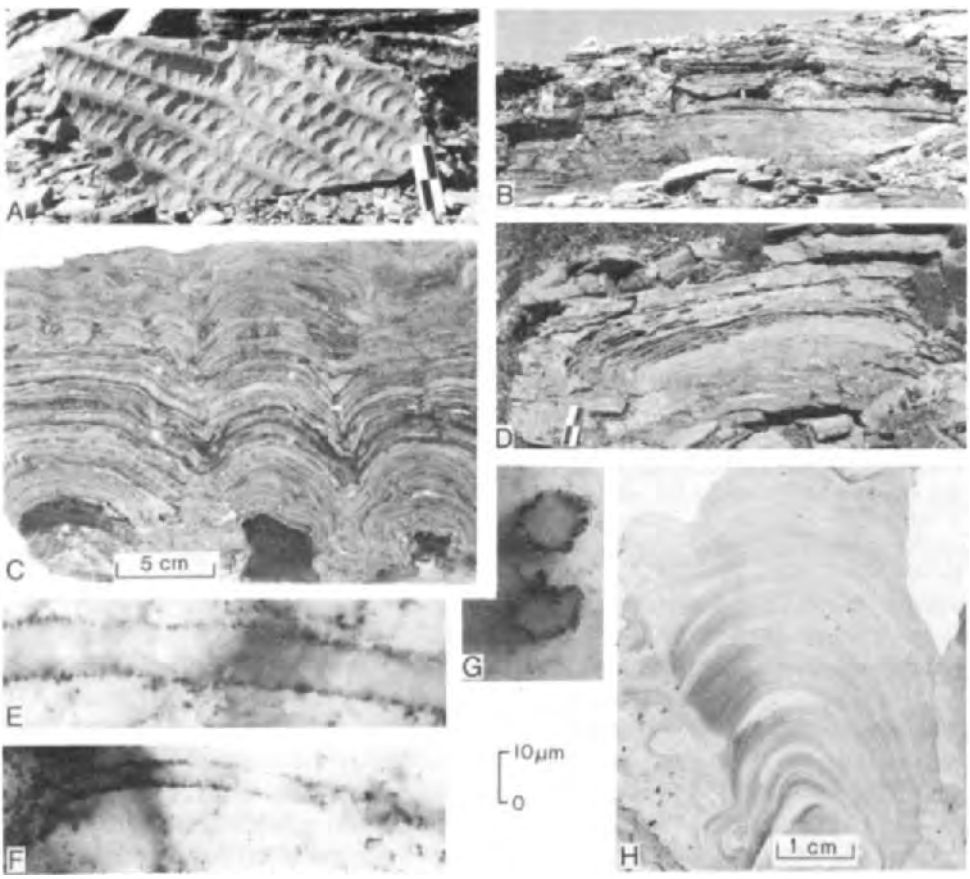

CONCLUSIONS

Glacier National Park, Montana provides some of the best exposed, most complete and structurally least complex sections of the Middle Proterozoic Belt Supergroup. These strata, attaining a thickness of ~2 900 m in central Glacier National Park, include offshore, peritidal, alluvial and possibly deltaic lithofacies. Stromatolites are very well developed in several Belt formations and those comprising the *Baicalia—Conophyton* Cycles in the Siyeh Limestone appear to be particularly promising for analyzing the northeastern part of the Belt Basin. Although studies of these stratigraphic units and stromatolites are not complete, preliminary information, particularly detailed measured sections, has been presented in this report with the hope that it will aid in attaining a more thorough understanding of the depositional history of the Belt Supergroup.

ACKNOWLEDGMENTS

The author thanks the National Park Service and gratefully acknowledges the cooperation and assistance provided by many Park Service rangers and

---

Fig. 20. Sedimentary structures, stromatolites or stromatoloids and microfossils from the Snowslip Formation, Glacier National Park, Montana. A. Ladder ripples in a muddy sandstone bed. Note that the larger ripples are flat crested. Scale is in 5 cm divisions. B. Calcitic stromatolites or stromatoloids in a sequence of green argillite, sandy argillite and muddy sandstone on the southwest side of Piegan Mountain. The mound-shaped stromatolite (or stromatoloid) to the right of the scale is about 40 cm high. C. Slabbed section through a calcitic, mound-shaped stromatolite or stromatoloid. Note that these mound-shaped laminae developed over topographic highs, which appear to represent eroded desiccation polygons. D. Stromatolite or stromatoloid composed of pure calcitic laminae, and occurring in muddy sandstone and sandy argillite. Scale is in 5 cm divisions. E—G. Microfossils from a calcareous stromatolite or stromatoloid located 55 cm above the second red argillite band in the lower Snowslip Formation, southwest side of Piegan Mountain. These unbranched tubular structures are defined by 0.2—1 μm diameter hematite particles that outline curved cylinders of hematite-free calcite. These microfossils occur in a matrix of 20—50 μm diameter pseudospar grains. Microfossils shown in E and F are oriented parallel to the surface of the thin section, those in G are oriented perpendicular to the surface of the thin section. Scale is given to the right. These specimens are deposited at the Department of Paleobiology, National Museum of Natural History, Smithsonian Institution, Washington, D.C. Specimen numbers and location of the microfossils (given in reference to a left-handed orthogonal Cartesian coordinate system positioned with its origin at the "x" inscribed on each glass slide and oriented with the x-axis parallel to the length of the slide and the y-axis parallel to the width of the slide) are as follows: E, USNM311322, 31.8 mm x, 15.4 mm y; F, USNM311324, 13.7 mm x, 26.7 mm y; G, USNM311323, 58.7 mm x, 4.0 mm y. 1 000-m Universal Transverse Mercator coordinates, zone 12, of the microfossil locality are 5 398 360 m N and 301 510 m E, obtained from U.S. Geological Survey Logan Pass (1968) 7.5′ Quadrangle. H. Thin section (viewed in transmitted light) of a stromatolite or stromatoloid from the lower Slip Formation. The laminae are composed largely of radial-fibrous calcite. Note the very smooth and even nature of these laminae.

personnel. Initial studies of the Belt Supergroup were conducted while a Ph. D. student and post-doctoral research associate directed by J.W. Schopf. Recent studies were funded by a grant from the Petroleum Research Fund of the American Chemical Society.

REFERENCES

Childers, M.O., 1963. Structure and stratigraphy of the southwest Marias Pass area, Flathead County, Montana. Geol. Soc. Am. Bull., 74: 141—164.

Douglas, R.J.W., 1952. Preliminary map, Waterton west of 4th meridian, Alberta. Geol. Surv. Can., Preliminary Map 52-10.

Fenton, C.L. and Fenton, M.A., 1931. Algae and algal beds in the Belt Series of Glacier National Park. J. Geol., 39: 670—686.

Fenton, C.L. and Fenton, M.A., 1933. Algal beds or bioherms in the Belt Series of Montana. Geol. Soc. Am. Bull., 44: 1135—1142.

Fenton, C.L. and Fenton, M.A., 1937. Belt Series of the north: stratigraphy, sedimentation, paleontology. Geol. Soc. Am. Bull., 48: 1873—1969.

Häntzschel, W., 1975. Trace fossils and problematica. In: C. Teichert (Editor), Treatise on Invertebrate Paleontology, 2nd Ed. Pt. W, Miscellanea, Geol. Soc. Am. and Univ. Kansas Press, Boulder, CO, and Lawrence, KS, 269 pp.

Harrison, J.E., 1972. Precambrian Belt Basin of northwest United States: its geometry, sedimentation, and copper occurrences. Geol. Soc. Am. Bull., 83: 1215—1240.

Harrison, J.E., 1974. Epilogue. In: Belt Symposium, 1973. Idaho Bur. Mines Geol., 2: 1—14.

Harrison, J.E., Griggs, A.B. and Wells, J.D., 1974. Tectonic features of the Precambrian Belt Basin and their influence on post-Belt structures. U.S. Geol. Surv. Prof. Pap. 866, 15 pp.

Horodyski, R.J., 1975. Stromatolites of the lower Missoula Group (Middle Proterozoic), Belt Supergroup, Glacier National Park, Montana. Precambrian Res., 2: 215—254.

Horodyski, R.J., 1976a. Stromatolites from the Middle Proterozoic Altyn Limestone, Glacier National Park, Montana. In: M.R. Walter (Editor), Stromatolites. Elsevier, Amsterdam, pp. 585—597.

Horodyski, R.J., 1976b. Stromatolites of the upper Siyeh Limestone (Middle Proterozoic), Belt Supergroup, Glacier National Park, Montana. Precambrian Res., 3: 517—536.

Horodyski, R.J., 1977. Environmental influences on columnar stromatolite branching patterns: examples from the Middle Proterozoic Belt Supergroup, Glacier National Park, Montana. J. Paleontol., 51: 661—671.

Horodyski, R.J., 1981. Pseudomicrofossils and altered microfossils from a Middle Proterozoic shale, Belt Supergroup, Montana. Precambrian Res., 16: 143—154.

Horodyski, R.J., 1982. Problematic bedding-plane markings from the Middle Proterozoic Appekunny Argillite, Belt Supergroup, northwestern Montana. J. Paleontol., 56: 882—889.

Horodyski, R.J. and Donaldson, J.A., 1980. Microfossils from the Middle Proterozoic Dismal Lakes Group, Arctic Canada. Precambrian Res., 11: 125—159.

Hunt, G., 1962. Time of Purcell eruption in southeastern Britsh Columbia and southwestern Alberta. J. Alberta Soc. Pet. Geol., 10: 438—442.

Idaho Bureau of Mines and Geology, 1973. Belt Symposium, 1973. Vol. 1, 322 pp.

Idaho Bureau of Mines and Geology, 1974. Belt Symposium, 1973. Vol. 2, 138 pp.

Klein, G. deV., 1977. Clastic Tidal Facies. Continuing Education Publication Company, Champaign, Illinois, 149 pp.

Knoll, A.H. and Golubic, S., 1979. Anatomy and taphonomy of a Precambrian algal stromatolite. Precambrian Res., 10: 115—151.

Maxwell, D.T., 1974. Layer-silicate mineralogy of the Precambrian Belt Series. In: Belt Symposium, 1973. Idaho Bur. Mines Geol., 2: 113—138.
McMannis, W.J., 1963. LaHood Formation — a coarse facies of the Belt Series in southwestern Montana. Geol. Soc. Am. Bull., 74: 407—436.
Mudge, M.R., 1970. Origin of the disturbed belt in northwestern Montana. Geol. Soc. Am. Bull., 81: 377—392.
Oehler, J.H., 1972. "Stromatoloids" from Yellowstone Park, Wyoming. Geol. Soc. Am. Abstracts with Programs, 4: 212—213.
Reineck, H.-E. and Wunderlich, F., 1968. Classification and origin of flaser and lenticular bedding. Sedimentology, 11: 99—104.
Rezak, R., 1957. Stromatolites of the Belt Series in Glacier National Park and vicinity, Montana. U.S. Geol. Surv. Prof. Pap., 294-D: 127—154.
Ross, C.P., 1959. Geology of Glacier National Park and the Flathead region, northwestern Montana. U.S. Geol. Surv. Prof. Pap., 296, 125 pp.
Schumm, S.A., 1968. Speculations concerning paleohydrologic controls of terrestrial sedimentation. Geol. Soc. Am. Bull., 79: 1573—1588.
Smith, A.G., 1968. The origin and deformation of some "molar-tooth" structures in the Precambrian Belt—Purcell Supergroup. J. Geol., 76: 426—443.
Walcott, C.D., 1914. Cambrian geology and paleontology, III. No. 2 — Precambrian Algonkian algal flora. Smithson. Misc. Collet., 64: 77—156.
Walker, R.G. and Cant, D.J., 1979. Sandy fluvial systems. In: R.G. Walker (Editor), Facies Models. Geosciences Canada Reprint Series 1. Geological Association of Canada, Toronto, pp. 23—31.
Walter, M.R., 1976. Introduction. In: M.R. Walter (Editor), Stromatolites. Elsevier, Amsterdam, pp. 1—3.
Walter, M.R., Bauld, J. and Brock, T.D., 1976. Microbiology and morphogenesis of columnar stromatolites (*Conophyton, Vacerrilla*) from hot springs in Yellowstone National Park. In: M.R. Walter (Editor), Stromatolites. Elsevier, Amsterdam, pp. 273—310.
White, B., 1974. Microfossils from the Late Precambrian Altyn Formation of Glacier National Park, Montana. Nature, 247: 452—453.
Willis, B., 1902. Stratigraphy and structure, Lewis and Livingston Ranges, Montana. Geol. Soc. Am. Bull., 13: 305—352.
Winston, D., 1973. The Precambrian Missoula Group of Montana as a braided stream and sea-margin sequence. In: Belt Symposium, 1973. Idaho Bur. Mines Geol., 1: 208—220.

This Page Intentionally Left Blank

THE EMERGENCE OF METAZOA IN THE EARLY HISTORY OF LIFE

MARTIN F. GLAESSNER

Department of Geology, University of Adelaide, South Australia 5000 (Australia)

ABSTRACT

Glaessner, M.F., 1983. The emergence of Metazoa in the early history of life. Precambrian Res., 20: 427–441.

After consideration of currently used time scales and their geochronometric calibration, the views of biologists on evolutionary events in the early history of the Metazoa are discussed, mainly on the basis of two examples from the abundant literature. The phylogenetic views of A.V. Ivanov on the origin and early evolution of Metazoa to the level of sponges, Cnidaria and Platyhelminthes, are outlined. A brief discussion of the subsequent coelomate radiation, based on the work of R.B. Clark follows. It is proposed that these evolutionary events, postulated by biologists, occurred in the time span of about 300 Ma preceding the appearance of large Metazoan body fossils in Ediacarian time, about 600–560 Ma ago. Palaeontological data from this pre-Ediacarian, Late Proterozoic time span are limited to few, mostly small trace fossils. The reasons for this paucity and the consequent need to give new dimensions to trace fossil studies are discussed. It is concluded that there is evidence for a pre-Phanerozoic 'prehistory' of the Metazoa. A full explanation of the events and processes leading to their diversification and of its chronologic sequence will only be possible when all interacting systems, including the lithosphere, hydrosphere and atmosphere, relevant to their evolution during the appropriate time interval have been more completely elucidated.

INTRODUCTION

Some 20 years ago I drew a diagram showing the distribution of 'Bacteria', 'Stromatolites' and 'Animals' in the record of the history of life (Glaessner, 1968). A similar, but more elaborate diagram was constructed independently by Schopf (1967). The most striking point made in these compilations was the great length of time during which (in modern terminology) only prokaryotes (bacteria and cyanophyta) existed in the biosphere, and the late appearance of (metazoan) animals. Going back in time, the line marked 'body fossils' (of animals) in my diagram becomes broken ~ 650 Ma ago while the line marked 'trace fossils' (which are almost exclusively the results of animal activities) continues as a thin line indicating rare occurrences, to 1000 Ma. Since then the view has been expressed, on various grounds (Cloud, 1968 and later works; Margulis, 1970; Schopf et al., 1973; Knoll and

Barghoorn, 1975, Stanley, 1976), that Metazoa appreared much later, perhaps between 700 and 650 Ma ago, not long before the dates assigned to Ediacarian fossil assemblages. These divergent views of the time of origination of the Metazoa will be discussed from viewpoints of biological (biohistorical) theory as well as a re-evaluation of the fossil record. This discussion will be kept free from terminological confusion about the time scale in which relevant geohistorical events are to be placed. A time framework is required for this purpose. No complete agreement about the relevant part of the standard scales has yet been reached, but much work, mainly by contributors to Subcommissions of the Commission on Stratigraphy of the International Union of Geological Sciences (I.U.G.S.) and Working Groups of the International Geological Correlation Programme (I.G.C.P.) is in progress and nearing completion.

TIME FRAMEWORK

The International Stratigraphic Guide (Hedberg, 1976) together with subsequent proposals by the Subcommission on Precambrian Stratigraphy and by the Working Group on the Precambrian—Cambrian Boundary will be the starting point of this brief discussion. The relevant time interval is at present classified according to Table I.

TABLE I

The relevant time interval of the Precambrian—Cambrian boundary

Eons	Eras	Periods	Approximate time calibration (Ma)
		Permian	
Phanerozoic	Palaeozoic		
?		Cambrian	
			550 — 570
		III (Late)	
			900
	Proterozoic	II (Middle)	
			1600
		I (Early)	
			2500

Cloud (1972, 1976 a,b) has moved away from such a strictly stratigraphic scale. Discussing the interrelations of atmospheric, lithospheric and biospheric evolution, he found it appropriate to divide the required time scale into 'lithospheric-historical divisions' explained as modes (or Eons), punctuated by events which rapidly changed surface conditions on the Earth. He named the relevant divisions Proterophytic (to ~ 2000 Ma), Palaeophytic (to ~ 700 Ma) and Phanerozoic. In his scales, the first two terms replace the

widely used Proterozoic. The Phanerozoic extends beyond the beginning of the Cambrian, hence the even more widely used term Precambrian must also disappear from this scale. It seems unlikely that geological practice will dispense with these terms.

The reason for the divergence is the conceptual difference between two different kinds of scales. In a geohistorical scale, required for the discussion of evolutionary processes, boundaries must be transitional, representing relatively short intervals of time, or times of rapid change, because instantaneous world-wide events seem to be of limited significance. In contrast, representation and analysis of other geological data requires a stratigraphic scale with operationally sharply defined boundaries between geological bodies. In geological mapping, which is the basis of such work, precise boundaries are an operational necessity and transitional zones are minimized. The two aspects of geological scales are metaphorically comparable to map legends v. chapter headings in a history text. They may or may not require different terms for certain sequences.

The term Phanerozoic, used for a historical division, should now include the Ediacarian Period which clearly precedes the Cambrian (Cloud and Glaessner, 1982). The Ediacarian represents the historical transition at the end of the Precambrian, after the end of the Late Precambrian glaciations and before the appearance of the abundant Early Cambrian shelly faunas. In terms of a stratigraphic scale the Ediacarian is therefore Late Precambrian. Cloud (1972, 1976a,b) favoured an extension of the traditional Palaeozoic Era to include the Ediacarian. It must be asked whether the stratigraphic scale in its map-legend aspect needs a formal Eon term to counterbalance the remaining 85% of geological time. The transitional character of the Ediacarian is consistent with its position at the end of the Precambrian and also at the beginning of the Phanerozoic historical unit. Harland and Herod (1975) who let the Phanerozoic begin with the Cambrian, have tentatively suggested subdivisions of the Late Precambrian (Table II).

The world-wide recognition of the postulated boundary between an earlier (Sturtian) and a later (Varangian) Late Precambrian division seems to be

TABLE II

Subdivisions of the Late Precambrian from Harland and Herod (1975)

Phanerozoic	Palaeozoic	Cambrian	
			? 570 ±
		Ediacarian	
	Vendian		? 650 ±
		Varangian	
Adelaidean			? 700 ±
	Karatauan	Sturtian	
	= U. Riphean		? 750 ±
	etc.	etc.	

fraught with difficulties even in glaciated areas, and impracticable elsewhere. A majority of stratigraphers in the U.S.S.R. have now accepted a stratigraphic scale separating the Vendian from the Riphean (at 650 or 680 ± 20 Ma, see Keller, 1979; Chumakov and Semikhatov, 1981), with equal ranking. Pending a decision on the terms of a global stratigraphic scale, the terms Proterozoic, Riphean and Vendian, and Ediacarian for post-glacial or 'lesser' Vendian, will be used in the following discussion. The term 'cryptozoic' will be used informally for the obscure time span of 'prehistoric' evolution of the Metazoa in Late Proterozoic, but pre-Ediacarian time.

CONJECTURES FROM BIO-HISTORY

Many students of the living marine invertebrates have discussed their possible evolutionary origins and relationships. Many phylogenetic diagrams have been published. (For a review of a few selected examples see Valentine, 1977, p. 21.) Few of them give time scales for the assumed sequences of diversification events. Most living phyla with fossilizable structures are represented in Palaeozoic strata and a number of them are highly differentiated in the Early Cambrian. Biologists have concluded that much of the metazoan evolution must have occurred in the Precambrian. The question of how much evolution occurred in how much of Precambrian time could not be seriously examined until the last 25 years, when Precambrian palaeontology began to develop. The inherently incomplete palaeontological record means that it cannot be relied upon alone, but must be considered in relation to biohistorical conjectures based on the study of the living fauna.

Among the many models of metazoan phylogeny, those based on extreme polyphyletic views, deriving different phyla separately from different, more or less hypothetical, Protozoa amount to agnosticism and need not be taken too seriously. Other models extend phyletic lineages represented in the Cambrian record downward into the Precambrian until they meet at some common hypothetical point of assumed monophyletic origin. Others again, which are based not only on comparative morphology, but also on embryology, biochemistry, biomechanics, bioenergetics and ecology, deserve more serious consideration. They cannot be reviewed here, but two examples will be briefly considered to show what, according to biologists, should have occurred in Precambrian time. Two different problems concern the student of the emergence of the Metazoa. One is the question of the origins of multicellular animals from eukaryote Protista and the origin of the lower Metazoa, including the Radiata or Diploblastica (Hanson, 1977; Sleigh, 1979). The other is their diversification into the higher Metazoa, including the coelomates (higher Metazoa). Of particular concern is the origination of the major groups represented in the Ediacarian faunas at the end of the Precambrian and their further evolution towards existing diversity.

Ivanov (1968, 1970) concluded that the Metazoa originated from colonial flagellate Protozoa of increasing complexity (Fig. 1). On the way, the Parazoa or sponges evolved as a sideline adapted to a sessile mode of life. The main line

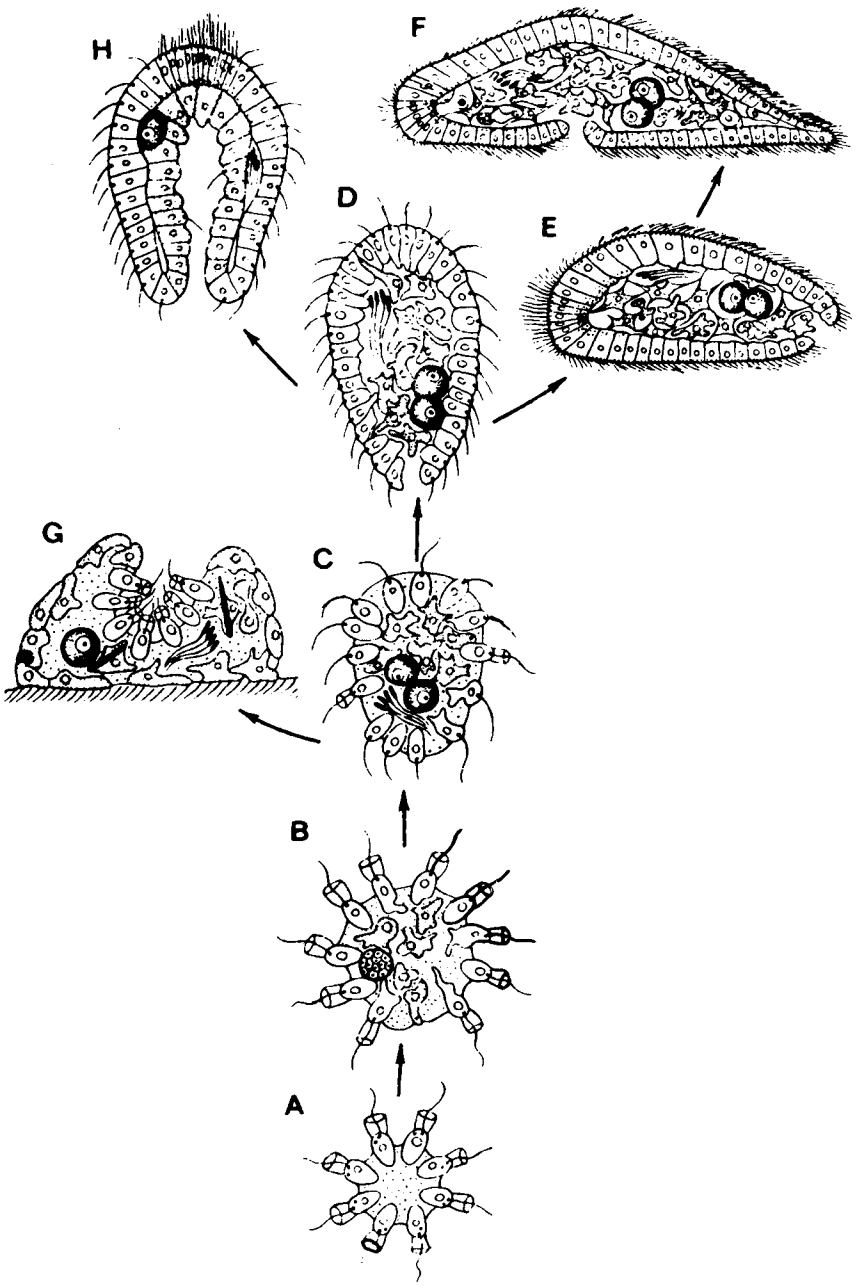

Fig. 1. Hypothetical stages in the phylogeny of the lower Metazoa. (After Ivanov, 1968, Fig. 118; 1970, Fig 8.) A — a colonial choanoflagellate (*Sphaeroeca*-type); B — same, *Proterospongia*-type; C — early Phagocytella; D — later Phagocytella; E — ancestral benthic turbellarian flatworm with mouth and bilateral symmetry; F — ancestral acoeloid turbellarian, with enhanced cell differentiation and ventral mouth. Sidelines from stage B leading to G — a primitive sponge, sessile, locomotion replaced by hydrokinetic function, and from stage D leading to H — a primitive coelenterate (Gastraea) (no scale, note small number of cells in each section, hence microscopic size of organisms).

is continued by a much discussed hypothetical organism, the 'Phagocytella'. It was postulated in the last century by the renowned Russian school of embryologists, on the basis of a widespread larval form of many Metazoa, the Planula. It developed ciliary locomotion, bilaterality, differentiation of tissues and a mouth. Further evolution went in two directions. One comprises the coelenterates, i.e., the Cnidaria which dominate in Ediacarian times, and the pelagic ctenophores which did not leave any fossil remains. The other leads to the Turbellaria which are flatworms (Platyhelminthes). During this course of evolution all animals must have been very small, otherwise they could not have been driven by ciliary movement, nor carried out other physiological functions at their low level of organization. Ivanov's (1968, 1970) views were criticised in detail, but accepted in essence by Salvini-Plawen (1978) who accepts monophyletic origination of the Metazoa. It was modified by Hanson (1977) and Sleigh (1979) who favour the alternative

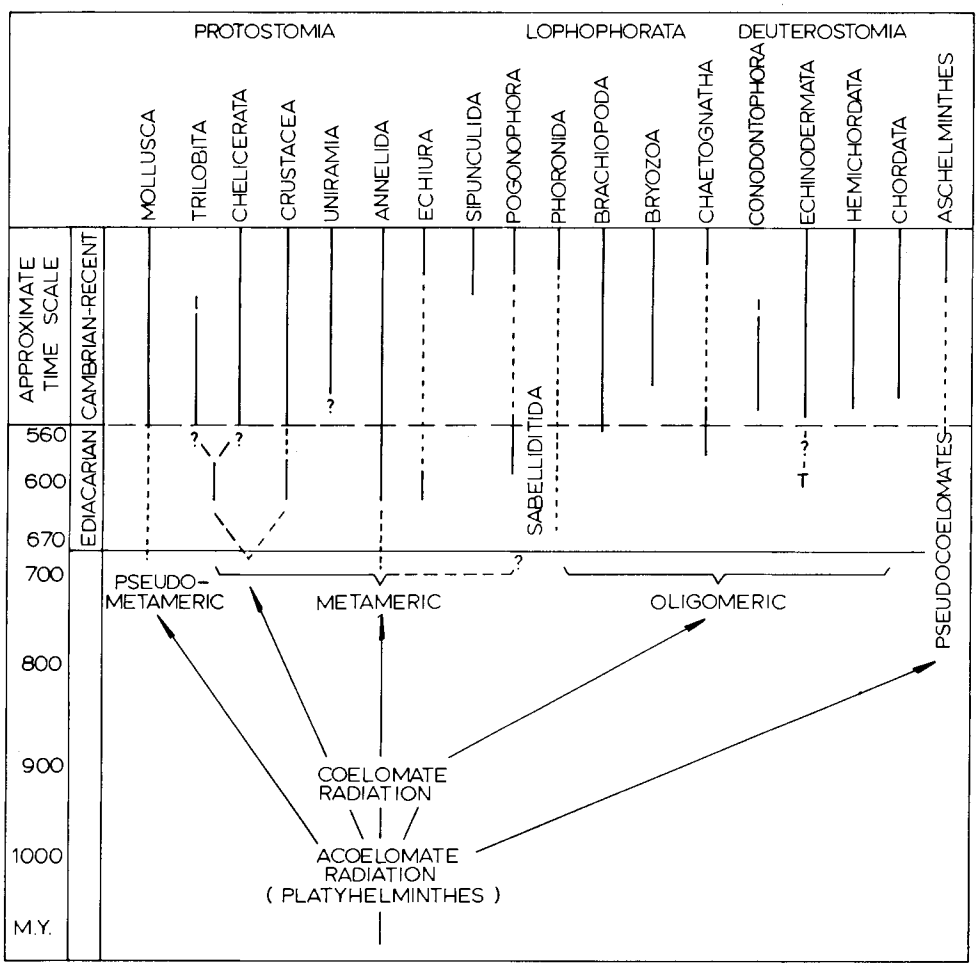

view of polyphyletic derivation. The sponges and the Cnidaria are derived from zooflagellates, including the choanoflagellate ancestors of the sponges, while the hypothetical ancestors of the Platyhelminthes and other Metazoa are the ciliates which are more advanced Protozoa. A further modification on biochemical grounds was suggested by Towe (1981).

Clearly, these evolutionary events, which are now obscured by the undoubted extinction of some lineages of Protozoa, must have occupied some of the time after the first appearance of the eukaryote protists. The age of the first appearance of eukaryote unicells is thought to be probably 1300–1500 Ma (Cloud, 1976a; Schopf and Oehler, 1976; Walter et al., 1976). Admittedly, 'compelling evidence' for the presence and diversity of eukaryote protists and algae comes from rocks which are only 800 Ma old. Before taking this date as evidence for the subsequent emergence of Metazoa and their diversification to the level of the Ediacarian faunas in the short time span of ~ 150 Ma, consideration has to be given to what biological theory has to say about the next stages of metazoan evolution, and then reconsider the palaeontological data. The widely accepted ideas of Clark (1964, 1979) are taken as a model.

On functional morphological grounds Clark (1964, 1979) demonstrates an evolutionary radiation of Metazoa without a true coelom, at the level of the Platyhelminthes, followed by a coelomate radiation, with the possible polyphyletic formation of a secondary body cavity, a coelom, of multiple kinds, functions, and possibly origins (Fig. 2). The body may be segmented throughout (metameric), for sound biomechanical reasons. The coelom can be divided into three parts (trimeric or oligomeric). This condition has been considered by some authors as primitive and described as archicoelomate (Ulrich,

---

Fig. 2. Hypothetical stages in the Late Proterozoic and later phylogeny of the higher Metazoa. The sequence of acoelomate and coelomate evolutionary radiations is based on the work of Clark, adapted to show possible origins of major Ediacarian taxa and admitting a possible multiple derivation of the coelom.

Explanatory notes: 1. Mollusca are here derived from Platyhelminthes. Some Ediacarian and possibly earlier trace fossils may originate from primitive, extinct, non-shellbearing molluscs. 2. Phylogenetic relations of the arthropods are highly controversial. A possible solution compatible with the Ediacarian arthropods is shown. Arthropods are thought to have unknown common ancestors with annelids. They may be represented by early trace fossils made by worm-like (coelomate?) metazoans. 3. Original metamerism, subsequently reduced or lost, of a number of living worm-like phyla is controversial. 4. The fossil record of the Phoronida and their origin is uncertain. The trace fossil *Skolithos* has been so interpreted. The Priapulida which are abundant in the Middle Cambrian Burgess Shale are omitted as their coelomate or pseudocoelomate character is uncertain. The Aschelminthes have no fossil record. 5. I have considered the Protoconodonts of the Precambrian–Cambrian transition (such as *Protohertzina*) as chaetognath spines; Repetski and Szaniawski (1981) presented a similar interpretation of early 'conodont assemblages'. 6. *Tribrachidium* (T) could be related to early echinoderms. 7. The Ediacarian phylogenetic relations of the phyla here grouped as oligomeric coelomates are still unknown. It should be noted that available data indicate early diversification of the 'Spiralia' and do not support the 'Archicoelomate' concept (Ulrich, 1972).

1972). Absent or incomplete segmentation may be interpreted as a primitive condition, or as lost or reduced. For this and many similar reasons of interpretation, biologists differ in their views on phylogenetic relations and factual data on living animals are insufficient to resolve the differences. What is of concern here is the degree of differentiation of the Ediacarian faunas in relation to the preceding radiations, rather than their precise course. Many metameric, some oligomeric, and possibly, from locomotion traces, some pseudometameric coelomates, at various stages of diversification are known. Therefore, it is known that both the acoelomate and the coelomate radiations must have preceded the Ediacarian Period. In the absence of identifiable fossil Metazoa of pre-Ediacarian age, the time which these events may have taken can only be estimated, but in any attempt the existing palaeontological data must be taken into consideration.

PALAEONTOLOGICAL DATA ON METAZOAN 'PREHISTORY'

Previous attempts of fitting evolutionary events into the Precambrian time scale (Valentine 1973, 1977; Valentine and Campbell 1975; Stanley 1976) were developed in the framework of genetic and ecological theories. Here, palaeontological data and biological models are considered in conjunction with an updated chronology of the evolutionary processes involved in the emergence of Metazoa.

Data on pre-Vendian palaeozoology are still extremely limited. From the time span between ~ 900 and 700 Ma a few trace fossils are known. A supposed medusoid, described as *Brooksella canyonensis* Bassler, from the Nankoweap Group of the Grand Canyon was considered a trace fossil of a burrowing worm (*Asterosoma?*, Glaessner, 1969) and apparently confirmed as such by Kauffman (Kauffman and Steidtmann, 1981, p.925) who gives the age as 1100—1300 Ma. A possible infaunal trail ~ 1 mm wide and a string of apparent ellipsoidal fecal pellets 0.5 mm wide and ~4 mm long were figured by Sabrodin (1971, 1972) from the Upper Riphean of the Ural. These faecal pellets, and possibly others described as microphytoliths, are at present the most convincing evidence for the existence of Metazoa, probably of coelomate grade, of Upper Riphean age (900 Ma or older, Sabrodin 1971, 1972; Krylov and Vassina, 1975). There are also small spiral trace fossils in relief, 2—3 mm in diameter, of the same age, from southern Siberia (Sokolov, 1975). Worm-like traces have been collected from the Wolstenholme and Dundas Formations of the Thule Group (Upper Riphean) of western North Greenland (Vidal and Dawes, 1980). Bioturbation has been reported from the Brioverian of the Channel Islands (Squire, 1973, tentative age 700 Ma). M.R. Walter (personal communication, 1981) found small worm-like traces in early Ediacarian rocks in central Australia.

Organic-walled fossils about 850 Ma old, from Anhui Province, eastern China, were found recently and considered to be *Sabellidites* (Wang, 1980). They are 30 mm long and 1.4 mm wide. They were collected by Zheng

Wenwu and will soon be further studied by him and Sun Weiguo (presently at the University of Adelaide) at Nanjing Palaeontological Institute. These fossils occur in an assemblage with *Chuaria* Walcott and *Tawuia* Hofmann which were also recently described from strata of apparently similar or greater (1000 Ma) age from western Canada (Hofmann and Aitken, 1979; Hofmann 1981). Similar forms were originally classified as medusae (*Beltanelloides*; Sokolov, 1975) or worms, but there is no evidence for them to be Metazoa. They have also been considered as plant microfossis (acritarchs) and lately as megascopic eukaryotic algae (Hofmann, 1981) and as multicellular (Duan Chenghua, 1982). I have observed a clear resemblance of some of the shape characteristics in photographs of the fossils considered to be *Sabellidites* and *Tawuia* from China. It is possible that there is only a superficial resemblance between these *Tawuia*-like fossils and the Vendian to Cambrian true *Sabellidites* tubes which resemble the tubes of living Pogonophora (Sokolov, 1972).

An intriguing question concerning possible trace fossils from quartzites more than 2000 Ma old from Wyoming was posed in the title and text of a recent paper by Kauffman and Steidtman (1981). As the authors state that there is no unequivocal evidence for biogenicity of these possible trace fossils, the question must remain open. There is no other evidence of burrowing animals of that age (see Cloud et al., 1980).

Why are there so few finds of ancient Metazoa? I suggest three reasons, based on their substance, size and probable number.

(1) Fossilization of animal cells and colonial protists is unlikely, because animal cells lack resistant cell walls.

(2) The first products of tissue-grade metazoan organization would have been small and remained so during the acoelomate radiation, for physiological and biomechanical reasons. In the Ediacara fauna there were large animals because cnidarians had developed a strong mesogloea and others had strong muscles or chitinous cuticles — and there were no macrophagous predators. All these considerations point to a long time span for metazoan 'prehistory', despite missing documentation.

(3) It is possible that in the evolution of the biosphere an increase in total biomass has occurred. When the necessary preconditions for the appearance of the Metazoa came into existence, on completion of the transition from cell colonies to organisms with tissues and organs, the total number of Metazoa grew slowly as they began to occupy new environments and to diversify accordingly. Even the known number of Ediacarian fossil localities is still very small, and in contrast to later Phanerozoic fossil localities a number of them have yielded only single specimens, despite repeated searches. Yet, the Late Precambrian sequences have many sediment types in common with the Phanerozoic and represent normal conditions for fossilization. The conclusion must be that early metazoan communities were much less numerous. For all these reasons we are still very far from an understanding of the evolution of the structure and functioning of animal *communities* at these early stages.

NEW DIMENSIONS OF TRACE FOSSIL STUDIES

How can knowledge of fossil remains from the period between 950 and 650 Ma (Late Riphean to Early Vendian in U.S.S.R. stratigraphic terminology) be increased? The hypothetical possibility exists of discoveries of remains of soft-bodied animals of greater age than the ones known, but the probability of such finds is low because early Metazoa would have been small, hardly recognizable as fossils and not sufficiently resistant to decay. They may have had little, if any, collagen available for the construction of resistant tissues (Towe, 1970). The inventory of fossil remains of this age given above (after elimination of non-metazoan remains, including numerous non-biogenic configurations) consists entirely of trace fossils. They are the results of the interference of animals with normal results of sedimentation, through locomotion, construction of dwellings, feeding and excretion.

Trace fossils are being described mainly from the viewpoint of morphology and topology of the traces rather than the effect of the animal on the sediment. From this evidence conclusions are drawn empirically on the palaeoenvironment and, mostly by actualistic methods, on the possible behaviour of the originators, i.e., feeding, grazing, locomotion, resting and dwelling, with or without due consideration of the possible interrelations or alternations of these forms of behaviour. An ethological classification is much used for these fossils, whose originators generally remain unknown or are at best guessed at. When each category is studied in its stratigraphic sequence, evolutionary trends appear (Seilacher, 1977). On this basis, Fedonkin (1980, 1981) has suggested that Ediacarian trace fossils are essentially two-dimensional. In the Cambrian they are vastly more abundant and include many three-dimensional structures indicating more complex behaviour. The traditional methodology of these studies, when not purely descriptive or palaeoenvironmental, is often palaeopsychological (Richter, 1927, 1928), i.e., trying to guess what the animal intended to do. Other potentially fruitful approaches may have been under-used or neglected. It would be desirable to determine how, and by what means, the animal interacted with the sediment. Such studies require close cooperation of sedimentologists, biochemists and palaeobiologists. To gain insight into animal-sediment relations at the time of metazoan diversification, three new approaches to the study of trace fossils are suggested.

(1) A re-definition of burrows. There are sessile burrowers which may be deposit feeders or filter feeders. Conveyor-belt feeders bring sediment to or from the surface, from vertical or U-tubes. Vagrant burrowers plough through the sediment, or through the still mobile surface layer, and either push it aside or pass it through their intestinal canal. Various feeding strategies by 'burrowers' may produce 4 or 5 different kinds of trace fossils which have not been consistently distinguished. Casts of surface trails should not be confused with infaunal burrowers. It is important to know whether a burrow was kept open and subsequently filled with sediment after the departure of

the animal, or whether the animal made the burrow by ingesting and excreting the sediment, backfilling the burrow by physiological rather than biomechanical means. Cylindrical fillings of these three kinds of burrow could be externally similar but they could not have been made by the same kind of animal.

(2) A study of mucus secretion in this context is particularly important. Mucus secretion is directly related to tube construction, feeding and locomotion. Many trace fossils are preserved only because grains of the burrow walls or locomotion trails are cemented by mucus which is hardened diagenetically. The same mechanism can apply to faecal pellets. Infaunal activity without temporary fossilization of mucus would result only in bioturbation sensu stricto, i.e., destruction of pre-existing stratification, without preservation of trace fossils.

(3) A study of faecal pellets from the viewpoint of structure and composition, particularly in relation to content of organic matter is important. Pelletizing is quantitatively significant on a muddy sea floor, including carbonate mud. A content of 90% gastropod pellets has been recorded in Bahamian lagoonal mud. Faecal pellets have frequently been considered during the last 50 years as sites of concentration of hydrocarbons and phosphates. It is amazing that there have been no satisfactory special studies of the palaeobiology of faecal pellets, particularly from Late Precambrian strata which contain the oldest productive oil deposits. It is likely that some of the common Precambrian (and Palaeozoic) so-called microphytoliths are faecal pellets, as has been claimed repeatedly, but without serious attempts at discrimination. If successful, a more satisfactory basis would be provided for their use as stratigraphic markers, than that which is presently available and practised mainly in the U.S.S.R. as an empirical method. It could also extend the proven range of Metazoa by several hundred million years.

Plants or Protista, whatever else they may do, do not walk on mucus trails, nor do they produce faecal pellets. In the study of the first appearance of animals in the geological record, their distinguishing features, i.e. locomotion and characteristic metabolism, in other words their physical and chemical interaction with the sediments, should receive far greater attention. The early animals must have influenced sediments sufficiently to keep not only sedimentologists and stratigraphers, but also organic geochemists busy looking in new directions for subtle but important traces of the first animal activities.

EVOLUTION OF DIVERSITY IN EARLY METAZOA

There will be some feedback from palaeobiology to zoological phylogenetic hypotheses. The Cnidaria, which are the most abundant and widely distributed animals of the Ediacarian, are represented by rather primitive 'Vendimedusae' (Wade, 1983) among the Scyphozoa, but also by soft corals and Hydrozoa. The presence of advanced pelagic Hydrozoa (Chondrophora)

contradicts the views of some zoologists of a late derivation of Hydrozoa from tetraradial Scyphozoa. It indicates the occurrence of one or more phases of diversification of the Cnidaria before Ediacarian time. Rates of evolution vary between and within grades of adaptive structural complexity. There are reasons to think that the Cnidaria and the annelids must have had a longer and more eventful 'prehistory' than the arthropods which are represented in the Ediacarian faunas by only a few kinds, of very 'primitive' appearance.

What determined the diversity of the Metazoa which must have originated in pre-Ediacarian times? Evolution occurs in a changing environment. The biosphere is a system which interacts with the hydrosphere, atmosphere and lithosphere. From each kind of interaction there were recently deduced ad hoc hyptheses for selected evolutionary events. However, it has not been shown convincingly that significant parameters of the hydrosphere changed just before it was populated by animals. The postulated quantum change in atmospheric oxygen did not occur at the beginning of the Cambrian as postulated by the original Berkner—Marshall theory, and if it had, it would have come too late to explain anything. The world-wide Late Precambrian glaciations did occur, during a long (over 350 Ma) time span including the Early Vendian and Late Riphean (Chumakov, 1981), and possibly ceased before or perhaps during the Ediacarian. Too little is known about the exact chronology and palaeogeographic distribution of these glaciations, and about their interactions with the hydrosphere and biosphere to explain on this basis any known biohistorical phenomena fully and satisfactorily.

What happened during Ediacarian—Cambrian times was an exponential increase in diversity of the emerging Metazoa which enabled them to occupy previously empty environmental niches in the sea (Brasier, 1979; Sepkoski 1978, 1979). I am convinced that this process began several hundred million years earlier than the exponential increase in diversity plotted by Sepkoski (1978, 1979). It required this long lead time because at that stage it was, to a large extent, a slow process of biochemical, biomechanical and bioenergetic improvement and consequent selection, helped perhaps by small population numbers. The spectacular morphological and less spectacular ethological effects are seen in palaeontological perspective as adaptations to environmental changes. The relations of cause and effect are less straightforward. The physiological, biochemical and biomechanical evolutionary processes which underlie them require more attention and further study.

CONCLUSIONS

(1) Historical data from biology and palaeontology confirm the existence of a metazoan prehistory, i.e., a cryptozoic era of metazoan evolution.

(2) Geochronological calibration of this era indicates its approximate coincidence with the Late Proterozoic, from ~ 950 Ma to the Ediacarian (~ 650 Ma).

(3) There are some indications that the total metazoan and probably the total animal biomass was small during cryptozoic time. It may have increased from Ediacarian to Cambrian time at a rapid rate, comparable to that of increasing diversity of the Metazoa.

(4) The evolution of metazoan community structure during the cryptozoic period is unknown. The sea floor was inhabited by Metazoa since early times. Nothing is known about the deep ocean.

(5) There are many ad hoc hypotheses in explanation of early evolutionary events. They invoke many variables in the environment such as geological cycles, non-glacial eustatic movements of the sea level, etc. Oxygen accession is the preferred factor, but nothing more than a gradual increase during the relevant time can be demonstrated. Without geologically improbable auxiliary hypotheses (such as a world-wide sulfide-rich marine habitat) no biologically significant passing of a threshold value is known to have occurred. Salinity seems to have been static and hence largely irrelevant. Speculating about temperature, the coincidence of the cryptozoic era with the total time span of the Late Precambrian glaciations is noted. However, credible inferences about their possible effects on life in the sea are lacking.

(6) The biosphere as a system was at all times interacting with the environment, i.e., the hydrosphere, atmosphere and lithosphere. Unifying theories will be possible only when the evolution of all these systems in the same time frame is better known and their interactions can be studied for each historical period on a quantitative basis.

ACKNOWLEDGEMENTS

This paper, prepared for the I.G.C.P. Meeting in Mexico, 1982, could not be presented there. It was given, in outline, at a seminar on 'The Earliest Animals' sponsored by the Baas Becking Geobiological Laboratory at the Bureau of Mineral Resources, Canberra, in December 1981. I am grateful to the organizers of these conferences and particularly R. Weber, Preston Cloud and M.R. Walter, for their encouragement; to Dr. Mary Wade and the participants of the seminar for helpful discussions; and to Dr. E.L. Yochelson for valuable and constructive criticism.

REFERENCES

Brasier, M.D., 1979. The Cambrian radiation event. In: M.R. House (Editor), The Origin of Major Invertebrate Groups. Systematics Assoc. Spec. Vol. 12, Academic Press, London, New York, pp. 103—159.

Chumakov, N.M., 1981. Upper Proterozoic glaciogenic rocks and their stratigraphic significance. Precambrian Res., 15: 373—395.

Chumakov, N.M. and Semikhatov, M.A., 1981. Riphean and Vendian of the U.S.S.R. Precambrian Res., 15: 229—253.

Clark, R.B., 1964. Dynamics in Metazoan Evolution, the Origin of the Coelom and Segments. Clarendon Press, Oxford, 313 pp.

Clark, R.B., 1979. Radiation of the Metazoa. In: M.R. House (Editor) The Origin of Major Invertebrate Groups. Systematics Assoc. Spec. Vol. 12, Academic Press, London, New York, pp. 55—102.

Cloud, P.E., Jr., 1968. Pre-metazoan evolution and the origins of the Metazoa. In: T. Drake (Editor), Evolution and Environment. Yale University Press, New Haven and London, pp. 1—72.

Cloud, P., 1972. A working model of the primitive Earth. Am. J. Sci , 272: 537—548.

Cloud, P., 1976a. Beginnings of biospheric evolution and their biogeochemical consequences. Paleobiology, 2: 351—387.

Cloud, P., 1976b. Major features of crustal evolution. Geol. Soc. S. Africa Annex to Vol. 79 (A.L. du Toit Memorial Lecture No.14), 33 pp.

Cloud, P. and Glaessner, M.F., 1982. The Ediacarian period and system: Metazoa inherit the Earth. Science, 217: 783—792.

Cloud, P., Gustafson, L.B. and Watson, J.A.L., 1980. The works of living social insects and the age of the oldest known Metazoa. Science, 210: 1013—1015.

Duan, Chenghua, 1982. Late Precambrian algal megafossils *Chuaria* and *Tawaia* in some areas of eastern China. Alcheringa, 6: 57—68.

Fedonkin, M.A., 1980. Early stages of evolution of Metazoa on the basis of paleoichnological data. Zh. Obshch. Biol., 2: 226—233 (in Russian).

Fedonkin, M.A., 1981. White Sea biota of Vendian (Precambrian non-skeletal fauna of the Russian Platform North). Trans. Geol. Inst. Acad. Sci. U.S.S.R. 342, 100 pp. (In Russian).

Glaessner, M.F., 1968. Biological events and the Precambrian time scale. Can. J. Earth Sci., 5: 585—590.

Glaessner, M.F., 1969. Trace fossils from the Precambrian and basal Cambrian. Lethaia, 2: 369—393.

Hanson, E.D., 1977. The Origin and Early Evolution of Animals. Wesley University Press, Middleton, CT and Pitman, London, 670 pp.

Harland, W.B. and Herod, K.N. 1975. Glaciations through time. Geol. J. Liverpool, Spec. Issue, 6: 189—216.

Hedberg, H.D. (Editor), 1976. International Stratigraphic Guide. Int. Subcomm. Strat. Classif. (ISSC), J. Wiley, New York, 200 pp.

Hofmann, H.J., 1981. Precambrian fossils in Canada — The 1970s in retrospect. In: Campbell F.H.A. (Editor), Proterozoic Basins of Canada. Geol. Survey Can. Pap., 81-10: 419—443.

Hofmann, H.J. and Aitken, J.D., 1979. Precambrian biota from the Little Dal Group, Mackenzie Mountains, northwestern Canada. Can. J. Earth Sci., 16: 150—166.

Ivanov, A.V., 1968. The origin of multicellular animals. Phylogenetic Essays. Nauka, Leningrad, 287 pp. (In Russian).

Ivanov, A.V., 1970. Verwandtschaft und Evolution der Pogonophoren. Z. Zool. Syst. Evolutionsforsch., 8: 109—119.

Kauffman E.G. and Steidtmann, R., 1981. Are these the oldest metazoan trace fossils? J. Paleontol., 55: 923—947.

Keller, B.M., 1979. Precambrian stratigraphic scale of the U.S.S.R. Geol. Mag., 116: 419—429.

Knoll, A.H. and Barghoorn, E.S., 1975. Precambrian eucaryote organisms: a reassessment of the evidence. Science, 190: 52—54.

Krylov, I.N. and Vassina, R.A., 1975. Oldest traces of life on Earth. All-Union Inst. Sci. Tech. Information, Moscow, Itogi Nauki i Tekhniki, Strat., Paleont. 6: 60—92. (In Russian).

Margulis, L., 1970. Origin of Eukaryotic Cells. Yale University Press, New Haven, London, 349 pp.

Repetski, J.E. and Szaniawski, H., 1981. Paleobiologic interpretation of Cambrian and earliest Ordovician conodont natural assemblages. U.S. Geol. Surv. Open File Rep., 81-7432: 169—172.

Richter, R., 1927. Die fossilen Fährten und Bauten der Würmer, ein Ueberblick über ihre biologischen Grundformen und deren geologische Bedeutung. Paläontol. Z., 9: 193—240.
Richter, R., 1928. Psychische Reaktionen fossiler Tiere. Palaeobiologica 1: 225—244.
Sabrodin, W., 1971. Leben im Präkambrium. Ideen Exakten Wiss., 12: 835—842.
Sabrodin, W., 1972. Leben im Präkambrium. Bild Wiss., pp. 586—591.
Salvini-Plawen, L., 1978. On the origin and evolution of the lower Metazoa. Z. Zool. Syst. Evolutionsforsch., 16: 40—88.
Schopf, J.W., 1967. Antiquity and Evolution of Precambrian Life. McGraw-Hill Yearbook of Science and Technology, McGraw-Hill, New York, pp. 47—55.
Schopf, J.W., Haugh, B.N., Molnar, R.E. and Satterthwait, D.F., 1973. On the development of metaphytes and metazoans. J. Paleontol. 47: 1—9.
Schopf, J.W. and Oehler, D.Z., 1976. How old are the eukaryotes? Science, 193: 47—49.
Seilacher, A., 1977. Evolution of trace fossil communities. In: A. Hallam (Editor), Patterns of Evolution. Developments in Palaeontology and Stratigraphy 5. Elsevier, Amsterdam, pp. 359—376.
Sepkoski, J.J., 1978. A kinetic model of Phanerozoic taxonomic diversity. I. Analysis of marine orders. Paleobiology, 4: 223—251.
Sepkoski, J.J., 1979. A kinetic model of Phanerozoic taxonomic diversity. II. Early Phanerozoic families and multiple equilibria. Paleobiology, 5: 222—251.
Sleigh, M.A., 1979. Radiation of the eukaryote Protists. In: M.R. House (Editor), The Origin of Major Invertebrate Groups. Systematics Ass. Spec. Vol. 12, Academic Press, London, New York, pp. 23—54.
Sokolov, B.S., 1972. Vendian and Early Cambrian Sabelliditida (Pogonophora) of the U.S.S.R. Proc. Int. Paleont. Union, 23rd Int. Geol. Congr. (1968), Warszawa, pp. 79—86.
Sokolov, B.S., 1975. Paleontological discoveries in Pre-Usolye deposits of the Irkutsk Amphitheatre. In: Analogues of Vendian Complex in Siberia. Acad. Sci. U.S.S.R., Sib. Branch, Inst. Geol. Geophys., Trans., 232: 112—117 (in Russian).
Squire, A.D., 1973. Discovery of Late Precambrian trace fossils in Jersey, Channel Islands. Geol. Mag., 110: 223—226.
Stanley, S.M., 1976. Ideas of timing of metazoan diversification. Paleobiology, 2: 209—219.
Towe, K.M., 1970. Oxygen-collagen priority and the early metazoan fossil record. Proc. Nat. Acad. Sci. Washington, 66: 781—788.
Towe, K.M., 1981. Biochemical keys to the emergence of complex life. In: J. Billingham (Editor), Life in the Universe, M.I.T. Press, Cambridge, MA, pp. 297—306.
Ulrich, W., 1972. Die Geschichte des Archicoelomatenbegriffs und die Archicoelomatennatur der Pogonophoren. Z. Zool. Evolutionsforsch., 10: 301—320.
Valentine, J.W., 1973. Evolutionary paleoecology of the marine biosphere. Prentice-Hall Inc., Englewood Cliffs, N.J., 511 pp.
Valentine, J.W., 1977. General patterns in metazoan evolution. In: A. Hallam (Editor), Patterns of Evolution. Developments in Palaeontology and Stratigraphy 5. Elsevier, Amsterdam, pp. 27—57.
Valentine J.W. and Campbell, C.A., 1975. Genetic regulation and the fossil record. Am. Sci., 63: 673—680.
Vidal G. and Dawes, P.R., 1980. Acritarchs from the Proterozoic Thule Group, North-West Greenland. Rapp. Grønlands Geol. Unders., 100: 24—29.
Wade, M., 1983. Fossil Scyphozoa, In: P.P. Grassé, (Editor), Traité de Zoologie. Masson et Cie, Paris (in press).
Walter, M.R., Oehler J.H. and Oehler, D.Z., 1976. Megascopic algae 1300 million years old from the Belt Supergroup, Montana: a re-interpretation of Walcott's *Helminthoidichnites*. J. Paleontol. 50: 872—881.
Wang, Y., (Editor), 1980. Research on Precambrian Geology, Sinian Suberathem in China. Tianjin Sci. Tech. Press, Tianjin. 400 pp.

This Page Intentionally Left Blank

DISTINCTIVE MICROBIAL STRUCTURES AND THE PRE-PHANEROZOIC FOSSIL RECORD

LYNN MARGULIS, BETSEY DEXTER DYER GROSOVSKY, JOHN F. STOLZ, ELIZABETH J. GONG-COLLINS and SUSAN LENK

Boston University, Department of Biology, Boston, MA 02215 (U.S.A.)

DOROTHY READ

Department of Biology, Southeastern Massachusetts University, North Dartmouth, MA (U.S.A.)

ALEJANDRO LÓPEZ-CORTÉS

Universidad Nacional de Mexico, Departmento de Ecologia Humana, Mexico D.F. (Mexico)

ABSTRACT

Margulis, L., Grosovsky, B.D.D., Stolz, J.F., Gong-Collins, E.J., Lenk, S., Read, D. and López-Cortés, A., 1983. Distinctive microbial structures and the pre-Phanerozoic fossil record. Precambrian Res., 20: 443—477.

The live and sedimentary components of the flat laminated microbial mat at Laguna Figueroa have been studied since the late sixties. This paper reports the observation and isolation of a variety of micro-organisms, both prokaryotes and eukaryotes. The microbes were taken from the flat laminated mats submerged under at least one meter of water due to the spring rains of 1979 and 1980. Both in situ and enrichment culture observations were made using light and electron microscopic techniques. New strains of the following microbes are reported here: *Bacillus megaterium, Bacillus licheniformis, Arthrobacter simplex* and *Paratetramitus jugosus.* Several pseudomonads were isolated, some of which form distinctive subsurface colonial structures. Regular distinctive colony morphologies and desiccation resistant cysts were often observed, several types of which grow to characteristically large sizes and resemble objects found in the pre-Phanerozoic fossil record.

Some colonies of manganese oxidizing bacilli and other bacteria are reminiscent of microfossils of the 2 Ga-old Gunflint Iron formation such as *Metallogenium, Eosphaera tyleri, Eoastrion* and *Huronispora.* Some manganese oxidizing bacteria form colonial structures that might be mistaken for individual organisms in the tens to hundreds of microns size range. The diversity of microbial structures, including those with preservation potential, must be kept in mind when interpreting the microfossil record.

INTRODUCTION

The organisms and structures described in this study were all observed in the field or were enriched on low nutrient culture media from mat inocula.

The mat inocula were from the flat laminated mat at Laguna Figueroa, Baja California which was first described as the *Microcoleus* mat by Horodyski et al., 1977. The texture of this mat has been compared with a pre-Phanerozoic banded chert from the Swartkoppie Zone in the 3.4 Ga-old Swaziland System of South Africa (Margulis et al., 1980). Ultimately, it will be of interest to know whether or not these live, modern, flat laminated mats are apt analogues of banded carbon-rich sedimentary rocks deposited over 3Ga- ago.

The work described here represents a continuation of efforts to understand the structural and temporal changes of the microbial composition of the flat mat (Stolz, 1983a, this issue), including identification of some of the heterotrophic micro-organisms (Margulis et al., 1980). Those identified so far include a prodigiosin-producing red marine vibrio (Giovannoni and Margulis, 1981); an extremely salt tolerant new strain of *Bacillus megaterium* and of *Arthrobacter* (Gong-Collins, 1982); a new species of the genus *Spirochaeta* (S.P. Fracek, Jr., personal communication, 1982); a euryhalic strain of *Bacillus licheniformis* (López-Cortés, 1982); and several marine ciliates including an encysting *Euplotes*, a *Cyclidium* and a *Paranophrys*. Progress is also underway in the determination of the extent of heat and desiccation resistance associated with the distinctive colony structure described here (Gong-Collins and Read, 1983).

The mats at Laguna Figueroa, north of San Quintin, Baja California del Norte, Mexico, lie in an enclosed hypersaline embayment. The northernmost portion of the hypersaline flat (North Pond or Charco del Norte) is periodically submerged and evaporated. The entire lagoon is ~ 16 km long and 1 km wide. The extent of the evaporite flat varies enormously, depending on seasonal weather conditions. During the heavy winter rains of 1979 and 1980 the flat was replaced by a fresh water lagoon which did not subside until late summer of 1981. The flood waters, which reached 3 m depths in March 1980, covered the mats entirely during the 1980 summer growing season. Profound changes, which are the subject of ultrastructural in situ studies (Stolz, 1983a), occurred in the submerged microbial mat communities during 1979 and 1980. This paper reports observations on in situ mats, and enrichments from them made in: August, 1977, 1978; May, 1979; August, 1979; March, 1980; December, 1980; and August, 1981.

Microbes isolated from these mats since 1977 exhibit diverse colony morphologies, including lens or disc-shaped structures that appear to penetrate and grow beneath the surface of 1.5% agar. Live bacteria and protists (primarily spore forming bacteria and cyst forming protists) have always been isolable from mat samples whether they are fresh from the field or have been stored for as long as four years at room temperature or at 4°C in sterile petri dishes, plastic bags or glass jars.

METHODS AND MATERIALS

Field observations and sample collection

All observations are based on field work which began in August 1977 and continued until 1982, at the intervals listed in the introduction. Unless otherwise stated the samples were taken from the flat laminated "*Microcoleus* mat" of the North Pond (site 1, Fig. 1; described by Horodyski et al., 1977) or the south salinas areas of Laguna Figueroa (site 2, Fig. 1). Samples were returned to the laboratory in the following forms: fixed in 4% formalin, fixed in 2.5% glutaraldehyde, unfixed, damp or wet in jars, dried in sterile petri plates, damp or wet in sterile petri plates and damp in plastic bags. The Nikon H (hand held compound microscope), binocular microscopes and hand lenses were taken into the field for in situ observations. Two types of agar plate media were utilized in these studies: K medium (Table I — modified from Nealson and Tebo, 1979) and manganese acetate medium (Table I) both made up in 1.5% bacto-agar. Growth on these manganese media represents a small subset of the organisms isolatable from the mat, primarily mineralized bacterial colonies and amoebic cysts.

An entire slice of the top laminated layer of the mat, always taken from the same North Pond site near the channels (Fig. 2) was generally placed in empty sterile petri plates or in sterile plates containing K or manganese acetate media. Damp mat samples, taken at various times, were placed in glass jars up to ~ 1 l in volume and closed. Samples of heterotrophic bacteria and amoebae have remained viable for over a year under these conditions. Mat samples were usually sliced in two: one was fixed with glutaraldehyde in the field (Stolz, 1983a, this issue) and the second retained for observations of live organisms and enrichments. The ciliates were enriched in ½ concentration artificial seawater, to which sterile filter paper was added as a source of cellulose carbon. After ~ 4 days a bacterial bloom was succeeded by a bloom of ciliates. Marine Cerophyll (2.5% solution in half strength seawater, Agri-Tech Inc. Kansas City, KS) was an even better method for enriching and culturing ciliates. The bacteria that formed distinctive colonies or subsurface colony structure were chosen for further study.

Microscopic and photographic techniques

Observations in the laboratory were made with Wild binocular and Nikon differential interference phase contrast microscopes to which 35 mm Nikon camera backs had been mounted. For spirochetes, dark field observations were made with a Zeiss RA microscope. Fluorescence observations were made with the Nikon Fluorophot. To make continuous observations of growing cultures, containing cysts and manganese oxidizing bacteria, sterile microscope slides were coated with modified K-agar and inoculated directly.

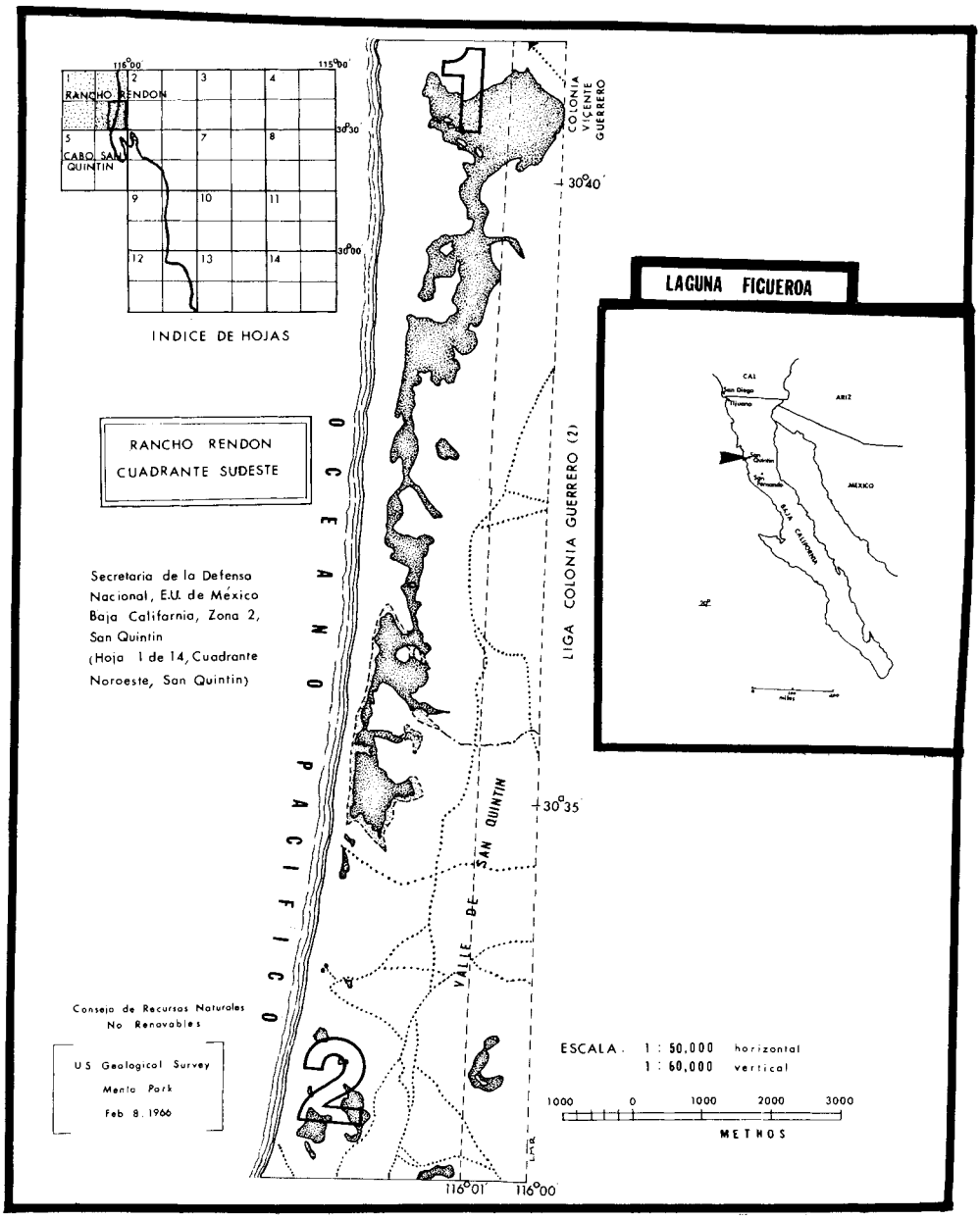

Fig. 1. Map of Baja California del Norte; North Pond (1) and south salinas (2) field sites are shown at bottom. Only North Pond was flooded in 1979 and 1980.

They were maintained for several days in autoclaved Coplin jars to which a few drops of sterile distilled water were added from time to time to prevent desiccation. The preparations were observed and photographed at approximately daily intervals for ~ 4 days and followed until growth ceased.

TABLE I

Media

Modified K medium	
$MnSO_4 \cdot 4H_2O$	0.1g
Bacto-Peptone	1.0g
Yeast extract	0.25g
Agar	7.5g
500 ml ASW (autoclaved together)	
Manganese acetate medium	
$Mn(C_2H_3O_2)_2 \cdot 4H_2O$	0.002% (w/v) in ASW
(unless other concentration specified, i.e., from 2×10^{-5} to 10^{-3})	
½ concentration artificial seawater (ASW)	
$CaCl_2 \cdot 2H_2O$	1.45g
$MgSO_4 \cdot 7H_2O$	12.35g
KCl	0.75g
NaCl	17.55g
Tris buffer (1.0 M, pH 7.5)	50 ml
Distilled water	950 ml
Iris buffer	
HCl (conc)	33.3 ml
Trizma Base	60.55g
Make up to 500 ml with distilled water	
Nutrient seawater agar	
Bacto Nutrient agar (Difco)	23.0g
in 1000 ml ASW	

For electron micrographs of the photosynthetic organisms, samples were fixed with 2.5% glutaraldehyde in sodium-citrate half strength seawater buffer (Stolz, 1983a, this issue), post-fixed with 2.0% osmium tetroxide, stained en bloc with 0.5% uranyl acetate, dehydrated with an ethanol series followed by propylene oxide, and embedded in Spurrs low viscosity embedding medium (Ladd Research Industries, Inc. Burlington Vt., P.O. Box 91). This medium also worked well for light micrographic sections of poorly consolidated mat. The amoebae and their cysts were fixed with 2.5% glutaraldehyde in artificial half strength seawater, post-fexed, dehydrated and embedded as described above. Grids of both materials were stained for 20 min in uranyl acetate (1.0%) and 15 min in lead citrate (Hayat, 1970).

Fig. 2. The *Microcoleus* desiccation polygons as they had been observed from ~ 1965 until spring 1979. (A) courtesy of R. Horodyski, scale 5 cm intervals. (B) May 1979, site 1 under 1 m of fresh water.

RESULTS AND DISCUSSION

Field observations

Our initial intentions were to characterize the flat laminated *Microcoleus* mat by documenting the presence of the active photosynthesizing microbes as well as distinctive heterotrophs that have potential for the future fossil record. Our studies were thwarted by a series of floods that began in the winter of 1978—79. The mats were flooded by at least 1 m of water from the time heavy rains began that season until late summer 1979, Fig. 2B. By August 1979 the flat laminated mats had re-emerged. However, heavy rains between December 1979 and summer 1980 resulted in permanent submergence during 1980.

The composition of the mat community has dramatically changed since 1977 because of the influx of fresh water and terrigenous sediment. The macroscopic appearance of the top few centimeters of mat, prior to and during the floods, is shown in Fig. 3. Since the rains did not abate in the winter—spring of 1980—81 there was sufficient rainfall to convert the evaporite flat into a lake which persisted throughout the growing season of 1980. The failure of the standing water to subside during the summer of 1980 led to burial of the surface of the mat with alluvial runoff, degradation of *Microcoleus* mats and cessation of productive cyanobacterial mat growth. The details of these alterations and their relevance to the interpretation of the pre-Phanerozoic fossil record are under study (Stolz, 1983a, b). Although laminated evaporite polygons had re-emerged by August 1981, the microbial community was different than before. *Microcoleus* and several other cyanobacterial species had vanished, the altered community was dominated by the coccoid *Thiocapsa* and other purple photosynthetic bacteria. This anaerobic photosynthetic community was covered by 2.5 cm of sediment which most likely severely limited the photosynthetic activity.

The fate of the mats is still being monitored with particular concern for potentially preservable microstructures. The mats have not returned to the original, relatively stable state known to have persisted for the decade prior to the floods. Such rapid mat burial by terrigenous sediment may be comparable to the earliest stages in diagenesis of fossil mats. Comparable differential growth of opportunistic bacteria and protists leading to mat degradation must have occurred in pre-Phanerozoic laminated microbial mats. The in situ and enrichment samples of microbes described here must, therefore, be correlated with the conditions of the mat at the time the samples were taken.

All of the colony structures described here have been seen in independent isolations at least twice and many in half a dozen or more different isolations. Even on plates containing little or no organic carbon (e.g., designed to isolate photosynthetic bacteria such as ASN III, Rippka et al., 1979) photosynthetic bacteria, protist cysts and distinctive colonies of heterotrophic

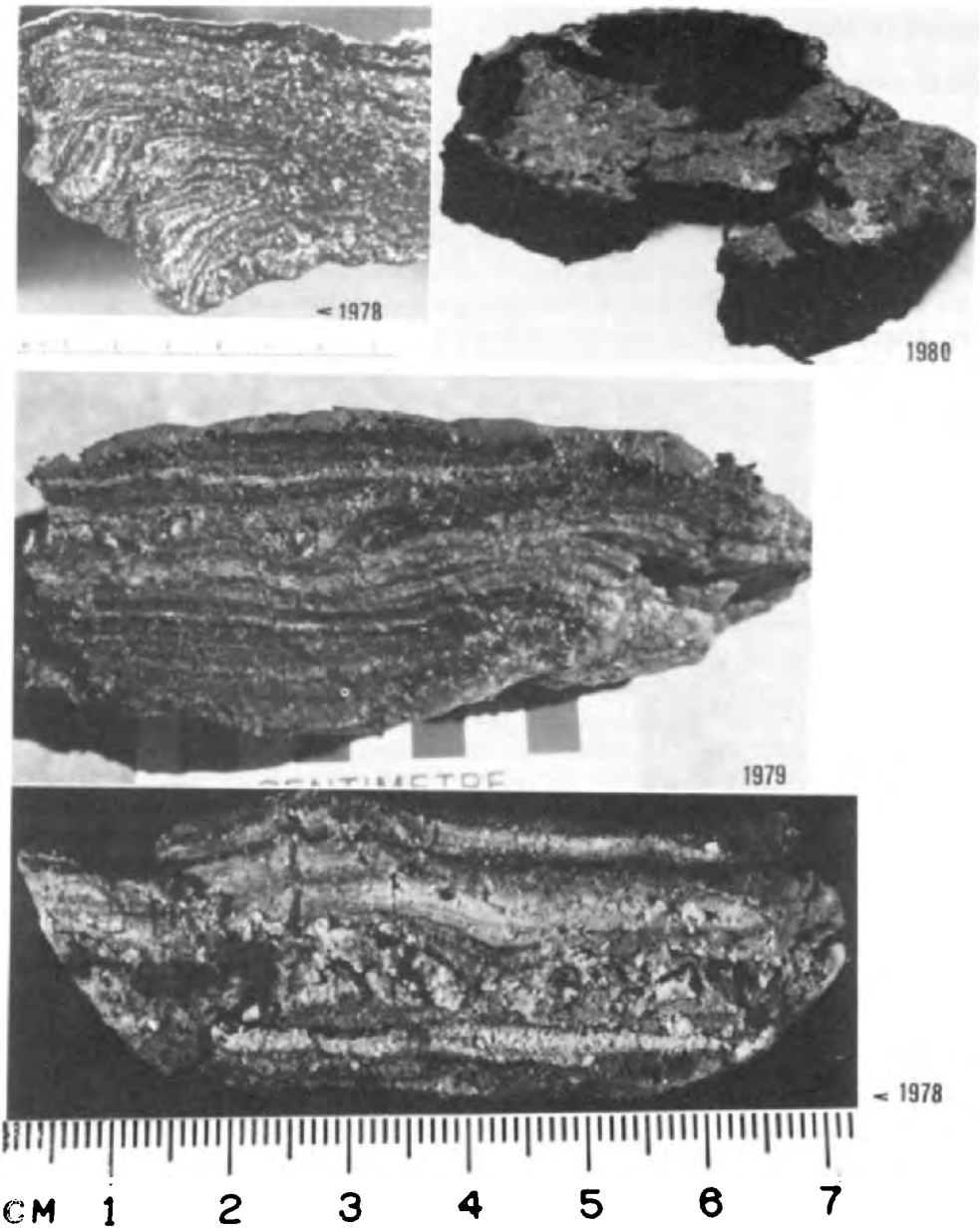

Fig. 3. The mat in 1977 showed typical fine colored laminae that had been observable in samples up to at least a decade prior to the flood. In mat samples artificially silicified with ethyl silicate (bottom, see Francis et al., 1979 for methods) laminae faithfully preserved their appearance. The 1979 submerged mat sample was recovered from beneath 1 m of fresh water during May 1979, off a small raft constructed to traverse the standing water. The 1980 mat sample was taken from a submerged sample 3 m below the surface of fresh standing water. The submerged surfaces of the former desiccation polygons could be recognized, but only two layers, yellow and black, could be distinguished. By mid-August 1981 laminated desiccation polygons composed of an entirely different photosynthetic community and covered with layers of fresh terrigenous sediment had re-emerged.

bacteria are seen in initial isolations. With continuing transfers the diversity of microbial life is sharply reduced.

Cysts

During the time in which there was fresh water on North Pond great numbers of spherical resistant structures were consistently recovered from mat samples. Most of our detailed observations concern the persistent, smaller and fast growing 10 μm spheres. These objects have been seen in the field (Fig. 4A) and in collection jars after a year in the laboratory, and can be isolated in enormous numbers from the fresh and damp mat. Two cysts of similar morphology have been observed in electron micrographs of in situ mat material from 1977, layer 2, between 2 and 4 mm below the surface (Stolz, 1983a, this issue). Even after 6 months storage at 4°C or at room temperature, when plated on low nutrient medium, either damp or dry mat material serves as inoculum for the growth of the micro-organisms that make these structures. If mat material is suspended in either distilled or ½ concentration artificial seawater for only a few minutes and this suspension is then plated on modified K medium, manganese acetate medium, or salt medium designed to grow marine photosynthetic bacteria, these 10 μm cysts appear in profusion (Fig. 4B, C).

Although most of the cyst-like objects have not been identified, at least two types are desiccation-resistant cysts of amoebae. On the basis of morphology, the cysts in Fig. 5B, 5D and 5H can be assigned to the genus

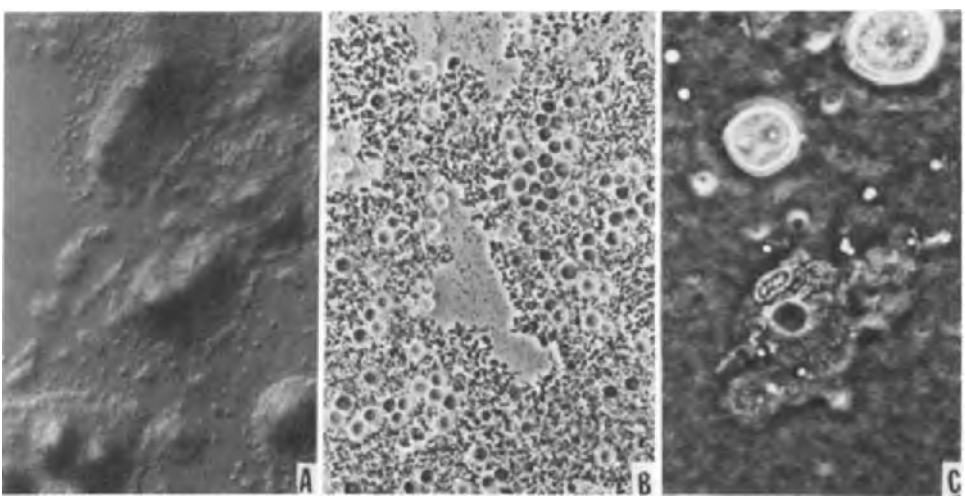

Fig. 4. Encysting protist, *Paratetramitus jugosus* on K medium: (A) cysts covering a bacterial colony taken from the mat, × 25 original magnification; each cyst is from 10 to 12 μm in diameter; (B) cysts at various stages within colonies of manganese oxidizing bacilli (original magnification × 400); (C) two cysts and vegetative amoeba containing a fecal pellet prior to expulsion.

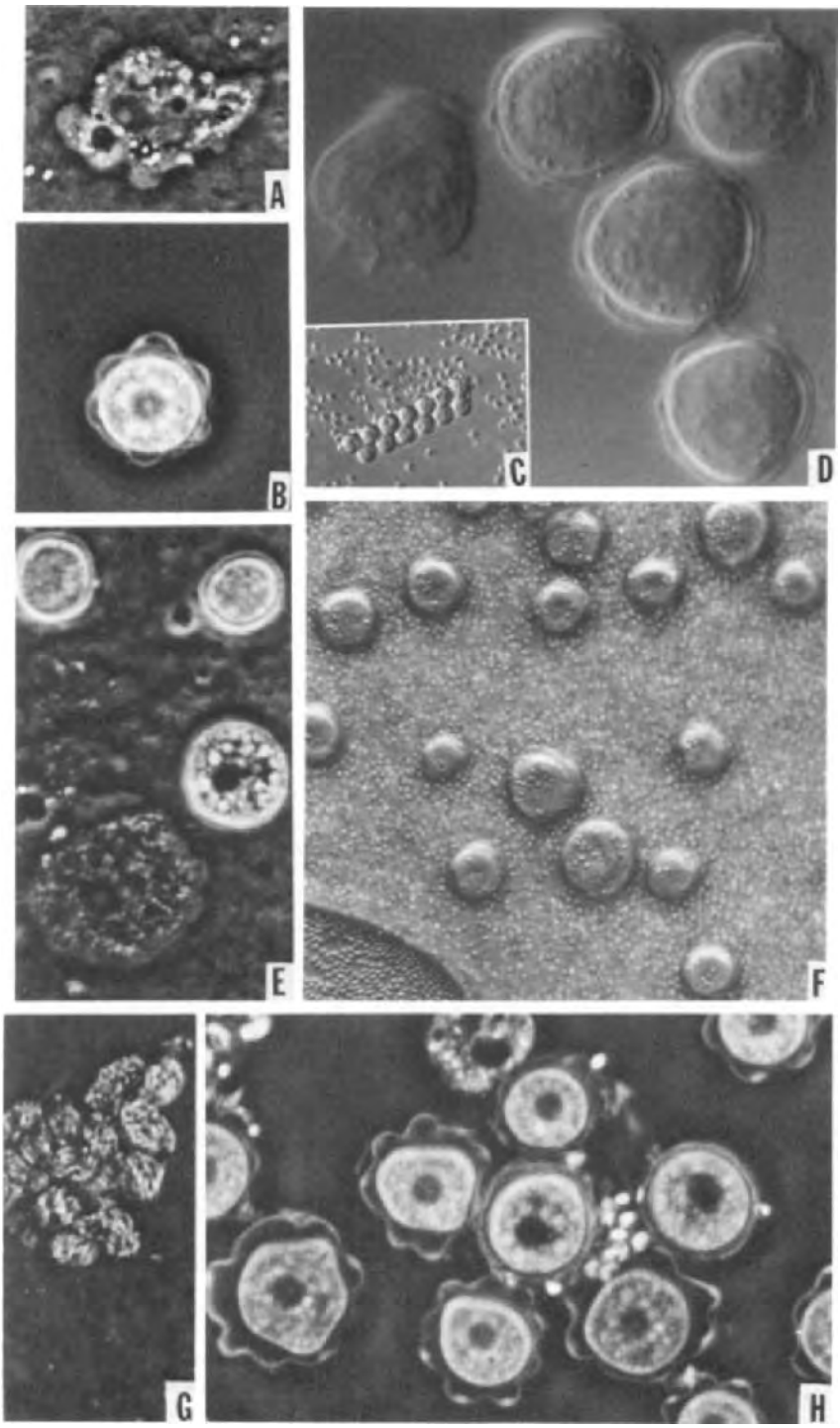
A
B
C
D
E
F
G
H

of fresh water soil amoebae, *Acanthamoeba.* On several occasions small amoebae have been seen to emerge from these 12 μm structures. Occasionally, huge clumps containing hundreds of these cysts develop on dry modified K plates taken from the field. Both T. Sawyer (Oxford, Maryland, see Bovee and Sawyer, 1979) and F. Page (of the Cambridge, England Collection of Algae and Protozoa) identified them as acanthamoebae (Page, 1981). Similar organisms were described by Singh and Das, 1970. We interpret the structures in Fig. 5D to be early stages in the formation of the resistant cyst wall.

The unidentified structures, ~ 5 μm in diameter (Fig. 5C) appeared on heterotrophic media on plates inoculated in the field and stored in the dark.

A major cyst-forming organism, shown on plates inoculated in the field (Fig. 6A, B, C, D), is an amoeboflagellate which has tentatively been assigned to the genus *Paratetramitus.* These, or very similar, 10 μm-diameter cysts have been seen in virtually every isolation from the mat and in fresh mat samples. They have appeared on media designed to isolate photosynthetic as well as heterotrophic microbes. These bacteriovores are able to grow vigorously on low nutrient media, and they especially feed on a bacillus which was a strong manganese oxidizer when first isolated (the "B" bacillus). Encysting amoebae have been observed growing side by side with algae of about the same size (Fig. 7). Algae and amoeba cysts, even if partially degraded, can be distinguished by fluorescence microscopy: the chlorophyll-containing structures when excited at 520—550 nm re-emitted in the red. Figure 5G shows structures frequently seen on plates harboring *Paratetramitus* cysts: they are interpreted as fecal pellets of the amoebae. This interpretation is strengthened by the observation, in rapidly growing cultures of amoebae grown on the "B" bacilli, of pellets prior to expulsion from the amoeba (Fig. 4C). Within less than a week colonies of the bacillus become riddled with cysts (Fig. 6B, C) and with longer incubation times the bacteria are completely digested.

Although this *Paratetramitus* (identified by F. Page, 1981 as *P. jugosis,* an organism isolated from fresh water and soil) has not yet been grown in the absence of live food, it can easily be removed to plates containing a minimum of other organisms, for example manganese acetate with unidentified bacilli (Fig. 6E). On modified K medium with a salinity of three quarters seawater and incubated from 22—31°C, not more than three morphotypes of bacteria and usually only one, that of the "B" bacillus, are seen.

A detailed description of this *Paratetramitus* is given by Read et al., 1983,

---

Fig. 5. Cysts and plaques all from a piece of mat placed on agar media designed for enrichment of manganese oxidizing bacteria: (A) amoeba, vegetative stage probably of an acanthamoeba; (B) *Acanthamoeba* sp. cyst; (C) unidentified spherical objects about 5 μm in diameter; (D) early stage in desiccation of cysts of *Acanthamoeba* sp.; (E) cysts and amoebae, probably *Paratetramitus jugosus*; (F) unidentified cysts and spores from field sample; (G) fecal pellets from amoeba in a cyst-riddled bacterial culture; (H) *Acanthamoeba* sp. cysts, amoebae and spores in early stage of desiccation.

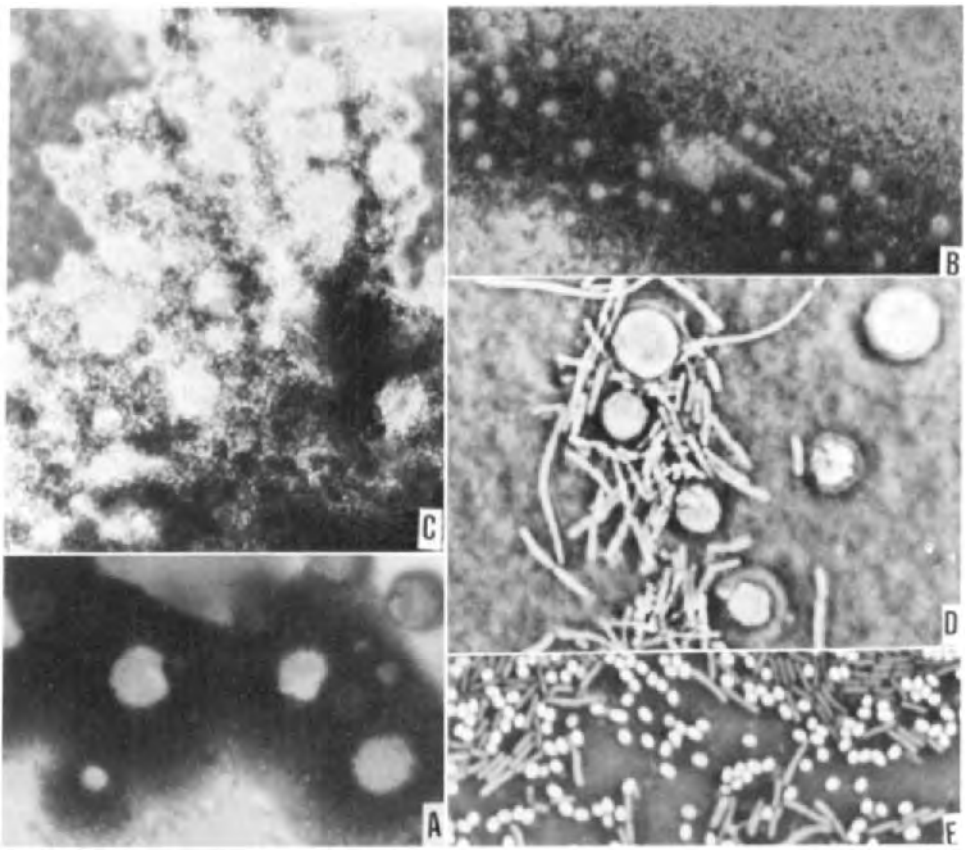

Fig. 6. Amoebae in cultures of manganese oxidizing bacteria: (A) plaques formed by holes in which amoebae have eaten away manganese coated spores; (B) the holes are due to amoebic cysts, ~ 10 μm in diameter, seen among the manganese-coated spores; (C) amoebae seem to be eating their way through colonies of this bacillus; (D) cysts at various stages of development seen in colonies of moribund bacilli; (E) "food" bacilli and their spores prior to attack by the encysting bacteriovoracious amoebae.

and is given here in brief. The appearance of holes within streaks or colonies of manganese-oxidizing bacteria provided the first evidence of this organism (Fig. 6A, B, C). Simultaneously, increasing number of amoebic cysts were seen on the same plates. The hypothesis that the amoebae forming these cysts were removing the bacillus spores was confirmed by electron micrographs of the amoebae (Fig. 8). In Fig. 8C, spores can be seen in the process of digestion within the naked amoebae. Figure 8A and 8D show the dense ultrastructure of the thick-walled cyst with autolysosomal bodies, and crystal-containing mitochondria that have been described for fresh water and soil amoeboflagellates (Bower and Korn, 1969). The electron micrograph of Fig. 8D, which corresponds to the light micrograph (Fig. 8E), shows the

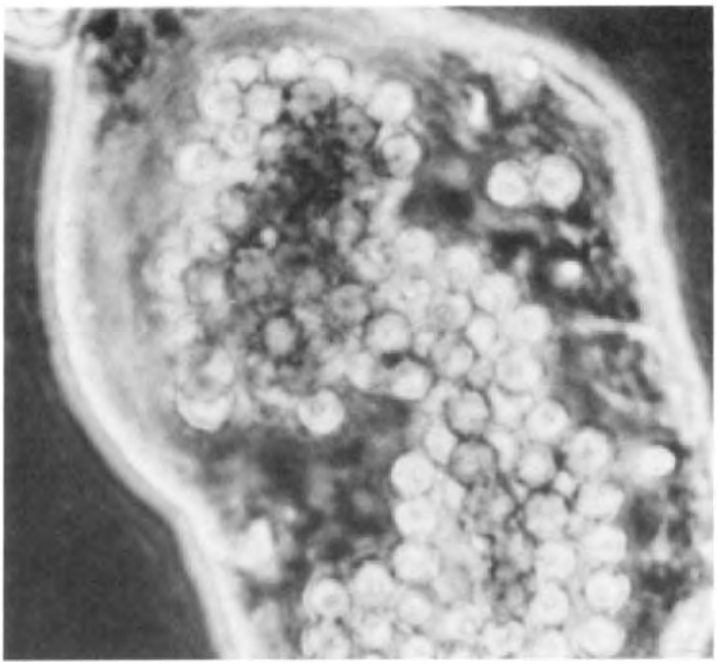

Fig. 7. Algae and cysts on field plate. The growth of 10—12 μm diameter chlorophytes and amoeba on enrichments for photosynthetic organisms was verified by electron microscopy.

"ectoplasmic" or "pseudocyst" that is extremely common in this material and which may represent a feeding, but walled stage in the complex development of the organism. This interpretation is offered to explain the overnight growth rate of cyst colonies that replace bacterial colonies where very few vegetative amoebae are observed, but in which the various cyst forms and damaged bacteria are abundant, such as in Fig. 6D. These *P. jugosus*, isolated and maintained on seawater plates, tolerate and grow at salinities up to 5.1 M sodium chloride, the highest value known for the species (F. Page, personal communication, 1982).

In field samples placed on modified K medium, such as those in Fig. 9, the development of spores (9A), clumps of spores coated with manganese precipitation (9A, C), spherical, elliptical and sometimes refractile structures (perhaps precipitates), and various cysts are seen. (Structures appearing on plates, such as those shown in Fig. 7, and in some cases verified with both electron microscopy and fluorescence microscopy, are cyanobacteria, chlorophytes or cyst-forming heterotrophic eukaryotes.) At the level of the light microscope, even with live material, spheroids are too similar to each other to be distinguished. In at least one case (Fig. 10A, B), smooth walled asexual cysts from *Dunaliella salina* which is extremely common on the surface of desiccation polygons (Fig. 2A) have been identified. The cysts

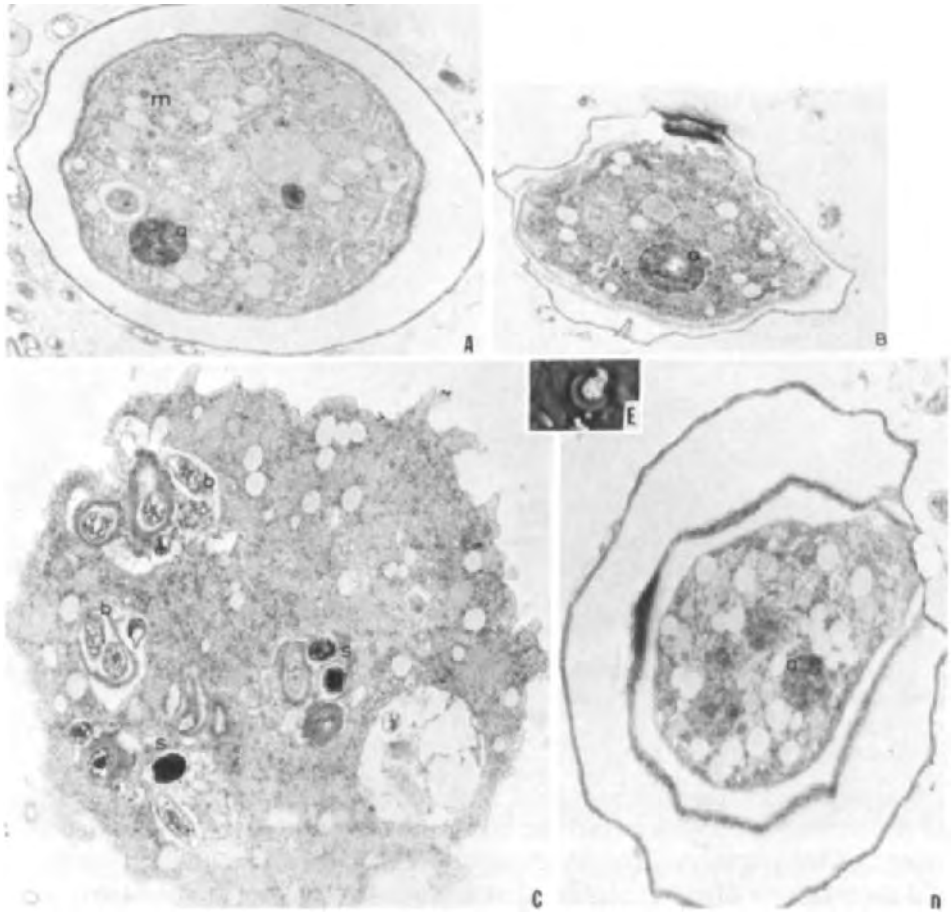

Fig. 8. *Paratetramitus jugosus:* (A) early stage of encystment (a= autolysosomal body, m= mitochondrion with crystal inclusion (× 12 500); (B) early cyst formation with irregular wall, prominent autolysomal body (a) (× 12 500); (C) vegetative amoebae with food vacuoles filled with bacteria (b) and spores (s) (× 12 500); (D) "ectoplasmic" or "pseudocyst" with autolysosomal bodies (× 12 500); (E) "ectoplasmic" or "pseudocyst" corresponding to electron micrograph in (D) (× 2000).

of this strain of *Dunaliella salina* form at salinities < 0.6 M or > 4.0 M NaCl. Germination and mitotic growth occur at intermediate salinities. A culture or field sample usually contained cysts of distinctly different sizes, but isolation of these organisms into monoalgal culture (Fig. 10) showed that all the organisms belong to the same strain. (See Margulis et al., 1980 for ultrastructural and other observations of this bright red mat surface organism).

Although encysted organisms have always been seen in material from the

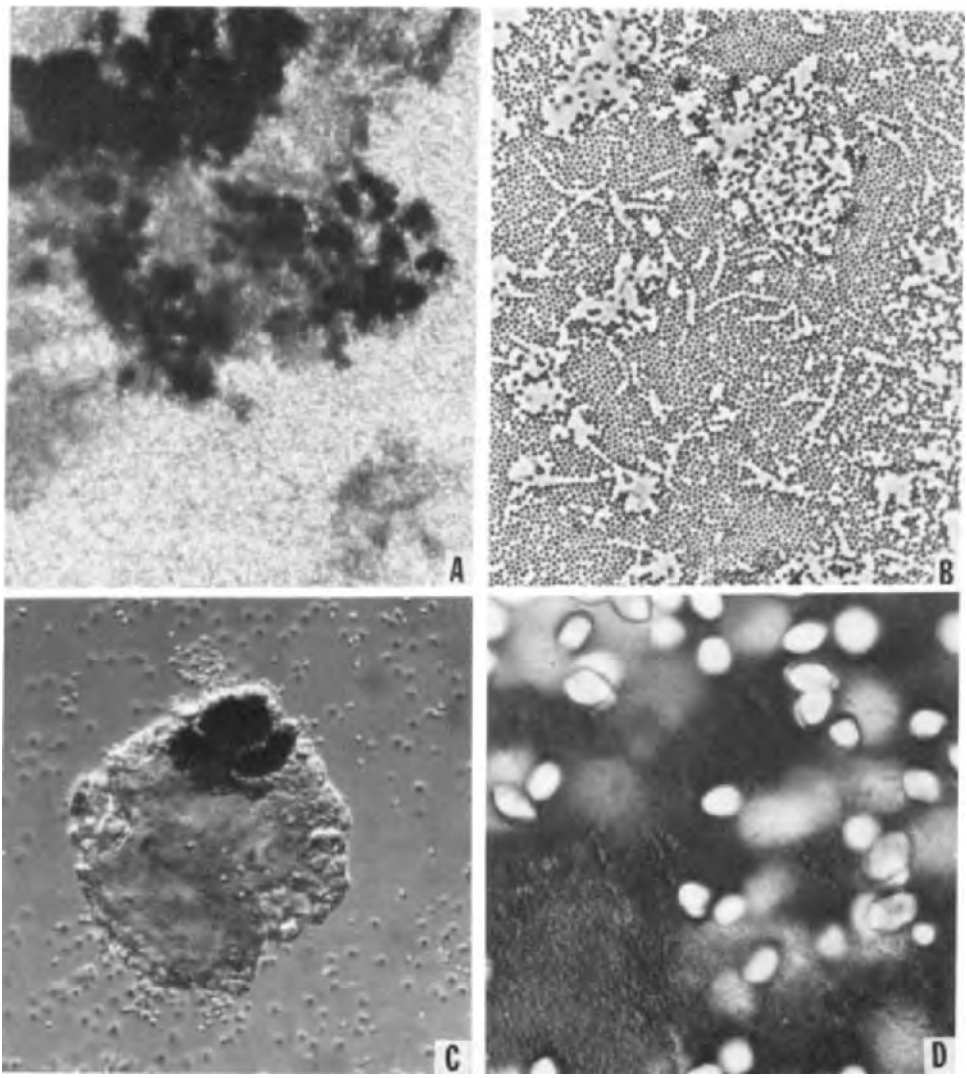

Fig. 9. Field samples from the 1980 mat taken from media designed to enrich for manganese oxidizing bacteria (K plates): (A) clumps of manganese precipitate associated with bacterial spores; (B) unidentified bacterial spores on field sample; (C) black manganese precipitate formed on clump of bacteria; (D) unidentified highly refractile biconvex lens-shaped objects frequently seen on fresh field samples and sometimes associated with bacterial colony surfaces. A March 1980 submerged enrichment sample on K medium from 3rd layer in mat, subcultured on K medium for 5 days produced filaments and these lens-shaped structures which were lost on subsequent transfer, although the bacterial isolate itself was viable indefinitely.

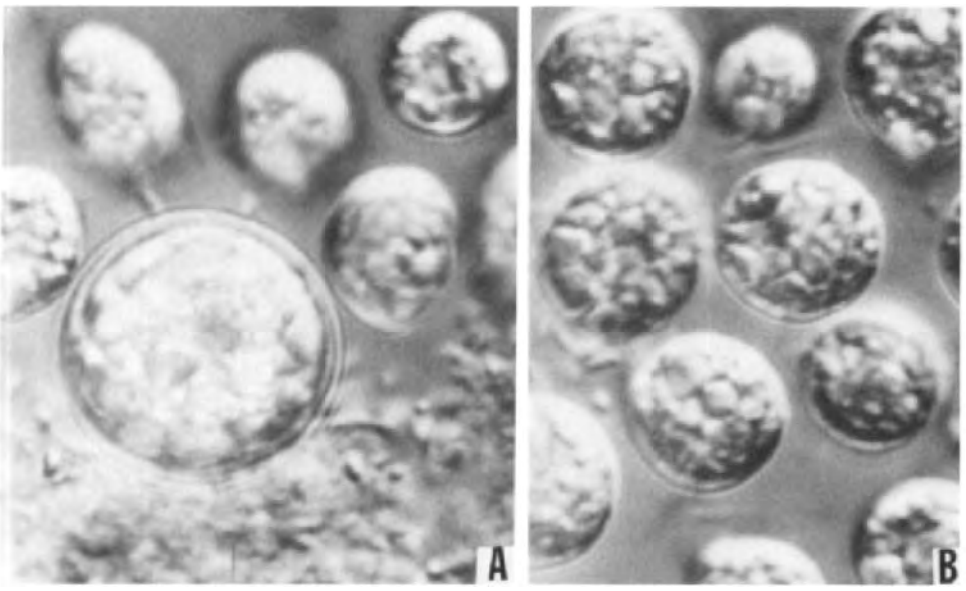

Fig. 10. *Dunaliella*, a green protist alga that encysts in seawater and grows vegetatively under hypersaline conditions: (A) a cyst 15 μm in diameter; (B) cysts from the same colony as (A), but only ~ 10 μm in diameter.

North Pond laminated mat, the diversity and abundance increased markedly with the influx of fresh water and the burial of the *Microcoleus* mat during the winters of 1979 and 1980.

Subsurface agar colonial structures

Subsurface bacterial colonies and structures within colonies, nearly all unidentified, are commonly seen to grow out if fresh mat material is placed on modified K medium (Figs. 11, 12, 13, 14). At least two of these colonies, which continued to make distinctive structures when transferred and isolated, are species of fluorescent Pseudomonas. These are probably new strains judging from comparisons between the data in Tables II and III, and characteristics listed in Bergey's manual (Buchanan and Gibbons, 1974) for pseudomonads. Chosen from dozens of colonies of heterotrophic bacteria, because they were recognizable enough to follow, three of the pseudomonad colonies have been in culture for several years. All formed distinctive lens-shaped or spherical colonial structures beneath the surface of the agar when streaked onto various nutrient seawater agar media (Table I).

These subsurface colonial structures form within 9—30 days after inoculation depending on the strain, temperature, salt, nutrient concentrations and the degree of dryness. The relationship between these variables and the formation of distinctive structures has been frustrated by the decrease of

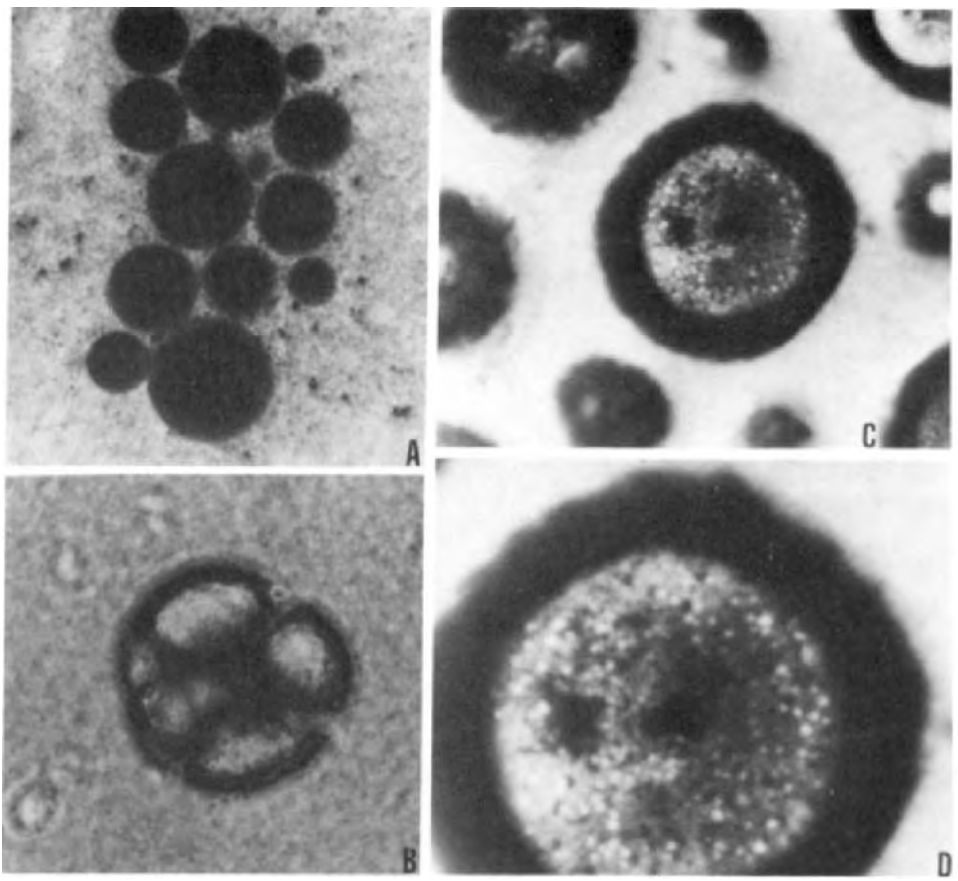

Fig. 11. Colony structures: (A) spherical subsurface agar bacterial colonies enriched from fresh mat samples on K medium (× 12); (B) desiccation resistant bacterial colony enrichable in fresh and dry mat samples; (C) spherical subsurface agar bacterial colonies enriched from fresh mat samples on K medium (× 25); (D) same as (C) (× 50).

the number and size of the structures formed with repeated subcultures. The original isolates that formed lens-shaped colonial structures were grown on seawater nutrient agar with any of a number of carbon sources. During the period of decreasing lens-shaped structure formation it was noted that distilled water and lowered NaCl (< 0.5 M) were most favorable for the appearance of these structures. However, since 1979 and 1980, four isolates progressively failed to make any lenses at all on any of the media on which they had previously formed them. With the exception of strain BC-2 of *Arthrobacter simplex* (Fig. 12, Gong-Collins and Read, 1983) which forms subsurface colonial structures under any conditions that permit it to grow, no partially characterized mat organism is now producing these structures. The distinctive structures of this new *Arthrobacter* stain with Alcian blue

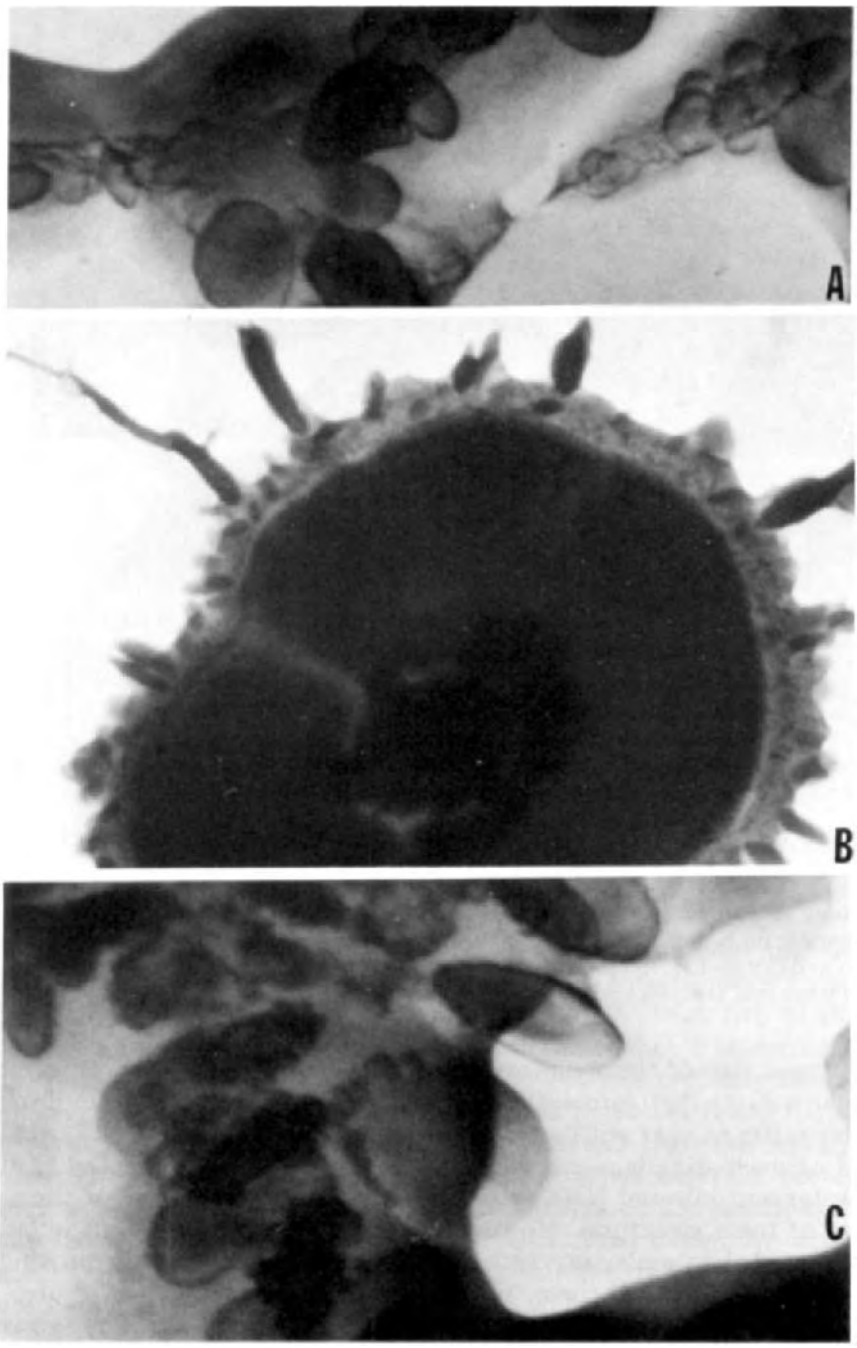

Fig. 12. *Arthrobacter simplex*, strain BC-1 (Gong-Collins and Read, 1983); (A) lens-shaped structures at the periphery of the freshly isolated colony; (B) lens-shaped colonial structures, some several hundred microns long, appear purple in transmitted light; (C) the subsurface agar colonial structures which vary from spherical to biconvex-lens shape, are most abundant at edges of colonies or along streaks.

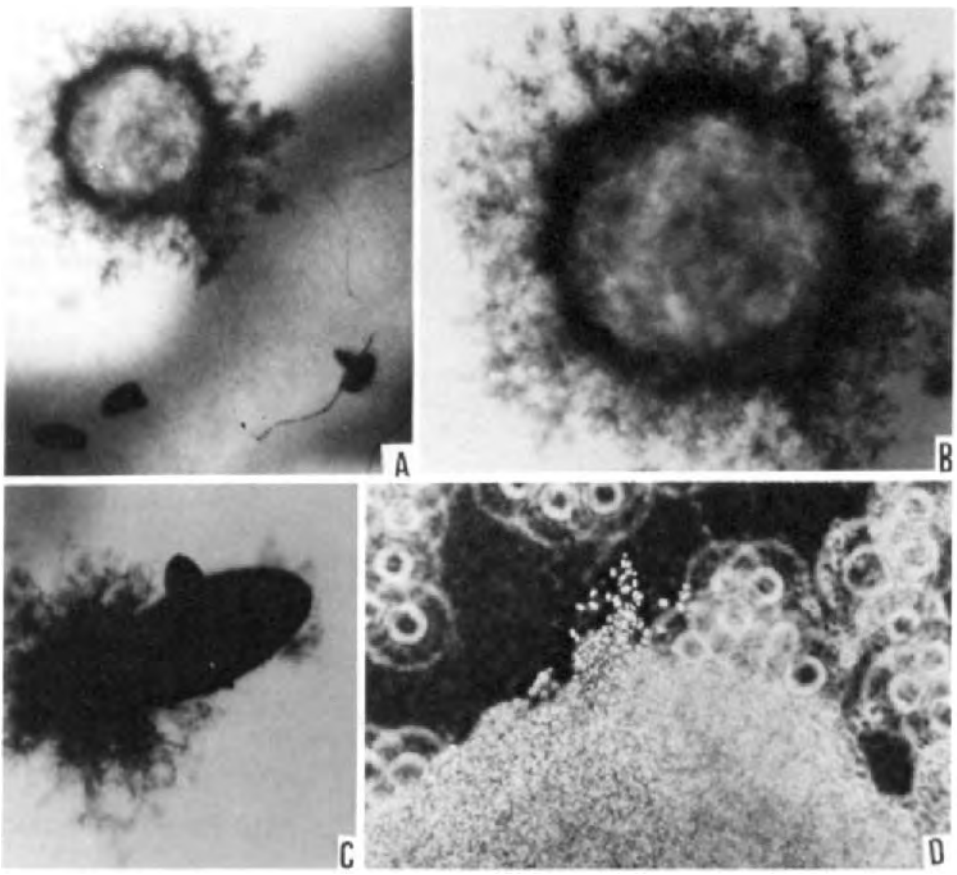

Fig. 13. Subsurface agar colonies from field samples: (A) unidentified spherical colonial structure embedded in agar (× 12); (B) same as (A) (× 25); (C) "phonograph records", disk-shaped black agar-embedded bacterial colonies (× 50); (D) edge of "phonograph record" colony composed of bacterial spores and the motile rods that form them. Packed spores and cell seen as dots (× 1000).

(thus they are composed, at least in part, of mucopolysaccharide) and it can be seen that they are composed of packed dead cells, and a material of mucous consistency which fluoresces in the green when excited with UV light at 450 nm (Gong-Collins, 1982).

Reisolations, especially of fresh mat bacteria, succeed in recovering isolates that do produce such subsurface colonial structures. In all cases studied so far, the structures are composed of densely packed nonmotile bacterial cells surrounded by mucous-appearing material. Prior to the formation of these colonial structures the bacteria are flagellated motile rods. The distinctive colonial structures, usually lens-shaped or spherical, may be embedded within the colonies themselves, in the agar below the colonies or, sometimes,

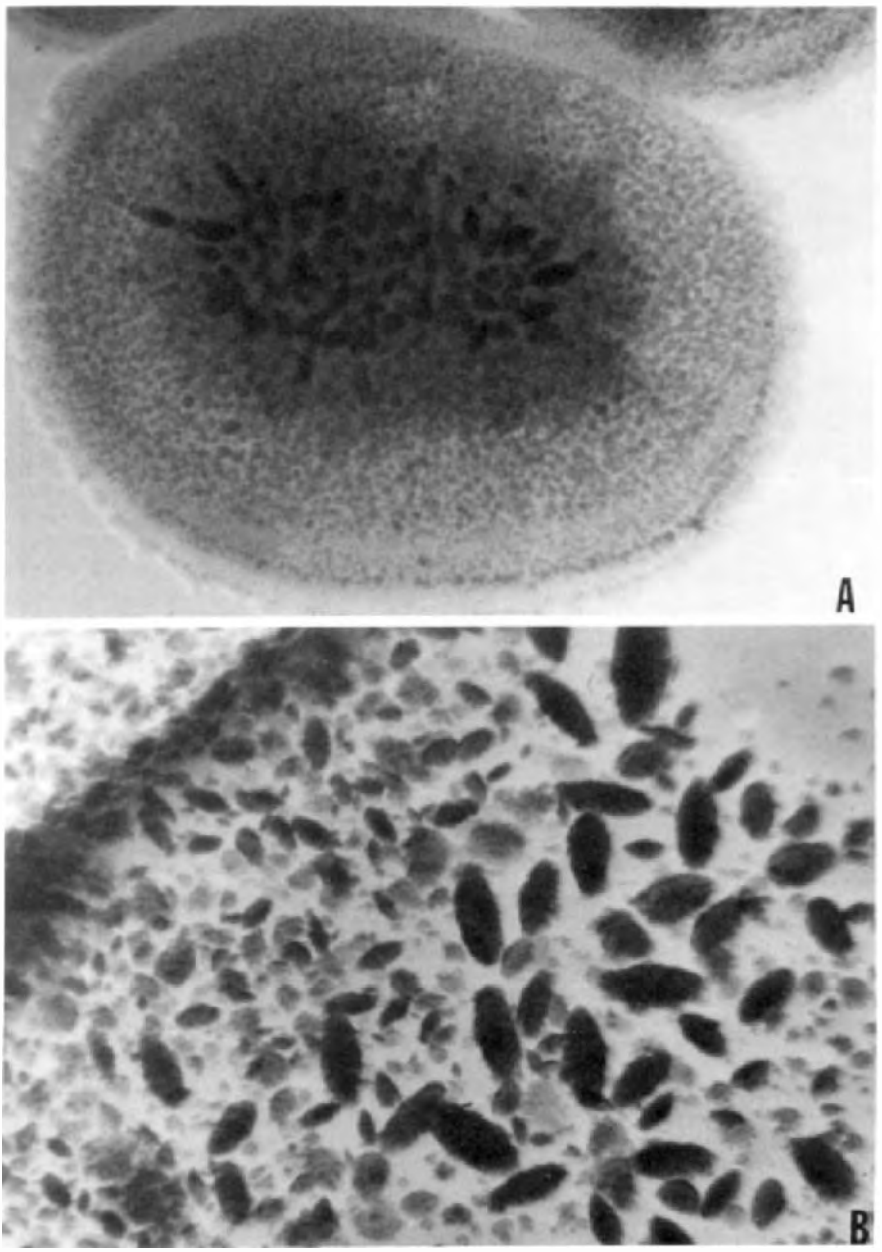

Fig. 14. *Pseudomonas* spp. BC-2 (see Tables I and II); (A) colony morphology showing lenses; (B) lenses of various sizes are embedded in the bacterial colony surface and in the agar.

TABLE II

Pseudomonads from the microbial mat: general characteristics

	Strain	
	BC-2	BC-3
shape	rod	rod
gram stain	—	—
aerobiosis	obl. aerobe	obl. aerobe
spores	—	—
motility	+	+
H_2S production	+	+
nitrate reduction	—	nt
gelatin hydrolysis	weak	+
starch hydrolysis	—	+
catalase	weak	+
oxidase	—	+
indole	—	—
fluorescence		
λ emission max=562	+	+
urease	—	—
citrate	+	—
casein	weak	+

(nt) = not tested; (λ) =562 nr. Each test was run at least twice.

TABLE III

Pseudomonads: compounds used as sole sources of carbon for growth

	BC-2	BC-3
Carbohydrates		
L-arabinose	-	+
D-cellobiose	nt	+
chitin	nt	+
D-fructose	+	+
D-fucose	-	-
D-galactose	-	+
D-glucose	+	+
lactose	-	+
D-levulose	+	+
D-maltose	-	+
D-mannose	-	+
raffinose	-	+
rhamnose	-	+
sucrose	-	+
trehalose	-	+
D-xylose	-	+

TABLE III (*continued*)

	BC-2	BC-3
Mono-, dicarboxylic acids		
D-gluconate	+	+
malonate	-	+
Hydroxy acids		
alpha-ketoglutarate	-	-
DL-lactate	-	+
D-tartrate	-	-
Miscellaneous organic acids		
L-ascorbate	-	+
Polyalcohols and glycols		
dulcitol	-	+
erythritol	-	-
D-mannitol	+	+
orcinol	-	-
D-sorbitol	-	-
Aliphatic amino acids		
L-alanine	-	-
L-asparagine	-	+
L-glycine	+	+
L-leucine	+	+
L-ornithine	-	+
Heterocyclic/aromatic amino acids		
L-histidine	+	-
DL-phenylalanine	+	+
L-proline	+	+
L-tryptophan	-	-
L-tyrosine	-	+
Basic amino acids		
L-arginine	+	+
L-lysine	+	+
Sulfur containing amino acids		
L-cysteine	-	-
L-cystine	-	-
L-methionine	+	+
Hydroxy amino acid		
L-serine	+	+
Nucleotide derivatives or precursors		
orotic acid	-	+
uracil	-	-

peripheral to the colonies. The structures fluoresce brightly with an absorption maximum of ~ λ =562 nm using the B (blue) filter with the Nikon Fluorophot microscope. They also fluoresce with the V (violet) filter, but not at all with the G (green) filter. Desiccation enhances the intensity of this intrinsic fluorescence.

Lens shaped colonies themselves are not unusual, as Stanier et al. (1957) state: "The shape of the eubacterial colonies that develop within a solid medium is largely determined by the manner in which the solid medium accomodates the expanding mass of cells. In agar media, the gel tends to split along a plane, through the center of the colony so that the colony usually develops in the shape of a biconvex lens."

The unusual aspect of these mat bacteria is that they seem to be burrowing themselves into the agar or into their own colonies. Unlike the phenomenon described by Stanier et al. (1957), in which the bacteria were inoculated under the surface, here the formation of subsurface mat colonies and colonial structures occurs spontaneously. Some colonies even occur in the shape of "phonograph records" suspended at various depths and angles in the agar (Fig. 13A, C, D). That the colony shape is determined by tightly packed bacteria is shown in Fig. 13D. Formation of these colonial structures may be a behavioral tendency of motile rods that travel together through the agar from the initial inoculum and become immobilized.

The colony morphology on agar may be parallelled in many mats which have been observed to have a consistency of agar gel. Fluorescent pseudomonads have been observed embedded in mucilage and decaying plant surfaces (Professor D. Caldwell, personal communication, 1980). The agar-like consistency is probably due to the abundance of mucopolysaccharide bacterial sheath material, especially of photosynthetic bacteria in soft sediment. The gelatinous consistency of the mat has been frequently noted (e.g., the 1980 mat sample, Fig. 3). In one sample the density was determined to be the same as that of 0.75% agar because the mat fragments, composed of several layers, neither floated nor sank in media containing that concentration of agar. The possibility that subsurface agar colony formation may be a behavior that confers heat and/or desiccation resistance on the bacterial colony is presently under investigation. The hypothesis of heat resistance conferred by the spherical and lens-shaped colonial structures has been verified in one case. The new isolate, *Arthrobacter simplex* (Gong-Collins and Read, 1983) is resistant to 70°C after it has formed colonial structures. The relative viability at this temperature is still 10% of that of the unheated bacteria, whereas 70°C is lethal to them before they produce the lens-shaped structures. The relative viability was reduced to less than one part in 10°C of that of untreated cells. However, in two other pseudomonad strains, BC-2 and BC-3 in which the relative viability was measured as a function of temperature, no differential viability associated with the presence of lens-shaped structures was observed. Further heat and desiccation studies were frustrated by the tendency of the colonies to lose the ability to form lens-shaped structures upon repeated transfer.

Although the detailed relationships between colony morphology and environmental constraints must be worked out, clearly the formation of distinctive colonial structures must be considered in the interpretation of sedimentary microstructure and texture, both for degrading microbial mats and the fossil record (these remarks are specifically applied to the case of *Metallogenium* below). Lens-shaped colonial structures (formed by the pseudomonad, strain BC-2) that showed enhanced structure formation at lower salt concentrations, are shown in Fig. 14. The numbers, sizes and shapes of these lenses vary from < 15 to > 150 μm in length, depending on the bacterial strain, growth conditions and, probably, other variables.

Metallogenium-like colonies

On many occasions we have seen colonies with the stellate structure attributed to *Metallogenium*, the supposed counterpart to *Eoastrion*, a 2 Ga- old microfossil (Awramik and Barghoorn, 1977). In some cases, spherical colonies surrounded by wispy stellate threads have been seen (Fig. 13A, B), and in others *Metallogenium*-like microcolonies have virtually covered portions of the plate or along the streak. The "*Metallogenium*-like" colonies may or may not be capable of oxidizing manganese to manganese dioxide (leucoberbelin blue positive). The size of the *Metallogenium*-like structures varies enormously. Bacterial colonies developing on the same petri plate may display "*Metallogenium*-like structures" that measure (from one edge to the other of the stellate structure) from hundreds to $< \sim 20$ μm. At least in the case shown in Fig. 15, the separated stellate colony morphology persisted to the limit of resolution of the light microscope, and was a reflection of the distribution of spores and vegetative cells in the colony. Although bacterial colonies that grow in the "*Metallogenium*-like" fashion may or may not oxidize manganese, vigorous manganese oxidizers are more distinctive due to the deposition of the dark MnO_2 precipitate on their spores.

It is clear to us that "*Metallogenium*" is a phenomenon of stellate colony growth and not a taxon of bacteria. This interpretation was confirmed by direct experience with G. Zavarzin's *Metallogenium* inoculum kindly provided by S.M. Awramik (Zavarzin, 1981). The striking similarity between *Metallogenium* and the Gunflint microfossil *Eoastrion* was confirmed (Fig. 16), but we know that these plates do not harbor pure cultures of bacteria.

Fig. 15. *Metallogenium:* (A) colony structures on K medium (× 25); (B) colony structures on K medium (× 50); (C) mixed colony of spore forming bacteria (× 50); (D) at higher magnification the "microcolonies" of (A), (B), (C) and (E) often appear as filamentous spore forming bacteria that with time, deposit manganese on their spores (bacteria that do not oxidize manganese, but are motile and form spores, also grow in a "*Metallogenium*-like fashion") (× 1000); (E) colony structure on K medium formed by a different bacterium than in (A)—(C) (× 25); (F) microcolonies that resemble *Metallogenium* are usually mixed cultures of spore formers with a "microcolony" growth habit (× 400).

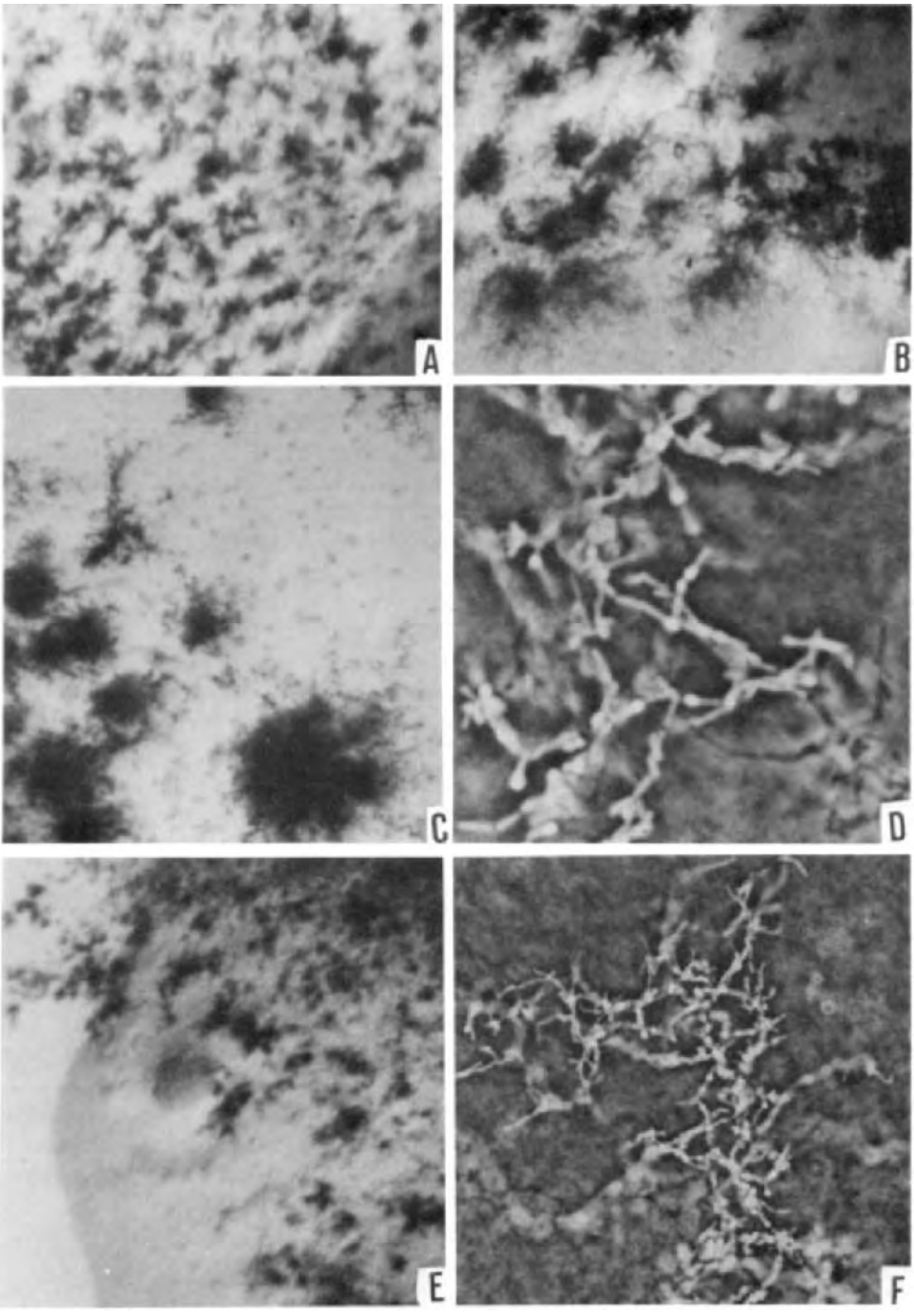
A
B
C
D
E
F

Indeed, when the inoculum was grown on manganese sulfate (1 part in 10^5 w/v) rather than manganese acetate (same concentration) another very distinctive bacterial colony emerged (Fig. 17). This colony varied from ~ 30 to 300 μm in diameter and formed spherical blastula-like structures that could easily have been mistaken for individual organisms. Unfortunately, although this bloom of subsurface agar structures lasted about a month they did not survive a transfer to fresh medium. When a richer medium, V-8, was used (Tousson and Nelson, 1968) with Zavarzin's *Metallogenium* inoculation, imperfect fungal hyphae appeared which formed conidia reminiscent of those of *Fusarium.* The *Metallogenium* inoculum survived repeated transfers in the presence of antibacterial antibiotics and surface sterilization of fungal spores with 3% (v/v) hydrogen peroxide, 3% (w/v) mercuric chloride and 70% (v/v) ethanol (Booth, 1977); although no manganese was deposited in the presence of the antibiotics (600 ug ml^{-1} chloraphenicol, tetramycin, erythromycin, or 300 ug ml^{-1} penicillin, streptomycin, tetracycline, chloramphenicol) the stellate underlying the microbial substructure and fungal hyphae could be seen. The antibiotics, which inhibit not only bacterial growth, but probably also manganese chelation were then removed. At that point the typical "*Metallogenium*" appearance reappeared. Thus, the *Metallogenium* habit survives repeated transfer in the absence of its expression.

In our hands at least, Zavarzin's "*Metallogenium*" is a mixed culture which contains a fungus and several kinds of bacteria, including a motile rod and a thin filamentous form. In spite of the claim that it is a mycoplasma (Dubinina, 1969; Zavarzin, 1981), structural evidence at the transmission electron microscopic level has not been published nor has the traditional evidence for a pure culture been presented. The mixed culture grows well, but slowly, on extremely low nutrients (all concentrations of manganese acetate are shown in Table I) and much less visibly, but at the same rate in sodium acetate at the same concentrations. For example, in both manganese and sodium acetate, colonies appeared after 4—5 days, and reached a maximum size and density in ~2 weeks. Of course the manganese-coated colonies were always far easier to see. Our *Metallogenium*-like bacterial colonies from the Baja California microbial mat are also mixed culture phenomena, but they lack a fungal component. Even in the cases shown in Fig. 15, two different bacterial isolates present the same morphological aspect. Although the stellate forms are colony structures, this stellate habit is retained to the level of high power magnification of the light microscope. This morphology is a reflection of the deposition of spores which form along thin filaments and tend to become coated with the manganese oxides or with brownish organic material. Given that the viscosity of mats and of our 1.5% agar plates are often quite comparable, it is possible that the pre-Phanerozoic *Metallogenium*-phenomenon also represents several different taxa.

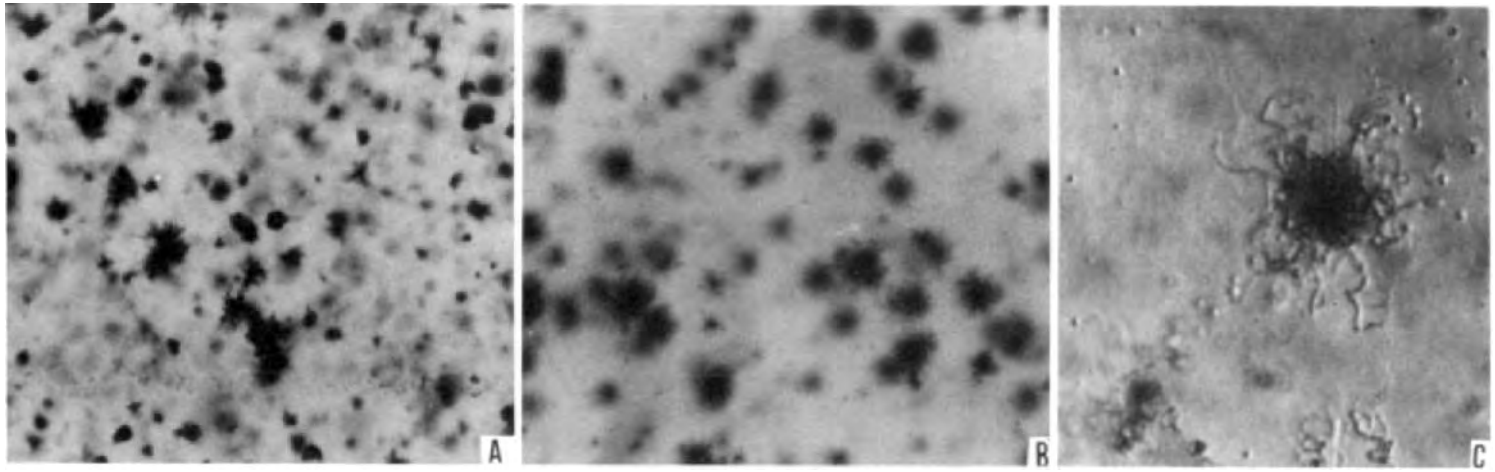

Fig. 16. *Eoastrion/Metallogenium*: (A) *Eoastrion*, from a petrographic thin section of the Gunflint chert, ~ 1.9 Ga-old, collected by E.S. Barghoorn (× 400); (B) "*Metallogenium*-like structure" growing on 1% manganese acetate (phase contrast photomicrograph of the three week old culture (× 400); (C) *Metallogenium*-like microcolony as in (B) (× 1000).

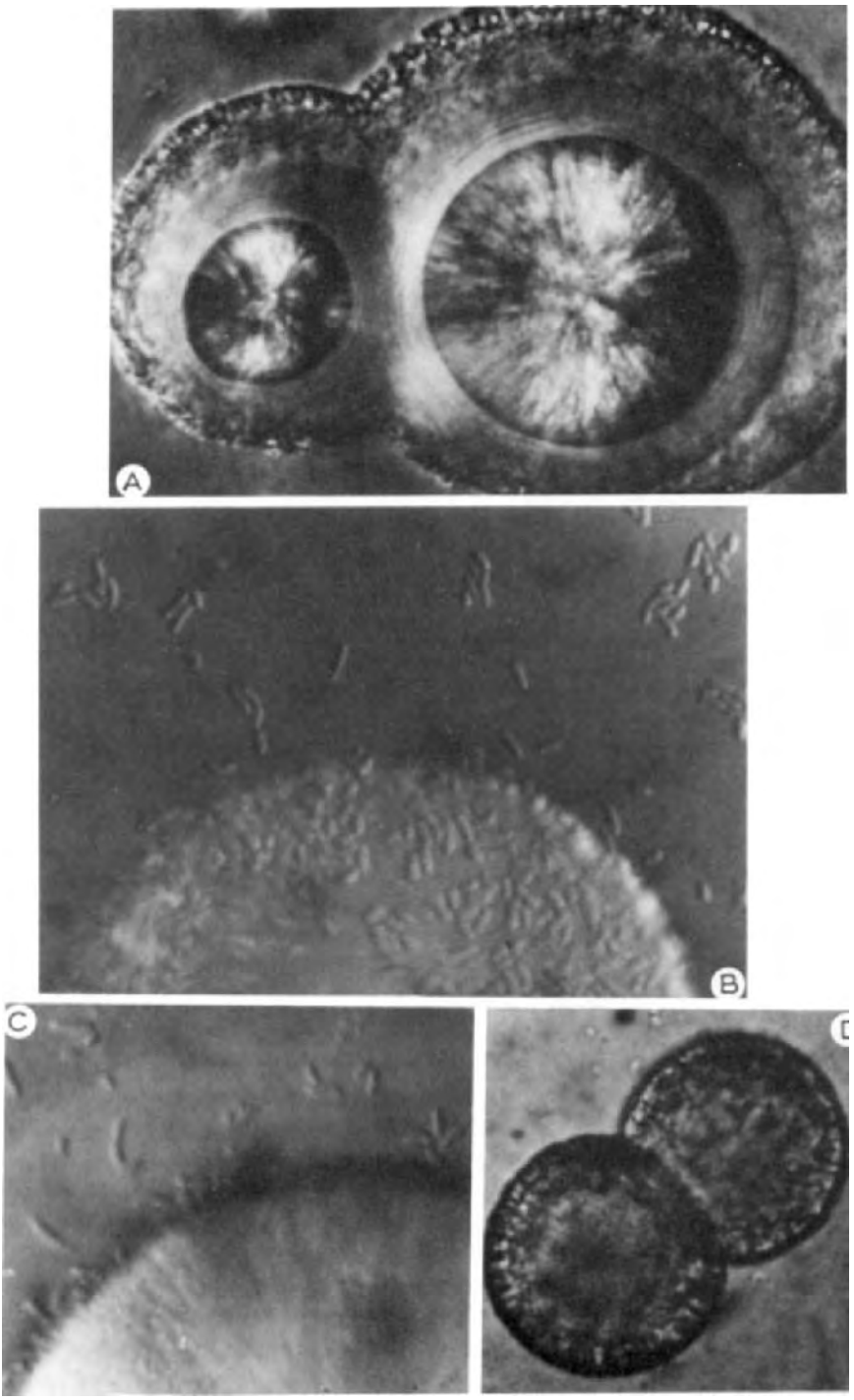

Fig. 17. *Eosphaera*-like bacterial colony: (A) colonial structures growing on manganese sulfate agar (× 40); (B) edge of "*Eosphaera*-like colony (× 100); (C) edge of another "*Eosphaera*-like" colony (× 100); (D) As in (C) (× 12).

Manganese oxidizing bacteria

Manganese oxidizing bacteria have been taken from each of the fresh mat samples. They are also recovered when dried mat samples, even after several years of storage, are moistened for only a few minutes in sterile seawater or distilled water and plated on K-agar (modified from Krumbein and Altman, 1973 as shown in Table I).

Fresh mat samples are extremely rich in manganese oxidizers: they usually contain several different kinds of oxidizers, each of which is represented many times. On modified K plates they make up ~ 10% of the total diversity. This abundance in fresh samples is far greater than that in dry or stored samples which yield a few manganese oxidizing colonies (all spore formers). We have stained intact mat samples with leucoberbelin blue (modified from Krumbein and Altman, 1973) and have, on several occasions, inoculated modified K medium with bacteria taken from various colored layers of the mat. On every occasion our impression that manganese oxidizers are concentrated in certain layers and that they are far from randomly distributed has been confirmed. Although detailed studies of field material have yet to be done, a sample experiment is shown in Fig. 18. The submerged mat of the spring of 1980 had two major layers (Fig. 3); strong manganese oxidizers (seen as dark lines along the streak in 18B) were far more prevalent in the lower black layer of the mat (18C) than they were in the upper layer (18A). It is possible that the oxidizers were brought in with terrigenous sediment and concentrated by burial in the black layer. Further information on manganese oxidizing bacteria from laminated sediment samples is given in the report of the summer course (Planetary Biology and Microbial Ecology, 1980. NASA Ames Research Center/University of Santa Clara, NASA Life Sciences Office, Washington D.C.). At least two of the manganese oxidizers have been identified as bacilli: *Bacillus licheniformis* (López-Cortés, 1982) and *Bacillus megaterium* (Gong-Collins, 1983).

Microbial mat samples: in situ transmission electron microscopical studies

Electron microscopic observations of fixed and embedded whole mat samples have permitted the study of the natural relations of micro-organisms to each other within the sediment (Stolz, 1983a, this issue). The new application of ultrastructural techniques has led to the discovery of organisms that have never been cultured: unicellular, sheet-forming, filamentous photosynthetic bacteria that are members of the genus *Thiocapsa* have been determined by combined light and electron microscopy. Ultrastructural observations showed at least one of these thiocapsas is *T. pfennigi* (Stolz, 1983b). Nearly all are deeply embedded in well developed sheaths (Fig. 19). The cells may occur as within sheath monads or dyads having total diameters of between 1.0 and 2.0 μm. The same purple sulfur bacteria which were major constituents of the 1979 microbial mat community

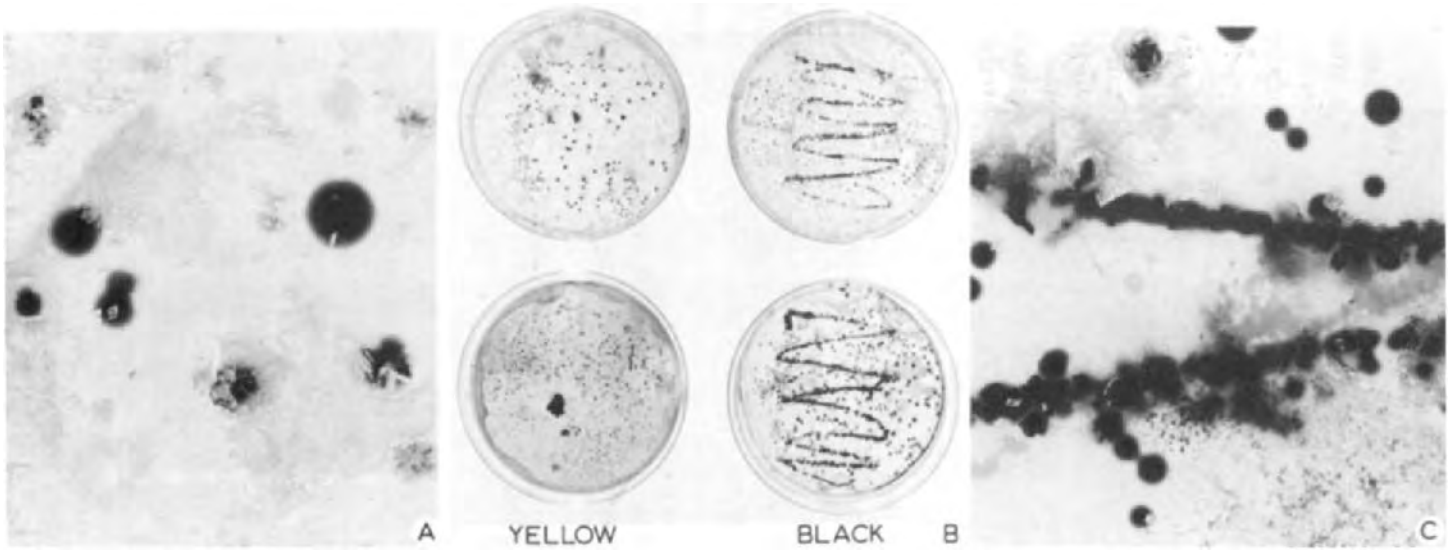

Fig. 18. Manganese oxidizing bacteria isolated from the submerged mat of 1980 (see Fig. 3): (A) dark colonies of manganese oxidizing bacteria along a streak taken from the yellow layer of the 1980 mat (× 12); (B) comparison between yellow (top) and black (lower) layers of the submerged mat (manganese oxidizing bacteria are far more prevalent in the lower layer); (C) dark colonies of manganese oxidizing bacteria along a streak taken from the black layer of the 1980 mat.

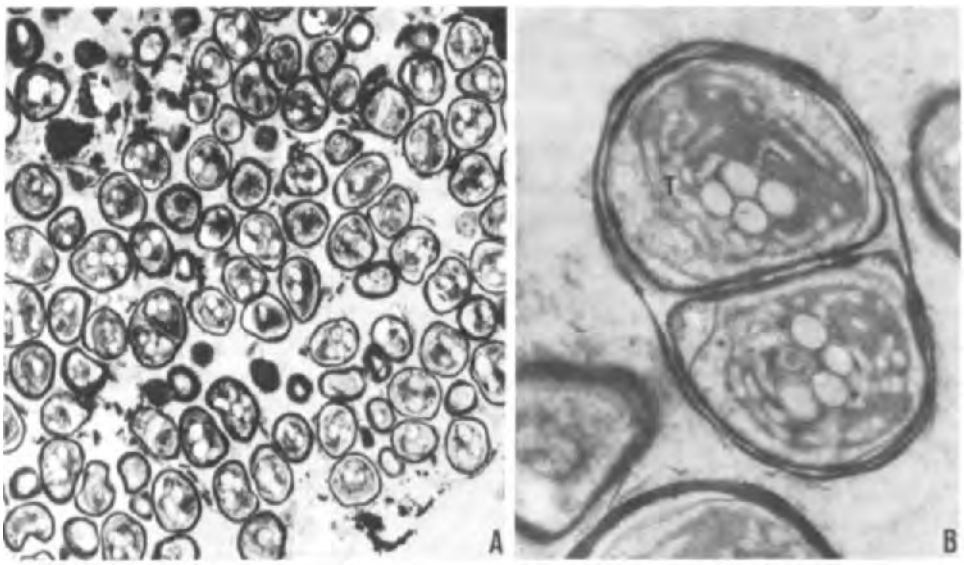

Fig. 19. *Thiocapsa*, electron micrographs of in situ mat: (A) *Thiocapsa* sp. from layer 5, 1.6 cm below surface of 1979 mat (× 6 500); (B) *Thiocapsa* sp. from layer 2, 1.2 cm below surface of 1979 mat. Note the tubular thylakoids (T) (× 37 500).

(Stolz, 1983, this issue) entirely dominate layer 2 of the mat. Their thick sheaths probably confer upon them high preservation potential. If found in the Archean fossil record they might possibly be misinterpreted as sheathed coccoid cyanobacteria. Further studies of the degradation pattern of these microbes within stratified sediment may clarify interpretation of possible pre-Phanerozoic analogues.

CONCLUSIONS

Micro-organisms isolated on low nutrient media from the flat laminated North Pond Laguna Figueroa mat exhibit distinctive structures, only a few of which have been studied in some detail. On media designed to grow photosynthetic bacteria or cyanobacteria, or on manganese rich media and under desiccating conditions, many species of bacteria and several of cyst-forming protists have been recovered. In situ studies of layers of the mat more than a cm or so from the surface reveal a number of morphologies apparently associated with mat burial and degradation. While only a very small fraction of the distinctive structures have been studied in detail, our experience is extensive enough to suggest that realistic interpretation of the late Proterozoic fossil record requires that such components of microbial mat communities be identified and their ecological role understood.

In this paper we have introduced objects measuring in size from one to several hundred μm that have been seen more than once in flat laminated

field samples or immediate enrichments from mat samples. The amoeba cysts were especially abundant in submerged mats during the periods of flood. Note that none of the microscopic objects are cyanobacteria, yet nearly all similar sized structures have been assumed to be cyanobacteria in descriptions of Proterozoic fossils found in cherts and macerations from shale (Schopf and Blacic, 1971; Awramik and Barghoorn, 1977; Vidal and Knoll, 1982a, b). As can be seen in Fig. 20, although microfossils may be derived from bona fide cyanobacteria, they may also be interpretable as cysts (compare Figs. 5, 7, 8, 10 and 20). Understanding of field relations, original environmental setting, mat position as well as the conditions of deposition and details of degradation (as noted by Knoll and Golubic, 1979; Vidal and Knoll, 1982a, b) are necessary for accurate interpretation

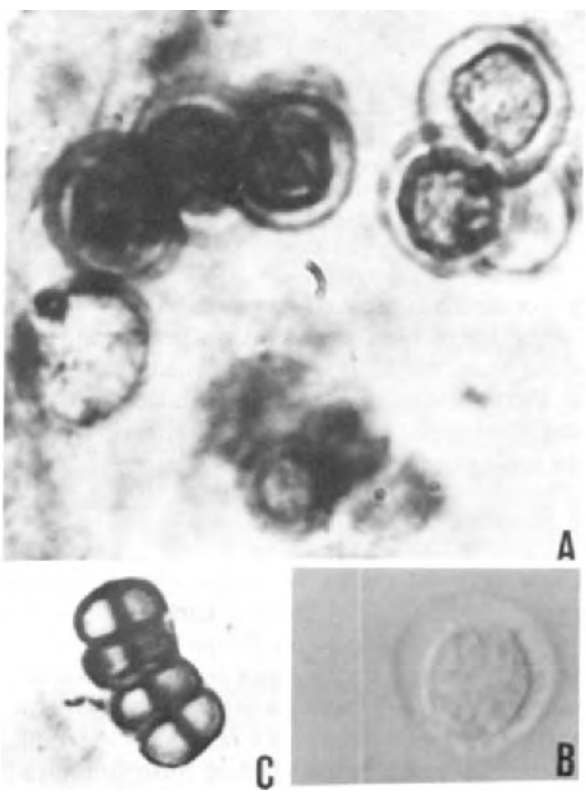

Fig. 20. Pre-Phanerozoic microfossils compared: (A) microfossils from the Bitter Springs Formation in Central Australia (~ 900 Ma-old) interpreted to be cyanobacteria, outer vesicle diameters approximately 15 μm in diameter (courtesy of Andrew Knoll); (B) cyst of *Paratetramitus jugosus* taken from Laguna Figueroa mat sample ~ 12 μm in diameter; (C) *Sphaerophycus wilsonii*, Proterozoic microfossil preserved in a silicifed microbial mat from Spitzbergen. The spheroids are ~ 4 μm in diameter (see Knoll, 1982 for details).

of the record. We have tried here to focus particularly on those objects which are abundant, regular members of the community which by virtue of metal deposition, thick walls or distinctive morphology are in some way more likely to be preserved. The goal of these studies is a complete characterization of microbial mat communities, precursors to stromatolites, in their natural sedimentary context as well as assessment of their geological and geochemical fates. Until more progress is made toward this goal it is unlikely that the interpretation of the microfossil record will be accurate.

ACKNOWLEDGEMENTS

We are grateful to Professor E.S. Barghoorn, Evelyn Ball, Robert Obar and Laurie Read for help with both the work and the manuscript, and Andrew Knoll for Fig. 20A, B. This work was begun in connection with the Planetary Biology and Microbial Ecology NASA Summer Research Program (including S. Chapnick and A. Lazcano-Araujo) and was later supported by NASA Life Sciences Grant NGR-004-025 and the Boston University Graduate School.

REFERENCES

Awramik, S.W. and Barghoorn, E.S., 1977. The Gunflint microbiota. Precambrian Res., 5: 121—143.

Booth, C., 1977. The genus *Fusarium*, a Laboratory Guide. Commonwealth Mycological Institute, Kew, Gt. Britain, 150 pp.

Bovee, E.C. and Sawyer, T.K., 1979. Marine flora and fauna of the Northeast United States. Protozoa: Sarcodina: Amoeba, NOAA Technical Report, NMFS Circular 419, Seattle, WA, 56 pp.

Bower, B. and Korn, E.D., 1969. The fine structure of *Acanthamoebae castellanae* (Neff strain), II. Encystment, J. Cell Biol., 41: 786—805.

Buchanan, R.E. and Gibbons, N.E. (Editors), 1974. Bergey's Manual of Determinative Bacteriology. 8th Edn., William and Wilkins, Baltimore, 1268 pp.

Darbyshire, J.F., Page, F.C. and Goodfellow, L.P., 1976. *Paratetramitus jugosus*, an amoeboflagellate of soils and freshwater, type species of Paratetramitus nov. gen. Protistologia, 12: 375—387.

Dubinina, G.A., 1969. Inclusion of *Metallogenium* among the Mycoplasmatales, Dokl. Akad. Nauk SSSR, 184: 1433—1436.

Francis, S., Margulis, L. and Barghoorn, E.S., 1978. On the experimental silicification of microorganisms: implications for the appearance of eukaryotes in the fossil record. Precambrian Res., 6: 65—100.

Giovannoni, S.J. and Margulis, L., 1981. A red *Beneckea* from Laguna Figueroa, Baja California, Mexico. Microbios, 30: 47—63.

Gong-Collins, E., 1982. Isolation and characterization of a new strain of *Bacillus megaterium* and a new species of *Pseudomonas* isolated from the microbial mats at Laguna Figueroa, Baja California del Norte, Mexico. M. Sc. Thesis, Boston University.

Gong-Collins, E., 1983. A euryhalic, manganese and iron oxidizing *Bacillus megaterium* Strain BC1 isolated from the microbial mats at Laguna Figueroa, Baja California del Norte. Int. J. Syst. Bacteriol., in press.

Gong-Collins, E. and Read, D., 1983. A desiccation resistant, euryhalic new strain of *Arthrobacter simplex* isolated from a laminated microbial mat at Laguna Figueroa, Baja California del Norte, Mexico.

Hayat, M.A., 1970. Principles and techniques of electron microscopy, biological applications. Vol. 1, Van Nostrand Reinhold, NY, 263 pp.

Horodyski, R.J., 1977. *Lyngbya* mats at Laguna Mormona, Baja California, Mexico: comparison with Proterozoic stromatolites. J. Sediment. Petrol., 47: 1305—1320.

Horodyski, R.J. and Vonder Haar, S.J., 1975. Recent calcareous stromatolites from Laguna Mormona (Baja California), Mexico. J. Sediment. Petrol., 45: 894—906.

Horodyski, R.J., Bloesser, B. and Vonder Haar, S., 1977. Laminated algal mats from a coastal lagoon, Laguna Mormona, Baja California del Norte, Mexico. J. Sediment. Petrol., 47: 680—696.

Knoll, A.H. and Golubic, S., 1979. Anatomy and taphonomy of a Precambrian algal stromatolite. Precambrian Res., 10: 115—151.

Knoll, A.H., 1982. Micro-organisms from the late Precambrian Draken Conglomerate, Ny Friesland, Spitzbergen. J. Paleontol., 56: 7755—7790.

Krumbein, W.E., Buchholtz, H., Franke, P., Giani, D., Giele, C. and Wonneberger, K., 1979. Oxygen and hydrogen sulfide co-existence in the sediments. A model for the origin of mineralogical lamination in stromatolites and banded iron formations. Naturwissenschaften, 66: 381—389.

Krumbein, W.E. and Altman, H.J., 1973. A new method for the detection and enumeration of manganese oxidizing and reducing micro-organisms. Helgol. Wiss. Meeresunters, 25: 347—362.

López-Cortés, A., 1982. Aislamento y caracterizacion de una cepa de *Bacillus* de las ecosïstemas microbianas de la Laguna Figueroa Baja California. Tésis de Licenciatura, Facultad de Ciencias, Universidad Nacional Autonoma de Mexico.

Margulis, L., Barghoorn, E.S., Asherdorf, D., Banerjee, S., Chase, D., Francis, S., Giovannoni, S. and Stolz, J., 1980. The microbial community in the layered sediments at Laguna Figueroa, Baja California, Mexico: Does it have Precambrian Analogues? Precambrian Res., 11: 93—123.

Nealson, K.H. and Tebo, B., 1980. Structural features of manganese precipitating bacteria. In: C.P. Ponnamperuma and L. Margulis (Editors), Limits of Life. D. Reidel, Holland, pp. 173—182.

Page, F.C., 1981. A light and electron microscopical study of *Protacanthamoeba caledonica*, n.sp., Type-species of Protacanthamoeba, n.g. (Amoebida, Acanthamoebidae). J. Protozool., 28: 70—78.

Read, L.K., Margulis, L., Stolz, J.F., Obar, R. and Sawyer, T.K., 1983. A new strain of *Paratetramitus jugosus* from Laguna Figueroa, Baja California, Mexico. Biol. Bull., in press.

Rippka, R., Deruelles, J., Waterbury, J.B., Herdman, M. and Stanier, R.Y., 1979. Generic assignments, strain histories and properties of pure cultures of cyanobacteria. J. Gen. Microbiol., 110: 1—61.

Schopf, J.W. and Blacic, J., 1971. New micro-organisms from the Bitter Springs Formation (Late Precambrian) of the North-Central Amadeus Basin, Australia. J. Paleontol., 45: 925—959.

Singh, B.N. and Das, S.R., 1970. Studies on pathogenic and non-pathogenic small free-living amoebae and the bearing of nuclear division on the classification of the Order Amoebidae. Phil. Trans. R. Soc. London, Ser. B, 259: 435—476.

Stanier, R.Y., Douderoff, M. and Adelberg, E.A., 1957. The Microbial World. 1st Edn., Prentice-Hall, Englewood Cliffs, NJ, 550 pp.

Stanier, R.Y., Palleroni, N.J. and Doudoroff, M., 1966. The aerobic pseudomonads: a taxonomic study. J. Gen. Microbiol., 43: 159—271.

Stolz, J.F., 1983a. Fine structure of the stratified microbial community at Laguna Figueroa, Baja California, Mexico. I. Methods of in situ study of the laminated sediments. Precambrian Res., 20: 479—492.

Stolz, J.F., 1983b. Fine structure of the stratified microbial community at Laguna Figueroa, Baja California, Mexico. II. Transmission electron microscopy as a diagnostic tool in studying microbial communities in situ. In: R. Castenholz, H. O. Halvorson and Y. Cohen (Editors), The Woods Hole Microbial Mat Symposium. Alan Liss, New York, 205 pp.

Tousson, T.A. and Nelson, P.E., 1968. A pictorial guide to the identification of *Fusarium* species according to the system of Snyder and Hansen. Penn. State University Press, University Park, PA, 51 pp.

Vidal, G. and Knoll, A.H., 1982. Radiations and extinctions of plankton in the late Proterozoic and Early Cambrian. Nature, 297: 57—60.

Vidal, G. and Knoll, A.H., 1983. Proterozoic plankton. Geol. Soc. Am. Mem., in press.

Zavarzin, G.A., 1981. The genus *Metallogenium.* In: M.P. Starr, H. Stolp, H.G. Trupper, A. Balows and H.G. Schlegel (Editors), The Handbook of Prokaryotes. Springer-Verlag, New York, pp. 524—530.

This Page Intentionally Left Blank

FINE STRUCTURE OF THE STRATIFIED MICROBIAL COMMUNITY AT LAGUNA FIGUEROA, BAJA CALIFORNIA, MEXICO. I. METHODS OF IN SITU STUDY OF THE LAMINATED SEDIMENTS

JOHN F. STOLZ

Boston University, Boston, MA 02215 (U.S.A.)

ABSTRACT

Stolz, J.F., 1983. Fine structure of the stratified microbial community at Laguna Figueroa, Baja California, Mexico. I. Methods of in situ study of the laminated sediments. Precambrian Res., 20: 479—492.

The microbial community of the flat laminated sediments in the hypersaline lagoon at Laguna Figueroa has undergone dramatic changes due to prolonged periods of submergence under fresh water. This paper describes the techniques used in the first comprehensive in situ ultrastructural study of a stratified microbial community formerly dominated by *Microcoleus* sp. and introduces the changes caused by flooding and burial. Flat mat desiccation polygons fixed in 2.5% buffered glutaraldehyde were studied by light and transmission electron microscopy. Typical pre-flood *Microcoleus*-dominated laminated mat from 1977 was compared to post-flood laminated mat from 1979. The technique faithfully preserves the various laminae with their associated organisms and sediment. Morphological identification of several genera of photosynthetic prokaryotes including cyanobacteria, purple, and green bacteria was made by analysis of cell membrane and wall structure. Amoebic cysts could also be recognized in situ. Bacteria of unknown generic affinity, but with distinctive ultrastructure were discovered. A filamentous purple photosynthetic bacterium was found to be a common component of the 1979 mat and two bacteria within a bacterium associations were seen in sections from the 1977 mat.

INTRODUCTION

The stratified microbial mat community in the laminated sediments of Laguna Figueroa, Baja California del Norte, Mexico has been the subject of several studies. The studies have compared these modern laminated sediments to those preserved in the pre-Phanerozoic fossil record (Horodyski et al., 1977; Margulis et al., 1980). Combining field studies and in situ microscopy with enrichment and isolation of microbes, the current research is on those members of the microbial community which form morphologically distinct structures with a high preservation potential, and includes manganese and iron-oxidizing bacteria (Giovannoni and Margulis, 1981;

Margulis et al., 1983, this issue). This study has been complicated by a series of fresh water floods which began in 1978 and have had a dramatic effect upon the mat microbiota. Although the laminae have been preserved, the microbial community has changed from domination by *Microcoleus* sp. and other cyanobacteria to a community dominated by anaerobic photosynthetic bacteria. Most of the organisms preserved in the laminated sediments and stromatolites of the pre-Phanerozoic have been interpreted as cyanobacteria (Knoll and Golubic, 1979; Golubic, 1980; Awramik, 1982). Understanding the complexity of stratified microbial mat communities and the effects of environmental changes (i.e., flooding) on them is necessary for an accurate interpretation of fossil micro-ecosystems.

Core samples, light microscopy, pigment analysis, carborundum marking (for growth rate), analyses of photosynthetic rates, and isolation and culturing of the mat organisms have been the standard techniques used in studies of microbial mats and living stromatolites (Brock, 1976). Recent studies have augmented these by measurements of acidity and oxidation-reduction state using micro-electrodes as well as in situ analysis by scanning electron microscopy (Krumbein et al., 1979). The fact that most laminated microbial mats and stromatolites are sites of calcium carbonate precipitation has hindered the use of transmission electron microscopy. The relatively low content of aragonite, 2—20% by volume (Horodyski et al., 1977), in the microbial mats at Laguna Figueroa make in situ ultrastructural studies possible, revealing details unattainable by light microscopy. Photosynthetic micro-organisms have distinctive ultrastructural characteristics. This is especially true for the photosynthetic membranes of cyanobacteria and anaerobic photosynthetic bacteria (Stanier et al., 1981; Trüper and Pfennig, 1981). Non-photosynthetic prokaryotes can be differentiated by their cell wall structures (Stanier et al., 1976).

This paper presents the techniques used to study the laminated microbial mat by transmission electron microscopy and discusses the changes in the microbial community induced by the flooding. Further discussion of the ultrastructure of the community can be found in Stolz (1983).

FIELD HISTORY

Laguna Figueroa is a lagoonal complex comprised of an evaporite flat, a salt marsh and a barrier dune which separates the flat and salt marsh from the ocean. Detailed descriptions are given in Horodyski and Vonder Haar

---

Fig. 1. The vertically stratified microbial community at Laguna Figueroa, Baja California, Mexico. (A) Desiccation polygons at field site 3 as they appeared in August 1979. (B) A typical cross section of a desiccation polygon as it appeared before the floods (courtesy of S.M. Awramik). Pencil on right side of photo for scale. (C) Light micrograph of the top layer of sediment from 1977 with bundles of *Microcoleus* sp.. (D) Light micrograph of coccoid cyanobacteria from top layer of sediment from 1977. (E) Light micrograph of the second layer of sediment from 1977 with purple photosynthetic bacteria. Bars 10 μm.

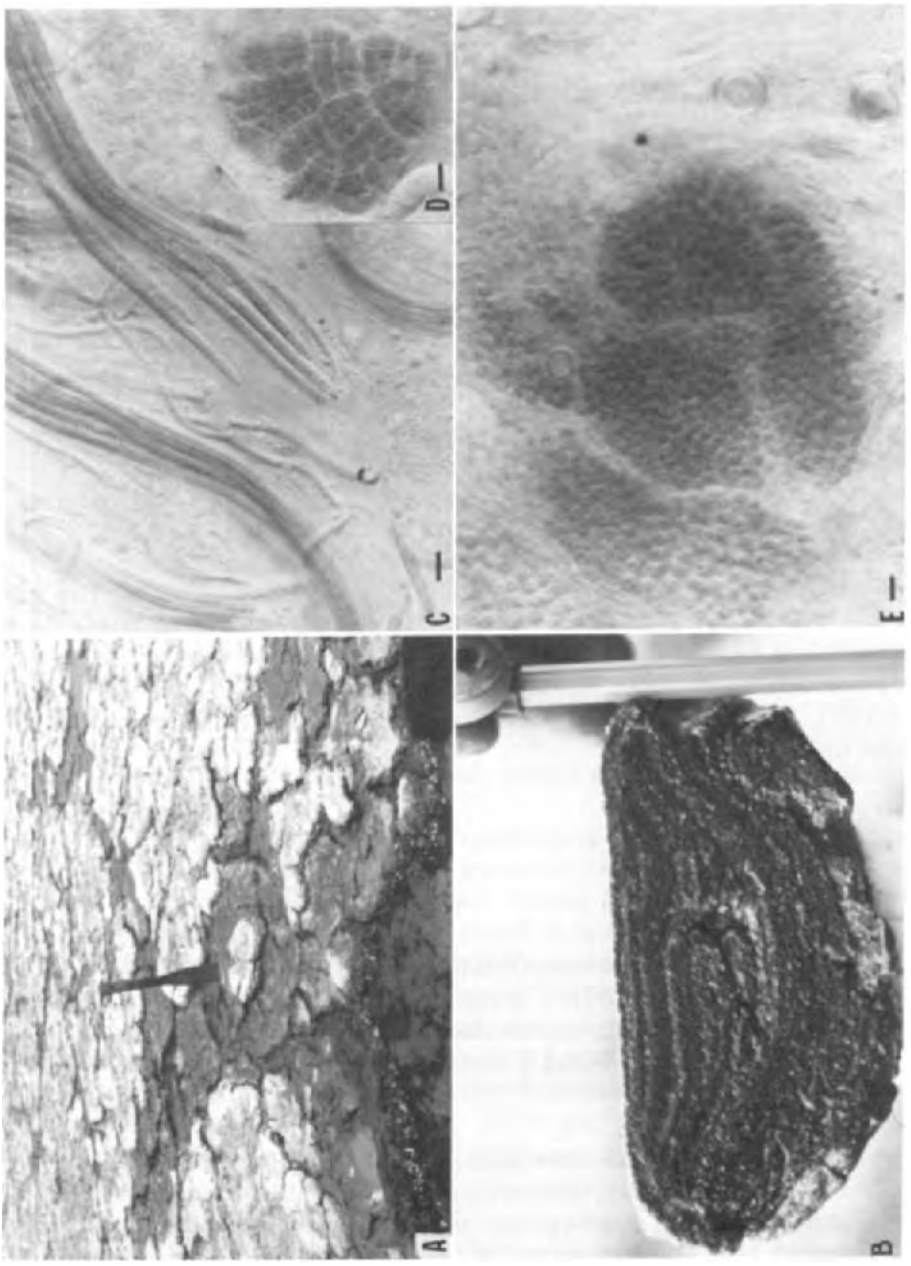
A
B
C
D
E

(1975), Horodyski (1977), Vonder Haar and Gorsline (1977) and Horodyski et al. (1977). Desiccation polygons were found in abundance at the evaporite flat/salt marsh interface (Fig. 1A). Transverse sections of these polygons revealed vertically laminated sediment and its associated microbial community (Fig. 1B). Beneath a thin (0.5—1.0 μm) veneer of sediment, an oxygenic photosynthetic layer dominated by *Microcoleus* sp. and other cyanobacteria was evident (Fig. 1C, D). A conspicuous red layer dominated by anaerobic photosynthetic bacteria lay below the *Microcoleus* layer (Fig. 1E). The re-remaining laminae were occupied by a great number of chemo-autotrophic and heterotrophic organisms and were underlain by odoriferous sulfide-rich mud (Margulis et al., 1980).

Over the course of at least ten years the evaporite flat was observed to be intermittently flooded for short periods of time due to late winter rains and spring high tides (Horodyski et al., 1977; Margulis et al., 1980). The duration of the flooding never exceeded several weeks (Vonder Haar and Gorsline, 1975). A dramatic change in environmental conditions occurred in 1979 and 1980 when the evaporite flat was flooded by an influx of fresh water, submerging the desiccation polygons for months and covering the mats with a thick (1—2.5 cm) layer of terrigenous mud and silt. The heavy rains during the winter of 1978—1979 submerged the mats under 1 m of water from December 1978 until the summer of 1979. The rains during the winter of 1979—1980 covered the mats with 3 m of water from December 1979 until the summer of 1981. Field samples for in situ electron microscopy were taken in August 1977, August 1979, May 1980 and August 1981. The results of the analyses of the 1977 and 1979 mats are discussed in this paper.

MATERIALS AND METHODS

Samples

August 1977

A 1.2 cm thick sample was taken from an emerged polygon at site 3 (Horodyski et al., 1977, p. 683). The top 2 mm formed a distinct blue green layer. The mat was sectioned horizontally into six 2 mm layers, labeled L-1, L-2, L-3, L-4, L-5 and L-6.

August 1979

A 2.6 cm thick sample was taken from a laminated emerged polygon at site 3. The top centimeter contained surface detritus composed of terrigenous clastics, including quartz grains, aragonite, gypsum and anhydrite, and was labeled L-0. The remaining 1.6 cm of well laminated microbial mat was sectioned horizontally into seven layers of different thicknesses: L-1A, 0.1 cm; L-1B, 0.1 cm; L-2, 0.1 cm; L-3, 0.1 cm; L-4, 0.25 cm; L-5, 0.25 cm; L-6, 0.75 cm.

Light microscopy

Light microscopic observations on fresh and fixed samples were made with a Wild dissecting microscope, Nikon Fluorphot with bright field and phase contrast optics, or a Nikon Optiphot with bright field and Nomarski optics to which a 35 mm camera back was mounted. Field material was examined with hand lenses and the Nikon H field microscope.

Transmission electron microscopy

Samples of laminated sediment were fixed with 2.5% glutaraldehyde in a solution devised by D. Chase: 40 ml 0.2 M sodium citrate, 10 ml 25% glutaraldehyde, 50 ml filtered seawater collected at the site and 1.47 g NaCl. The 1977 sample was left in glutaraldehyde and stored at 4°C until January 1982, when the procedure was completed. The 1979 sample was fixed for 2 h, washed and transported to the laboratory in buffer (25 ml distilled water, 25 ml seawater, 0.73 g sodium citrate and 1.175 g NaCl). Samples were washed in fresh sodium citrate buffer and post-fixed in 2% osmium tetroxide in 0.5 M sodium acetate buffer for 1 h. After washing twice in 0.5 M sodium acetate buffer, the sample was stained en bloc with 0.5% uranyl acetate in H_2O overnight. After washing three times in distilled water for a total of 1 h and dehydrated in an ethanol series (50, 70, 90, 95, 100%) the sample was placed in propylene oxide for 20 min (2 × 10 min) followed by a mixture of propylene oxide and Spurr's embedding media (1:1) for 30 min. The samples were then left in Spurr's (Ladd Research Industries Inc.) for 5 h (or overnight), cut into smaller pieces, placed into beam capsules or plastic molds with fresh Spurr's medium and polymerized for 8 h at 70°C.

The block faces were trimmed specifically avoiding clastic and aragonitic material. Thick and thin sections were cut on a Sorvall Porter Blum MT-2 ultra-microtome using 1/4 inch glass knives. Single sections were cut routinely, but serial sections were impossible as the knife edge dulled quickly. After several cuts the sections would fragment, in blocks which contained a great deal of sediment. Parlodian and carbon coated grids were used to salvage these sections. Sections were stained with 1% uranyl acetate (in distilled water) for 20 min followed by 15 min in lead citrate (Hayat, 1970). They were observed on a JEOL 100B transmission electron microscope at 60 kV. Thick sections (200 nm in thickness) were stained with toluidine blue and used for orientation and light microscopic observation (Hayat, 1970).

Whole mount sections

Samples (5 mm^2), fixed in 2.5% glutaraldehyde, post-fixed in 2% osmium tetroxide and stained en bloc, were embedded with Spurr's medium in large

plastic molds. They were then mounted onto microscope slides (75 × 25 mm) with Permount, ground to 300 μm in thickness with a Sears Craftsman verticle mill (Model 527-21411) fitted with a Dremel cutting bit, and hand polished with plastic polishing powder (Carolina Biological Supply). Care was taken in polishing because the powder contained diatomaceous earth which had to be removed before mounting the coverslip.

RESULTS AND DISCUSSION

A diagramatic comparison of the August 1977 and August 1979 mat is shown in Fig. 2. The 1977 mat, as described by Horodyski (1977), was a well laminated microbial community covered by a thin layer of evaporitic minerals (gypsum, anhydrite, halite) and quartz sand. The top 2 mm formed a blue green layer dominated by the cyanobacterium *Microcoleus* sp.. In hand samples of mat, broken perpendicular to the laminae, sheaths and filaments of *Microcoleus* sp. could be seen along the fracture line. The second 2 mm of sediment formed a reddish layer dominated by anaerobic photosynthetic bacteria such as *Chromatium* sp., *Thiocapsa* sp. and *Chloroflexus* sp.. The underlying well-laminated sediment, which was black and highly sulfurous, contained species of anaerobic heterotrophic microbes.

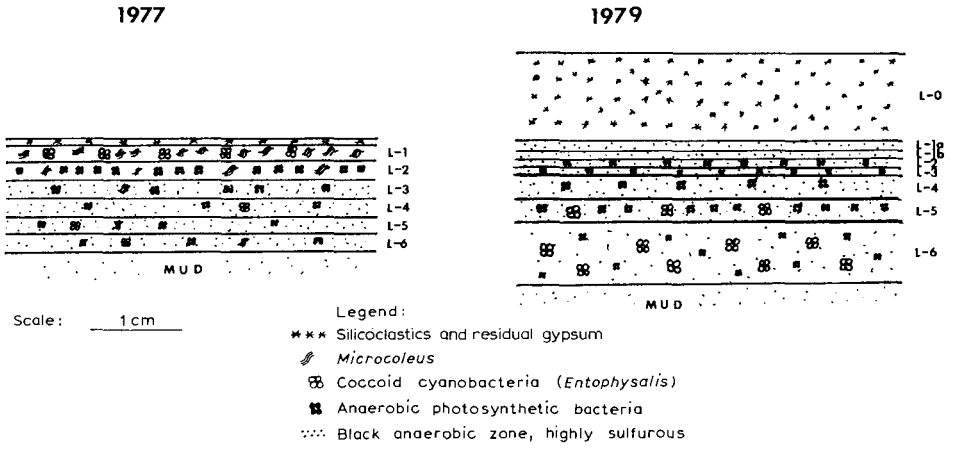

Fig. 2. Comparison of transverse sections of desiccation polygons from August 1977 and August 1979 mat samples.

Fig. 3. In situ sections of microbial mat from 1977. (A) Light micrograph of a bundle of *Microcoleus* sp. from layer 1. Toluidine blue stained section of fixed and embedded material (bar 5 μm). (B) Transmission electron micrograph of *Microcoleus* sp. corresponding to the group in lower left hand corner (arrow) of light micrograph (3A). Note radiating thylakoids (bar 5 μm). (C) Transmission electron micrograph of three different types of photosynthetic prokaryotes from layer 2. (M) = *Microcoleus* sp. (cyanobacterium), (P) = purple bacterium, (G) = *Chloroflexus* sp. (green bacterium), arrow points to chlorosomes (bar 0.5 μm). (D) Transmission electron micrograph of coccoid cyanobacteria (*Pleurocapsalean*) with parietal thylakoids (arrow) (bar 2 μm).

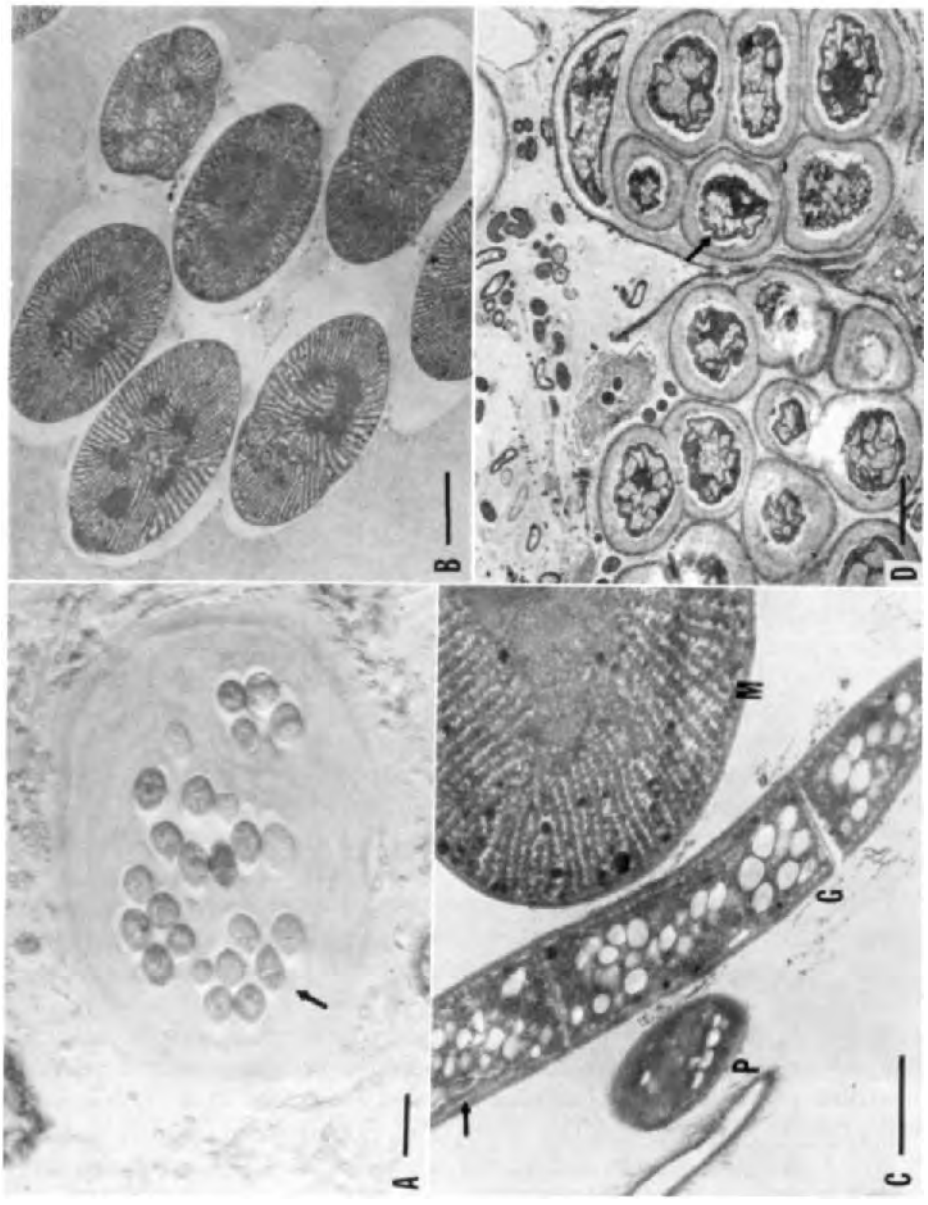
A
B
C
D
M
G
P

The well defined desiccation polygons of the 1979 microbial mat resembled the 1977 mat, but differed in microbial composition. The first distinguishing feature was the top centimeter of silicoclastic sediment. The distinctive blue green layer was entirely replaced by a black layer. Broken mat revealed no filaments. The anaerobic photosynthetic layer was 1.2 cm below the surface because of the increase in surface sediment. If the top centimeter of sediment is discounted, the laminated sediments of both mats are approximately the same thickness (1.5 cm).

Field observations of the stratified sediments in the evaporite flat for 1977 and 1979 showed typical polygons. They were both well laminated sediments with an active microbiota, although the 1979 mat showed signs of degradation. However, in situ light and transmission electron microscopy revealed significant changes in the community. Bundles of *Microcoleus* sp. predominated in the top 2 mm of sediment in the 1977 mat (Fig. 3). The multiple trichomes within a common sheath were easily recognised in thick (Fig. 3A) and thin (Fig. 3B) sections of embedded material. Trichomes of *Microcoleus* sp. were also present in the second 2 mm of mat, but were less abundant, and anaerobic photosynthetic bacterial species such as *Chromatium* sp., *Thiocapsa* sp. and *Chloroflexus* sp. predominated (Fig. 3C). Coccoid cyanobacteria were also common in this layer. Krumbein and Giele (1979) noted that many of the coccoid cyanobacteria identified by Horodyski and Vonder Haar (1975) as a species of *Entophysalis* were probably *Pleuracapsa.* The cyanobacteria in Fig. 3D is a *Pleuracapsa* sp., based on the description of the group given in Waterbury and Stanier (1979).

Light microscopic observations revealed the underlying layers of the mat to be composed of a large variety of heterotrophic bacteria and photosynthetic bacteria in various stages of degradation.

The microbial community in the degrading 1979 mat was dramatically different. Light microscopic analysis of embedded samples prepared as whole mounts and ultrastructural studies revealed a sparsity of microbes within the first 1.2 cm. The top centimeter of sediment was non-laminated and represents a substantial increase in the previously thin veneer of surface sediment. It was devoid of any photosynthetic organisms. Layer L-1A and L-1B, which represents the 2 mm formerly dominated by *Microcoleus* sp., contained only empty sheaths, degraded material, and empty diatom frustules. Analysis of layer 2 (L-2), 1.2 cm below the surface (the layer previously dominated by anaerobic photosynthetic bacteria) showed *Thiocapsa* sp. and *Chromatium* sp. well preserved throughout this layer. The cyanobacteria which were active and abundant in these uppermost layers in the 1977 mat were conspicuously absent in the 1979 material.

Photosynthetic anaerobic bacteria and some small (1—2 μm) cyanobacteria (probably an *Aphanothece* sp.) persisted in layer 3. The first layer in which anaerobic photosynthetic organisms appeared active and abundant was layer 4. Bundles of *Chromatium* sp. and *Thiocapsa* sp. were present with some small filamentous cyanobacteria. Coccoid photosynthetic anaerobic bacteria sur-

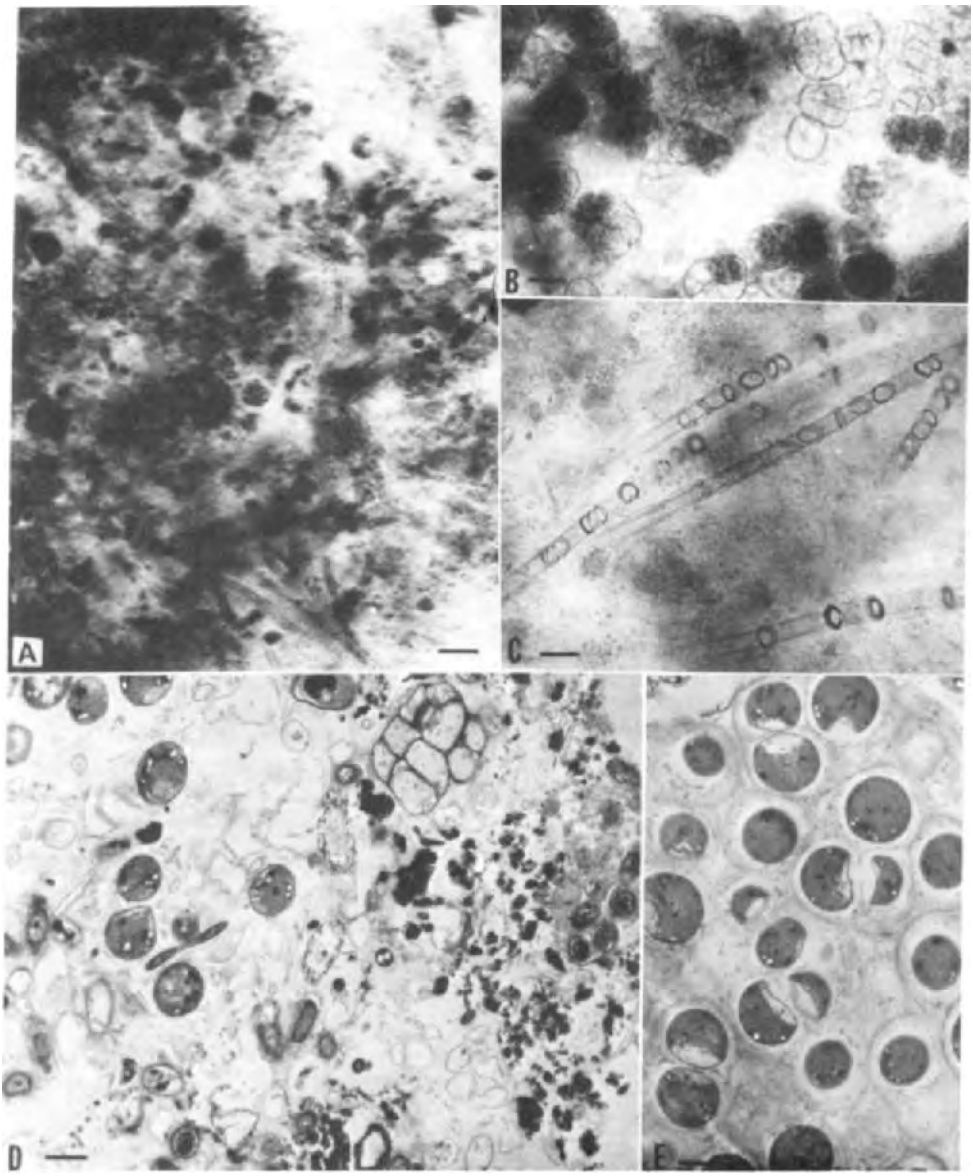

Fig. 4. In situ sections from layer 6 of microbial mat from 1979. Light micrograph of whole mounted section showing empty sheaths of filamentous cyanobacteria and protokerogenous material (bar 20 μm). (B) Light micrograph of the empty sheaths of a coccoid cyanobacteria (*Entophysalis* sp.) (bar 10 μm). (C) Light micrograph of empty sheaths of a filamentous cyanobacteria (bar 10 μm). (D) Transmission electron micrograph showing empty sheaths and degrading purple photosynthetic bacteria (bar 1 μm). (E) Transmission electron micrograph of *Thiocapsa* sp. in various stages of degradation (bar 1 μm).

rounded by thick sheaths and coccoid cyanobacteria within a common sheath (*Entophysalis* sp.) were tightly packed to form layer 5. The *Entophysalis* sp. in layer 5 was in various stages of degradation. The most diverse assemblages of micro-organisms comprised layer 6. Large groups of *Entophysalis* sp., *Thiocapsa* sp., and *Chromatium* sp. predominated in this layer, all in various stages of degradation. The remarkable preservability of sheath material is shown in Fig. 4. Abundant well-preserved, but degrading sheaths were seen in the whole mounted section (Fig. 4A). Large numbers of degraded *Entophysalis* sp. (Fig. 4B) as well as empty sheaths of filamentous cyanobacteria (Fig. 4C) predominated. Purple photosynthetic bacteria could also be recognized in various stages of degradation (Fig. 4D, E).

In situ analysis of the laminated sediments reveals organisms with remarkable ultrastructural features, most of which are indistinguishable at the light microscopy level (Figs. 5, 6). Several filamentous bacteria 0.5 μm in diameter had inclusion bodies that appeared to be smaller bacteria (Fig. 5A, B). An amoebic cyst similar to those isolated from the mat in large quantities (Margulis et al., 1983 this issue) was seen in situ (Fig. 5C). An unidentified rod-shaped bacterium with distinctive cell wall structures at its tip is shown in Fig. 6A and B. The filamentous organisms in Fig. 6C probably represent a new species of purple photosynthetic bacteria.

Although they lack intracellular organelles and membrane bounded nuclei, prokaryotic micro-organisms can be distinguished from each other on the basis of ultrastructure. Differences in cell wall structure, and specialized cell membranes can be recognized by transmission electron microscopy, especially in photosynthetic prokaryotes (Remsen, 1978; Drews et al., 1978). Gram positive and gram negative bacteria which lack specialized internal membranes can nevertheless be differentiated by their cell wall structure. Gram positives have only two layers, an inner cell membrane and an outer peptidoglycan layer, whereas gram negatives have an inner cell membrane and an outer cell membrane separated by a peptidoglycan layer (Stanier et al., 1976). Most cyanobacteria have extensions of the cell membrane differentiated into the photosynthetic membranes, thylakoids, which contain globular proteinaceous units called phycobilisomes (Stanier et al., 1981). The anaerobic photosynthetic bacteria form two groups, the purple and the green bacteria (Stanier et al., 1981).

The purple photosynthetic bacteria possess intracytoplasmic membranes arranged in five possible configurations: vesicles, tubes, bundled tubes, stacks and flat membranes (Trüper and Pfennig, 1981). The green bacteria contain chlorosomes closely apposed to the cell membrane (Pierson and Castenholz, 1978).

Tentative identification of the mat organisms to genus level could be made on the basis of ultrastructural classification. This analysis of the microbial community at Laguna Figueroa, Baja California, Mexico shows that the useful technique of transmission electron microscopy can be applied to in situ studies. A great diversity of micro-organisms undetectable by any

other method is revealed. The numbers and kinds of organisms crucial to the functioning of the microbial ecosystem must be recognized by ultrastructural detail. In situ analysis allows recognition of differential degradation and preservation of members of the community, such as coccoid cyanobacteria. Since most micro-organisms cannot be cultivated in the laboratory, nor are they distinguishable with light microscopy, ultrastructural methods provide the only hope for complete analyses of a community.

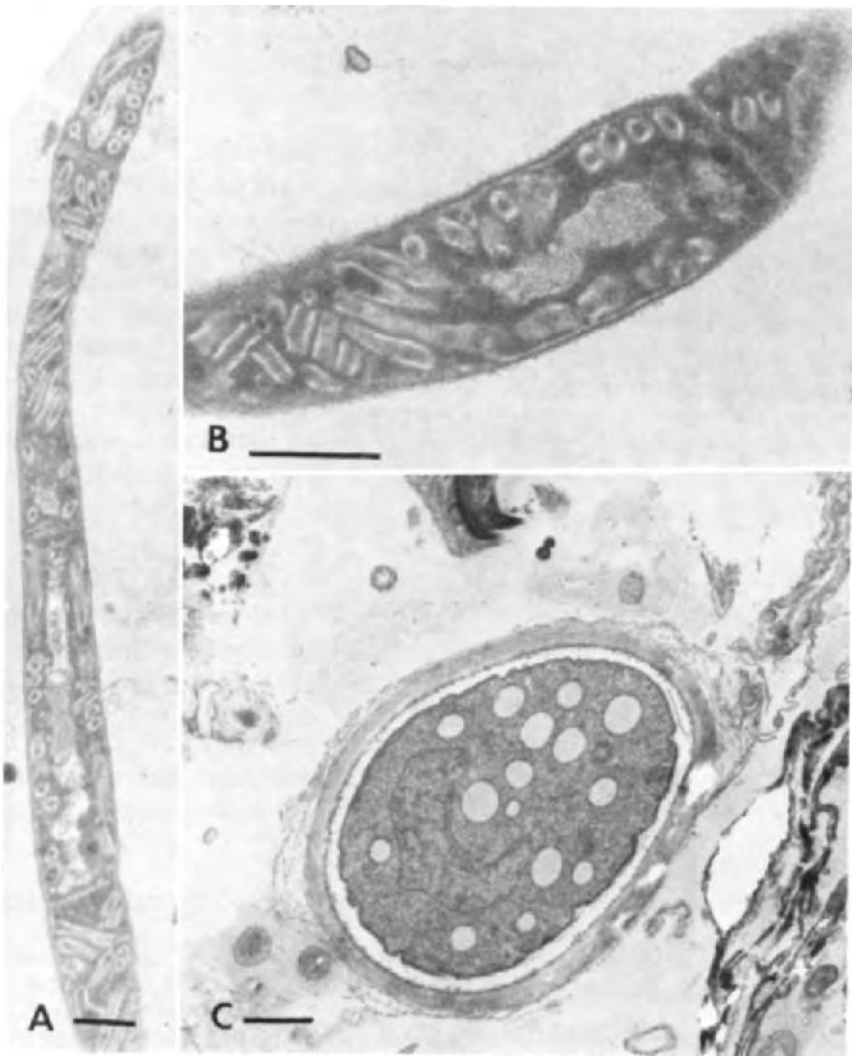

Fig. 5. Transmission electron micrographs of organisms with distinctive ultrastructural characteristics from layer 2 of 1977 microbial mat. (A) and (B) Bacteria within a bacteria association (bar 0.5 μm). (C) Amoebic cyst (bar 0.5 μm).

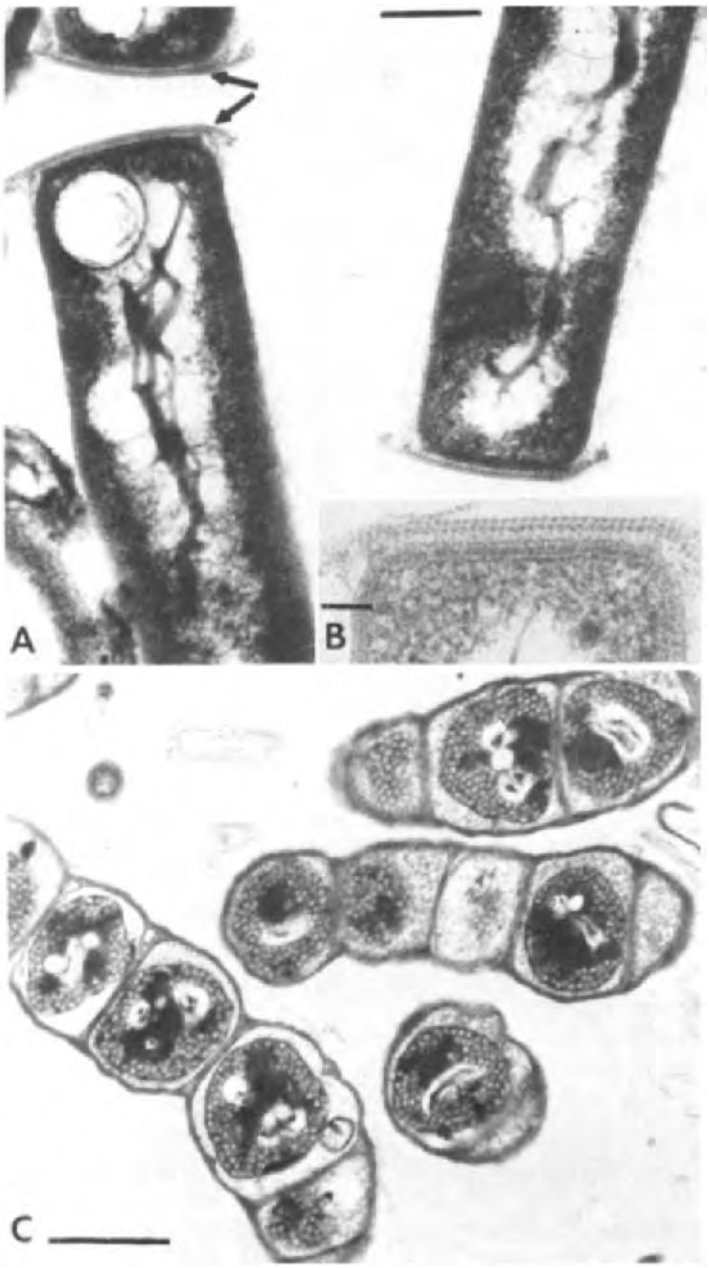

Fig. 6. Transmission electron micrographs of organisms with distinctive ultrastructural characteristics from layer 6 of 1979 microbial mat. (A) Gram negative rod with modified ends (arrows) (bar 0.25 μm). (B) Higher magnification of same type of cell in 6A (bar 0.05 μm). (C) Unidentified filamentous purple photosynthetic bacteria (bar 1 μm).

Furthermore, the flooding of the microbial mats at Laguna Figueroa has provided a unique opportunity to study a microbial ecosystem under stress. Implications for the interpretation of the fossil record are significant. The microbiota of the 850 Ma-old hypersaline lagoon, the Gillen member in Australia, was described as a community with a low microbial diversity (Oehler et al., 1979). The authors attributed this lack of diversity to the harsh environment and the paucity of preservable organisms under these conditions. Understanding the preservability of organisms and structures formed by organisms in the laminated sediments of Laguna Figueroa will provide a better interpretation of fossil microbiotas such as the Gillen member.

CONCLUSIONS

Techniques developed primarily for ultrastructural studies of animal and plant tissue can be applied to stratified microbial communities in laminated sediments. The abundance, complexity and diversity of micro-organisms in the microbial mat of Laguna Figueroa has been explored using these techniques. The major components of the mat community could be identified to genus level. The influx of fresh water and sediment into the hypersaline lagoon was shown to have a dramatic effect on the microbial community. The organism primarily responsible for the trapping and binding of sedimentary particles and establishing the laminated fabric of the sediment, (i.e., *Microcoleus* sp.) disappeared after the storm. If these sediments were preserved during or immediately after a storm, the laminated structure would be preserved with little evidence of the organisms that built them.

ACKNOWLEDGEMENTS

The research reported in this paper was supported by a grant from NASA (NASA 004-025) and the Boston University Graduate School. This work was inspired by the interaction between the faculty and students in the NASA summer program in Planetary Biology and Microbial Ecology, 1980. The author is grateful to L. Margulis, D. Chase, R.C. Fuller, S. Awramik, D. Phillips, F. Craft, B.D.D. Grosovsky and J.T. Albright for valuable comments and assistance in both the work and the preparation of the manuscript for publication.

REFERENCES

Awramik, S.M., 1982. The pre-Phanerozoic fossil record. In: H.D. Holland and M. Schidlowski (Editors), Mineral Deposits and the Evolution of the Biosphere. Springer-Verlag, Berlin, pp. 67—82.

Brock, T.D., 1976. Biological techniques for the study of microbial mats and living stromatolites. In: M.R. Walter (Editor), Stromatolites. Elsevier, Amsterdam, pp. 21—30.

Drews, G., Weckesser, J. and Mayer, H., 1978. Cell envelopes in photosynthetic bacteria. In: R.K. Clayton and W.R. Sistrom (Editors), The Photosynthetic Bacteria. Plenum Press, New York, pp. 61—77.

Giovannoni, S.J. and Margulis, L., 1981. A red Benekea from Laguna Figueroa, Baja California. Microbios, 30: 47—63.

Golubic, S., 1980. Early photosynthetic micro-organisms and environmental evolution. In: R. Holmquist (Editor), COSPAR Life Sciences and Space Research, Pergamon, New York, pp. 101—107.

Hayat, M.A., 1970. Principles and Techniques of Electron Microscopy Biological Applications. Vol. 1, Van Nostrand Reinhold, New York.

Horodyski, R.J., 1977. *Lyngbya* mats at Laguna Mormona, Baja California, Mexico; comparison with Proterozoic stromatolites. J. Sediment. Petrol., 47: 1305—1320.

Horodyski, R.J., Bloesser, B. and Vonder Haar, S.J., 1977. Laminated algal mats from a coastal lagoon, Laguna Mormona, Baja California, Mexico. J. Sediment. Petrol., 47: 680—696.

Ladd Research Industries Inc., Spurr's low viscosity embedding media: information brochure. P.O. Box 901, Burlington, Vermont, 4 pp.

Knoll, A.H. and Golubic, S., 1979. Anatomy and taphonomy of a Precambrian algal stromatolite. Precambrian Res., 10: 115—151.

Krumbein, W.E. and Giele, C., 1979. Calcification in a coccoid cyanobacterium associated with the formation of desert stromatolites. Sedimentology, 26: 593—604.

Krumbein, W.E., Buchholz, H., Franke, P., Giani, D., Giele, C. and Wonneberger, K., 1979. O_2 and H_2S co-existence in stromatolites: a model for the origin of mineralogical lamination in stromatolites and banded iron formations. Naturwissenschaften, 66: 381—389.

Margulis, L., Barghoorn, E.S., Ashendorf, D., Banerjee, S., Chase, D., Francis, S., Giovannoni, S. and Stolz, J., 1980. The microbial community in the layered sediments at Laguna Figueroa, Baja California, Mexico: does it have Precambrian analogues? Precambrian Res., 11: 93—123.

Margulis, L., Grosovsky, B.D.D., Stolz, J.F., Gong-Collins, E.J., Lenk, S., Read, D. and López-Cortés, A., 1983. Distinctive microbial structures and the pre-Phanerozoic fossil record. Precambrian Res., 20: 443—477.

Oehler, D.Z., Oehler, J.H. and Stewart, A.J., 1979. Algal fossils from a late Precambrian hypersaline lagoon. Science, 205: 388—390.

Pierson, B.K. and Castenholz, R.W., 1978. Photosynthetic apparatus and cell membranes of green bacteria. In: R.K. Clayton and W.R. Sistrom (Editors), The Photosynthetic Bacteria. Plenum Press, New York, pp. 179—197.

Remsen, C.C., 1978. Comparative subcellular architecture of photosynthetic bacteria. In: R.K. Clayton and W.R. Sistrom (Editors), The Photosynthetic Bacteria. Plenum Press, New York, pp. 31—60.

Stanier, R.Y., Adelberg, F.A. and Ingraham, J., 1976. Microbial World. 4th Edn., Prentice Hall, Englewoods Cliffs, New Jersey.

Stanier, R.Y., Pfennig, N. and Trüper, H.G., 1981. Introduction to the photosynthetic prokaryotes. In: M.P. Starr, H. Stolp, H.G. Trüper, A. Balows and H.G. Schlegel (Editors), The Prokaryotes, A Handbook on the Habitats, Isolation and Identification of Bacteria. Springer Verlag, Berlin, pp. 197—211.

Stolz, J.F., 1983b. Fine structure of the stratified microbial community at Laguna Figueroa, Baja California, Mexico. II. Transmission electron microscopy as a diagnostic tool in studying microbial communities in situ. In: R. Castenholz, H.O. Halvorson and Y. Cohen (Editors), The Woods Hole Microbial Mat Symposium. Alan Liss, New York, 205 pp.

Trüper, H.G. and Pfennig, N., 1981. Characterization and identification of anoxygenic phototrophic bacteria. In: M.P. Starr, H. Stolp, H.G. Trüper, A. Balows and H.G. Schlegel (Editors), The Prokaryotes, A Handbook on the Habitats, Isolation and Identification of Bacteria. Springer Verlag, Berlin, pp. 299—312.

Vonder Haar, S.P. and Gorsline, D.S., 1975. Flooding frequency of hypersaline coastal environments using orbital imagery, geological implications. Science, 190: 147—149.

Vonder Haar, S.P. and Gorsline, D.S., 1977. Hypersaline lagoon deposits and processes in Baja California, Mexico. Geosci. Man, 18: 165—177.

Waterbury, J.B. and Stanier, R.Y., 1978. Patterns of growth and development in *Pleurocapsalean* cyanobacteria. Microbiol. Rev., 42: 2—44.

STROMATOLITES – THE CHALLENGE OF A TERM IN SPACE AND TIME

W.E. KRUMBEIN

Geomicrobiology Division, University of Oldenburg, P.O. Box 2503, D-2900 Oldenburg (W. Germany)

ABSTRACT

Krumbein, W.E., 1983. Stromatolites — the challenge of a term in space and time. Precambrian Res., 20: 493–531.

Several definitions of stromatolites are discussed and Kalkowsky's most important statements about stromatolites are translated from German to English. A new definition for stromatolites is proposed, namely "Stromatolites are laminated rocks, the origin of which can clearly be related to the activity of microbial communities, which by their morphology, physiology and arrangement in space and time interact with the physical and chemical environment to produce a laminated pattern which is retained in the final rock structure". Unconsolidated laminated systems, clearly related to the activity of microbial communities and often called "recent stromatolites" or "living stromatolites", are defined as "potential stromatolites".

The main microbial activities which are important in the formation of potential stromatolites and stromatolites are described and examples of stromatolites of various types, including iron stromatolites, are also described.

INTRODUCTION

There are four good reasons to discuss ancient and "recent stromatolites" in "Precambrian Research". (1) The term itself has been applied to many different structures and has found many different interpretations. (2) Knowledge of fossil and recent biogenic laminated structures has increased. (3) Our view of the evolutionary significance of stromatolites is now more definitive and (4) views on the evolution of the physiology and the ecology of stromatolite forming micro-organisms have also changed considerably.

It is, however, inappropriate to use the term "recent stromatolite" for structures that are not "rock structures" or lithified (cemented) structures. Unconsolidated rocks or sedimentary structures cannot be regarded as stromatolites, but, perhaps, as unconsolidated stromatolites. If the term "living stromatolite" (Brock, 1976) is considered, then the conclusion may be drawn that rocks are alive. Continuing this play on words, the terms "fossil" and "recent algal mat" may also be considered. By definition, algae

are eukaryotic photosynthetic organisms, which rarely if ever form mats or laminated deposits. The term blue-green algae was replaced by the more appropriate term cyanobacteria or blue-green bacteria. Good reasons for using such terms were already known 110 years ago (Cohn, 1872; Krumbein, 1979b; Rippka et al., 1979; Starr et al., 1981). Cyanobacteria, in contrast to algae, are able to survive and thrive under a wide range of different environmental conditions and, consequently, interpretations of algal rocks must differ from those of cyanobacterial rocks.

"Extant stromatolite-building cyanophytes" are known (Golubic, 1976), and there are abiogenic "stromatolite-like structures" (Walter, 1976b) which have also been called "geyserites", "speleothems" or "calcretes" (Read, 1976; Walter, 1976b; Thrailkill, 1976). Alternatively, some laminated calcretes and speleothems have been shown to form biologically, sometimes also via cyanobacteria activity (Kretzschmar, 1982; Krumbein and Lange-Giele, 1979; Danielli and Edington, 1983). Thus lithoclasts, speleothems, manganese nodules, calcretes, even silcretes and rock varnishes or ironstones are placed by some authors, into the "non-living" and by others into the "extant", i.e. really "living stromatolite" group. Monty (1977) summarized the state of the art for the period between 1960 and 1970 as follows: "stromatolites were regarded as (1) intertidal algal mats that (2) trap and bind carbonates and that (3) the laminated structure of stromatolites is governed, however, by inorganic environmental factors." However, the latest publications (Walter, 1976; Flügel, 1977; Krumbein, 1978; Awramik, 1981; Monty, 1981; Holland and Schidlowski, 1982) have taken, more or less, the opposite point of view, namely, that the lamination pattern of stromatolites is biologically produced.

From these rather randomly selected remarks on stromatolites and the organisms or "processes" that produce them, it seems logical (1) to go back (75 years) to the original definition of stromatolites by Kalkowsky (1908) and (2) to look at recent environments, where potential stromatolites are forming and (3) to try to understand what kind of organisms and events govern the formation of laminated rock structures, called stromatolites.

It is the aim of this paper to analyse the different uses of the term stromatolite. I will (1) present several different definitions given in the literature; (2) redefine stromatolites according to present day knowledge of such structures and in relation to former definitions and (3) define the communities, and arrangement and ecology of communities, that may form stromatolitic structures.

DEFINITIONS

Stromatolites

According to Plato, the paradox of all search for a definition is that we already know what we are seeking to define. The paradox cannot be solved by restating that we already perceive, what we want to conceive, for the con-

ception is apriori. The use of the term stromatolite for many laminated rocks and especially for those from the Precambrian, rests on the unconscious recognition of those common qualities which are to be expressed in the definition. In defining, the object is to clarify and organise a precedent for knowledge that is obscure, confused and inarticulate. Kalkowsky (1908) says that stromatolites are made by micro-organisms. Others (Bricker, 1971) have pointed out for carbonate cementation in general, that "occult micro-organisms may be the villains explaining a lot in the variability of beachrock cements". In the case of biogenic beachrock cements, Krumbein (1979a), however, tried to drag the villains into the light of day. In the case of stromatolites this may be dangerous, because many geologists believe, that the light of day, i.e., photosynthetic CO_2 uptake, makes most of the stromatolitic carbonates. In reality, the chemo-organotrophic bacteria involved in carbonate precipitation in laminated "stromatolitic beachrocks" as well as in "carbonate stromatolites" are "the villains" which avoid the light of day and produce carbonates in the dark, via degradation of organic matter previously produced by bacterial photosynthesis (Krumbein, 1979a). Others escape the truth by being obscure and talking about abiogenic and biogenic stromatolites.

Hence, consistency of perception makes the process of defining easy, but the absence of such conditions for stromatolites presents practical difficulties. In the absence of a homogenous group, no common quality exists. Therefore, it can be assumed that "Precambrian stromatolites" are difficult to define, the main difficulty being that no logical way has yet been found for defining the ideal system(s) for producing stromatolites.

The expressions "more stromatolitic" and "less stromatolitic" are often used (Walter, 1976a). It seems, however, better to ask: Is the structure in question stromatolitic? rather than how stromatolitic is it? It is certainly possible to say about laminated rocks of the Precambrian, that they might be stromatolites. It is, however, impossible to deduce a biological origin from the fact that some authors call Precambrian laminites stromatolites.

The problem of a deductive definition for stromatolites is the disagreement concerning the denotation of the term, which is derived from subjective perception or choice of descriptive data. Which aspect, then, focusses interest? The lamination? The origin of lamination? The rarity of the specimen, the name of the describer, his reputation or the place of publication? Finally, is there only one stromatolite definition or are there several? These words of introduction are clarified by citing several "classical" definitions.

Let me start with the translation of the most prominent and meaningful passages of the first publication in which the term stromatolite was used. Kalkowsky (1908) studied lower Triassic "Buntsandstein deposits" of the Harz area, a region close to the shores of the former Permian Zechstein evaporite sea.

Kalkowsky in his classic paper discusses stromatolites and stromatolite associated oolites in the following way:

"The name stromatolite shall designate (define) masses of limestone, which possess a fine, more or less, planar lamination in contrast to the concentric lamination of oolite grains. ..."

"Oolites and stromatolites of the North German Buntsandstein are produced by plants; from the very beginning of my description I will have to use terms related to organisms. The mineral composition of the rocks has to be considered, however, as well as in any limestone produced with the aid of plants or animals. The intimate combination of phenomena of the organic world with those of the inorganic, which gives its peculiar character to many fields of geology certainly has to be considered in this case. ..."

"In general use the — properly speaking silly — term oolite designates the rock as a whole, while ooid is used for the single grains of rocks with these typically spherical grains. The single grain is named ooid from similar to an egg. ... In both cases the primary structure of the oolite, as well as of the stromatolite, is visible in thin sections by the size of the carbonate particles, as well as by the form and arrangement of allochthonous materials, i.e. sand grains and clay dusts. In no place, however, can one see organic structures comparable to those of other zoogenic or phytogenic limestones."

"The organic creators of oolites and stromatolites have been so small, that only the structure of their aggregates is preserved. ..."

"Stromatolites, basically, are remarkable for their macroscopic structure. The structure of calcareous stromatolites is characterized basically by less important allochthonous compounds and ooids. The most important structural units are more or less planar layers of carbonate, which built the stromatolitic rock or stromatolite. The stromatolite generally lacks the clearly defined all embracing structure of the ooid. In analogy to ooid and oolite, however, the individual layers of carbonate could be named stromatoid inasmuch they can be related in a similar way to the organic producer as the individual grain of an oolite. The two types of organisms may even be related to each other inasmuch we can see a gradual relationship between ooid, polyooid, ooid-bag and stromatoid. Following the sequence ooid, polyooid, ooid-bag and stromatoid we can state that the product always consists of thin layers, which are less and less related to a centerpoint of formation (concentric—to convex—to planar)."

In the following passages, Kalkowsky describes the intimate relations between oolitic parts of the Buntsandstein and stromatolitic ones, and states that both have been formed in situ. These findings have been stated recently for the Solar Lake microbial mats which include stromatoids as well as ooids and ooid bags (Friedman et al., 1973; Krumbein et al., 1977; Krumbein and Cohen, 1974, 1977). Kalkowsky continues:

"All stromatolites in vertical section expose a typical layered pattern, macroscopically visible especially in weathered surfaces. The individual stromatoid layers are composed of very thin threads, which often have the tendency of radial composition. The layers are not totally planar, the fibrous structure is not always visible. After decalcification the laminae of sand and clay clearly mirror the original layered structure. The stromatolite as a whole is relatively poor in allochthonous particles, of which only few were encoated during growth, similar to the thin layers of allochthonous material in ooids.

There is a general tendency of accretion of sand and clay on specific spots, contributing to the finely undulated structure of the stromatoid. ..."

"In comparing the structure of the ooids with the stromatoids one comes to the conclusion that the stromatoid structure in general is coarser. It is perhaps justified to conclude that the organisms forming the stromatoid were bigger than those forming the ooid."

From more recent literature it is derived that organic macromolecules and (small) chemo-organotrophic bacteria are creating the ooids while (relatively larger) cyanobacteria or fungi are often forming the stromatoids (Grosovsky et al., 1983; Krumbein and Cohen, 1974; Krumbein et al., 1977; Krumbein, 1974, 1979a).

Thus, it has been established that Kalkowsky's "feeling" was more or less justified for certain classes of oolites and stromatolites (see also Young, 1981). Kalkowsky continues:

"Stromatoids in contrast to ooids always show upwards directed unidirectional growth. It can always be discerned, in which direction the stromatoid was growing. The stromatolite, thus, is a limestone grown in situ. Its essential component is the stromatoid, whose single layer can extend very far and bind very tightly whatever foreign components are added. ..."

"The stromatoid grows upwards in more or less planar layers with a general tendency towards upwards convex forms. From this pattern the multiple structures of most stromatolites can be derived.
This multiple structure, derived from the tendency of building into upwards convex layers, may vary so much that one is tempted in the beginning to distinguish several classes of stromatolites. The more examples of stromatolites one sees, the more, however, one comes to the conclusion that all stromatolites are nothing but differences in the habitus of one and the same principle organism, and that the differences in habitus are basically caused by external influences (not by different species or organisms)."

"Analysing the structure of stromatolites one also has to consider interruptions of the layering by more or less vertically oriented parts. These shall be named interstices. The interstices correspond somehow to the inter-radial structures of the ooids. They differ from the latter since they contain little or no carbonate. The interstices are layers of clay, sand, small ooids or embryonal ooids. Additionally, one sees small amounts of carbonate cement, which may be derived or mobilised from the ooids or from the adjacent stromatoids. Interbedding with stromatoids layers of ooids may also occur within a stromatolite. Besides the ooid participation in the interlayers, these are mostly poor in carbonate and, thus, weather faster than the stromatoid itself. Completely planar layers of stromatoids are very rare and of small horizontal extension. Even within planar layers wavy structures are observed. From this wavy layering the layers above evolve small convex hummocks of a few mm width. Layers above these small hummocks may equalize again. Real interstices occur only when the hummocks get larger. When they reach 20—25 mm width, it is possible that a generally plain stromatolite is inter-

rupted by tubular interstices, towards which the individual stromatoid turns down. These interstices are not continuous, they may be interrupted by overgrowth by new stromatoids, which divide then at other places to form new interstices. The combination of waviness of the individual layer or stromatoid with the interstices leads to the multitude of domal branching and cauliflower type structures. ..."

"*Genesis*

The preferential explanation of the formation of ooids in agitated water fails completely under these conditions of interbedding of ooids with stromatoids in a stromatolite. Bacterial colonies grown in agar look similar to the ooids. If one cultivates bacteria in a beaker in gelatine they take completely bead shaped structures. That Sphaerocodium is nothing else than bacteriogenic ooids which were bored by blue-green algae will be demonstrated at another place."

Kalkowsky describes here, very carefully, the in situ genesis of ooids by bacterially degrading (putative) precipitation of carbonates and subsequent boring by blue-green bacteria (Bathurst, 1971; Krumbein, 1974; Krumbein and Cohen, 1974; Krumbein, 1979a) and says, he will later explain this phenomenon in more detail. However, he never came back to this observation in his scientific work. He finishes:

"If somebody insists on the inorganic genesis of ooids, (like Campbell, 1982; insert of translator) he will, however, never find a good explanation for the ooid-bags, i.e. aggregates of ooids embedded in a common mucous sheath. These bags of ooids often form the initiating stage of thin or rather thick stromatolites. (We found these bags to be often derived from decay of slime embedded coccoid cyanobacteria within microbial laminated mats, e.g., Krumbein and Cohen (1974). The convex growth of stromatolites, their tendency to diverge into branches or individual hives with convex apexes and marginally widening leaves, all these are characteristics which indicate the struggle (Streben) for light and nutrients expressed by Oskar Schmidt. We have to assume in conclusion that lowest plant type organisms must have created the stromatolites. One might think of recent plant species, that form cushions. I will not cite literature here. Here it was only my task to demonstrate that ooids and stromatolites of the Lower Triassic of North Germany ascribe themselves an organic origin."

I have translated the major statements and findings of Kalkowsky in order to demonstrate that his original definition was restricted to calcareous stromatolites, which are closely connected to ooids and oolitic parts of the same rock. He calls ooids the individual grain and oolite the rock composed of ooids. He names stromatoid the individual layer of a stromatolite, interstice the inorganic parts between stromatoids and stromatolite branches, and stromatolite the final rock structure composed of many individual stromatoids and often stromatolite branches. Also, oncoid and oncolite should be used in the same way (Heim, 1916; Pia, 1926, 1928; Gary et al., 1972). Un-

fortunately, in English oncoid and oncolite, ooid and oolite, as well as stromatoid and stromatolite are not always used in this way (Buick et al., 1981; Flügel, 1982).

Furthermore, Kalkowsky states that "stromatolites are organogenic, laminated, calcareous rock structures, the origin of which is clearly related to microscopic life, which in itself must not be fossilised."

It was initially intended to add a few photographs of Kalkowsky's material. However, J. Paul and T. Peryt (personal communication) plan a detailed re-examination of the outcrops and of Kalkowsky's material which is to be published in due course (see also Paul, 1982).

Thus, Kalkowsky (1908) has described stromatolites with great care and insight. He has also clearly described the phenomenon of in situ formation of ooids as part of a stromatolite system. He probably never knew that exactly this type of microbial mat, made up of a large variety of micro-organisms, exists in the Solar Lake and the Ras Muhammed Pool (Sinai) and in the benthic microbial mats of Lake Hoare in Antarctica (Krumbein and Cohen, 1974; Krumbein et al., 1977; Young, 1981; Parker and Simmons, 1981). The similarity between these two recent types of microbial mats is that they form stromatoids (carbonate flakes) interbedded with allochthonous material layers and autochthonous biogenic ooids, and some oncoids. Also gradual lateral developments can be observed, where oncolites (microbial biscuits) merge into flat stromatolites (Krumbein, unpublished data). So much for Kalkowsky (1908).

Walter (1976a, p. 1) gives a genetic rather than descriptive definition of stromatolites, which has been widely used since that time. This definition is in my opinion no more "genetic" than Kalkowsky's and, also, does not embrace all aspects of microbially produced laminites.

"Stromatolites are organosedimentary structures produced by sediment trapping, binding, and/or precipitation as a result of the growth and metabolic activity of micro-organisms, principally cyanophytes."

The definition is perhaps too brief and this may lead to confusion. The term stromatolite clearly names a rock, i.e., a consolidated (cemented) structure. The term cyanophyte is misleading and has been replaced by cyanobacteria. Organosedimentary does not specifically imply the microbial origin. The widely used "Glossary of Geology" gives another less genetic and, somehow, more confusing all-embracing definition (Gary et al., 1972):

"Stromatolites are variously shaped (often domal), laminated, calcareous sedimentary structures formed in a shallow water environment under the influence of a mat or assemblage of sediment-binding blue-green alga that trap fine (silty) detritus and precipitate calcium carbonate, and commonly develop colonies or irregular accumulations of a constant shape, but with little or no microstructure. They have various gross forms, from nearly horizontal to markedly convex, columnar and subspherical. Stromatolites were originally regarded as animal fossils, and although they are still regarded as "fossils" because they are the result of organic growth, they are not fossils

of any specific organism, but consist of associations of different genera and species of organisms that can no longer be recognized and named, or that are without organic structures. "The various generic names given to these structures are apparently invalid since the names apply only to various forms assumed by the accumulated entrapped sediment and may not be directly related to specific organisms" (Pettijohn, 1957, p. 221)." The reference refers only to the part of the definition given in quotation marks.

Friedman and Sanders (1978) describe stromatolites as follows:

"Stromatolites are laminated lithified deposits consisting of alternating layers of material formed by micro-organisms, usually algae, and of extraneous particles that have been cemented. The material formed by micro-organisms may consist of soft organic matter, or its fossil analogue, or of thin layers of precipitated carbonate material. The extraneous particles may consist of anything, but among these, fine grained carbonate particles typically predominate."

During the reviewing procedure of this article, Buick et al. (1981) have published an excellent paper which regards stromatolites in almost the same way as I wish them to be regarded, except for the recent microbially influenced systems and some special cases of stromatolites. They also find a lot of abuse in the currently proposed mixed genetic—morphological definition of stromatolites. This abuse is clearly recognized in statements like: "If the proposed new definition of Krumbein (e.g., Krumbein, 1982) were to be strictly followed, many if not most Proterozoic "stromatolites" and virtually all Archean "stromatolites" would not fall under his definition of a stromatolite". Buick et al. (1981) repeat exactly my introductory remarks on definitions derived from Plato, i.e., they state that geologists use the term stromatolite in the field in a morphological sense and then: "often these structures are subsequently assumed to be biogenic, because a name that asserts biogenicity has already been applied to them or no evidence for or against biogenicity can be found." This results in many inorganic structures being wrongly called biogenic. Buick et al. (1981) propose the use of two terms, i.e. stromatolites for really biogenic structures and stromatoloid (Oehler, 1972) for structures that are morphologically similar to stromatolites, but of uncertain origin. Furthermore, I propose to use a third term for structures that are not stromatolites yet, but may become stromatolites in the process of diagenesis. Buick et al. (1981) excellently summarize the criteria for the recognition of stromatolites in ancient rocks. These differ only slightly from the criteria proposed here, especially as far as recent structures which may become stromatolites are concerned.

From the above definitions and from many detailed descriptions of fossil and recent examples it is concluded that the present day definition of stromatolites should not be restricted to the microbial mat type of "potential stromatolites" of Solar Lake, Sinai, and Lake Hoare, Antarctica, or Shark Bay, Australia, (i.e., carbonate stromatolites) but should also apply to many other biogenic laminated structures and rock structures. Kalkowsky's defini-

tion only needs to be revised in this respect. Several features of stromatolites and recent microbial laminated systems which should be considered in defining stromatolites are summarized below.

(1) Stromatolites are alternatingly or evenly laminated consolidated rocks.

(2) Their lamination is related to the activity of micro-organisms.

(3) The intracellular and extracellular products of the micro-organisms as well as their physiology contribute to the final structure, e.g., by trapping, binding or precipitation of minerals and mineral grains.

(4) The micro-organisms associated with the laminated structure may or may not be fossilized.

(5) The environment of formation must be suitable for the growth of micro-organisms (temperature, pressure, light etc.).

(6) The micro-organisms do not produce the bulk of the stromatolite, but they produce or influence its lamination and some of its chemical characteristics.

(7) In a sedimentary stromatolitic environment the rate of inorganic sedimentation must allow the formation of a substantial microbial community.

(8) The microbial community or its products must accrete faster or more efficiently than they are destroyed by destructive forces, such as boring and burrowing organisms, or physical and chemical forces.

(9) Photosynthetic microbial communities may or may not be involved in the formation of stromatolitic structures.

(10) The organisms involved in stromatolite formation should be of microscopic scale. Otherwise their product could be included, as a special case, into the group of bioherms or biostromes or reefs, which is actually done by some authors.

With regard to these characteristics of stromatolites and recent stromatolitic environments it becomes clear that a broader approach than Kalkowsky's, and also a more precise and broader approach than Walter's (1976a) is needed in order to define stromatolites. Also more detail information is needed in order to distinguish stromatolites from inorganically produced laminites (e.g., Flügel, 1982, limonite laminites), or rhythmites.

The new definition proposed here is based on several previous definitions, and the exchange of ideas, views and information among biologists, chemists, geochemists, geologists and paleontologists.

I suggest:

Stromatolites are laminated rocks, the origin of which can clearly be related to the activity of microbial communities, which by their morphology, physiology, and arrangement in space and time interact with the physical and chemical environment to produce a laminated pattern which is retained in the final rock structure.

In addition:

Unconsolidated laminated systems, clearly related to the activity of microbial communities, often called "recent stromatolites" or "living stromatolites" are defined as "potential stromatolites".

This definition is basically similar to that given by Kalkowsky (1908). However, it needs some careful consideration and in the following paragraphs I discuss in more detail some aspects and terms used in previous works and in my definition.

Laminated. In sedimentological terms, stratified rocks have layers, which are called beds when the individual strata are thick, and laminae when they are thin. Still bed and laminae are relative terms. In potential stromatolites I have found laminae ranging from 50 μm to a maximum of 4 cm. With reference to this I cite Ingram (1954) who defines the borderline between laminae and beds as 1 cm, and Campbell (1967) who extends very thick laminae to a maximum of 15 cm, whereas very thin beds may have only 1—3 cm thickness.

Clearly related. If no microfossil is found in laminated rock structures, it must be established by other analytical means or indication that the lamination of the rock in question is derived, at least in part, from biological activities. Even the presence of organic compounds alone is not sufficient (e.g., Freund et al., 1982).

Microbial community is preferred to terms such as algal mat or microbial mat, because the aspect of formation by micro-organisms has to be included without any prejudice as to whether one or more microbial communities make up the ecosystems, whether or not they were originally laminated, photosynthetic, benthic, or formed mats. I exclude the term "principally prokaryotic" organisms suggested by Buick et al. (1981), because fungi are also micro-organisms, build stromatolites (e.g., Kretzschmar, 1982) and are eukaryotic in nature. All the latter systems may, however, be associated with the production of ultimate stromatolitic structures by geodynamic accumulation of individual laminae.

Photosynthetic and algae. These terms are deliberately excluded from the general definition, since neither photosynthesis nor algae are needed for the formation of stromatolites, although many stromatolites are in fact produced via photosynthetic activity of cyanobacteria in association with other phototrophic bacterial communities, which form microbial mats or laminated microbial mats (e.g., Kretzschmar, 1982; Grosovsky et al., 1983).

Macro-organisms are excluded from the definition as possible contributors to the formation of stromatolites, although many macro-organisms occur within recent and fossil Phanerozoic laminated microbial systems and their fossil remainders. The dominant organisms imposing the structure, however, are definitely micro-organisms. Laminated products of macro-organisms, however, (e.g., the laminated products of *Placunopsis ostracina* which have laminae of 0.4—1.5 mm thickness and form stratiform, domal and cauliflower shaped branched systems in the Middle Triassic of south-west Germany (Fig. 1)) are usually called bioherms (when mound-shaped), biostromes (when laminar) or (when rigid and wave resisting) reefs (e.g., Krumbein, 1963). On the other hand stromatolites may also be regarded as skeletal or non-skeletal microbial bioherms, biostromes or even reefs. This concept of microbial bioherms or reefs has never gained wide acceptance, apparently because the reef-building

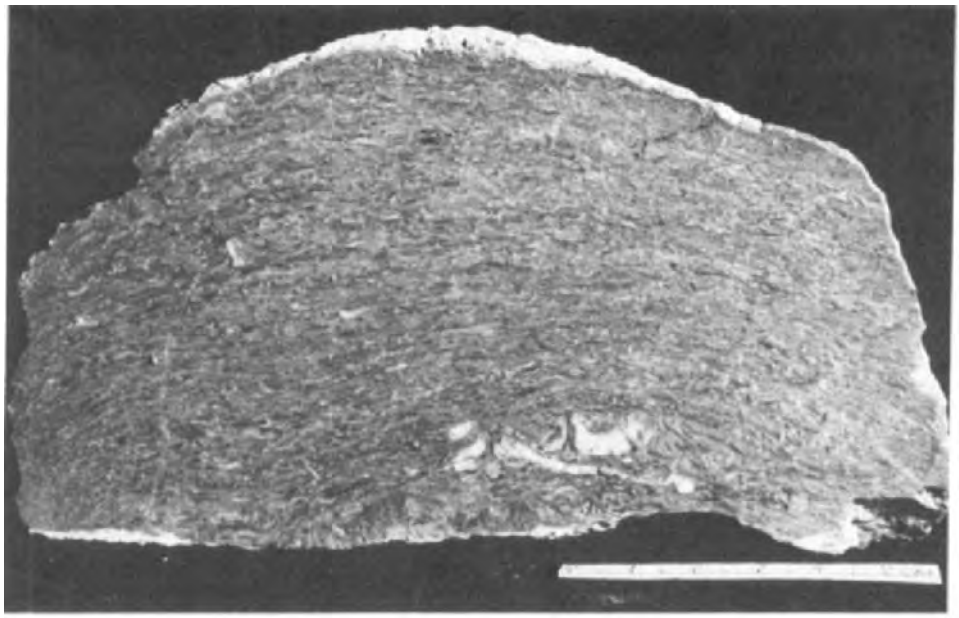

Fig. 1. Finely laminated dome shaped carbonate rock with detrital interstices. Cauliflower type branched and stromate structures occur also in the same environment. The lamination is on the 0.5 mm scale. The organism is *"Placunopsis ostracina"* of the German Triassic. Only two features differentiate this structure from stromatolite definitions, i.e., (1) macro-organisms, not micro-organisms have produced the laminated biogenic rock structure and (2) *Placunopsis* forms skeletal carbonates, a feature sometimes used to exclude structures from the term stromatolite. However, skeletal structures are sometimes included (Riding, 1977).

organisms are so minute that it did not seem worthwhile to include them into the general picture and definitions of bioherm, biostrome and reef. However, Eggleston and Dean (1976) have used the term "stromatolite bioherms" for domal recent stromatolites of Green Lake, New York and other locations. *The physiology (and metabolic activity)* of the microbial community directs the growth and motility of individual structures as well as of the whole community (e.g., pinnacle motility or upwards migration of a mat through a new thin sediment layer), thus sometimes defining the spacing and the production of individual laminae. In addition, physiology and metabolism also produce the physical (e.g., slime production and trapping of particles) and chemical changes in the environment which cause the lamination (e.g., pH-changes regulating dissolution and precipitation of carbonates, silica etc.; O_2-production by oxygenic photosynthesis yielding gas bubbles that are instrumental in pinnacle and dome formation or in the upward floating of mats and parts of mats; ferric mineral formation, sulfate reduction and sulfur reduction yield H_2S-production, solubilisation of gypsum crystals and nodules, pseudomorph formation, ferrous mineral and carbonate formation, transformation of aragonite into celestite, Mg-calcite and dolomite, and possibly silica trans-

formations). Physical and chemical changes produced via the physiological activity of the stromatolite forming micro-organisms are, therefore, of utmost importance to the final rock structure. Perhaps even large amounts of phosphates may be deposited by microbial communities yielding stromatolites (Krajewski, 1981).

The arrangement in space and time of the stromatolite producing microbial community is important for several reasons. Stromatolite generating microbial communities may not necessarily be laminated benthic communities, but can still produce a final laminated rock structure. They also need not to be water covered. Monolayered microbial communities may grow upwards in space and with time thus producing laminae according to sedimentation and migration pattern. Also a single-layer community may thrive for a certain period of the year. During the time of its existence it may trap, bind or precipitate minerals. During the rest of the year, in the absence of the microbial community, inorganic sediments will accumulate. The laminae-producing community may also be planktonic and may precipitate calcium carbonate or other minerals in summer, while abiogenic minerals may be deposited in winter. This cycle creates laminated "organosedimentary" structures of the "potential stromatolite" type with only small influences of benthic microbial activity. In terms of this, and other definitions, such structures are often not easy to distinguish from "classical biostromate stromatolites". Laminites may also be produced in and on sporadically wetted soils or rocks, in caves and cavities via laminated or monolayered communities of bacteria, photosynthetic micro-organisms or fungi.

The average recent "potential stromatolite", however, is made up of 1—4 layers of different photosynthesizing communities and 1—3 layers of different non-photosynthesizing communities, thus predetermining in situ the ultimate laminated structure of the stromatolitic rock. Cases of multilayered communities yielding only a single lamina in the final rock structure are also known (e.g., Krumbein and Cohen, 1977).

The interaction with the physical and chemical environment is included in the definition because former inorganic, e.g. evaporative laminations, may be destroyed or altered by interaction with laminated or layered microbial communities within the sediments. Structureless carbonate, gypsum and silicoclastic, even halite beds can become laminated by the activity of microbial communities living within them or on top of them. Precipitation and dissolution patterns may cause laminations and clay layers may alternate with benthic or planktonic carbonate producing communities. Laminations of chemical fossils (e.g., carotenoids, humic matter, oil and tar or any other kind of bitumen) can also be embedded in otherwise structureless evaporitic or other sedimentary beds. In the "Wadden Sea" (North Sea), thick beds of otherwise structureless silicoclastic sediments may be defined as "potential stromatolites", because these sediments trap smaller particles in the slime of microbial communities living at the surface. Alternations of ferrous and ferric layers may additionally be caused by oxygenic and anoxygenic layers of the community

(P. Rongen, 1979). Thus, the normal graded bedding of silicoclastic sediments is transformed by the microbial benthic mat into irregularly (undular) graded upwards convex stromatolites with alternations of ferric and ferrous minerals, similar to laminations in the banded iron formations (see also Kretzschmar, 1982; Grosovsky et al., 1983).

Organosedimentary. This term has been excluded from the definition because stromatolites may not always form in classical sedimentary environments, and the lamination pattern can be produced without leaving organic compounds behind. Biosedimentary may be an alternative term. Organosedimentary also implies the participation of all kinds of organisms. Stromatolites, however, by definition are made by micro-organisms.

The term principally by cyanophytes has also been excluded from the new definition because stromatolites do exist which have not been produced by photosynthetic micro-organisms, and because "potential stromatolites" exist which are formed by photosynthetic micro-organisms other than cyanobacteria. Examples of stromatolites exist which are formed by fungi, chemoorganotrophic and chemolithotrophic bacteria, and by obligate anoxygenic phototrophic bacteria.

The new definition proposed here, together with these explanatory remarks, points out that a stromatolite is a rock structure, the lamination of which is caused by microbial communities rather than by algae or cyanobacteria alone, and also they need not be organic nor sedimentary structures. Any laminated rock structure which cannot be defined as the result of interaction with microbial communities shall hitherto be regarded as "stromatoloid" (Buick et al., 1981). The terms "inorganic stromatolite" or "abiogenic stromatolite" appear to be a sort of compromise and should be avoided. The terms stromatactis and thrombolite (Flügel, 1982) are related to stromatolites, but should be discussed separately, as should the problem of skeletal or non-skeletal micro-organisms associated with stromatolite formation or bioherm and biostrome formation (Krumbein, 1983).

Microbial communities actively participating in the formation of stromatolites

The definition, description and study of microbial communities actively participating in the formation of potential and consolidated stromatolites is rather complicated. Several means of description have to be used in order to circumscribe the biological features of stromatolites.

Firstly, it has to be repeated that following the five kingdom classification (Margulis and Schwartz, 1982) and according to the definitions of prokaryotes (Starr et al., 1981), most stromatolites are produced by prokaryotes, i.e., bacteria, and only sometimes by fungi. Algal stromatolites are improbable and no example of the recent or fossil record can be given here. Some diatoms, red algae and planktonic algae may, however, be part of laminated prokaryotic microbial communities. These frequently produce oncoids and/or oncolites rather than stromatolites.

Besides the RNA group analysis and protein tree derived evolutionary system of classification of prokaryotes and eukaryotes (e.g., Stackebrandt, 1981; Stackebrandt and Woese, 1981; Trüper, 1982) the most useful scheme of classification and recognition of micro-organisms and microbial effects is based on the metabolic activities of micro-organisms rather than on morphology. The insight into metabolic capabilities of micro-organisms is also necessary for the understanding of geomicrobiological processes, i.e., the role of micro-organisms in specific geochemical reactions and in the production of geological structures via microbial activities. Therefore, the basic principles of microbial metabolic activity are presented here in order to further understanding of the multiple biochemical processes occurring in the microcosm of a laminated microbial community, or a "potential stromatolite", that lead to the formation of lithified consolidated stromatolites.

The stromatolite ecosystem is almost exclusively occupied by prokaryotes because they can live (1) in completely anaerobic environments, and (2) have adapted themselves to extreme conditions of light (high and low), temperature, acidity and salinity, in which eukaryotes cannot live. Furthermore they have unique metabolic capacities which are either absent from or only present in rudimentary form in eukaryotes. This uniqueness includes the modes of energy conversion, the wide range of growth substrates and oxidation—reduction couples used, as well as tolerance to extreme conditions (Schlegel and Jannasch, 1981).

The processes of recovering energy, reducing power and substances essential for microbial growth and multiplication, are given the term "trophe", which means nutrition or related to nutrition. Whether or not micro-organisms use certain biochemical pathways, depends on their capability to adapt to a certain environment. The capability of adaptation is expressed by the terms "phily" = friendship, or tolerance = forbearing. An organism that grows optimally in 30% salinity is a halophilic organism, an organism that can grow at such salinity, but does grow better or the same way at much lower salinities, is halotolerant.

All micro-organisms in order to live and to multiply need:

(1) An energy source in order to maintain a steady state equilibrium (thermodynamic stabilization against entropy).

(2) Sources of hydrogen, protons or electrons (i.e., reducing power) in order to regulate the energy flow through the cell and to build reduced carbon compounds for metabolic, morphology and motility purposes.

(3) Sources of carbon, nitrogen, phosphorus and other nutrients in order to build the necessary cell compounds. Usually this is restricted to carbon because carbon makes up $>50\%$ of the dry cell mass.

(4) Terminal electron acceptors for energy conversions and final steps of the oxidation—reduction reactions going on within the microbial cell.

Reactions in respect of 1—3 are named assimilatory and those with regard to 4 are called dissimilatory.

Energy sources

The two ways of obtaining energy for growth are called (a) phototrophy, when the organism uses light energy and (b) chemotrophy, when the organism uses chemical bond energy as an energy source. A phototrophic bacterium exerts photosynthesis, a chemotrophic bacterium exerts chemosynthesis.

I define photosynthesis and chemosynthesis accordingly: "photosynthesis is the production of energy rich chemical compounds or membrane potential useful for the microbial metabolism from appropriate light energy." Appropriate light energy means not too high, not too low and of the right spectral qualities. The generation of reducing power and of organic carbon compounds is not restricted to phototrophy and is not an overall principle of photosynthesis. "Chemosynthesis is the production of energy rich chemical compounds or membrane potential useful for the microbial metabolism from appropriate reduced (inorganic or organic) compounds." Appropriate means that the organism is capable of introducing the "activation energy" for oxidation and liberation of energy from the reduced compound and that the compound liberates more energy, then "activation energy" is needed.

The definition of photosynthesis includes the halobacteria, which produce membrane potential for cation pumping and proton gradient driven ATP by photoactivation of membrane bound bacteriorhodopsin. The definition excludes direct photoreduction of nicotinamid adenine dinucleotide phosphate (NADP), because it usually proceeds via several steps which are also hydrogen donor related. NADPH-recovery is not exclusively restricted to phototrophs and photosynthesis and may be included into the so-called light-independent dark reactions.

Hydrogen (or electron) sources

The hydrogen or electron donor related classification is termed (a) lithotrophy in the case of inorganic proton or electron donors and (b) organotrophy in the case of organic proton or electron donors. Ultimately, within the cell, electrons or hydrogen coming from lithotrophic or organitrophic sources are serving to build up reducing power or reduction equivalents in combination with the energy derived from photosynthesis or chemosynthesis.

Nutrient (carbon) sources

The types of carbon or any other nutrient source are divided into: (a) autotrophy, when the organism uses inorganic carbon, nitrogen or phosphorus compounds and (b) heterotrophy, when the source of the nutrient is an organic compound. It is possible to talk about heterotrophy and autotrophy without connotation. In this case the carbon source is inferred. It is, however, possible to talk about carbon autotrophy and nitrogen heterotrophy in one and the same organism. For example, this is the case in insect digesting plants such as *Drosera*, which is a carbon autotroph and nitrogen heterotroph, because it derives its nitrogen from the digested insects and its carbon from atmospheric carbon via carbon dioxide fixation (humans are phosphorus-heterotrophs).

Electron acceptors

The terminal electron acceptor for metabolic activities of micro-organisms can be (a) oxygen. In this case the organism exerts aerobic respiration, i.e., oxidative phosphorylation. The term (b) anaerobic respiration (also oxidative phosphorylation when energy is gained during this process) applies when the terminal electron acceptor is another inorganic oxidized compound (in special cases also organic compounds) which is reduced by the cell (dissimilative reduction) during the transfer of electrons from the cell's respiratory chain. Anaerobic respiration is very important in the structure and growth of microbial mats inasmuch classical electron acceptors are sulfate, nitrate, ferric iron, carbon dioxide and other oxidized compounds, which are reduced in large quantities by the deeper laminae of many stromatolitic microbial communities.

The third kind of electron acceptor, known as (c) fermentation or substrate level phosphorylation, are organic compounds (mostly present in the cell). One organic carbon compound, or one part of an organic carbon compound, is oxidized under energy and electron gains, and another part, or another

TABLE I

Nutritional requirements of laminated microbial communities

Energy source	Electron donor	Carbon source	Term (examples)[a]
Light	Inorganic	Inorganic	Photolithoautotroph (Cyanobacteria)
Light	Inorganic	Organic	Photolithoorganotroph (*Rhodospirillum*)
Light	Organic	Inorganic	Photo-organoautotroph (*Chloroflexus*)
		Organic	Photo-organoheterotroph (Rhodopseudomonas)
Bond energy of inorganic and organic compounds	Inorganic	Inorganic	Chemolithoautotroph (*Thiobacillus*)
	Inorganic	Organic	Chemolithoheterotroph (*Desulfovibrio*)
Bond energy of inorganic and organic compounds	Organic	Inorganic	Chemo-organoautotroph (heterotroph CO_2-fixation)
	Organic	Organic	Chemo-organoheterotroph (most chemo-organotrophic bacteria)

[a]The examples are taken randomly using species of bacteria known to be able to live under the given nutritional requirements and to be involved in stromatolite formation.

compound, is further reduced while serving as an electron acceptor. This is referred to as substrate level phosphorylation concerning energy gains. Terminal products and substrates of fermentation are very important in microbial mats, since these compounds are sometimes delivering protokerogen, gases and other substances important for early diagenesis, and because fermentation is usually less efficient in degradation and oxidation of organic materials, thereby leaving many detectable compounds within the rock forming system (Edmunds et al., 1982). Hereby the microbial origin of a given laminite may be demonstrated.

Besides these terms, the use of which is summarized in Table I, other important definitions have been changed and adapted to new findings in physiology and ecology, and are needed in order to understand stromatolite formation.

Photosynthetic communities

In cases where the recovery of reducing power is coupled directly to the photosynthesis process, anoxygenic may be separated from oxygenic photolithotrophy or photo-organotrophy. Phototrophic micro-organisms, capable of using water as an electron donor are oxygenic photolithotrophs and those using other reduced inorganic compounds, such as hydrogen sulfide, elementary sulfur or hydrogen, are called anoxygenic photolithotrophs. Those which use organic electron donors are defined as anoxygenic photo-organotrophs. The photosynthetic bacteria involved in stromatolite formation can thus be subdivided into the anoxygenic photosynthetic bacteria and the oxygenic photosynthetic bacteria (mainly cyanobacteria).

Facultative and obligate

The metabolic capabilities of micro-organisms may further be defined by the terms facultative and obligate. Some cyanobacteria can use water and hydrogen sulfide alternatively as electron donors. In this case they may be called facultative anoxygenic photolithotrophs. Some cyanobacteria are even capable of using organic compounds as electron and/or carbon donors. In these cases they may be called facultative photo-organotrophs or photo-organoheterotrophs, i.e., they are capable of switching from inorganic to organic electron donors as well as from carbon dioxide to sugars as carbon source.

It is clear that in a sedimentary environment which may be deprived of sufficient light, and where poisoning by hydrogen sulfide may occur, it is an advantage to be metabolically flexible. Most algae (green algae) are, on the contrary, obligate oxygenic and obligate photolithotrophs and, therefore, poor candidates for stromatolite formation.

A recently discovered filamentous obligate anoxygenic phototrophic sulfur bacterium has still another adaptation pattern. *Chloroflexus*, a green or red filamentous phototrophic bacterium, lives by anoxygenic photolitho-autotrophy under anaerobic conditions. It occurs in thermal "potential stroma-

TABLE II

Micro-organisms occurring in "potential stromatolites"

Group	Example	Photo-troph	Pigment s	Oxygenic	Anoxy-genic	Lithotroph (electron donor)
Prokaryotes						
Archaebacteria	Halobacter	+	b-rn[a]	–	+	–
Chorobiaceae	Chlorobium	+	b chc[b]	–	+	S, H_2SH_2
Chloroflexcaceae	Chloroflexus	+	b chlc	–	+	(H_2S)
Rhodospirillaceae	Rhodopseudomonas	+	b chlb	–	+	$S_2O_3^-$
Chromatiaceae	Thiocapsa	+	b chl a	–	+	S, H_2S
Chromatiaceae	Ektothiorhodospira	+	b al a	–	+	H_2S, H
Cyanobacteria	Synechococcus	+	chl a[c]	+	–	H_2O
Cyanobacteria	Phromidium	+	chl a	+	(+)	H_2O, H_2S
Beggiatoaceae	Beggiatoa	–	–	–	–	H_2S
Cytophagaceae	Pelonema	–	–	–	–	–
Prosthecate bacteria	Hyphomicrobium	–	–	–	–	–
Sulfate reducers	At least 6 species	–	–	–	–	(H_2)
Sulfur reducers	At least 3 groups	–	–	–	–	(H_2)
Spirochaetes	Spirochaeta halophila	–	–	–	–	–
Aerobic and anaerobic	Rods and cocci[e]	–	–	–	–	H_2S, S^0 $H_2S_2O_3^{2-}$
Eukaryotes						
Diatoms	Nitzschia	+	chl a,b[d]	+	–	H_2O
Fungi	Mucorales e.g.	–	–	–	–	–

[a] Bacteriorhodopsin.
[b] Bacteriochlorophyll; [c] chlorophyll a; [d] chlorophyll a and b (all chlorophylls are so similar in structure that a nomenclature of chlorophylls may soon be available which no longer separates "plant" and

tolites" as well as in marine hypersaline "potential stromatolites". The change of metabolic activity can be experimentally produced by changing the light conditions. Thereby the whole structure and morphology of the mat is changed. The bacterium comes to the surface and switches to aerobic chemo-organotrophy (Starr et al., 1981; Krumbein et al., 1983).

In summary, the micro-organisms occurring in and regulating the physico-chemistry of "potential stromatolites" (Table II) can be described by the combination of the following pairs of terms, thereby also defining their geo-chemical activities in stromatolite formation.

(1) Phototroph and chemotroph (energy source).
(2) Lithotroph and organotroph (hydrogen or electron source).
(3) Autotroph and heterotroph (carbon and other nutrient sources).
(4) Aerobic and anaerobic (life in the presence and absence of oxygen).
(5) Oxygenic and anoxygenic (using water as an electron donor or not).
(6) Aerobic and anaerobic respiration and fermentation.
(7) Facultative or obligate use of one of the above-mentioned capabilities.

Finally, it is stressed that the frequently used partition between bacterial and plant photosynthesis is completely obsolete. All species of photosynthetic pigments and all types of photosynthesis occur in bacteria. The obligate

Organo-troph	Aerobic	Micro-aero-philic	An-aerobic	Chemo-troph	Auto-troph	Hetero-troph	Terminal electron acceptor	Respi-ration	Halo tolerance
+	+	(+)	–	(+)	–	+	O_2	+	+
(+)	–	–	+	–	+	–	C org	–	+
+	+	+	+	+	+	+	O_2	+	+
+	(+)	(+)	+	+	(+)	+	O_2	+	+
+	(+)	(+)	+	(+)	+	(+)	(?)	?	+
+	–	(+)	+	–	+	–	–	–	+
(+)	+	+	–	(+)	+	(+)	O_2	+	+
(+)	+	+	+	(+)	+	(+)	O_2(S)	+	+
(+)	+	(+)	–	+	(+)	+	O_2	+	+
+	–	–	+	+	–	+	–	–	+
+	+	(+)	–	+	–	+	O_2	+	+
+	–	–	+	+	–	+	SO_4^{2-}	+	+
+	–	–	+	+	–	+	S^0	+	+
+	(+)	–	+	+	–	+	C org	–	+
+	+	+	+	+	+	+	O_2, H_2S $NO_3^-CD_2$	+	+
–	+	–	–	–	+	–	O_2	+	(+)
+	+	–	–	+	–	+	O_2	+	+

"bacterial" chlorophylls, but one chlorophyll with a definition of the changed radicals).
[e]In this list the chemo-organotrophic and chemolithotrophic bacteria have been summarized with all capacities which have been shown to occur in microbial mats.

anoxygenic or micro-aerophilic phototrophic bacteria use bacteriochlorophylls a—e and associated pigments. The anoxygenic aerobic photosynthetic bacterium *Halobacter halobium* uses bacteriorhodopsin for the production of membrane potential or ATP from light energy. The cyanobacteria use chlorophyll a and phycobilins associated with special phycobiliproteins for photosynthesis. The cyanobacterium *Prochloron*, recently found as ectosymbiont of Ascidians, uses chlorophyll a and chlorophyll b as is the case in any higher plant chloroplast.

Some cyanobacteria can switch from linear to cyclic photophosphorylation in the presence of high concentrations of hydrogen sulfide (Krumbein and Cohen, 1974, 1977). It is essential, therefore, to look carefully into the microbial communities forming photosynthetic microbial mats, because the geochemistry of the resulting stromatolite may utterly depend on the species occurring and on the principles of growth realized in such a mat. Furthermore, chemolithotrophs and chemo-organoheterotrophs as well as chemolithoheterotrophs may additionally, or independently, occur within the mats and largely modify the chemical environment. This in turn greatly influences our understanding of stromatolites as indicators of an oxygenated or anoxic atmosphere.

This excursion into the basic definitions of microbial metabolism was necessary in view of the fact that today "algal mats" are still regarded as the producers of "stromatolites".

Definition of various microbial communities initiating the genesis of "potential" and consolidated stromatolites

After describing the multiple metabolic pathways involved in the formation of "potential stromatolites" and ultimately lithified stromatolites, the different microbial (mainly cyanobacterial) communities which are known to produce "potential stromatolites" are now defined.

Fig. 2. Large patches of cyanobacterial mats floating up in a sabkha environment of the Gulf of Aqaba. These patches and many other macrostructures e.g., the Nostoc "eggs" of Mare's egg in Oregon may be misinterpreted as eukaryote macro-organisms in sedimentary rocks.

Terms which may be useful are: (1) microbial ecosystems, or (2) laminated microbial ecosystems, or (3) laminated microbial community. The latter term is preferred, because it does not imply that the whole system is an entirely microbial ecosystem (since Late Precambrian eukaryotes are present and do modify the microbial community as a part of the total ecosystem).

Stromatolite forming microbial communities can be subdivided into:

(a) microbial mats (monolayered);

(b) photosynthetic microbial mats;

(c) laminated microbial mats;
(d) photosynthetic laminated microbial mats;
(e) oxygenic photosynthetic microbial mats;
(f) anoxygenic photosynthetic microbial mats;
and their laminated examples in cases where several laminae of microbial populations occur or accumulate with time.

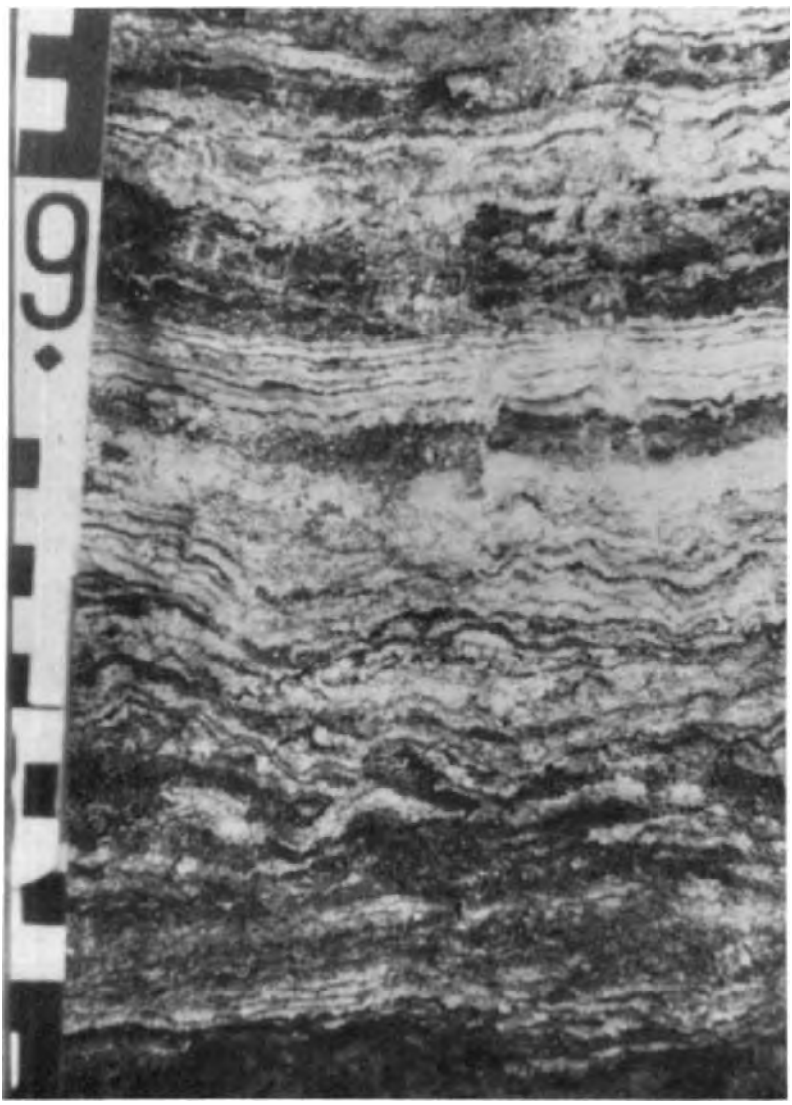

Fig. 3. Finely laminated carbonate, gypsum, clay rock of a fossil sabkha at Devil's Head (Ma'aganah), Sinai. The lamination may be biogenic. Biological origin of or influence in the lamination has not yet been fully established. The material is under biogeochemical study. No fossils have been shown (see also Krumbein and Cohen, 1977). Therefore, it is suggested to call this sequence stromatoloid. Scale in cm.

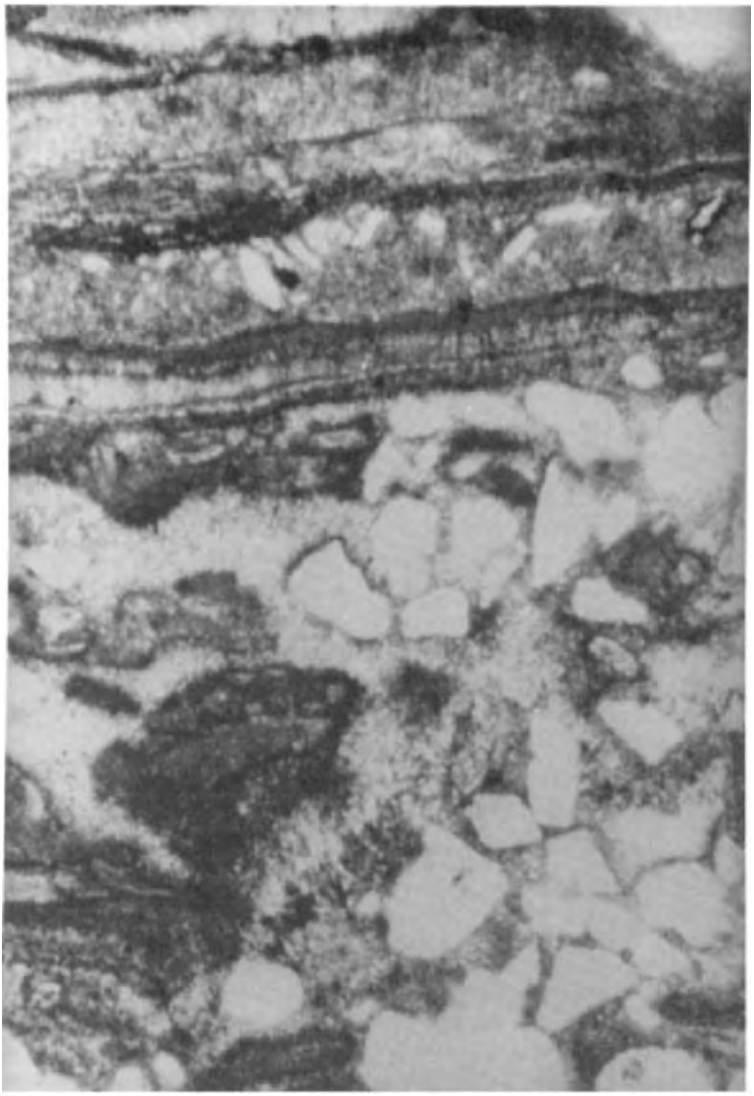

Fig. 4. Thin section of laminated stromatolitic beachrock of El Hamira Bay (Sinai). In several places the beachrock is forming as stromatolite and in other places as structureless carbonate cemented bank, the original lamination is then not preserved. According to the new definition, "potential stromatolites" for several reasons have or have not been transformed into extant stromatolites (see also Krumbein, 1979a). Scale ~1 × 2 mm. This example is both a beachrock and a stromatolite at the same time.

Fig. 6. Oncoidal "potential stromatolite" (non-lithified) of the Sabkha Gavish (Sinai). The oncoidal laminated granules may reach domal shapes of up to 5 cm and may gradually pass into forms similar to those in Fig. 7 (see Krumbein et al., 1979a). Scale: at the lower left a halophila seaweed leaf of 7 cm length is visible (see Friedman and Krumbein, 1983).

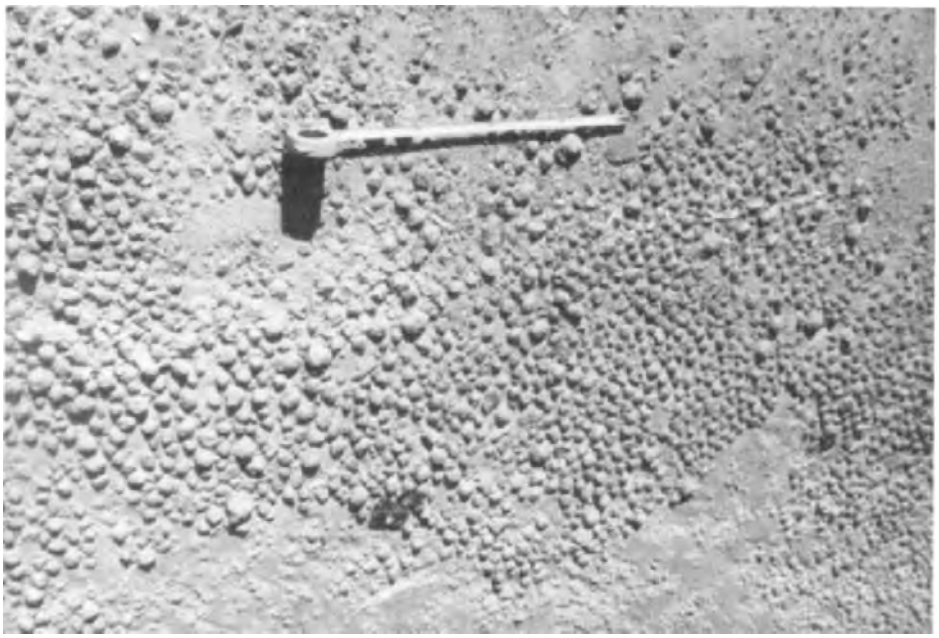

Fig. 5. Laminated oncoidal stromatolites (lithified) fusing partially into stromate laminites. Individual domes may reach 5 cm diameter. The stromatolite system has been formed and cemented on the shores of a slightly hypersaline bay at the Ras Muhammed Peninsula of Southern Sinai (Gavish et al., 1978) and is very similar to beachrocks and oncolites included in the stromatolite definition by Kalkowsky (1908).

In desert environments, the following terms may be applied to rocks exposed to air, and in soils: photosynthetic microbial crusts and laminated photosynthetic microbial crusts etc.

In Figs. 2—16 I have shown several examples of laminated rock structures and "potential stromatolites" clearly related to the activity of different microbial communities in order to widen the scope of possible sources and environments of stromatolitic structures.

It may sound absurd to differentiate so many microbial systems that produce stromatolitic structures. With respect to some recent and fossil examples, e.g. cave laminites related to the activity of fungi and chemo-organotrophic bacteria (Pochon et al., 1964; Danielli and Edington, 1983), or laminated ironstones of the Miocene, which are clearly produced by laminated mats of fungi (Figs. 12—16) (Gygi, 1981; Kretzschmar, 1982), or the not yet settled discussion of Pacific hot vent laminites and Precambrian banded iron formations (BIF) (Kretzschmar, 1982; Krumbein et al., 1979a; Grosovsky et al., 1983), it seems important, however, to stress that the microbial communities which produce undular laminated rock structures are not exclusively photosynthetic ones and are very variable in physiology, structure, morphology and taxonomy. It is also important to state that they are neither necessarily intertidal nor always depth dependent (Jannasch and Wirsen, 1981).

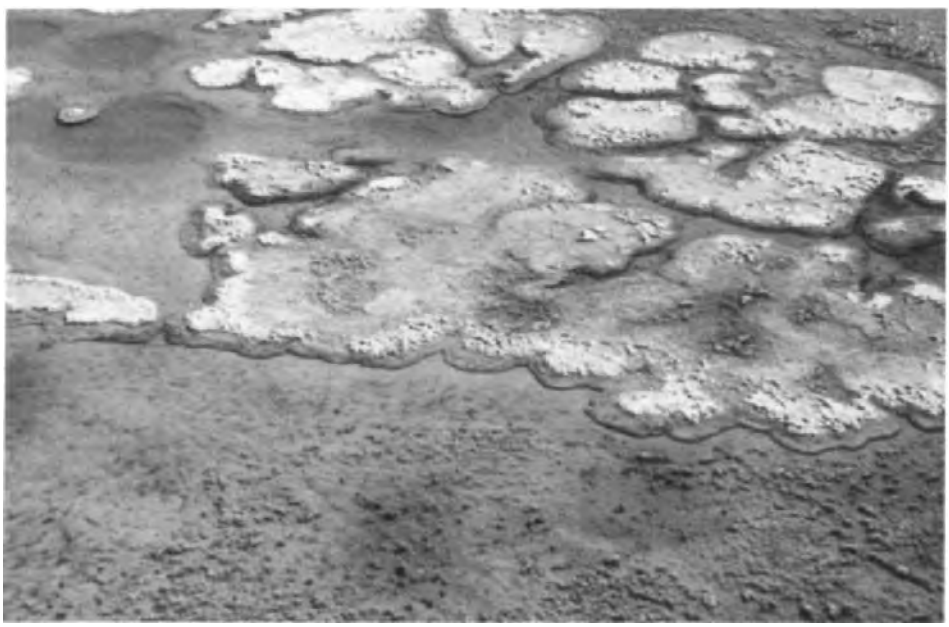

Fig. 7. Dome shaped "potential stromatolites" built by cyanobacteria, *Chloroflexaceae*, *Chromatiaceae* and several other bacteria. The depth of lamination is ~1—3 mm per lamina. The living system consists of ~5 layers extending over a depth of 12 mm (see also Krumbein et al., 1979a). Scale: one individual dome has a diameter between 20 and 50 cm. The maximum elevation above ground is 7 cm. The system is non-lithified, except for some thin carbonate layers and summer gypsum formation which isr edissolved in winter.

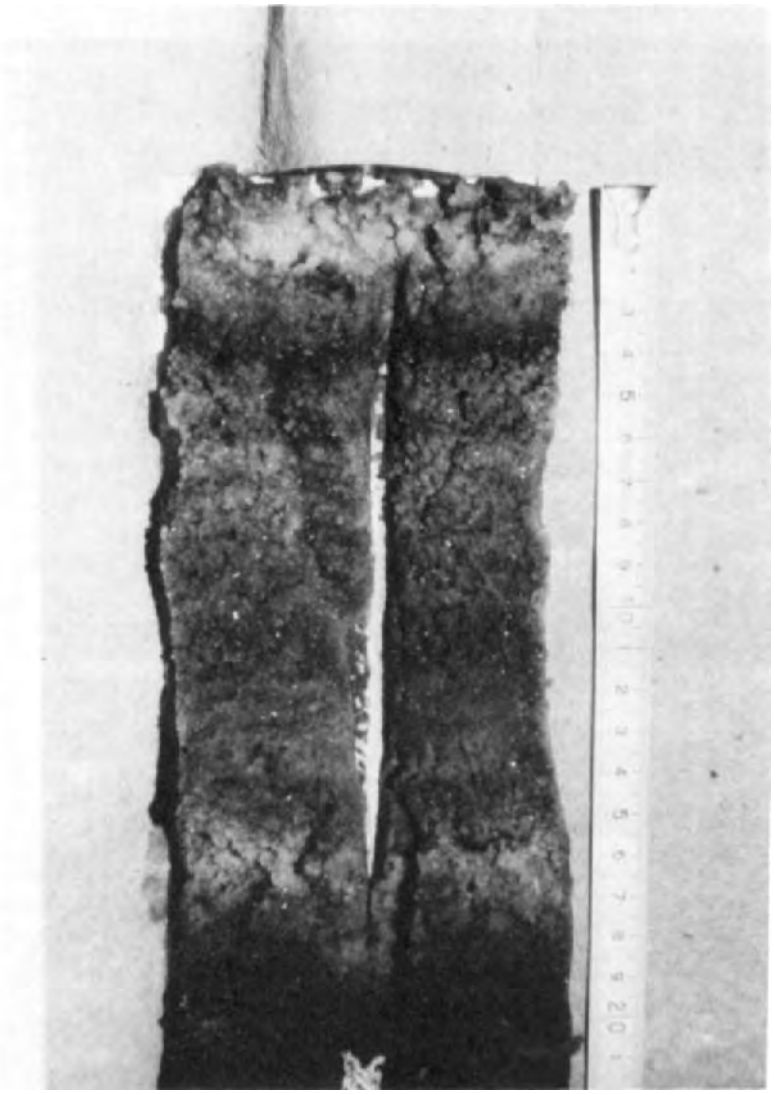

Fig. 8. "Potential stromatolite" of the Sabkha Gavish (Sinai). The bright zones, from 0—2 cm and from 6—7 cm, reflect surface halite precipitation of the central parts of the Sabkha. Besides halite, gypsum, celestite, traces of baryte and other salts occur. The crystallization sequence is interrupted by a desert sheet flood layer at 14—15 cm depth. The uppermost 2 cm are orange red (*Halobacterium halobium* and square bacteria). The region between 2 and 3.5 cm is olive green and dark green because of coccoid and filamentous cyanobacteria, the dark line at 3.5—4.5 cm is violet coloured in its upper parts, because of the *Chromatiaceae* and in its lower parts it is black, because of sulfate reducing bacteria and iron sulfide formation. The whole sequence is repeated from 15 cm to 22 cm. Lamination is imposed on an evaporation sequence by biological activity under simultaneous chemical changes (gypsum dissolution, carbonate precipitation). Also, the sulfides and organic remainders will colour the eventually lithifying sequence into dark and bright layers, as is often observed in sabkha type stromatolites. The depth of the living photosynthetic system of more than 5 cm is caused by the high light penetration rate into the crystalline salt deposit (glass fibre effect as in etiolated plants, e.g., Mandoli and Briggs, 1982).

Fig. 9. Finely laminated "potential stromatolite" of the Solar Lake (Sinai). The bright interlayers are desert sheet flood sediments, the fine dark and bright lamination is caused by different microbial communities of many years piled one on top of the other. The present photosynthetically active layer is the very thin black top layer (Krumbein and Cohen, 1974, 1977).

DESCRIPTION OF "POTENTIAL STROMATOLITES"

Many descriptions of stromatolites and "potential stromatolites" have been given over the years (Kalkowsky, 1908; Pia, 1928; Black, 1933; Johnson, 1937; Cloud, 1942; Shrock, 1948; Rutte, 1953; Ginsburg and Lowenstam, 1958; Logan, 1961; Seibold, 1962; Korolyuk, 1963; Krylov, 1964; Barghoorn and Tyler, 1965; Bertrand-Sarfati, 1966; P.F. Hoffman, 1967; Gebelein and Hoffman, 1968; H.J. Hoffman, 1969; Neumann et al., 1970; Bathurst, 1971; Awramik et al., 1972; Golubic, 1973; Krumbein and Cohen, 1974; Schwarz et al., 1975; Walter, 1976; Flügel, 1977; Krumbein, 1978; Trudinger and Swaine, 1979; Nissenbaum, 1980; Monty, 1981; Holland and Schidlowski, 1982). As the expert can see, I have tried to summarize, sequentially, the most important aspects and authors or editors over the past 75 years. The wide scope and the tremendous amount of literature written about

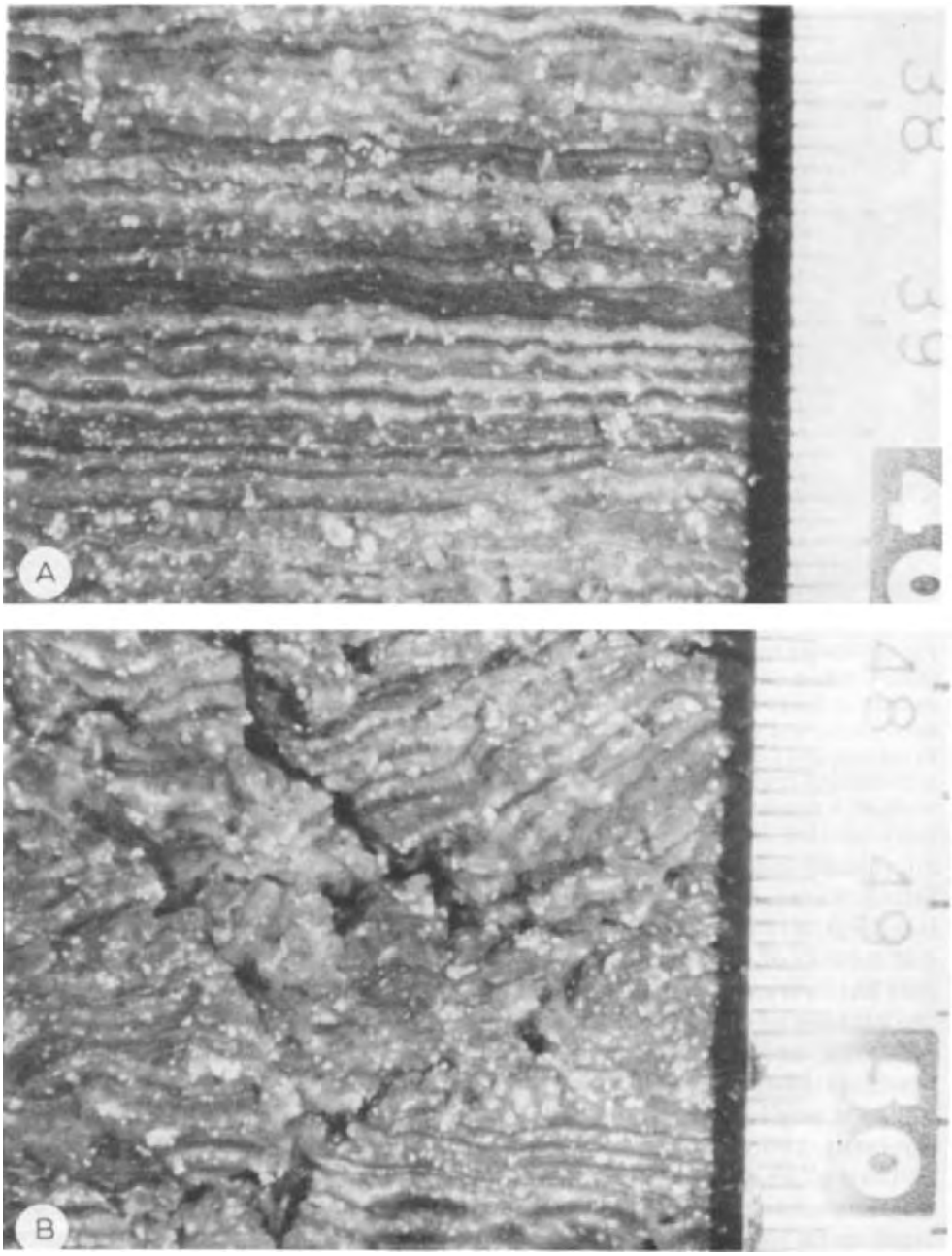

Fig. 10. (a, b) Sections of deeper parts of the core in Fig. 9, enlarged. Dark laminae are composed mainly of the empty sheaths of *Microcoleus*. The bright parts originate from *Chloroflexus* and from empty sheaths of coccoid cyanobacteria of the *Synechococcus* type as well as from coccoid purple sulfur bacteria. The former sulfate reduction zone is no longer visible because iron sulfides have been transformed into pyrite (see also Krumbein et al., 1977). The lamination in (b) is disturbed by dry cracks and sampling. It is difficult to identify the stromatolitic structure in this section. Bright spots in (a and b) designate bacteriogenic ooids (Krumbein, 1974, 1979a).

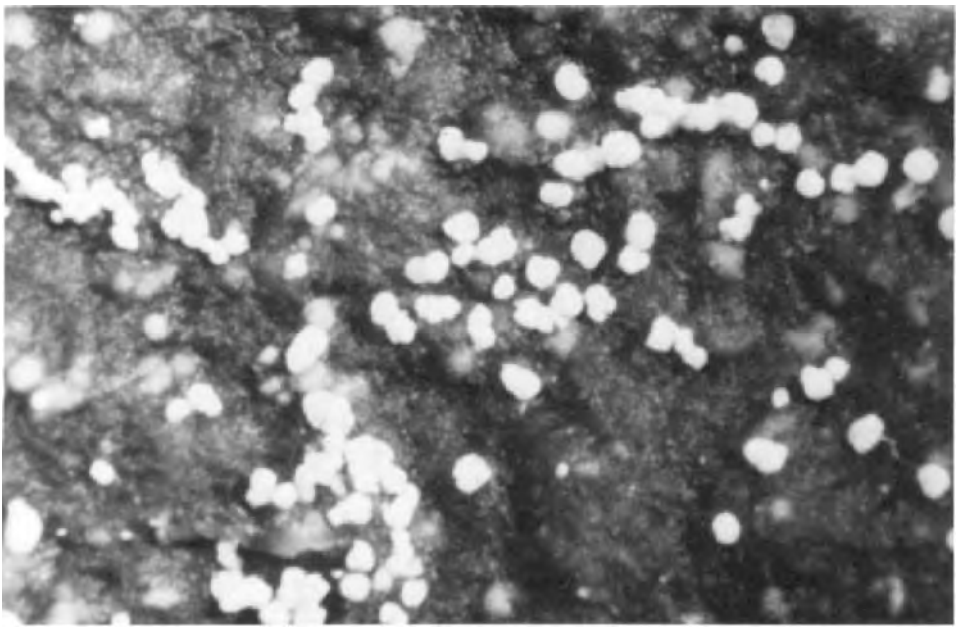

Fig. 11. Ooids formed in situ in the layers of "potential stromatolites" of the Solar Lake (Sinai). The ooids and "ooid bags" encoated into individual slime sheaths correspond exactly to Kalkowsky's (1908) description of ooids and oncoids merging upwards into stromatoids and stromatolites. The structure and genesis of the ooids is explained in Krumbein and Cohen (1974, 1977) and Krumbein et al. (1977). The mineralogy is given in Krumbein (1974) and Friedman et al. (1973). Scale: the ooids measure between 30 and 500 μm in diameter.

microbially influenced geological structures is certainly not exhausted in this listing. Views, descriptions, theories, analyses, unfortunately also misunderstandings, and many other aspects can be gained from the cited books, articles and reviews of the topic. It may also be noteworthy, however, that stromatolites have very recently gained interest amongst scientists not at all related to the geology of stromatolites, nor even to the biology of these rock structures. M. Calvin, known for his work on the Calvin-cycle has stimulated much of the biogeochemical research on stromatolites (e.g., Philp et al., 1978) via Eglinton (e.g., Edmunds et al., 1982) or Burlingame (e.g., Burlingame and Simoneit, 1968). Roger Stanier, one of the most outstanding microbiologists of the era, who died untimely in 1982, was excited about the wide distribution and ecological importance of cyanobacteria in stromatolites. He stimulated much research along the biological and biogeochemical side, and gave very interesting suggestions during his visit of the Solar Lake and Ras Muhammed microbial laminated systems. He also exchanged opinions with Ourisson about this topic (e.g., Ourisson et al., 1979). Biochemists (e.g., Lehninger, 1972), molecular biologists (Stackebrandt and Woese, 1981) and many microbiologists also became interested in the documents of microbial

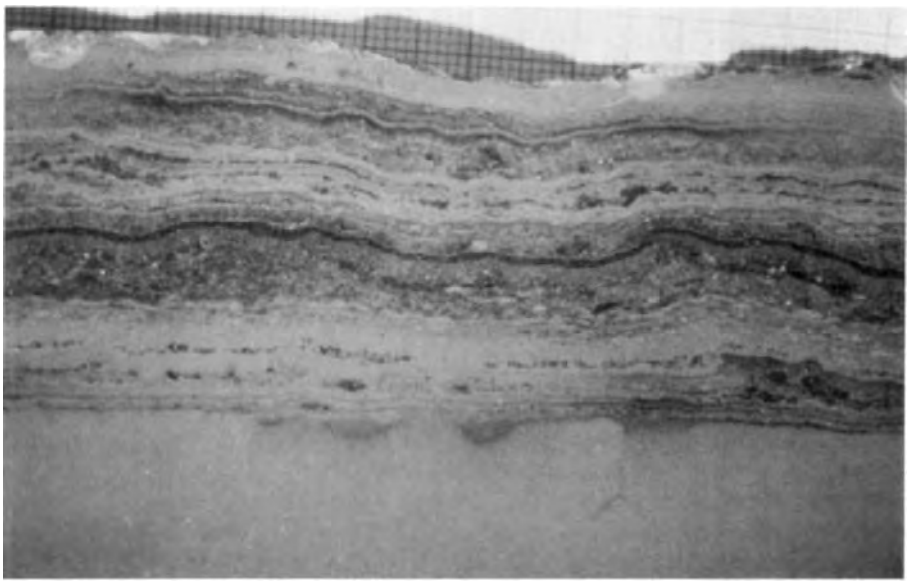

Fig. 12. Iron stromatolite of Warstein (Germany) (Kretzschmar, 1982). The biogenic finely laminated ironstone consists mainly of iron oxides and quartz. The lamination is mainly produced by a fungal iron precipitating microbial community (Krumbein, 1971; Krumbein and Jens, 1981; Krumbein and Altmann, 1973).

life in the Precambrian and of the recent analogues in present day deposits (e.g., Starr et al., 1981; Trüper, 1982; Nealson, 1982). There is no doubt, that cell biologists who have a deep interest in the evolution of cellular structures and capacities, and symbiosis have reason to study stromatolites (Margulis et al., 1980; Margulis, 1981).

Literature on methods to study "potential stromatolites" in the field and in the laboratory has also expanded, with incredibly refined, and focussed approaches to the cellular and molecular biology level (Brock, 1976, 1978; Krumbein et al., 1977, 1979b; Potts et al., 1978; Bauld, 1979; Javor, 1979; Shilo, 1979, 1980; Jorgensen et al., 1979, Wickstrom, 1980; Trudinger and Walter, 1980; Skyring and Johns, 1980; Schubert et al., 1980; Stal and Krumbein, 1981, 1982a, b; Lorenz et al., 1981; Oehler et al., 1982; Stal et al., 1982; Schopf, 1983).

The major aspects of methodology refinement in the study of "potential stromatolites" are: (1) microelectrode studies in the field with electrodes measuring $<8\ \mu m^2$ (Jorgensen et al., 1979); (2) field studies of carbon dioxide fixation (Krumbein et al., 1979); (3) nitrogen fixation, and oxygen and hydrogen turnover at the nanomolar and picomolar level, and on areas of $<200\ \mu m^2$ (Jorgensen et al., 1979; Stal and Krumbein, 1981); (4) analysis of picomolar concentrations of organic molecules (Edmunds et al., 1982); (5) precise determination of nucleic acids in the mat material (Lorenz et al.,

Fig. 13. Thin section of an iron stromatolite as given in Fig. 10. Fungal iron encrusted filaments are visible, as well as dark and bright layers of more or less iron encrusted hyphae embedded in the later intruded hydrothermal quartz. Perhaps these iron stromatolites can also throw light on biogenicity of iron in older sequences (e.g., Knoll and Simonsen, 1981). Scale from bottom to top ~1 mm.

1981); and (6) movements of organisms in response to changes of light, salinity and temperature in the micrometer scale, and with response times of < 1 min (Holtkamp, personal communication, 1982). All this information on photosynthetic as well as on non-photosynthetic microbial mats and potential stromatolites yield views that are extremely important for the hypothetical interpretation of the life conditions of micro-organisms influencing the formation of Precambrian stromatolites. The information known at present on non-photosynthetic stromatolites may also be very useful for

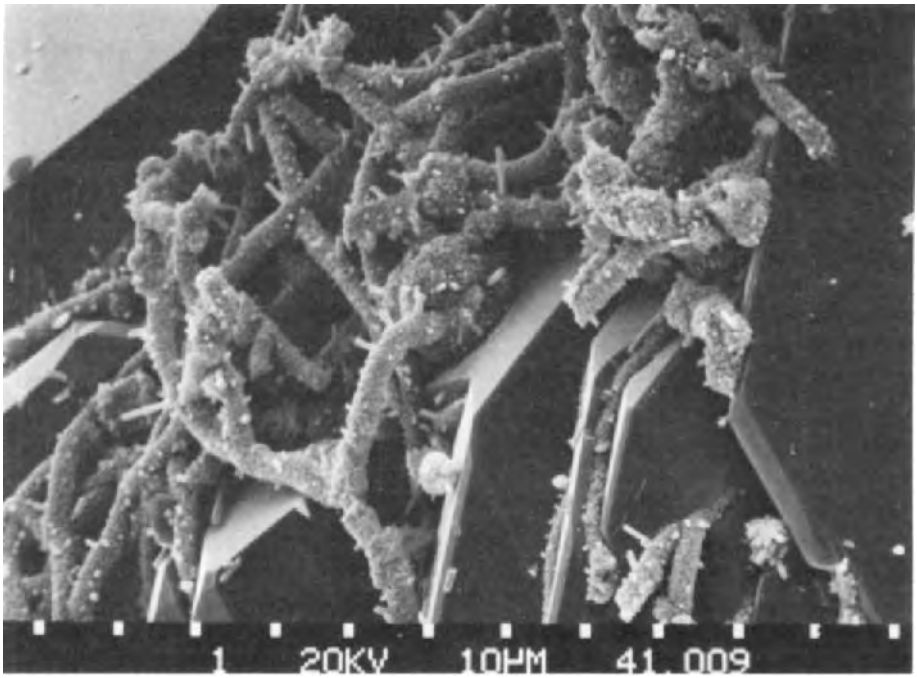

Fig. 14. Iron oxide encrusted fungal filaments showing the good preservation of the quartz embedded oxide material. The fungal material is completely degraded, the iron encrusted tubes are preserved and now look very similar to other filamentous micro-organisms. The quartz impregnation does not deform the previous biogenic iron encrustations. Deflation of fungal filaments can be attributed to decay environments prior to the quartz impregnation. The scale is 100 μm across.

the interpretation of non-carbonate and non-evaporite iron-chert stromatolites. The question is still very much debatated of whether they are stromatolites or abiogenic laminites, e.g. Kretzschmar (1982). A similar question has to be raised concerning evaporative salt—iron—manganese laminites of the Dead Sea (Friedman, 1980; Druckman, 1981).

Microbial mats, laminated microbial mats and laminated (stratified) microbial communities largely influence many sedimentary systems, and also rock, soil and crust systems without permanent water cover.

The extension of photosynthetic microbial systems with depth is largely regulated by light penetration. Light penetration can be enhanced by light scattering effects into the sediment and/or rock, thus creating laminated microbial systems between ~50 μm and a maximum of 8 cm in sedimentary systems. An easy experiment of system expansion can be done by using quartz wool fibres, which initiate systems of up to 10 cm in depth (Sprague and Krumbein, unpublished data), comparable to etiolated plant tissue light

Fig. 15. Iron stromatolite of Fig. 12, thin section. Fungal microcolonies (alternate with free spiral shaped conidiophore hairs or pro-conidiophores. All fungal filaments are iron oxide encrusted. Scale: 700 μm across. The structures vaguely resemble structures found in BIF's of the Precambrian.

traps (Mandoli and Briggs, 1982). However, on average, a laminated photosynthetic microbial community of a marine sedimentary environment usually ranges between 2 and 5 mm depth from the surface layer to the black sulfate reduction zone, into which no light penetrates. The maximum observed extension, to my knowledge, is 8 cm in evaporitic Sabkhas of tropical areas.

Photosynthetic laminated microbial communities usually consist of several characteristic layers. The top layer is often a sediment layer either without micro-organisms or with highly light resistant ones, such as diatoms, Halobacteria and coccoid cyanobacteria with high ratios of red carotenoid pigments admixed. The second layer usually consists of either coccoid or filamentous cyanobacteria. Underneath these, *Chloroflexaceae* or purple sulfur phototrophic bacteria occur. These are capable of using low light intensities and light of different wave lengths to those used by cyanobacteria. Underneath the obligate anoxygenic photosynthetic bacteria, a black sulfate reducing layer is usually observed. Sulfate and sulfur reducing bacteria furnish the sulfide, which the obligate anoxygenic photosynthetic bacteria (photosynthetic sulfur bacteria) and some facultatively anoxygenic photosynthetic bacteria (cyanobacteria) use as an electron donor. The *Chloroflexaceae* and

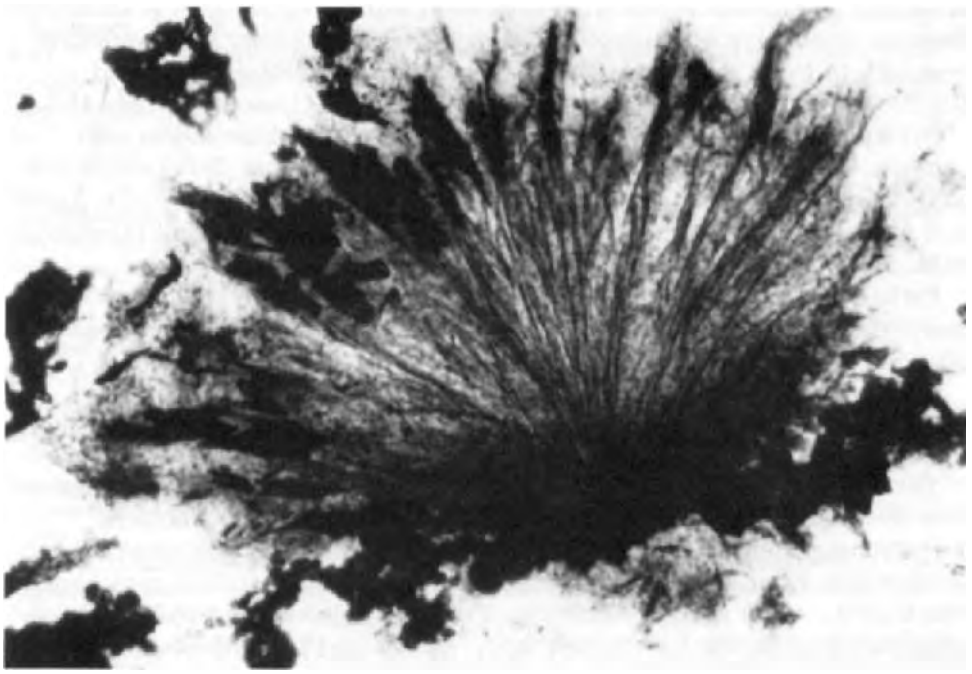

Fig. 16. Enlarged section of the thin section of Fig. 15. It shows the typical pattern of fungal mycelia, which have alternately heavily encrusted and less encrusted parts. The scale is 170 μm across (courtesy of Kretzschmar).

Chromatiaceae often act as a buffer system for the cyanobacteria to which excessive H_2S may be poisonous, especially when they cannot switch to anoxygenic photosynthesis or when they are incapable of producing storage oxygen bubbles (Krumbein et al., 1979a).

Finally, some suggestions may be given concerning further work, and classification of stromatolites and "potential stromatolites". It is very important to analyse recent laminated systems, i.e., "potential stromatolites" according to their genesis and physico—chemical environment in relation to the participating organisms. From these findings and from careful organic geochemical analyses of the "potential stromatolites" answers may be derived to questions such as:

(1) Are the Precambrian stromatolites really stromatolites or are many of them abiogenic laminated evaporite series which can only be regarded as stromatoloids (Friedman and Krumbein, 1983)?

(2) Have they been formed by anoxygenic or oxygenic photosynthetic communities or by photosynthetic communities at all (Jannasch and Wirsen, 1981; Krumbein, 1983)?

(3) Do some of the banded iron formations (BIF's) contain stromatolites or only stromatoloids? Have they been formed by phototrophic planktonic

or benthic communities? Or have they been formed by fungi or filamentous chemo-organotroph or chemolithotroph bacteria or merely by evaporative processes in fresh water or seawater (Kretzschmar, 1982; Holland and Schidlowski, 1982; Friedman and Krumbein, 1983; Grosovsky et al., 1983)?

(4) Are stromatolites genetically related to hydrocarbon and/or ore deposits, and to the accumulation of heavy metals such as the uranium and gold deposits of the ancient cratonic shields in Africa, Canada, South America and Australasia (Friedman, 1980; Friedman and Krumbein, 1983; Grosovsky et al., 1983)?

Perhaps these questions and future studies derived from them may be of more practical importance than those related to the origin and the time sequence of lamination in stromatolites.

ACKNOWLEDGEMENTS

Parts of the field and laboratory work leading to the conclusions presented here have been financed by grants 333/13 to 333/16 of the Deutsche Forschungsgemeinschaft (DFG). Also "Niedersächsisches Zahlenlotto" and Volkswagen-Foundation have sponsored work on stromatolitic environments. Much of the work was stimulated by IGCP-projects 157 and 160. I acknowledge the aid of K. Oetken, S. Seufer, A. Sievers and I. Raether. All my coworkers have continuously discussed the problems with me. I especially acknowledge the advice and criticism of Lynn Margulis (Boston), Jaap Boon (Amsterdam) and J. Paul (Göttingen). The part on iron stromatolites is mainly dependent on material worked out jointly with M. Kretzschmar of the University of Bochum. S. Awramik, G. Gerdes, A. Knoll, G. Skyring and L. Stal reviewed the first versions and made many suggestions for changes and improvements of the manuscript. I am also indebted to the reviewers of the various versions of this manuscript.

REFERENCES

Awramik, S.M., 1981. The pre-Phanerozoic biosphere — three billion years of crises and opportunities. In: Biotic Crises in Ecological and Evolutionary Time. Academic Press, New York, pp. 83—102.

Awramik, S.M., Golubic, S. and Barghoorn, E.S., 1972. Blue-green algal cell degradation and its implication for the fossil record. Geol. Soc. Am. Abstr. Program, 4: 438.

Barghoorn, E.S. and Tyler, S.A., 1965. Micro-organisms from the Gunflint Chert. Science, 147: 563—577.

Bathurst, R.G.C., 1971. Carbonate Sediments and their Diagenesis. Elsevier, Amsterdam, pp. 620.

Bauld, J., 1979. Primary productivity, sulfate reduction and sulfur isotope fractionation in algal mats and sediments of hamel in Pool, Shark Bay, W.A. Aust. J. Mar. Freshwater Res., 30: 753—764.

Bertrand-Sarfati, J., 1966. Essai de classement d'échantillons de stromatolites des séries précambriennes de l'Ahaggar occidental. Bull. Soc. Geol. Fr., 8: 158—164.

Black, M., 1933. The algal sediments of Andros Island, Bahamas. Philos. Trans. R. Soc. London, Ser. B, 22: 165—192.

Bricker, O.P. (Editor), 1971. Carbonate Cements. John Hopkins University Press, Baltimore, 376 pp.
Brock, T.D., 1976. Environmental microbiology of living stromatolites. In: M.R. Walter (Editor), Stromatolites — Developments in Sedimentology, 20. Elsevier, Amsterdam, pp. 21—30.
Brock, T.D., 1978. Thermophilic micro-organisms and life at high temperatures. Springer, New York, 465 pp.
Buick, R., Dunlop, I.S.R. and Groves, D.I., 1981. Stromatolite recognition in ancient rocks: an appraisal of irregularly laminated structures in an Early Archean chert-bante unit from North-Pole, Western Australia. Alcheringa, 5: 161—181.
Burlingame, A.L. and Simoneit, B.R., 1968. Analysis of the mineral entrapped fatty acids isolated from the Green River Formation. Nature, 218: 252—256.
Campbell, C.V., 1967. Lamina, lamina set, bed and bedset. Sedimentology, 8: 7—26.
Campbell, S.E., 1982. Precambrian endoliths discovered. Nature, 299: 429—431.
Cloud, P.E., 1942. Notes on stromatolites. Am. J. Sci., 240: 363—379.
Cohn, F., 1872. Untersuchungen über Bakterien. Beitr. Biol. Pflanz., 2: 127—224.
Danielli, H.M.C. and Edington, M.A., 1983. Bacterial calcification of limestone caves. Geomicrobiol. J., in press.
Druckman, Y., 1981. Sub-Recent manganese-bearing stromatolites along shorelines of the Dead Sea. In: C. Monty (Editor), Phanerozoic Stromatolites. Springer, Berlin, pp. 197—208.
Edmunds, H.L.H., Brassel, S.C. and Eglinton, G., 1982. The organic geochemistry of benthic microbial ecosystems. In: Holland and Schidlowski (Editors), Mineral Deposits and the Evolution of the Biosphere. Springer, Berlin, pp. 31—51.
Eggleston, J.R. and Dean, W.E., 1976. Fresh water stromatolitic bioherms in Green Lake, New York. In: M.R. Walter (Editor), Stromatolites — Developments in Sedimentology, 20. Elsevier, Amsterdam, pp. 479—488.
Flügel, E. (Editor), 1977. Fossil Algae, Recent Results and Developments. Springer, Berlin, 375 pp.
Flügel, E., 1982. Microfacies Analysis of Limestones. Springer, Berlin, 633 pp.
Freund, F., Knobel, R., Wengeler, H., Kathrein, H., Oberheuser, G. and Schaefer, R.G., 1982. Organic compounds in the early atmosphere formed abiotically from atomic carbon. Geol. Rundsch., 72: 1—31.
Friedman, G.M., 1980. Review of depositional environments in evaporite deposits and the role of evaporites in hydrocarbon accumulation. Bull. Cent. Rech. Explor. Prod. Elf-Aquitaine, 4: 590—608.
Friedman, G.M. and Krumbein, W.E. (Editors), 1983. The Sabkha Gavish — a model of a coastal hypersaline ecosystem. Ecological Studies. Springer, Berlin, in press.
Friedman, G.M., Amiel, A.J., Braun, M. and Miller, D.S., 1973. Algal mats, carbonate laminites, ooids, oncolites, pellets and cements in hypersaline sea-marginal pool, Gulf of Aqaba, Red Sea. Bull. Am. Assoc. Petrol. Geol., 56: 618.
Friedman, G.M. and Sanders, J.E., 1978. Principles of Sedimentology. Wiley, New York, 792 pp.
Gary, M., MacAfee, R., Jr. and Wolf, C.L. (Editors), 1972. Glossary of Geology. Am. Geol. Inst., Washington, 805 pp.
Gavish, E., Krumbein, W.E. and Tamir, N., 1978. Recent clastic carbonate sediments and sabkhas marginal to the gulfs of Elat and Suez. In: X. Int. Congress of Sedimentology, Guidebook. J.F.S., Jerusalem, pp. 309—329.
Gebelein, C.D. and Hoffman, P., 1968. Intertidal stromatolites from Cape Sable, Florida. Geol. Soc. Am. Spec. Pap., 121: 109 (abstract).
Ginsburg, R.N. and Lowenstamm, H.A., 1958. The influence of marine bottom communities on the depositional environment of sediments. J. Geol., 66: 310—318.
Golubic, S., 1973. The relationship between blue-green algae and carbonate deposits. In: N.G. Carr and B.A. Whitton (Editors), The Biology of Blue-Green Algae. Blackwell, Oxford, pp. 434—472.

Golubic, S., 1976. Biology of stromatolites. Organisms that build stromatolites. In: M.R. Walter (Editor), Stromatolites — Developments in Sedimentology, 20. Elsevier, Amsterdam, pp. 113—126.

Grosovsky, B.D.D., Kretzschmar, M., Krumbein, W.E. and Lorenz, M., 1983. Possible microbial pathways playing a role in the formation of Precambrian ore deposits. Geology J., in press.

Gygi, R.A., 1981. Oolitic iron formations: marine or not marine? Eclogae Geol. Helv., 74: 233—254.

Heim, A., 1916. Monographie der Churfürsten-Mattstock Gruppe, 3. Teil, Lithogenese. Beitr. Geol. Karte Schweiz, NF 20, Basel, pp. 369—662.

Hoffman, P.F., 1967. Algal stromatolites: use in stratigraphic correlation and paleocurrent determination. Science, 157: 1043—1045.

Hofmann, H.J., 1969. Attributes of stromatolites. Geol. Surv. Can. Pap., 69-39: 58 pp.

Holland, H.D. and Schidlowski, M. (Editors), 1982. Mineral deposits and the evolution of the biosphere. Report of the Dahlem Workshop on Biospheric Evolution and Precambrian Metallogeny. Berlin 1980, September 1—5, Springer, Berlin, 332 pp.

Ingram, R.L., 1954. Terminology for the thickness of stratification and parting units in sedimentary rocks. Geol. Soc. Am. Bull., 65: 937—938.

Jannasch, H.W. and Wirsen, C.O., 1981. Morphological survey of microbial mats near deep-sea thermal vents. Appl. Environ. Microbiol., 41: 528—538.

Javor, B.J., 1979. Ecology, physiology and carbonate chemistry of blue-green algal mats, Laguna Guerrero Negro, Mexico. Ph.D. Thesis, Dept. Biol. and Graduate School Univ. Oregon.

Johnson, J.H., 1937. Algae and algal limestones from the Oligocene of South Park, Colorado. Bull. Geol. Soc. Am., 48: 1227—1236.

Jørgensen, B.B., Revsbech, N.P., Blackburn, T.H. and Cohen, Y., 1979. Diurnal cycle of oxygen and sulfide microgradients and microbial photosynthesis in a cyanobacterial mat sediment. Appl. Environ. Microbiol., 38: 46—58.

Kalkowsky, E., 1908. Oolith and Stromatolith im norddeutschen Buntsandstein. Z. Dtsch. Geol. Ges., 60: 68—125.

Knoll, A.H. and Simonson, B., 1981. Early Proterozoic microfossils and penecontemporaneous quartz cementation in the Sokoman Iron Formation, Canada. Science, 211: 478—480.

Korolyuk, I.K., 1963. Stromatolites of the Late Precambrian. In: B.M. Keller (Editor), Stratigrafiya S.S.S.R.; Verkhnii dokembrii. Gosgeoltekhizdat, Moscow, pp. 479—498 (in Russian).

Krajewski, K.P., 1981. Phosphate microstromatolites in the High-Tatric Albian Limestones in the Polish Tatra Mts. Bull. Acad. Pol. Sci. Ser. Sci. Terre, 29: 175—183.

Kretzschmar, M., 1982. Fossil fungi in iron stromatolites from Warstein, Rhenish massif, Northwestern Germany. Facies, 7: 237—260.

Krumbein, W.E., 1963. Über Riffbildung von Placunopsis ostracina im Muschelkalk von Tiefenstockheim bei Marktbreit in Unterfranken. Abh. Naturwiss. Ver. Würzburg, 4: 1—15.

Krumbein, W.E., 1971. Manganese-oxidizing fungi and bacteria in recent shelf sediments of the Bay of Biscay and the North Sea. Naturwissenschaften, 58: 56—57.

Krumbein, W.E., 1974. On the precipitation of aragonite on the surface of marine bacteria. Naturwissenschaften, 61: 167.

Krumbein, W.E. (Editor), 1978. Environmental Biogeochemistry and Geomicrobiology. Vol. 3, Ann Arbor Sci., Ann Arbor, MI, 1055 pp.

Krumbein, W.E., 1979a. Photolithotrophic and chemo-organotrophic activity of bacteria and algae as related to beachrock formation and degradation (Gulf of Aqaba, Sinai). Geomicrobiol. J., 1: 139—203.

Krumbein, W.E. (Editor), 1979b. Cyanobakterien — Bakterien oder Algen? I. Oldenburger Symposium über Cyanobakterien, 1977. Taxonomische Stellung und Ökologie, Schriftenreihe der Universität Oldenburg (Oldb), 128 pp.

Krumbein, W.E., 1982. Work report. Stromatolite Newsl., 9: 26—27.
Krumbein, W.E., 1983. Biogene Lamination — Stromatolith und Biostrom. Festschrift E. Rutte, Weltenburger Akademie, Gruppe Gescnichte, Kelheim/Weltenburg, pp. 133—141.
Krumbein, W.E. and Altmann, H.J., 1973. A new method for the detection and enumeration of manganese oxidizing and reducing micro-organisms. Helgol. Wiss. Meeresunters., 25: 347—356.
Krumbein, W.E. and Cohen, Y., 1974. Biogene, klastische und evaporitische Sedimentation in einem mesothermen monomiktischen ufernahen Sea (Golf von Aqaba). Geol. Rundsch., 63: 1035—1065.
Krumbein, W.E. and Cohen, Y., 1977. Primary production, mat formation and lithification: contribution of oxygenic and facultative anoxygenic cyanobacteria. In: E. Flügel (Editor), Fossil Algae, Springer, Berlin, pp. 37—56.
Krumbein, W.E. and Jens, K., 1981. Biogenic rock varnishes of the Negev Desert (Israel). An ecological study of iron and manganese transformation by cyanobacteria and fungi. Oecologia, 50: 25—38.
Krumbein, W.E. and Lange-Giele, C., 1979. Calcification in a coccoid cyanobacterium associated with the formation of desert stromatolites. Sedimentology, 26: 593—604.
Krumbein, W.E., Buchholz, H., Franke, P., Giani, D., Giele, C. and Wonneberger, C., 1979a. O_2 and H_2S co-existence in stromatolites. A model for the origin of mineralogical lamination in stromatolites and banded iron formations. Naturwissenschaften, 66: 381—389.
Krumbein, W.E., Cohen, Y. and Shilo, M., 1977. Solar Lake (Sinai). 4. Stromatolitic cyanobacterial mats. Limnol. Oceanogr., 22: 635—656.
Krumbein, W.E., Rippka, R. and Waterbury, J.B., 1979b. Schematische bakteriologische Gliederung der Cyanophyten im Vergleich zur phykolotischen. In: W.E. Krumbein (Editor), Cyanobakterien — Bakterien oder Algen? Universität Oldenburg, Littman-Druck, p. 107.
Krylov, I.N., 1964. Stromatolity. In: Tommotskii Yarus i Problema Nizhnei Granitsy Kembriya. Tr. Geol. Inst. Akad. Nauk. S.S.S.R., 206(2): 323.
Lehninger, A.L., 1972. Biochemistry. Worth, New York, 1103 pp.
Logan, B.W., 1961. Cryptozoan and associate stromatolites from the Recent of Shark Bay, Western Australia. J. Geol., 69: 517—533.
Lorenz, M.G., Aardema, B.W. and Krumbein, W.E., 1981. Interaction of marine sediment with DNA and DNA availability to nucleases. Mar. Biol., 64: 225—230.
Mandoli, D.F. and Briggs, W.R., 1982. Optical properties of etiolated plant tissues. Proc. Natl. Acad. Sci. U.S.A., 79: 2902—2906.
Margulis, L., 1981. Symbiosis in cell evolution. Freeman, San Francisco, 417 pp.
Margulis, L. and Schwartz, K.V., 1982. Five Kingdoms. Freeman, San Francisco, 338 pp.
Margulis, L., Barghoorn, E.S., Giovannoni, S.J., Banerjee, S., Francis, S., Ashendorf, S., Stolz, J. and Chase, D., 1980. The microbial community at Laguna Figueroa, Baja California, Does it have Precambrian analogues? Precambrian Res., 11: 93—123.
Monty, C., 1977. 2 evolving concepts on the nature and the ecological significance of stromatolites, Liège, Belgium. In: E. Flügel (Editor), Fossil Algae. Springer, Berlin, pp. 15—36.
Monty, C., 1981. Phanerozoic Stromatolites, Case Histories. Springer, Berlin, 249 pp.
Nealson, K.H., 1982. Microbiological oxidation and reduction of iron. In: P. Westbroek and E.W. de Jong (Editors), Biomineralization and Biological Metal Accumulation. Reidel, Dordrecht, pp. 459—479.
Neumann, A.C., Gebelein, C.D. and Scoffin, T.P., 1970. The composition, structure and erodability of subtidal mats, Abaca, Bahamas. J. Sediment. Petrol., 40: 274—297.
Nissenbaum, A. (Editor), 1980. Hypersaline Brines and Evaporitic Environments. Elsevier, Amsterdam, 270 pp.

Oehler, J.H., Arneth, J.-D., Eglinton, G., Golubic, S., Hahn, J.H., Hayes, J.M., Hoefs, J.W., Hollerbach, A., Junge, C.E., Krumbein, W.E., McKirdy, D.M., Schidlowski, M. and Schopf, J.W., 1982. Reduced Carbon Compounds in Sediments. In: H.D. Holland and M. Schidlowski (Editors), Mineral Deposits and the Evolution of the Biosphere. Springer, Berlin, pp. 289—307.

Ourisson, G., Albrecht, P. and Rohmer, M., 1979. The hopanoids, paleochemistry and biochemistry of a group of natural products. Pure Appl. Chem., 51: 709—729.

Parker, B.C. and Simmons, G.M., Jr., 1981. Blue-green algal mats — living stromatolites — from frigid, light-limited Antarctic lakes. Trend in Biological Sci., pp. 111—112.

Paul, J., 1982. Der Untere Buntsandstein des Germanischen Beckens. Geol. Rdsch., 71: 795—811.

Pettijohn, F.J., 1957. Sedimentary Rocks, 2nd Edn. Harper, NY, 718 pp.

Philp, R.P., Brown, S., Calvin, M., Brassel, S. and Eglinton, G., 1978. Hydrocarbon and fatty acid distributions in recently deposited algal mats at Laguna Guerrero, Baja California. In: W.E. Krumbein (Editor), Environmental Biogeochemistry and Geomicrobiology. Ann Arbor Sci., Ann Arbor, MI, pp. 255—270.

Pia, J., 1926. Pflanzen als Gesteinsbildner. Bornträger, Berlin, 355 pp.

Pia, J., 1928. Die Anpassungsformen der Kalkalgen. Paläobiologie, 1: 211—244.

Pochon, J., Chalvignac, M.A. and Krumbein, W.E., 1964. Recherches biologiques sur le mondmilch. C.R. Acad. Sci. Paris, 258: 5113—5115.

Potts, M., Krumbein, W.E. and Metzger, J., 1978. Nitrogen fixation rates in anaerobic sediments determined by acetylene reduction, a new ^{15}N field assay, and simultaneous total N ^{15}N determination. In: W.E. Krumbein (Editor), Environmental Biogeochemistry and Geomicrobiology, 3: Methods, Metals and Assessment. Ann Arbor Sci., Ann Arbor, MI, pp. 753—769.

Read, J.F., 1976. Calcretes and their distinction from stromatolites. In: M.R. Walter (Editor), Stromatolites — Developments in Sedimentology, 20. Elsevier, Amsterdam, pp. 55—71.

Riding, R., 1977. Skeletal stromatolites. In: E. Flügel (Editor), Fossil Algae, Recent Results and Developments. Springer, Berlin, pp. 57—60.

Rippka, R., Deruelles, J., Waterbury, J.B., Herdman, M. and Stanier, R.Y., 1979. The cyanobacteria, generic assignments, strain histories and properties of pure cultures of cyanobacteria. J. Gen. Microbiol., 111: 1—61.

Rongen, P., 1979. Das Farbstreifen-Sandwatt als rezentes Beispiel von Stromatolithen. In: W.E. Krumbein (Editor), Paläontologische Gesellschaft, 49. Jahresversammlung, Kurzfassungen und Exkursionsführer Oldenburg (Oldb), pp. 24—25.

Rutte, E., 1953. Süsswasserkalke aus dem Kaiserstühl und Breisgau. Ber. Naturforsch. Ges. Freiburg im Breisgau, 43: 1—38.

Schlegel, H.G. and Jannasch, H.W., 1981. Prokaryotes and their habitats. In: M.P. Starr et al. (Editors), The Prokaryotes. Springer, New York, pp. 43—82.

Schopf, J.W. (Editor), 1983. Origin and Evolution of the Earth's Earliest Biosphere. Princeton Press, in press.

Schubert, W., Giani, D., Rongen, P., Krumbein, W.E. and Schmidt, W., 1980. Photoacoustic in-vivo spectra of recent stromatolites. Naturwissenschaften, 67: 129—132.

Schwartz, H.-U., Einsele, G. and Herm, D., 1975. Quartz-sandy, grazing-contoured stromatolites from coastal embayments of Mauritania, West Africa. Sedimentology, 22: 539—561.

Seibold, E., 1962. Untersuchungen zur Kalkfällung und Kalklösung am Westrand der Great Bahama Bank. Sedimentology, 1: 50—74.

Shilo, M. (Editor), 1979. Strategies of Microbial Life in Extreme Environments. Verlag Chemie, Weinheim, p. 11.

Shilo, M., 1980. Strategies of adaptation to extreme conditions in aquatic microorganisms. Naturwissenschaften, 67: 384—389.

Shrock, R.R., 1948. Sequence in Layered Rocks, McGraw-Hill, New York, NY, 507 pp.
Skyring, G.W. and Johns, I.A., 1980. Iron in Cyanobacterial Mats. Pergamon, Oxford, pp. 407—408.
Stackebrandt, E., 1981. Neue Aspekte zur Evolution der Zelle. Progress Naturwissen. Biol., 11: 331—342.
Stackebrandt, E. and Woese, C.R., 1981. The evolution of prokaryotes. In: Carlile, Collins and Moseley (Editors), Molecular Aspects of Microbial Evolution. Cambridge University Press, Cambridge, pp. 1—31.
Stal, L.J. and Krumbein, W.E., 1981. Aerobic nitrogen fixation in pure cultures of a benthic marine *Oscillatoria* (cyanobacteria). Microbiol. Lett., 11: 295—298.
Stal, L.J. and Krumbein, W.E., 1982a. Nitrogen fixation in a laminated microbial ecosystem. Zentralbl. Bakteriol. Mikrobiol. Hyg. Abt. 1, Orig. Reihe C, 3: 564.
Stal, L.J. and Krumbein, W.E., 1982b. Nitrogen fixation in a benthic *Oscillatoria* under aerobic and oxygenic conditions. IV. Int. Symp. Photosynthetic Prokaryotes. Abstracts A 27 a—b.
Stal, L.J., van Gemerden, H.G. and Krumbein, W.E., 1982. Characterization of mixed microbial populations by photopigment analysis. IV. Int. Symp. Photosynthetic Prokaryotes. Abstracts A 28 a—b.
Starr, M.P., Stolp, H., Trüper, H.G., Balows, A. and Schlegel, H.G. (Editors), 1981. The Prokaryotes. Springer, New York, 2284 pp.
Thrailkill, J., 1976. Speleothems. In: M.R. Walter (Editor), Stromatolites — Developments in Sedimentology, 20. Elsevier, Amsterdam, pp. 73—86.
Trudinger, P.A. and Swaine, D.J. (Editors), 1979. Biogeochemical Cycling of Mineral-Forming Elements. Elsevier, Amsterdam, 612 pp.
Trudinger, P.A. and Walter, M.R. (Editors), 1980. Biogeochemistry of Ancient and Modern Environments. Australian Acad. Sci., Canberra, 723 pp.
Trüper, H.G., 1982. Microbial processes in the sulfur cycle through time. In: H.D. Holland and M. Schidlowski (Editors), Mineral Deposits and the Evolution of the Biosphere. Springer, Berlin, pp. 5—30.
Walter, M.R. (Editor), 1976a. Stromatolites — Developments in Sedimentology, 20. Elsevier, Amsterdam, 790 pp.
Walter, M.R., 1976b. Geyserites of Yellowstone National Park: an example of abiogenic "stromatolites". In: M.R. Walter (Editor), Stromatolites — Developments in Sedimentology, 20. Elsevier, Amsterdam, pp. 87—112.
Wickstrom, C.E., 1980. Distribution and physiological determinants of blue-green algae nitrogen fixation along a thermal gradiant. J. Phycol., 16: 436—443.
Young, P., 1981. Thick layers of life blanket lake bottoms in Antarctica valleys. *BioScience*, pp. 53—60.

This Page Intentionally Left Blank

STRATIFORM COPPER DEPOSITS AND INTERACTIONS WITH CO-EXISTING ATMOSPHERES, HYDROSPHERES, BIOSPHERES AND LITHOSPHERES

A.C. BROWN and F.M. CHARTRAND

Dept. of Mineral Engineering, Ecole Polytechnique, P.O. Box 6079, Station "A", Montreal H3C 3A7 (Canada)

ABSTRACT

Brown, A.C. and Chartrand, F.M., 1983. Stratiform copper deposits and interactions with co-existing atmospheres, hydrospheres, biospheres and lithospheres. Precambrian Res., 20: 533–542.

Fundamental evidence from world-class stratiform copper deposits repeatedly indicates that they originated by a two-stage mineralization process: a syn-diagenetic enrichment of the host sediment in iron sulfide, followed by a sub-surface addition of copper during early diagenesis of the sediment. In contrast to the previously favored syngenetic hypothesis, which suggested an open equilibration between atmosphere, hydrosphere, biosphere and upper lithosphere during mineralization, the two-stage model implies that only the initial deposition of iron sulfides should take place with open exchanges between the upper "spheres". The sub-surface emplacement of copper should occur in relative isolation from surface environments and, therefore, the occurrence and distribution of stratiform copper deposits through time and space should not be used to make direct interpretations of contemporaneous conditions in the upper "spheres".

INTRODUCTION

In general, the sedimentary character of stratiform copper mineralization suggests that these deposits are reaction products of their local surface environments and might, therefore, form a basis for interpretation of the nature of their contemporaneous atmospheres, hydrospheres, biospheres and/or lithospheres. This possibility would be especially appropriate if indeed stratiform copper deposits had syngenetic, syn-sedimentary origins, analogous to sedimentary iron-formations which have been used to model the iron–oxygen balance at the Earth's surface in Precambrian time (e.g., Cloud, 1968; Garrels, 1981).

However, over the past two decades, diagnostic evidence has been accumulating against the concept of strictly syngenetic deposition of copper in so-called "stratiform" copper deposits. Nevertheless, at the present time, the syngenetic–epigenetic controversy continues (Gustafson and Williams,

1981). The term "stratiform" is not entirely satisfactory for the type of sediment-hosted copper mineralization discussed here because on close examination the cupriferous zone is generally found to be pene-conformable to the host strata. Unfortunately, a simple alternative term has not yet been found to identify the deposit-type referred to in this paper (examples: the Central African copperbelt; the Kupferschiefer ores of the German—Polish copperbelt). Note as well that the deposits discussed here do not include continental red-bed deposits of the "sandstone U—V—Cu" type. In this paper, further evidence is given in support of a post-sedimentary, early diagenetic introduction of copper to the host sediment. Consequently, concepts of open interactions between the upper "spheres" (atmosphere, hydrosphere, biosphere and upper lithosphere), such as might be expected in syngenetic models, must be modified to suit diagenetic aspects of the post-sedimentary model.

In the generalized conceptual model described here (Fig. 1), the initial sulfide enrichment of the host sediments is still largely considered to be a product of open interaction between the uppermost "spheres" of an active sedimentary marine basin. However, the subsequent enrichment in copper (forming copper-bearing sulfides by reaction with the earlier emplaced sulfide) is considered to be a sub-surface process, isolated to a significant degree from conditions in the overlying basin and atmosphere. The generation of sub-surface cupriferous solutions, now commonly believed to result from leaching of metal from adjacent immature red-bed sediments, may be only indirectly related to conditions in the upper "spheres". These general concepts are developed in greater detail below.

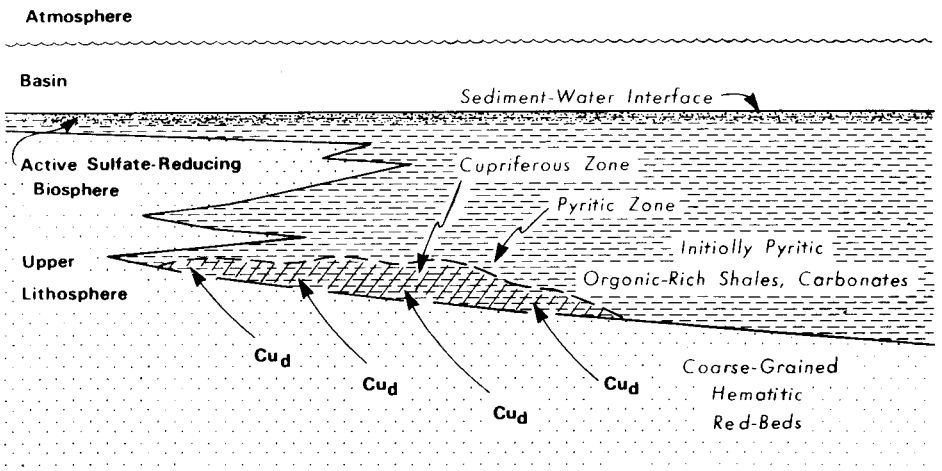

Fig. 1. Schematic model for stratiform copper mineralization showing locations of (1) syn-diagenetic iron sulfide accumulation beneath an active sediment—water interface, and (2) early diagenetic copper deposition by a sub-surface influx of dissolved copper (Cu_d) into the initially pyrite sediment.

THE DIAGENETIC (EPIGENETIC) ORIGIN OF STRATIFORM COPPER DEPOSITS

General

For over 200 years, the famous Kupferschiefer ores of Germany were considered to be syngenetic in origin and, in post-World War II years, the Northern Rhodesian (now Zambian) Copperbelt ores have also been thought of as syn-sedimentary deposits (e.g., Garlick, 1961, 1981; Fleischer et al., 1976). While studies on these impressive European and African deposits still suggest to some geologists that the origin of stratiform copper deposits is syngenetic, recent investigation of these and other stratiform copper deposits around the world now indicate that a post-sedimentary addition (Brown, 1981) of copper to the host-strata would be more consistent with observed details of their mineralization.

Without citing all of the evidence for a diagenetic origin, a summary is given of a few of the more outstanding features supporting this hypothesis. In his petrographic analysis of the Zairian portion of the Central African Copperbelt, Bartholomé (1962) was among the first to provide compelling evidence (now substantiated by several independent investigations of other stratiform copper deposits) that the Zairian deposits exhibit a step-by-step diagenetic replacement of iron-rich sulfides by copper-rich sulfides. The sequence pyrite → chalcopyrite → bornite → digenite → chalcocite indicates a post-sedimentary addition of copper to formerly pyritic sediments. Bartholomé and Katekesha (1971), Bartholomé et al. (1972) and Bartholomé (1974) present additional textural interpretations supporting this concept of diagenetic copper emplacement, and propose that the copper was introduced from red-beds underlying the ore horizons.

White (1960) noted that the cupriferous zone at the White Pine stratiform copper deposit of northern Michigan is not strictly conformable with bedding, and that the top of the cupriferous zone is characterized by a narrow zone of pyrite—chalcopyrite—bornite—chalcocite overlain by anomalous concentrations of cadmium sulfide. Studies by Brown (1965, 1971) and White and Wright (1966) describe the emplacement of this copper by an upward advancing mineralization front. It was concluded that copper was derived from the underlying red-beds, and copper deposition resulted from an encounter of cupriferous brines with syn-diagenetic pyrite in the basal portion of organic-rich host "shales".

While the laterally extensive Kupferschiefer mineralization has long been considered the classic example of syngenetic stratiform copper deposits, many authors (e.g., Schouten, 1946; Rentzsch and Knitzschke, 1968; Rentzsch, 1974) have drawn attention to the diagenetic replacement textures showing pyrite replacement by copper-bearing sulfides in the Kupferschiefer, and have demonstrated that the mineralization is significantly discordant relative to bedding. A vertical and lateral zoning of copper, lead and zinc above subjacent red-beds once more suggests copper infiltration from permeable continental beds underlying the ore horizon.

The above examples represent only a few of the features which argue for the post-sedimentary emplacement of copper in stratiform copper deposits. A more complete compilation of these features is given by Brown (1978, 1981). The following description of the Redstone copper deposits results from an additional detailed investigation of another important stratiform copper deposit, and illustrates once again that mineralization took place during diagenesis of the host strata. The significance of this conclusion relative to interactions in the upper "spheres" is described in subsequent sections.

The Redstone example

A recent study by Chartrand (1981), and Chartrand and Brown (1981) has resulted in the identification of four distinct stages in the syngenetic and early diagenetic history of carbonate horizons hosting the stratiform copper mineralization at the Coates Lake deposits of the Redstone Copperbelt, Northwest Territories, Canada. In this well-preserved example of Upper Proterozoic copper mineralization, the carbonate host-rocks have been recognized as coastal sabkha horizons interbedded with reddish continental siltstones at the transition from a major continental red-bed unit into overlying marine carbonates (Ruelle, 1982). Close examination of the carbonate beds has revealed numerous features equivalent to those found in intertidal and supratidal zones of modern sabkha sediments found along the Trucial coast of the Persian Gulf. The following is a summary of the principal features which led Chartrand to propose a post-sedimentary deposition of copper at Coates Lake.

Stage I (syn-diagenesis)

(1) Dolomicritic beds overlying algal-laminated limestones of intertidal origin are characterized by blade-like crystals of anhydrite pseudomorphic after gypsum (Fig. 2). The transformation of virtually syngenetic gypsum to anhydrite is a commonly observed feature in the uppermost few centimetres of modern intertidal sediments.

(2) By analogy with dolomitization observed in modern sabkhas, the dolomicrites mentioned above should also have formed at the earliest syn-diagenetic stage when the loss of Ca^{+2} from the tidal waters during gypsum—anhydrite precipitation would have generated residual dolomitizing surface waters on the tidal plains.

(3) Syn-diagenetic pyrite forms disseminated euhedra in the carbonate beds and replaces gypsum—anhydrite in the blade-like grains described above. This iron-sulfide probably precipitated under anoxic conditions existing in decaying algal mats slightly beneath the sedimentary interface.

Stage II (very early diagenesis)

(4) The disseminated pyrite euhedra (Fig. 3) are rimmed by epitaxial calcite.

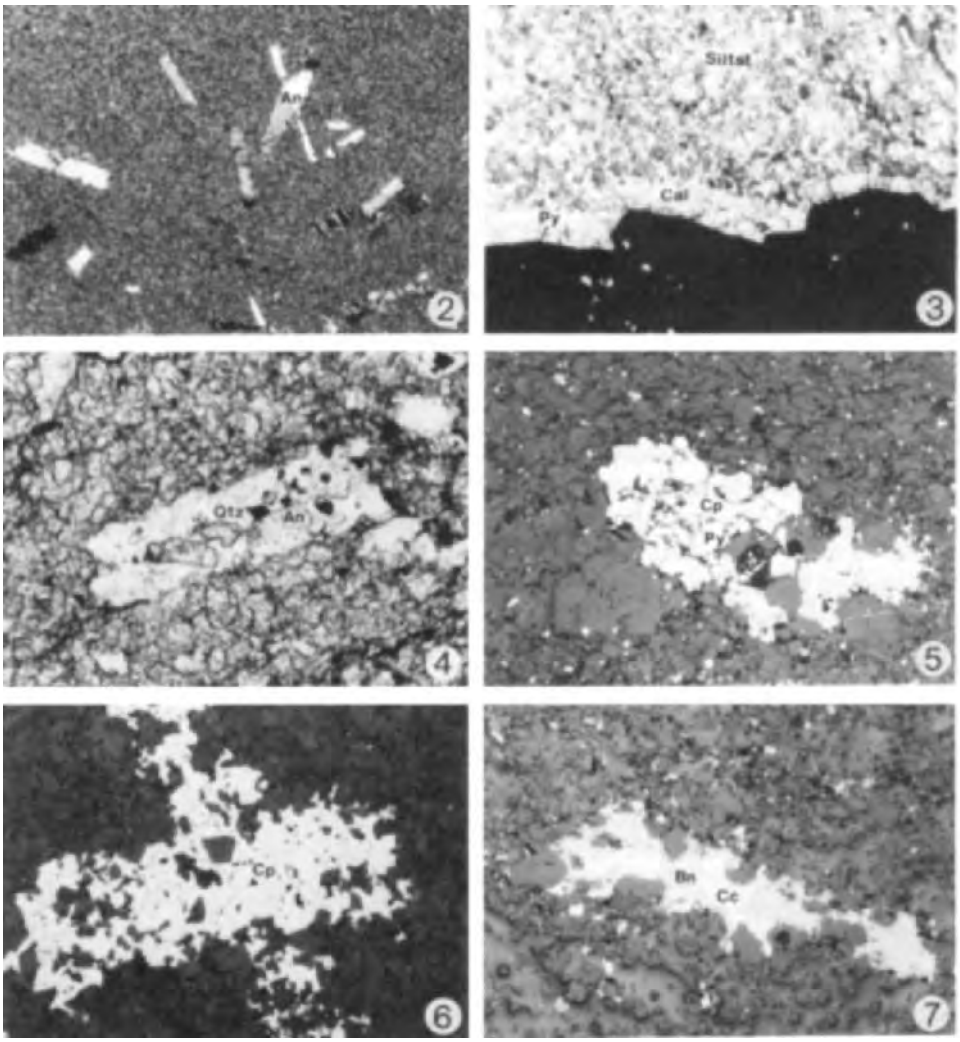

Figs. 2—7. (2) Anhydrite pseudomorphic after gypsum laths in dolomicritic beds, Redstone area, N.W.T. (transmitted light, crossed polars, 40X, B2-04. (3) Epitaxial calcite rimming the border of pyrite euhedra in greenish siltstone (transmitted light, 40X, FC-3). (4) Quartz replacing anhydrite pseudomorphic after gypsum laths in dolomicritic beds (transmitted light, 160X, FC-22). (5) Chalcopyrite replacing pyrite within pseudomorphs after gypsum laths (reflected light, 125X, B3-45). (6) Chalcopyrite pseudomorphic after gypsum laths (reflected light, 125X, FC-52). (7) Bornite and chalcocite pseudomorphic after gypsum laths (reflected light, 125X, B1-10).

(5) Partial replacement of gypsum—anhydrite blades by calcite, quartz and feldspars is illustrated in Fig. 4. Quartz and feldspars also form authigenic grains in the algal-laminated layers. Overgrowth textures indicate the presence of more than one generation of stage II quartz.

Stage III (ore-stage diagenesis)

(6) Copper-bearing sulfides replace remnants of anhydrite, quartz and pyrite from stages I and II above (Fig. 5).

(7) Blade-like grains of gypsum—anhydrite origin are partially or totally filled by copper-bearing sulfides (chalcopyrite, bornite, digenite and chalcocite; Figs. 6 and 7).

Stage IV (post-ore diagenesis)

(8) Pores of the mineralized carbonates are filled with neomorphic calcite. This calcite probably reduced the porosity and permeability of the algal-laminated layers, and arrested the influx of cupriferous solutions.

From the above, it is obvious that copper emplacement at Coates Lake occurred after identifiable syngenetic and very early diagenetic events (as observed in the studies of the other stratiform copper deposits mentioned earlier). Furthermore, this mineralization exhibits a zoning of sulfides similar to other deposits of this type: copper-rich sulfides, such as chalcocite and digenite, are most abundant in its lowermost strata; intermediate Cu—Fe sulfides, such as bornite and chalcopyrite occur at higher stratigraphic levels; and the iron-rich sulfide, pyrite, predominates in the overlying unmineralized beds. It has also been noted that copper reaches higher stratigraphic levels in some drill-hole profiles than in others, suggesting that the sulfide zoning is moderately transgressive to bedding, as found in many other stratiform copper deposits. While the Coates Lake deposit of the Redstone Copperbelt does exhibit many unique features of its own, its genesis appears to conform closely to a general model for this deposit-type.

THE GENERALIZED ORE-FORMING MODEL

As a result of the numerous studies cited above, the syngenetic origin of stratiform copper mineralization is rejected in favor of copper emplacement during early diagenesis of the host strata. The general model, applicable to most stratiform copper deposits, is characterized by the following fundamental features.

(1) The host-rock is initially enriched in sulfides. Depending on the local sedimentary environment, this sulfide could be deposited directly as disseminated iron-sulfides during earliest diagenesis of the uppermost levels of recently deposited organic-rich muds. Alternatively, the sulfur of the sulfide may be deposited initially as evaporitic gypsum—anhydrite which subsequently experiences partial or complete replacement during very early diagenesis; the dissolved sulfate would then be reduced to sulfides by bacterial activity.

(2) Subsequently, mineralizing solutions percolate through the sulfide-rich beds and deposit copper-bearing sulfides (with variable amounts of lead, zinc and other sulfophile metals) by replacement of the earlier iron sulfides. The final configuration of the mineralized zone is moderately cross-cutting relative to bedding, and the sulfides exhibit a zonal distribution within the mineralized zone. The mineral zone is typically located in the lowest beds of reducing, organic-rich, sulfide-rich sediments and occurs adjacent to oxidized red-beds from which the copper was derived. While various explanations may be given for the ultimate source of copper, the most obvious source would be immature clastic debris in the red-beds. Mafic volcanic clasts, for example, could contribute up to 400 ppm copper by leaching with chloride-rich brines under oxidizing conditions.

This two-stage general model (early, syngenetic sulfide enrichment, and subsequent additions of copper during diagenesis) has been referred to as a diplogenetic process (Lovering, 1963). Its implications regarding interactions between the contemporaneous atmosphere, hydrosphere, biosphere and upper lithosphere are discussed below.

INTERACTIONS OF THE ATMOSPHERE, HYDROSPHERE, BIOSPHERE AND LITHOSPHERE — CONSEQUENCES OF THE GENERALIZED ORE-FORMING MODEL

Several interactions should occur between the upper "spheres" during the step-by-step formation of stratiform copper deposits. Other potential interactions should be restricted or even prevented where certain environments are physically isolated from each other. The following is a discussion of the more obvious interactions which should exist at various stages in the formation of these stratiform deposits.

(1) The "ground preparation" of the host-strata involves the syn-diagenetic, pre-ore accumulation of sulfides, which subsequently react with introduced copper to form mineralized beds. The sulfide precipitation is initiated by an influx of seawater sulfate across the sedimentary interface and into the uppermost bottom muds. Sulfate-reducing bacteria, thriving under anoxic conditions in the presence of organic food, reduce this sulfate to sulfide through metabolical processes (Berner, 1971). Obviously this environment calls for quiet, stagnant conditions within the muds in order to exclude the possibility of oxidation by overlying seawater which may be in equilibrium with an oxidizing(?) atmosphere.

(2) The bacterially-produced sulfide reacts quickly in situ with iron-bearing minerals of the soft muds to form primitive iron sulfides which soon crystallize and recrystallize to form what is commonly called syngenetic or syndiagenetic pyrite. Again, this reaction takes place in isolation from possible oxidizing atmospheres and hydrospheres overlying the sedimentary interface. Obviously this precipitation and accumulation of initial iron sulfides occurs in the presence of an active biosphere, and involves interactions with pore waters and solid constituents of the sediment.

(3) The chloride-rich brines called upon for the sub-surface transport of copper may have diverse origins (e.g., see White, 1968, 1981): e.g., ultrafiltration of connate waters, or equilibration of meteoric waters with rock units during deep circulation. The dominant interaction involves pore water and solid mineral phases deep within the basin sediments. In the case of descending oxygenated meteoric waters, there should be initial interactions between the surface water (hydrosphere) and the atmosphere, then interactions between the descending water and the near-surface sediments. Equilibration of the interstitial meteoric water with the sediments should modify the chemistry of the water. The surficial origin of the descending water would be masked to such an extent that recognition of the former association of the water with the atmosphere would become increasingly difficult. Some studies, such as isotopic analyses (e.g., S, D/H, O, Sr, C) have attempted to determine the origins of certain modern metalliferous brines. In general, these investigations have failed to identify the sources of the brine constituents without encountering serious ambiguities (White, 1981). These difficulties probably arise from complexities in sub-surface hydrologic systems and uncertain lithologies at depth (e.g., presence or absence of evaporitic units).

(4) Once an oxygenated interstitial chloride-rich brine has been generated, it should be able to leach trace amounts of metals from the enclosing sediments due to the formation of stable metal—chloride complexes (e.g., $CuCl_3^{-2}$). Large volumes of immature sediments containing mafic detritus could provide important quantities of cupriferous brine. This sub-surface rock/water interaction would tend to be more efficient at depth where higher temperatures would be expected. Mineralization would be especially effective if the enclosing sediments were porous and permeable (i.e., if the ore fluid were formed in an aquifer, as is the case for coarse-grained redbeds commonly found to underlie stratiform copper deposits). Furthermore, it would be important that this brine circulate within the aquifer so that large amounts of metals could be transported to the site of copper emplacement in adjacent sulfide-bearing "shales". Transport mechanisms involving pressure and temperature gradients, recycling of brines, ultrafiltration processes, etc. have been discussed by White (1968), Brown (1970) and others.

(5) The final interaction responsible for stratiform copper deposition is the early diagenetic replacement of original syn-diagenetic iron sulfide by copper-bearing sulfides under the reducing conditions present in an organic-rich host-rock. The result is a simple exchange of sulfur derived from pyrite to form a zoned array of chalcopyrite, bornite, diagenite and chalcocite, with a moderate transgression of bedding by the cupriferous zone as described earlier.

Thus, the emplacement of copper in its stratiform host takes place in isolation from the atmosphere, the surface hydrosphere, the active biosphere and the sediments still being deposited at the overlying sediment/water interface. Nevertheless, it is obvious from this brief account that copper

deposition is ultimately dependent on several processes in which both surface and sub-surface environments and interactions are vitally significant.

CONCLUSIONS

Investigations concluding that stratiform copper mineralization is due to post-sedimentary processes impose many constraints on any postulated direct interactions between the contemporaneous atmosphere, hydrosphere, biosphere and lithosphere. Nevertheless, if the syngenetic model is adhered to, then of course the suggested constraints may be disregarded. On the other hand, for those who adopt the diagenetic model supported here, these same constraints may be seen as guidelines to an improved understanding of the complexities involved in this diplogenetic mineralization process.

Considering the mounting evidence in favor of the diagenetic model, it would seem wise to give more thought and effort to definitive studies of detailed features within this model (e.g., the sub-surface generation of cupriferous ore solutions with or without associated metals such as lead, zinc, silver and cobalt). As this research progresses, it would be expected that the present four-fold classification of the upper "spheres" would give way to a more detailed series of surface and sub-surface environments. Reactive constituents from two or more "spheres" should combine to define and control local sub-environments for each step in the mineralizing process. It is hoped that this report may aid in the design of such studies.

ACKNOWLEDGMENTS

This paper benefits from numerous studies and countless discussions on the genesis of stratiform copper deposits over past years, and we wish to thank all who have contributed directly and indirectly to the development of our current concepts on such mineralization. Of course, we remain responsible for the particular interpretations and conclusions expressed here.

We are especially grateful to Shell Canada Resources Ltd. for financial and logistical support during our studies of the Redstone deposits. The generous assistance and guidance of A.B. Baldwin and J.C.L. Ruelle have been particularly appreciated. A.C.B. is also supported by a grant from the National Science and Engineering Research Council of Canada for continuing studies on the metallogeny of stratiform copper mineralization.

REFERENCES

Bartholomé, P., 1962. Les minerais cupro-cobaltifères de Kamoto (Katanga—Ouest). Partie I, pétrographie. Partie II, paragenèse. Studia Univ.Louvanium, Fac. Sci., 14: 1—40; 16: 1—24.

Bartholomé, P., 1974. On the diagenetic formation of ores in sedimentary beds, with special reference to the Kamoto deposits. In: P. Bartholomé (Editor), Gisements Stratiformes et Provinces Cuprifères. Soc. Géol. Belgique, Liège, pp. 203—214.

Bartholomé, P. and Katekesha, F., 1971. Cobalt zoning in microscopic pyrite from Kamoto, Republic of the Congo (Kinshasa). Miner. Deposita, 6: 167—176.

Bartholomé, P., Evrard, P., Katekesha, F., Lopez-Ruiz, J.M. and Ngongo, M., 1972. Diagenetic ore-forming processes at Kamoto, Katanga, Republic of the Congo. In: G.C. Amstutz and A.J. Bernard (Editors), Ores in Sediments. Springer-Verlag, Berlin, pp. 21—41.

Berner, R.A., 1971. Principles of Chemical Sedimentology. McGraw-Hill, New York, 240 pp.

Brown, A.C., 1965. Mineralogy at the top of the cupriferous zone, White Pine mine, Ontonagon County, Michigan. Univ. Michigan, M.Sc. Thesis, 81 pp.

Brown, A.C., 1970. Environments of generation of some base-metal deposits (discussion). Econ. Geol., 65: 60—61.

Brown, A.C., 1971. Zoning in the White Pine copper deposit, Ontonagon County, Michigan. Econ. Geol., 66: 543—573.

Brown, A.C., 1978. Stratiform copper deposits — evidence for their post-sedimentary origin. Miner. Sci. Eng., 10: 145—163.

Brown, A.C., 1981. The timing of mineralization in stratiform copper deposits. K.H. Wolf (Editor), Handbook of Strata-bound and Stratiform Ore Deposits. Elsevier, Amsterdam, pp. 1—23.

Chartrand, F., 1981. Evolution diagénétique des dépôts stratiformes de cuivre du Lac Coates, ceinture cuprifère de Redstone, Territoires du N.O., Canada. Ecole Polytechnique de Montréal, M.Sc. Thesis, 137 pp.

Chartrand, F. and Brown, A.C., 1981. Diagenetic stratiform copper deposits, Redstone area, N.W.T., Canada. Geol. Soc. Am., Abstr. with Programs, 13: 426.

Cloud, P.E., 1968. Environments and organisms on the primitive Earth. In: The Primitive Earth, a Symposium. Miami Univ., Oxford, Ohio.

Fleischer, V.D., Garlick, W.C. and Haldane, R., 1976. Geology of the Zambian copperbelt. In: K.H. Wolf (Editor), Handbook of Strata-bound and Stratiform Ore Deposits. Elsevier, Amsterdam, pp. 253—406.

Garlick, W.C., 1961. The syngenetic theory. In: F. Mendelsohn (Editor), The Geology of the Northern Rhodesian Copperbelt. MacDonald, London, 523 pp.

Garlick, W.C., 1981. Sabkhas, slumping and compaction at Mufulira, Zambia. Econ. Geol., 76: 1817—1847.

Garrels, R.M., 1981. Waters of the Early Proterozoic. In: Early Crustal Genesis. International Proterozoic Symposium. Univ. Wisconsin—Madison (Abstracts), May 1981.

Gustafson, L.B. and Williams, N., 1981. Sediment-hosted stratiform deposits of copper, lead and zinc. Econ. Geol., 75: 139—178.

Lovering, T.S., 1963. Epigenetic, diplogenetic, syngenetic and lithogene deposits. Econ. Geol., 58: 315—331.

Rentzsch, J., 1974. The "Kupferschiefer" in comparison with deposits of the Zambian copperbelt. In: P. Bartholomé (Editor), Gisements Stratiformes et Provinces Cuprifères. Soc. Géol. Belgique, Liège, pp. 403—418.

Rentzsch, J. and Knitzschke, G., 1968. Die Erzmineralparagenesen des Kupferschiefers und ihre regionale Verbreitung. Freiberg. Forschungsh. C, 231: 189—211.

Ruelle, J.C.L., 1982. Depositional environments and genesis of stratiform copper deposits of the Redstone copper belt, Mackenzie Mountains, N.W.T. In: R.W. Hutchinson, C.D. Spence and J.M. Franklin (Editors), Precambrian Sulphide Deposits. Geol. Assoc. Can. Spec. Pap., 25: 701—737.

Schouten, C., 1946. The role of sulfur bacteria in the formation of the so-called sedimentary copper ore and pyritic ore bodies. Econ. Geol., 41: 517—538.

White, D.E., 1968. Environments of generation of some base-metal ore deposits. Econ. Geol., 61: 402—410.

White, D.E., 1981. Active geothermal systems and hydrothermal ore deposits. Econ. Geol., 75: 392—423.

White, W.S., 1960. The White Pine copper deposit (discussion). Econ. Geol., 55: 402—410.

White, W.S. and Wright, J.C., 1966. Sulfide-mineral zoning in the basal Nonesuch Shale. Econ. Geol., 61: 1171—1190.

ORIGIN AND DISTRIBUTION OF GOLD IN THE HURONIAN SUPERGROUP, CANADA — THE CASE FOR WITWATERSRAND-TYPE PALEOPLACERS

D.J. MOSSMAN

Department of Geology, Mount Allison University, Sackville, New Brunswick EOA 3CO (Canada)

G.A. HARRON

DuPont of Canada Exploration Ltd., Suite 102, 1550 Alberni Street, Vancouver, British Columbia V6G 1A5 (Canada)

ABSTRACT

Mossman, D.J. and Harron, G.A., 1983. Origin and distribution of gold in the Huronian Supergroup, Canada — the case for Witwatersrand-type paleoplacers. Precambrian Res., 20: 543—583.

Field observations and experimental results show that gold is mobile under a wide range of natural conditions in the surficial environment. However, the extent to which, and the form(s) in which gold was mobile in ancient placers remains speculative. Rather more convincing is the extent to which diagenetic and metamorphic processes have been active in redistributing the gold.

Huronian paleoplacer gold deposits span a critical transition in Earth history, namely, the oxyatmoversion, evidence for which exists in the upper Gowganda Formation dated at 2.288 Ga. Prior to this transition, deposition of gold occurred under reducing atmospheric conditions, with transportation of the more finely-divided material possibly as organic-protected colloids, as has been suggested for the Witwatersrand. Following the oxyatmoversion, gold deposition will have been subject to secondary enrichment, like many Phanerozoic placer gold occurrences. For this reason, and on purely sedimentological grounds, upper Huronian strata ought to have as much potential for hosting economic deposits of gold as the basal units.

A total of 121 Au and Au—U occurrences, including several past and presently producing mines from the Huronian Supergroup, are examined. These are classified according to whether mineralization is: in or adjacent to diabase dikes (11 cases); in (quartz, quartz—carbonate) veins (85 cases); stratiform (25 cases). Of the non-diabase-hosted occurrences, 41.3% occur in the Cobalt Group, 15.7% in the Quirke Lake Group, 24.9% in the Hough Lake Group and 9% in the Elliott Lake Group.

Frequency of occurrence can be related to transgressive sedimentary cycles, with deposits concentrated in the Matinenda, Mississagi and Gowganda Formations, which immediately overlie the Archean—Huronian unconformity. Most of the deposits occur in the Gowganda Formation, although none of these is stratiform.

In terms of Au content, there is a large overlap in class intervals of stratiform vein deposits. Vein deposits are, in general, richer than stratiform by a factor of 10. Selected stratiform deposits in the Matinenda, Mississagi and Serpent Formations are examined in

light of available geological and geochemical data. In these deposits, anomalous gold values in dominantly quartzitic metasediments are accompanied by fine-grained pyrite and other heavy minerals, including uranium, which occurs in most, but not all cases. Metamorphic grade ranges from upper greenschist to lower amphibolite facies. A few of the stratiform occurrences are accompanied by accumulations of carbonaceous material, an association reminiscent of the Witwatersrand goldfields.

Results of electron-microprobe study indicate that much of the gold in the Huronian metasediments occurs as low level concentrations in pyrite of morphologically different types, in arsenopyrite, chalcopyrite, and in pyrrhotite variously altered to marcasite. It is clear that Huronian paleoplacer gold deposits exist, but only in conditions much modified by diagenetic and metamorphic processes.

INTRODUCTION

A great deal of interest is currently being shown in the potential of the Huronian Supergroup for hosting not only stratiform uranium deposits, but also stratiform gold. Most of the occurrences are located well to the east of the well known uranium camps of Elliot Lake and Blind River; in particular, they appear concentrated in the area known as the Cobalt Embayment northeast of Sudbury (Figs. 1 and 2).

Some of the Au occurrences are associated, not only with heavy-mineral suites such as pyrite, uranium and Fe—Ti oxides, but also with concentrations of carbonaceous material. This relationship may be significant in light of the fact that in the Witwatersrand nearly 50% of all payable conglomerate sheets contain carbonaceous matter (Tankard et al., 1982, p. 133). The South African material is more properly termed kerogen (Zumberge et al., 1978).

The nature of the Huronian material, generally referred to as "thucholite", is less well understood. It has long been known from the Elliot Lake ores, although it has evidently not been considered common (Theis, 1979, p. 32). Recently, numerous new occurrences of U—C have been located in the Huronian between Agnew and Elliot Lakes (V.R. Ruzicka, personal communication, 1981). These occurrences are similar to material described by Ruzicka and Steacy (1976); particulate gold is absent in this so-called thucholite.

In the case of the Witwatersrand, the results of research carried out by Hallbauer (1976) and Hallbauer and Warmelo (1974) indicate that at least some of the Rand's gold-bearing kerogen originated as primitive organic form(s) of life. Pretorius (1974) describes the material as algal mats. It is intriguing to consider the possibility that, in addition to the many geological and sedimentological similarities that the basal Huronian has with the Witwatersrand, a similar sort of organic connection may exist between C and Au and/or U in the Huronian rocks.

The search for gold in the Huronian Supergroup raises many questions in addition to those of origin and distribution. How closely do the pyritic U—Au conglomerates and sandstones of the Lower Huronian resemble

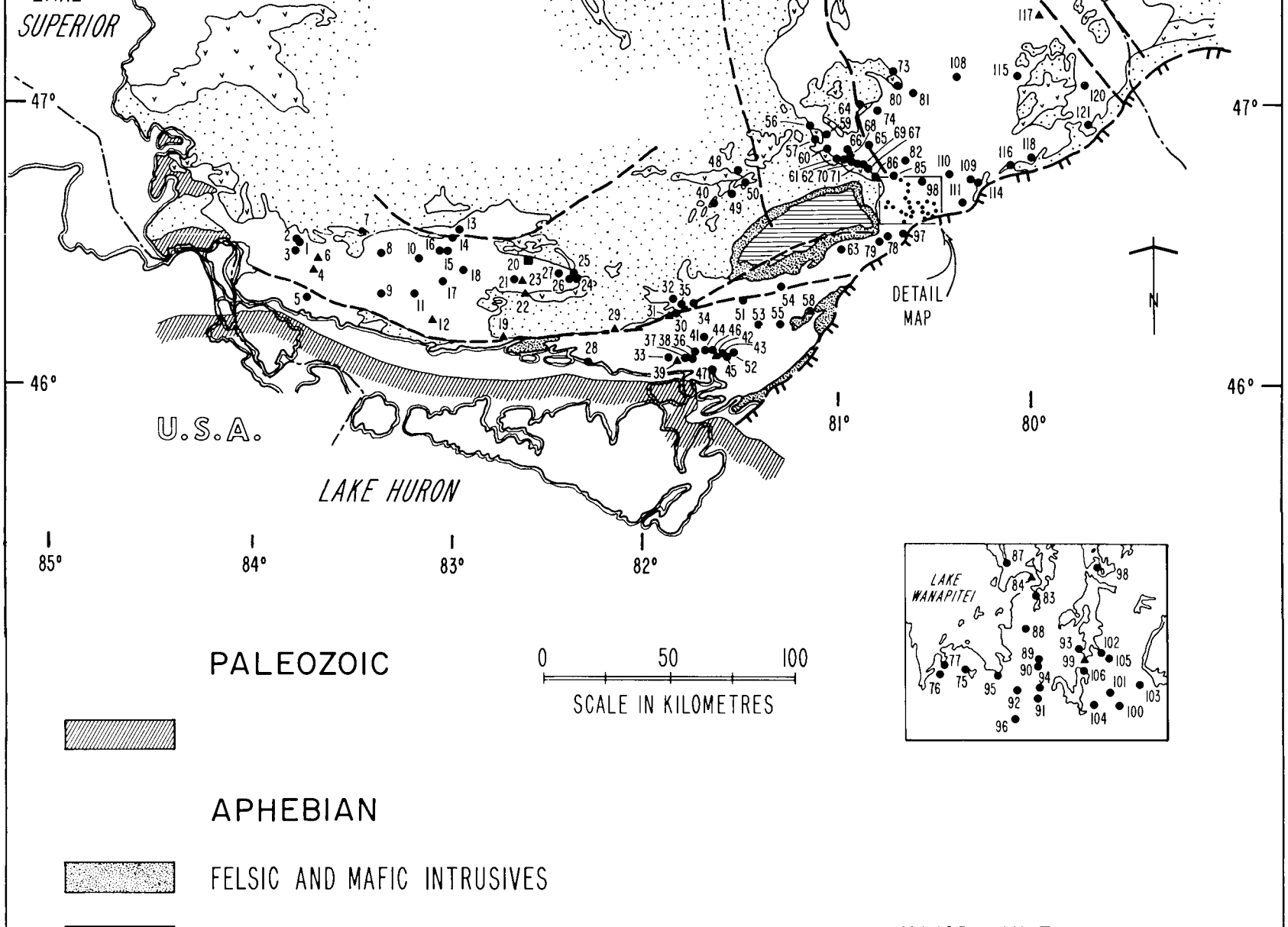
LAKE SUPERIOR
47°
46°
U.S.A.
LAKE HURON
85°
84°
83°
82°
81°
80°
DETAIL MAP
N
LAKE WANAPITEI
PALEOZOIC
0 50 100
SCALE IN KILOMETRES
APHEBIAN
FELSIC AND MAFIC INTRUSIVES
WHITEWATER GROUP METASEDIMENTS
MAJOR FAULTS

the Witwatersrand? Is uranium typically associated with the gold? To what extent was gold soluble and were appreciable amounts precipitated by organic or inorganic activity? In which respects has the geology of Proterozoic gold been modified by diagenetic and metamorphic processes? These and related questions bear directly on the development and interactions of the late Precambrian (Proterozoic) lithosphere, biosphere and atmosphere. The purpose of this paper is to attempt to throw some light on these questions by examining: (1) some aspects of the geochemistry of gold; (2) spatial distribution of gold in the Huronian; (3) the possible connection of the geology of Huronian gold with the oxyatmoversion.

ASPECTS OF THE GEOCHEMISTRY OF GOLD

Increasing attention is being paid to the extent to which Au is soluble under surficial conditions. Experiments have confirmed that the element is in fact geochemically rather versatile in the weathering cycle. The fact that it is capable of combining with a large number of anions to form complex ions, a few of which are stable under geologically reasonable conditions of Eh and pH, means that gold is likely to be mobile to variable degrees (at least when present as a complex ion under oxidizing conditions) and is capable of becoming secondarily enriched in a manner common to many metallic ore deposits.

Thus, gold readily forms complex ions, for example with chloride, thiosulfide and cyanide ions (Table I). Acidic oxidation of pyritic gold deposits yields Au Cl_4^-, according to

$$Au^\circ + 4\ Cl^- = AuCl_4^- + 3\acute{e};\ E^\circ = +1.00\ v \qquad (1)$$

Assuming an activity of 10^{-5} moles l^{-1} for the lower limit of the solubility of gold, Cloke and Kelly (1964) showed that gold is soluble in acid chloride solutions where pH> 5 and Eh> 0.90, and chloride ion activity $>10^{-3.2}$ moles l^{-1}. The combination of these conditions, while uncommon, may account for immobility of Au in oxide zones and is a possible explanation for the spectacular enrichment reported from many gold occurrences (placer and otherwise) associated with laterites (Le Count Evans, 1981).

Thiosulfates are transient products of biological activity in soils and probably seldom reach substantial proportions. In a carbonate environment, oxidation of pyrite may produce enough $S_2O_3^{2-}$ to dissolve gold; similarly in an oxidizing environment, pH 5—8, $S_2O_3^{2-}$ will dissolve gold according to (Lakin et al., 1974)

$$Au^\circ + 2\ S_2O_3^{2-} = Au\ (S_2O_3)^{3-} + \bar{e};\ E^\circ = -0.6\ v\ to\ -0.7\ v \qquad (2)$$

Cyanides are produced in soils by hydrolysis of cyanogenic glycosides which are normally quite abundant. Gold becomes mobile as $Au(CN)_2^-$ because the presence of CN^- reduces the oxidation potential of Au from -1.5 v to -0.2 v and because the dissolved oxygen becomes a sufficiently strong oxidant to dissolve the gold (Lakin et al., 1974). Thus, in an oxygenated

TABLE I

Experimental evidence regarding the conditions under which gold is mobile

Form	Conditions	Reference
$AuCl_4^-$	$Fe(SO_4)_3$,MnO_2,$Cl^- \pm H_2SO_4$, low pH, high Eh	Cloke and Kelly, 1964
$Au(S_2O_3)_2^{3-}$	In soils under vegetation; alkalic oxidation of pyritic gold	Lakin et al., 1974
$Au(CN)_2^-$	HCN formed in soil by hydrolysis of cyanogenic glycosides produced by plants	Lakin et al., 1974
Colloidal Au	Gold sols stabilized with protective coatings by organic acids	Ling Ong and Swanson, 1969

environment, ample HCN, formed by hydrolysis of cyanogenic plants, animals and fungi, results in solution of gold according to (Lakin et al., 1974)

$$Au^\circ + 2CN = Au(CN)_2^- + \bar{e}; \; E^\circ = -0.2v \qquad (3)$$

The gold cyanide thus formed may, to a degree, be subsequently concentrated in the structure of the organism (Table II); whether in protein, organometallic complex or porphyrin, has not been determined (Boyle, 1979).

Experimental evidence also indicates that gold is commonly bound in a relatively stable form by organic acids, at least in slightly acid to basic waters, where the organic acids are soluble (Ling Ong and Swanson, 1969). This process is accomplished by organic concentrations in the range 3—30 ppm, which reduce gold chloride solutions to negatively-charged colloids of metallic gold by forming a protective coating of hydrophilic organic molecules around the colloidal particles. In this form the gold is reported stable for over 8 months (Ling Ong and Swanson, 1969); precipitation of the organic-protected colloids will only occur with a change in environment, e.g., entry to seawater, brackish water, or an acid environment.

TABLE II

Examples of concentrations of gold in organisms during life processes

Medium	Assay (max)	Reference
Lichen	1.0 ppm	Razin and Rozhkov, 1966
Fungi	11.6 ppm	Boyle, 1979
Wormwood	125.0 ppm	Aripova and Talipov, 1966
June bugs	25.0 ppm	Babička, 1943
Marsh horsetails	8.5 ppm	Boyle, 1979
Human hair	43.0 ppb	Bate and Dyer, 1965
Marine organisms	126.0 ppb	Bowen, 1968

Thus, transportation of gold as an organic-protected colloid and its subsequent deposition is not dependent on high Eh as are the other reactions shown in Table I. It is a geochemically feasible process under reducing conditions, and for this reason it is the explanation preferred by Hallbauer (1976, p. 126) to account for the concentration of gold in kerogen on the Rand.

Abundant field evidence also indicates that gold is not only soluble, but is capable of becoming secondarily enriched as a result of repeated redox reactions, such as occur under lateritic conditions. The mode of occurrence of gold in many placers (Table III) demands a process of secondary enrichment similar to the alternating transport (dissolution) and deposition (precipitation) which characterizes other oxidized and secondarily-enriched metallic ore deposits.

TABLE III

Mode of occurrence of gold in placers; field evidence bearing on the problem of the mobility of the element under surficial conditions

Euhedral crystals in (some) placers	Warren, 1979
Gold "paint" on placer boulders	Dirk Templeman-Kluit, personal communication
Extreme fineness of most placer gold	Clark, 1979
Large size of nuggets cf. mother lode	Clark, 1979
Presence of wire gold in some placers	Le Count Evans, 1981
Presence of fibrous, crystalline gold in placers on laterite	Le Count Evans, 1981
Common concentration of Au in gossans	
Examples of biogenic gold	

It is widely recognized that the size of gold particles in placers decreases as the age of the placer increases. Thus, many Tertiary and modern placers contain some coarse gold, whereas in all Precambrian placers the gold is very fine-grained. That of the Witwatersrand, for example, ranges from 50 to 100 μm in diameter. Boyle (1979) suggested that in the Precambrian rocks, the natural milling process has been through many cycles, thus grinding up and dispersing the gold. According to Boyle (1979), this situation contrasts with younger rocks where sediments are typically first or second generation. While this suggestion is appealing, it may very well be that some other process, such as oxidation and secondary enrichment, more vigorous in post-Precambrian sedimentary cycles, may have played a significant role.

DISTRIBUTION OF GOLD IN THE HURONIAN SUPERGROUP

Introduction

Remnants of Aphebian sediments exist in various parts of the Canadian Shield although, with the exception of those in the Montgomery Lake—Padlei area of the Northwest Territories (Roscoe, 1973), few exhibit the unique features of the lower Huronian rocks. These features include: the presence of pyrite in coarse clastic sediments; the absence of iron oxides and red coloration; the occurrence of extensive thick tillites and of radioactive quartz — pebble conglomerate beds.

The classic lower Proterozoic Huronian Supergroup (Fig. 2) is preserved along a belt ~ 325 km long × 60 km wide from Sault Ste. Marie, Ontario, to Noranda, Quebec. It is a very thick (maximum 15 km), complex, sedimentary suite of rocks (Colvine, 1981), deposited 2.45—2.25 Ga- ago (Roscoe, 1973), generally along south—southeasterly drainage patterns into non-marine—paralic environments.

According to Young (1981) and Fralick and Miall (1981), Huronian sediment older than the Gowganda Formation accumulated in an easterly-trending fault-bounded trough. In contrast, the Upper Huronian, i.e., rocks younger than the Gowganda Formation, are more widespread and record deposition under conditions of crustal downwarping east and northeast of Sudbury in the Cobalt Embayment region. Also, a mounting body of evidence indicates that the areas of deposition outlined by the Upper Huronian rocks do not necessarily define the original sedimentary basins of the Lower Huronian sediments (Card and Lumbers, 1977; Wood, 1979).

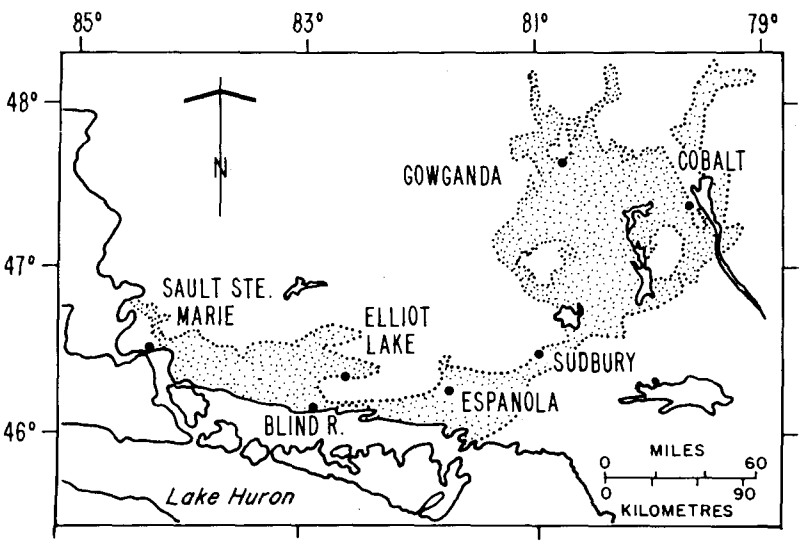

Fig. 2. Index map of distribution of Huronian Supergroup (stippled); the bulge northeast of Sudbury is the Cobalt Embayment.

According to Roscoe (1973), reddish coloration is present in some units in the Cobalt Group, suggesting that free oxygen had begun to accumulate at that time. Specifically, the appearance of red beds at about the middle of the Firstbrook Member (the thick, upper, non-conglomeratic part of the Gowganda Formation consisting mainly of laminated argillite) provides good evidence for oxyatmoversion within the Gowganda Formation (John Wood, personal communication, 1981; see also Owsiacki, 1981, p. 217). In contrast, rocks older than the Upper Gowganda are drab in colour, have detrital pyrite and uraninite, overlie iron-deficient paleosols and are interpreted as having been deposited under anoxygenic conditions.

The Huronian Supergroup are the most ancient Aphebian strata known in Canada (Roscoe, 1973). Their original distribution was much larger than the area indicated in Fig. 2. The basins of deposition are believed to have been far larger and possibly extended as much as 1000 km to the northeast into central Quebec (Frarey and Roscoe, 1970).

The Huronian Supergroup includes (Fig. 3) four Groups of metasediments. Gold occurrences are reported from all four groups. One hundred and

		NUMBER OF OCCURRENCES
COBALT GROUP	BAR RIVER	0
	GORDON LAKE	0
	LORRAIN	3
	GOWGANDA	47
QUIRKE LAKE GROUP	SERPENT	8
	ESPANOLA	6
	BRUCE	5
HOUGH LAKE GROUP	MISSISSAGI	29
	PECORS	1
	RAMSAY LAKE	0
ELLIOT LAKE GROUP	McKIM	2
	MATINENDA	9
	ARCHEAN	

Fig. 3. Outline of the stratigraphy of the Huronian Supergroup (after Robertson et al., 1969). Maximum thickness of the respective Groups is: Elliot Lake, 4000 m; Hough Lake, 3500 m, Quirke Lake, 1500 m; Cobalt, 6000 m. A total of 110 gold occurrences are distributed among the formations, as indicated; the remaining 11 of the 121 total occur in diabase.

twenty-one Au or Au—U occurrences were researched during the present survey (Fig. 1, Table IV). Eleven of the occurrences are in, or adjacent to, diabase. Of the remainder: 41.3% occur in terrain mapped as the Cobalt Group; 15.7% in the Quirke Lake Group; 24.9% in the Hough Lake Group, and 9% in the Elliot Lake Group. These data, together with some exciting new finds of stratiform gold in the Lorrain Formation (see addendum) support the suggestion (Meyn, 1979; Innes and Colvine, 1979; Wood, 1980) that the Matinenda, Mississagi, Serpent, Espanola and Lorrain Formations have the highest potential for paleoplacer gold.

Of the 121 occurrences, the majority (47) occur in the Gowganda Formation (Fig. 3). This possibly reflects its greater areal extent relative to the other formations. No stratiform deposits are recorded in the Gowganda and only two in the Lorrain Formation. This may be due to the fact that diabase intrusions increase in abundance to the northeastern portion of the Cobalt Embayment. Thus, many of the vein or diabase related deposits probably represent remobilization of original paleoplacer gold.

Of interest here is our observation that mineralization in the "diabase-related" deposits is the same whether the diabase cuts the Archean or the Huronian (e.g., compare Massey Mine and Hermina Copper in Salter Township). Thus, the proximity of paleoplacer gold must not be implied by the presence of gold in a diabase-related deposit.

Type distribution of Au and Au—U in the Huronian (Table IV) indicates that 25 are stratiform and 96 occur in veins. Frequency of occurrence can be related to transgressive sedimentary cycles. Thus, most occurrences are in the Matinenda, Mississagi and Gowganda Formations which immediately overlie the Archean—Huronian unconformity in a transgressive mode.

With respect to tenor of Au, the data for Table V indicate a large overlap in class intervals of stratiform V. vein deposits. Vein deposits are, in general, richer than stratiform by a factor of ~10.

As knowledge of metallogenic processes has grown, especially during the last decade, the concept that many of the diabase-associated gold occurrences owe their origin to remobilization of paleoplacer gold has gained momentum (Roscoe, 1969, p. 165; Innes and Colvine, 1979). One good example, examined in this paper, is the Long Lake Mine of Eden Township. Others, east of Sudbury, are described by Innes and Colvine (1979) as associated with gold-bearing quartz veins in Nipissing diabase. The McLean-Watt (Northgate) deposit in the Serpent Formation of Scadding Township is believed to have formed by remobilization of syngenetic gold contained in siltstone and siliceous greywacke, as well as by enrichment from diabase (Martins et al., 1979).

Several instances of possible remobilization of gold have been investigated in quartzite of the Lorrain Formation (Innes and Colvine, 1979). Altogether, there is a great body of evidence which points to the existence of a syngenetic zonation of various metals (Cu, Co, Ag and even Ni) in addition to gold (Card and Pattison, 1973; Innes and Colvine, 1979) in the Huronian.

TABLE IV

List of 121 Au, Au—U occurrences investigated in the Huronian Supergroup. (Cat.) Categories of deposits: P = prospect (●, Fig. 1); PP = past producer (▲, Fig. 1); MP = active mine (■, Fig. 1). (V) vein; (DR) diabase related; (S) stratiform. The most recent available data were used in the present study and every effort made to use the correct information (tons (t) = 2000 lb)

No.	Name	Township	Cat.	Host rock formation	Morphology			Mineral assemblage[c]	Assays, Reports	Reference
					V[a]	DR[b]	S			
1	Hugli L.	McMahon	P	Gowganda	x	x		cpy—py—hem	0.01% Cu, 0.4 oz/t Ag, Tr Au	Chandler, 1973, p. 53
2	Stuart L.	McMahon	P	Gowganda	x			cpy—py—hem	0.21% Cu, 0.02 oz/t Ag, Tr Au	Chandler, 1973, p. 59
3	Kirk	Aberdeen	P	Diabase	x	x		py	no record	Ferguson et al., 1971, p. 18
4	Red Rock	Aberdeen	PP	Gowganda	x	x		py—cpy	0.11—0.51% Cu, Tr Au, Tr Ag/5—45′	Shklanka, 1969, p.14
5	McGregor Rd	Plummer Add	P	Lorrain	x	x		py—hem	0.02 oz/t Au, 0.03% U_3O_8, 0.04% ThO_2	Bennett and Leahy, 1979, p. 99
6	Havilah	Galbraith	PP	Mississagi	x	x		cpy—py	0.16 oz/t Au, 0.03 oz/t Ag in 6600 t	Ferguson et al., 1971, pp. 18—19
7	Burden L	Otter	P	Diabase	x	x		Co—Ag—Bi—Ni sulphides	1.22 oz/t Au/4′	Giblin and Leahy, 1979, p. 94
8	Rothsay	Gould	P	Gowganda	x	x		cpy—py—hem	0.62% Cu, 0.01 oz/t Au	Siemiatkowska, 1977, p. 49
9	Lot 1, con III	Wells	P	Gowganda	x	x		cpy—py	0.02 oz/t Au	Shklanka, 1969, p.105
10	Ridgefield	Nouvel	P	Gowganda	x			cpy—py	0.05% Cu, 0.02 oz/t Au/2′	Shklanka, 1969, p.98
11	Corbold L	Montgomery	P	Bruce			x	cpy	0.24% Cu, 0.05 oz/t Au	Shklanka, 1969, p.102
12	Brady	Patton	PP	Gowganda	x	x		cpy—py	3.6—4.9% Cu, 0.08—0.22 oz/t Au	Robertson, 1963a, p.61
13	Stanford	Albanel	P	Lorrain	x	x		cpy—py	15.6% Cu, 0.24% Zn, 0.36 oz/t Ag, 0.02 oz/t Au	Siemiatkowska, 1978, p.69
14	Ventures	Albanel	P	Diabase	x	x		Cu—Pb—Zn—Co—Bi sulphides	1.56% Cu, 0.63% Pb, 0.26% Zn, 0.1% Co, 0.05% Bi, 3.46 oz/t Ag, 0.1 oz/t Au	Siemiatkowska, 1978
15	Copper Prince	Kamichisitit	P	Gowganda	x			cpy—py	4.1% Cu, 0.03 oz/t Au/7.1′	Siemiatkowska, 1978, pp. 66—67
16	Pathfinder	Kamichisitit	P	Gowganda	x			cpy—py	4.1% Cu, 0.01 oz/t Au/3′	Shklanka, 1969, p.95

TABLE IV (*continued*)

No.	Name	Township	Cat.	Host rock formation	Morphology			Mineral assemblage[c]	Assays, Reports	Reference
					V[a]	DR[b]	S			
17	Matinenda L	Juliette	P	Matinenda	x			cpy—py	1.85% Cu, 0.012 oz/t Au	Shklanka, 1969, p.111
18	Picton U	Jogues	P	Mississagi			x	cpy—py—po	1.2% Cu, 0.002 oz/t Au	Robertson, 1963b, pp. 72—73
19	Pronto	Long	PP	Matinenda			x	py—po—RA	0.12% U_3O_8, Tr Au	Robertson, 1970, p.85
20	Denison	Bouck	MP	Matinenda			x	py—RA	0.08—1.73%U_3O_8, 0.07—0.3% ThO_2, 0.005—0.032 oz/t Au	Roscoe, 1969, Appendix C
21	Silvermaque	Gunterman	P	Bruce and Mississagi			x	py—RA	0.01 oz/t Au	Robertson, 1968a, p.136
22	Nordic	Gunterman	PP	Matinenda			x	py—RA	0.01 oz/t Au, 0.06 oz/t Ag	Robertson, 1968a, p.101
23	Stanleigh	Gunterman	PP	Matinenda			x	py—RA	0.043—0.63% U_3O_8, 0.007—0.18% ThO_2, 0.005—0.03 oz/t Au	Roscoe, 1969, Appendix C
24	Payton	Gaiashk	P	Mississagi	x			py—aspy—cpy	0.74 oz/t Au/2 1/2′	Robertson, 1962, pp. 76—77
25	B.C. Exploration No. 2	Gaiashk	P	Matinenda			x	py—RA	0.006% U_3O_8, 0.02 oz/t Au/1′	Robertson, 1962, pp. 70—71
26	Whitefish	Gaiashk	P	Mississagi	x	x		py—cpy	2.0% Cu, 0.16 oz/t Au	Robertson, 1962, pp. 88—89
27	McCool L	Gaiashk	P	Serpent	x	x		cpy—py	1.5% Cu, 0.02—0.04 oz/t Au+Ag	Robertson, 1962, pp. 85—86
28	Frechette Is.	(L.Huron)	P	Diabase	x	x		cpy—po—py	0.94% Cu, 0.145 oz/t Au/1.9′	Robertson, 1976, p.104
29	Massey	Salter	PP	Pecors	x	x		cpy—py	2.5% Cu, 0.5 oz/t Ag, 0.02 oz/t Au in 20 000 t	Robertson, 1976, pp. 111—116
30	White	Shakespeare	P	Matinenda	x	x		po—cpy	0.06% Cu, 0.06% Ni, 0.29 oz/t Ag, 0.01 oz/t Au	Shklanka, 1969, p.282
31	Shakespeare	Shakespeare	PP	Matinenda	x			cpy—po—aspy	1.12—1.85 oz/t Au/3-5 9000 t mined	Card and Palonen, 1976, pp. 39—40
32	Noranda	Shakespeare	P	Matinenda	x			po—py—cpy—gal	1.55—8.45% Cu, Tr—0.02 oz/t Au	Card and Palonen, 1976, p.41
33	Tough	McKinnon	P	Serpent	x			py—cpy—aspy	0.17 oz/t Au/8.5′	Gordon et al., 1979, p.73
34	Cons. Monclerg	Baldwin	P	Mississagi			x	py—RA	0.008% U_3O_8, 1.01% Cu, 0.01 oz/t Au	Robertson, 1968b, p.67

35	Springer	Baldwin	P	Mississagi	x	x		cpy—py—po	0.93% Cu, 0.08 oz/t Au	Shklanka, 1969, p.231
36	Fox L	Mongowin	P	Serpent + Gowganda	x			py—cpy—aspy	1.91% Cu, 0.94 oz/t Ag, 0.83 oz/t Au	Ferguson et al., 1971, p.76
37	Majestic	Mongowin	P	Gowganda	x	x		py—cpy—aspy	no records	Card, 1976a, pp. 56—57
38	Jo-Ami	Mongowin	P	Gowganda	x			py—aspy	0.52—14.1 oz/t Au/1—3′	Card, 1976a, p.57
39	McMillan	Mongowin	PP	Gowganda	x			py—po—cpy—aspy	0.18 oz/t Au in 60 140 t	Card, 1976a, pp. 54—55
40	Lot 7, Con V	Hart	P	Espanola	x	x		gal—sph—py—cpy	7.32% Ni, 16.9% Co, 3.3% Bi, 0.03% Cu, 0.06 oz/t Au	Sergiades, 1968, p.55
41	Stratton L	Foster	P	Serpent	x			py—po—aspy	0.04 oz/t Au	Card, 1976a, p.58
42	Bosquet	Curtin	PP	Gowganda	x	x		py—cpy—aspy	0.27 oz/t Au in 17 400 t	Card, 1976a, pp. 51—52
43	Bridger	Curtin	P	Gowganda	x			py—aspy	0.07 oz/t Au	Card, 1976a, pp. 52—53
44	Pond	Curtin	P	Gowganda	x			py—aspy	0.19 oz/t Au/18′	Card, 1976a, p.53
45	Howry Crk.	Curtin	P	Gowganda	x	x		py—aspy	0.08—0.51 oz/t Au/1 1/2′	Card, 1976a, p.55
46	Upsala	Curtin	P	Gowganda	x			py—cpy—gal	0.4% Cu, 0.11 oz/t Au	Card, 1976a, p.57
47	Iroquois Is.	I.R. 4	P	Espanola	x			po—py—cpy—aspy	0.01—0.07 oz/t Au/4′	Card, 1976b, p.51
48	B and M Exploration	Munster	P	Gowganda	x	x		py	0.14% Zn, 0.01% Pb, 0.01% Cu, 0.002 oz/t Ag, 0.002 oz/t Au	Card and Innes, 1981, pp. 104—105
49	Hess L.	Hess	P	Espanola			x	mag—cpy—gal	0.5% Pb, 0.12% Cu, 0.18 oz/t Ag, 0.002 oz/t Au	Card and Innes, 1981, pp. 103—104
50	Central Hess	Hess	P	Espanola	x			sph—gal—py—cpy	10.6% Zn, 4.95% Pb, 0.97% Cu, 1.6 oz/t Ag, 0.002 oz/t Au/15′	Card and Innes, 1981, pp. 97—98
51	Turpeinen	Lorne	P	Mississagi	x			cpy—py	3.48% Cu, 0.02 oz/t Au	Ginn, 1965, p.38
52	Harwood L.	Roosevelt	P	Gowganda	x			py—aspy	0.88 oz/t Au/28″	Gordon et al., 1979, p. 81
53	Chellew	Dieppe	P	Espanola	x			py—cpy	0.5% Cu, 0.001 oz/t Au/40′	Card et al., 1975, p.56
54	Simpson	Graham	P	McKim	x			py	0.35 oz/t Au	Gordon et al., 1979, p.101
55	L. Panache	I.R.6	P	Mississagi	x			py—po—cpy—aspy	no records	Card et al., 1975, p.59

TABLE IV (*continued*)

No.	Name	Township	Cat.	Host rock formation	Morphology			Mineral assemblage[c]	Assays, Reports	Reference
					V[a]	DR[b]	S			
56	Roberts L.	Roberts	P	Mississagi			x	py—RA	0.19% U_3O_8, 0.02 oz/t Au	Meyn and Matthews, 1980, p.196
57	Nordic	Roberts	P	Mississagi			x	py—RA	0.11% U_3O_8, 0.02 oz/t Au	Meyn and Matthews, 1980, p.196
58	Long Lake	Eden	PP	Mississagi	x			py—po—aspy—cpy	0.26 oz/t Au in 221 000 t	Gordon et al., 1979, pp. 61—62
59	Leslie	Creelman	P	Mississagi			x	py—RA	0.05% U_3O_8, 0.003 oz/t Au	Meyn and Matthews, 1980, p.196; Meyn, 1971
60	North Hutton	Hutton	P	Mississagi			x	py—RA	0.44% U_3O_8, 0.003 oz/t Au	Meyn and Matthews, 1980, p.196
61	Central Hutton	Hutton	P	Mississagi			x	py—RA	0.17% U_3O_8, 0.01 oz/t Au	Meyn and Matthews, 1980, p.196
62	Banagan L.	Hutton	P	Mississagi			x	py—RA	0.19% U_3O_8, 0.003 oz/t Au	Meyn and Matthews, 1980, p.196
63	La Salle	McKim	P	McKim	x	x		py	0.77% Cu, 0.13% Ni, 0.18 oz/t Ag, 0.001 oz/t Au	Innes, 1978
64	C.J.M.	Grigg	P	Mississagi			x	py—RA	0.009% U_3U_8, 0.01 oz/t Au	Meyn, 1972, p.11
65	Towers	Fraleck	P	Diabase	x	x		gal—cpy—py—aspy	12.9% Pb, 1.5% Cu, 1.49 oz/t Ag, 0.91 oz/t Au	Dressler, 1979b, p.43
66	Flesher L.	Parkin	P	Mississagi			x	py—RA	0.004% U_3O_8, 0.002 oz/t Au	Meyn and Matthews, 1980, p.196
67	Mataris	Parkin	P	Bruce	x			py—aspy	no records	Gordon et al., 1979, p.113
68	Powerline Rd.	Parkin	P	Serpent			x	py—RA	0.015% U_3O_8, 0.001 oz/t Au	Meyn and Matthews, 1980, p.196
69	Parkin	Parkin	P	Bruce	x			py—gal	0.34 oz/t Au/5′	Gordon et al., 1979, p.114
70	Bouma	Parkin	P	Mississagi			x	py—RA	0.002% U_3O_8, 0.0003 oz/t Au	Meyn and Matthews, 1980, p.196

71	Aro	Parkin	P	Mississagi	x			po	6.21 oz/t Ag, 0.08 oz/t Au	Meyn, 1970, pp. 51—52
72	British-Matachewan	Powell	P	Gowganda	x			py	0.09 oz/t Au	Gordon et al., 1979, p.163
73	Solace L.	Selkirk	P	Gowganda	x			gal—py—cpy	10.2% Pb, 4.08 oz/t Ag, 0.06 oz/t Au	Card et al., 1973, p.99
74	C.J.M.	Stobie	P	Mississagi			x	py—RA	0.021—0.08% U_3O_8, 0.005 oz/t Au	Meyn, 1972, p.32
75	Bonanza	Maclennan	P	Mississagi	x	x		py	0.04 oz/t Au	Thomson, 1961, p.28
76	Skead	Maclennan	P	Mississagi	x			py—cpy	0.62% Cu, 0.27 oz/t Au/6.1′	Thomson, 1961, p.27
77	Sheppard	Maclennan	P	Mississagi	x			py	0.23 oz/t Ag, 5.43 oz/t Au	Gordon et al., 1979, pp. 108—109
78	Falcon	Falconbridge	P	Serpent	x			py	0.32 oz/t Au in 18 000 t reserve	Phemister, 1939, p.20
79	Copper Prince	Falconbridge	P	Mississagi	x			py—cpy	no records	Shklanka,1969, p.275
80	W R 90	Turner	P	Gowganda	x	x		gal—sph—cpy	4.2% Pb, 0.24% Zn, 1.1% Cu, 0,22 oz/t Au	Card et al., 1973, pp. 93—94
81	T. Saville	Turner	P	Mississagi			x	py—RA	0.06% U_3O_8, 0.01 oz/t Au	Card et al., 1973, p.113
82	Wolfe L.	Mackelcan	P	Lorrain	x			py	0.002—2.25 oz/t Au	Dressler, 1978b, 1979a,
83	Comstock	Rathburn	P	Gowganda	x			py	3.5—12.9 oz/t Au	Gordon et al., 1979, p.80
84	Crystal	Rathburn	PP	Gowganda	x	x		py—cpy	0.53 oz/t Au in 730 t	Gordon et al., 1979, pp. 80—81
85	McVittie	Rathburn	P	Diabase	x	x		py—cpy	0.01—0.42 oz/t Au/3—10′	Dressler, 1978a
86	Bennett	Rathburn	P	Gowganda	x			py	no records	Dressler, 1978a
87	Rathburn L.	Rathburn	P	Diabase	x	x		py—po—cpy	14.3% Cu, 2.86% Ni, 0.61% Pt, 0.83% Pd, 0.28 oz/t Ag, 0.16 oz/t Au	Shklanka, 1969, p.261
88	Alwyn Porcupine	Scadding	P	Gowganda	x	x		py—cpy	1.11% Cu, 0.085 oz/t Au/6 1/2′	Thomson, 1961, p.28
89	Mid Continental	Scadding	P	Diabase	x	x		py	0.14 oz/t Au/15′	Kindle, 1933, p.43
90	Red Rock	Scadding	P	Gowganda	x	x		py—aspy	no records	Thomson, 1961, p.29
91	Northgate	Scadding	P	Serpent	x			py—po—cpy—aspy	0.26 oz/t Au in 260 750 t reserve	Martins et al., 1980, pp. 111—115
92	Alkins	Scadding	P	Gowganda	x	x		py	no records	Kindle, 1933, p.44
93	Midas	Scadding	P	Gowganda	x	x		gal—cpy—py	0.02—0.07% Cu, 0.04—0.36 oz/t Ag, 0.0—0.66 oz/t Au	Dressler, 1979b, p.112
94	Wanapitei	Scadding	P	Serpent	x			py	0.37 oz/t in 42 000 t reserve	Gordon et al., 1979, p.82

TABLE IV (*continued*)

No.	Name	Township	Cat.	Host rock formation	Morphology			Mineral assemblage[c]	Assays, Reports	Reference
					V[a]	DR[b]	S			
95	Potvin	Scadding	P	Espanola	x	x		py	0.09 oz/t Au	Gordon et al., 1979, p.117
96	Scadding	Scadding	P	Bruce	x			py	no records	Gordon et al., 1979, p.118
97	McVittie	Street	P	Mississagi	x			py—cpy	1.12% Cu, 0.01 oz/t Au	Shklanka, 1969, p.282
98	Kukagami L.	Kelly	P	Gowganda	x	x		py—cpy—gal	0.73% Cu, 5.18% Pb, 1.0 oz/t Ag, 0.09 oz/t Au	Shklanka, 1969, pp. 251—252
99	Mac-Auer	Davis	PP	Gowganda	x			py—cpy	0.87 oz/t Au in 7 700 t reserve	Gordon et al., 1979, p.58
100	McLeod	Davis	P	Gowganda	x	x		py—aspy	0.50 oz/t Au/4 1/2′	Thomson and Card, 1963, p.16
101	Norstar	Davis	P	Gowganda	x			py—cpy—aspy	1.5% Cu, 0.41 oz/t Au in 275 000 t reserve	Thomson and Card, 1963, pp. 15—16
102	Taylor	Davis	P	Gowganda	x	x		py	no records	Gordon et al., 1979, p.59
103	Washagami	Davis	P	Gowganda	x	x		py—cpy	10% Cu, 0.04 oz/t Au	Gordon et al., 1979, p.98
104	Crerar	Davis	P	Gowganda	x			py—cpy	4.09% Cu, 0.09 oz/t Au	Gordon et al., 1979, p. 97
105	Tecumseh	Davis	P	Gowganda	x	x		py—cpy	Au over 20″	Thomson and Card, 1963, p.18
106	Handy	Davis	P	Gowganda	x			py	no records	Thomson and Card, 1963, p.17
107	Tomlinson	Bompass	P	Gowganda	x			py—cpy—gal	no records	Gordon et al., 1979, p.192
108	Delhi-Pacific	Delhi	P	Gowganda	x	x		gal—py—cpy	7.13% Pb, 5.58 oz/t Ag, 0.25 oz/t Au in 54 000 t reserve	Gordon et al., 1979, pp. 59—60

109	T. Saville	McNish	P	Mississagi			x	py	no records	Dressler, 1979b, pp. 81—82
110	A.E. Jerome	McNish	P	Gowganda	x	x		py—po—cpy—sph—gal	2.98% Cu, 0.53% Zn, 1.88 oz/t Ag, 0.02 oz/t Au	Dressler, 1979b, p.76
111	P.C.E.	Janes	P	Diabase	x	x		cpy—po	0.77% Cu, 0.28% Ni, 0.035 oz/t Au/15′	Shklanka, 1969, p.251
112	Paramount	Tudhope	PP	Diabase	x	x		cpy—py	Cu, Ag, Au in 43 t	Shklanka, 1969, p.373
113	Sauve	Tudhope	P	Gowganda	x	x		cpy—hem	1.56% U_3O_8 with Cu, Au	Shklanka, 1969, p.373
114	Pickle Crow	Pardo	P	Mississagi			x	py	0.028% U_3O_8, 0.05 oz/t Au	Gordon et al., 1979, p.24
115	Hardie	Cynthia	P	Gowganda	x	x		py—cpy—po	2.15% Cu, 0.14 oz/t Ag, 0.14 oz/t Au	Simony, 1964, p.23
116	Wright	Vogt	P	Mississagi			x	py—RA	0.052% U_3O_8, 0.40 oz/t Au/2′	Grant, 1964, pp. 20—21
117	Cobalt-Kittson	Kittson	PP	Gowganda	x	x		Co—Ni—Fe arsenides	0.08 and 0.20 oz/t Au	Johns, 1979, p.114
118	Cross Lake	Torrington	P	Gowganda	x			py—cpy—gal	5.03% Cu, 2.39% Pb, 3.26 oz/t Ag, 0.03 oz/t Au	Grant, 1964, p.21
119	Marshall	Ingram	P	Gowganda	x	x		cpy—py—gal	0.36% Cu, 0.24% Pb, 0.41% Co, 1.72 oz/t Ag, 0.98 oz/t Au	Gordon et al., 1979, p.140
120	E D 61	Cassels	P	Diabase	x	x		py—aspy	1.08 oz/t Au/4″	Gordon et al., 1979, p.27
121	Rabbit L.	Askin	P	Gowganda	x			Co—Ni sulphides	0.44 oz/t Au	Gordon et al., 1979, p.27

[a]Vein, refers to quartz or quartz and carbonate veins.
[b]Diabase related refers to mineralization in or adjacent to diabase dykes.
[c]Abbreviations py = pyrite; po=pyrrhotite; cpy=chalcopyrite; gal=galena; sph=sphalerite; hem=hematite; mag=magnetite; RA=radioactive minerals.

TABLE V

Statistics on (available) Au assay data for 81 vein deposits and 24 stratiform deposits in the Huronian Supergroup (see text for discussion)

Vein deposits (N = 81)		Stratiform deposits (N = 24)		All assay data (N = 105)	
Interval (oz/t) Au	Frequency	Interval (oz/t) Au	Frequency	Interval (oz/t) Au	Frequency
0.0001— 0.00099		0.0001— 0.00099	1	0.0001— 0.00099	1
0.001 — 0.0099	6	0.001 — 0.0099	9	0.001 — 0.0099	16
0.01 — 0.099	31	0.01 — 0.099	13	0.01 — 0.099	44
0.1 — 0.99	37	0.1 — 0.99	1	0.1 — 0.99	37
1.0 — 9.99	5	1.0 — 9.99		1.0 — 9.99	5
10.0 —99.9	2	10.0 —99.9		10.0 —99.9	2

Thus an excellent case is documented for palingenesis of various ores, including gold. The resurrection of elements/minerals from ancient terrains and their subsequent concentration in younger rocks is in fact well established by examples of uranium ores (e.g., Athabasca, Saskatchewan) and classic Pb—Zn districts (e.g., Coeur d'Alene, Idaho). Evidently, the lithosphere exercised great control over distribution of Huronian gold, in a manner entirely consistent with the principle of uniformitarianism.

Presently, research on, and exploration for, Huronian gold has reached the stage where the existence of paleoplacers of gold, uranium and associated minerals are no longer in doubt. It remains to delineate the extent of the paleoplacers, to evaluate the degree to which they have been modified, and to assess their economic potential. Ideally, an understanding will be gained of the geological processes which helped localize the gold, to the extent that it can be used in a predictive way to locate new deposits.

Eden Township

The best known gold occurrence here, located at Long Lake, ~ 20 km south of the Sudbury Irruptive, has always been believed to be closely associated with Nipissing Diabase. Cettainlym the host Mississagi sandstones are intruded by diabase and the main orebody is in the shape of an inverted funnel, having scarcely any obvious original surface expression, geochemical or otherwise. Mineralization consists mainly of arsenopyrite and pyrite-rich metasediments. The most arkosic units contain up to 8% thorium-poor monazite (M. Jones, personal communication, 1982). Potassium—argon dating of coarse-grained muscovite from the ore shoot yields 1361 ± 35 Ma (R.L. Armstrong, personal communication, 1981), indicating that the mineralization is not likely to be related to a (2.1 Ga) Nipissing event (see also Gibbins and McNutt, 1975).

In the immediate vicinity of the Long Lake Mine, as well as regionally, the predominant rock type is subarkosic sandstone of the Mississagi Formation. Thicker, more coarse-grained, commonly cross-bedded units (for details see Card et al., 1975, p. 11) alternate with relatively thin (typically 2—5 cm), darker, fine-grained, argillaceous bands. Regionally, conglomerates are rare and in the area of this study are non-existent.

Typical Mississagi sandstone, located at 1 km distance from the mine site, shows predominant albite—oligoclase, quartz and lesser amounts of K-feldspar. In this rock, which has been metamorphosed to upper greenschist facies, the heavy mineral grains, chiefly pyrite (Fig. 4), outline the relict sedimentary framework of the subarkosic sandstone.

Results of a modest regional geochemical survey of metasediments, in an ~ 0.5 km^2 area, immediately south of the mine reveal (Fig. 5) a very high background value (155 ppb) for Au in the area (neglecting the two "erratic high" assays to the right of the diagram). In contrast, the average terrestrial abundance of Au is 5 ppb. The histogram reflects anticipated

log-normal behaviour of gold values and an increased percentage of heavy minerals in those samples with the higher gold content. The latter feature is entirely compatible with the concept of a placer distribution of the gold.

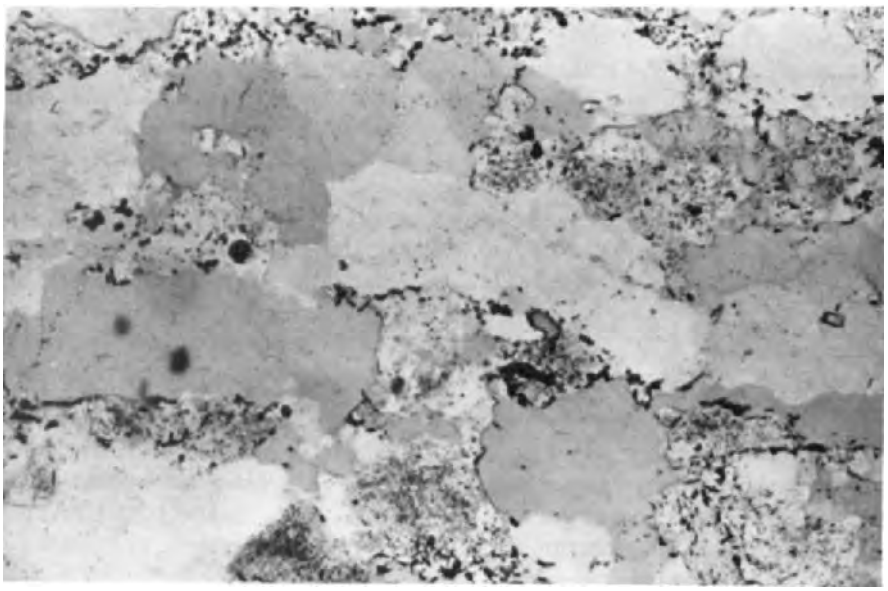

Fig. 4. Mississagi sandstone, plane polarized transmitted light, width of field of view is 0.5 mm. Opaques (chiefly pyrite) outline the relict sedimentary framework of the rock.

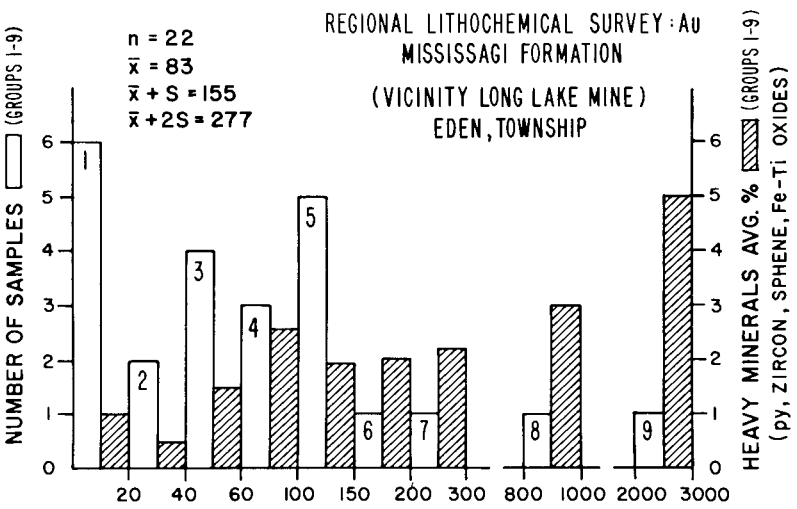

Fig. 5. Results of a reconnaissance lithochemical survey conducted over a 0.5 km² area immediately south of the Long Lake Mine, Eden Township (see text for details).

It is also instructive to note that here, and apparently elsewhere throughout Eden Township, uranium does not accompany the gold. It is a situation resembling the Witwatersrand, where uraninite values are restricted to conglomeratic units (for further discussion see Fralick and Miall, 1981).

Gold values at the mine site and in the surrounding region are almost invariably associated with graphite. There is little startling about this fact per se, for the affinity of the two elements under a wide variety of geological circumstances is well known. At one location, 1 km south of the mine, anomalous Au values occur directly adjacent to (but evidently not within) a metre-thick graphitic horizon. Graphite composes ~ 40% of this rock and occurs as well crystallized fibres in a cell-like matrix enclosing inequigranular detrital silicate grains. The material bears little resemblance to Au—U bearing carbonaceous material from either the Witwatersrand (Hallbauer, 1976) or elsewhere in the Huronian (Ruzicka and Steacy, 1976).

TOWNSHIPS IN THE COBALT EMBAYMENT

Introduction

The results of the survey by Meyn and Matthews (1980) in the southern part of the Cobalt Embayment revealed anomalous concentrations of gold up to 800 ppb. They suggested that the source of this gold is in the Abitibi greenstone belt located to the north. This seems reasonable in view of deduced directions of sediment transport (Innes and Colvine, 1979) and, also, because throughout much of the Cobalt Embayment (Plain) the conglomerates are polymictic, with subangular pebbles of quartz, quartzite, granite, and volcanic and metasedimentary clasts. Likewise, the matrix of these conglomerates typically ranges from fine-grained, dark, chloritic argillite to grey, medium-grained sandstone (Meyn and Matthews, 1980). In contrast, the Elliot Lake rocks, also believed to have been derived from the north, but from a predominantly granitic terrain, are classic oligomictic quartz-pebble conglomerates.

North of the Sudbury irruptive, metasediments traditionally assigned to the Mississagi Formation (Collins, 1925; Robertson et al., 1969) form the basal part of the Huronian Supergroup. Long (1976) suggested that part, at least, of the sequence is probably equivalent to the Matinenda Formation. Whatever the truth of this matter, there are some interesting gold occurrences in the region, as illustrated (Fig. 6) by the following examples. .

In each of Turner, Vogt, Pardo, Grigg and Roberts Townships, uranium, the easier metal to prospect for, turns up in argillite, siltstone, sandstone and conglomerates. In most, but apparently not all cases (Meyn and Matthews, 1980), it is closely associated with pyrite. Autoradiographs confirm that the radioactivity coincides with the concentration of heavy minerals, including zircon, ilmenite, rutile, brannerite, uraninite and coffinite.

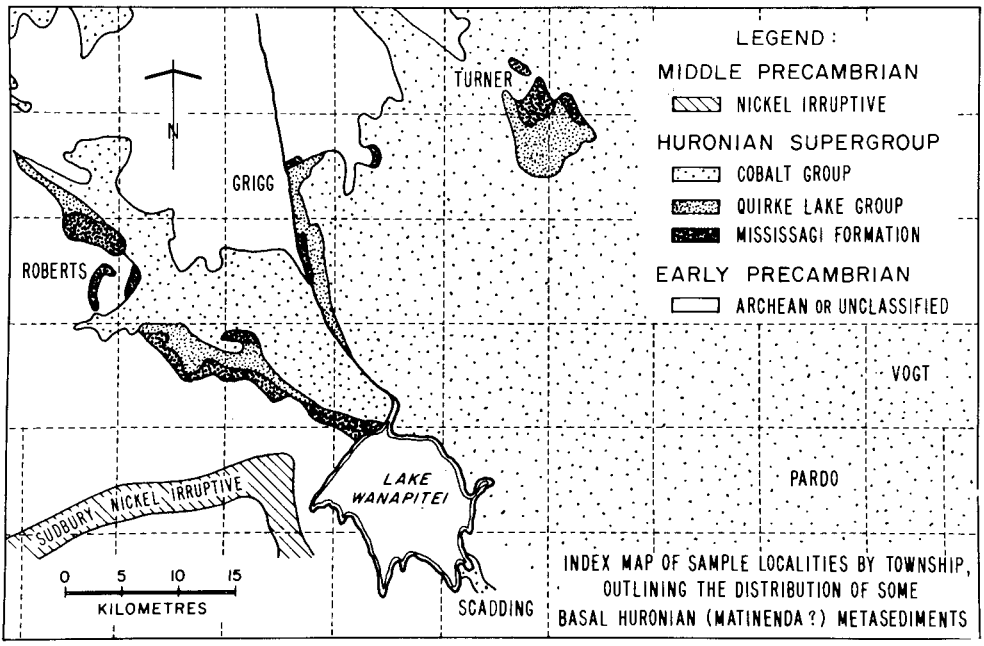

Fig. 6. Index map to the Townships: Turner; Vogt; Pardo; Grigg, Roberts and Scadding, outlining the distribution of some lower Huronian (Matinenda?) metasediments in the Cobalt Embayment (modified from Meyn and Matthews, 1980).

As far as can be determined, gold accompanies the uranium in this setting, although in highly variable, generally low, amounts. It is instructive to note that most properties currently being investigated for Au were located by scintillometer (e.g., Long, 1981). As shown by the example of Long Lake (Eden Township), where uranium is lacking, the occurrence of gold may be far more widespread than presently understood. In fact, on purely sedimentological grounds (Long, 1981) there is little reason to believe that paleoplacer gold is restricted to the basal Huronian in the Cobalt Embayment.

Turner Township

Several occurrences of uranium in siltstone have been investigated in recent years in Turner Township. Some, such as the "Discovery Pond" prospect, (No. 81, Table IV) contain up to 0.2% U_3O_8 ton^{-1}, as well as gold values up to 160 ppm (Sullivan, 1979). In this instance the link with a paleoplacer origin is certainly not evident. On the contrary, Sullivan (1979) has argued vigorously for a genetic link with basic igneous rocks.

Elsewhere in the area, however, a paleoplacer mode of some of the gold and uranium is less equivocal. Long (1981, p. 220), for example, described the occurrence (not listed in Table IV) of a large pebble conglomerate

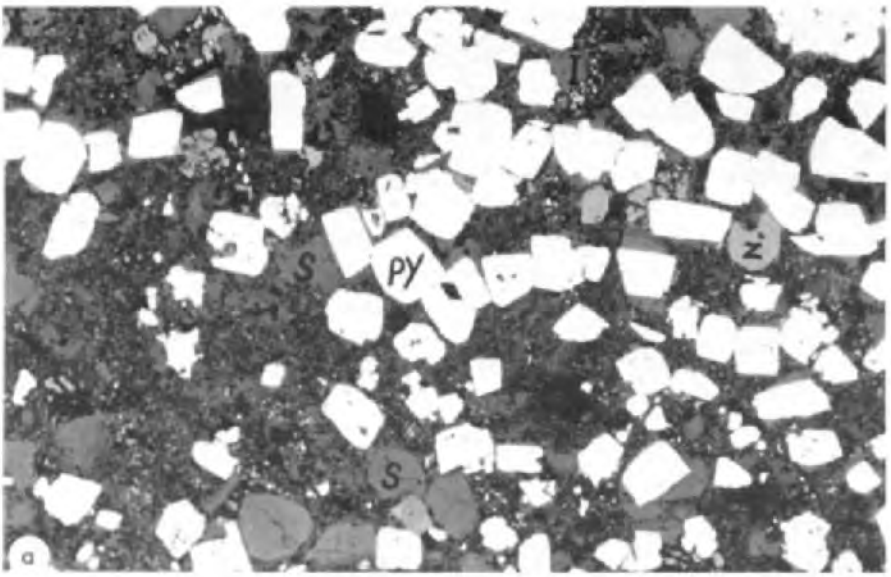

Fig. 7a. Photomicrograph of auriferous pyritic-pebble conglomerate, Turner Township. Note subrounded pyrite grains (PY); rounded zircon (Z); composite Fe—Ti minerals after ilmenite or titanomagnetite (I); silicates (S). Pyrite closely resembles that of the Roberts Township example (Fig. 11a). Plane polarized reflected light. Width of field of view = 1.5 mm.

Fig. 7b. Electron microprobe seam at 15 kv, 30 nano amps of a portion of the above field containing pyrite grains set in matrix of silicate minerals. Width of field of view = 0.3 mm (see text for details).

unit with subrounded and rounded clasts (maximum 12 cm, median 4.2 cm) forming the base of a fining-upward sequence in the lower 100 m of a section. This uraniferous, polymictic, cobble and pebble conglomerate carries 170 ppb gold. Coarse sandstones immediately above the conglomerate carry variable amounts of gold up to 350 ppb and are commonly pyritic along bedding-planes. Metamorphic grade is lower amphibolite facies.

Examination of several polished thin sections in reflected light revealed no visible gold. Upon examination with an electron-microprobe, minute sub-microscopic specks of gold appeared in one section in the silicate groundmass (Fig. 7a, b). It is unlikely, however, that these tiny, highly dispersed specks are in hydraulic equilibrium with the other minerals present. Pyrite grains show low level enrichment in gold.

Vogt Township

A conglomerate bed, carrying U and Au mineralization, located near the south end of Lake Timagami first attracted attention as a uranium project (No. 16, Table IV). It has been the subject of intermittent exploration for several decades and gold values well above background have been reported. Grant (1964) noted assays of up to 1700 ppb U in the rock. The conglomerate is reported to be located close to a deposit of graphite (not seen by the writers).

According to Long (1981, p. 220), the conglomerate carrying highest gold values is ~ 55 cm thick and contains pebbles of quartz, schist and various sedimentary and volcanic clasts. It has been subject to lower amphibolite facies metamorphism and has clasts with a maximum intermediate diameter of 5.1 cm, in a medium-grained pyritic sand matrix.

The conglomerate carries 240 ppb gold, an amount significantly less than reported by Grant (1964). Long (1981) has suggested that this indicates high lateral variability in the conglomerate; associated sandstone also carries high gold (60 ppb), indicative of possible localized high gold concentrations. The auriferous conglomerate is probably located stratigraphically within 15—20 m of the basement. According to D.G.F. Long (personal communication, 1981) it is likely a braided stream deposit, possibly mid—distal fan. Thus, the type of environment envisaged is not unlike that pictured by Pretorius (1974) as one supporting extensive growths of "algal mats" during sedimentation on the Witwatersrand.

A photomicrograph of the Vogt Township conglomerate (Fig. 8) reveals rounded to sub-rounded grains of pyrite resembling those commonly ascribed to detrital origin, e.g., some of the Witwatersrand "buckshot" pyrite. Graphite is absent in this specimen. Overall, distribution of gold in this rock is identical to that of the sample from Turner Township.

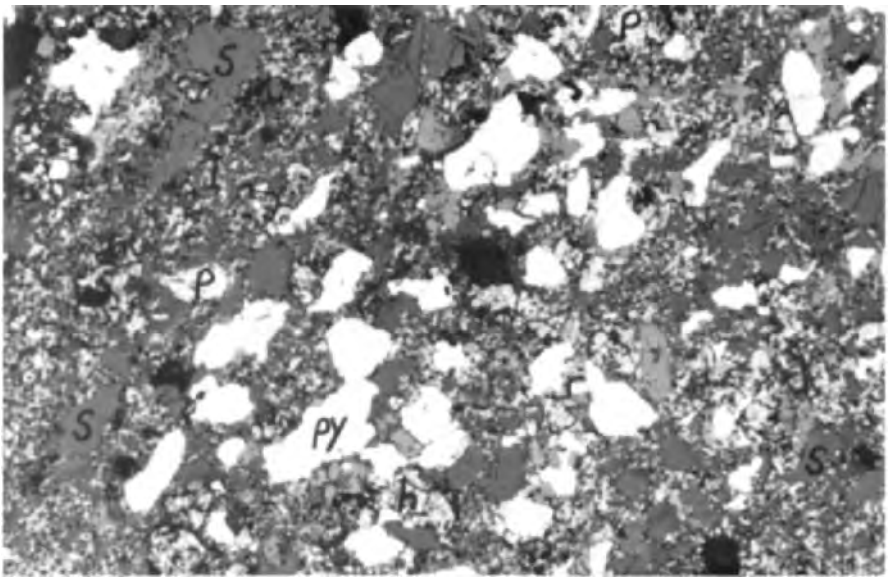

Fig. 8. Auriferous pyritic conglomerate from Vogt Township. Photomicrograph shows "buckshot" pyrite (PY) partly oxidized here to hematite (h) (pyrite is slightly anisotropic); alteration after detrital ilmenite or titanomagnetite (I); pyrrhotite (P); silicates (S). Reflected light. Width of field of view = 1.5 mm (see text for details).

Pardo Township

The paleoplacer (No. 114, Table IV) of Pardo Township has been investigated primarily on account of its uranium content. Long (1981) describes it as a polymictic, large pebble conglomerate. The clasts (maximum 7 cm, median 2.5 cm) are of predominantly local origin and include well rounded vein quartz and argillite, together with lesser amounts of black chert and some metavolcanic clasts not observed in the immediate basement. The matrix is a medium to coarse sand with very little pyrite (Long, 1981). Like the example from Vogt Township, it is part of a braided-stream deposit (Long, personal communication, 1981) probably formed in a mid-fan environment. According to Long (1981, p. 222), the highest concentrations of Au (165 ppb) do not occur in the most proximal facies, but in large pebble conglomerates like this with high U concentrations and usually with a high pyrite content. Metamorphic grade is upper greenschist facies.

Examination under the ore microscope reveals very few heavy minerals, litte pyrite, and no visible gold or carbon. The most conspicuous opaque mineral is pyrrhotite heavily altered to marcasite. Chalcopyrite is also present, as shown in Fig. 9. Electron-microprobe examination of this material indicates that gold is present at low levels of concentration in all of these opaque phases, presumably in solid solution.

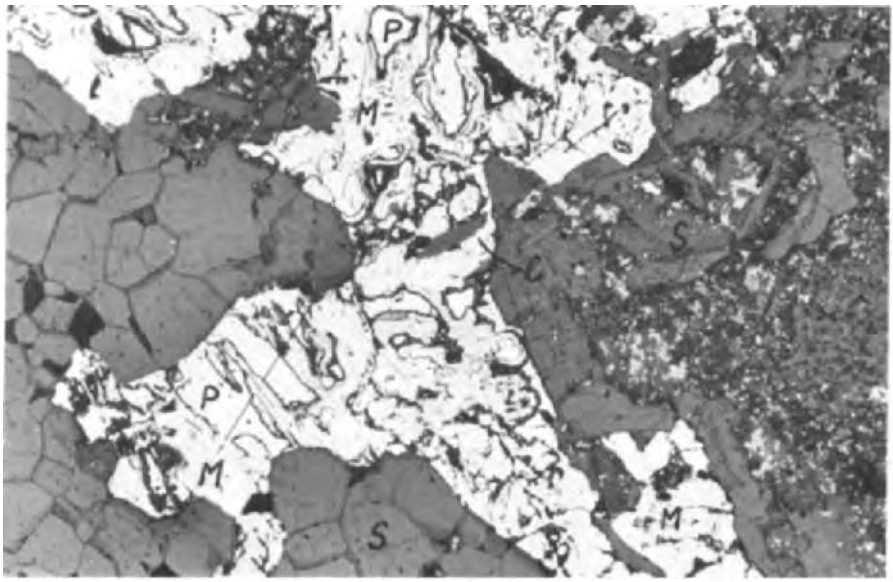

Fig. 9. Photomicrograph in plane polarized reflected light of auriferous, weakly pyritic conglomerate from Pardo Township. Pyrrhotite (P) is here heavily replaced by marcasite (M); chalcopyrite (C) occurs as scattered unaltered blebs; silicates (S) form groundmass. Width of field of view = 1.5 mm.

Grigg Township

In the "Mississagi" of Grigg Township, concentrations of heavy minerals occur in dark, radioactive siltstones and conglomerates. For example, Wood (1979, p. 63) reported that one sample of "dark siltstone" assayed 70 ppb Au; 0.14% Co; 0.17% Cr; 0.03% Cu; 0.02% Ni; 0.02% Pb and 0.1% U. This mineralization may be derived from an area of highly radioactive granite located 4 km west and from mafic volcanic rocks which discontinuously underlie the area.

A polymictic (Fig. 10) conglomerate with clasts of granite, quartz and basic schist, unlike the oligomictic, quartz-pebble conglomerates of the Witwatersrand and Elliot Lake, is located at the "CJM property" (Fig. 11), in the centre of the Township. It is a 2 m-thick radioactive conglomerate which occurs at the base of an ~30 m-thick sequence of uranium-enriched metasediments (No. 64, Table IV). The clasts are supported in a dark, fine-grained matrix, rich in biotite and chlorite. The composition of the conglomerate evidently reflects the underlying predominantly "greenstone" basement, whereas the provenance of the Blind River—Elliot Lake metasediments is granite.

Fig. 10. Polymictic conglomerate, Grigg Township ("CJM" Prospect). Note subrounded matrix-supported clasts of granite (G), quartz (Q), basic schist (S). The dark bands are biotite-rich laminations.

Thin layers of interbedded dark siltstone are conspicuous in the conglomerate from Grigg Township. At first these were believed to be carbonaceous. However, graphite is lacking in representative rocks from this property; nor was gold observed in the several polished thin-sections examined. Typically, the rock is studded with opaque mineral grains and judging from the pleochroic haloes developed in adjacent biotites many of them are radioactive. Metamorphic grade is lower amphibolite facies.

In this specimen, gold occurs at very low levels within the few sporadic pyrite grains.

Roberts Township

Meyn and Matthews (1980, p. 198) reported that, in this southern portion of the Cobalt Embayment, some of the highest U and Au values are located in Roberts Township. High assays reported from selected sampling of the Nordic prospect (No. 57, Table IV) yield: 8200 ppm U; 1640 ppm Th; 800 ppb Au. Meyn and Matthews (1980) attributed the anomalous Au values to a fluviatile, possibly braided stream, placer mode of concentration, with the provenance being the Abitibi greenstone belt to the north.

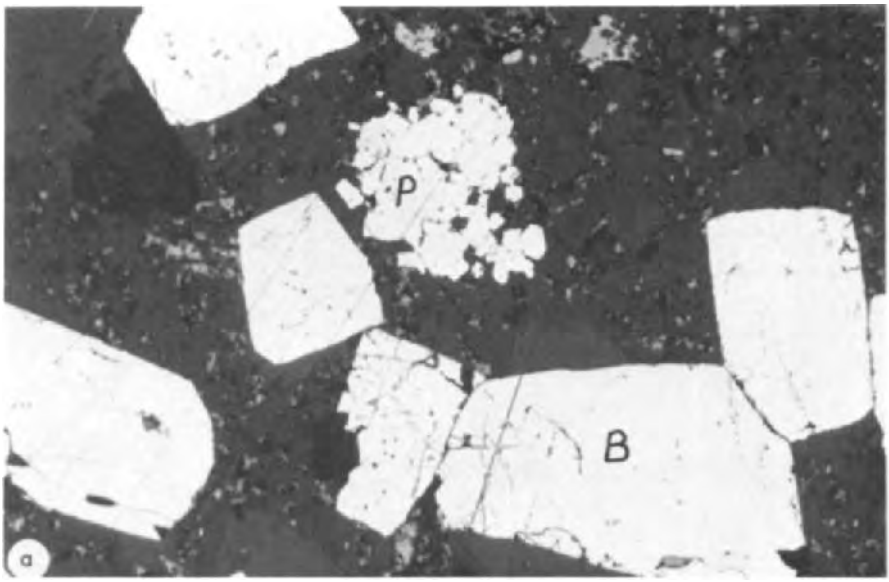

Fig. 11a. Photomicrograph, in plane polarized reflected light, of pyritic horizon of pebbly, medium sandstone from Roberts Township shows two kinds of pyrite: buckshot (B) and porous (P). Comparable low levels of concentrations of gold occur in pyrite of both types. Width of field of view = 0. 5 mm.

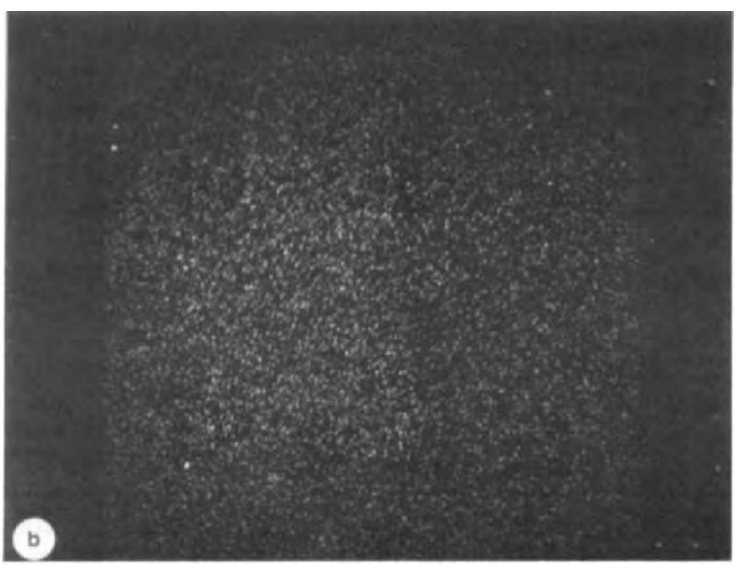

Fig. 11b. Electron microprobe scan of portion of the above field at 15 kv, 30 nano amps indicates low level concentrations of gold in pyrite grain (left of center) set in a matrix of silicate minerals. Width of field of view = 0.3 mm.

The sample reported on here was taken within a few tens of metres of the basement. It has been described by D.G.F. Long (personal communication, 1981) as part of a 10 cm-thick pyritic horizon in a ripple-laminated, pebbly, medium sandstone. Pebbles are predominantly chert and iron formation of local derivation. Metamorphic grade approximates upper greenschist—lower amphibolite facies. The host rock assays 350 ppb Au.

Two kinds of pyrite are evident (Fig. 11a). The most abundant kind is the rounded grains of "buckshot" pyrite of presumed detrital origin (see also Theis, 1979, p. 14). The other, also possibly analogous to the Witwatersrand, is a porous pyrite of presumed authigenic origin.

Detrital zircon is also present, along with rutile and ilmenite. Carbon (graphite) is not present in the rock. Electron-microprobe examination shows that gold is fairly evenly concentrated, though at very low levels, within pyrite grains (Fig. 11b). No discrete grains of gold, submicroscopic or otherwise, appear in the groundmass. Nor was any difference detected in the amount of gold concentrated in "buckshot" pyrite and in the "porous" variety.

THE ASSOCIATION C—U—(AU?) ELSEWHERE IN HURONIAN

In the Huronian Supergroup, some of the closest analogues to the Witwatersrand kerogen are the occurrences of thucholite reported from the Elliot Lake region. For example, Hallbauer has reportedly (in Theis, 1979) photographed filamentous carbonaceous material from the Rio Algom Nordic mine which resembles that of the Witwatersrand.

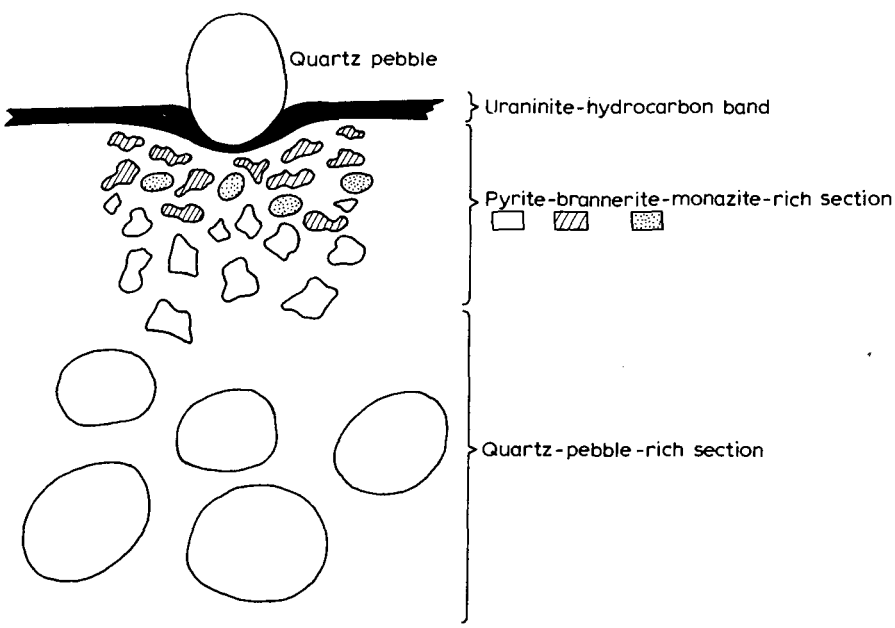

Fig. 12. "Conglomeratic uranium ore" (after Ruzicka and Steacy, 1976, p. 346) (see text for details).

Another example reproduced in Fig. 12 is a feature discovered by Ruzicka and Steacy (1976) in uranium ore at Denison mine, Elliot Lake. Briefly, their interpretation is that the ore constituents separated hydraulically and that the hydrocarbon, derived from some primary organic matter and acting as a collector or natural flotation agent for the uraninite, accumulated at the end of the depositional cycle.

Hattori et al. (1981) challenged Ruzicka and Steacy's (1976) interpretation on the basis of stable isotopic evidence, which apparently favours introduction of the organic matter after the original sedimentation of the conglomerate. A further cautionary note should be recalled by Boyle and Steacy's (1973) description of columnar thucholite containing specks of uraninite and gold from a skarn gold deposit at the Richardson mine, Ontario.

GEOLOGY OF HURONIAN GOLD AND THE OXYATMOVERSION

The transition from a reducing atmosphere to an oxidizing atmosphere was delayed a long time, according to the working model shown in Fig. 13. Yet it was well before Cloud's (1972, p. 543) designated "transitional stage" that the greatest concentrations of uranium and gold were deposited in early Proterozoic sediments.

In the Witwatersrand rocks, Hallbauer (1976) favours a reducing atmosphere during sedimentation, with transport of some Au as organic-supported colloids and extraction of the gold by (plant) micro-organisms. In the

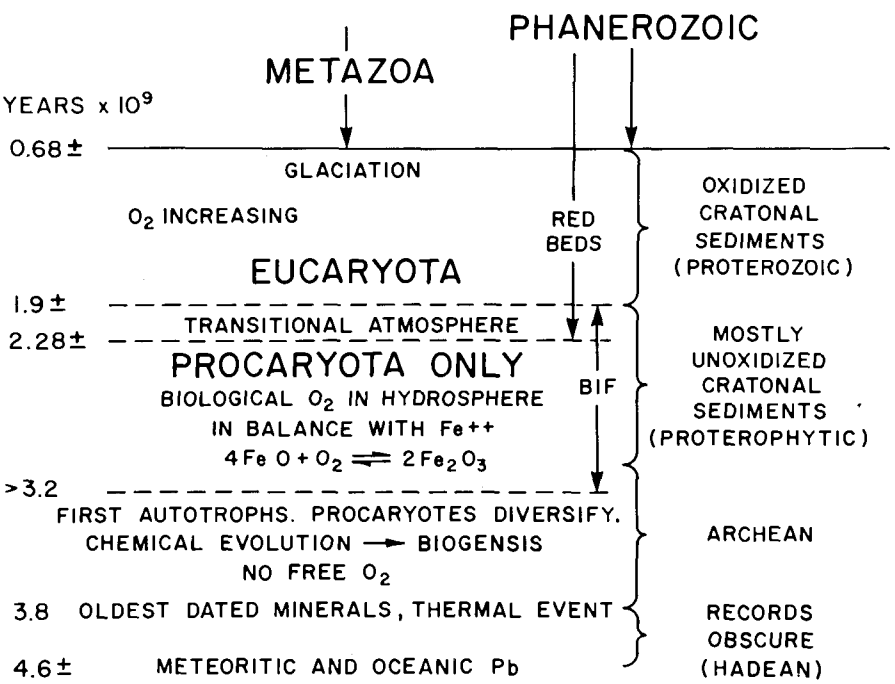

Fig. 13. Model of early Earth evolution (modified after Cloud, 1972, p. 543).

Huronian metasediments, carbonaceous material accompanies numerous concentrations of uranium and associations of carbon—uranium and gold are known from several localities. However, unequivocal evidence that any of that carbonaceous material is of fossil origin, in the sense of the Witwatersrand analogue, has not been demonstrated. Neither has the possibility been ruled out.

The question of just how reducing the atmosphere was during deposition of Proterozoic gold remains a controversial one. However, regardless of whether a direct connection between Au precipitation and life processes existed or not, the extent to which redox reactions were possible almost certainly would have affected the distribution of gold in those ancient sediments.

According to Garrels' (1981) calculations, the partial pressure of oxygen prior to banded iron formations (BIF's) was $<10^{-4}$ atmosphere. Yet even this figure is a long way from the "zero O_2 until ~ 2.3 Ga- ago" currently favoured by Cloud (1981).

Results of sulfur isotopic work also indicate minimal oxidation in the sedimentological regime of the Witwatersrand (Hoefs et al., 1968). In contrast, the results of Hattori et al.'s (1981) study of pyrites from the basal Huronian indicate a uniform source for the sulfur and crystallization in a metamorphic environment of secondary pyrite without oxidation and reduction.

It may be precisely because of the lack of any appreciable oxidation that the gold of early Proterozoic placers is, without exception, very fine-grained. This is in contrast to younger placers, particularly modern ones, where large nuggets are not uncommon. It is in these deposits where, for example, conditions of high Eh combined with low pH are capable of effecting the repeated solution and redeposition of gold necessary for secondary enrichment.

In the Huronian Supergroup there is excellent evidence for placing the oxyatmoversion at the base of the Firstbrook Member of the Gowganda Formation, with the first appearance of red beds (Owsiacki, 1981: Wood, personal communication, 1981). These same argillaceous rocks of the Gowganda have yielded a Rb/Sr isochron of 2.288 Ga ± 87 Ma according to Fairbairn et al. (1969).

The above data is virtually coincident with the 2.3 Ga figure currently favoured by Cloud (1981) as the time when free oxygen first began to build up in the atmosphere. This being the case, it seems possible that in sediments post-dating the lower Gowganda, paleoplacers of gold may exhibit features of enrichment comparable to some of the geologically younger deposits. Lovell and Grabowski (1981, p. 106) have suggested that Western Australian desert-type auriferous soil horizons may be preserved in the Lorrain Formation. A similar possibility applies to the Gordon Lake and Bar River Formations. These are precisely the rocks in which secondary enrichment of ore deposits would first have occurred.

DISCUSSION AND CONCLUSIONS

Geochemical behavior of gold in the surficial environment indicates that the element is relatively mobile under oxidizing conditions and therefore subject to processes of secondary enrichment. This situation is favored under lateritic conditions and it may also apply to many placer gold deposits. However, it does not apply to the Witwatersrand and to much of the Huronian Supergroup, which were deposited under reducing atmospheric conditions.

Huronian metasediments younger than mid-Gowganda (2.288 Ga) were deposited post-oxyatmoversion. In these, like the Tarkwa deposits of Ghana, where highest Au values occur in the most hematite-rich conglomerates (Boyle, 1979), conditions may have been favourable for forming economic paleoplacers of gold.

In the first instance, basement provenance will have determined the extent to which gold and its companion heavy minerals are distributed in the Huronian metasediments. Whether that gold occupies a demonstrably paleoplacer niche today also depends, in addition to those factors already discussed, on the degree to which diagenesis and metamorphism (regional and contact) have effected remobilization of gold.

In the case of the Witwatersrand, regional metamorphic grade is low greenschist facies (Pretorius, 1981). Opinions differ concerning the extent to which distribution of pyrite and gold has resulted from the processes of diagenesis and metamorphism (Saager, 1969; Feather and Koen, 1975; Dimroth, 1979). However, few if any investigators would deny that some reworking did take place.

With respect to pyrite in the Witwatersrand, the rounded, porous, occasionally concretionary type is generally acknowledged as diagenetic in origin, formed within the basin of deposition and possibly aided by the action of sulfate-reducing bacteria. The fact that its distribution is limited (Saager, 1970) is seen as compatible with a non-oxidizing atmosphere for these ores.

Theis (1979) has presented evidence to support a predominantly detrital origin of pyrite at Elliot Lake. Ninety percent of the grains are subrounded or subangular; the remaining grains (Theis, 1979, pp. 7—8) are either large and porous (replacements) or fine-grained euhedral crystals (crystallized in situ). The grouping is essentially the same as that favored for Witwatersrand pyrite (Saager, 1970). The types of grains and their relative abundances are similar to that observed in the present study.

According to Saager (1969), remobilization of Witwatersrand gold occurred due to a combination of processes including: alteration in streams; wave action and erosion; supergene enrichment; metamorphic reconstitution. Among other things, these processes are held to account for the exceptionally constant Ag/Au values of ~ 0.0812 for individual grains of gold (Saager, 1969).

In the Huronian, such data can only be determined when an economic paleoplacer deposit is located. Unfortunately, the discrete gold particles located during the present study are too finely dispersed to allow a quantitative estimate of the silver content.

The Huronian is renowned as a silver province, particularly in the northeastern part of the Cobalt Embayment. The situation is an interesting contrast to the Witwatersrand where gold ore samples commonly have high Ag/Au values, suggesting the presence of discrete silver minerals (Saager, 1969). Possibly, segregation of Ag from Au in the Huronian went further toward completion than in the Witwatersrand. That this should be the case is not unreasonable in view of the differences in regional metamorphic grade between the two terrains.

If diagenetic processes are credited with affecting relatively minor redistribution of gold in lower Aphebian sediments, the role of metamorphism seems likely also to have effected substantial change, particularly in the case of the Huronian Supergroup. Here, in the Southern Superior Province, regional metamorphism is complex (Card, 1978). Overall, the regional metamorphic grade ranges from lower greenschist to middle amphibolite facies, but the boundary between these facies, based as it is on the chloritoid—staurolite transition, is not easy to delineate with certainty.

At the higher metamorphic grades it is virtually certain that mobilization of gold will have been promoted well beyond that achieved through diagenesis. Fyfe and Henley (1973, p. 301) have shown that it is specifically under temperature conditions of 400°C (2 kb total pressure) that gold will move out of a system in waters saturated with respect to Au. The main provision is that chloride be present in the water moving out of the rock. Thus, in a predictive sense, no matter what the origin of the gold, the prospects diminish for locating modified paleoplacer gold in rocks of amphibolite grade and higher within the Huronian Supergroup.

ACKNOWLEDGEMENTS

Preparation of this paper has been greatly facilitated through discussions with many people including: P.E. Giblin, northeastern region resident geologist, Sudbury; D.G. Innes, consulting geologist, Sudbury; J. Wood and A.C. Colvine of the Ontario Geological Survey; R.A. Cameron and D.G.F. Long, Department of Geology, Laurentian University, Sudbury; V.R. Ruzicka, Geological Survey of Canada, Ottawa. Especially, we wish to acknowledge sample materials freely provided for our study by J. Wood, D.G.F. Long and V.R. Ruzicka.

We gratefully acknowledge financial support provided throughout the course of this study by Du Pont of Canada Exploration Ltd. and by the National Sciences and Engineering Council of Canada in the form of a grant in aid of research to D.J.M.

Addendum

Since this paper went to press several interesting new occurrences of paleoplacer gold have been located in the Huronian Supergroup and are detailed in Table A1.

TABLE A1

No.	Name	Township	Cat.	Host Rock Formation	Morphology			Mineral Assemblage	Assays, Reports	Reference
					V	DR	S			
122	Inco deep drilling; hole no. 54060	Telfer	P	Mississagi			X	diss. py in arkosic wacke	Highest value 0.004 oz/t Au/1′	Dressler, 1979a
123	Inco deep drilling; hole no. 54061	DeMorest	P	Serpent and Mississagi			X	diss. py	to 0.021 oz/t Au/2′ in Serpent; to 0.032 oz/t Au/2′ in Mississagi	Card et al., 1973
124	Inco deep drilling; hole no. 54062	DeMorest	P	Mississagi			X	py	to 0.026 oz/t Au/2.2′ in subarkose, minor pebble beds	Card et al., 1973
125	—	Lundy (north half)	P	Lorrain (Firstbrook Member)			X	—	180 ppb in laminated argillites	Owsiacki, 1982
126	—	Dufferin and North Williams	P	Lorrain			X	hem	to 0.04 oz/t Au (enrichment 700X background)	Colvine, 1982
127	Cullis Lake	Day	P	Quartz-pebble conglomerate at base of Thessalon Formation, a dominantly volcanic unit — believed equivalent to the Matinenda Formation (Frarey, 1977)			X	py	4300 ppb grab sample of conglomerate at unconformity with Livingstone Creek sandstone	Bennett, 1982

REFERENCES

Aripova, Kh. and Talipov, R.M., 1966. Concentration of gold in soils and plants in the southern part of the Tamdyn Mountains. Ubz. Geol. Zh., 10: 45—51 (Chem. Abstr., 66: 48364 m).

Babička, J., 1943. Gold in living organisms. Mikrochemie Ver. Mikrochim. Acta, 31: 201—253.

Bate, L.C. and Dyer, F.F., 1965. Trace elements in human hair. Nucleonics, 23: 74—81.

Bennett, G., 1982. Gold in radioactive quartz pebble conglomerates of the Thessalon area District of Algoma (Abstract). In: E.G. Pye (Editor), Geoscience Research Seminar, Dec. 8—9, 1982 (Abstracts). Ont., Geol. Surv., Toronto, 15 pp.

Bennett, G. and Leahy, E.J., 1979. Report of the Sault Ste. Marie resident geologist. In: C.R. Kustra (Editor), Annual Report of the Regional and Resident Geologists, 1979. Ont. Geol. Surv. Misc. Pap., 91: 97—102.

Bowen, H.J.M., 1968. The uptake of gold by marine sponges. J. Mar. Biol. Assoc. U.K., 48: 275—277.

Boyle, R.W., 1979. The geochemistry of gold and its deposits. Geol. Surv. Can. Bull. 280, 584 pp.

Boyle, R.W. and Steacy, H.R., 1973. An auriferous radioactive hydrocarbon from the Richardson mine, Eldorado, Ontario. In: Report of Activities, April—October, 1972. Geol. Surv. Can. Pap., 73-1A: 282—285.

Card, K.D., 1976a. Geology of the Espanola—Whitefish Falls Area, District of Sudbury, Ontario. Ont. Div. Mines Geol. Rep. 131, 70 pp.

Card, K.D., 1976b. Geology of the McGregor Bay—Bay of Islands Area, Districts of Sudbury and Manitoulin. Ont. Div. Mines Geol. Rep. 138, 63 pp.

Card, K.D., 1978. Geology of the Sudbury—Manitoulin Area, Districts of Sudbury and Manitoulin. Ont. Geol. Surv. Rep. 166, 238 pp.

Card, K.D. and Innes, D.G., 1981. Geology of the Benny Area, District of Sudbury. Ont. Geol. Surv. Rep. 106, 117 pp.

Card, K.D. and Lumbers, S.B., 1977. Sudbury—Cobalt, District of Algoma, Manitoulin, Nipissing, Sudbury and Temiskaming. Ont. Geol. Sur., Map 2361, Geol. Compilation Ser., Scale 1:253 440.

Card, K.D. and Palonen, P.A., 1976. Geology of the Dunlop—Shakespeare Area, District of Sudbury. Ont. Div. Mines Geol. Rep. 139, 52 pp.

Card, K.D. and Pattison, E.F., 1973. Nipissing Diabase of the Southern Province, Ontario. In: G.M. Young (Editor), Huronian Stratigraphy and Sedimentation. Geol. Assoc. Can. Spec. Pap., 12: 7—30.

Card, K.D., McIlwaine, W.H. and Meyn, H.D., 1973. Geology of the Maple Mountain Area, Districts of Temiskaming, Nipissing, and Sudbury. Ont. Div. Mines Geol. Rep., 106, 133 pp.

Card, K.D., Palonen, P.A. and Semiatkowska, K.M., 1975. Geology of the Louise—Eden Lake Area, District of Sudbury. Ont. Div. Mines Geol. Rep. 124, 66 pp.

Chandler, F.W., 1973. Geology of McMahon and Morin Townships, District of Algoma. Ont. Div. Mines Geol. Rep. 112, 77 pp.

Clark, W.B., 1979. Fossil river beds of the Sierra Nevada. Calif. Geol., July, 3: 143—149.

Cloke, P.L. and Kelly, W.C., 1964. Solubility of gold under inorganic supergene conditions. Econ. Geol., 59: 259—270.

Cloud, P., 1972. A working model of the primitive Earth. Am. J. Sci., 272: 537—548.

Cloud, P., 1981. Aspects of Proterozoic biogeology — weaving the fabric. International Proterozoic Symposium, Univ. Wisconsin-Madison, May 18—21, Abstract.

Collins, W.H., 1925. North shore of Lake Huron. Can. Geol. Surv. Mem. 143, 160 pp.

Colvine, A.C., 1981. Reconnaissance of the Lorrain Formation, northern Cobalt Embayment. In: J. Wood, O.L. White, R.B. Barlow and A.C. Colvine (Editors), Summary of Field Work, 1981, Ontario Geological Survey. Ont. Geol. Surv., Misc. Pap., 100: 187—190.

Colvine, A.C., 1982. Summary of activities, Mineral Deposits Section. In: J. Wood, O.L. White, R.B. Barlow and A.C. Colvine (Editors), Summary of Field Work, 1982 by the Ontario Geological Survey. Ont. Geol. Surv. Misc. Pap., 106: 172—175.

Dimroth, E., 1979. Significance of diagenesis for the origin of Witwatersrand-type uraniferous conglomerates. Philos. Trans. R. Soc. London, Ser. A, 291: 277—287.

Dressler, B.O., 1978a. Rathburn Township, District of Sudbury. Ont. Geol. Surv., Prelim. Map P 1609, Geol. Compilation Ser., Scale 1:15840.

Dressler, B.O., 1978b. Mackelcan Township and Southern Wanapitei Lake Area, District of Sudbury. In: V.G. Milne, O.L. White, R.B. Barlow and J.A. Robertson (Editors), Summary of Field Work, 1978, Ontario Geological Survey. Ont. Geol. Surv. Misc. Pap., 82: 112—115.

Dressler, B.O., 1979a. Mackelcan Township, District of Sudbury, Ontario. Ont. Geol. Surv., Map P 2227, Geol. Compilation Ser., Scale 1:15840.

Dressler, B.O., 1979b. Geology of McNish and Janes Townships, District of Sudbury. Ont. Geol. Surv. Rep. 191, 91 pp.

Fairbairn, H.W., Hurley, P.M., Card, K.D. and Knight, C.J., 1969. Correlation of radiometric ages of Nipissing Diabase and Huronian metasediments with Proterozoic orogenic events in Ontario. Can. J. Earth Sci., 6: 489—497.

Feather, C.E. and Koen, G.M., 1975. The mineralogy of the Witwatersrand reefs. Miner. Sci. Eng., 7: 189—224.

Ferguson, S.A., Groen, H.A. and Haynes, R., 1971. Gold deposits of Ontario, part 1. Ont. Dept. Mines Misc. Rep. 13, 315 pp.

Fralick, P.W. and Miall, A.D., 1981. Sedimentology of the Matinenda Formation. In: E.G. Pye (Editor), Geoscience Research Grant Program, Summary of Research, 1980—1981, Ontario Geological Survey. Ont. Geol. Surv. Misc. Pap., 98: 80—89.

Frarey, M.J., 1977. Geology of the Huronian belt between Sault St. Marie and Blind River, Ontario. Geol. Surv. Can. Mem. 383, 87 pp.

Frarey, M.J. and Roscoe, S.M., 1970. The Huronian Supergroup north of Lake Huron. In: A.J. Baer (Editor), Symposium on Basins and Geosynclines of the Canadian Shield. Geol. Surv. Can. Pap., 70-40: 143—157.

Fyfe, W.S. and Henley, R.W., 1973. Some thoughts on chemical transport processes, with particular reference to gold. Miner. Sci. Eng., 5: 295—303.

Garrels, R.M., 1981. Waters of the early Proterozoic. International Proterozoic Symposium, Univ. Wisconsin-Madison, May 18—21, Abstract.

Gibbins, W.A. and McNutt, R.H., 1975. Rubidium—strontium mineral ages and polymetamorphism at Sudbury, Ontario. Can. J. Earth Sci., 12: 1990—2003.

Giblin, P.E. and Leahy, E.J., 1979. 1978 Report of northeastern regional geologist and Sault Ste. Marie resident geologist. In: C.R. Kustra (Editor), Annual Report of the Regional and Resident Geologists, 1978. Ont. Geol. Surv. Misc. Pap., 84: 89—98.

Ginn, R.M., 1965. Geology of Nairn and Lorne Townships, District of Sudbury. Ont. Dept. Mines Geol. Rep. 35, 46 pp.

Gordon, J.B., 1977. Gold deposits of Ontario, east central sheet, districts of Thunder Bay, Algoma, Cochrane, Sudbury, Temiskaming and Nipissing. Ont. Geol. Surv., Prelim. Map P 1228, Mineral Deposits Series, Compilation 1974, 1975, 1976, Scale 1: 1 013 760 or 1 inch to 16 miles.

Gordon, J.B., Lovell, H.L., De Grijs, J. and Davie, R.F., 1979. Gold deposits of Ontario, part 2. Ont. Geol. Surv. Misc. Rep., 18: 253 pp.

Grant, J.A., 1964. Vogt—Hobbs area. Ont. Dept. Mines Geol. Rep. 22 (accompanied by Map 2048, Scale 1 inch to 1/2 mile) 24 pp.

Hallbauer, D.K., 1976. The plant origin of the Witwatersrand carbon. Miner. Sci. Eng., 7: 111—131.

Hallbauer, D.K. and Van Warmelo, K.T., 1974. Fossilized plants in thucholite from Precambrian rocks of the Witwatersrand, South Africa. Precambrian Res., 1: 199—212.

Hattori, K., Campbell, F.A. and Krouse, H.F., 1981. Stable isotope study on uraniferous conglomerate in Elliot Lake (abstract). Geol. Assoc. Can. — Min. Assoc. Can. — Can. Geophys. Union Joint Ann. Mtg., Calgary, p. A24.

Hoefs, J., Nielson, H. and Schidlowski, M., 1968. Sulfur isotope abundance in pyrite from the Witwatersrand conglomerates. Econ. Geol., 63: 975—977.

Innes, D.G., 1978. McKim Township, District of Sudbury. Ont. Geol. Surv., Prelim. Map P 1978, Geol. Compilation Ser., Scale 1:15840.

Innes, D.G. and Colvine, A.C., 1979. Metallogenetic development of the eastern part of the Southern Province of Ontario. In: V.G. Milne, O.L. White, R.B. Barlow and C.R. Kustra (Editors), Summary of Field Work, 1979, Ontario Geological Survey. Ont. Geol. Surv. Misc. Pap., 90: 184—189.

Johns, G.W., 1979. Firstbrook Lake Area, District of Timiskaming. In: V.G. Milne, O.L. White, R.B. Barlow and C.R. Kustra (Editors), Summary of Field Work, 1979, Ontario Geological Survey. Ont. Geol. Surv. Misc. Pap., 90: 112—115.

Kindle, L.F., 1933. Moose Mountain—Wanapitei Area. In: A. West (Editor), 41st Annual Report, Vol. XLI, Part IV. 1932, Ont. Dept. Mines, pp. 29—49.

Lakin, H.W., Curtin, G.C., Hubert, A.E., Shacklette, H.T. and Doxtader, L., 1974. Geochemistry of gold in the weathering cycle. U.S. Geol. Surv. Bull. 1330, 80 pp.

Le Count Evans, D., 1981. Laterization as a possible contribution to gold placers. Eng. Min. J., 82: 86—91.

Ling Ong, H. and Swanson, V.E., 1969. Natural organic acids in the transportation, deposition and concentration of gold. Colo. Sch. Mines Q., 64: 395—425.

Long, D.G.F., 1976. The stratigraphy and sedimentology of the Huronian (lower Aphebian) Mississagi and Serpent Formations. Ph.D. Thesis, Univ. Western Ont., London, Ont., 291 pp.

Long, D.G.F., 1981. The sedimentary framework of placer gold concentrations in basal Huronian strata of the Cobalt Embayment. In: J. Wood, O.L. White, R.B. Barlow and A.C. Colvine (Editors), Summary of Field Work, 1981, Ontario Geological Survey. Ont. Geol. Surv., Misc. Pap., 100: 218—223.

Lovell, H.L. and Grabowski, G.P.B., 1981. Report of the Kirkland Lake resident geologist: In: C.R. Kustra (Editor), Annual Report of the Regional and Resident Geologists. 1980, Ontario Geological Survey. Ont. Geol. Surv., Misc. Pap., 95: 86—107.

Martins, J.M., Horst, R.E. and Giblin, P.E., 1980. Report of Sudbury resident geologist. In: C.R. Kustra (Editor), Annual Report of the Regional and Resident Geologists, 1979, Ontario Geological Survey. Ont. Geol. Surv. Misc. Pap., 91: 103—116.

Meyn, H.D., 1970. Geology of Hutton and Parkin Townships. Ont. Dept. Mines Geol. Rep. 80, 78 pp.

Meyn, H.D., 1971. Geology of Roberts, Creelman and Fraleck Townships, District of Sudbury. Ont. Dept. Mines North. Aff. Geol. Rep. 191, 48 pp.

Meyn, H.D., 1972. Geology of Grigg and Stobie Townships, District of Sudbury. Ont. Dept. Mines North. Aff. Geol. Rep. 100, 39 pp.

Meyn, H.D., 1979. Uranium deposits of the Cobalt Embayment. In: V.G. Milne, O.L. White, R.B. Barlow and C.R. Kustra (Editors), Summary of Field Work, 1979, Ontario Geological Survey. Ont. Geol. Surv. Misc. Pap., 90: 218—221.

Meyn, H.D. and Matthews, M.K., 1980. Uranium deposits of the Cobalt Embayment. In: V.G. Milne, O.L.White, R.B. Barlow, J.A. Robertson and A.C. Colvine (Editors), Summary of Field Work, 1980, Ontario Geological Survey. Ont. Geol. Surv. Misc. Pap., 96: 195—199.

Owsiacki, L., 1981. Geology of Lundy Township, District of Temiskaming. In: J. Wood, O.L. White, R.B. Barlow and A.C. Colvine (Editors), Summary of Field Work, 1981, Ontario Geological Survey. Ont. Geol. Surv., Misc. Pap., 100: 214—217.

Owsiacki, L., 1982. Geology of Lundy Township (Northern Half), District of Temiskaming. In: J. Wood, O.L. White, R.B. Barlow and A.C. Colvine (Editors), Summary of Field Work, 1982 by the Ontario Geological Survey. Ont. Geol. Surv. Misc. Pap., 106: 201—206.

Phemister, T.C., 1939. Notes on several properties in the District of Sudbury. In: 48th Annual Report. Vol. XLVIII, Part X, Ont. Dept. Mines, pp. 16—28.
Pretorius, D.A., 1974. Gold in the Proterozoic sediments of South Africa. Systems, paradigms, and models. Univ. Witwatersrand, Econ. Geol. Res. Unit, Inf. Circ., 87: 1—22.
Pretorius, D.A., 1981. Gold and uranium in quartz-pebble conglomerates. Econ. Geol., 75: 117—138.
Razin, L.V. and Rozhkov, I.S., 1966. Geochemistry of gold in the crust of weathering and the biosphere of gold-ore deposits of the Kuranakh type. Nauka, Moscow, (Reviewed in Econ. Geol., 62: 437—438) 254 pp.
Robertson, J.A., 1962. Geology of Townships 137 and 138, District of Algoma. Ont. Dept. Mines Geol. Rep. 10, 94 pp.
Robertson, J.A., 1963a. Geology of the Iron Bridge Area, District of Algoma. Ont. Dept. Mines Geol. Rep. 17, 69 pp.
Robertson, J.A., 1963b. Townships 155, 156, 161, 162, parts of 167, 168, District of Algoma. Ont. Dept. Mines Geol. Rep. 13, 88 pp.
Robertson, J.A., 1968a. Geology of Township 149 and Township 150, District of Algoma. Ont. Dept. Mines Geol. Rep. 57, 162 pp.
Robertson, J.A., 1968b. Uranium and thorium deposits of northern Ontario. Ont. Div. Mines Misc. Rep. 9, 106 pp.
Robertson, J.A., 1970. Geology of the Spragge Area, District of Algoma. Ont. Dept. Mines Geol. Rep. 76, 109 pp.
Robertson, J.A., 1976. Geology of the Massey Area, District of Algoma, Manitoulin and Sudbury. Ont. Div. Mines Geol. Rep. 136, 130 pp.
Robertson, J.A., Card, K.D. and Frarey, M.J., 1969. The Federal—Provincial Committee on Huronian Stratigraphy progress report. Ont. Dept. Mines Misc. Pap. 31, 26 pp.
Roscoe, S.M., 1969. Huronian rocks and uraniferous conglomerates. Geol. Surv. Can. Pap. 68-40, 205 pp.
Roscoe, S.M., 1973. The Huronian Supergroup, a Paleoaphebian succession showing evidence of atmospheric evolution. Geol. Assoc. Can. Spec. Pap., 12: 31—47.
Ruzicka, V. and Steacy, H.R., 1976. Some sedimentary features of conglomeratic uranium ore from Elliot Lake, Ontario. Geol. Surv. Can. Pap., 76-1A; 343—346.
Saager, R., 1969. The relationship of silver and gold in the Basal Reef of the Witwatersrand System, South Africa. Miner. Deposita, 4: 93—113.
Saager, R., 1970. Structures in pyrite from the Basal Reef in the Orange Free State Gold Field. Geol. Soc. S. Afr. Trans., 73: 29—46.
Sergiades, A.O., 1968. Silver—cobalt—calcite vein deposits of Ontario. Miner. Resour. Circular 10, 23 pp.
Shklanka, R., 1969. Copper, nickel, lead and zinc deposits of Ontario. Ont. Dept. Mines Misc. Rep. 12, 394 pp.
Siemiatkowska, K.M., 1977. Geology of the Wakaomata Lake Area, District of Algoma. Ont. Div. Mines Geol. Rep. 151, 57 pp.
Siemiatkowska, K.M., 1978. Geology of the Endikai Lake Area, District of Algoma. Ont. Geol. Surv. Rep. 178, 79 pp.
Simony, P.S., 1964. Geology of Northwestern Timagami Area, District of Nipissing. Ont. Dept. Mines Geol. Rep. 28, 30 pp.
Sullivan, C.J., 1979. Intracratonic basins and ore deposits. Bull. Can. Inst. Mining Met., 72: 75—80.
Tankard, A.J., Jackson, M.P.A., Eriksson, K.A., Hobday, D.K., Hunter, D.R. and Minter, W.E.L., 1982. Crustal Evolution of Southern Africa. The Golden Proterozoic. Springer-Verlag, Berlin, pp. 115—150.
Theis, N.J., 1979. Uranium-bearing and associated minerals in their geochemical and sedimentological context, Elliot Lake, Ontario. Geol. Surv. Can. Bull. 304, 50 pp.

Thomson, J.E., 1961. Maclennan and Scadding Townships. Ont. Dept. Mines Geol. Rep. 2, 34 pp.

Thomson, J.E. and Card, K.D., 1963. Geology of Kelly and Davis Townships. Ont. Dept. Mines Geol. Rep. 15, 20 pp.

Warren, H.V., 1979. Supergene gold crystals at Stirrup Lake, B.C. Western Miner, 52(6): 9—14.

Wood, J., 1979. Regional geology of the Cobalt Embayment, Districts of Sudbury, Nipissing and Temiskaming. In: V.G. Milne, O.L. White, R.B. Barlow and C.R. Kustra (Editors), Summary of Field Work, 1979, Ontario Geological Survey. Ont. Geol. Surv. Misc. Pap., 90: 79—81.

Wood, J., 1980. Regional geology of the Cobalt Embayment, Districts of Sudbury, Nipissing and Temiskaming. In: V.G. Milne, O.L. White, R.B. Barlow, J.A. Robertson and A.C. Colvine (Editors), Summary of Field Work, 1980, Ontario Geological Survey. Ont. Geol. Surv. Misc. Pap., 96: 61—63.

Young, G.M., 1981. Tectono-sedimentary history of early Proterozoic rocks of the northern Great Lakes region. International Proterozoic Symposium, Univ. Wisconsin-Madison, May 18—21.

Zumberge, J.E., Sigleo, A.C. and Nagy, B., 1978. Molecular and elemental analysis of the carbonaceous matter in the gold- and uranium-bearing Vaal Reef carbon seams, Witwatersrand sequence. Miner. Sci. Eng., 10: 223—246.

This Page Intentionally Left Blank